



This work is protected by copyright and other intellectual property rights and duplication or sale of all or part is not permitted, except that material may be duplicated by you for research, private study, criticism/review or educational purposes. Electronic or print copies are for your own personal, non-commercial use and shall not be passed to any other individual. No quotation may be published without proper acknowledgement. For any other use, or to quote extensively from the work, permission must be obtained from the copyright holder/s.

THE PETROGENESIS OF THE ST. MALO MIGMATITE BELT,

NORTH-EASTERN BRITTANY, FRANCE

MICHAEL BROWN BA, FGS

Thesis submitted for the Degree of Doctor of Philosophy

at

The University of Keele

December, 1974

IMAGING SERVICES NORTH

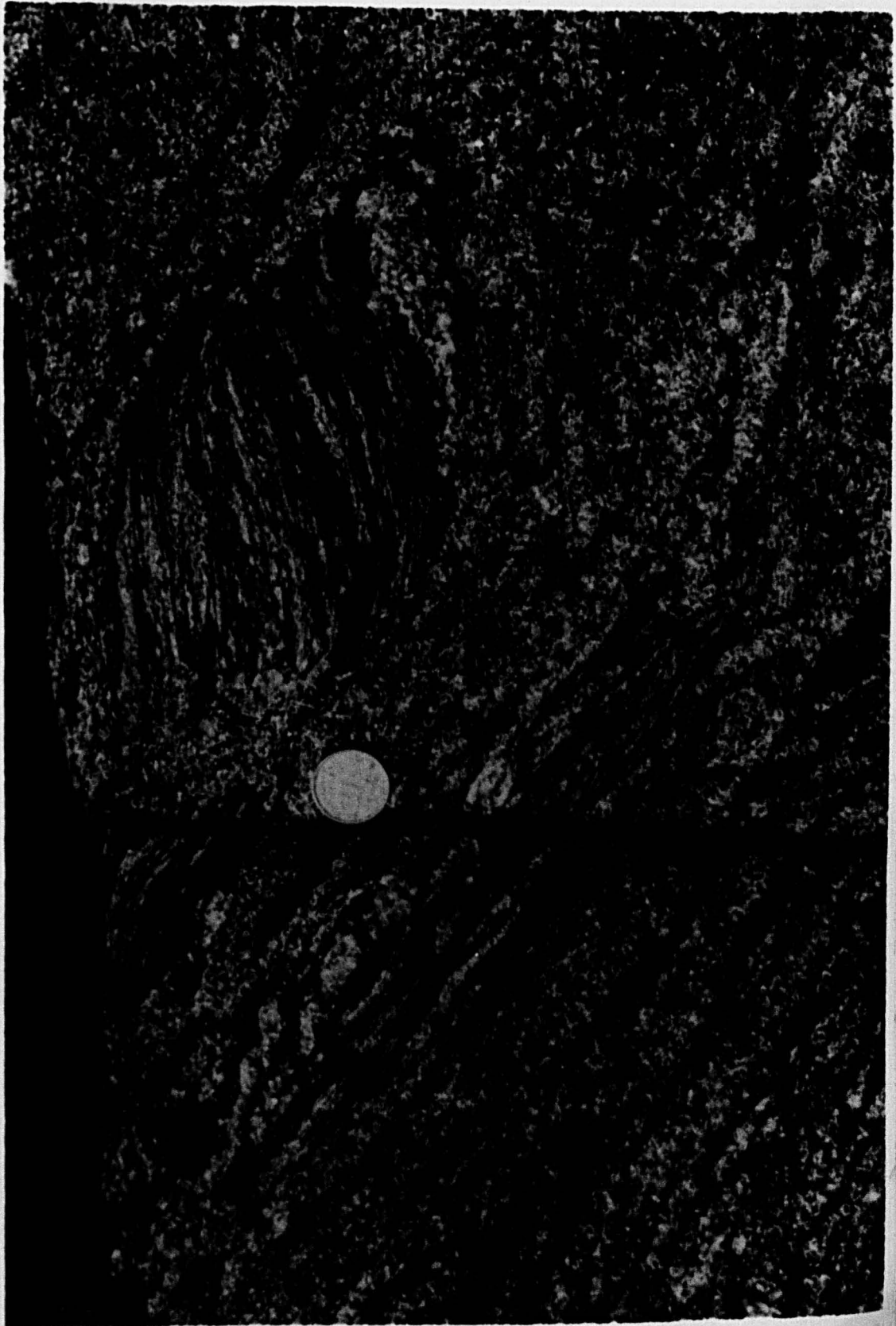
Boston Spa, Wetherby
West Yorkshire, LS23 7BQ
www.bl.uk

BEST COPY AVAILABLE.

VARIABLE PRINT QUALITY

FRONTISPIECE 1

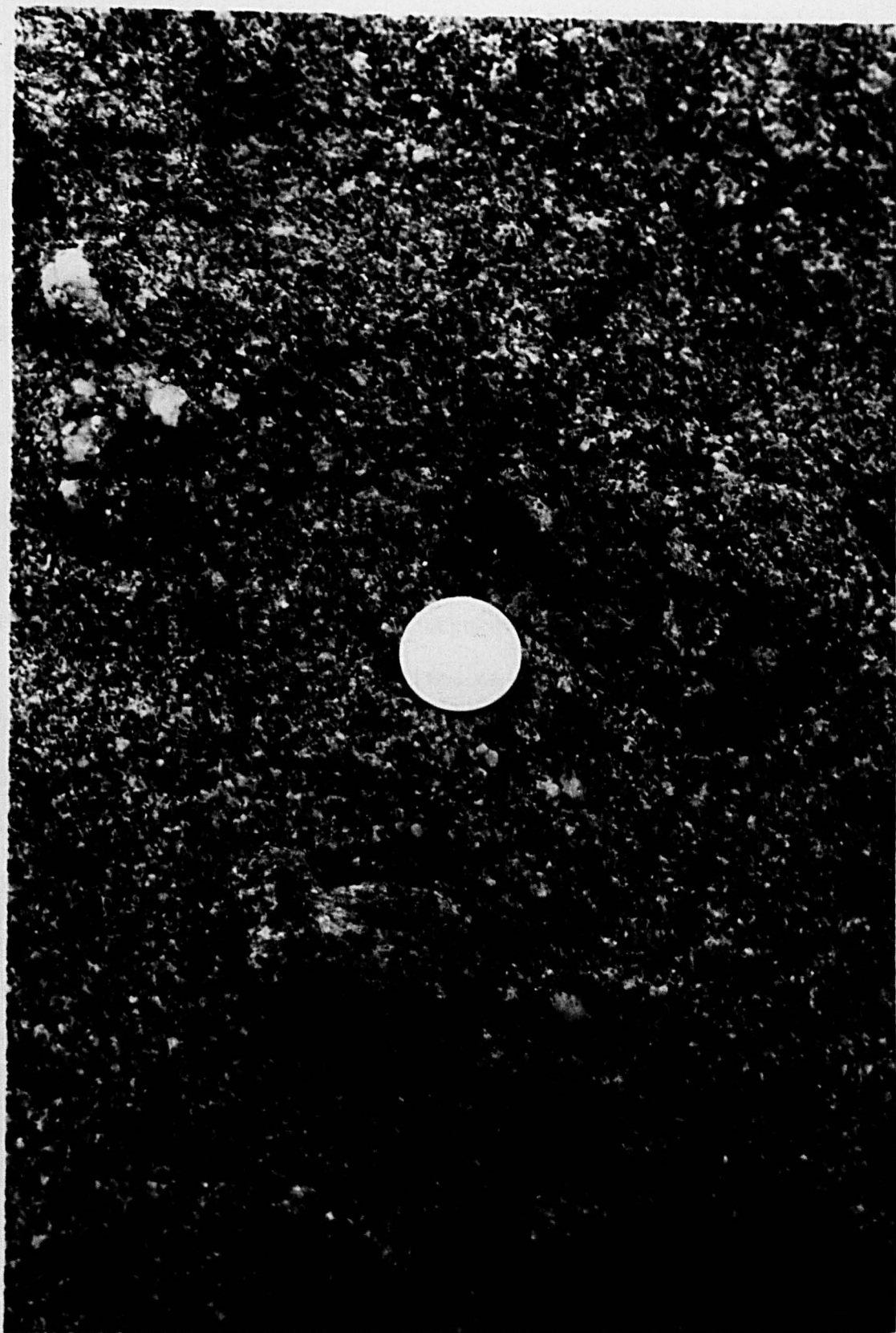
THE TRANSITION FROM METATEXITE TO DIATEXITE
WEST OF POINTE DE LA GARDE GUERIN



FRONTISPIECE 2

INHOMOGENEOUS DIATEXITE

HAVRE DE ROTHENEUF



Abstract

The St. Malo migmatite belt is located along the north Brittany coast between the towns of N. D. du Guildo (Cotes-du-Nord) and Cancale (Ille-et-Vilaine). The belt, which has a north-east trend and structural grain, has been assigned to the Hercynian (Abrard, 1923), Caledonian (Graindor, 1962) and Cadomian (Leutwein, 1968 and Jeannette, 1971) earth movements. Detailed structural and metamorphic studies have shown, however, that rocks within the St. Malo migmatite belt have a longer structural history and a higher metamorphic grade than adjacent Brioverian supracrustal rocks (Brown, Barber & Roach, 1971). The St. Malo migmatite belt represents part of the Pentevrian basement within the Armorican Massif.

Included within the St. Malo migmatite belt are metasediments, metatexites, diatexites and, locally, sheets of granite and trondhjemite. The terms metatexite and diatexite are used according to the definitions proposed by Brown (1973). Metatexis is defined as "... the process of segregation (usually of quartz and feldspar) by metamorphic differentiation and partial fusion" and a metatexite is therefore a rock "... produced by metatexis and in which the migmatitic banding is evident". Diatexis is defined as "... high-grade anatexis in which fusion may be complete" and a diatexite is therefore a rock "... produced by diatexis and in which there is no continuous migmatitic banding".

The western half of the St. Malo migmatite belt comprises approximately equal proportions of metatexite and diatexite at the present level of erosion. Mesoscopic patches of diatexite are common within the metatexite and often fragment the metatexite to give schollen structure. Granite sheets are common within the metatexites. The

eastern half of the St. Malo migmatite belt is dominated by diatexite at the level now exposed. The diatexite forms a core to the migmatite belt and on its south-eastern side has punched through the metatexite envelope to intrude Pentevrian metasediments. The River Rance provides a transverse section through the St. Malo migmatite belt and allows the transition from Pentevrian metasediment to metatexite to diatexite to be studied in detail. Similar rocks are exposed around St. Cast and upstream along the Rance near Dinan.

Brioverian metasediments are exposed on the north-western side of the St. Malo migmatite belt. They comprise a sequence of turbidites. Shear belts of Cadomian age cut the Pentevrian basement.

The major element chemistry of the diatexites shows a closer affinity with sediments of greywacke type rather than with sediments of arkose type and one sample of Pentevrian metasediment is similar to calcium-poor greywacke. The St. Malo rocks have K/Rb ratios near the average for upper crustal rocks and Th/U ratios similar to amphibolite facies granite gneisses. Twenty four separated biotites have been analysed for a selection of major and trace elements and have allowed an estimate to be made of the prevailing temperature and fugacity of water during diatexis.

Four episodes of deformation are recognized within the Pentevrian metasediments prior to the Cadomian orogeny. Initial metatexis was broadly concomitant with D_1 whilst later diatexis was broadly concomitant with D_3 . Three episodes of deformation are recognized within the Brioverian supracrustal rocks and within shear belts developed in the Pentevrian basement in response to the Cadomian orogenic episode.

Mesonormative Q-Ab-Or ratios of the diatexites show a close relationship with points of minimum melt composition determined

experimentally within the $\text{NaAlSi}_3\text{O}_8$ - KAlSi_3O_8 - $\text{CaAl}_2\text{Si}_2\text{O}_8$ - SiO_2 - H_2O system and projected from An onto the Q-Ab-Or face of the Q-Ab-Or-An tetrahedron. Mesonormative Ab-Or-An ratios of the diatexites lie within the plagioclase feldspar field on the ternary feldspar face of the Q-Ab-Or-An tetrahedron. A variety of evidence suggests that the diatexites crystallised under variable water vapour pressures in the range 2-5 kb. Consideration of the water saturated phase relations in the Q-Ab-Or-An tetrahedron shows that the mesonormative compositions of the diatexites generally lie within the primary phase volume of quartz close to the quartz-feldspar surface. Crystallization of the diatexites would have proceeded with the early appearance of quartz and plagioclase feldspar which would have moved the liquid composition down the quartz-feldspar surface to the intersection with the two feldspar surface when K-feldspar would have appeared. This is consistent with the observed textural relationships between the felsic phases. P-T conditions during diatexis were within the stability field of sillimanite and probably above the stability of muscovite (breakdown possibly by the vapour absent reaction plagioclase + muscovite + quartz = sillimanite + K-feldspar + liquid) at the level now exposed and probably above the stability of biotite (breakdown possibly by the vapour absent reaction biotite + sillimanite + quartz = cordierite + K-feldspar + liquid) at deeper levels within the belt.

during the course of this work I extend my thanks. In particular, G.J. Lees (Keele), G.M. Power (Portsmouth) and A.J. Barber (Chelsea) have willingly provided valuable advice and encouragement.

My thanks go to Mrs Jane Massey for typing this thesis.

Contents
Acknowledgements

The research for this thesis was undertaken during the tenure of a Research Studentship from the Natural Environment Research Council which is gratefully acknowledged. Professor F. Wolverson Cope provided research facilities in the Department of Geology and I extend my thanks to him and his staff for their assistance and encouragement. The provision of research facilities and financial assistance by Oxford Polytechnic through its Research Committee to facilitate the completion of this thesis is gratefully acknowledged. My thanks go to my parents for assistance between 1969 and 1972 through the provision of a car which enabled the fieldwork in Brittany to be completed with minimum inconvenience.

The research topic was suggested by Dr R.A. Roach as part of his research project on the Precambrian rocks of the Armorican Massif. Dr Roach supervised the research topic and I am grateful for this and the innumerable stimulating discussions that have taken place between us during the last five years - may they continue.

To the many members of the Department of Geology at Keele and the Geology Section at Oxford who have provided advice and assistance during the course of this work I extend my thanks. In particular, G.J. Lees (Keele), G.M. Power (Portsmouth) and A.J. Barber (Chelsea) have willingly provided valuable advice and encouragement.

My thanks go to Mrs Jane Massey for typing this thesis.

Contents

	1. Plage de Quatre Vaux	III.14
	2. Pnte de la Garde	III.17
CHAPTER I		
	Introduction	I.1
	Previous Views on the Geology	I.4
	Methods of Research	I.16
	Discussion on Nomenclature	I.22
	Definition of Terms	I.31
	The Succession of Rock Types	I.34
	Biotite Chemistry and Genesis	IV.15
CHAPTER II		
	General Distribution of the Rock Types	II.1
	Field Description of the Rock Types	
	A. The Pentevrian Basement	V.1
	1. The Metasediments	II.6
	2. The Metatexites	II.10
	3. The Diatexites	II.16
	4. The Colombière Granite	II.21
	5. The Granitoid Sheets	II.23
	B. The Cataclastic Rocks	II.24
	C. The Brioverian Supracrustal Rocks	II.27
	D. The Cadomian Igneous Rocks	II.30
CHAPTER III		
	Petrography of the Rock Types	VI.1
	A. The Pentevrian Basement	VI.2
	1. The Metasediments	III.1
	2. The Metatexites	III.2
	3. The Diatexites	III.4
	4. The Colombière Granite	III.11
	5. The Granitoid Sheets	III.12

B. The Cataclastic Rocks	
1. Plage de Quatre Vaux	III.14
2. Pnte de la Garde	III.17
C. The Brioverian Supracrustal Rocks	III.22
D. The Cadomian Igneous Rocks	III.23
The Feldspars	III.24

CHAPTER IV

Whole-rock Major and Trace Element Chemistry	IV.1
Biotite Chemistry and Genesis	IV.15

CHAPTER V

Structural Relationships

Preliminary Statement	CHAPTER 1	V.1
A. The Pre-Cadomian Structures		
1. The Metasediments		V.3
2. The Metatexites and Diatexites		V.7
B. The Cadomian Structures		
1. The Brioverian Supracrustal Rocks		V.9
2. The Pentevrian Basement		V.11

CHAPTER VI

Petrogenesis

Introductory Statement	VI.1
The St. Malo Rocks and the System Q-Ab-Or-An-H ₂ O	VI.2
The Genesis of the St. Malo Rocks	VI.7

CHAPTER VII

Discussion	VII.1
------------	-------

Introduction

The Armorican Massif of north-west France is one of several Hercynian Massifs within Europe. It is of great interest because its northern part has escaped major orogenic reworking during Phanerozoic time (Roach, Adams, Brown, Power and Ryan, 1972). It is thus possible to study the Precambrian basement to the Hercynian orogen without having to consider, except locally, Phanerozoic deformation and metamorphism. The research area forms part of the Armorican Massif - a region of some 100,000 km² comprising Precambrian and Palaeozoic rocks and bounded to the east and south by the unconformable Mesozoic sediments of the Paris and Aquitaine basins (see Figure I.1). The Precambrian of the Armorican Massif has been divided into two fundamental tectonic units by Cogné (1959 & 1962) and Roach et al (op. cit.): the Pentevrian¹, a pre-900 m.y. crystalline basement with a complex orogenic history, and the Brioverian¹, a supracrustal sequence of possible age range 900 m.y. to 700 m.y. or 650 m.y. (see Bishop, Roach and Adams, in press). Both the Pentevrian basement and the Brioverian cover were deformed, metamorphosed and intruded by igneous material during the late Precambrian to early Palaeozoic Cadomian¹ orogenic episode.

CHAPTER I

The area studied is located along the north Brittany² coast between the towns of St. Cast and Cancale and is centred around Dinard and St. Malo (Figure I.2). It extends inland along the River Rance

¹ Anglicised versions of the French 'Pentévrien', 'Briovérien' and 'Cadomien'.

² Brittany is the major geographical region within the Armorican Massif of France.

Introduction

The Armorican Massif of north-west France is one of several Hercynian Massifs within Europe. It is of great interest because its northern part has escaped major orogenic reworking during Phanerozoic time (Roach, Adams, Brown, Power and Ryan, 1972). It is thus possible to study the Precambrian basement to the Hercynian orogen without having to consider, except locally, Phanerozoic deformation and metamorphism. The research area forms part of the Armorican Massif - a region of some 100,000 km² comprising Precambrian and Palaeozoic rocks and bounded to the east and south by the unconformable Mesozoic sediments of the Paris and Aquitaine basins (see Figure I.1). The Precambrian of the Armorican Massif has been divided into two fundamental tectonic units by Cogné (1959 & 1962) and Roach et al (op.cit.): the Pentevrian¹, a pre-900 m.y. crystalline basement with a complex orogenic history, and the Brioverian¹, a supracrustal sequence of possible age range 900 m.y. to 700 m.y. or 650 m.y. (see Bishop, Roach and Adams, in press). Both the Pentevrian basement and the Brioverian cover were deformed, metamorphosed and intruded by igneous material during the late Precambrian to early Palaeozoic Cadomian¹ orogenic episode.

The area studied is located along the north Brittany² coast between the towns of St. Cast and Cancale and is centred around Dinard and St. Malo (Figure I.2). It extends inland along the River Rance

¹ Anglicised versions of the French 'Pentévrien', 'Briovérien' and 'Cadomien'.

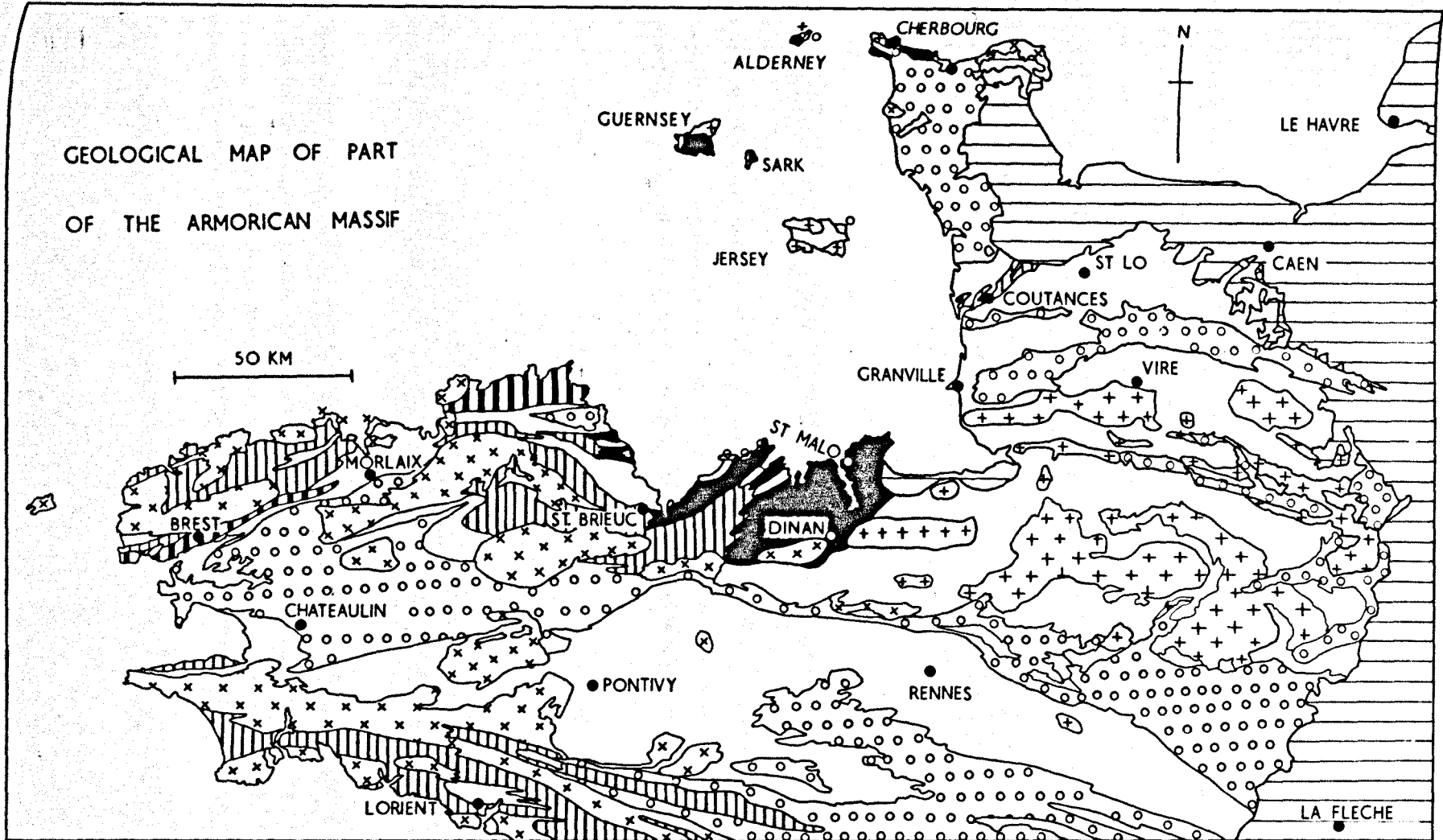
² Brittany is the major geographical region within the Armorican Massif of France.

Figure I.1

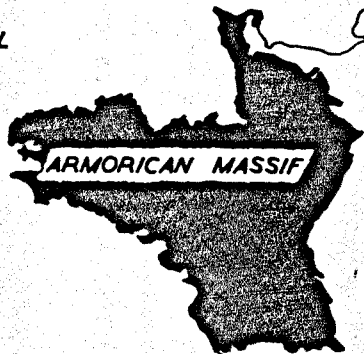
Simplified geological map of the northern and central parts of the Armorican Massif, France. The Armorican Massif comprises Brittany, Vendée and the western parts of Normandy, Maine and Anjou.

GEOLOGICAL MAP OF PART
OF THE ARMORICAN MASSIF

50 KM



CHANNEL



PARIS
BASIN

BAY OF BISCAY

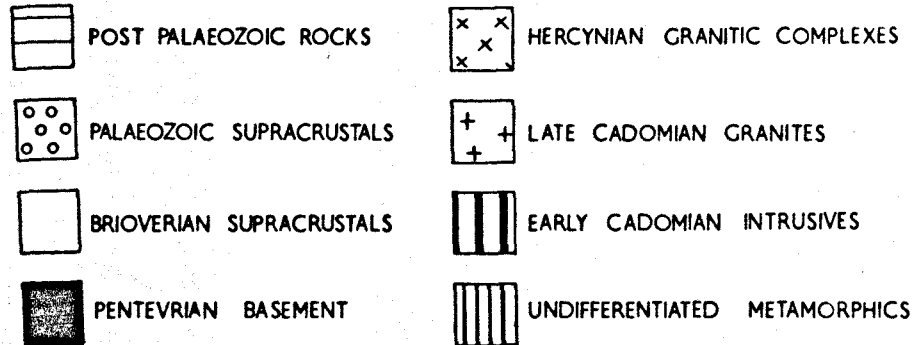
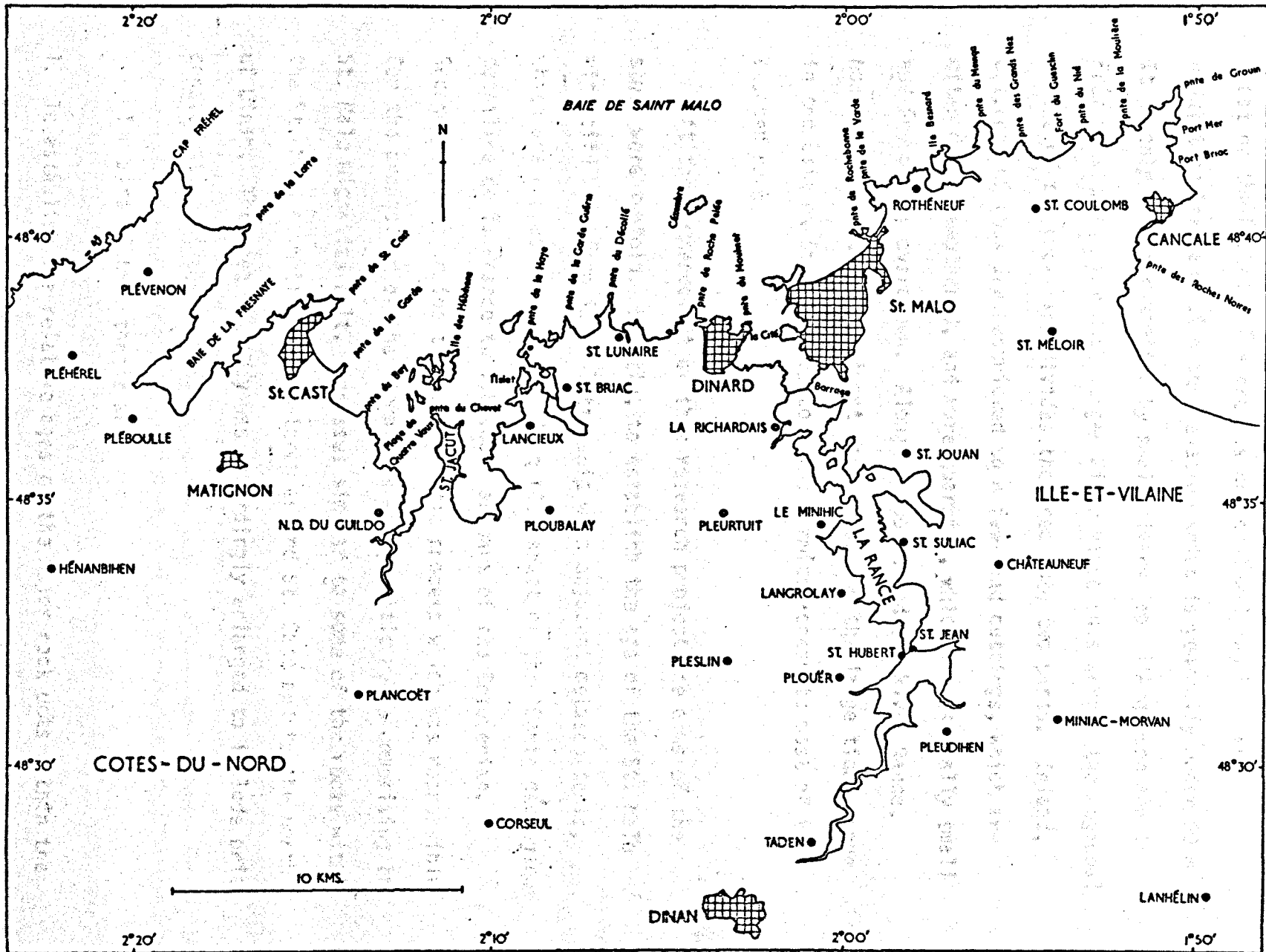


Figure I.2

The main towns and villages and the prominent headlands of the area studied for this thesis.



2°20'

2°10'

2°00'

1°50'

48°40'

48°35'

48°30'

48°40'

48°35'

48°30'

COTES-DU-NORD

BAIE DE SAINT MALO

ILLE-ET-VILAINE

10 KMS.

DINAN

PLÉVENON

PLÉHÉREL

PLÉBOULLE

HÉNANBIHEN

MATIGNON

N.D. DU GUILDO

PLANCOËT

CORSEUL

St. CAST

LANCIEUX

PLOUBALAY

St. BRIAC

St. LUNAIRE

DINARD

LA RICHARDAIS

PLEURTUIT

LANGROLAY

PLESLIN

St. HUBERT

Plouër

PLEUDIHEN

TADEN

St. Brieuc

St. LUNAIRE

St. BRIAC

DINARD

LA RICHARDAIS

PLEURTUIT

LANGROLAY

PLESLIN

St. HUBERT

Plouër

PLEUDIHEN

TADEN

St. MALO

LA RICHARDAIS

St. JOUAN

LE MINIHIC

LANGROLAY

St. HUBERT

Plouër

PLEUDIHEN

TADEN

ROTHÉNEUF

St. COULOMB

St. MÉLOIR

St. JOUAN

LE MINIHIC

LANGROLAY

St. HUBERT

Plouër

PLEUDIHEN

TADEN

CANCALE

CHÂTEAUNEUF

MINIAC-MORVAN

LANHÉLIN

Port Mer

Port Brioc

Cancale

St. Méloir

St. Jouan

Le Minihic

Langrolay

St. Hubert

Plouër

Pleudihen

Taden

penne de Grouen

penne des Roches Noires

penne de la Moulière

penne du Néel

penne de la Grande Motte

penne de la Vierge

penne de la Roche

penne de la Haye

penne de la Grande Motte

penne de la Vierge

penne de la Roche

penne de la Vierge

penne de la Roche

penne de la Haye

penne de la Grande Motte

penne de la Vierge

penne de la Roche

penne de la Haye

penne de la Grande Motte

penne de la Vierge

penne de la Roche

penne de la Haye

penne de la Vierge

penne de la Roche

penne de la Haye

penne de la Grande Motte

penne de la Vierge

penne de la Roche

penne de la Haye

penne de la Grande Motte

penne de la Vierge

penne de la Roche

penne de la Haye

towards Dinan and includes part of the département of Cotes-du-Nord (west of the Rance) and part of the département of Ille-et-Vilaine (east of the Rance). The area is one of low-lying but gently undulating farmland with an elevation which is generally under 50 m. It is only poorly dissected by small rivers (eg. l'Arguenon and le Frémur) although the much larger River Rance cuts across the regional strike of the rocks and divides the area into two parts. Inland, outcrops of rock are restricted to a few road cuttings, which are often deeply weathered, and rare quarries, which are generally small and frequently overgrown. Along the coast and the River Rance, however, the outcrop is almost continuous and the large tidal range in the Baie de St. Malo (up to 12 m) permits access to most of the exposed rock.

At the commencement of this research project the aims of the study were twofold. Firstly, to establish the age of the St. Malo migmatite belt from its relationship with adjacent metasediments, which are represented on the Dinan (60) sheet of the 'Carte géologique détaillée de la France au 1:80.000' as part of the Brioverian. Secondly, to determine the petrogenetic process which was responsible for the production of the migmatites and granitic rocks comprising the St. Malo migmatite belt. Gneisses similar to some of the rocks within the St. Malo migmatite belt outcrop around St. Cast and to the north of Dinan. The area of study was accordingly enlarged to include brief consideration of these rocks.

The aims of this thesis are:

1. To establish the relative ages of the major rock units within the research area.

2. To determine the petrogenesis of the migmatites and granitic rocks within the St. Malo migmatite belt.

3. To make comparisons with other areas of Precambrian within the Armorican Massif.

The St. Malo migmatite belt and associated metasediments (ie. the metasediments forming the palaeosome to the migmatites), the St. Cast gneisses and the Dinan gneisses are correlated with the Pentevrian basement. Younger supracrustal rocks are correlated with the Brioverian cover. A summary of the evidence which demonstrates the Pentevrian age of the St. Malo migmatite belt has been presented by Brown, Barber and Roach (1971).

Previous Views on the Geology

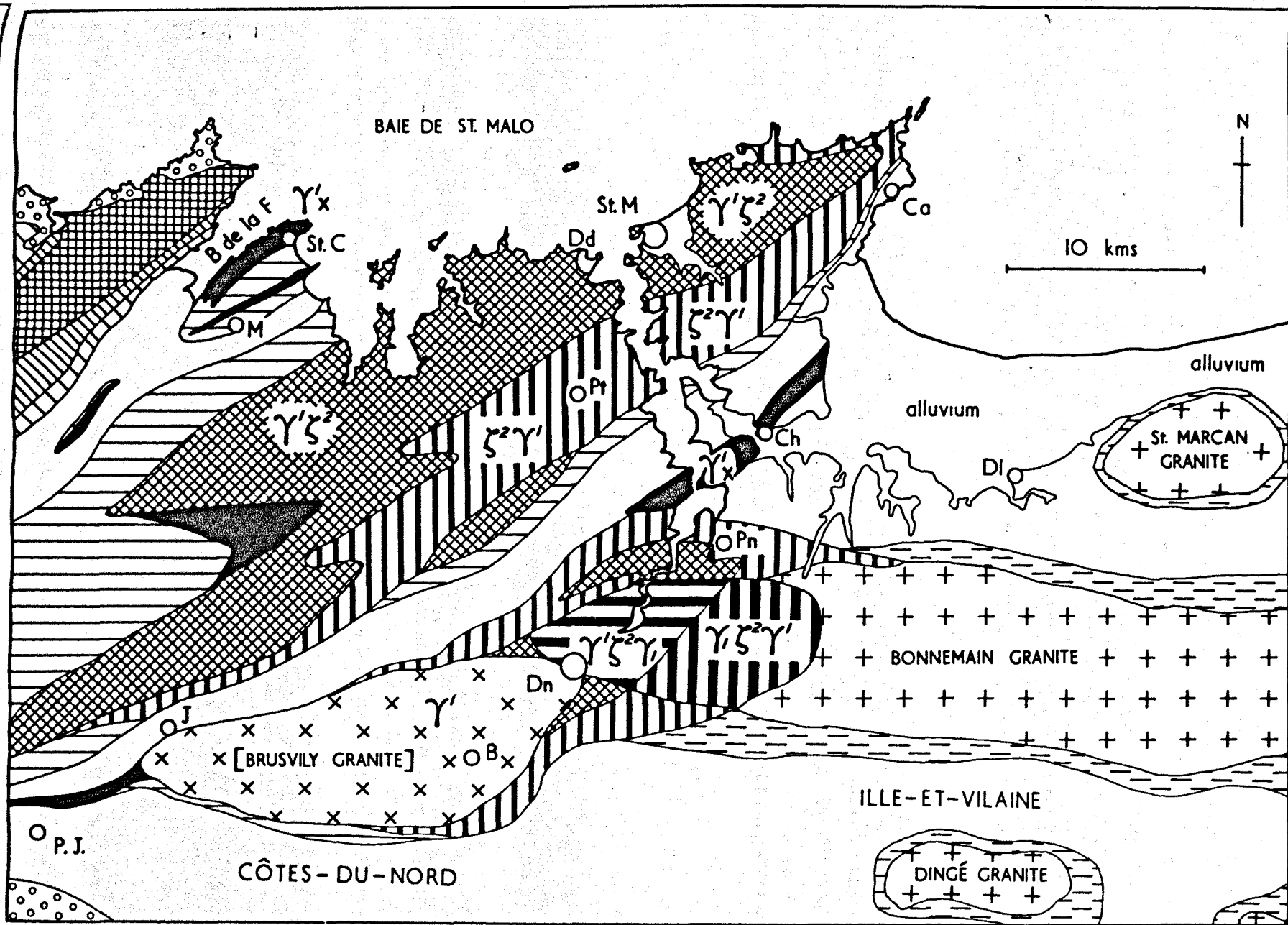
The Precambrian stratigraphy of the Armorican Massif has been summarised by Roach et al (1972) and Bishop et al (in press). It was Charles Barrois (1892 & 1893) who made the first major contribution to the geology of north-east Brittany with the publication of the Dinan sheet (No. 60) of the 1:80,000 geological map of France. Abrard (1923) provided the first detailed petrological account of the rocks which comprise the St. Malo migmatite belt. More recently, Cogné (1951) has described the section along the Rance from Langrolay to Dinard and along the coast to the west. He has made frequent reference to the St. Malo migmatite belt (Cogné, 1964, 1966, 1967, 1970 & 1971) in review articles. However, the most detailed piece of work in recent years on north-east Brittany is that of Jeannette (1971) who undertook a structural analysis of the Precambrian rocks.

Barrois (1892 & 1893) grouped all non-feldspathized schists and phyllites from lower Normandy and northern Brittany into one lithostratigraphic group which he called the "schistes et phyllades de St.-Lo", which later became part of the Brioverian (Barrois, 1895). The "schistes et phyllades de St.-Lo" consist of blue-grey phyllites which alternate with bands of feldspathic greywacke. In the area covered by the Dinan geological map rocks assigned to this group by Barrois (1892 & 1893) occur in three bands (Figure I.3, unit 12). The first of these, south west from the Baie de la Fresnaye, is characterised by quartzites and carbonaceous quartzites ("phtanites"); the second band, from Jugon to Cancale, comprises bluish argillaceous phyllites with beds of quartz-rich greywacke and only rare "phtanites"; the third band, from Plenee-Jugon to Dol, comprises bluish phyllites and greywackes but no "phtanites". Carbonaceous rocks have been

Figure I.3

Geological map of the Dinan area after Barrois (1892)
without major modification (dykes and limon omitted).

1. Granulite
2. Granulite feuilletée
3. Granulite feuilletée
4. Granulite granitique feuilletée
5. Schistes micacés et feldspathisés
6. Micaschistes et gneiss granulitique
7. Granite feuilletée granulitisé
8. Granite
9. Syénite de Coutance
10. Schistes amphibolique granitisés
11. Schistes micacés et leptynolithes
12. Schistes et phyllades de St.-Lo
13. Schistes cornés amphibolique et épidiorites
14. Palaeozoic rocks



	1		8
	2		9
	3		10
	4		11
	5		12
	6		13
	7		14

- B de la F BAIE DE LA FRESNAYE
- St.C ST. CAST
- M MATIGNON
- J JUGON
- P.J. PLENEE JUGON
- Dd DINARD
- Pt PLEURTUIT
- Dn DINAN
- B BOBITAL
- St M ST. MALO
- Ch CHATEAUNEUF
- Pn PLEUDIHEN
- Ca CANCALE
- DI DOL



considered by some workers to be diagnostic of Middle Brioverian sequences (eg. Cogné, 1962; and Jeannette, 1971).

The high-grade metamorphic rocks of the Dinan area were placed by Barrois (1892 & 1893) into two main groups with further subdivisions. The more important of these groups is the "granulite" (two mica granite) which lies in three principal belts. Barrois considered these rocks to occupy anticlinal zones parallel to the fold trend in the 'schistes et phyllades de St.-Lo' and to represent its deeper metamorphic equivalent, a view which persists in recent French literature on the area (Cogné, 1971; Jeannette, 1971; and Auvray et al., 1972). The first belt of "granulite" is that passing through St. Cast which consists of "granulite feuilletée" or gneissified schist (Figure I.3, unit 2, γ^1_x) and comprises bands of schist alternating with feldspathic schist. The second belt of "granulite" passes through St. Malo and is also given the name "granulite feuilletée" although of a different type (Figure I.3, unit 3, $\gamma^1_{\beta^2}$). This variant, Barrois suggested, was produced by injection so intimate that the original schists have been reduced to scattered debris within foliated granite. The third belt of "granulite" is that trending north-east from Dinan and which presents different variants over its outcrop. These include both the previous types and also an area of "granulite granitique feuilletée" (Figure I.3, unit 4, $\gamma^1_{\beta^2}\gamma_1$) thought by Barrois to be produced by the "influence" of the Bonnemain granite. Clearly the "granulite" is both varied and complex.

The second main group of high-grade metamorphic rocks are the "micaschistes et gneiss granulitique" (schists with interbanded feldspathic schists and gneisses) (Figure I.3, unit 6, $\beta^2\gamma^1$). These rocks are often gradational into the "granulite" and may be difficult to delimit from it with precision. The rocks of this group occupy

two important belts, the first passing through Pleutuit and the second through Pleudihen (see Figure I.3).

In a summary of the geology of the département of Ille-et-Vilaine Kerforne (1921) has followed the stratigraphic divisions established by Barrois. Kerforne's comments on the Precambrian are essentially correct though often uninspired, for example "le soubassement du département, comme dans tout le Massif du reste, est formé de sédiments très anciens désignés par M. Ch. Barrois sur le nom Briovérien. Nous n'en connaissons pas la limite inférieure. Aucune discordance ne les sépare des Gneiss et Micaschistes et, par suite, il est impossible de différencier un terrain plus ancien". He considered the St. Malo and Dinan belts of gneissose rocks to be "... plutôt formé de gneiss que de micaschistes et constitue un massif de roches injectée de granulite parallèlement à la stratification". Kerforne noted that the gneisses contained a substantial quantity of secondary (sic) sillimanite.

Abrard (1923) has provided the only comprehensive petrographic description of the various rock types within the St. Malo Massif, a study which took some ten summers to complete. No detailed map is provided but the division into rock types follows Barrois' original works (1892 & 1893). Abrard considered that the St. Malo Massif comprised ancient schists and gneisses which had suffered granitization late in their history. He suggested that this Massif formed an anticlinal core to the adjacent synclines of feldspathised schist. The Massif has a Caledonoid trend but was considered by Abrard to be of Hercynian age. He noted the sharp junction between the gneisses of the Massif and schists in the north-west (at Plage de Quatre Vaux) and the transition nature of the change from gneiss to schist upstream along the Rance.

Cogné (1951) described the section from Langrolay, alongside the Rance, to St. Briac, west of Dinard (see Figure I.2). He noted the gradual change from phyllites with siliceous horizons which outcrop around Langrolay-St. Suliac, within the Jugon-Cancale belt of Barrois (see above and Figure I.3), northwards into finely banded schists then into interbanded schists and gneisses and finally into migmatites and homogeneous granites around Dinard and westwards along the coast. Although Cogné found that it was impossible to map the embrechite³ and anatexite⁴ migmatite types into zones, due to their intimate interpenetration within metres, he did distinguish for descriptive purposes veinites, agmatites⁵, arterites, nebulites and homogeneous biotite-rich granites. He considered that this sequence from phyllites through schists and migmatites to homogeneous granites was produced by segregation, essentially in the solid state, to produce veinites, and by anatexis at higher grades of metamorphism, to produce nebulites, both without extensive change in chemical composition.

- ³ Embrechite: gneiss with a granitic facies and a regularly parallel stratification or schistosity. Often with phenoblasts of feldspar (augen structure) or lenses and small layers of granite.
- ⁴ Anatexite: rock formed by anatexis. Migmatite with granitic facies, rather homogeneous, often nebulitic.
- ⁵ From Cogné's figure this type is schollen structure and not agmatite structure.

Cogné (1962) has summarized the stratigraphy, palaeogeography, metamorphic and structural history of the Brioverian within the Armorican Massif. The regional stratigraphic divisions of the Brioverian proposed are based upon the supposed correlation of horizons of similar (distinctive) lithology within the Brioverian of Lower Normandy, northern Brittany and southern Brittany. Graindor (1962a) was critical of this extension of his well established stratigraphic column for the Brioverian of Lower Normandy to the discontinuous outcrops of supposed Brioverian in Brittany. However, since later French authors (eg. Jeannette, 1968 & 1971; and Hameurt and Jeannette, 1971) adhere to the succession given by Cogné (1962) it is presented in Table I.1.

The most detailed piece of work on this part of the Armorican Massif since Barrois' original survey (1892 & 1893) is that by Jeannette (Jeannette, 1968; Jeannette and Cogné, 1968; Jeannette, 1971; and Hameurt and Jeannette, 1971) on the structural geology of the Precambrian of north-eastern Brittany. Jeannette (1971) has divided the St. Malo migmatite belt into a central core of migmatitic gneisses extending from N. D. du Guildo to Rotheneuf which is surrounded by a variety of non-migmatitic gneisses (see Figure I.4). These non-migmatitic gneisses are divided into four types by Jeannette: cordierite-sillimanite gneiss; microcline gneiss; plagioclase gneiss; and albite gneiss (Figure I.4). He assigned all the metasediments within north-east Brittany to the Brioverian. No rocks of Pentevrian age are recognized by Jeannette in the St. Malo area. He has divided the Cadomian orogeny into two phases - Cadomian I and Cadomian II - which are separated by uplift and erosion after the deformation and metamorphism of the Lower and Middle Brioverian but before the deposition of the Upper Brioverian. Each phase has developed a set of

TABLE I.1

THE BRIOVERIAN SUCCESSION IN NORTH-EASTERN ARMORICA (AFTER COGNÉ, 1962)

ORDOVICIAN

'Grès Armoricaïn' quartzites.

TECTOGENESIS

Laize slates and sandstones.

UPPER
BRIOVERIAN

Granville conglomerates.

OROGENESIS

BRIOVERIAN

MIDDLE
BRIOVERIAN

St. Lo schists and phyllites
with sandy intercalations.

Lamballe slates with phthanites.

LOWER
BRIOVERIAN

Erquy volcanic series.

Cesson conglomerates and
arkoses.

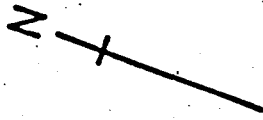
PENTEVRIAN

Granodioritic gneiss.

Figure I.4

The geology of the St. Malo region. Taken from Jeannette (1971, Fig. 44) without major modification.

8. Alluvions
7. Schistes séricito-chloriteux
6. Micaschistes à biotite et muscovite
5. Gneiss albitiques
4. Gneiss plagioclasique
3. Gneiss à microcline
2. Gneiss à cordierite et sillimanite
1. Gneiss migmatitique

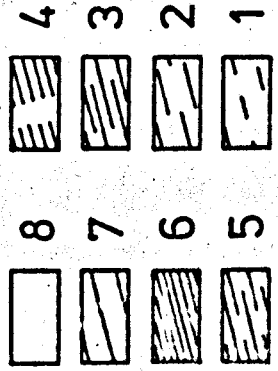


St. CAST

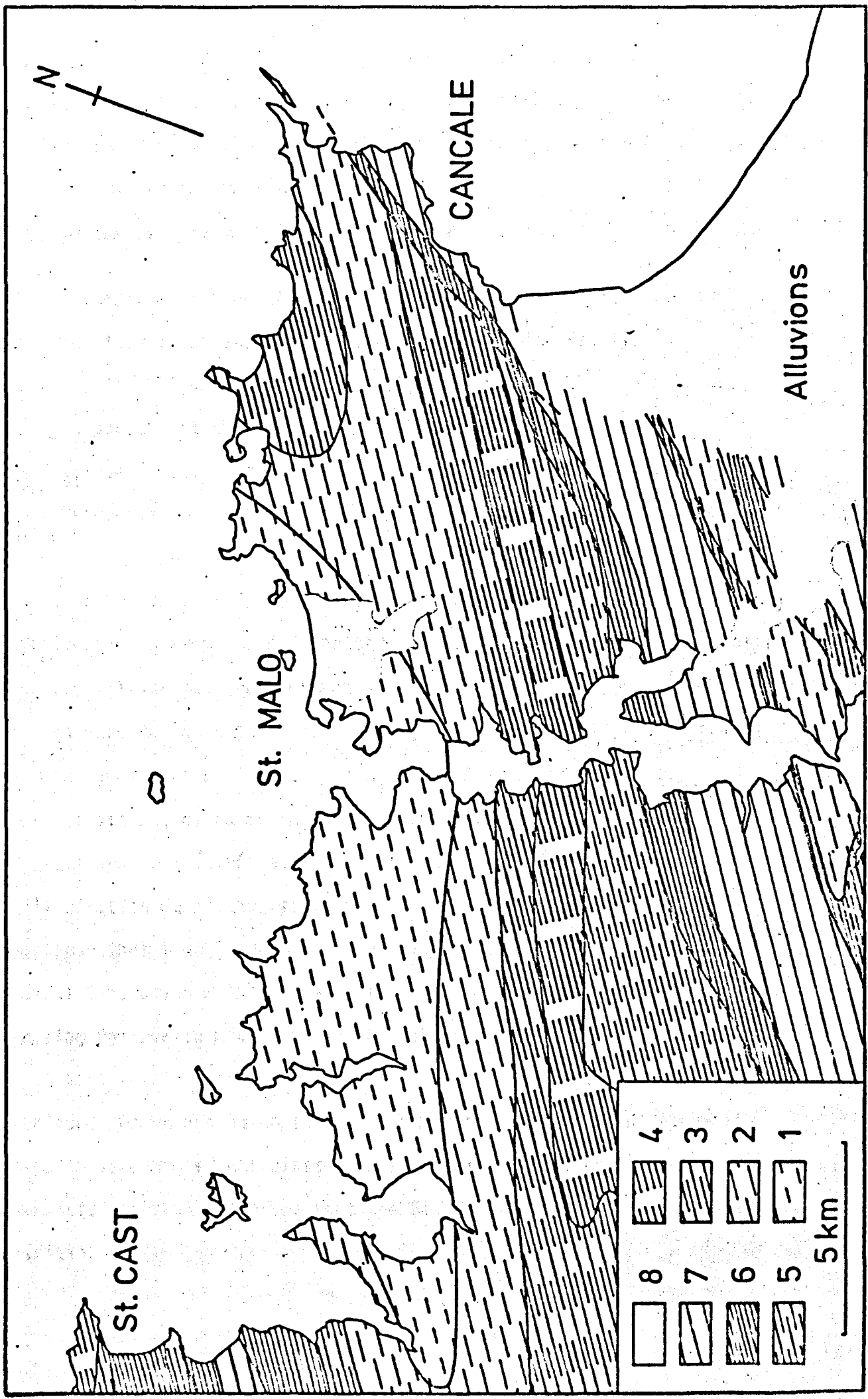
St. MALO

CANCALE

Alluvions



5 km



folds and is associated with an episode of metamorphism. The development of the migmatites within the St. Malo belt of gneisses is regarded as the result of anatexis during the high temperature - low pressure metamorphism associated with Cadomian II. Jeannette recognizes late to post Cadomian II shearing and regional cataclasis.

Hameurt and Jeannette (1971) consider that they can recognize in the vicinity of St. Cast, within the "granulite feuilletée" of Barrois (see Figure I.3), a sequence of conglomeratic meta-arkoses. They suggest that this sequence should be called the "Groupe détritique de St. Cast" and regarded as the lowermost subdivision of the Brioverian. The gneisses of the St. Malo belt, those which outcrop along the Rance and parts of the 'Gneiss de Brest' some 200 km to the west of St. Cast are placed within this new subdivision of the Brioverian. Hameurt and Jeannette suggest that it is strong deformation at the sillimanite grade of metamorphism which gives a migmatitic appearance to these gneisses. They write "... les trainées micacées de ces gneiss ne sont donc en général ni les résidus à une granitisation, ni du mélanosome métatectique, mais les témoins des galets argileux étirés et largement recristallisés, ou ceux de la dilacération de niveaux schisteux qui ont subi le même sort". They propose that the "Groupe détritique de St. Cast" represents part of a basal Brioverian molasse sedimentation deposited on both sides of the rising Pentevrian mountain chain - now represented by the Pentevrian gneisses which outcrop along the eastern flank of the Baie de St. Brieuc. Brown and Roach (1972a) thought that Hameurt and Jeannette must have confused cataclastic rocks within a major shear belt for arkosic rocks and asserted that the St. Malo gneisses were of anatectic origin.

The only detailed account of the Pentevrian basement of the French mainland is that by Ryan (1973) who has examined an area comprising both Pentevrian basement and Brioverian cover rocks from the west side of the Baie de St. Briec, Côtes du Nord. In this area the Pentevrian consists of the Port Goret gneisses (staurolite bearing paragneisses), the Plouha Series (metasediments and metavolcanics) and the Port Moguer tonalite. Ryan (op.cit.) and Ryan and Roach (in press) have recognized four major fold phases and four episodes of regional metamorphism within the Pentevrian prior to the deposition of the Brioverian. The structural and metamorphic histories may be more complex locally. The Brioverian comprises a thick sequence of turbidites, termed the Binic-Bréhec Series, and a restricted sequence of metasediments and metavolcanics, termed the Palus Plage Brioverian. It is thought that the original unconformable relationship between the Pentevrian and the Brioverian is partly preserved to the east of Palus Plage where the Palus Plage Brioverian overlies the Port Goret gneisses (Ryan, op.cit. and Ryan and Roach, op.cit.). The Cadomian orogeny has developed two main phases of folding, with the local development of a third phase, within the Brioverian and has caused local deformation of the Pentevrian basement.

Before any summary of the various ages that have been postulated for the St. Malo migmatite belt is attempted, it is necessary to review current opinions concerning the geochronology and stratigraphy of the Precambrian rocks in the northern part of the Armorican Massif. It was only in 1959 that a basement older than the Brioverian was recognized within the mainland part of the Armorican Massif (Cogné, 1959), although basement gneisses had been recognized on Guernsey (Roach, 1957). Cogné demonstrated the unconformable relationship between the Brioverian (a supracrustal sequence comprising phyllites and spilitic volcanic rocks) and an older crystalline basement (locally granite

gneiss but more commonly quartz-dioritic gneiss), which he named the Pentevrian, at Jospinet on the eastern side of the Baie de St. Brieuc. Since this important first step Adams has undertaken a radiometric age study of northern Brittany and the Channel Islands (Adams, 1967a; Adams, 1967b; Adams in Bishop et al, 1969; Adams in Roach et al, 1972; and Bishop, Roach and Adams, in press) and enabled a Precambrian stratigraphy to be established.

Two isotopic events have been recognized within the Pentevrian basement of Guernsey, part of the Armorican Massif, by Adams using the Rb/Sr isochron method (Adams, 1967b; Roach et al, 1972; and Bishop et al, in press). Leutwein et al (1973) have confirmed the existence of Pentevrian basement within the mainland part of the Armorican Massif. They obtained an Rb/Sr isochron age of $2,500 \pm 100$ m.y. from gneisses at la Hague, near Cherbourg. This compares favourably with the older Rb/Sr isochron age of $2,620 \pm 50$ m.y. which Adams obtained from the Icart gneiss on Guernsey (Adams, 1967b; Roach et al, 1972; and Bishop et al, in press).

Recent work in west Finistère (Bradshaw, Renouf and Taylor, 1967; and Bishop, Bradshaw, Renouf and Taylor, 1969) has shown that during the Cadomian orogeny two phases of folding preceded the main regional metamorphism in this area. Furthermore the ENE-WSW trend of the main Cadomian deformation was a significant control over post-Cadomian sedimentation and deformation. Limits on the age of the Brioverian supracrustal sequence and the time span of the Cadomian orogenic episode in west Finistère have been given by Adams (in Bishop et al, op.cit.). The Gneiss de Brest, which intrudes and hornfelses

Brioverian sediments⁶ and predates the main regional metamorphism (Bradshaw et al, op.cit.) gives an Rb/Sr isochron age of 690 ± 40 m.y. and the post-metamorphic Renards granite gives an Rb/Sr isochron age of 565 ± 40 m.y. Brioverian sedimentation is therefore considered to have terminated by 700 m.y. (see Roach et al, 1972) or possibly 650 m.y. (see Bishop et al, in press) and the tectono-metamorphic phase of the Cadomian orogeny had essentially finished by Cambrian times.

Vidal, Auvray, Cogné, Hameurt and Jeannette (1971) obtained an Rb/Sr isochron age of 466 ± 10 m.y. for the Erquy spilite group which outcrops on the eastern side of the Baie de St. Brieuc and which formerly had been regarded as a part of the lowermost Brioverian in this area (eg. Cogné, 1959, 1962 & 1970; Auvray, 1968 & 1969; and Table I.1). Vidal et al regard the spilitic mineralogy of these rocks as a primary igneous assemblage with an igneous texture and regard their isochron age as dating the time of extrusion. Accordingly, the Erquy spilite group has been taken out of the Precambrian by Vidal and his colleagues and placed within the lower Ordovician. These results and conclusions were the subject of criticism by Brown and Roach (1972a) who considered that the Rb content of many of the samples dated was so low that the measured values might be in error. This criticism of analytical technique was rightly refuted by Vidal (in Auvray, Cogné, Hameurt, Vidal and Jeannette, 1972). Far more important were the criticisms by Brown and Roach of the interpretation of this isochron age, especially the failure of Vidal et al (op.cit.) to consider the regional palaeogeography and the tectonic environment of post-Cadomian

⁶ The Gneiss de Brest cannot therefore represent a metamorphosed lower Brioverian molasse sequence as suggested by Hameurt and Jeannette (1971) (see above p. I.9).

sedimentation over the northern part of the Armorican Massif. Moreover, earlier K/Ar age determinations by Leutwein and his colleagues (Leutwein and Sonet, 1965 and Leutwein, 1968) had confirmed a Precambrian age for the Erquy spilite group. In their reply (Auvray et al, op.cit.) to Brown and Roach (op.cit.) the French geologists pointed out that it is the Rb/Sr ratio which is more important than the absolute value of Rb in a rock for an accurate age determination. They reasserted the primary nature of the mineral assemblage and texture and restated that the age obtained was that of extrusion. Brown and Roach (1972b) could not accept this interpretation and suggested that although the measured age could possibly date a reheating and subsequent rehomogenisation of Sr isotopes during the Lower Palaeozoic the deformation and metamorphism of the Erquy spilite group were of Cadomian age. Hameurt (personal communication, 1972) has suggested that "le flanc est de la Baie de Saint-Brieuc se présente comme un fragment des Calédonides gréffé sur une Bretagne demeurée totalement à l'écart de la crise calédonienne". In view of the problems inherent in any analysis of pillow lavas (see, for example, Hart, Erlank and Kable, 1974) the age of the Erquy spilite group must remain an open question.

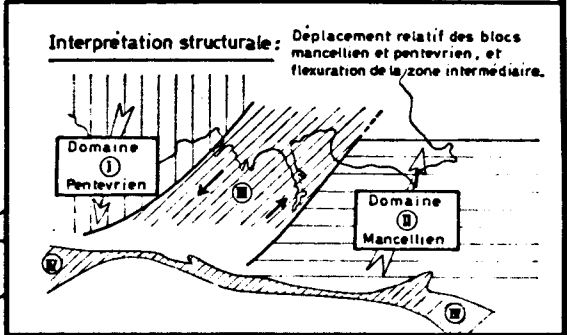
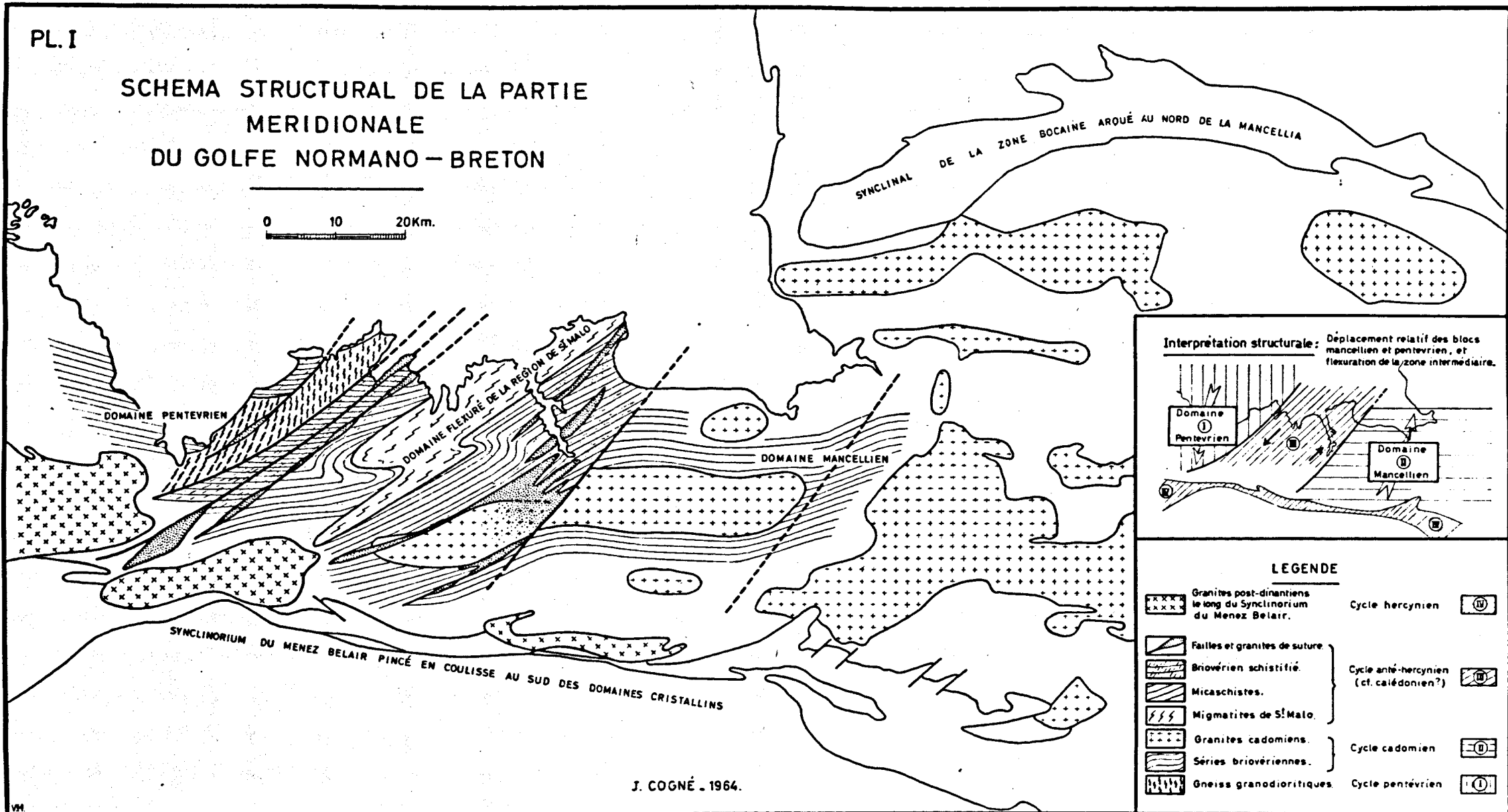
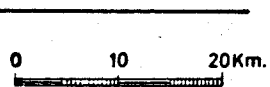
Within this uncertain framework of ages from the Precambrian of the Armorican Massif the age of the St. Cast, St. Malo and Dinan belts of migmatitic gneisses may be discussed. Abrard (1923) and Mathieu (1944) both considered the migmatites to be Hercynian in age, whilst Graindor (1962b) and Graindor and Wasserberg (1962) suggested a Silurian age from Rb/Sr "whole rock" and mica age determinations. Cogné (1964) considered the NE-SW trending zone between Matignon and Cancale to be a zone of post-Cadomian shearing between the 'Domaine Pentévrien' to the west and the 'Domaine Mancellien' on the east (Figure I.5). According to Cogné local metamorphism and granitization

Figure I.5

Map from Cogné (1964) to show the St. Malo-Dinan zone of Caledonian shearing between the Pentevrian and Mancellian blocks.

PL. I

SCHEMA STRUCTURAL DE LA PARTIE
MERIDIONALE
DU GOLFE NORMANO - BRETON



LEGENDE

	Granites post-dinantiens le long du Synclinorium du Menez Belair.	Cycle hercynien	
	Failles et granites de suture.	} Cycle anté-hercynien (cf. calédonien?)	
	Briovérien schistifié.		
	Micaschistes.		
	Migmatites de S' Malo.	} Cycle cadomien	
	Granites cadomiens.		
	Séries briovériennes.	} Cycle pentevrien	
	Gneiss granodioritiques.		

J. COGNÉ - 1964.

within this zone was responsible for the production of migmatites. He suggested that the metamorphism was of Silurian age (Caledonian) on the basis of Graindor's age determinations and because he maintained that the zone of migmatites cut the Mancellian granites (Mancellian granites - late Cadomian granites, see Adams, 1967b), but was limited to the south by the Hercynian Menez-Belair syncline (see Figure I.5).

Leutwein and Sonet (1965) considered the rocks of the St. Malo region to be polymetamorphic anatectic gneisses. They were able, with their greater number of age determinations, to place the Silurian age of Graindor (412 m.y.) in perspective: "... ces âges comme lié à certains processus de rejeunissement des migmatites plus anciennes, vraisemblablement cadomiennes". Rb/Sr orthoclase ages of 1,000 m.y. from the Ile de Cézambre, north of Dinard, might indicate a longer history for these rocks than Leutwein and Sonet have postulated. In a later review Leutwein (1968) considered the St. Malo paragneisses to have been Brioverian metasediments affected by Cadomian anatexis, with later isotopic rejuvenation during the Caledonian and Hercynian earth movements. A similar rejuvenation was postulated for the Dinan gneisses though here Leutwein was uncertain of their true age. The orthoclase ages were not mentioned in this later review.

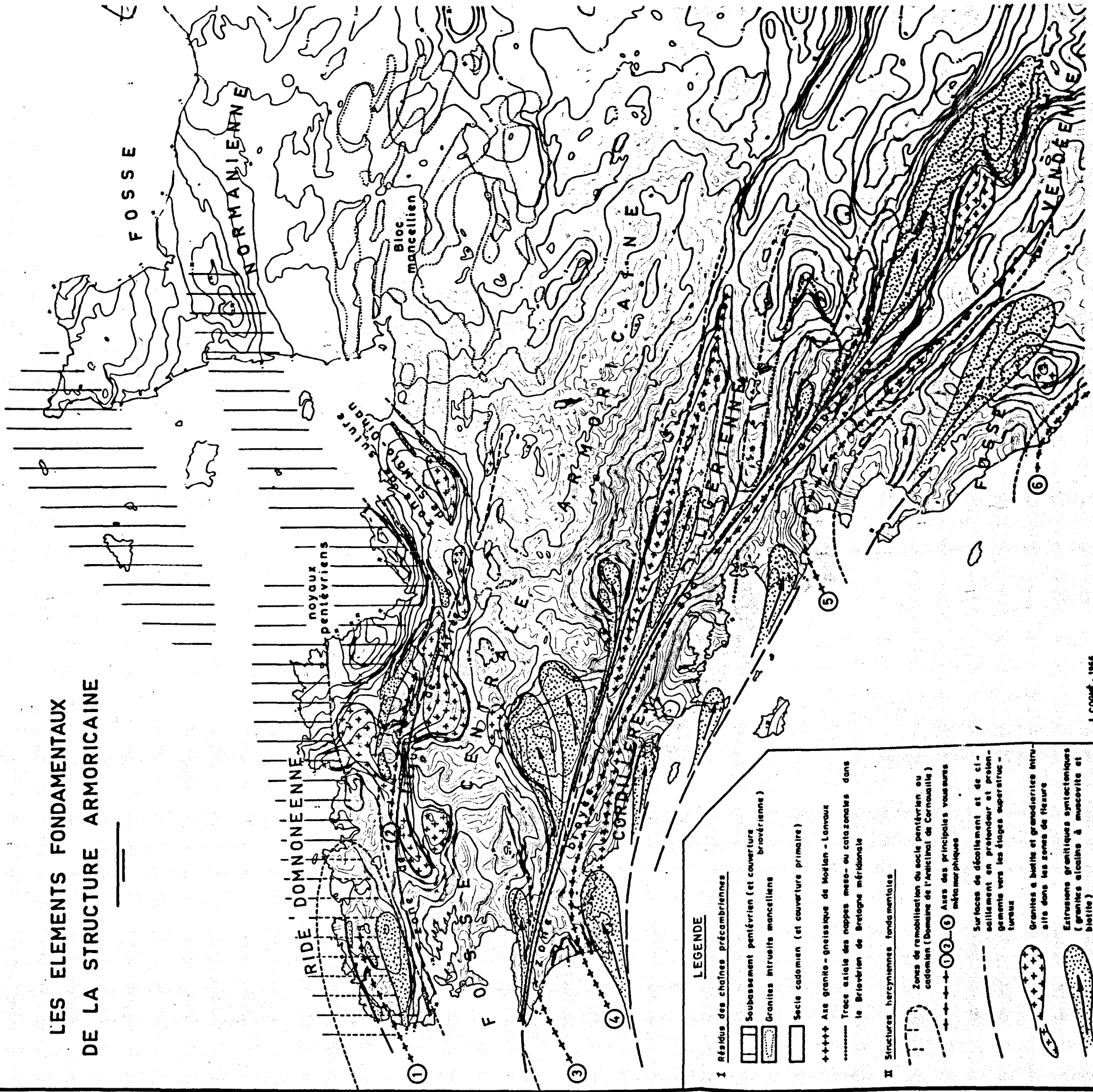
Cogné (1966, 1967 & 1970) revised his opinion on the age of the St. Malo migmatites and associated rocks as a result of the work by Leutwein and Sonet. He concluded that Graindor's Caledonian age was the result of local Hercynian reactivation of Cadomian migmatites with concomitant syntectonic granite intrusion (Figure I.6). This theme was continued (Cogné, 1971) and the following synthesis proposed: "La limite septentrionale de ce domaine (Domaine Mancellian⁷) contre le

⁷ My additional information

Figure I.6

The main elements of Armorican structure according to
Cogné superimposed on the 'Carte Gravimétrique du Massif
Armoricain' (Cogné, 1967).

LES ELEMENTS FONDAMENTAUX
DE LA STRUCTURE ARMORICAINE



LEGENDE

I Résidus des chaînes précambriennes

- Subassement pentévrien (et couverture bravérienne)
- Granites intrusifs manceilliens
- Socle cadomien (et couverture primaire)

+++++ Axe granito-gneissique de Moëlan - Lannoux

..... Trace axiale des nappes méso- ou catazonales dans le Briovérien de Bretagne méridionale

II Structures hercyniennes fondamentales

- Zones de remobilisation du socle pentévrien ou cadomien (Domaine de l'anticlinal de Cornouaille)
- Axes des principales voûtures métamorphiques

Surfaces de décollement et de cisaillement en profondeur et prolongement vers les étages supérieurs - tureaux

Granites à biotite et granodiorites intrusifs dans les zones de flexure

Extrusions granitiques syntectoniques (granites alcalins à muscovite et biotite)

bloc domnonéen (the 'Domaine Pentévrien' of 1964, compare Figure I.5 with I.6⁷) est jalonnée par des granitisations localement intenses disséminées au long de cette flexure, d'âge cadomien précoce, mais reprises dans des déformations plus tardives bien qu'antérieures cependant à la mise en place du pluton mancellien (Jeannette, 1971). Ce sont les migmatites et les gneiss migmatitiques de St. Malo les grano-diorites plus or moins orthogneissiques de St. Cast, de Dinan et de Cancale". Clearly the migmatites are now thought to be of early Cadomian age with some reworking later in the Cadomian orogeny.

Brown, Barber and Roach (1971) have shown that the St. Malo migmatite belt must be Pentevrian in age. They have described a longer structural history and a higher metamorphic grade for the diatexites and metatexites of the St. Malo belt than for adjacent Brioverian metasedimentary schists at the Plage de Quatre Vaux (see Figure I.2) on the north-western side of the St. Malo belt (cf. Abrard, 1923 - see p. I.6 above). They suggest that the St. Malo belt probably represented the basement to the Brioverian supracrustal sequence although the junction between the two at Plage de Quatre Vaux is now tectonic. This is completely opposed to the views of Hameurt and Jeannette (1971), summarized above, who regard the rocks of the St. Malo belt as a lower Brioverian molasse sequence metamorphosed and deformed during the Cadomian orogeny. Brown and Roach (1972a & 1972b) and Auvray et al (1972) have debated this fundamental difference in interpretation but have failed to reach agreement.

for research purposes to determine the minerals present, their mutual relationships and textures and their approximate proportions. To enable easier identification of the mineral assemblages in some of the specimens a standard staining technique

⁷ My additional information.

A later five-axis universal stage was employed in the determination of

Methods of Research

The coastal outcrop was mapped at a scale of 1:15,000 on base maps constructed from a mosaic of aerial photographs kindly made available by the Geography Department at Keele. Selected sections of the coast were mapped at a scale 1:5,000 on maps constructed from a mosaic of x3 enlargements of the aerial photographs. Inland, outcrops were mapped on the 1:25,000 'Carte de France' topographic sheets, which were the largest scale available. A Brunton compass-clinometer was used to measure the orientation of structures which included foliation, lineation and fold orientation, together with certain non-penetrative planar discontinuities such as granitoid sheet margins and dyke margins. Lineations were measured on the foliation surface either in terms of their pitch, where the foliation was steep, or their plunge, where the foliation was shallow. The structural data obtained in the field were analysed statistically where appropriate using an equal area stereographic net in the manner described by Turner and Weiss (1963).

The various rock types studied in the field have been further examined in the laboratory with the aid of approximately six hundred thin sections. The rock specimens were cut at right angles to the foliation and lineation where present and also in other orientations when this was considered useful. The thin sections were examined by conventional methods using a Leitz research microscope to determine the minerals present, their mutual relationships and textures and their approximate proportions. To enable easier identification of the alkali feldspar in some of the specimens a standard staining technique for K-feldspar using sodium cobaltinitrite was utilised (Chayes, 1952). A Leitz five axis universal stage was employed in the determination of

the extinction angle of plagioclase feldspar albite twin lamellae; the composition was then determined from the Michel-Levy curve.

Specimens for possible geochemical and mineralogical study were collected during routine field mapping. With the exception of one specimen (211) the grain size of the rocks is always less than 1 cm, and specimens of about two kilograms were therefore considered representative (cf. Smales and Wager, 1960). The freshest possible material was always selected at each suitable locality. Specimens for analysis were split into pieces approximately five cubic centimetres in size and all weathered crust removed. These pieces were then reduced to the size of peas in a Sturtevant jaw crusher. Approximately 500 gm of this broken rock were crushed for 25 seconds in a Tema ring mill using a tungsten-carbide pot. The resultant mixture of minerals, composite grains and rock flour was thoroughly homogenised, coned and quartered and one half reserved for mineral separation. The other half was pulverised for a further 2 minutes in the Tema ring mill, thoroughly homogenised, coned and quartered and one portion stored in a predried glass bottle. 6 gm of powder were taken and mixed with an organic binding agent (12 drops of 2% mowiol solution), pressed between two highly polished tungsten-carbide patters in a hydraulic press for 5 minutes at 25 tons pressure and the resultant pellet dried overnight at 110°C.

Many of the major elements (SiO_2 , TiO_2 , Al_2O_3 , total iron (T. Fe as Fe_2O_3), MnO , CaO , K_2O and P_2O_5) and all of the chosen trace elements (Ba, Cu, La, Pb, Rb, Sr, Th, U, Y, Zn and Zr) were determined on these sample pellets using a Phillips PW 1212 15 channel automatic X-ray fluorescence spectrometer (XRF) with simultaneous punched tape and printed roll output. A PDP-8 digital computer with 4K of store was used to sort and average data from the punched tape output. Major

element analyses were based on calibration curves constructed from international standard rocks (U.S.G.S. and B.R.G.M.) for which recommended values are available (Flanagan, 1969 and Roubault et al, 1968) with the exception of SiO_2 for which a calibration curve was constructed from wet chemical analyses of ten of the samples. Trace elements were calibrated by a standard addition or 'spiking' technique (cf. Leake et al, 1969 and Jenkins and De Vries, 1967). Selected international standard rocks (U.S.G.S. standard rocks G2, GSP1 and AGV1 and B.R.G.M. standard rocks GA and GH) were analysed for the trace elements at the same time as the unknowns to provide a check on the accuracy of the method, which was found to be acceptable (see Table I.2 and the discussion below). The XRF methods used in this work are in most respects similar to those used by Leake et al (1969). The machine operating conditions used are summarised in Tables I.3, I.4 and I.5.

The theoretical aspects of precision and accuracy in XRF work have been discussed in detail by Jenkins and De Vries (1967) and Leake et al (1969) and are considered to be outside the scope of the present study. Leake et al write "... the precision in general is limited chiefly by counting statistics and by pellet surface variation. The accuracy of the results is mainly dependent on the accuracy of the calibrations used and the effects of mineralogical variations within the sample analysed". These remarks have been taken into consideration throughout the work. Sample preparation and the pelleting technique used in this study are given above and minimise pellet surface variation. Errors due to counting statistics have been kept to a minimum by the choice of operating conditions to give a low relative deviation consistent with an acceptable counting time. Long and short term machine variation was reduced to the minimum by adopting a ratio

Table I.2

The results of trace element determinations by the author for certain standard rocks compared with the results obtained by other workers and with the recommended values.

	G2					GSP 1					AGV 1					GA			GH		
	1	2	3	4	6	1	2	3	4	6	1	2	3	4	6	1	5	6	1	5	6
Ba	1970			1950	2134	1545			1360	1481	1320			1410	1337	900	850	906	75	24	16
Cu	7			11	4	35			35	29	64			64	75	N.D.			N.D.		
La	113			112	76	146			280	95	34			43	29	N.D.			N.D.		
Pb	42			29	54	76			52	95	N.D.					45	26	51	62	50	67
Rb	170	173	169		195	249	251	255		293	78	68	67		146	177	175	200	408	390	451
Sr	502	486	475		515	214	232	235		242	578	662	657		1086	323	325	329	8	10	9
Th	47			25	51	N.D.					20			7	11	35		32	N.D.		
U	2.25			1.99		3.00			1.98		2.90			1.94		*				19	
Y	8			12	14	26			37	36	14			25	19	19		28	79		114
Zn	115			75	99	130			143	116	107			112	119	82	85	112	N.D.		
Zr	395			316	348	618			544	518	277			227	243	N.D.			178	170	164

N.D. - Not determined.

* - Positive result but below calculated detection limit.

1. This work (analyst - M. Brown)
2. Fairbairn & Hurley (1971)
3. Laeter & Abercrombie (1970)
4. Flanagan (1969)
5. Roubault et al (1968)
6. Leake et al (1969/70)

TABLE I.3

OPERATING CONDITIONS AND RESPONSE FOR THE CHROMIUM TUBE

ELEMENT	Al	Si	P	K	Ca	Ti
ATOMIC NUMBER	13	14	15	19	20	22
PEAK	K α					
VOLTS (kv)	60	60	60	40	40	60
CURRENT (mA)	24	24	24	16	8	24
COLLIMATOR	C	C	F	C	C	F
CRYSTAL	P.E.	P.E.	P.E.	P.E.	LiF	LiF
PRESET COUNTS	1x10 ⁵	1x10 ⁵	3x10 ³	3x10 ⁵	1x10 ⁵	1x10 ⁵
PEAK:BACKGROUND	50:1	333:1	14:1	838:1	197:1	142:1
RELATIVE DEVIATION	0.5%	0.5%	1%	0.25%	0.5%	0.5%

COLLIMATOR - C COARSE; F FINE

P.E. - PENTA-ERYTHRITOL

LiF - LITHIUM FLUORIDE (200)

GAS FLOW PROPORTIONAL COUNTER AND VACUUM PATH THROUGHOUT

PEAK - BACKGROUND CALIBRATION THROUGHOUT

GAS FLOW PROPORTIONAL COUNTER

SCINTILLATION COUNTER

SCINTILLATION COUNTER

SCINTILLATION COUNTER

VACUUM PATH THROUGHOUT

TABLE I.4

OPERATING CONDITIONS AND RESPONSE FOR THE TUNGSTEN TUBE

ELEMENT	Mn	Fe	Zr	Ba	La
ATOMIC NUMBER	25	26	40	56	57
PEAK	K α	K α	K α	L β_2	L α_1
VOLTS (kV)	60	40	100	50	60
CURRENT (mA)	32	16	16	40	32
COLLIMATOR	F	F	F	C	C
DETECTOR	BOTH	G.F.P.C.	S.C.	BOTH	G.F.P.C.
PRESET COUNTS	1x10 ⁴	1x10 ⁶	1x10 ⁴	1x10 ⁴	3x10 ³
PEAK:BACKGROUND	8:1	2500:1	2.2:1	2.4:1	1.2:1
RELATIVE DEVIATION	0.6%	<0.1%	1%	1.3%	4%
P or B	P	P	B	P	B
LOWER LIMIT OF DETECTION			5 ppm	20 ppm	3 ppm
COLLIMATOR - C COARSE; F FINE					

CRYSTAL - LiF (220) THROUGHOUT

G.F.P.C. - GAS FLOW PROPORTIONAL COUNTER

S.C. - SCINTILLATION COUNTER

P = PEAK - BACKGROUND

B = (PEAK/BACKGROUND) - 1

VACUUM PATH THROUGHOUT

Serial No. and weight of sample, and date of analysis, are given in Table 1.5.

An acceptable accuracy by **TABLE 1.5** for different elements is shown in the caption; the values in the parentheses are the recommended values for the

international standard range used for calibration of the calibration.

OPERATING CONDITIONS AND RESPONSE FOR THE MOLYBDENUM TUBE

ELEMENT	Cu	Zn	Rb	Sr	Y	Pb	Th	U
ATOMIC NUMBER	29	30	37	38	39	82	90	92
PEAK	K α	K α	K α	K α	K α	L α	L α	L α
VOLTS (kV)	80	80	80	80	80	95	80	80
CURRENT (mA)	24	24	24	24	24	20	24	24
COLLIMATOR	F	F	F	F	F	F	F	F
G.F.P.C.	IN	IN	OUT	OUT	OUT	OUT	OUT	OUT
PRESET COUNTS	1×10^4	1×10^4				1×10^4	1×10^4	1×10^4
PRESET TIME			40 secs	40 secs	40 secs			
PEAK:BACKGROUND	2:1	2.5:1	6:1	7.5:1	2.5:1	1.8:1	1.1	1.4:1
RELATIVE DEVIATION	1.5%	1.2%	0.7%	0.5%	1.4%	5%	4%	2.5%
P or B	B	B	B	P	B	B	B	B
LOWER LIMIT OF DETECTION	2 ppm	2 ppm	1 ppm	1 ppm	1 ppm	4 ppm	2 ppm	1.4 ppm

The lower limit of detection is defined by 1.64σ and is given in Table 1.5.

CONCENTRATION - concentration given a count rate equivalent to twice the standard deviation of the background.

SCINTILLATION COUNTER AND VACUUM THROUGHOUT - the background count rate in the scintillation counter may be 10^4 counts per minute.

G.F.P.C. - GAS FLOW PROPORTIONAL COUNTER - the background count rate in the G.F.P.C. may be 10^4 counts per minute.

P - PEAK - BACKGROUND - the peak may be calculated by using the square root of the background count rate divided by the slope factor of the calibration curve.

B - (PEAK/BACKGROUND) - 1 - the relative mass fraction of the element in the sample.

The approximate mass fraction correction outlined above is also applied in the calculation of the lower limit of detection. The calculated lower limits of detection for the above elements are given in tables 1.3, 1.4 and 1.5.

technique and an internal reference standard (cf. Leake et al., 1969).

An acceptable accuracy for the major element determinations is dependent upon the accuracy of the recommended values for the international standard rocks used in construction of the calibration curve. The accuracy of the recommended values for such standard rocks has been considered by Flanagan (1969) and need not be reiterated here. The 'spiking' technique used in the trace element determinations ensures an accurate result for unknowns with a similar matrix to that of the spikes (that is, where there is little mineralogical variation), in the case of this study a mixture of specimen 204 (micaceous schist) and 205 (inhomogeneous diatexite), provided that the quantity of the element added is of the same order of magnitude as the amount expected in the unknowns (Jenkins and De Vries, 1967). For most of the trace elements determined in this work the accuracy was improved by ratioing the number of peak counts against the number of background counts. In effect this applies an approximate mass absorption correction (cf. Anderman and Kemp, 1958) and Tables I.3, I.4 and I.5 show the elements to which this has been applied.

The lower limit of detection is defined by Jenkins and Dr Vries (1967) as "that concentration which gives a count rate equivalent to a background reading plus twice the standard deviation of the background". The standard deviation of the background may be approximated to the square root of the background counts and thus the lower limit of detection may be approximated to twice the square root of the background counts divided by the slope factor of the calibration curve. When the approximate mass absorption correction outlined above has been applied, it must also be applied in the calculation of the lower limit of detection. The calculated lower limits of detection for the trace elements analysed are given in tables I.3, I.4 and I.5.

Significant interferences both between elements and from tube contamination have been corrected (cf. Leake et al, 1969). The Y results have been corrected for the interference of $RbK\beta$ but the $SrK\beta$ interference on Zr noted by Leake et al was not apparent even up to Sr contents of 1,500 ppm. The mutual interference of Pb and Th has not been corrected since the differences are only small (approximately 2 ppm/100 ppm according to Leake et al, 1969). Some of the U results are very close to the calculated lower limit of detection and should accordingly be used with caution. Interference from Cu contamination in the Mo tube was apparent for Cu and the second order $MoK\alpha$ peak interfered with Zn. Using a "spectrosil" pure silica pellet values of 49 ppm Cu and 14 ppm Zn were measured for these interferences and subtracted from the results for the unknowns.

Ferrous iron was determined by titration with dichromate solution, using diphenylamine sulphonic acid as the indicator, after decomposition of the sample by boiling in a hydrofluoric-sulphuric acid mixture (after Shapiro and Brannock, 1962). Na_2O and MgO were determined by standard wet chemical methods on a solution prepared using the Teflon decomposition vessel method of Bernas (1968). Na_2O was determined by flame photometry (Riley, 1958) and MgO by atomic absorption spectrometry using calibration curves constructed from standard solutions of known concentration.

The portion of the mixture of minerals, composite grains and rock flour (see above p. I.17) reserved for mineral separation was sieved and the 60-120 mesh size fraction was chosen as suitable for separation in all cases after a microscopic examination. Each sample was thoroughly elutriated in distilled water to remove all the rock flour adhering to the mineral grains and then dried overnight at $110^{\circ}C$. A better than 99% pure concentrate of biotite (zircon was the main

impurity) was separated from this fraction using a Cook isodynamic magnetic separator after several runs at different currents and different angular settings (for both dip and pitch). From the felsic portion remaining an alkali feldspar concentrate (with slight quartz impurity) was obtained using heavy liquid techniques (a mixture of tetrabromoethane and dimethylformamide adjusted to give a specific gravity of 2.60). A concentrate of plagioclase and quartz was also obtained.

The biotite separates were analysed for most of the major elements by the Geochemistry Laboratory Staff at Keele University using standard rapid wet silicate analysis techniques. The trace elements were determined on a Hilger and Watts Large Quartz Spectrograph employing a standard addition or 'spiking' technique using a biotite matrix for the construction of calibration curves. The determinations were made in duplicate and the average of the two taken as the value for the unknown. Technical assistance with the spectrograph is acknowledged.

The structural state of the separated alkali feldspars was determined using the X-ray diffraction methods of Wright (1968), Tilling (1969), Ragland (1970), and Vorma (1971). A Siemens Kristalloflex IV counter tube diffractometer employing $\text{CuK}\alpha$ radiation was used for the diffraction of the feldspar powders. The feldspar separates were ground to a fine flour with a hand pestle and mortar and a small quantity mixed with CaF_2 in the ratio 5:1 as an internal standard to calibrate the diffractogram, spread evenly on a glass plate with a little distilled water and left to dry. This alkali feldspar - CaF_2 smear was diffracted from $52^\circ 2\theta$ to $18^\circ 2\theta$ twice at a chart recorder speed of $\frac{1}{2}^\circ 2\theta/\text{minute}$, the peak positions measured (at $\frac{2}{3}$ peak height and $\frac{1}{2}$ peak width) and the two values averaged. The

structural state of the alkali feldspars may be estimated from a plot of 2θ (060) against 2θ ($\bar{2}04$) prepared for feldspars of known structural state (Wright, 1968). The obliquity (Goldsmith and Laves, 1954) of the alkali feldspars and Ragland's parameter (1970) based on Wright's three peak method (1968) have been calculated and compared with results from the literature (Tilling, 1969; Ragland, 1970; and Vorma, 1971). Albite-rich domains were detected in some of the feldspars (cf. Vogel, 1969).

The plagioclase-quartz mixtures were prepared in a similar way to the alkali feldspars except that the quartz already present was used as an internal standard. The plagioclase-quartz smears were X-ray diffracted and the composition of the plagioclase determined from the curves of Smith (1956: 2θ (111)-(1 $\bar{1}1$)) and Bambauer et al (1967: 2θ (131)-(1 $\bar{3}1$)).

Accordingly a genetic classification of rock types has been used for the migmatitic basement gneisses within the area of study.

Discussion on Nomenclature

A consistent and workable scheme of rock types is necessary for field mapping and also for representation of data collected in the field and analysed in the laboratory on the final map. In the ideal case a scheme of rock types for field use would be neutral (ie. non-genetic). This ideal is often impracticable and never more so than in the case of large areas of migmatitic basement gneisses. A classification based upon the interpenetration structures of migmatites (as defined by Mehnert, 1968, for example and shown in Figure I.7)⁸ is often unsuitable simply because of the rapid change

⁸ Not all the structures given by Mehnert, 1968, as typical of migmatites can be considered within the migmatite spectrum properly defined. See the discussion later in this section.

from one structure to another and even interpenetration between these structures (cf. Cogné, 1951 - summarized above p. I.7). Equally any classification based upon the petrographic nature of the neosome in migmatitic basement gneisses (for example, pegmatitic, granitic and dioritic as suggested by Mehnert, 1968) requires a sufficient and significant variation in that neosome both on a scale which can be represented on the final map and over the whole of the area to be mapped.

A reconnaissance survey of the area studied herein suggested that both of the methods of classification discussed above were unsuitable for these migmatitic basement gneisses. Furthermore, this reconnaissance also suggested that segregation and anatexis were the main petrogenetic processes responsible for the development of the St. Malo migmatite belt⁹. Accordingly a genetic classification of rock types has been used for the migmatitic basement gneisses within the area of study. The migmatites and associated homogeneous gneisses have, therefore, been mapped into metatexites, inhomogeneous diatexites and homogeneous diatexites according to the definitions of these rock types by Brown (1973) which are summarized below. The basement has thus been mapped in a similar way to that adopted by Mehnert in the Black Forest (1953-1963; 1968).

The role of anatexis in the formation of migmatites has remained controversial since the well known debate between Sederholm (1907, 1923, 1926; 1967) and Holmquist (1916, 1921). The term anatexis was

⁹ Further work has confirmed this early conclusion (see Chapters II, III, IV & VI).

Figure I.7

Summary of typical migmatite interpenetration structures according to Mehnert (1968) and without modification.

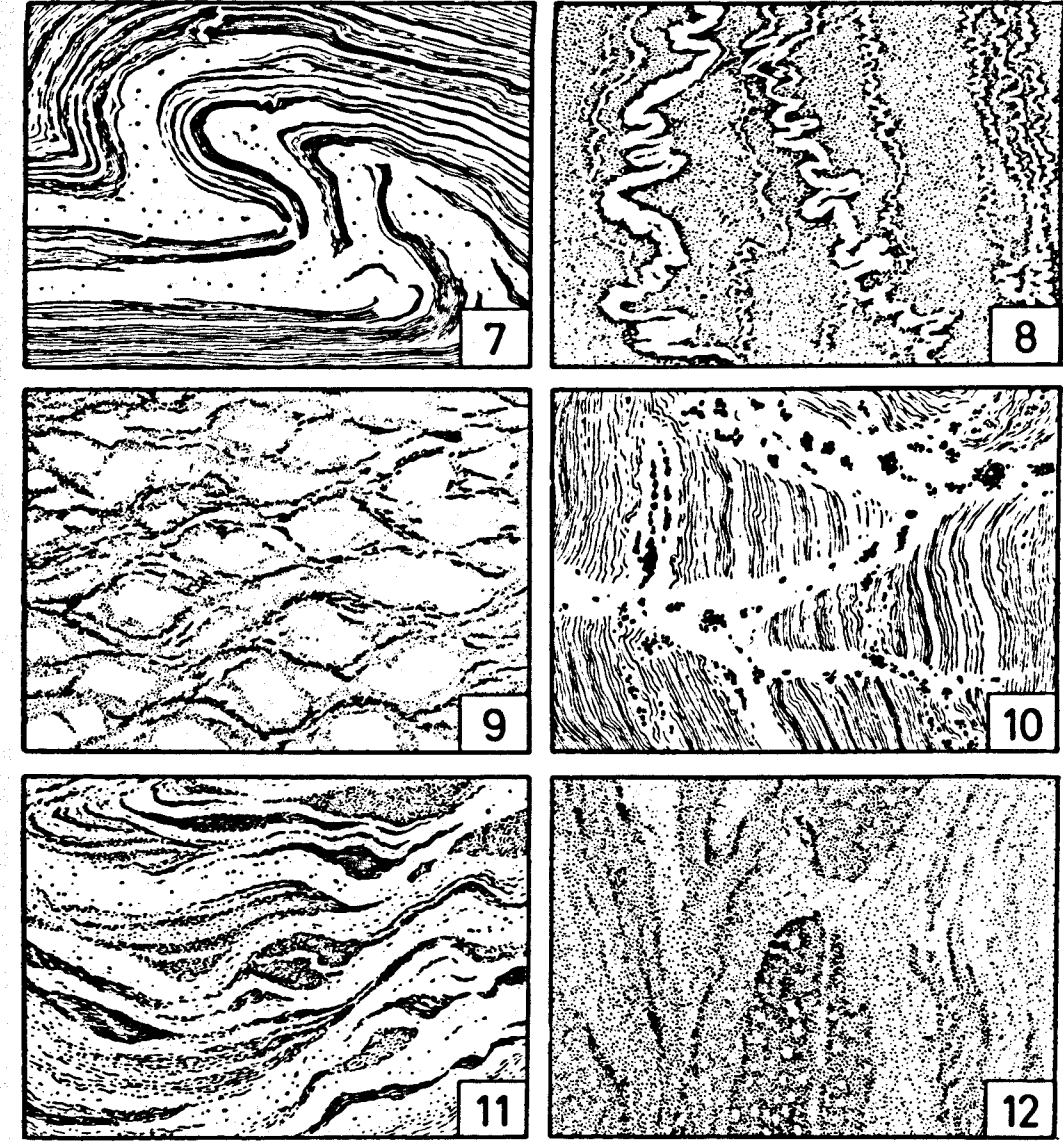
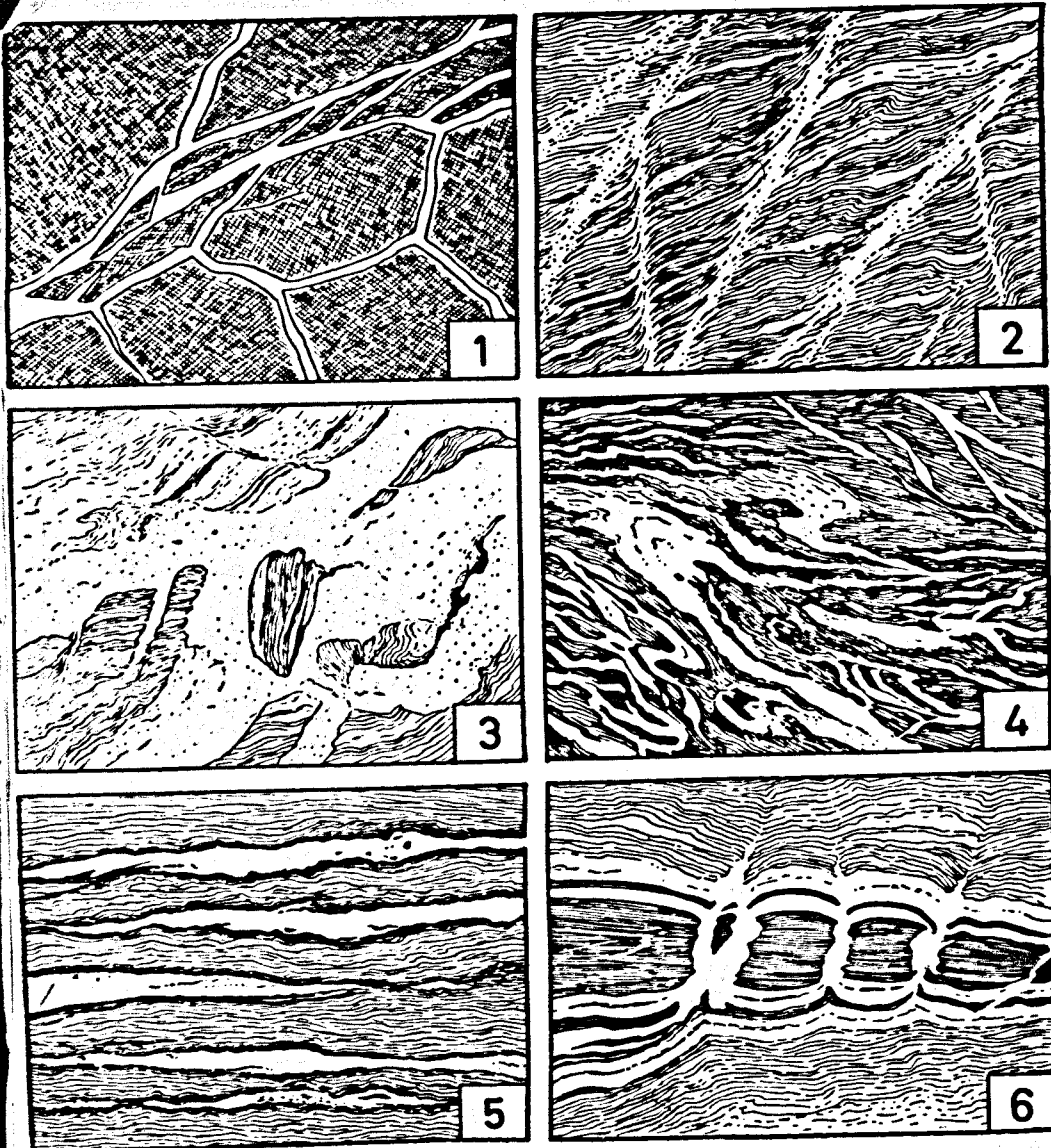


Fig. 1a. Summary of typical migmatite structures.
 1. Agmatic (breccia) structure.
 2. Diktyonitic structure.
 3. Schollen (raft) structure.
 4. Phlebitic (vein) structure.
 5. Stromatic (layered) structure.
 6. Surreitic (dilatation) structure.

Fig. 1b. Summary of typical migmatite structures.
 7. Folded structure.
 8. Ptygmatic structure.
 9. Ophthalmitic (augen) structure.
 10. Stictolithic (fleck) structure.
 11. Schlieren structure.
 12. Nebulitic structure.

proposed by Sederholm (1907; 1967, p.49) for the process of refusion of material. Many authors (for example, Von Platen, 1965; Lundgren, 1966; Winkler, 1967 & 1970; Mehnert, 1968; Sharma, 1969; James and Hamilton, 1969; Fyfe, 1970; Brown and Fyfe, 1970 & 1972; Tobschall, 1971; Blattner, 1971; and Rutishauser, 1973) consider that anatexis of metasediments is likely under the conditions of temperature and load pressure attributed to the amphibolite facies of metamorphism. Anatexis, however, is not the sole process by which migmatites can be developed. Magmatic injection (eg. Lowman, 1965), metamorphic differentiation (eg. White, 1966) and metasomatism (eg. Misch, 1968; and Brown, 1967 & 1971) are possible alternative mechanisms. It is apparent, however, that there are many areas of migmatitic rocks which are similar in appearance but for which a variety of origins have been proposed. This situation has arisen mainly because it is difficult to distinguish between certain petrogenetic processes by which banding can be developed in a rock during high-grade metamorphism.

It is difficult to distinguish between segregation by metamorphic differentiation and segregation by partial melting either on field criteria or chemical criteria (see White, 1966; Whitney, 1969 and Chapter IV of this thesis). Hughes (1970) has postulated that biotite selvages, so common in migmatites, form at the boundary between two contrasting intergranular fluid phases (hydrothermal and silicate) and mark the beginning of anatexis. Perhaps there is a continuum between segregation in the solid state and segregation by partial fusion of quartz and feldspar. If this is the case, then the rock types metatexite and diatexite as they are defined at the present, have a restricted application. It is for this reason that the processes of metatexis and diatexis are re-evaluated and redefined below.

The term metatexis was introduced by Scheumann (1936 & 1937) and added to an already confused nomenclature based on Loewinson-Lessing's syntexis (1899), Gurich's diatexis (1905), Sederholm's palingenesis and anatexis (1907), Holmquist's ultrametamorphism (1916) and Backlund's rheomorphism (1937). Metatexis is defined by Mehnert (1968) as "partial, differential or selective anatexis of the low-melting components of a rock (generally quartz and feldspar)". No satisfactory criterion is available to distinguish between the processes of metamorphic differentiation (segregation in the solid state) and metatexis as defined by Mehnert (segregation by partial fusion). Indeed, can they be considered as separate processes since segregation begins well below the temperatures necessary for anatexis to begin (eg. Williams, 1972) but may then become accentuated by anatexis when the appropriate conditions are attained (Hughes, 1970)? Chemical data on this point is inconclusive and the distribution of K, Rb and Ba cited as evidence for metamorphic differentiation by White (1966) is also consistent with segregation by partial fusion (see discussion in Chapter IV). Recent experimental work suggests (Beswick, 1973) that the K/Rb distribution coefficients for biotite-matrix and alkali feldspar-matrix pairs may be used to confirm or deny the presence of a melt. Mehnert's suggestion (1968, p.247) that "crystallization from a melt is very probable when the quantitative mineral composition strictly or nearly corresponds to the eutectic ratio of the chemical system involved" does not in itself constitute a proof that a melt ever existed. It is for these reasons that it is considered that the process of metatexis is too narrowly defined by Mehnert (above). The following definition is proposed:

Metatexis is the process of segregation (usually of quartz and feldspar) by metamorphic differentiation and partial fusion.

It follows that:

A metatexite is a rock produced by metatexis and in which the migmatitic banding is evident.

Metatexis, as defined here, thus covers the segregation process by which the Palmer migmatites were developed (White, 1966), and which are therefore metatexites. A metatexite comprises three parts: the palaeosome or parent rock (generally schistose or gneissose); the leucosome or light coloured element (generally granitic); and the melanosome or dark margins (mainly mafic and generally biotite selvages). The leucosome and melanosome together constitute the neosome or new rock and represent the segregated portion.

The term diatexis was introduced by Gurich (1905) to refer to the advanced stages of anatexis when fusion was essentially complete and thus covers the same ultrametamorphic process for which Loewinson-Lessing (1899) has earlier suggested the term syntexis. Diatexis is defined by Mehnert (1968) as "high grade anatexis which includes the mafic minerals". Thus melting of the mafic components of a rock must be proved before diatexis can have occurred. But, how does one distinguish between a rock in which there has been extensive anatexis but in which the mafic component, for example biotite, has remained in equilibrium with the anatectic melt and has not suffered fusion and a rock formed by anatexis in which the mafic component, again biotite for example, has melted incongruently but then reappears during cooling and solidification of the anatectic melt? The presence of cordierite and/or garnet together with alkali feldspar does not in itself constitute a proof that the rock was originally an anatectic melt. Similarly, the absence of both cordierite and garnet from a

rock whose field relations suggest anatexis does not preclude that rock from having passed through a melt stage. Melting of the mafic component of a rock is not so much a prerequisite of diatexis, but, in some instances, more a consequence of diatexis. Diatexis should logically refer to that degree of partial fusion which exceeds that required to produce a metatexite, that is when the extent of the melting is such that the metatextitic banding is destroyed. It is an extension of the metatectic process with which it is associated in both space and time. The following definition is proposed:

Diatexis is high grade anatexis in which fusion may be complete.

It follows that:

A diatexite is a rock produced by diatexis and in which there is no continuous migmatitic banding.

In a diatexite the palaeosome no longer represents a significant proportion of the total rock, the texture is commonly igneous and mafic schlieren are frequently present, representing the melanosome, and may define a foliation. There is no continuous banding. The components of the neosome are intimately associated with each other and the palaeosome of the metatexites is represented only by schistose or gneissose enclaves within the neosome.

The term migmatite was introduced by Sederholm (1907, 1967) with the following words (1967, p.86): "Because the mixture of different constituents is the characteristic feature of all these different rocks, I would suggest for them the name migmatites, from migma, a mixture. This rock group occupies in a sense a transitional position between the granites and the crystalline schists of partly sedimentary,

partly igneous eruptive origin, and has no sharp boundary with any of them". In 1916 Holmquist proposed the term ultrametamorphism for "... a partial or complete recrystallization of .. gneisses, through which they are converted into pegmatitic gneisses and granites". This conversion was effected by Sederholm's anatexis since Holmquist also considered that "... a general segregation of the quartz feldspar material from the rocks took place at this high degree of regional metamorphism, and that it marks the first steps of remelting of the crust" (metatexis!). Read confirmed the sagacity of the above observations with his statement (1957) that "... one of the most firmly established facts in metamorphic geology is the close association in the field of the highest-grade metamorphic rocks and migmatites".

Migmatites clearly straddle the fields of metamorphism and magmatism. It is less clear how rocks produced by anatexis during ultrametamorphism fit within the migmatite spectrum. Should "... diatexite where the rocks have an igneous texture, containing scattered biotite schlieren" (Brown, Barber and Roach, 1971) be included within the migmatite spectrum as they are, for example, by Mehnert (1968) or do these rocks lie outside the overlap between the metamorphic and magmatic fields and within the magmatic field proper? They correspond to the autochthonous granites of Read (1957) and ought to lie outside the migmatite spectrum.

The recommended definition of the term migmatite is that given by Dietrich and Mehnert at the 21st International Geological Congress in 1960 and quoted by Mehnert (1968): "A migmatite is a megascopically composite rock consisting of two or more petrographically different parts, one of which is the country rock in a more or less metamorphic stage, the other is of pegmatitic, aplitic, granitic or generally plutonic appearance". It is uncertain whether Dietrich and Mehnert

originally intended that diatexites should be included within their concept of a migmatite, although the fact that the country rock is only represented by few scattered remnants argues against. However, it is quite certain that Mehnert (1968) regards both schlieren structure and rebulitic structure as "typical migmatite structures" and diatexites as "typical migmatites" (see Mehnert, 1968, chapters 2 and 9). These structures are plainly not migmatitic since the necessary heterogeneity of the mixed rock as envisaged by Sederholm, that is the migmatite banding has been destroyed. A narrower definition of the term migmatite than that quoted above is required. Any new proposal must retain the non-genetic character of Dietrich and Mehnert's definition and yet remain compatible with Sederholm's original intentions (1907). The following definition is proposed:

A migmatite is a megascopically composite rock comprising alternating layers or lenses of granitoid and schist or gneiss.

Fundamental to the concept of a migmatite is the alternation, as well as the mixture, of two rock types, and implicit within it is a high degree of structural concordance between the two rock types.

Diatexites cannot be considered migmatites, and migmatites cannot be formed by diatexis. Metatexites, on the other hand, are migmatites, but metatexis is only one process by which migmatites may be formed (although it is probably the most common). Agmatites, as defined by Sederholm (1923, 1967), are excluded by this definition from the migmatite spectrum and are better considered as xenoliths, whether cognate or foreign, within magma - they are the intrusion breccias of Harker (1908).

Since the processes of metatexis and diatexis are distinguished according to the presence or absence of a migmatitic banding, which

in itself reflects the degree of melting which has occurred, it follows that metatexites grade gradually and almost imperceptibly into diatexites, often with a mixed transition zone, in migmatitic terrains developed predominantly by anatexis. Moreover, there is generally no significant change in bulk chemical composition although there may be differences in detail (Mehnert, 1968, Tables X and XIII; and Chapter IV this thesis). Thus although the beginnings of metatexis, preserved in low-grade metatexites, are easily distinguished from the later stages of diatexis, preserved as schlieric to nebulitic diatexites, this distinction becomes blurred in the middle ranges of anatexis, preserved as high-grade metatexites and schollen structure.

The distinction between metatexite and diatexite used in this work is based upon the nature of the neosome and the presence or absence of continuous zones of palaeosome (see Brown, Barber and Roach, 1971). Thus a metatexite is recognized by the presence of more or less continuous zones of palaeosome (schistose to gneissose) which are separated by more or less continuous zones of neosome comprising pegmatitic to granitic leucosomes generally bordered by thin biotite melanosomes (selvedges). Banding is ubiquitous, if occasionally discontinuous, in metatexites and even in the highest grades of metatexis biotite-rich bands can be distinguished from granitoid bands although bands of palaeosome may be quite rare. Inhomogeneous diatexites are characterised by the presence of biotite-rich schlieren which define a swirling foliation (see Brown, Barber and Roach, 1971). They often contain enclaves of both metatexite and schistose palaeosome but there is no migmatitic banding. Homogeneous diatexites have the appearance of foliated granitoid rocks, the swirling foliation being defined by discrete biotite crystals and small aggregates of biotite. Enclaves are absent. On the scale of an outcrop mesoscopic

areas of metatexite and mesoscopic areas of diatexite often penetrate intimately, frequently with local structural discordance - that is the diatexite cross-cuts the metatextitic banding. The diatexites were clearly mobile (see Frontispiece 1). For purposes of representation on a map this type of outcrop is classified according to the dominant rock type¹⁰.

Definition of Terms

Certain terms used with ambiguity in the literature or with uncertain or imprecise meaning are defined as they are used throughout this work. Many of the definitions are taken, with only minor modification, from Mehnert (1968), where the definitions were based upon Dietrich and Mehnert (1960), and Higgins (1971). Certain terms have been redefined by Brown (1973) and these new definitions are adhered to here. Purely French terms and French usage of some terms have been defined or expanded as appropriate in the text and may be further expanded by reference to Jung and Roques (1936 & 1952).

Anatexis: Melting of rock (modified by supplementary terms such as: differential, selective, partial or complete melting or fusion).

Anatexite: Rock formed by anatexis.

Augen: A lenticular or rounded mineral or aggregate of minerals larger than the general groundmass grain size of a rock.

¹⁰ This section on nomenclature is based on a recent paper by the author (Brown, 1973).

Cataclasis: The process by which rocks are broken and granulated due to stress and movement during faulting and shearing.

Cataclastic rock: Rock formed by cataclasis.

Diatexis: High-grade anatexis in which fusion may be complete.

Diatexite: Rock formed by diatexis, may be inhomogeneous or homogeneous.

Fluxion structure: Foliation produced by cataclasis.

Foliation: Any s-surfaces of metamorphic origin.

Gneiss: Coarse-grained metamorphic rock exhibiting a parallel structure (banding, foliation or lineation) and in which felsic minerals dominate over mafic minerals. The distinction from schist on the one hand and granitoid on the other is arbitrary and gradational.

Granitoid: A general term for any medium-to-coarse-grained, hypabyssal or plutonic-appearing, granite-like rock.

Granitization: Process, involving addition and removal of components, by which pre-existing solid rocks of any composition and origin are transformed into granitoid rocks.

Intrusive: Applies to a rock body that has moved from its place of origin into another rock.

Injection: Forcible intrusion of a fluid into a solid rock.

Leucosome: Leucocratic, quartz and feldspar rich, part of a migmatite.

Melanosome: Melanocratic, rich in mafic minerals, part of a migmatite.

Metablastesis: Preferred crystallization of a mineral or a group of minerals either by isochemical recrystallization or metasomatism.

Metamorphic differentiation: Process by which contrasting mineral assemblages are developed from an initially uniform rock during solid-state recrystallization.

Metatect: Leucocratic segregated part of a metatexite.

Metatexis: The process of segregation (usually of quartz and feldspar) by metamorphic differentiation and partial fusion.

Metatexite: Rock formed by metatexis, a migmatitic banding is evident.

Migmatite: Megascopically composite rock comprising alternating layers or lenses of granitoid and schist or gneiss.

Mobilizate: Geochemically mobile phase formed by mobilization.

Mobilization: Petrogenetically neutral term for the formation of mobile minerals or groups of minerals in pre-existing rocks by the geochemical migration of mobile components, eg. in melts, in solutions or in a gas phase.

Neomineralization: The process of metamorphic transformation of the old mineral constituents of a rock into new minerals of different composition; new mineral growth.

Neosome: Newly formed part of a migmatite.

Palaeosome: Parent rock of a migmatite.

Porphyroblast: A relatively large crystal or mineral grain developed during metamorphism by neomineralization and/or recrystallization. Porphyroblasts are larger than the matrix which encloses them.

Porphyroclast: A relatively large fragment of a crystal, mineral grain, or aggregate of crystals or grains, in a cataclastic rock. They are not produced by neomineralization or recrystallization.

Schlieren: Irregular streaks or masses, generally of mafic minerals, in migmatites or granitoids.

s-surface: Any kind of penetrative planar structure in rocks.

Schist: A foliated metamorphic rock in which the main constituent minerals are visible to the naked eye and in which platy and/or micaceous minerals are generally the most important and abundant.

Shear belt: A zone of shearing in rocks; essentially like a fault zone but more specific because it excludes zones of faulting not associated with shear.

Granite

The Succession of Rock Types

Metasediments without primary sedimentary structures but with a complex history of deformation including an early metamorphic foliation generally parallel to the lithological banding (bedding?) are assigned to the Pentevrian basement. Metatexites and diatexites derived from this metasedimentary sequence and associated granitoid rocks are also placed within the Pentevrian basement on structural-metamorphic evidence (see Brown et al, 1971). Metasediments with preserved primary sedimentary structures and a simple history of multiple deformation and associated igneous rocks are correlated with the Brioverian cover. There is a north-south dolerite dyke swarm of Palaeozoic age.

The principal rock types in the area studied approximately in order of decreasing age are:

A. The Pentevrian Basement.

1. The Metasediments - semi-pelites with psammities.
2. The Metatexites - migmatites (sensu Brown, 1973).
3. The Diatexites - inhomogeneous and homogeneous anatexites.
4. The Colombière Granite.
5. The Granitoid Sheets - granites, granite pegmatites and trondhjemites.

- B. The Cataclastic Rocks - shear belts within the Pentevrian basement.
- C. The Brioverian Supracrustal Rocks - turbidites with minor volcanics.
- D. The Cadomian Igneous Rocks.

General Distribution of the Rock Types

The main rock units comprising the part of north-eastern Brittany under discussion are shown in Figure II.1 - drawn from the author's own field observations with the exception of the Palaeozoic cover and Pentevrian diorite gneiss block which are taken directly from the Dinan (60) sheet of the "Carte géologique détaillée de la France au 1.80,000" published in 1964. The main rock units recognized are: the Pentevrian basement comprising the metasediments, the three belts of migmatitic gneisses (the St. Malo migmatite belt, the Dinan gneiss belt and the St. Cast gneiss belt), and the Pentevrian diorite gneiss block in the north-west; the Brioverian supracrustal rocks in two narrow fault blocks; and the Palaeozoic cover. The Bonnemain granite, a post-kinematic Cadomian intrusion, is exposed in working quarries around the village of Lanhélin.

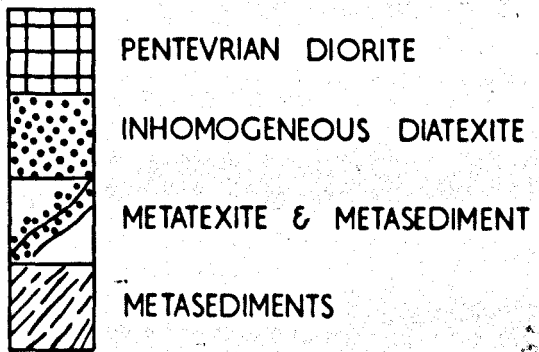
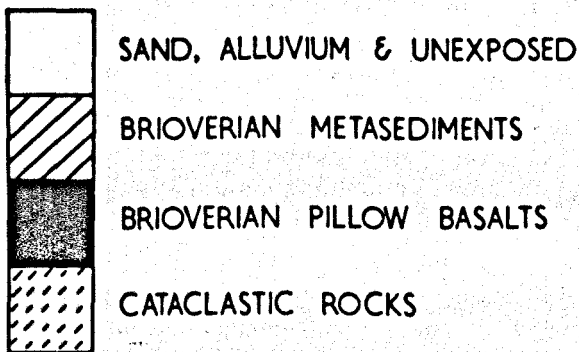
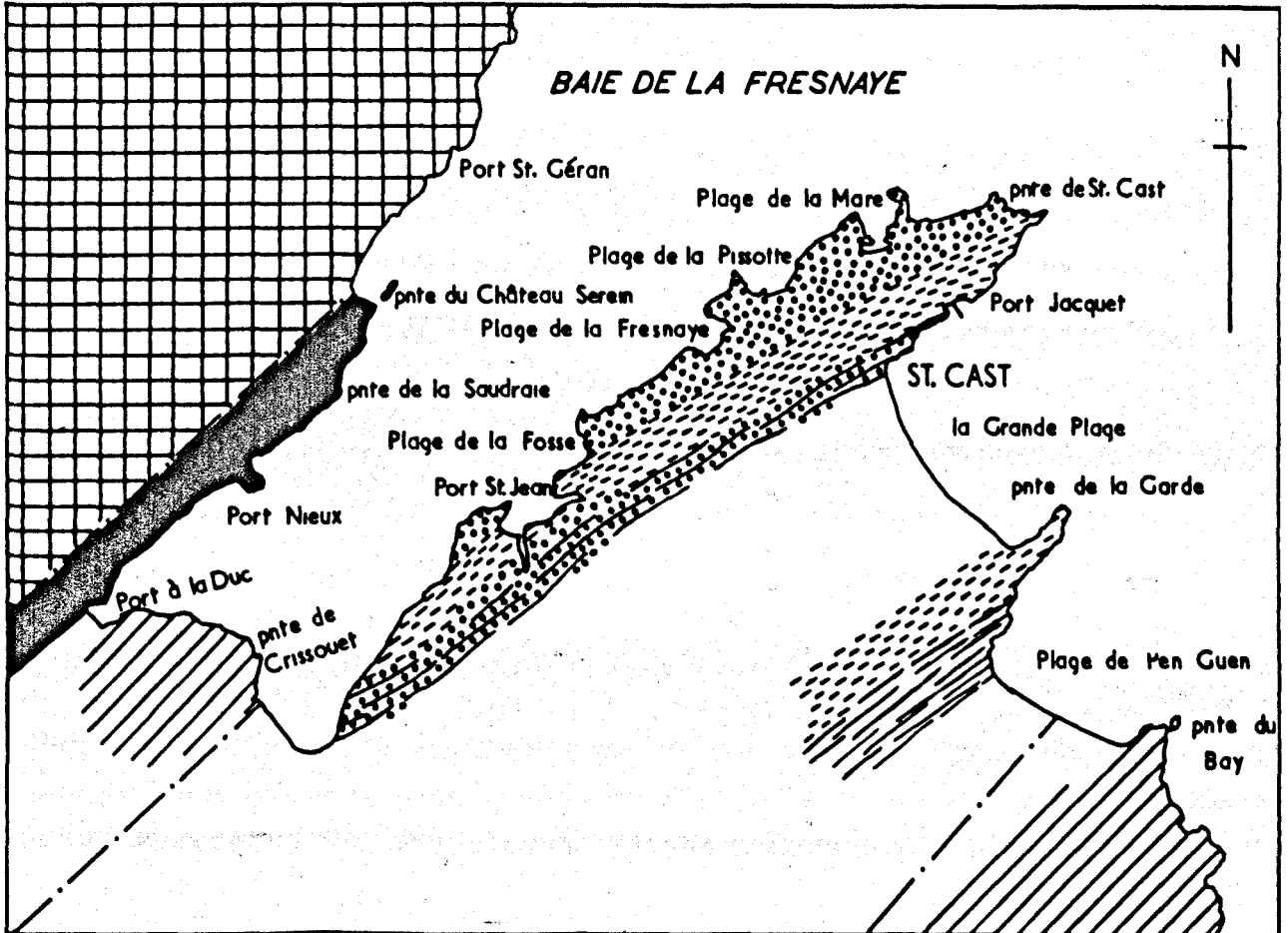
The exposed parts of the St. Cast gneiss belt (comprising the 'granulite feuilletée' and 'schistes micacés et feldspathisés' of Barrois, 1892; see also Figure I.3), the neighbouring Brioverian supracrustal rocks and the Pentevrian diorite gneiss are all shown in more detail in Figure II.2. The Pentevrian diorite gneiss (also called the Plevenon quartz-dioritic gneiss) comprises quartz, plagioclase, hornblende and biotite. According to Cogné (1964) it represents a horst of Pentevrian basement. The Brioverian pillow lavas in faulted contact with the diorite gneiss on its south-eastern side are exposed along part of the north-western flank of the Baie de la Fresnaye. They contain thin intercalations of cleaved muds and silts. The volcanic sequence includes spilitic pillow lavas,

Figure II.1

The main rock units of north-eastern Brittany.

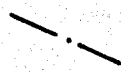
Figure II.2

The St. Cast gneiss belt and its relationship with the two belts of Brioverian supracrustal rocks.



5 KMS.



 CONJECTURAL FAULT

sills and hyaloclastites; occasional discrete pillows are found enclosed in silty sediment. The slaty cleavage in the metasediments and a variably developed fracture cleavage in the volcanics strikes ENE-WSW and dips steeply. To the south-east of Port à la Duc Brioverian supracrustal rocks again outcrop and comprise laminated muds, silts and sandy horizons which have features typical of sediments deposited from turbidity currents (eg. graded bedding and ripple lamination). Volcanics are not represented here. The contact between the predominantly volcanic succession characterised by pillow lavas and these turbidites is not exposed but their structural histories and grade of metamorphism are similar. The turbidite metasediments are folded about ENE-WSW axes and cut by a steep metamorphic cleavage which has an axial planar relationship to the folds. The junction between these Brioverian supracrustal rocks exposed at the head of the Baie de la Fresnaye and the gneisses of the St. Cast belt exposed along the south-eastern flank of the Baie is nowhere exposed but is thought to be faulted.

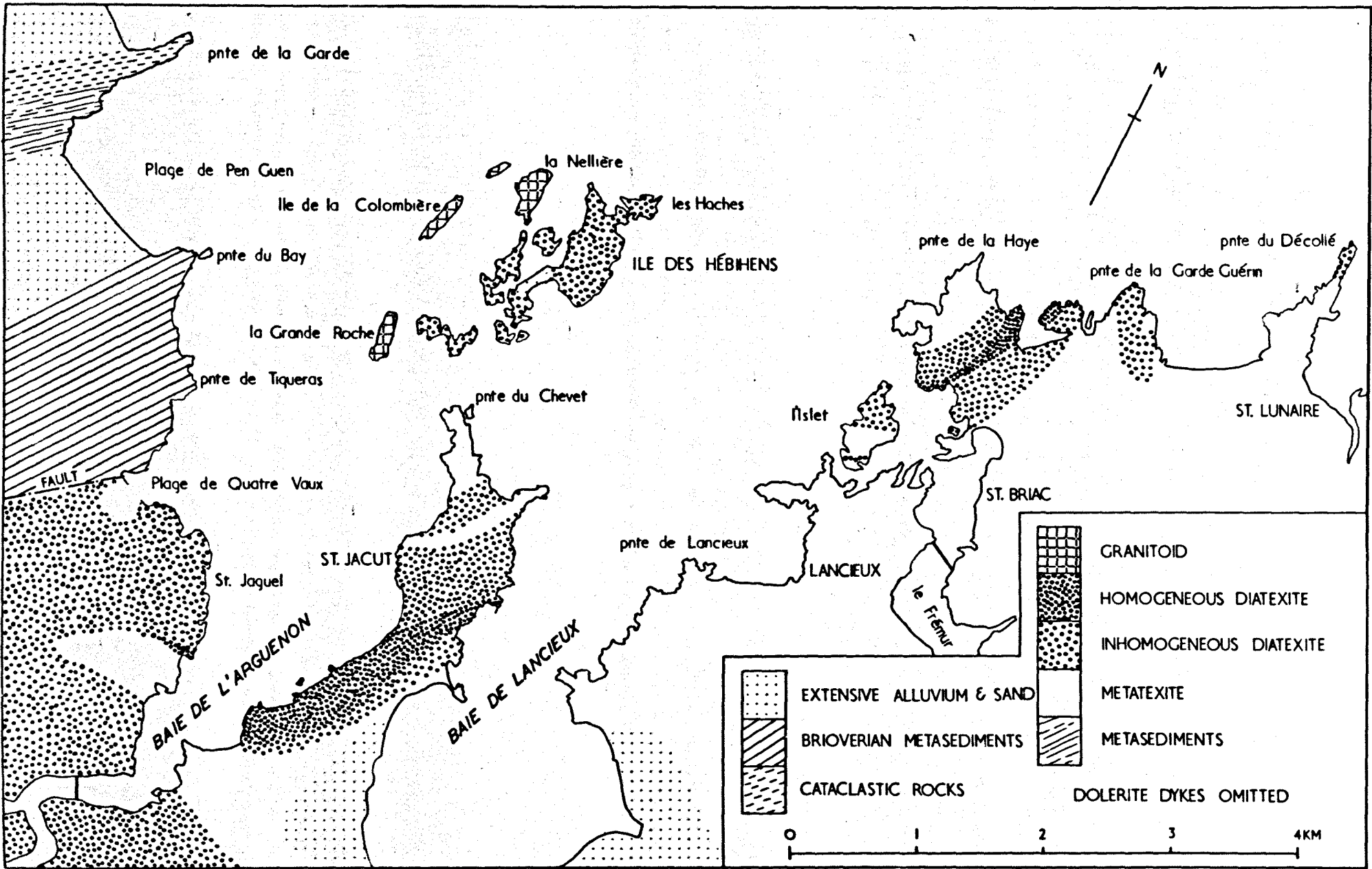
The St. Cast gneiss belt is well exposed around the pnte de St. Cast, south-west from the small fishing harbour of Port Jacquet and around the pnte de la Garde which lies to the south of la Grande Plage (Figure II.2). The north-western side of the belt is dominated by diatexites, mainly inhomogeneous diatexite which is occasionally sheared to give a protomylonite, but metatexite and some metasediment are present. A major shear belt is exposed along the south-eastern side of the pnte de St. Cast in which mylonite schists and gneisses have been produced from synkinematic leucogranites and the metatexite. On the south-eastern side of the shear belt, at the northern end of la Grande Plage, metasediments with some metatexites crop out. Diatexites are exposed alongside the road leading from la

Grande Plage to Port Jacquet and also in the harbour area. A broad expanse of sand flats separates the main part of the St. Cast gneiss belt from the sheared rocks and metasediments of pnte de la Garde at the south end of la Grande Plage (Figure II.2). Here the north-western and central parts of the headland are formed of cataclastic rocks within a second major shear belt. The rocks are predominantly mylonite schists and gneisses produced from a variety of parent materials but synkinematic leucogranites are present only in minor quantity. Complexly folded semi-pelitic metasediments with thin psammite ribs and sheared metasediments are exposed around the south-eastern parts of the pnte de la Garde bordering the northern end of the Plage de Pen Guen. This magnificent stretch of unspoiled beach backed by extensive sand flats separates the gneisses of the St. Cast belt from structurally simple metasediments assigned to the Brioverian supracrustal sequence which are exposed around the pnte du Bay at the south-eastern end of the Plage. Thus no contact between the two units may be observed and a faulted junction is postulated.

This second fault block of Brioverian, Figure II.3, consists of psammites with well preserved grading and laminated semi-pelites around the pnte du Bay. To the south the semi-pelites dominate with minor psammite horizons and occasional intraformational conglomerates. The evidence strongly suggests that these rocks represent a turbidite sequence. Synkinematic tourmaline-granite and granite pegmatite sheets (= Cadomian felsic sheets) have been intruded into the Brioverian sediments between the pnte de Tiqueras and the Plage de Quatre Vaux. Within the sediments two distinct phases of folding are recognized but are separated by a phase of flattening. The first phase of folding recognized, the main phase

Figure II.3

The north-western part of the St. Malo migmatite belt and its relationship with the adjacent Brioverian supracrustal rocks.



of folding, is accompanied by a penetrative metamorphic foliation which is axial plane to the folds produced and strikes between N-S and E-W with a steep dip. A superimposed homogeneous strain has tightened these main folds and produced folds with the same orientation in discordant quartz veins and thin pegmatites. The Cadomian felsic sheets were intruded between these two phases of deformation and have suffered boudinage by the second phase of deformation. The second phase of folding recognized has produced open folds which deform the metamorphic foliation on the macroscopic and mesoscopic scales and which generally have an associated axial plane crenulation foliation which deforms the metamorphic foliation on the mesoscopic-to-microscopic scale. These Brioverian supra-crustal rocks are not seen in direct contact with the gneisses of the St. Malo migmatite belt exposed on the south-east side of the Plage de Quatre Vaux but the junction is thought to be faulted (Brown, Barber and Roach, 1971). This north-western margin to the St. Malo belt underwent heterogeneous deformation during the Cadomian orogenic episode.

The western part of the St. Malo migmatite belt is shown in Figure II.3 and consists, for the most part, of metatexite but with all gradations between metasediment and diatexite present. Diatexites dominate the marginal part of the belt. There are two areas of homogeneous diatexite, the larger, south of St. Jacut-de-la-Mer, can be seen to grade into inhomogeneous diatexite on its southern margin, and the smaller north of St. Briac, which can be seen passing into inhomogeneous diatexite on both flanks. The granitoid mapped in Figure II.3 is the Colombière granite which outcrops as islands to the west of the Ile des Hébihens. It is not seen in direct contact with the inhomogeneous diatexites but probably

represents a third area of homogeneous diatexite, more fractionated than the other two. A large raft of metasediment is contained within the granite on the west side of la Nellière. This part of the St. Malo belt corresponds to part of the second belt of 'granulite feuilletée' mapped by Barrois (1892) (see Figure I.3).

Figure II.4 shows the eastern half of the St. Malo belt where diatexite is dominant and an extensive area of homogeneous diatexite occurs. This homogeneous diatexite 'core' has a simple intrusive contact with multiply folded Pentevrian metasediments at Port Briac, north of the picturesque fishing port of Cancale. The northern side of the homogeneous diatexite grades almost imperceptibly into inhomogeneous diatexites which are partially cataclased to the west of the pnte de Grouin. Relationships on the south side of the homogeneous diatexite are made obscure by the lack of rock exposed although the junction between it and the metasediments can be traced with some confidence about five kilometres inland. The St. Malo migmatite belt extends southwards up the River Rance changing successively from diatexite to metatexite and then into unmigmatized metasediments (Figure II.5). These metasediments, best exposed near the towns of Langrolay and St. Suliac, preserve within them a complex history of multiple folding and are accordingly assigned to the Pentevrian (see Brown & Roach, 1972b). This eastern part of the St. Malo belt was divided into two groups by Barrois (1892) - the 'granulite feuilletée' and the 'micaschistes et gneiss granulitique' (see Figure I.3).

The belt of metasediments stretching from Cancale on the coast across to the Rance at St. Suliac - Langrolay separates the St. Malo migmatite belt from the Dinan belt of high-grade gneisses (Figure II.5). The relationship of the metasediments to the gneisses

Figure II.4

The eastern part of the St. Malo migmatite belt and its relationship with the Pentevrian metasediments.

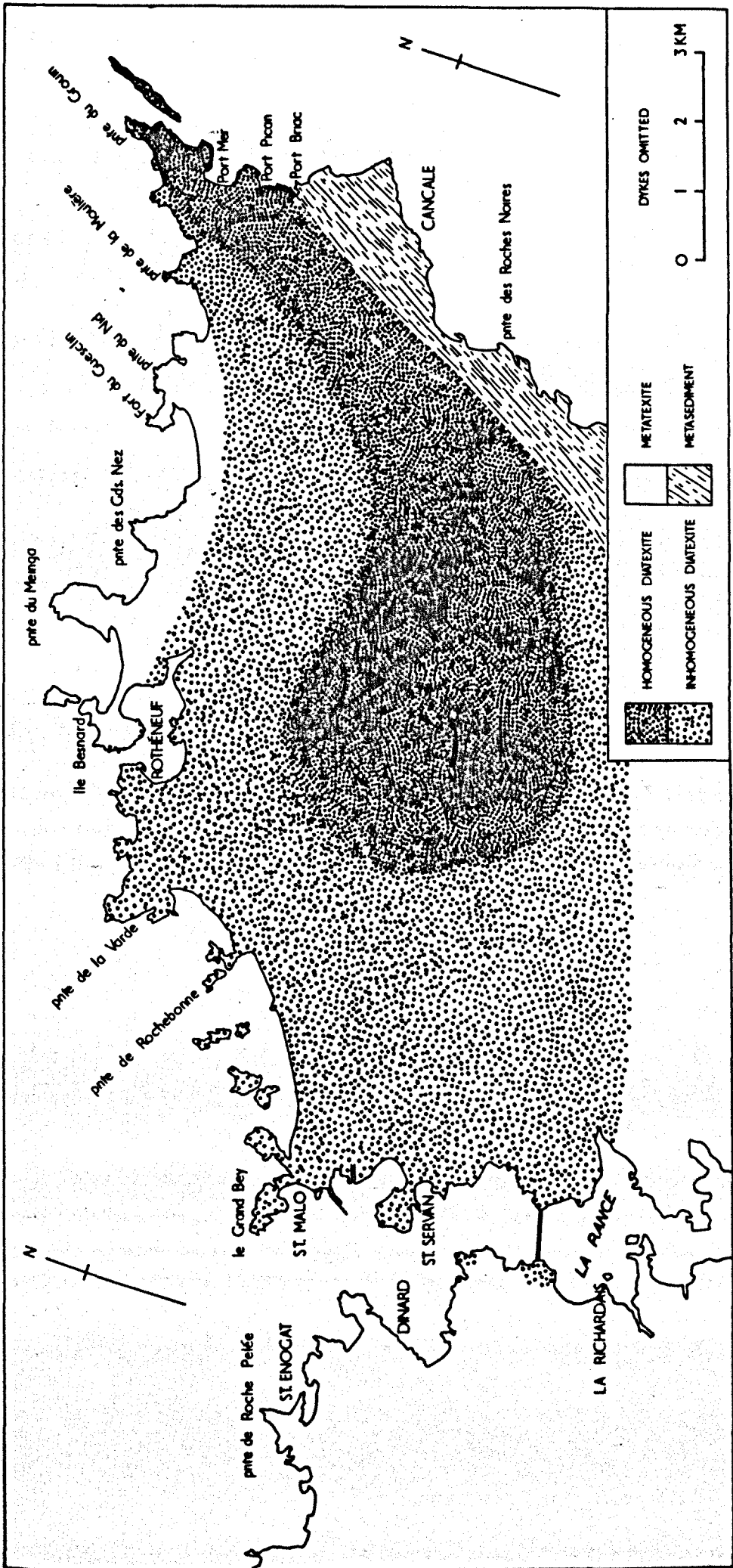
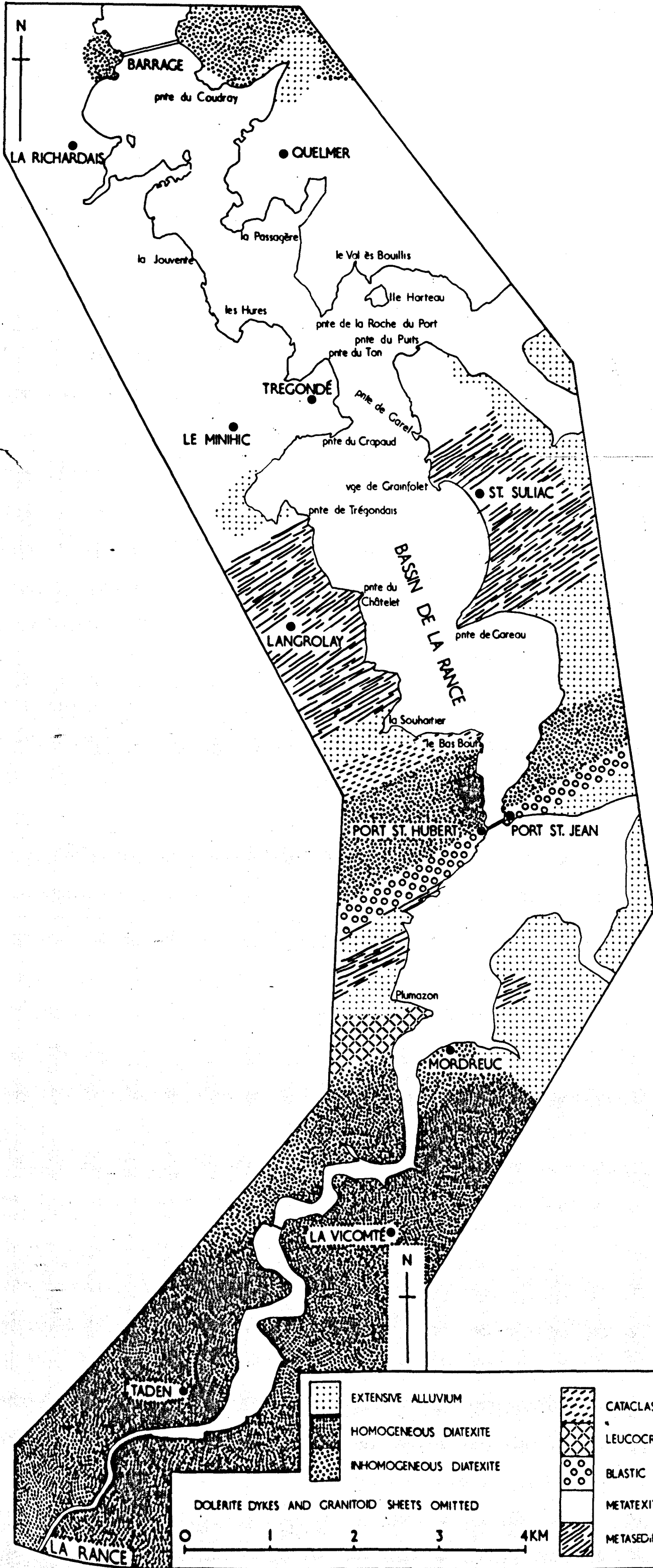


Figure II.5

The Rance section through the St. Malo and Dinan migmatite belts and the associated Pentevrian metasediments.



comprising the Dinan belt is obscured by alluvium. The Dinan belt, only exposed along the Rance, comprises mainly homogeneous diatexites in the south and inhomogeneous diatexites in the north but cataclastic rocks, blastic schists, metasediments and leucocratic gneiss are represented. The rocks of this belt were described as 'granulite feuilletée', 'granulite feuilletée' and 'granulite granitique feuilletée' by Barrois (1892) (see Figure I.3).

Field Description of the Rock Types

A. The Pentevrian Basement

1. The Metasediments

Metasediments attributed to the Pentevrian basement outcrop on the south-eastern side of the pnte de la Garde (Figure II.2), alongside the River Rance around the towns of Langrolay and St. Suliac (Figure II.5), within the Dinan migmatite belt as small isolated outcrops (Figure II.5) and along the coast to the north and south of the port of Cancale (Figure II.4). The outcrops around Cancale and along the Rance may be regarded as parts of the same belt of metasediments (see Figure II.1) and equates with the Jugon-Cancale belt of Barrois (1892) who considered them to be Brioverian in age (see Figure I.3). These metasediments predate the migmatites forming the palaeosome of the metatexites and occurring as enclaves within the inhomogeneous diatexites; they represent the oldest rocks found within the area of study. The nature of this metasedimentary sequence may be seen in Plates II.1, II.2 and II.3.

Plate II.1

a: General view of multiply folded Pentevrian semi-pelitic metasediments (23/18).

Pnte de la Garde, near St. Cast.

b: Closed structure within the Pentevrian metasediments shown in 'a'. The metamorphic foliation is parallel to the long dimension of the eye (23/11).

Pnte de la Garde, near St. Cast.

c: Ramsay 'type 2' interference structure within the Pentevrian metasediments shown in 'a' (23/6).

Pnte de la Garde, near St. Cast.

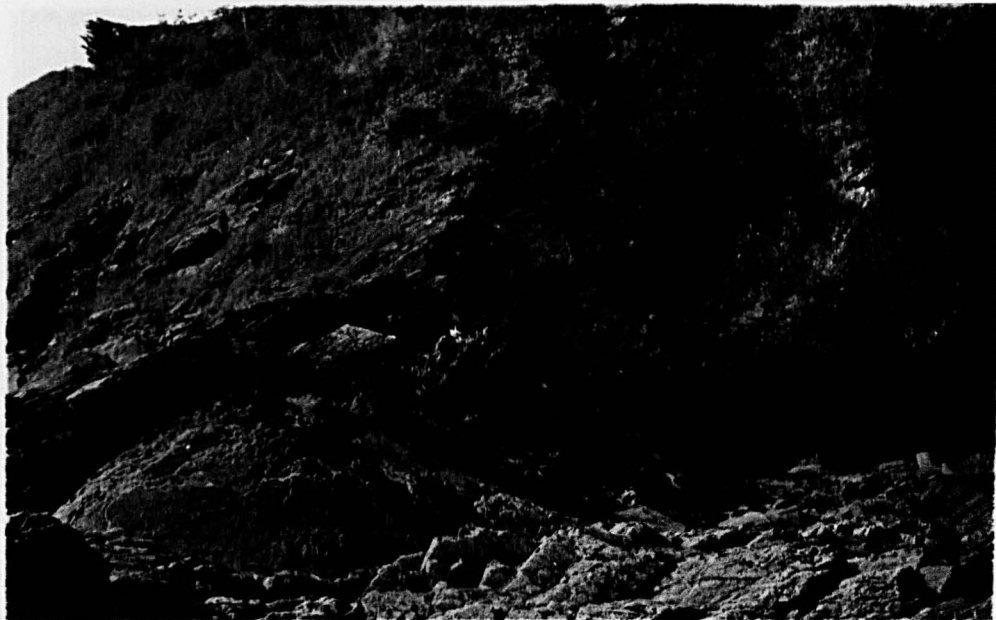


Plate II.2

- a: Pentevrian metasediments which here comprise thick (up to 1 metre) psammitic units separated by thinner semi-pelitic units (13/4).

Between pnte de Garel and vge de Grainfolet, north of St. Suliac.

- b: Pentevrian metasediments comprising psammite and semi-pelite layers and showing small late-Pentevrian folds (12/28).

Pnte de Garel, north of St. Suliac.

- c: More general view of the Pentevrian metasediments shown in detail in 'b'. Note the late-Pentevrian upright folds (12/26).

Pnte de Garel, north of St. Suliac.

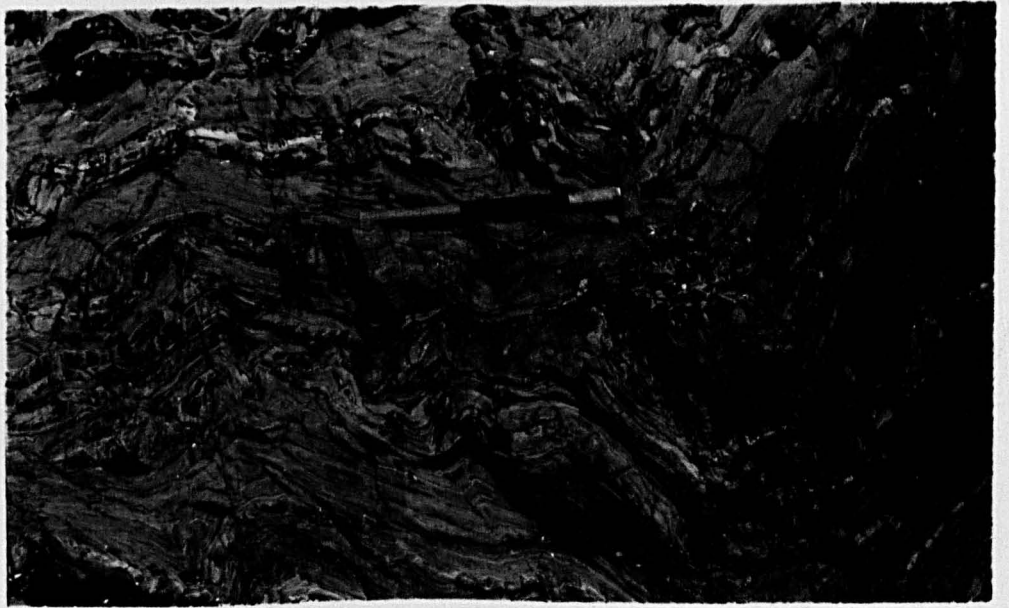
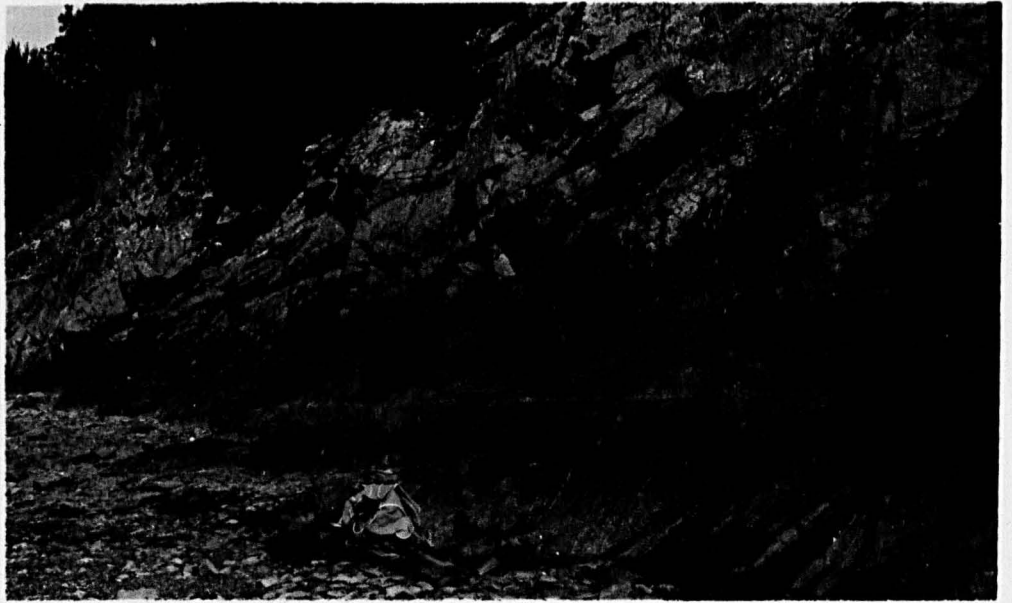
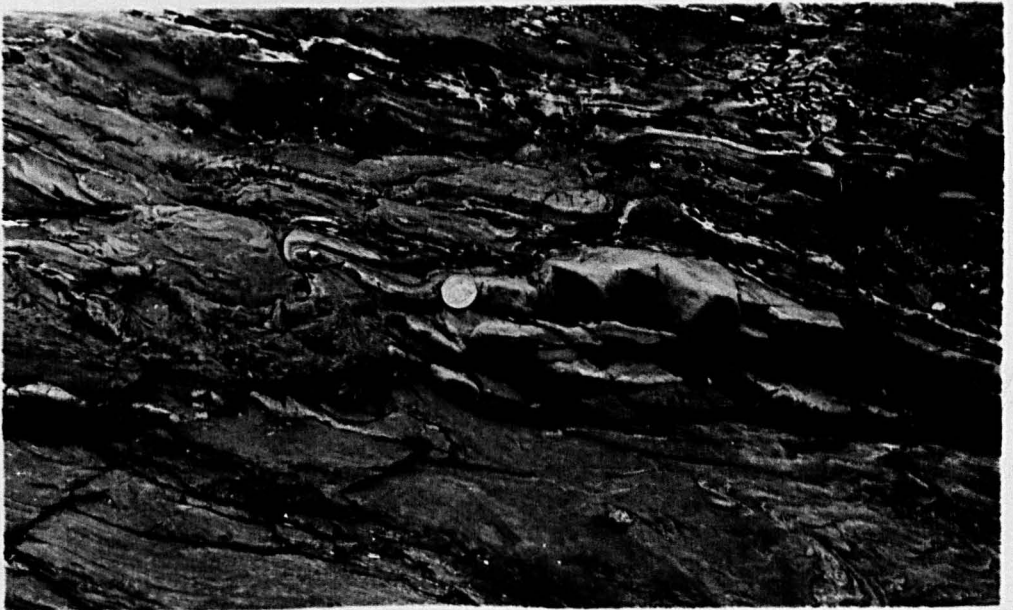
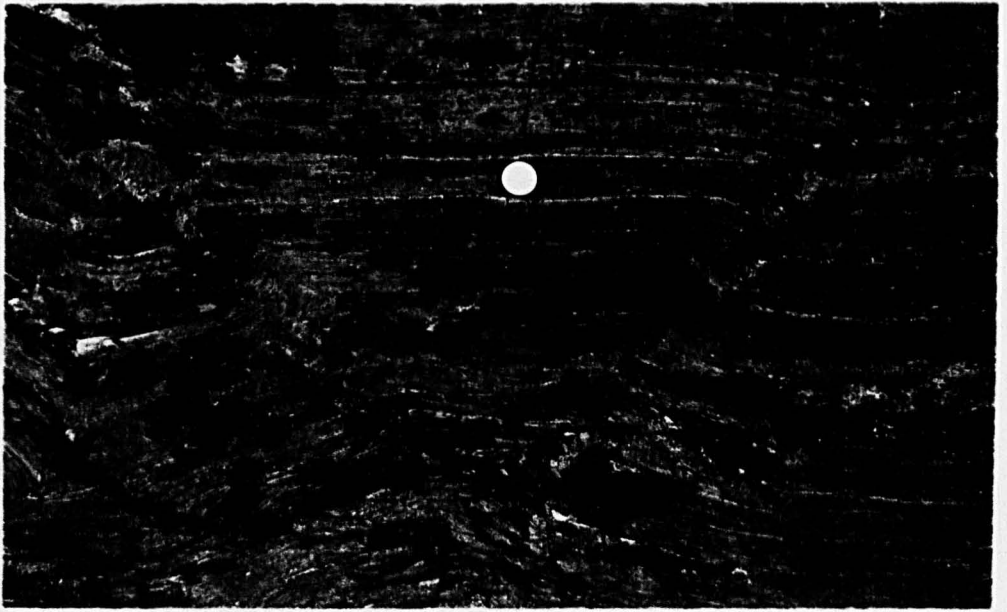


Plate II.3

- a: Pentevrian semi-pelitic metasediments with a late conjugate kink set (8/27).
Port Briac, north of Cancale.
- b: Thin psammite layers within Pentevrian metasediments of dominant semi-pelitic lithology. Note the Pentevrian fold hinges which are defined by the psammite layers (19/23).
La Houle, Cancale.
- c: Pentevrian semi-pelitic metasediments with late-Pentevrian folds (18/20).
South of la Houle, Cancale.



The pnte de la Garde:

Metasediments from the south-eastern side of the pnte de la Garde are shown in Plate II.1 where interference structures (of the type attributed by Ramsay (1967) to the effects of multiple folding) give some indication of the complex structural history preserved within these rocks. These metasediments comprise medium to fine grained dark grey semi-pelites with medium grained grey to light grey psammities. This alternation of psammite and semi-pelite probably represents an original lithological banding although no structures of possible sedimentary origin have been seen. There is a ubiquitous early metamorphic foliation which parallels this lithological banding, a feature which is considered to characterise the Pentevrian metasediments of north-eastern Brittany (Brown and Roach, 1972b). The sand flats backing the Plage de Pen Guen unfortunately prevent the junction between the Pentevrian metasediments and the Brioverian metasediments which lie to the south from being examined. It is assumed to be faulted. Small shear zones cut the metasediments and to the north-west they suffer extensive cataclasis and pass into the cataclastic rocks of the major shear belt which comprises the central and north-western parts of the headland.

Along the Rance:

The metasediments which crop out along both banks of the Rance (see Figure II.5) comprise laminated buff to grey pelites within a sequence of fine to medium grained grey semi-pelites and thick (up to one metre) medium grained grey to light grey psammitic layers. They are shown in Plate II.2. An early metamorphic foliation parallel to the lithological banding is omnipresent and a complex history of

deformation is recorded in the rocks (see Chapter V). Depositional textures and structures, however, are nowhere preserved. The lithological variation producing a regular coarse banding is thought to reflect the sedimentary bedding. There are occasional thin (ca 10 cm) concordant pegmatite layers within the metasediments and rare discordant granitoid sheets some tens of centimetres in thickness. The southern margin of this main belt of metasediments is not exposed along the Rance but lies obscured by alluvium. However, since the rocks outcropping to the south of la Souhaiter (Figure II.5) have been sheared and give way to inhomogeneous diatexites of the Dinan belt the junction may well be tectonic. Downstream from Langrolay - St. Suliac unmigmatized metasediments of the type shown in Plate II.2 gradually give way to metasediments which have suffered metatexis. It is stressed that there is a gradual increase in the amount of granitoid intruding the metasediments accompanied by the beginning of segregation in the metasediments. The division between metasediment and metatexite along the Rance is therefore somewhat arbitrarily drawn in Figure II.5 and extensive areas of semi-pelitic and psammitic metasediment occur within the metatexites as far north as la Richardais. However, the metasediments within the 'metasediment zone' show no segregation phenomena whatsoever and represent the unaltered palaeosome to the metatexites and diatexites comprising the St. Malo migmatite belt.

Around Cancale:

The metasediments which outcrop in the cliffs and along the foreshore both north and south of Cancale (Figure II.4) represent the north-eastern extension of the belt of metasediments outcropping along the Rance. However, since the regional plunge of the structures within the metasediments is generally to the NE-ENE the

rocks around Cancale, some fifteen kilometres to the north-east from the Rance, represent a somewhat higher structural level within the metasediments. The metasediments are again mainly medium to fine grained grey to black semi-pelites with thin medium grained grey to light grey psammite ribs (see Plate II.3). The junction between these metasediments and the homogeneous diatexite which forms the 'core' to the eastern part of the St. Malo belt is well exposed along the south edge of a wave cut platform on the north side of the small beach at Port Briac to the north of Cancale (Figure II.4). The contact appears intrusive and is structurally concordant (Plate II.4), the foliation in the diatexite parallels the lithological lamination and metamorphic foliation in the metasediments and the lineation in both is also parallel. Occasional thin veinlets (under 2 cm thick) of the diatexite occur within the metasediments on the foreshore. They are always structurally concordant. One slightly thicker vein parallels the junction between the diatexite and the metasediments but has no visible connection to the diatexite at the present erosion level (Plate II.4c). Whilst the actual contact between these two rock units is never seen inland, it can be traced to within a few metres for some five kilometres to the south-west. Concordant junctions between gneissic rocks and older metasediments are common within basement complexes (Roach, 1957 & 1966). To the south of Cancale the metasediments eventually pass under the alluvium which surrounds the Baie de Mont St. Michel (see Figure I.1).

Small isolated outcrops of metasedimentary rocks occur along the Rance between the bridge at Port St. Hubert - Port St. Jean and Mordreuc (Figure II.5). They are mainly medium grained grey semi-pelites with a ubiquitous foliation parallel to the lithologic lamination but they are distinctive in that they carry dark grey

Plate II.4

- a: The junction between intrusive homogeneous diatexite and Pentevrian semi-pelitic metasediments (8/24).
North side of the beach at Port Briac, north of Cancale.
- b: Concordance between the lineation in the metasediments and that in the diatexite (8/23).
North side of the beach at Port Briac, north of Cancale.
- c: Concordance between the foliation in the diatexite (at the bottom of the photograph) and that in the metasediments. Note the concordant vein of diatexite, now boudinaged (8/25).
North side of the beach at Port Briac, north of Cancale.

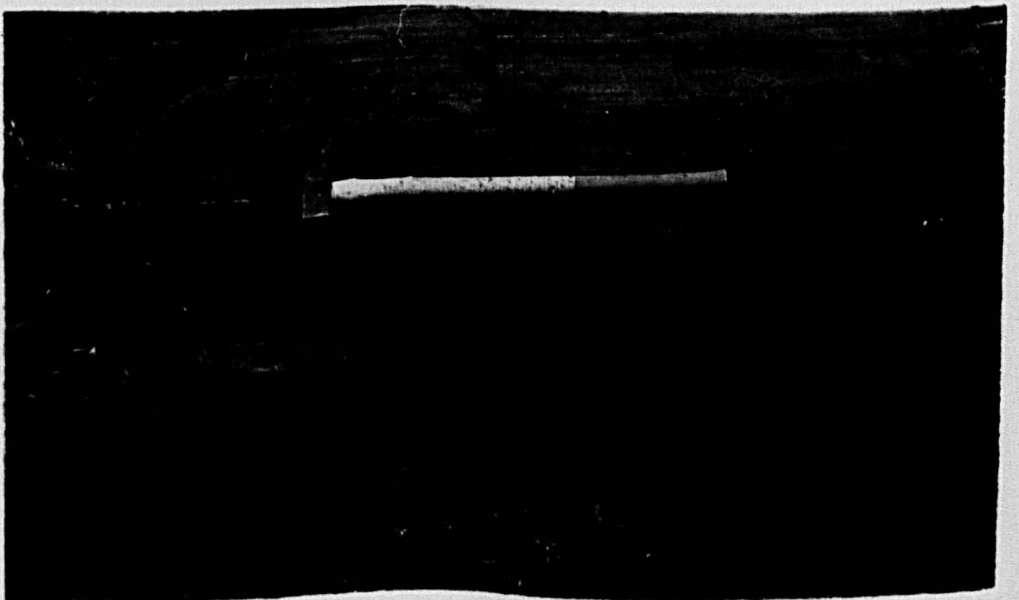
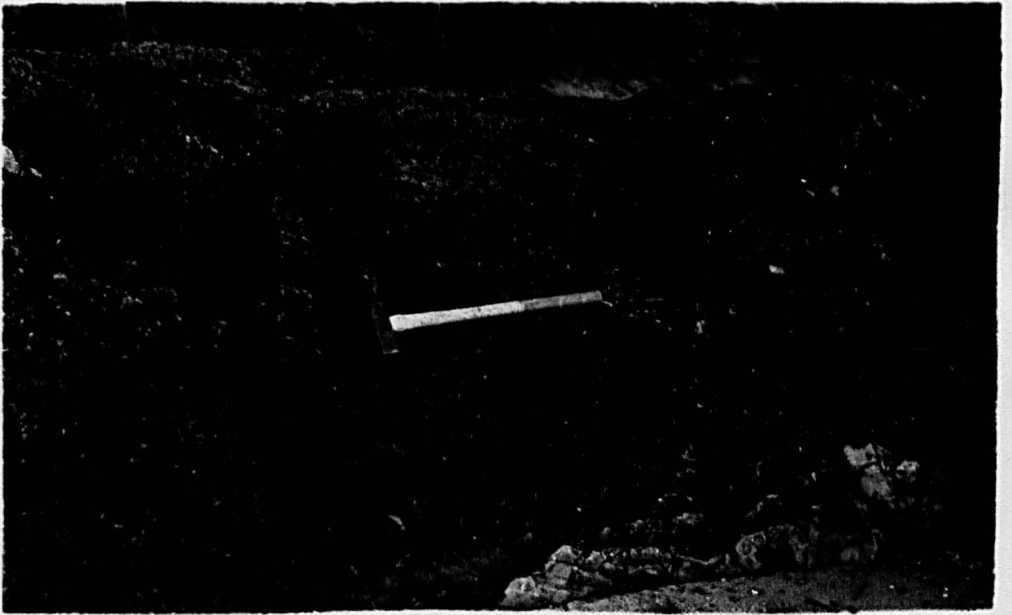


Plate II.5

a: Pentevrian semi-pelite with retrogressed cordierite
porphyroblasts (913).

La ville Ger, near Mordreuc. x 1.0

b: Pentevrian semi-pelite with retrogressed cordierite
porphyroblasts (1003).

La ville Ger, near Mordreuc. x 1.0



ovoid porphyroblasts of retrogressed cordierite (?) (Plate II.5). Folds are not seen within these small outcrops but on the basis of lithological similarity and the 'bedding' foliation these metasediments are thought to be Pentevrian also.

Thus the Pentevrian metasediments comprise semi-pelites with thin ribs of psammite giving way at a structurally lower level to thicker psammite layers. Depositional textures and structures are absent but a metamorphic foliation parallel to the lithologic banding is omnipresent. They are characterised by multiple folding.

2. The Metatexites

The metatexites, which make up about half the St. Malo migmatite belt at the present erosion level, form a partial envelope around the diatexite core to the belt. They are well displayed along the coast on the north-western side of the belt and dominate the western half of the belt (see Figures II.3 & II.5). The northern part of this metatexite envelope is represented by the narrow strip of metatexites exposed along the coast to the east of Rotheneuf (see Figure II.4). It was the river and coastal outcrop from le Minihic sur Rance to St. Briac, west of Dinard, that Cogné described in 1951 when he postulated segregation and anatexis of metasediments to produce the migmatites and rebulites. The metatexites are true migmatites (see discussion in Brown, 1973 and Chapter I) and are the rocks after which the St. Malo migmatite belt takes its name. Included under the group heading of 'metatexites' are rocks which display all gradations of segregation phenomena from schists with ptygmatic veins or quartz segregations to coarsely banded migmatitic gneisses in which no schist is preserved. The problems of nomenclature have already been discussed (Brown, 1973 and

Chapter I) and need not be reiterated here. Examples of the variety of rocks included within this group are shown in Plates II.6 to II.15 inclusive. The following typical migmatite structures (after Mehnert, 1968, Ch. 2) are represented within the St. Malo metatexites: schollen (raft) structure (eg. frontispiece 1 and Plate II.9a); phlebitic (vein) structure (eg. Plates II.8c & II.9c); stromatic (layered) structure (eg. Plates II.8a, II.8b & II.10c); folded structure (eg. Plates II.13a & II.13b); ptygmatic structure (eg. Plates II.10a, II.11a, II.11b, II.11c & II.14a); and rarely pseudo-ophthalmitic (augen) structure (eg. Plates II.12b & II.12c). Structures such as those represented by Plates II.6a, II.6b, II.8a & II.8b) are termed high-grade stromatic structure since the essential layering has almost broken to give schollen structure or the schlieren structure of inhomogeneous diatexites and little palaeosome remains (see Plate II.7c). It is stressed at this point that areas represented as metatexite in Figures II.3, II.4 & II.5 are predominantly composed of metatexite but that minor amounts of psammitic metasediment, inhomogeneous diatexite and sheets of granitoid are all present. These areas have suffered extensive metatexis during their complex history.

The relations of the metatexites to the metasediments described above are best seen along the transverse section of the St. Malo belt provided by the River Rance (Figure II.5). This is one point upon which both French geologists (Auvray, Cogné, Hameurt, Vidal and Jeannette, 1972) and British geologists (Brown and Roach, 1972b) agree even though their respective interpretations of the available evidence differ (this will be more fully discussed in Chapter V). Completely unmigmatized metasediments are exposed along both banks of the Rance around the towns of Langrolay and St. Suliac (Figure

Plate II.6

a: High-grade stromatic structure within metatexite, almost
an inhomogeneous diatexite (13/18)

La Justice, St. Jacut.

b: High-grade stromatic structure within metatexite
(13/21).

La Justice, St. Jacut.

c: Metatexite (13/26).

La Justice, St. Jacut.

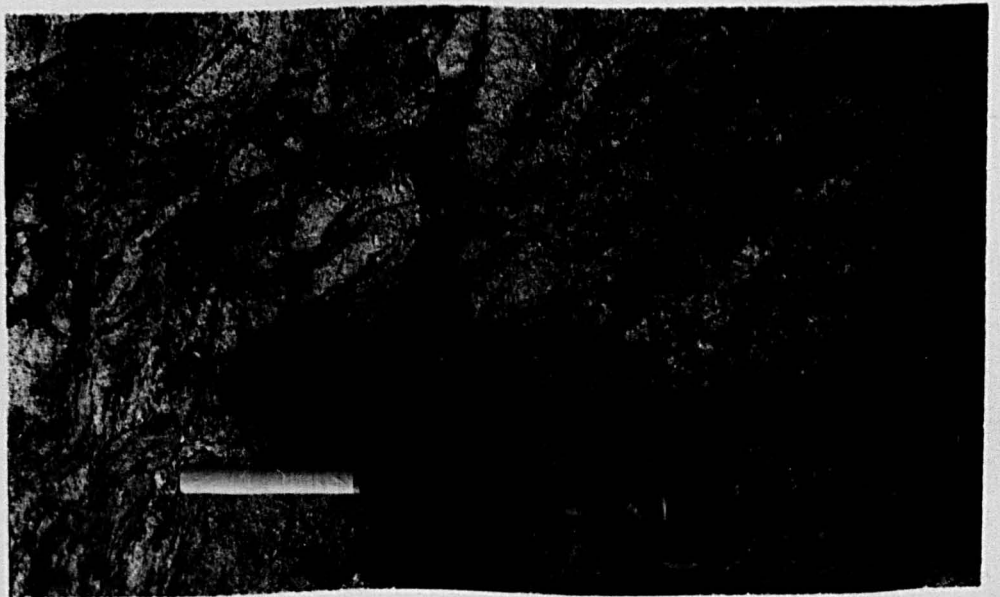
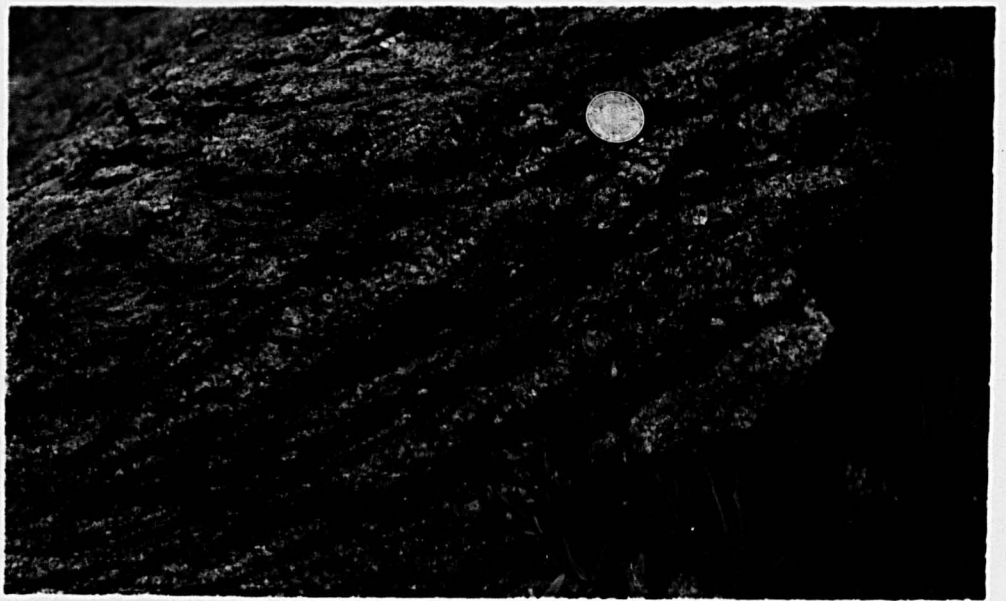


Plate II.7

- a: Enclave of metasediment, slightly metatexitic, within coarsely inhomogeneous diatexite (25/12).
Le Tertre Corieau, south of Lancieux.
- b: Metatexitic cut by concordant sheets of granite pegmatite (2/7).
North of Le Tertre Corieau, south of Lancieux.
- c: Thin granite sheets, metatexite and inhomogeneous diatexite from within the metatexite of the Island at Port l'Islet (2/18).
Port l'Islet, near Lancieux.

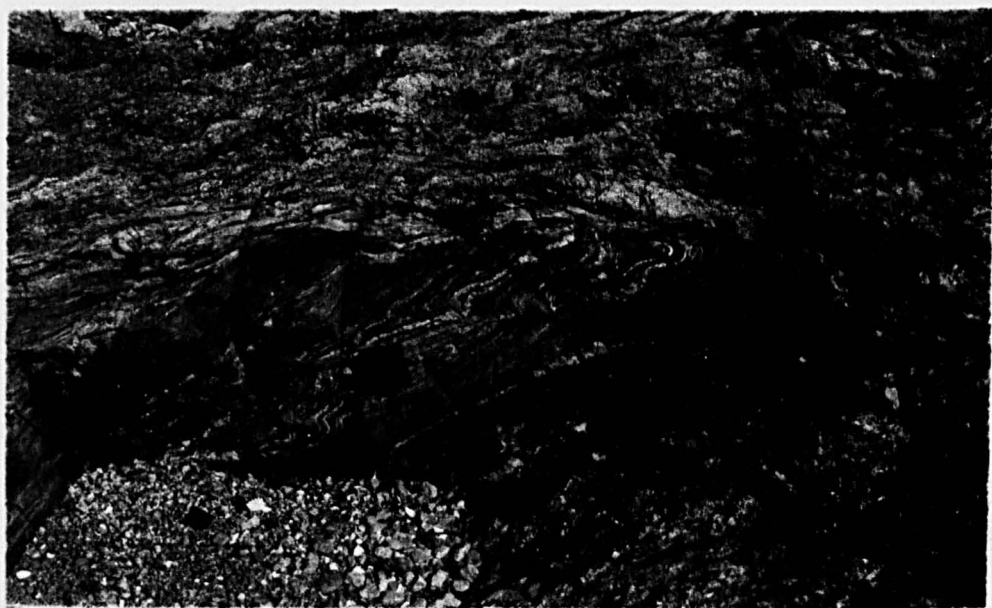


Plate II.8

a: High-grade stromatic structure within metatexite. Note the pegmatite leucosomes and the thinner biotite melanosomes (11/34).

North of Le Tertre Corieu, south of Lancieux.

b: High-grade stromatic structure within metatexite. Note the granite leucosomes and the biotite-rich melanosome layers and schlieren (2/20).

Port l'Islet, near Lancieux.

c: Phlebitic structure within metatexite (3/6).

Pnte de la Garde Guérin, near St. Lunaire.

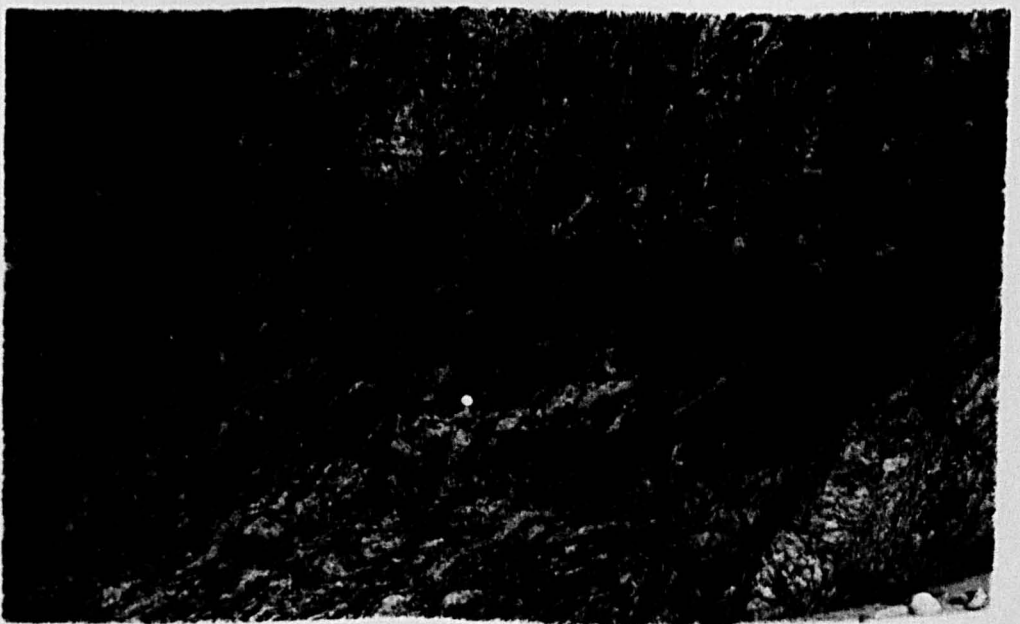
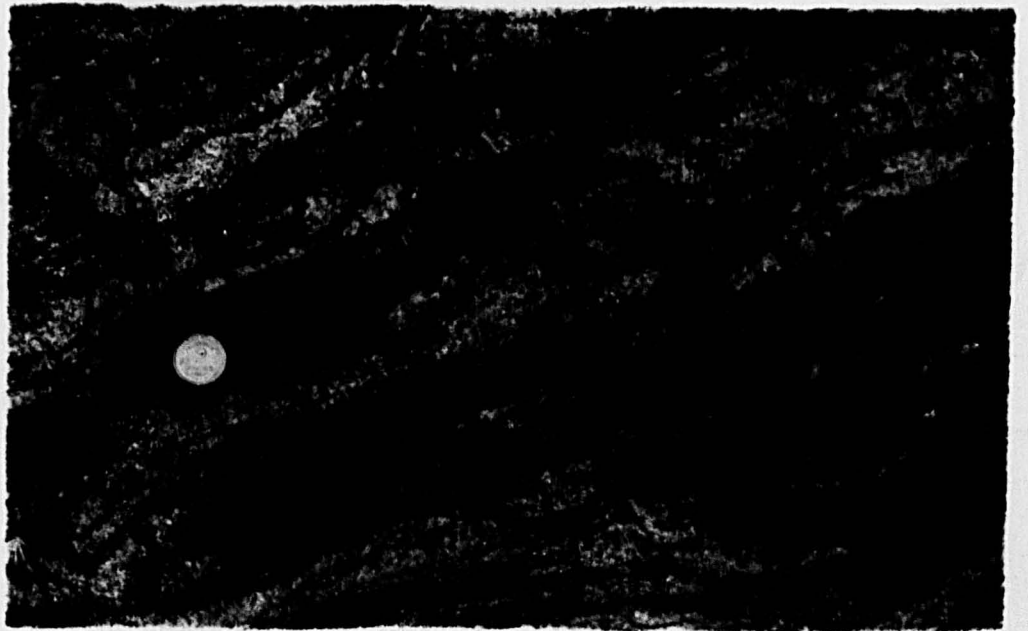
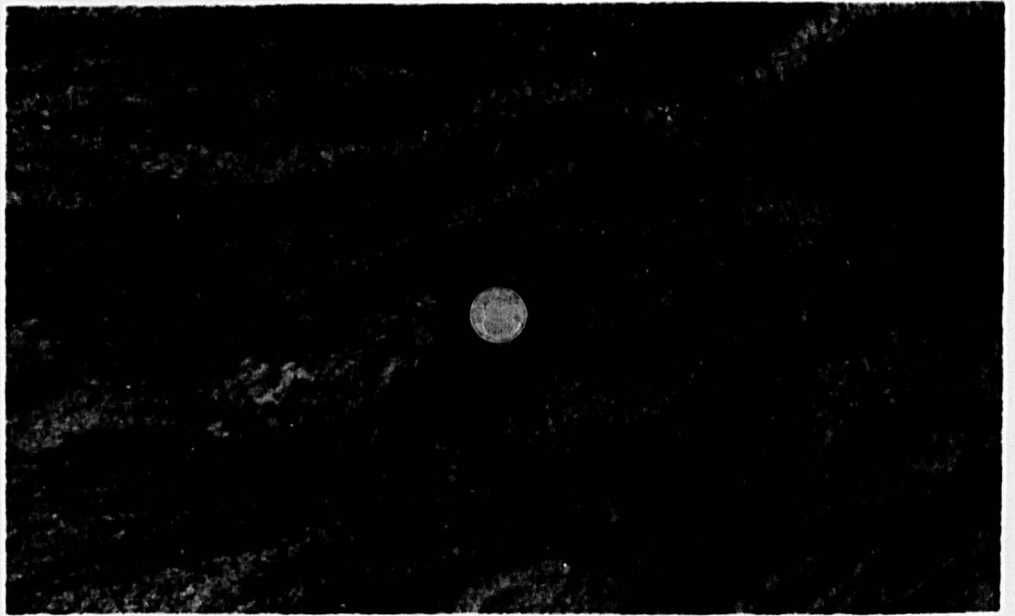


Plate II.9

a: Slight development of schollen structure (to the right of the hammer for example) as the inhomogeneous diatexite breaks up the metatexitic migmatite banding (10/22).

Pnte de la Garde Guérin, near St. Lunaire.

b: Stromatic structure developed within metatexite, near change over to inhomogeneous diatexite (10/25).

Pnte de la Garde Guérin, near St. Lunaire.

c: High-grade metatexite showing a folded structure or almost phlebitic structure (7/8).

St. Malo.

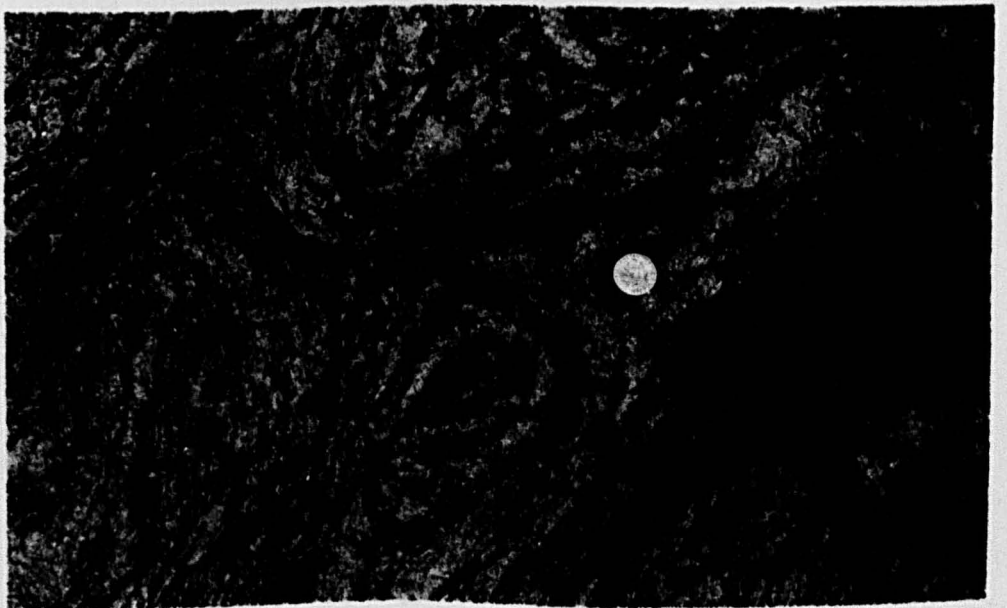
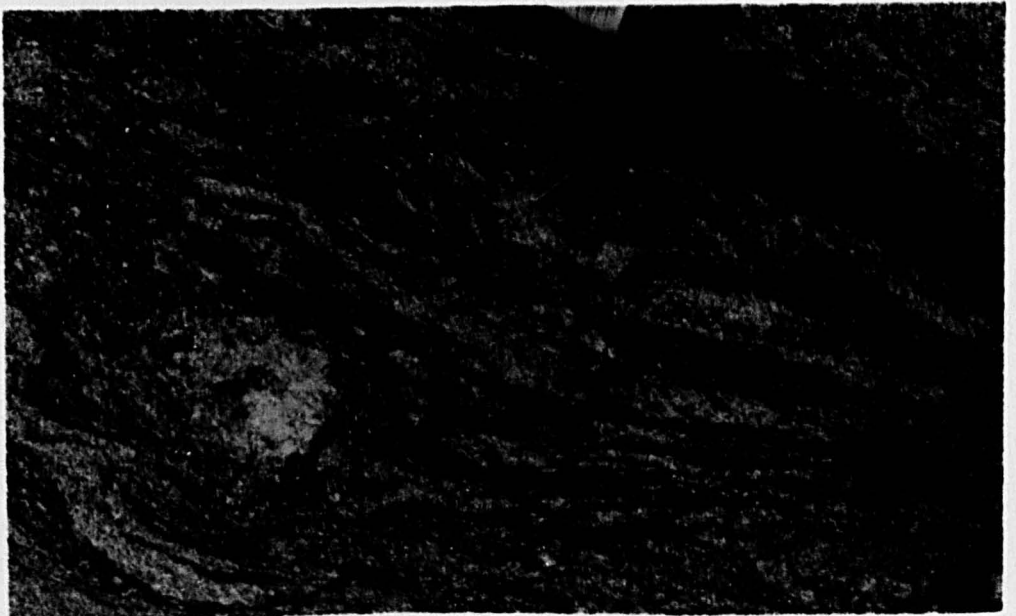


Plate II.10

a: Stromatic structure and pygmatic structure developed on either side of a small shear zone within metatexite (10/28).

Pnte de Cancanal, la Richardais.

b: Folded structure within metatexite; note small shear zone (10/31).

Pnte de Cancanal, la Richardais.

c: Stromatic structure within metatexite. Note the layers of palaeosome (under the coin and to the right) and the pegmatite leucosomes with thinner biotite melanosomes (4/29).

South of St. Servan.

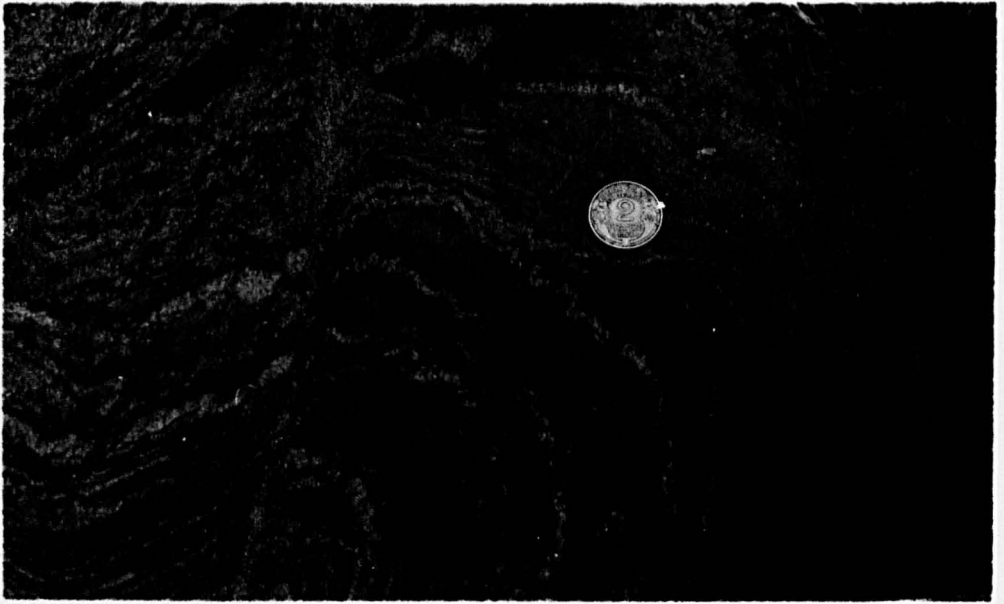


Plate II.11

a: Ptygmatic structure within metatexite. The quartzo-feldspathic ptygmas have thin biotite selvages and are within a semi-pelitic palaeosome (238).

Le Val es Bouillis, la Rance.

b: As 'a' (239).

c: As 'a' (240).

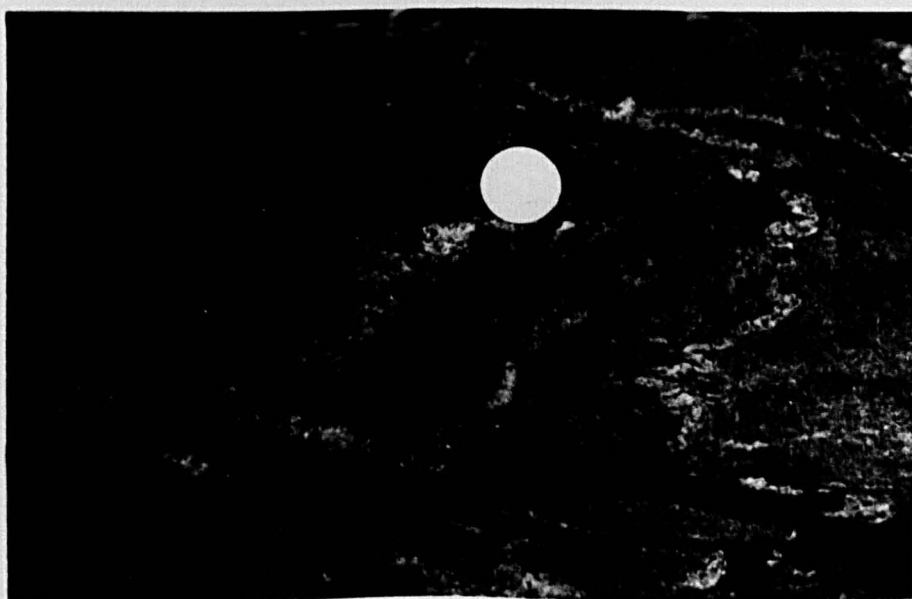
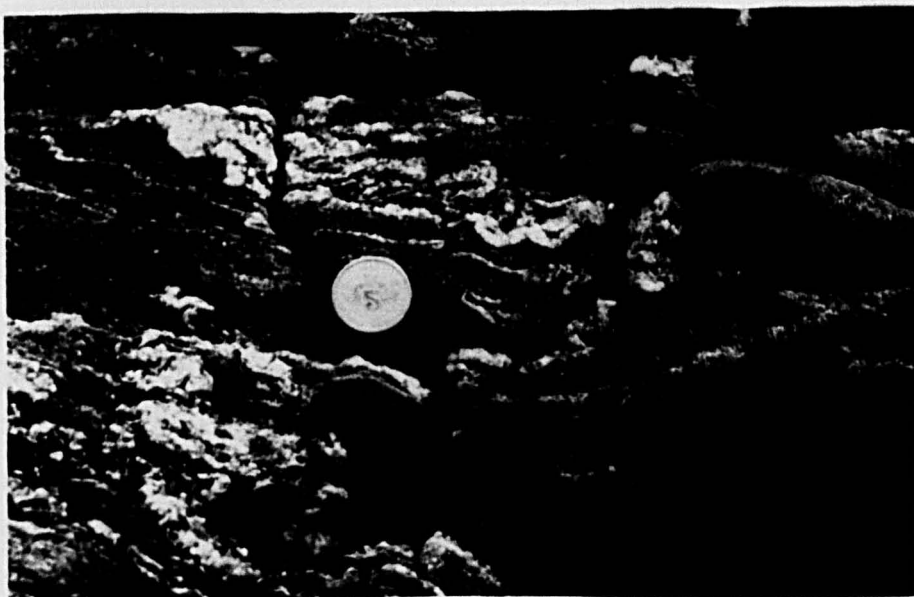


Plate II.12

a: Stromatic structure within metatexite. Note the very narrow low-angle shear zones (5/9).

Pnte de Rochebonne, Paramé.

b: Stromatic structure with hydrothermal and pegmatitic mobilizates and occasional quartz or quartz-feldspar augen giving a pseudo-opthalmitic structure within metatexite (8/2).

Pnte de Meinga, near Rotheneuf.

c: Stromatic structure with some pseudo-opthalmitic structure within metatexite. Note the quartz augen below the coin (8/8).

Pnte de Meinga, near Rotheneuf.

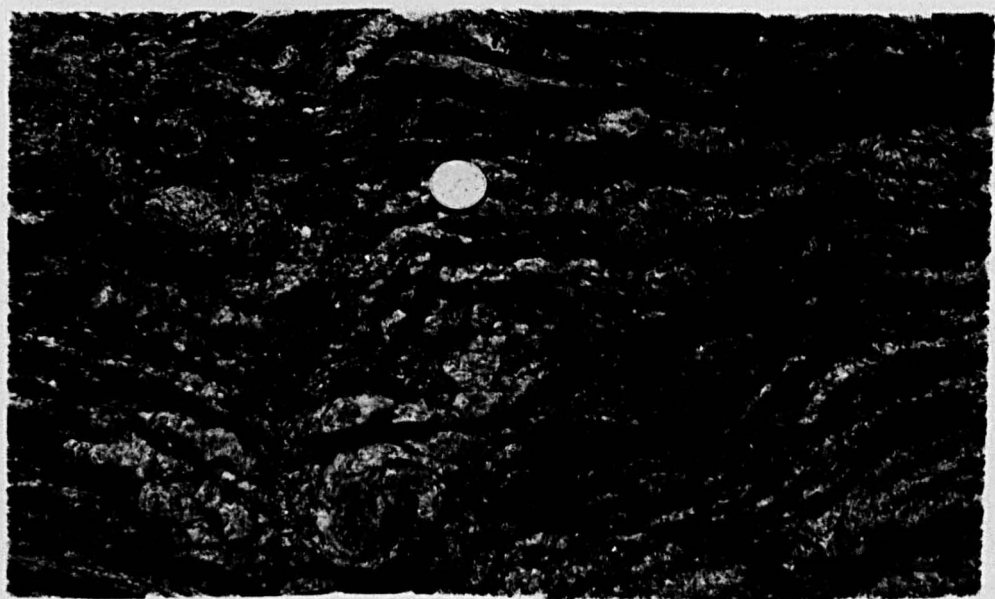
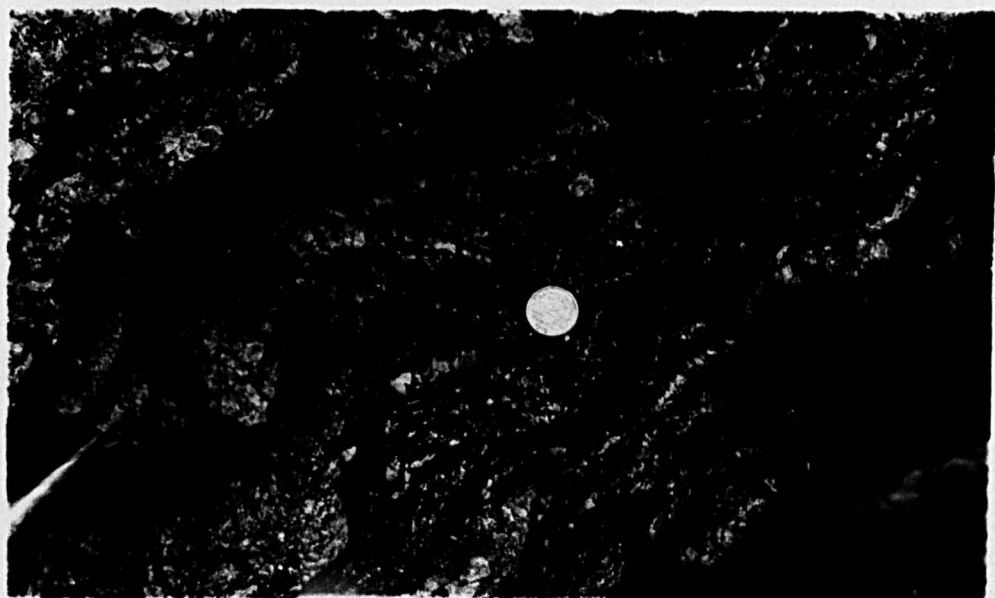
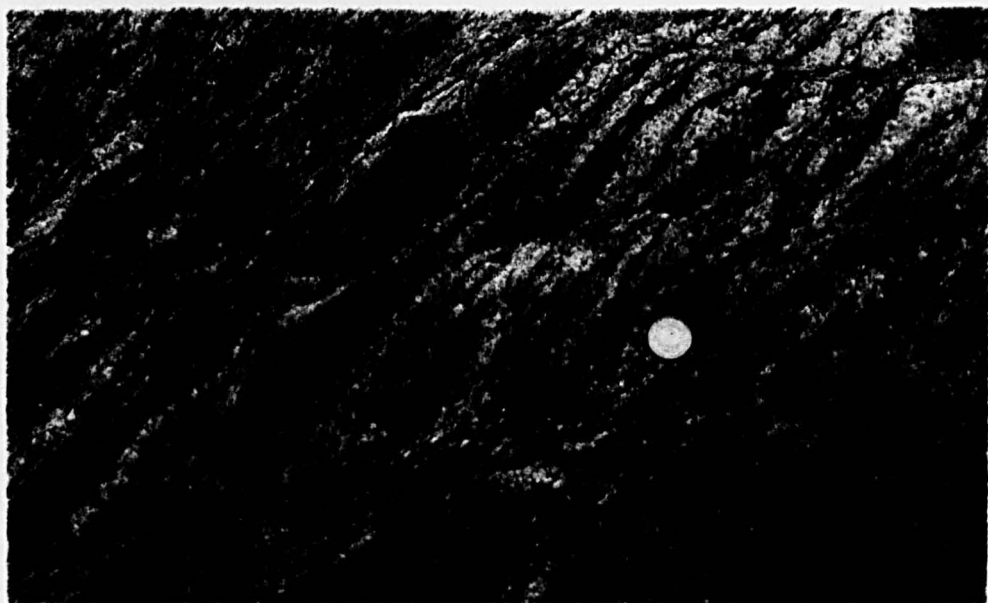


Plate II.13

a: Folded structure with slight pseudo-ophthalmitic structure tendency. Pegmatitic (quartz+feldspar) mobilizates with thin biotite selvages and schistose palaeosome (7).

Fort du Guesclin, east of Rotheneuf.

b: Folded structure with pseudo-ophthalmitic structure within metatexite. Note the omnipresent biotite selvages to the quartz-feldspar mobilizates and the steep lineation defined by the fold axes (8).

Fort du Guesclin, east of Rotheneuf.

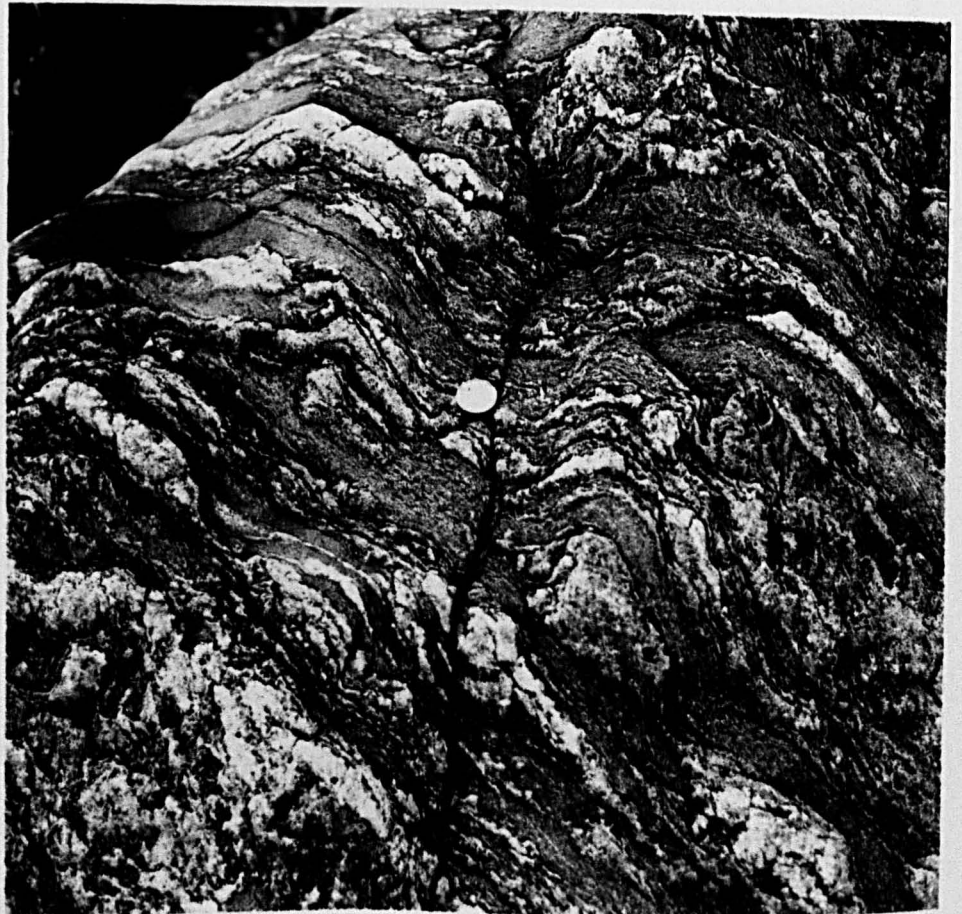


Plate II.14

a: Ptygmatic structure within metatexite. The quartz-feldspar ptygma has a thin biotite selvage on both sides (301).

Le Val es Bouillis, la Rance.

x 0.7

b: Low-grade metatexite with thin quartz-feldspar segregations and biotite selvages. Note the discordant quartz-feldspar vein (308).

Quarry south of le Minihic, la Rance.

x 0.7



Plate II.15

a: Small-scale folded structure within metatexite. The quartz-feldspar leucosomes are separated by thin biotite selvages (melanosomes) from the schistose palaeosome (V 20).

Western end of Plage du Guesclin, east of Rotheneuf.

x 0.5

b: Small-scale stromatic structure within metatexite. The quartz-feldspar leucosomes have thin biotite melanosomes (V 16).

Pnte du Meinga, near Rotheneuf.

x 0.5

c: Fine stromatic structure within metatexite. The fine schistose palaeosome has segregated into a thin quartz-feldspar leucosome with thin biotite selvages (melanosomes) (761).

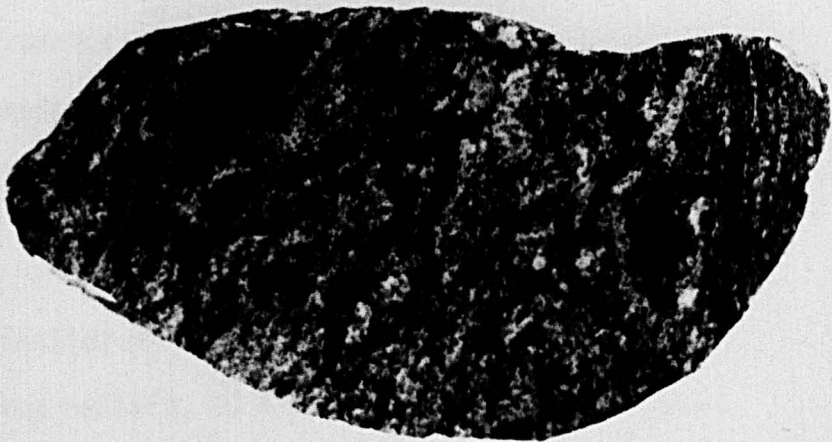
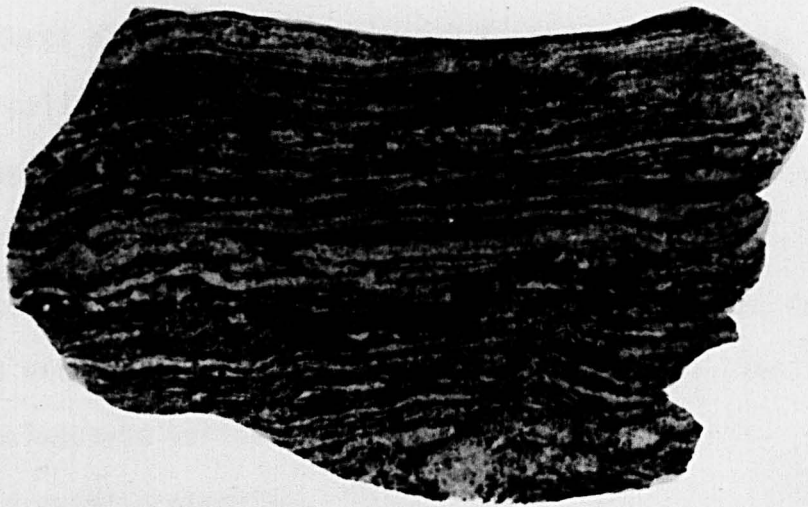
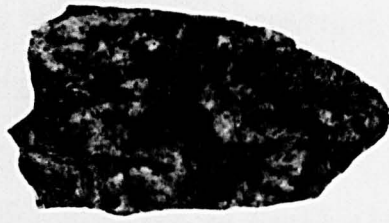
Pnte de la Garde Guerin, near St. Lunaire.

x 0.5

d: Metatexite with rather diffuse structure although the larger view provided by the wave-cut platform suggests stromatic structure (731).

Western end of Plage du Guesclin, east of Rotheneuf.

x 0.5



II.5) and comprise semi-pelites with psammites and some pelites (see above). With the onset of metatexis (segregation of quartz and quartzo-feldspathic material) there is a concomitant increase in the availability of outside material since intruded granitoid sheets (mainly trondhjemitic) become more frequent, notably in the outcrops to the north of pnte du Crapaud and pnte de Garel along the Rance (Figure II.5). This introduced granitic material will be discussed below in a later section. Metatexis affects the component lithologies of the original sedimentary sequence in different ways according to composition and produces different penetration structures as a result. Phlebitic structure is characteristic of rocks which were originally pelitic. Stromatic, folded and ptygmatic structures are typically developed in rocks which were originally semi-pelitic and consequently represent the most common structures. Ptygmatic structure is the characteristic response of the psammitic component of the sequence to metatexis. Thus the palaeosome content of the rocks mapped as metatexites along the Rance can vary between extremes according to composition, moreover the nature of this palaeosome varies from gneissose-schist of semi-pelitic origin to massive psammite. The neosome of the metatexites exposed along the Rance habitually comprises a quartzo-feldspathic leucosome of variable thickness (ca 1-2 cm in ptygmatic structure to ca 5 cm in stromatic structure) and a thin biotite selvage or biotite-rich melanosome, though this relationship may be less well defined in phlebitic structures (reference should be made to the plates).

The metatexites of the Rance thus include a range of migmatite structures which reflect, to a certain extent, the original lithological variation of the sedimentary sequence and also,

therefore, the degree of segregation which has taken place. Since it is not yet possible to distinguish between the process of metamorphic differentiation and that of partial melting (see Brown, 1973 and Chapter I this thesis) as ways of developing a banded migmatitic rock, it has been proposed (Brown, 1973) that all processes of segregation be included within the sphere of metatexis. Thus the structures described above, from the Rance, where the neosome comprises two parts suggesting a segregated relationship, are both migmatites and metatexites. Moreover, it is difficult to envisage any fundamental genetic difference between these structures - phlebitic structure, stromatic structure, folded structure and pygmatic structure - although this is implied by Mehnert (1968, Ch. 2).

The relationship of the metatexites to the inhomogeneous diatexites is best examined on the north-western side of the St. Malo migmatite belt, where small areas of diatexite are exposed within the metatexites, and on the northern side of the St. Malo migmatite belt to the east of Rotheneuf (see Figures II.3 & II.4). The change from predominantly metatexite to predominantly diatexite is not sharp but transitional through a zone where the two are thoroughly intermingled. Indeed Mehnert (1968, p.276) writes "... anatectic massifs show no sharp boundaries but merge continuously into the surrounding country rock". However, distinction can be drawn between areas dominantly comprising metatexite and those dominantly comprising inhomogeneous diatexite; Brown (1973) has stressed the gradual transition from a banded metatexite structure to a foliated schlieren structure characteristic of the diatexites. In the area between St. Jacut and Dinard (Figure II.3) the dominant rock type is metatexite, that is there is generally a migmatitic

banding preserved which is defined by the interlayering of palaeosome and neosome. Within the metatexite two mappable areas of diatexite are recognized whilst mesoscopic areas of inhomogeneous diatexite are frequent within the dominant metatexite (see frontispiece 1 and Plates II.7c and II.9a, for example). It is this complex mixture of rock types to the east of St. Briac to which Cogné (1951) made the following reference: "Les faciès décrits se répètent, s'interfèrent, sur quelques dizaines de mètres, et ceci depuis le front situé dans les micaschistes. Il faut noter cependant que dans l'ensemble ce sont les artérites et les nébulites qui sont les plus fréquentes, ce qui, zonéographiquement, paraît placer ces migmatites au niveau des anatexites". This is also the part of the St. Malo belt where Auvrey, Cogné, Hameurt, Vidal and Jeannette (1972) will admit that anatectic mobilization has occurred!

The metatexites are again seen in contact with diatexites to the east of Rotheneuf, especially on the east and north sides of the Havre de Rotheneuf (Figure II.4). The change from metatexite to inhomogeneous diatexite at the eastern end of the Havre is gradual and similar to that described above. However, the junction between the two rock types is seen to be quite sharp on the south and west sides of Ile Besnard on the northern side of the Havre. Here the metatexites are clearly seen to rest structurally above the diatexites but both maintain structural concordance. The dip is moderate towards the Baie de St. Malo, that is it is away from the diatexite 'core' to the belt.

Metatexites are well exposed in three main areas within the St. Malo migmatite belt: along the coast between the Presqu'Isle de St. Jacut-de-la-mer and Dinard; along the River Rance upstream from the

Barrage; and on the north side of the belt to the east of Rotheneuf. The metatexites in each of these areas have certain distinctive characteristics. The main distinction lies between the metatexites exposed in the two coastal areas and those exposed along the Rance section. The differences are due to an original difference in the composition of the parent rock or palaeosome of the metatexites. These differences will now be discussed.

The metatexites outcropping along the coast west of Dinard and around St. Jacut have predominantly a stromatic structure, in which the mobilizate varies from a hydrothermal (quartz) mobilizate to a granitic (quartz-feldspar-mica) mobilizate, although areas of inhomogeneous diatexite are developed and often give rise to schollen structure and rare phlebitic structure occurs. To the east of Rotheneuf the metatexites comprise predominantly stromatic structure (or folded structure, there is no essential difference) with both hydrothermal (quartz) and pegmatitic (quartz-feldspar) mobilizates being developed; areas of diatexite within these metatexites are extremely rare. Quartz pods occasionally give rise to a kind of pseudo-ophthalmitic structure. The rarity of ptygmatic structure in both areas is noteworthy, ptygmas only being developed in psammitic enclaves within the inhomogeneous diatexites. Granite and granite-pegmatite sheets are common in the western part of the belt around Lancieux and St. Lunaire but are not found within the northern outcrop of metatexites.

In contrast, the metatexites which crop out alongside the Rance upstream from the Barrage are dominated by the equal development of ptygmatic structure and stromatic (or folded) structure. This is reflected in the larger proportion of metasediment preserved as schist and schistose palaeosome and reflects an original difference

in sedimentary lithologies. The parent rocks of the metatexites exposed in the Vallée de la Rance must have originally contained a high proportion of psammitic lithology within the sequence. The increase of psammitic lithologies structurally downwards within the unmigmatized metasediments has been commented on above. Thus it is likely that the greater proportion of psammitic lithologies within the metatexites of the Rance section reflects a lower structural level within the sedimentary pile than that which gave rise to the metatexites exposed along the coast. Trondhjemite sheets are present within the metatexite zone of the Rance.

In the majority of the St. Malo metatexites the palaeosome may be distinguished from the neosome which itself comprises a leucosome of variable thickness (ca 1-2 cm in the case of ptigmatic structure up to ca 5 cm in the case of stromatic or folded structures) and either a biotite selvedge or a biotite-rich melanosome. This relationship suggests segregation in situ rather than injection of a melt or an aqueous fluid, though the relationship may not necessarily represent a melt - restite pair (see Hughes, 1970).

3. The Diatexites

Inhomogeneous and homogeneous diatexites together make up about half of the St. Malo migmatite belt at the present erosion level and completely dominate the eastern part of the belt (see Figure II.4). Smaller, but significant areas of diatexite are exposed on the extreme north-western side of the belt, at St. Jacut and at St. Briac (see Figure II.3) whilst mesoscopic areas of inhomogeneous diatexite are common within the metatexites which dominate the western part of the belt. Diatexites, mainly inhomogeneous, are also exposed along the south-eastern flank of the Baie de la Fresnaye

within the St. Cast gneiss belt (see Figure II.2 and the figure in Brown and Roach, 1972a). South of the Pentevrian metasediments which outcrop along the Rance diatexites are again encountered (see Figure II.5), they are grouped into the Dinan gneiss belt which is dominated by diatexite. The diatexites are equivalent to the "anatexites" of French geologists (see Jung and Roques, 1952) and represent migmas produced by Backlund's (1937) "rheomorphism" - they are parautochthonous granites (Read, 1957).

The diatexites are distinguished from metatexites on the basis that a regular banding has been destroyed by extensive anatexis (see Brown, 1973 and Chapter I) and as such are not true migmatites. However, they do represent the products of migmatization by anatexis and are intimately associated with true migmatites. Schlieren and nebulite structures (after Mehnert, 1968, Ch. 2) are characteristic, although schollen structure is not uncommon in areas of transition from metatexite to diatexite and is caused by the breaking up of the metatexite by more mobile diatexite (see frontispiece 1 and Plate II.9a). Typical examples of inhomogeneous diatexites showing variably developed schlieren structure from within the St. Malo belt are shown in Plates II.16-II.25. Inhomogeneous and homogeneous diatexite from within the St. Cast gneiss belt are represented in Plate II.26. Homogeneous diatexites, mainly from the St. Malo belt, showing a foliated structure without schlieren are given in Plates II.27-II.30.

The north-western junction of the St. Malo migmatite belt against Brioverian supracrustal rocks is tectonic (Brown, Barber and Roach, 1971) and the diatexites, which have undergone Cadomian cataclasis, will be described in a later section. Of the two small areas of diatexite within the dominant metatexite in the western

Plate II.16

a: Inhomogeneous diatexite with metatexitic band. Note the variable size of the schlieren within the left-hand half of the boulder (7/10).

South-east from Plage de Quatre Vaux, near N. D. du Guildo.

b: Variable inhomogeneous diatexite to homogeneous diatexite. Note the preserved metatexitic banding (stromatic structure) on the bottom right-hand side of the outcrop (25/19).

South of pnte du Chateau Parlant, St. Jacut.

c: Thin pegmatite veins within slightly inhomogeneous diatexite (11/8).

South of pnte du Chateau Parlant, St. Jacut.

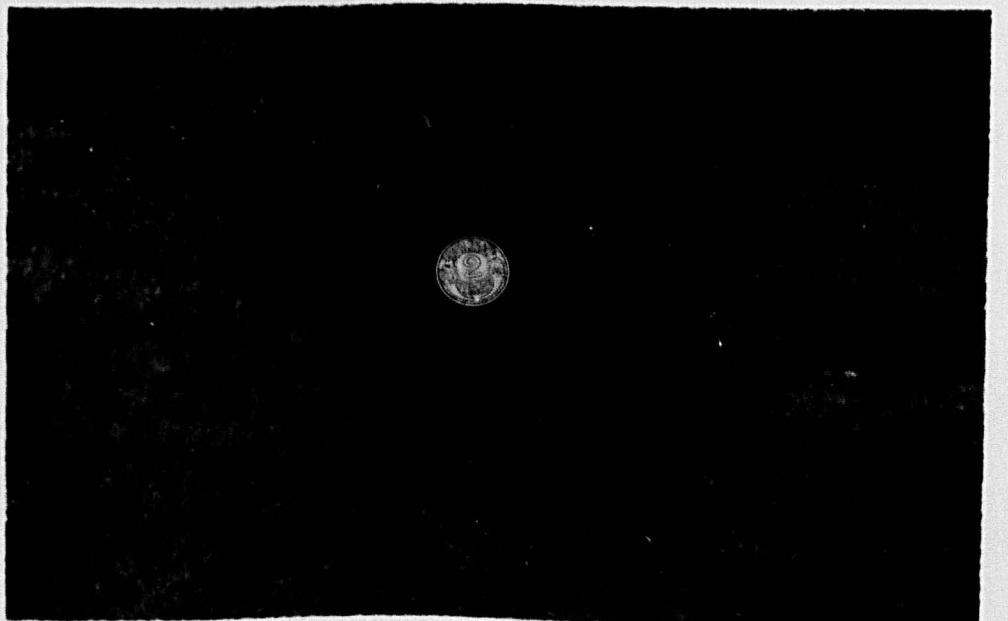
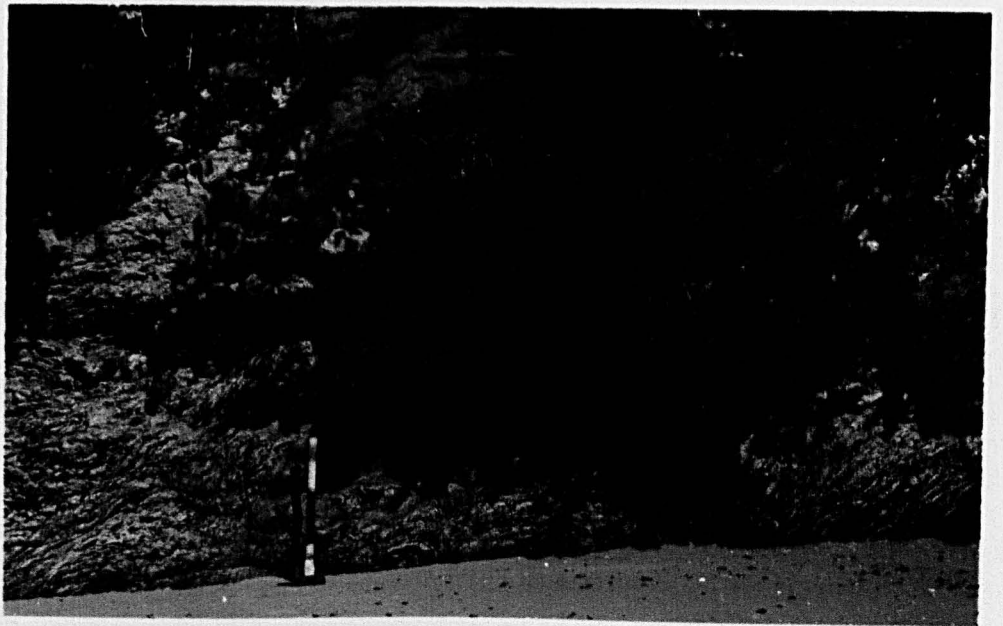


Plate II.17

a: Slightly inhomogeneous diatexite (development of biotite schlieren) bordering the south-western side of the St. Jacut homogeneous diatexite (11/10).

Northern end of Plage de Vauvert, St. Jacut.

b: Inhomogeneous diatexite with typical schlieren structure (1/27).

Pnte du B chet, St. Jacut.

c: Psammitic schist enclave contained within well foliated inhomogeneous diatexite. Notice that the schlieren of biotite are flattened in the foliation plane (1/28).

Pnte du B chet, St. Jacut.

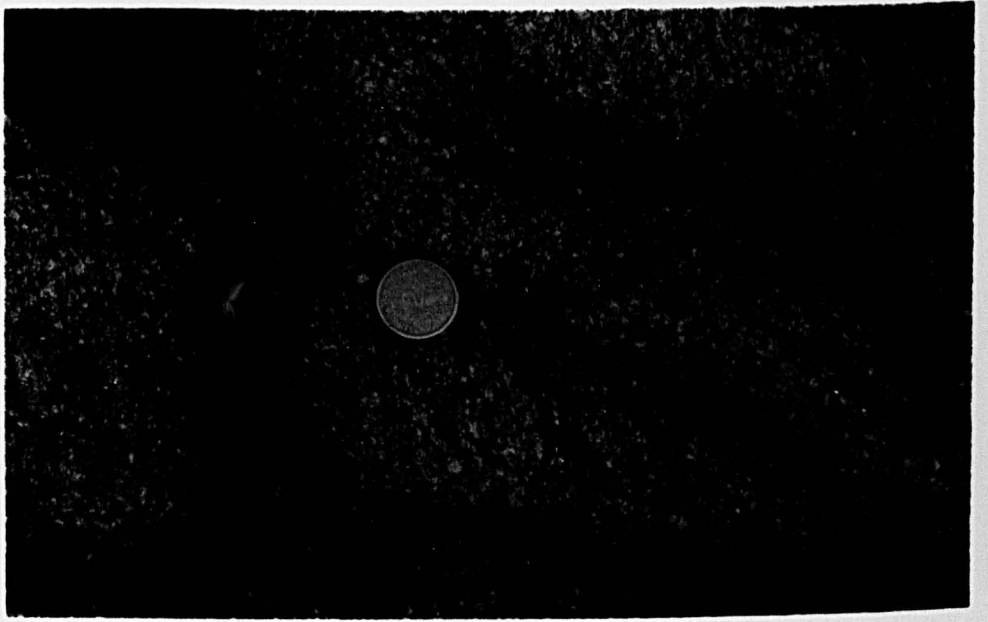


Plate II.18 ✓

a: Small area of inhomogeneous diatexite within metatexites exhibiting high-grade stromatic structure. Note the development of schlieren from bottom-left to top-right across the plate (13/25).

La Justice, St. Jacut.

b: Foliated inhomogeneous diatexite cut by a later narrow shear zone (13/28).

South from Plage de la Pissott, St. Jacut.

c: Poorly foliated inhomogeneous diatexite with variably developed schlieren structure (13/31).

South from Plage de la Pissott, St. Jacut.

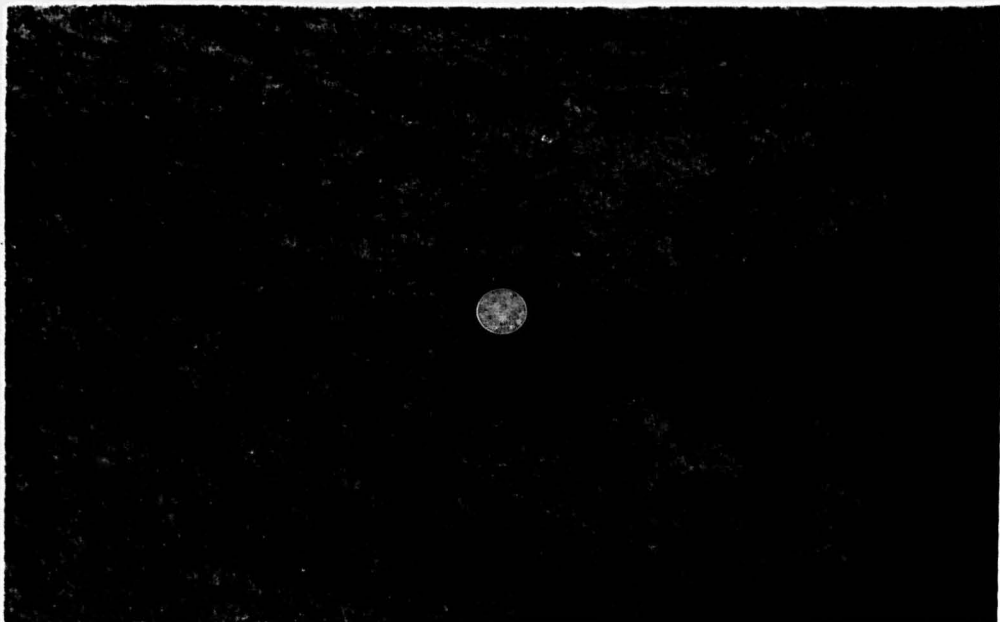


Plate II.19

a: Folded biotite layers within inhomogeneous diatexite exhibiting schlieren structure (1/29).

Pnte du Béchet, St. Jacut.

b: The beginning of the break up of the migmatitic banding - the transition from metatexite to inhomogeneous diatexite (3/4).

Western side of pnte de la Garde Guérin, near St. Lunaire.

c: Well foliated inhomogeneous diatexite (3/5).

Western side of pnte de la Garde Guérin, near St. Lunaire.

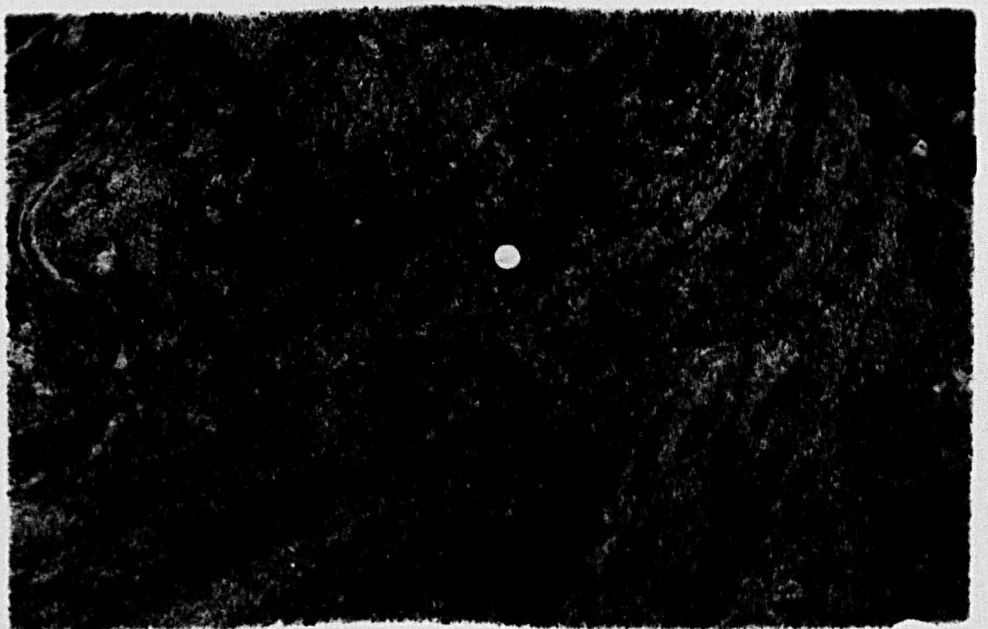
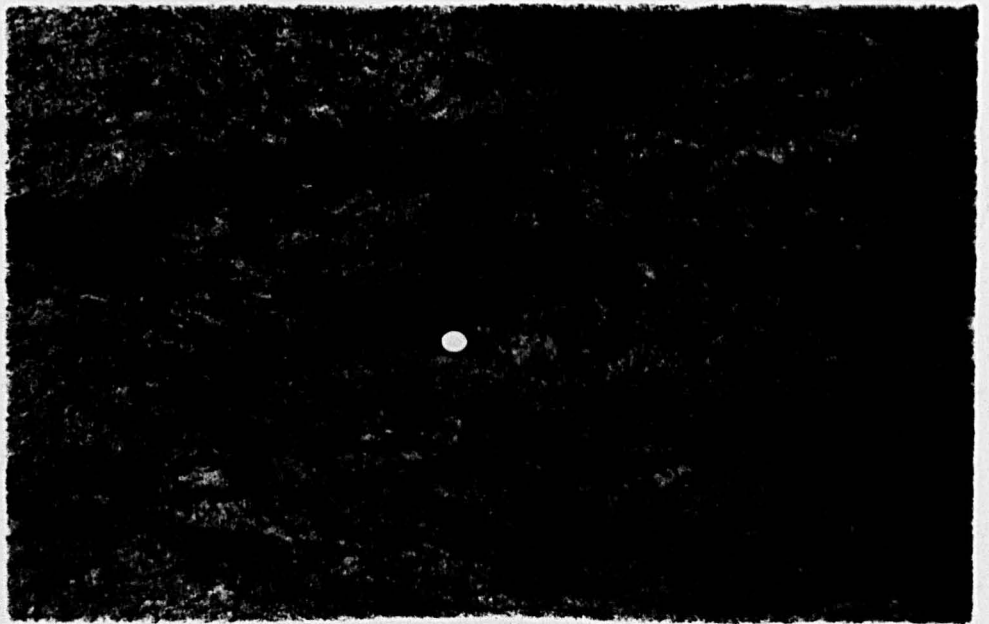


Plate II.20

a: Foliated inhomogeneous diatexite (3/18).

Pnte du Décollé, St. Lunaire.

b: Foliated inhomogeneous diatexite (3/21).

Pnte du Décollé, St. Lunaire.

c: Foliated inhomogeneous diatexite (5/15).

Pnte du Nicet, near Rotheneuf.

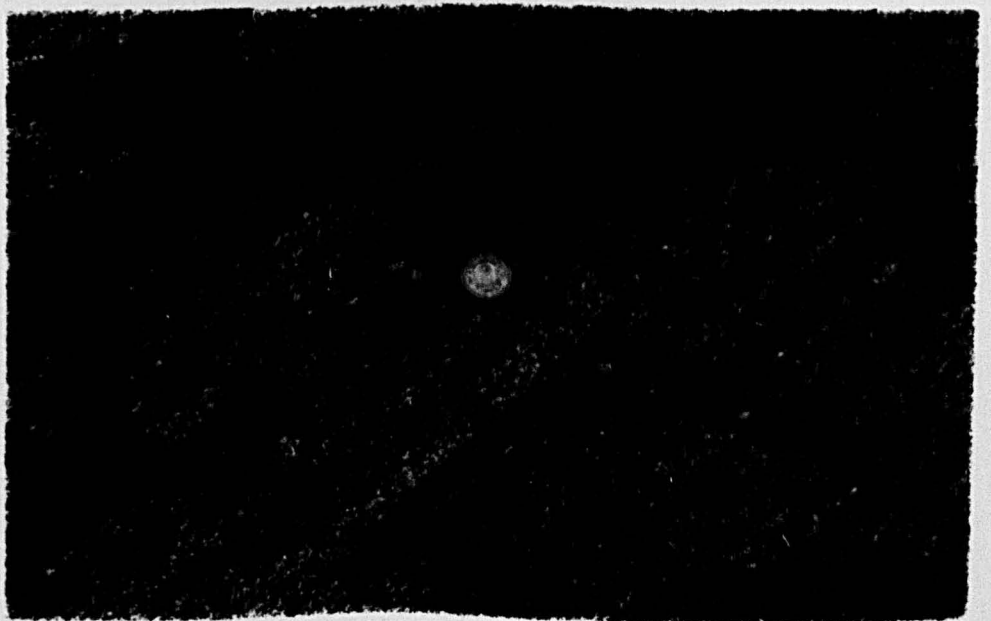
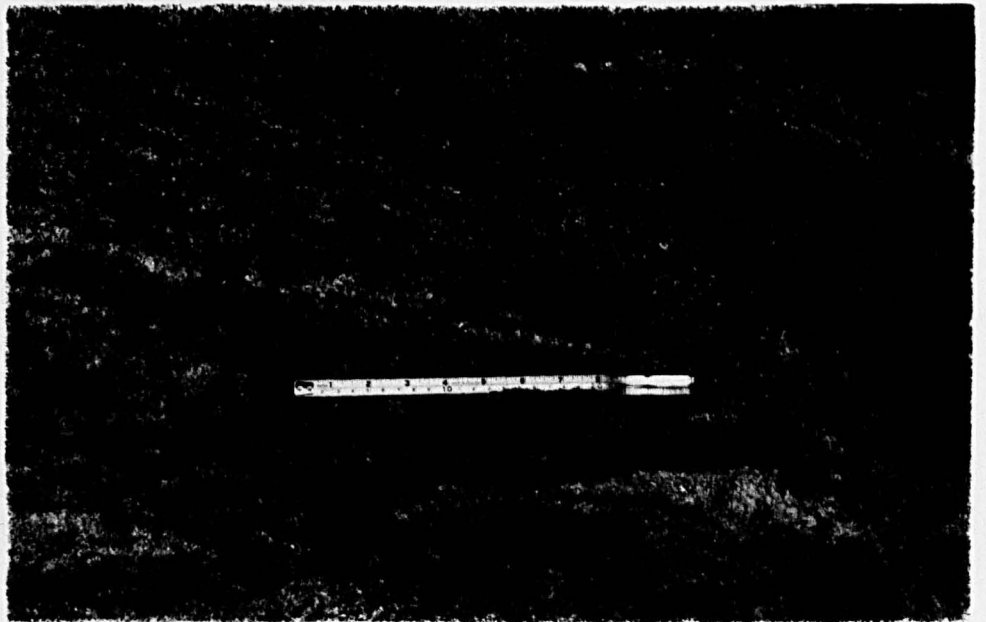


Plate II.21

- a: Inhomogeneous diatexite with prominent schlieren structure (4/25).
South-east of Dinard.
- b: Inhomogeneous diatexite with small biotite schlieren (5/8).
Pnte de Rochebonne, Paramé.
- c: Inhomogeneous diatexite with prominent schlieren structure (5/10).
Pnte de Rochebonne, Paramé.

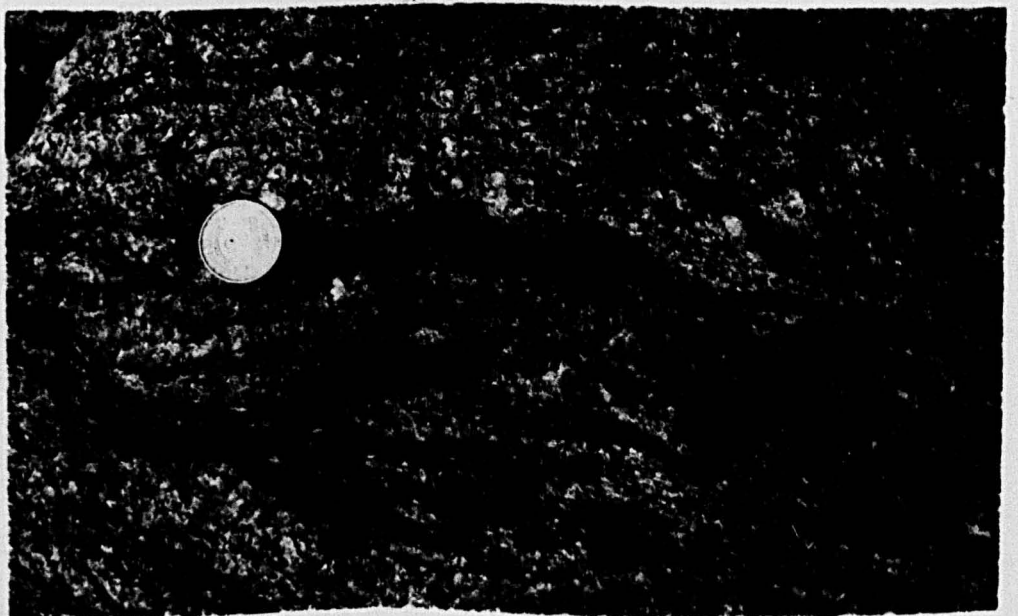
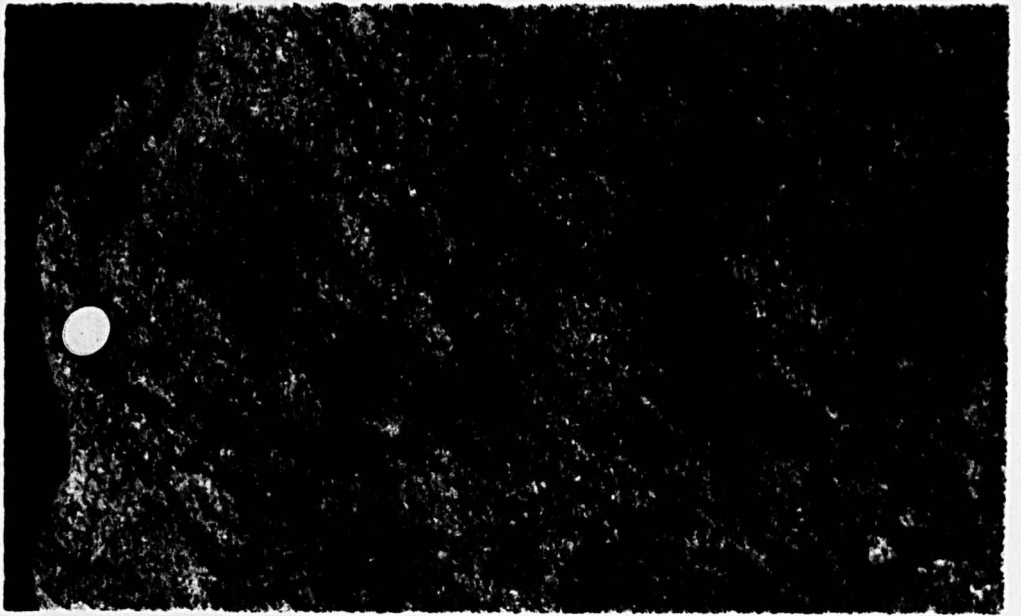


Plate II.22

a: Inhomogeneous diatexite with schlieren structure to the left of the coin and with a rodding lineation around the coin - within metatexite (4/25).

South-east of Dinard.

b: Inhomogeneous diatexite with well developed schlieren structure (5/13).

Pnte de la Varde, near Paramé.

c: Typical inhomogeneous diatexite with schlieren structure (5/19).

Havre de Rotheneuf.

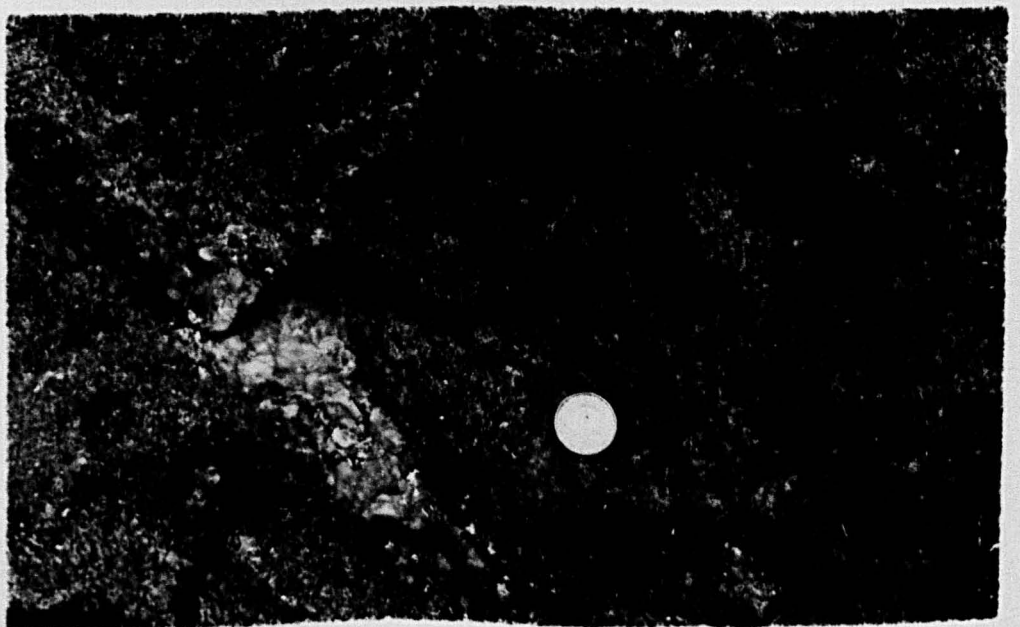


Plate II.23

- a: Inhomogeneous diatexite (12/8).
Eastern end of the Havre de Rotheneuf.

- b: Inhomogeneous diatexite (12/9).
Eastern end of the Havre de Rotheneuf.

- c: Inhomogeneous diatexite (12/11).
Eastern end of the Havre de Rotheneuf.

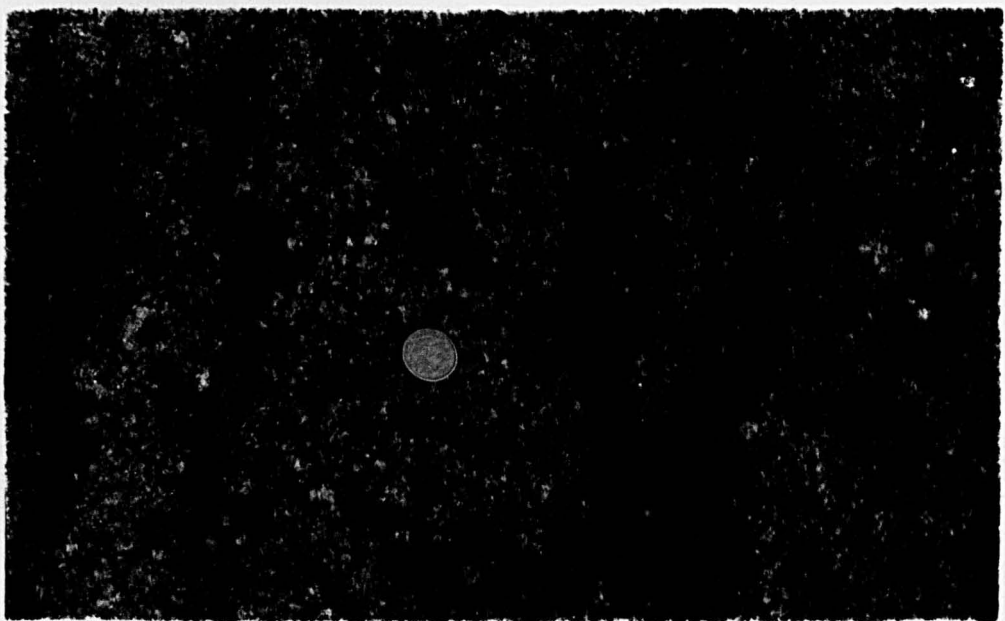


Plate II.24

- a: Inhomogeneous diatexite with small biotite schlieren
(309).
Western bank of l'Arguenon, le Guildo. x 0.5
- b: Inhomogeneous diatexite with small biotite schlieren
(704).
Northern end of Plage des Haas, St. Jacut. x 0.6
- c: Inhomogeneous diatexite with schlieren (SJ 16).
Plage de Rougeret, St. Jacut. x 0.5
- d: Inhomogeneous diatexite with schlieren structure (762).
Eastern side of pnte de la Garde Guérin, near St.
Lunaire. x 0.5
- e: Inhomogeneous diatexite with small biotite schlieren
(D 5).
St. Lunaire. x 0.5
- f: Slightly inhomogeneous diatexite with small biotite
clusters and schlieren (207).
Eastern bank of La Rance near the Barrage. x 0.5

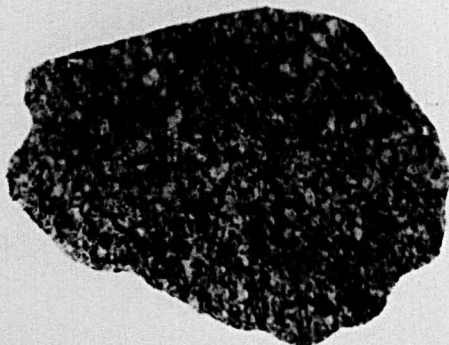
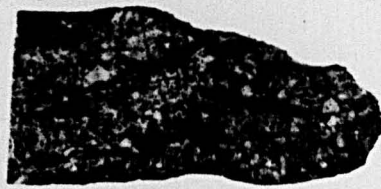
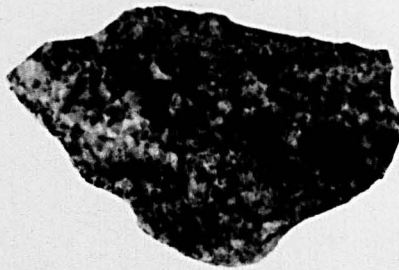
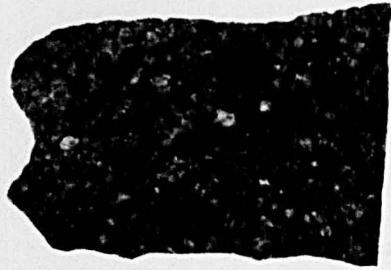


Plate II.25

- a: Slightly inhomogeneous diatexite with small schlieren
(208).
Quarry at Montagne St. Joseph, St. Malo. x 0.6
- b: Inhomogeneous diatexite with schlieren structure (726).
West of pnte de Grouin, north of Cancale. x 0.6
- c: Inhomogeneous diatexite with biotite schlieren (902).
North of Port St. Jean, la Rance. x 0.7
- d: Slightly inhomogeneous diatexite (914).
Western bank of la Rance near la Vicompté. x 0.6

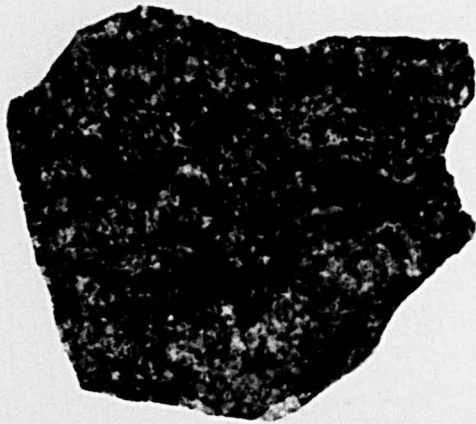


Plate II.26

- a: Homogeneous diatexite (1038).
South of Plage de la Fosse, near St. Cast. x 1.0
- b: Homogeneous diatexite (1037).
South of Port St. Jean, near St. Cast*. x 1.0
- c: Inhomogeneous diatexite with schlieren structure (1046).
Western side of Plage de la Mare, near St. Cast. x 1.0

* Do not confuse with Port St. Jean, la Rance.

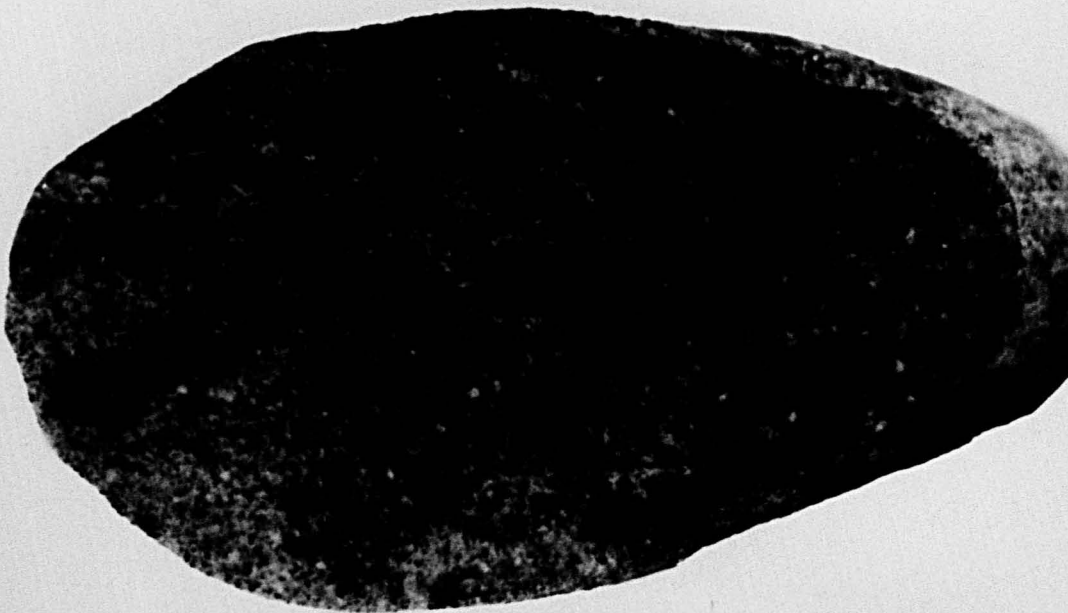
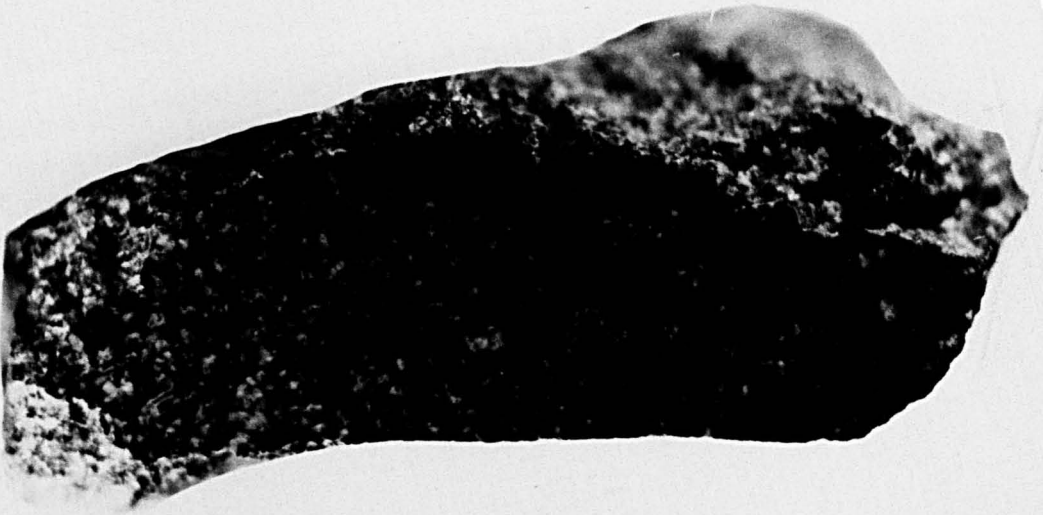


Plate II.27

a: Tourmaline-rich pegmatite cutting foliated homogeneous diatexite. Note the local feldspathisation under the scale (1/25).

Le Rocher Plat, St. Jacut.

b: Tourmaline-rich pegmatite cutting foliated homogeneous diatexite (8/28).

Le Rocher Plat, St. Jacut.

c: Coarse perthite patches and local feldspathisation within foliated homogeneous diatexite. Note the complete absence of biotite schlieren (11/17).

South from Plage de Ruet, St. Jacut.

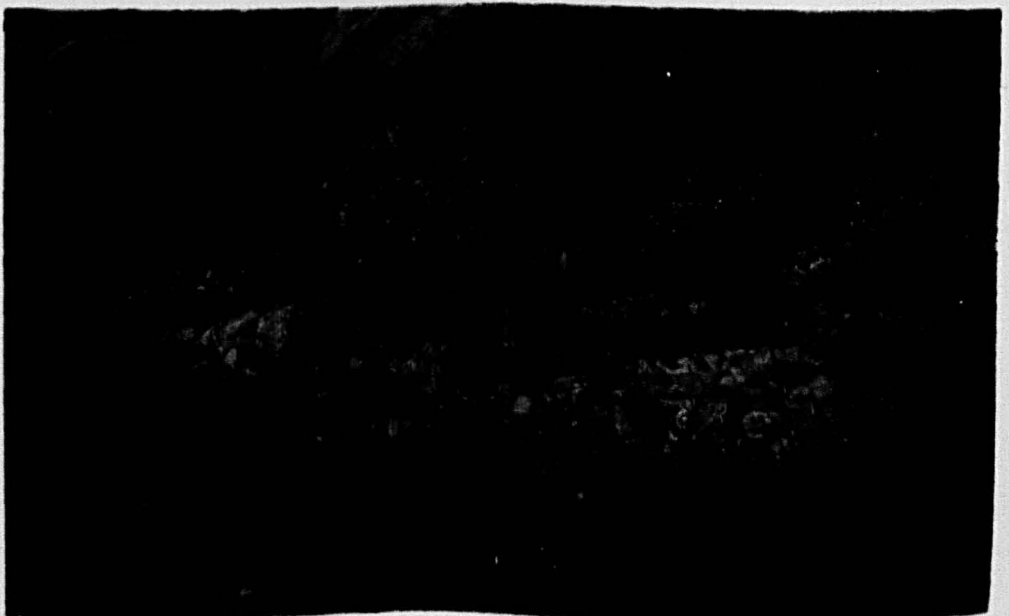
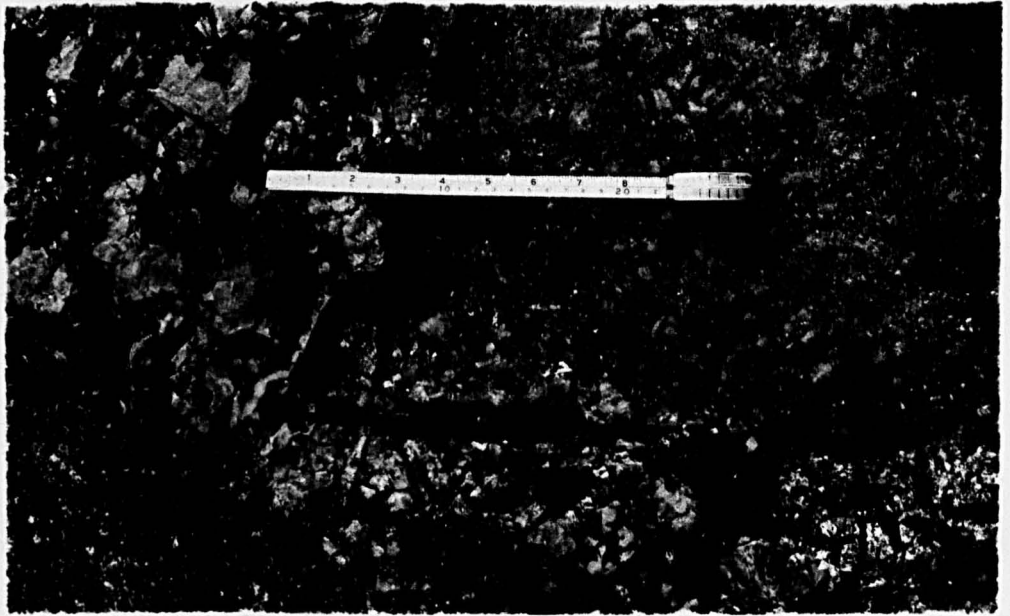


Plate II.28

- a: Homogeneous to slightly inhomogeneous diatexite (901).
North of Port St. Jean, Ia Rance. x 0.9
- b: Homogeneous diatexite (720).
West of pnte de Grouin, north of Cancale. x 0.8
- c: Foliated homogeneous diatexite (701).
Le Rocher Plat, St. Jacut. x 0.8
- d: Homogeneous diatexite (765).
South-eastern end of Plage de Quatre Vaux, near N.D.
du Guildo. x 0.8

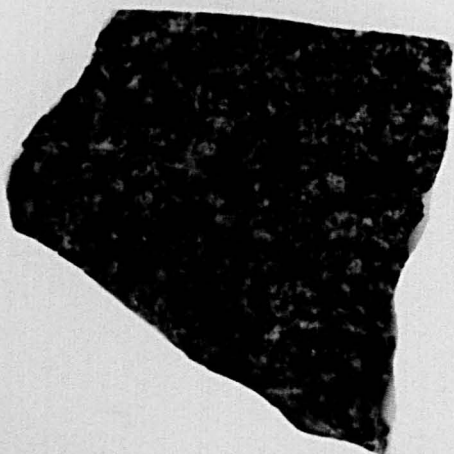
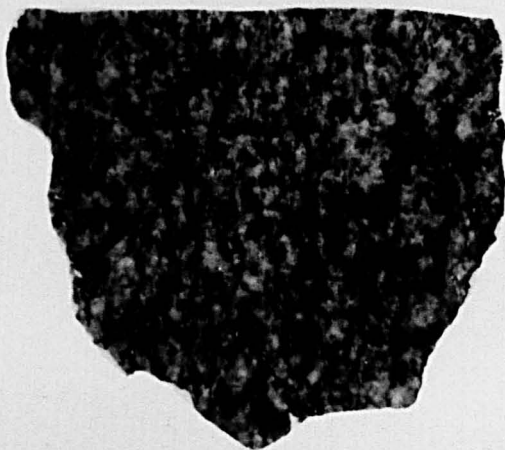
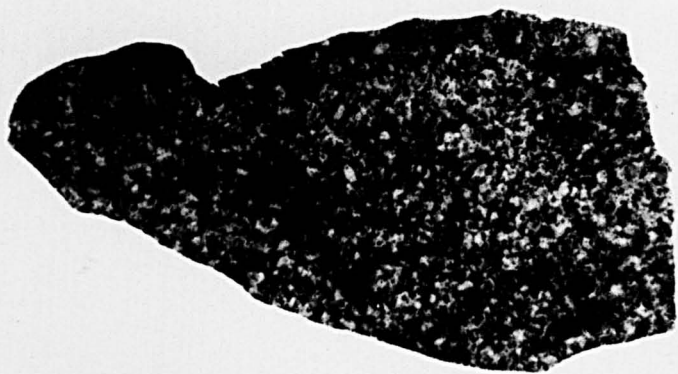


Plate II.29

- a: Foliated homogeneous diatexite (8/21).
Port Briac, north of Cancale.
- b: Raft of Pentevrian semi-pelite within foliated
homogeneous diatexite (18/11).
Port Briac, north of Cancale.
- c: Flattened xenolith within foliated homogeneous
diatexite (18/13).
Port Briac, north of Cancale.

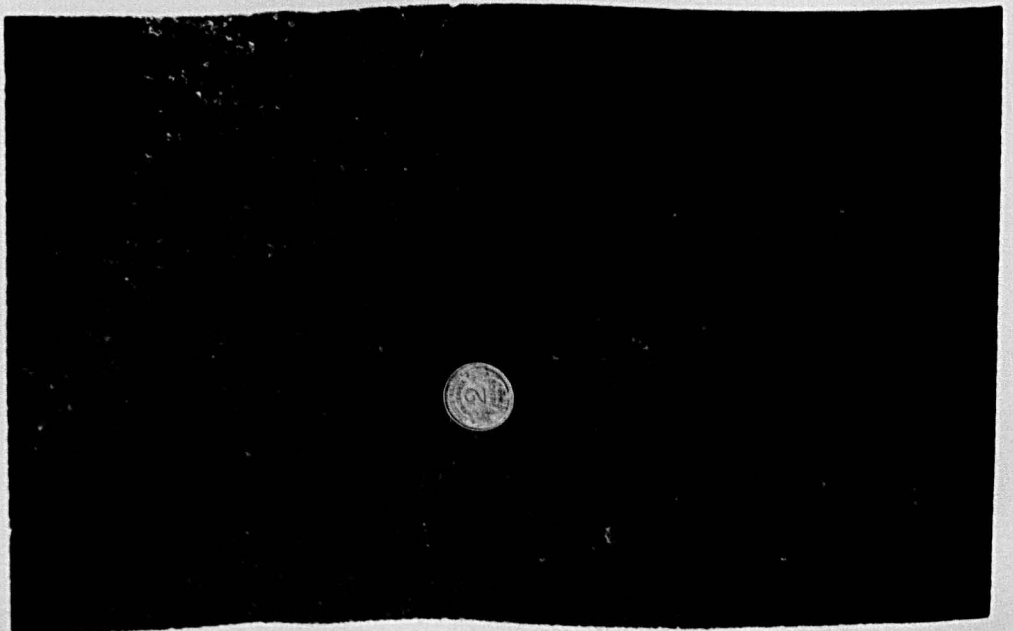
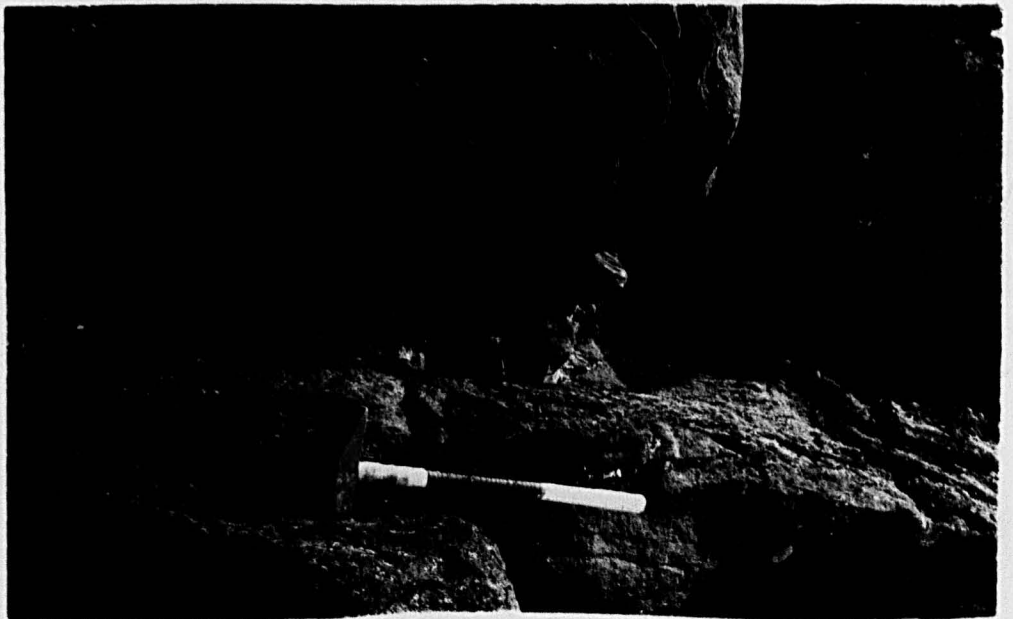
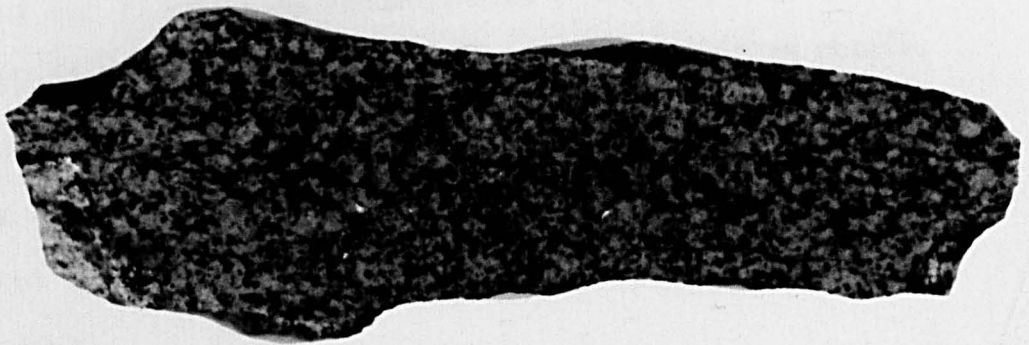
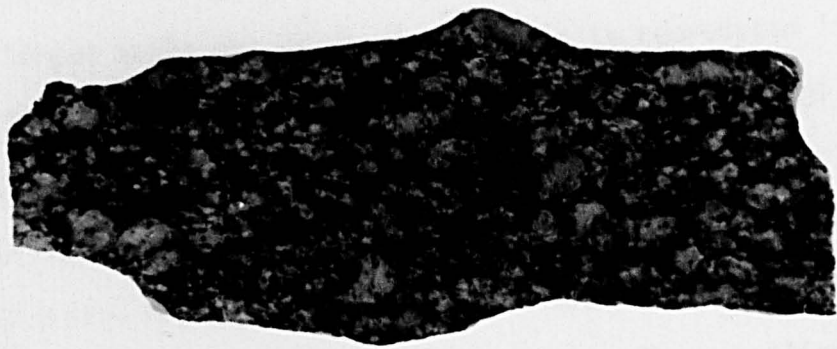


Plate II.30

- a: Well foliated homogeneous diatexite about 10 metres from its contact with the Pentevrian metasediments (C 1).
Port Briac, north of Cancale. x 1.0
- b: Slightly finer and more leucocratic homogeneous diatexite (711).
Pnte de Grouin, north of Cancale. x 1.0
- c: Semi-pelite from the raft of metasediments within the homogeneous diatexite. Note the fine segregation in the upper part of the specimen (CAN).
Port Briac, north of Cancale. x 0.9



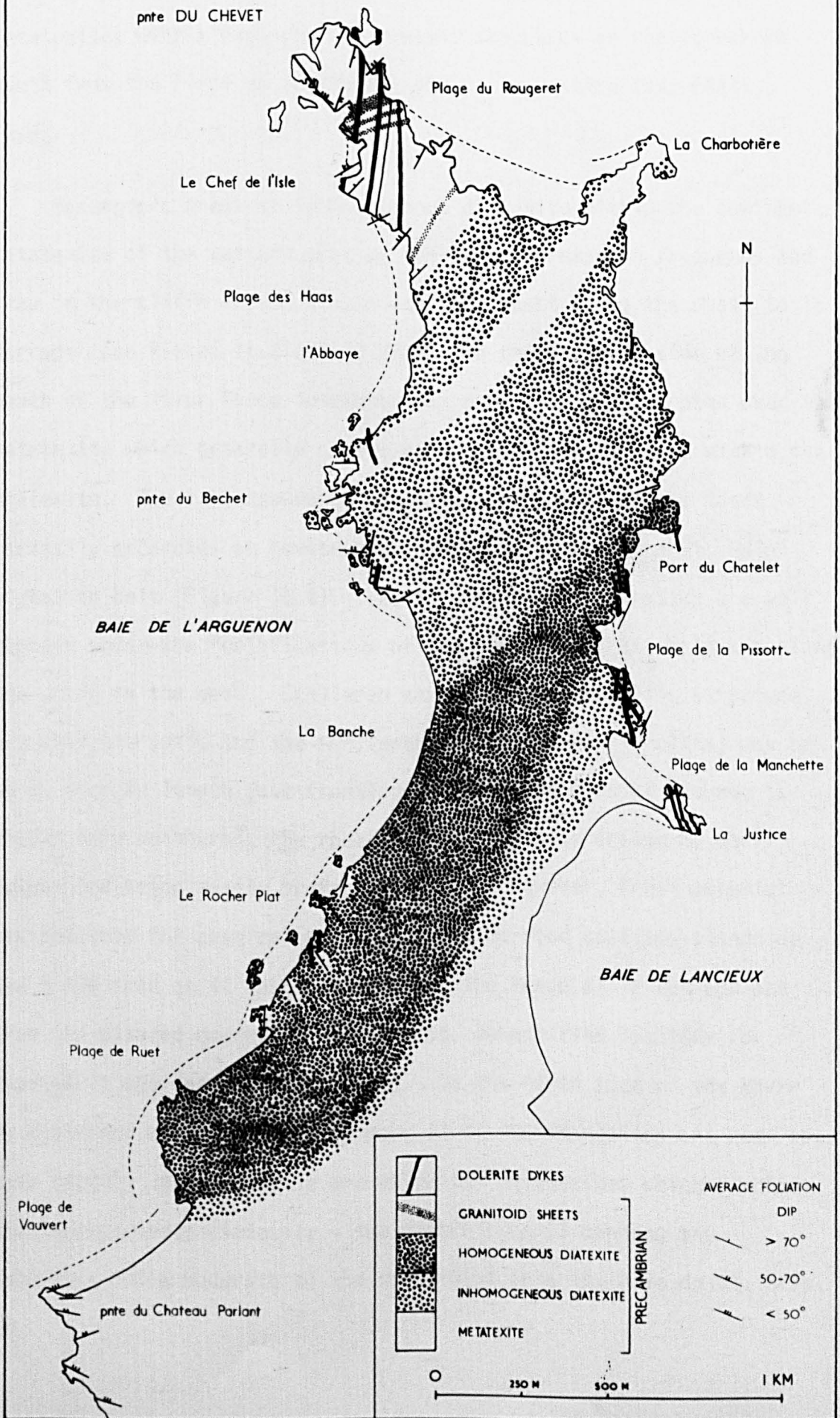
part of the belt that crossing the Presqu'Isle de St. Jacut-de-le-Mer is slightly the larger and demonstrates the relationship between metatexites, inhomogeneous and homogeneous diatexites admirably. A larger scale map of the Presqu'Isle is reproduced in Figure II.6. The inhomogeneous diatexites are well exposed in the shallow cliffs of the pnte du B chet and along the coast north of the camping site at la Justice. The inhomogeneous diatexites are medium-grained granodioritic rocks which contain schlieren of biotite of variable size up to about 5 cms in long dimension. These schlieren define a foliation within the rocks, often a swirling foliation (see Plates II.17 and II.18). The inhomogeneous diatexites weather to an orange-buff colour, entirely fresh material is difficult to obtain, and often break easily under the hammer as a result of this weathering. Enclaves of psammitic metasediment are contained within the foliated inhomogeneous diatexite as boudin-like structures (Plate II.17c).

The relationship between the inhomogeneous diatexites, with the psammitic enclaves representing the included relict palaeosome, and the metatexites, with their migmatitic banding between neosome and palaeosome, is best examined either along the foreshore to the north of the Plage des Haas or along the foreshore immediately north of the Plage de la Manchette on the Presqu'Isle de St. Jacut-de-le-Mer (Figure II.6). On the north side of the Plage des Haas, just north of l'Abbaye, inhomogeneous diatexite is seen to give way over a zone of transition some 100 m in outcrop width to metatexite. Within this transition zone the two rock types are interbanded but with local discordance as the more mobile diatexite cross cuts the metatexitic banding. To the south of the Plage des Haas, a zone of metatexites exhibiting high-grade stromatic structure lies within

Figure II.6

Large-scale map to show the diatexites of the Presqu'Isle de St. Jacut-de-la-Mer on the north-western side of the St. Malo migmatite belt (see Figure II.3).

THE PRESQU'ISLE DE ST. JACUT-DE-LA-MER



	DOLERITE DYKES] PRECAMBRIAN	AVERAGE FOLIATION DIP
	GRANITOID SHEETS		
	HOMOGENEOUS DIATEXITE		
	INHOMOGENEOUS DIATEXITE		
	METATEXITE		
			 > 70°
			 50-70°
			 < 50°

0 250 M 500 M 1 KM

the inhomogeneous diatexite (Figure II.6). On the south-eastern side of the Presqu'Isle the inhomogeneous diatexites quickly give way to metatexites with a high-grade stromatic structure on the foreshore south from the Plage de la Pissott and on la Justice (see Plate II.6).

Mesoscopic areas of inhomogeneous diatexite within the dominant metatexite of the western part of the belt increase in frequency and size in the cliffs around Dinard and south-east along the coast to la Barrage (see Plates II.21a & II.22a). On the opposite side of the mouth of the River Rance inhomogeneous diatexite predominates over the metatexite which generally occurs as large raft-like areas within the diatexite. The inhomogeneous diatexite to the east of the Rance partially encircles an homogeneous diatexite core to the St. Malo migmatite belt (Figure II.4). The inhomogeneous diatexites are well exposed under the fortifications of the old cité of St. Malo and along the coast to the east. Schlieren structure and nebulitic structure are characteristic and the schlieren of biotite (\pm fibrolite) may be up to 6 cm in length (see frontispiece 2). The coastal outcrop is always very weathered, the rocks having a typical orange to buff colour and being easily broken by hammer. However, fresh material was obtained for chemical analysis from the road cuttings alongside the N 138 road as it descends to cross the Rance at la Barrage and from the disused quarry at Montagne St. Joseph (the locality for Graindor's age date samples, 1962). On the north side of the Havre de Rotheneuf at Ile Besnard (Figure II.4) the diatexites are seen to pass rapidly into stromatic and phlebitic metatexites which overlie the inhomogeneous diatexite - the general dip of banding and foliation being moderate to the north-west into the Baie de St. Malo.

Homogeneous diatexites form the cores to each of the three areas of inhomogeneous diatexite. The homogeneous diatexite of the Presqu' Isle de St. Jacut-de-la-Mer is shown in Figure II.6. The rock is a medium-grained foliated granodiorite which weathers to a buff-yellow colour; enclaves are absent (Plates II.27 & II.28). There are rare tourmaline-pegmatite or perthitic orthoclase feldspar patches within the homogeneous diatexite and also thin (under 10 cm thick) pegmatite sheets infilling joints within the diatexite (see Plates II.27 & II.28). The change from inhomogeneous to homogeneous diatexite is best seen on the eastern side of the Presqu' Isle to the north and south of the small Port du Châtelet. On both sides the transition from inhomogeneous diatexite with schlieren to homogeneous diatexite devoid of schlieren is rapid - the schlieren become both smaller and less dense over a zone of a few metres before dying out. The width of the surrounding inhomogeneous diatexite outcrop on the southern side of the homogeneous diatexite is much narrower than that on the northern side and reflects the regional asymmetry seen in the outcrop of the main diatexite mass to the east.

The main area of homogeneous diatexite is well exposed in the cliffs forming the pnte de Grouin north of Cancale. It stretches some 12 km inland to the south-west and reaches a maximum width of 4 km, at the present erosion level, just south-east of Parame-St. Malo (Figure II.4). The rock is a buff coloured, medium-to-coarse grained granodiorite with a pronounced foliation defined by biotite and feldspar. It is very strongly foliated and lineated near its junction with Pentevrian metasediments at Port Briac (see Plate II.30). It is thought to be intrusive into the Pentevrian metasediments (see discussion above and Plate II.4). Within the diatexite just north of the plage at Port Briac are several small xenoliths of metasediment

flattened in the plane of the foliation (see Plate II.29c). There are also two much larger rafts of semi-pelitic metasediment preserved within the diatexite as large boudin-like structures (Plate II.29b). The foliation within the metasediments in the rafts, within the homogeneous diatexite and within the Pentevrian metasediments forming the host is parallel and dips steeply to the south-east. There is a marked lineation in all three which plunges at a low to moderate angle to the north-east.

The north-western part of the St. Cast gneiss belt, exposed along the length of the south-east flank of the Baie de la Fresnaye (see Figure II.2), comprises mainly inhomogeneous diatexites with small schlieren and minor homogeneous areas. Plate II.26 shows the nature of these rocks in hand specimen. It is these rocks and their cataclased equivalents to the south-east of the pnte de St. Cast that Hameurt and Jeannette (1971) have confused with arkoses. The present interpretation, based upon reconnaissance field mapping in 1971, is given in Figure II.2 and has been briefly described by Brown and Roach (1972a). The diatexites are orange-buff coloured medium-grained granodioritic rocks with small schlieren of biotite which give way to garnet around the pnte de St. Cast. They are cut by narrow shear zones of the type described by Ramsay and Graham (1971) and give way to thoroughly cataclastic rocks, developed from leucogranite and metatexite, on the south-east side of the pnte de St. Cast and north from the Port Jacquet (Figure II.2).

4. The Colombière Granite

North of the Presqu'Isle de St. Jacut-de-la-Mer lie a series of islands and small isolated rock outcrops which are normally either covered by the sea or cut-off from the Presqu'Isle by the sea.

However, for a short time either side of very low low-tides these outcrops are accessible for examination. The largest of the islands, Ile des Hébihens, is some 1.5 km from south to north and about the same from east to west - though only about 1 km² of rock outcrops through the sand. The islands of La Grande Roche, la Colombière and la Nellière are accessible only during the lowest of low-tides. The discontinuous nature of the outcrop, the fact that it spends most of the time below water and the short time available for its study all conspire to obscure the relationship between these island outcrops and the mainland outcrop (see Figure II.3).

Figure II.7 summarizes the geology of these islands. There is clearly a change in rock type from east to west across the discontinuous outcrop though no actual junction is seen. On the east of the Ile des Hébihens the rocks are slightly inhomogeneous medium-grained granodioritic rocks which are very similar to the diatexites of St. Jacut. They are not foliated. On the north-eastern corner of the Island a band of metatexite of variable thickness up to ca 10 m is contained within this diatexite (see Plate II.31). On the north and western sides of the Island the diatexite contains an increasingly greater number of small xenoliths the further north-west that it is seen (see Plate II.32). These xenoliths, which are fragments of rock and do not therefore equate with the biotite schlieren of the inhomogeneous diatexites, vary in size from under a centimetre to some tens of centimetres in length and may be of semi-pelite or metatexite. At la Nellière the rock type has changed gradually and without any definite junction to a granite rather than a granodiorite in composition and contains less biotite. The granite is a pink-buff in colour and the medium-grained rock is unfoliated. Contained within this granite are two rafts of banded psammite/semi-pelite

Figure II.7

Sketch geological map of the islands to the north of the
Presqu'Isle de St. Jacut-de-la-Mer.

1000 metres

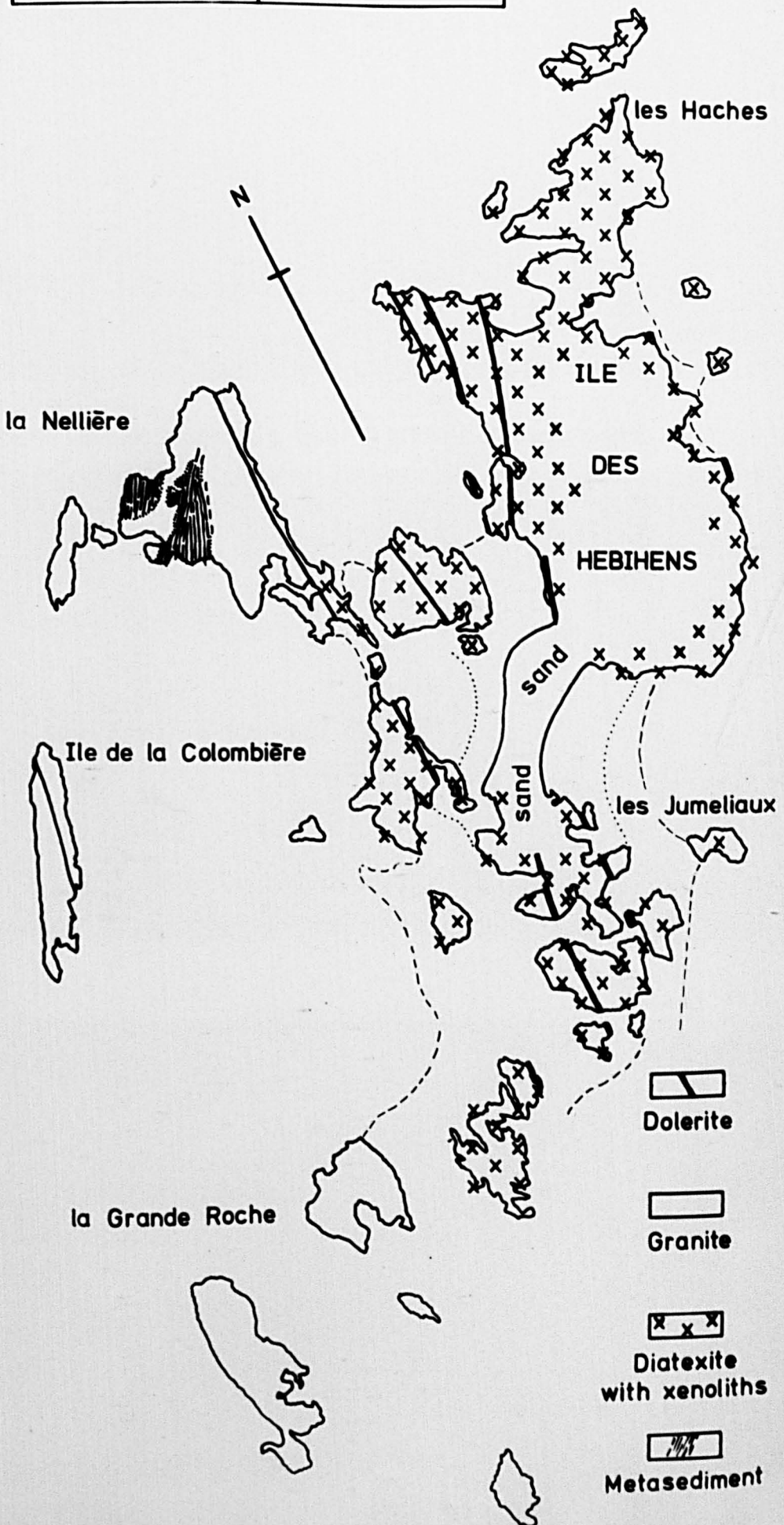


Plate II.31

- a: Inhomogeneous diatexite with biotite-rich schlieren (10/3).
North of Ile des Hébihens.
- b: Slightly inhomogeneous diatexite with small enclave of metatexite (10/5).
Western side of Ile des Hébihens.
- c: Fine stromatic structure within metatexite layer in diatexite. Note the leucosomes with thin biotite selvages (melanosomes) and the schistose palaeosome (10/9).
North-eastern corner of Ile des Hébihens.

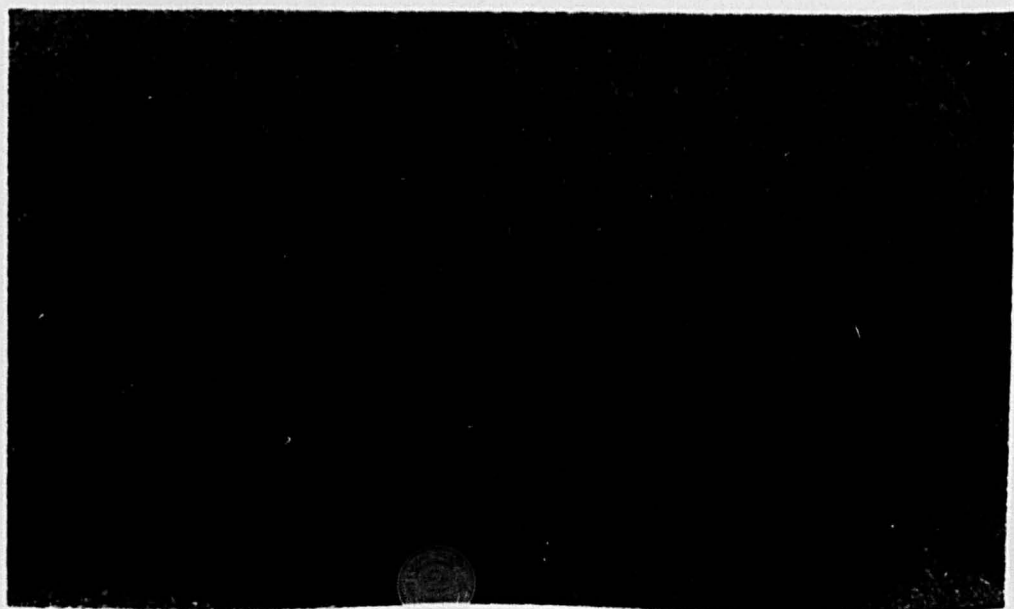
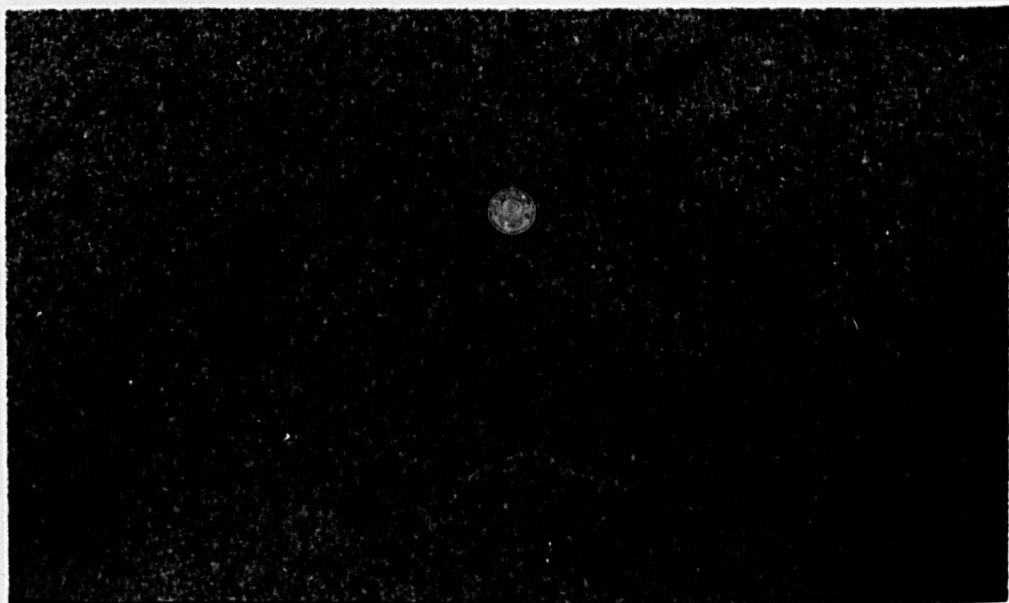


Plate II.32

a: Metasedimentary xenoliths in homogeneous diatexite
(10/2).

Western side of Ile des Hébihens.

b: Metasedimentary xenoliths in homogeneous diatexite
(10/4).

Western side of Ile des Hébihens.

c: Metasedimentary xenoliths weathering out from
homogeneous diatexite (10/11).

North-western corner of Ile des Hébihens.

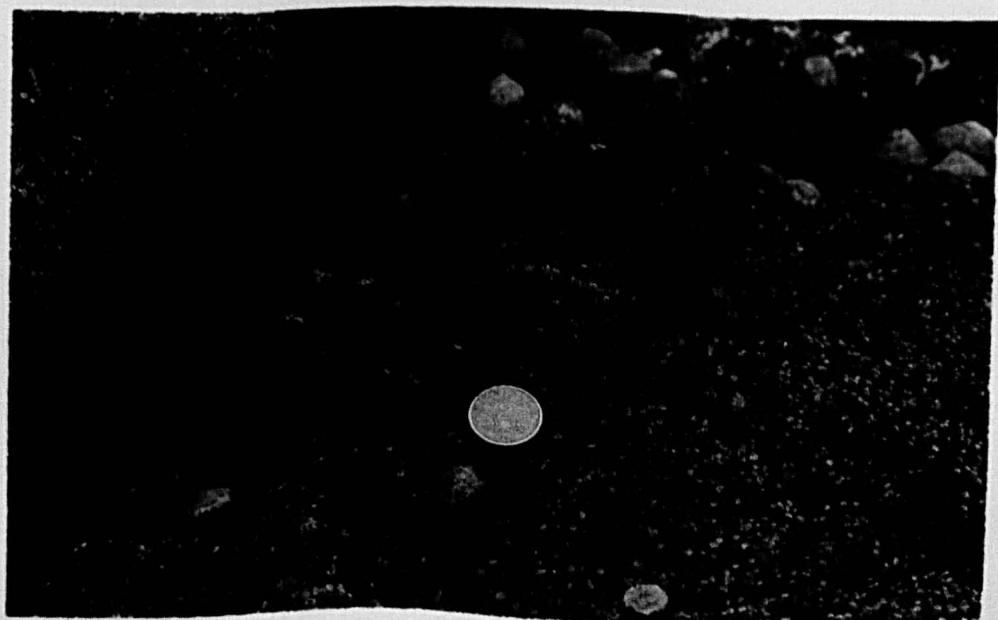
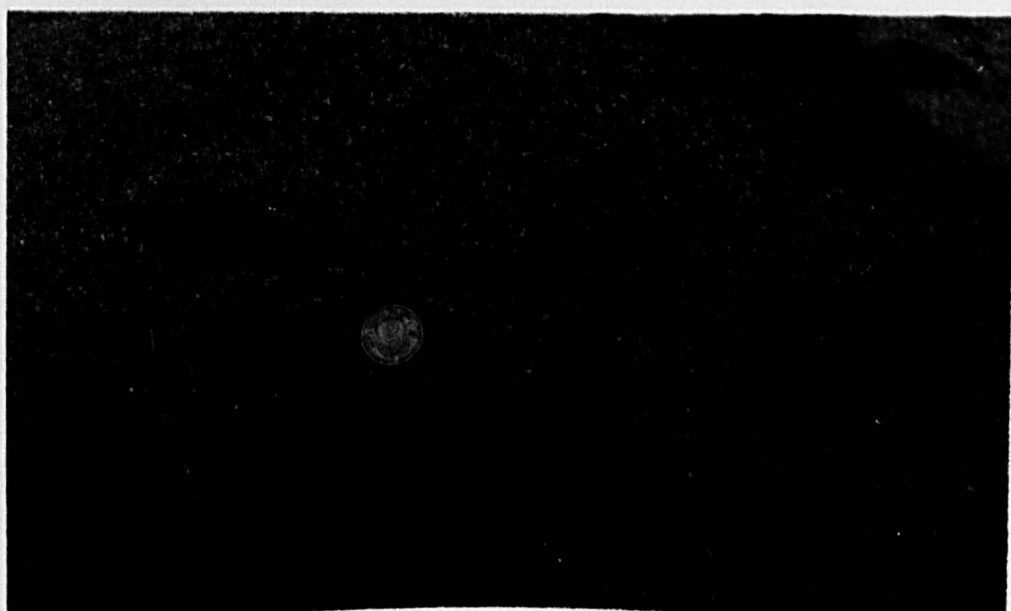


Plate II.33

a: Xenoliths in homogeneous granitoid at the edge of the raft of metasediments (18).

La Nellière, north of St. Jacut.

b: Xenoliths in homogeneous granitoid at the edge of the raft of metasediments (17).

La Nellière, north of St. Jacut.



Plate II.34

a: The banded psammites and semi-pelites comprising the raft of metasediments (3/32).

La Nellière, north of St. Jacut.

b: The western part of the raft of metasediments in the homogeneous granitoid (3/37).

La Nellière, north of St. Jacut.



metasediment; the more easterly of the two is invaded and broken up by the granite giving rise to a narrow zone of large xenoliths (see Plates II.33 & II.34). Finally, the two islands of la Colombière and la Grande Roche are comprised of a pink to white biotite granite, medium-grained and unfoliated, which contains only very rare biotite enclaves.

5. The Granitoid Sheets

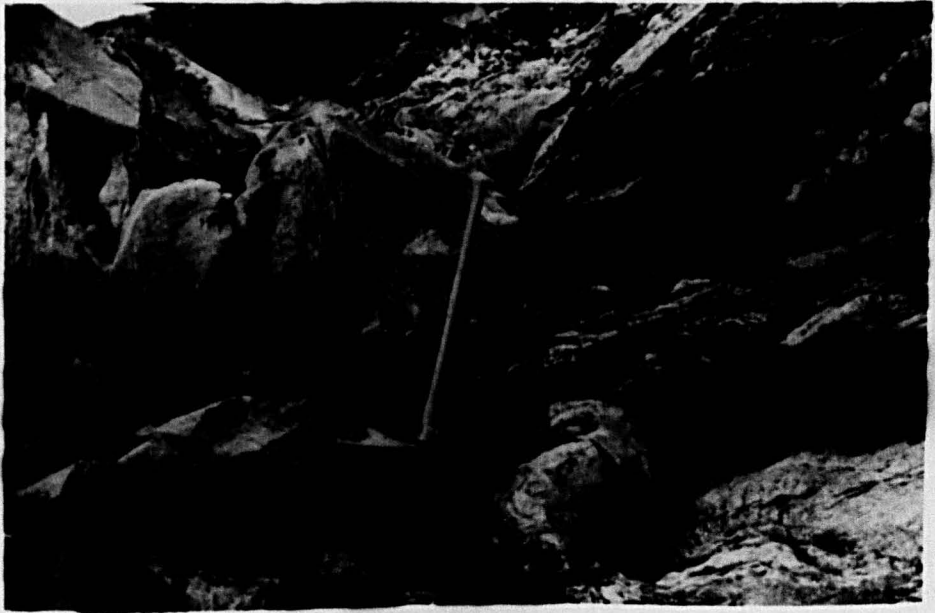
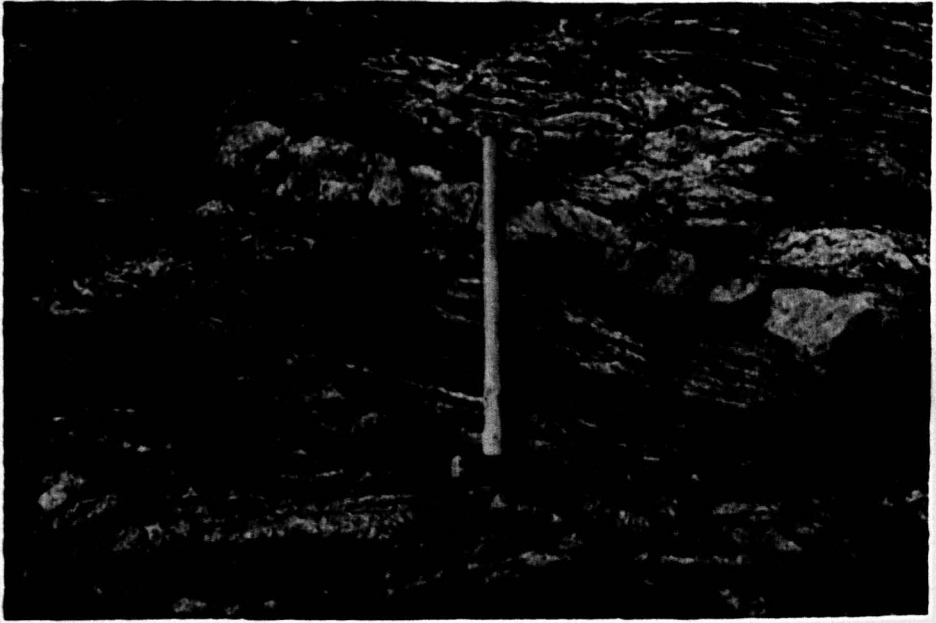
There are three types of granitoid sheet which occur within the St. Malo migmatite belt, each of quite restricted occurrence. The first type are the true granite sheets which cut the metatexites of the northern part of the Presqu'Isle de St. Jacut-de-la-Mer (see Figure II.6) and the metatexites to the west of Lancieux. They are generally concordant with the migmatite banding and may rarely contain xenoliths of metatexite close to their margins. The granite sheets, which may be up to 10 m thick, are a pink-buff colour and medium-grained - they resemble the granite of la Nellière. Secondly, there are thin, under 3 m thick, granite-pegmatite sheets. They are found within the metatexites of St. Jacut and to the west of Lancieux. Whilst the granite-pegmatite sheets are generally concordant with respect to the migmatite banding they can locally cut across the banding. These granitic rocks are coarse-grained and leucocratic, they may be white or buff in colour (see Plates II.7b & II.35a). The third type of granitoid sheet are restricted to the metatexites outcropping along the Rance, especially around the village of le Minihic sur Rance (see Figure II.5 and Plate II.35). These sheets are mainly trondhjemitic in composition, cream in colour, medium-grained and leucocratic. They are broadly concordant with the migmatite banding but may locally cross cut that banding and contain xenoliths of metatexite, especially near the margins.

Plate II.35

- a: Granite-pegmatite sheet within metatexite (42).
North from le Tertre Corieu, south of Lancieux.

- b: Strongly discordant trondhjemite sheet cutting
metatexite (36).
North from pnte du Crapaud, la Rance.

- c: Trondhjemite veining psammitic metasediment (38).
West of pnte du Crapaud, la Rance.



B. The Cataclastic Rocks

Six shear belts and minor shear zones cut the Pentevrian basement within the area studied and contain a variety of cataclastic rocks all with a well developed and thoroughly transposive fluxion structure. Cataclastic rocks have been reviewed in detail by Higgins (1971) and his proposals on nomenclature are followed in this work. Brown, Barber and Roach (1971) recognized that the St. Malo migmatite belt had suffered cataclasis on its north-western margin in a shear belt of Cadomian age and then been faulted against the now adjacent Brioverian supracrustal rocks. They observed that the metatexites and inhomogeneous diatexites exposed on the south-eastern side of the Plage de Quatre Vaux (see Figure II.3) were cut by narrow shear zones ca 30 cm wide, in which the high-grade gneisses (diatexites and metatexites) were broken down to schists, similar to those described by Ramsay and Graham (1970). These small shear zones gave way to a larger shear belt some tens of metres wide and comprising schistose rocks. Plate II.36a shows one of the narrow shear zones transposing the diatexite foliation and producing a protomylonite. Protomylonite, mylonite and ultramylonite are all developed within the larger shear belt (Plates II.36b & II.36c). Plate II.37 shows examples of the protomylonite and mylonite from the south-east side of the beach at Plage de Quatre Vaux and compares them with the sillimanite schists of the metatexites exposed there. The cataclasis clearly destroys the diatexite foliation and any banding that may have been present but the schistose rocks produced may be distinguished from the Pentevrian palaeosome and the Brioverian cover exposed on the north-west side of the beach. The buff-to-grey protomylonites and grey-to-black mylonites have prominent feldspar porphyroclasts and a well developed fluxion structure. A late crenulation foliation developed in the

Plate II.36

- a: Transition, from right to left across the plate, from the well foliated inhomogeneous diatexite with its schlieren structure into the protomylonite with its fluxion structure (17/32).
South-eastern end of the Plage de Quatre Vaux.
- b: Protomylonite from within the main shear belt. Note the feldspar clasts, the quartz-feldspar augen and the flattened biotite schlieren (7/14).
Just south from Plage de Quatre Vaux.
- c: Mylonite with crenulated fluxion structure from within the main shear belt. Note the streaked out quartz-feldspar layers and only rare feldspar clasts visible to the naked eye (7/15).
Just south from Plage de Quatre Vaux.

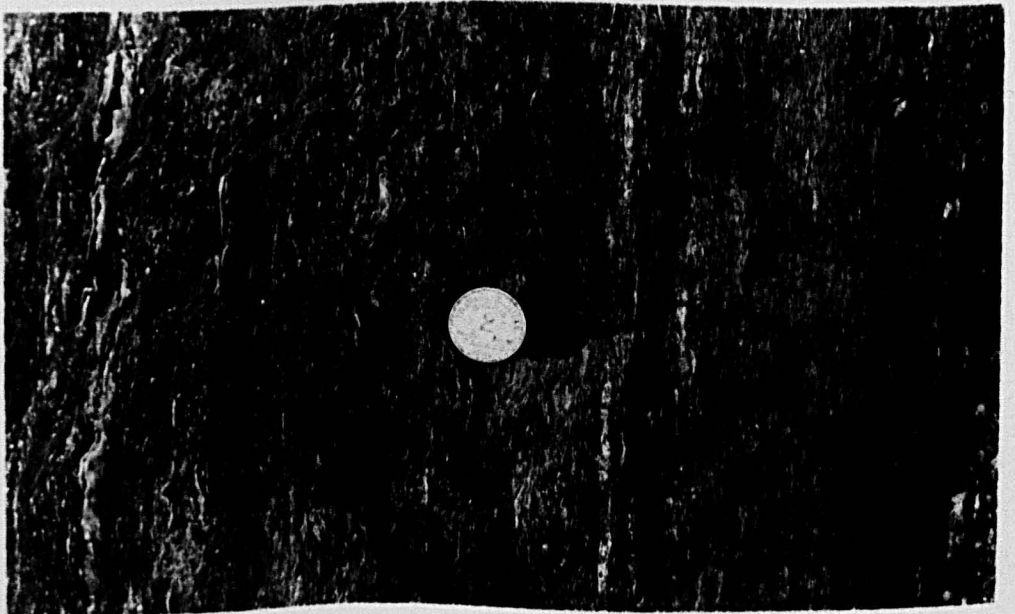
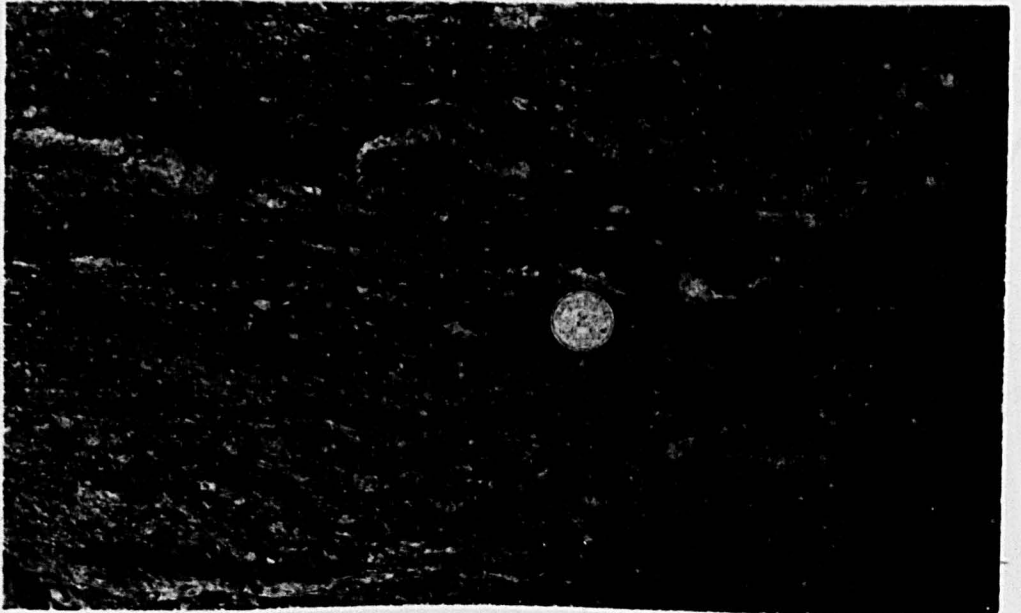
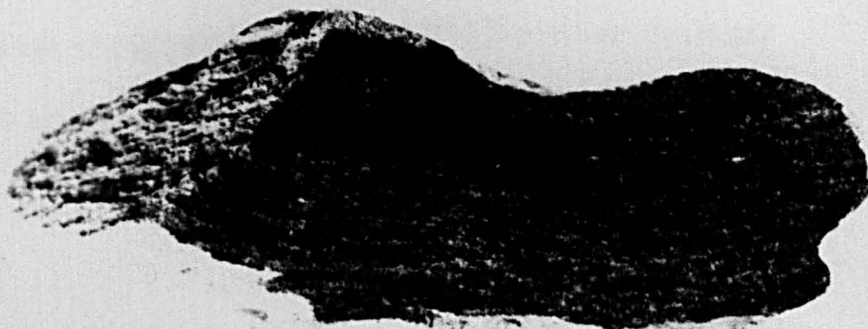
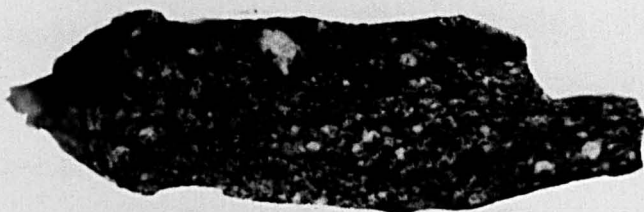


Plate II.37

- a: Protomylonite (1067).
Plage de Quatre Vaux, near N. D. du Guildo. x 0.7
- b: Mylonite (1068).
Plage de Quatre Vaux, near N. D. du Guildo. x 1.4
- c: Protomylonite - slightly cataclased diatexite (925).
Plage de Quatre Vaux, near N. D. du Guildo. x 1.4
- d: Sillimanite schist palaeosome (1070).
Plage de Quatre Vaux, near N. D. du Guildo. x 0.8
- e: Protomylonite (926).
Plage de Quatre Vaux, near N. D. du Guildo. x 0.9
- f: Sillimanite schist palaeosome (1069).
Plage de Quatre Vaux, near N. D. du Guildo. x 0.8



sillimanite schists, mylonites and ultramylonites was equated by Brown et al (1971) with that developed in the Brioverian cover. Thus a higher metamorphic grade and a longer structural history together with the late transpressive structures suggested that the St. Malo migmatite belt represented Pentevrian basement. This view is still held.

One kilometre to the west of the pnte de Grouin (north of Cancale) the inhomogeneous diatexites become sheared over an outcrop width of about 500 m. Within this zone mylonite gneisses with a marked fluxion structure are developed (Plate II.38a). This new foliation is deformed by mesoscopic open folds and large kink bands. Preserved in the fluxion structure are rare intrafolial folds - relicts of an earlier deformation (Plate II.38b). Occasional boudins of garnet gneiss are contained within the mylonite gneiss but are only of restricted extent (see Plate II.39).

The northern junction of the Dinan gneiss belt with the Pentevrian metasediments is not exposed but lies hidden under Rance alluvium (Figure II.5). It may well be tectonic since the first rocks which outcrop to the south of the metasediments are grey mylonite schists with quartzo-feldspathic ribs and stringers which seem to have been produced by the cataclasis of metatexites, (Plate II.38c). There is a strong lineation developed in the mylonite schists and the foliation is deformed by mesoscopic open folds. Only a kilometre to the south around Port St. Hubert and Port St. Jean mylonite schists with a prominent fluxion structure and characteristic cream feldspar porphyroclasts are developed within and from the blastic schists (see Plate II.40).

Plate II.38

a: Mylonite gneiss produced by the partial cataclasis of inhomogeneous diatexite. Note the strong foliation and the streaked out schlieren of biotite (12/14).

To the west of pnte de Grouin, north of Cancale.

b: Mylonite gneiss derived from inhomogeneous diatexite and with a preserved intrafolial fold of palaeosome (12/16).

To the west of pnte de Grouin, north of Cancale.

c: Mylonite schist with strong rodding lineation produced by cataclasis of metatexite (16/11).

Le Bas Bout, north of Port St. Jean, la Rance.



Plate II.39

- a: Garnet gneiss (1030).
West of pnte de Grouin, near Cancale. x 0.8
- b: Garnet gneiss (1029).
West of pnte de Grouin, near Cancale. x 0.8
- c: Garnet gneiss (1027).
West of pnte de Grouin, near Cancale. x 0.7

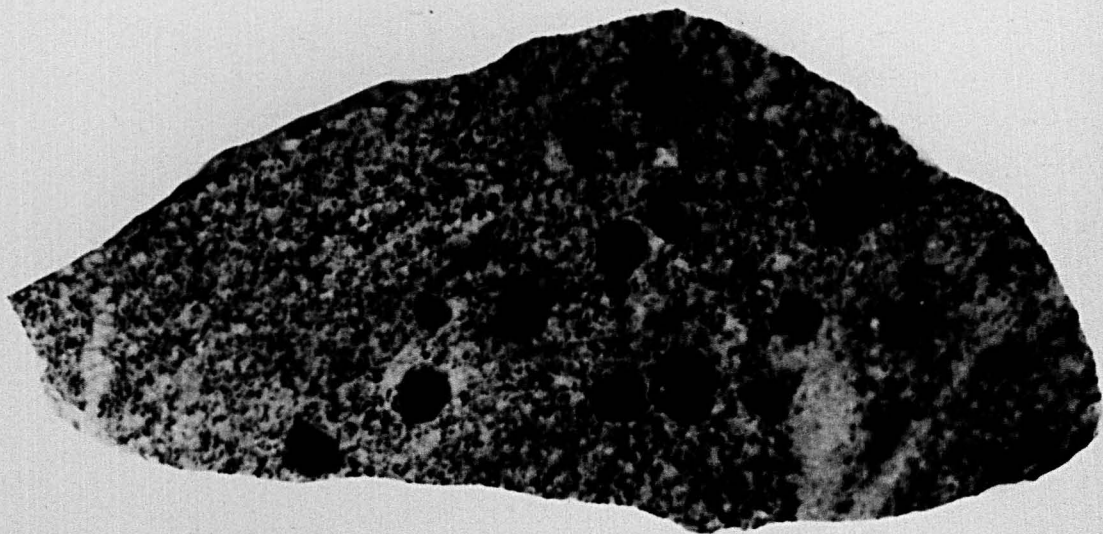
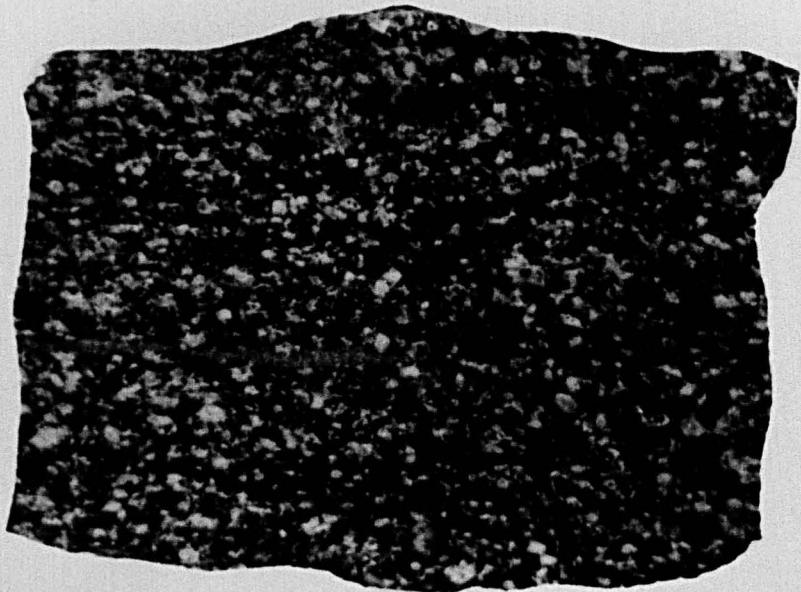
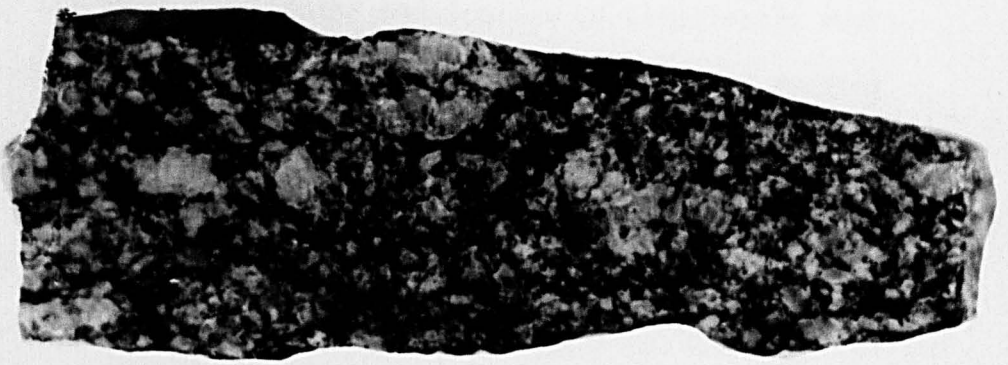


Plate II.40

- a: Blastic gneiss (903).
Port St. Jean, 1a Rance. x 1.2
- b: Blastic gneiss (904).
Port St. Jean, 1a Rance. x 1.2
- c: Protomylonite (905).
West of Port St. Hubert, 1a Rance. x 1.1



By far the most spectacular development of cataclastic rocks, however, are those produced by the two major shear belts cutting through the St. Cast belt of gneisses (Figure II.2). Both of the shear belts are ca 500 m in outcrop width. The first is exposed on the headland of pnte de St. Cast, along the roadside down to the Port Jacquet and along the wave cut platform between the headland and the Port. It is this belt of rock which has been the subject of a debate in Nature between Brown and Roach (1972a & 1972b) and French geologists (Auvray et al, 1972). The second shear belt is exposed along the north-western side and central part of the pnte de la Garde. Both shear belts are comprised of mylonite schist and mylonite gneiss with well developed fluxion structure and occasional contemporaneous intrafolial folding of the fluxion banding. There is a prominent mineral lineation. The foliation and lineation are deformed by later open folds. The pnte de St. Cast shear belt contains mainly medium-to-dark grey mylonite schists derived from metatexites and metasediments similar to those exposed below the Port and white and light grey mylonite schists derived from synkinematic leucogranite and granite sheets which have been intruded up the shear belt and themselves suffered cataclasis (Plate II.41). The mylonite schists of the pnte de la Garde shear belt are of variable colour - buff, grey, grey-green or creamy-buff - according to the original lithology. Dark grey-green mylonite schists with red garnets and creamy-orange feldspar porphyroclasts are prominent on the south-eastern side of the central part of the headland (Plate II.42), whilst buff coloured mylonite schists, again with cream feldspar porphyroclasts±garnets, are prominent on the north-western side of the headland. Thin bands of grey mylonite schist are common throughout the shear belt and may represent cataclased palaeosome or metasediment. Mylonite gneisses in which the original metatextitic banding is still partly preserved are found on the south-east side of

Plate II.41

a: Mylonite schist produced by cataclasis of leucogranite
(1086).

Pnte de St. Cast.

x 0.9

b: Mylonite schist produced by cataclasis of granite
(1087).

Pnte de St. Cast.

x 0.9

c: Mylonite gneiss with retrogressed areas after
porphyroblasts of garnet (1082).

Pnte de la Garde, south of St. Cast.

x 0.9

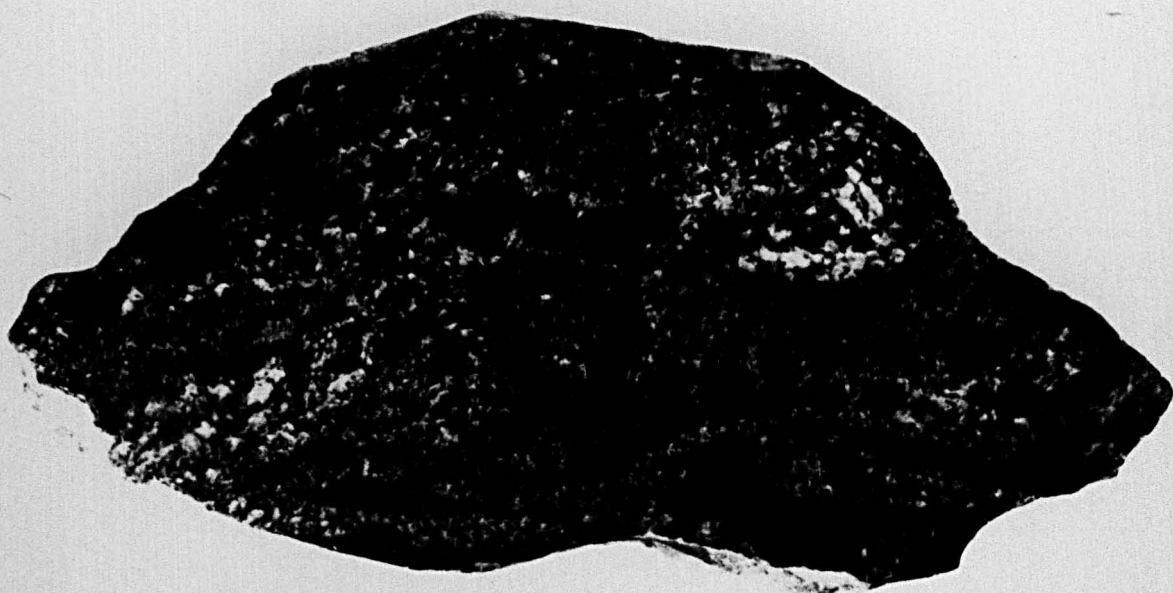


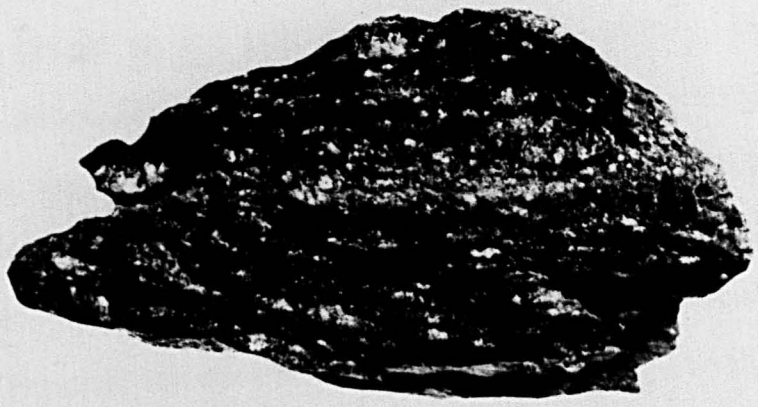
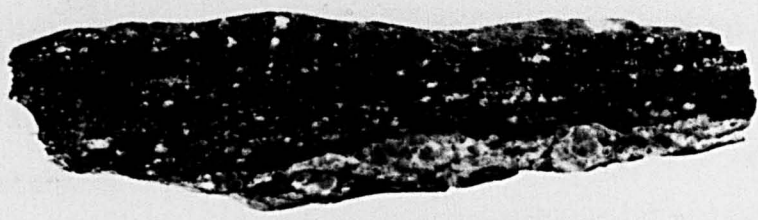
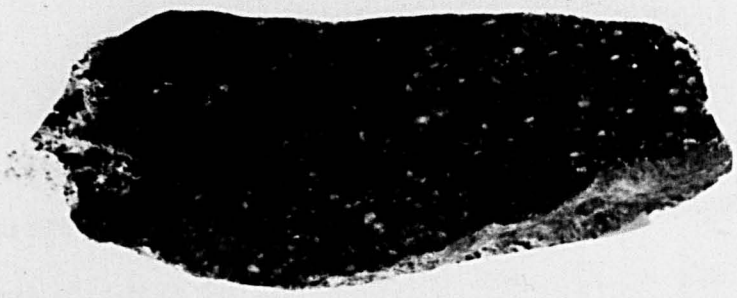
Plate II.42

- a: Dark grey-green mylonite schists with red garnet
(medium grey in photograph) and creamy-orange (white-
to light grey in photograph) porphyroclasts (1017).
Pnte de la Garde, south of St. Cast. x 1.0
- b: As 'a'. Note garnet left-centre (black due to
reflected light) and larger feldspar porphyroclasts
(1016).
Pnte de la Garde, south of St. Cast. x 1.0



Plate II.43

- a: Sheared diatexite (mylonite gneiss) (1050).
Pnte de la Garde, south of St. Cast. x 0.7
- b: Mylonite schist (1014).
Pnte de la Garde, south of St. Cast. x 0.7
- c: Mylonite schist (1054).
Pnte de la Garde, south of St. Cast. x 0.7
- d: Sheared metatexite (mylonite gneiss) (1049).
Pnte de la Garde, south of St. Cast. x 0.7
- e: Sheared metatexite (mylonite gneiss) (1051).
Pnte de la Garde, south of St. Cast. x 0.6



the headland near the junction with the Pentevrian metasediments. Plate II.43 shows various mylonite schists and gneisses from the pnte de la Garde shear belt. Synkinematic white tourmaline bearing granite sheets cross cut the new foliation but have been themselves sheared to a folded form with the foliation axial planar to the folds developed. Clearly more than one phase of movement has occurred within these shear belts. These two shear belts are thought to be of Cadomian age for reasons which will be expanded later (Chapter V).

C. The Brioverian Supracrustal Rocks

Rocks attributed to the Brioverian by the author are exposed along two small stretches of coast on the north-western side of the area of study and represent the north-eastern ends of two narrow fault blocks of cover within a large area of Pentevrian basement rocks (see the first section of this chapter and figures II.1, II.2 & II.3). Although the recent age determination on the Erquy volcanic rocks has raised the possibility that parts of the Brioverian sequence may not be of Precambrian age (Vidal et al, 1971 and Auvray et al, 1972), it is a possibility for which Brown and Roach (1972a & 1972b) can find little support from the geology nor from their palaeogeographic and tectonic interpretation of the northern part of the Massif Armoricaïn during the Lower Palaeozoic. However, whilst this younger series of metasediments is regarded as Precambrian by the author and also by the French workers (Hameurt and Jeannette, 1971 and Jeannette, 1971) some doubts must remain until the true stratigraphic position of the Erquy volcanic rocks is confirmed.

The more southerly belt of Brioverian metasediments outcropping along the coast between Plage de Quatre Vaux and Plage de Pen Guen (to

the east of N. D. du Guildo, see Figures II.2 & II.3) has been studied in more detail by the author than the second belt to the north which was examined during reconnaissance field mapping of the St. Cast area in the summer of 1971. A detailed description of the second belt of Brioverian metasediments has been given by Jeannette (1968 & 1971). The lithological, and to some extent the structural, nature of the metasediments within these two belts is shown in Plates II.44, II.45 and II.46. Comparison should be made with Plates II.1, II.2 and II.3 which demonstrate the lithological and structural characteristics of the Pentevrian metasediments. Clearly there are marked differences between the two groups of metasediments both in terms of non-diastraphic structures and in terms of tectonic structures, though there are similarities in lithology.

The most obvious feature of these Brioverian metasediments is the preservation of sedimentary structures which are typical of deposits from turbidity currents (Allen, 1970). The series of photographs in Plate II.44 shows that around the Pnte du Bay the Brioverian sequence comprises very thick, up to 1 metre thick, turbidite units (Bouma, 1962) which are dominated by coarse psammite - divisions A, B and C (Bouma, 1962 and Allen, 1970). The thin pelite top of one unit (division E) and the irregular base of coarse sand to the bottom graded part (division A) of another unit is clear from Plate II.44c. One single turbidite unit, almost complete, is shown in Plate II.45a. The A division is dominant and is well graded, it is some 50 cm thick, and gives way to a parallel laminated division without grading some 30 cm thick. No ripple lamination is seen in this area though rare evidence of slump structures is found in the finer beds. The features described, especially the prominence of division A, are characteristic of proximal turbidites (Allen, 1970). These turbidite units can be recognized

Plate II.44

a: Graded psammite units within the Brioverian supracrustal sequence (25/28).

Pnte du Bay, south of St. Cast.

b: Close-up of the graded psammite units showing the dominance of the graded division ('A') of turbidites. The top of the sequence is to the south-east (right in the photograph) (25/29).

Pnte du Bay, south of St. Cast.

c: Pelitic top ('E' division) to one turbidite unit and coarse greywacke base ('A' division) to the next turbidite unit (25/33).

Pnte du Bay, south of St. Cast.

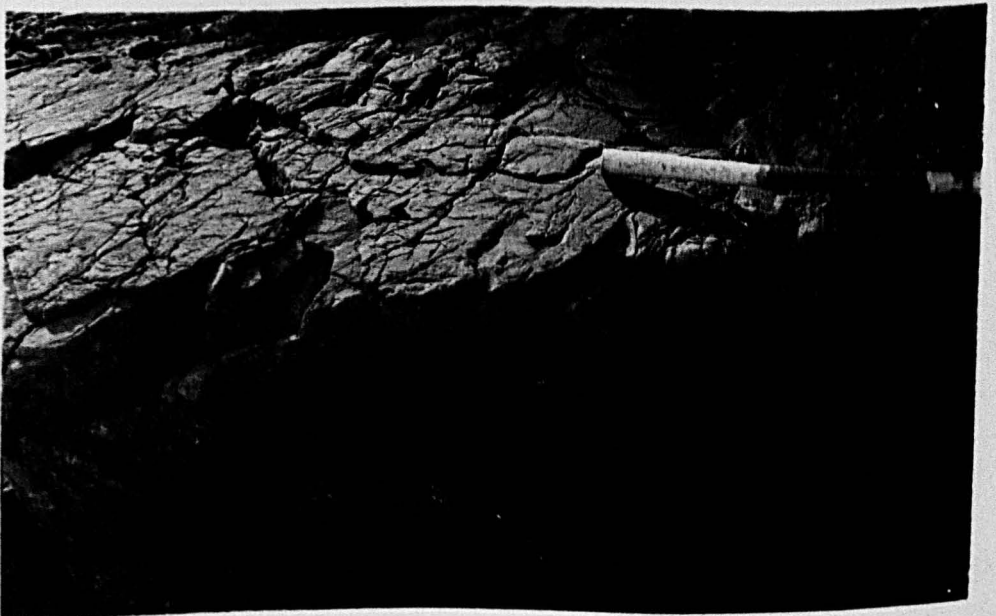
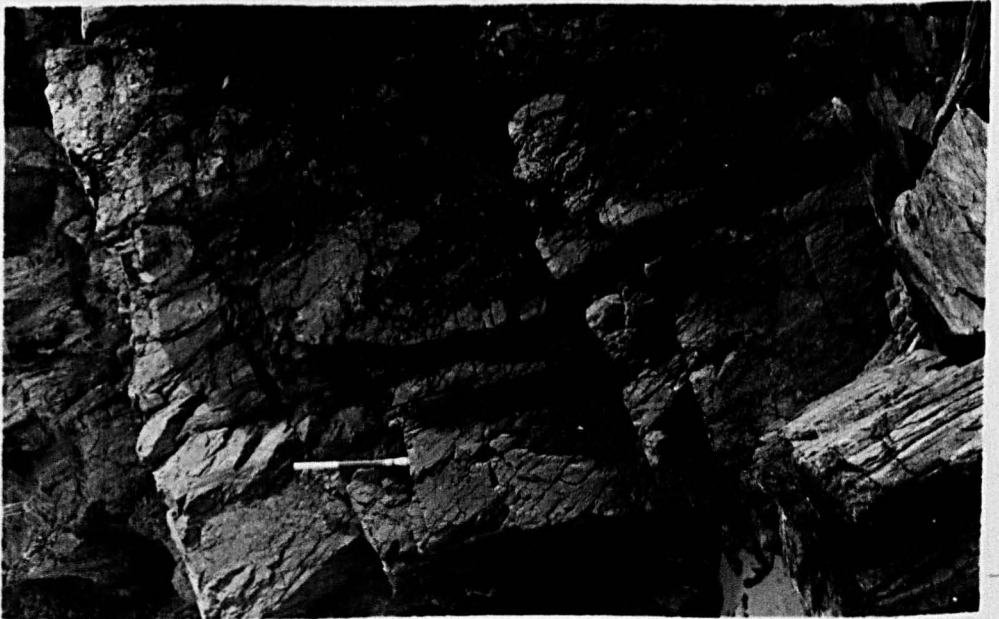


Plate II.45

a: Single turbidite unit from the sequence shown in Plate II.44a. Note the coarse greywacke base to the 'A' division which grades up into the semi-pelite of the 'B' (+ 'C' division ?). The metamorphic cleavage becomes progressively better developed from left to right across the photograph (25/30).

Pnte du Bay, south of St. Cast.

b: Intraformational conglomerate within the Brioverian turbidite sequence (17/22).

North of pnte de Tiqueras, north from Plage de Quatre Vaux.

c: Quartz veined Brioverian semi-pelitic schists which dominate the sequence between pnte de Tiqueras and Plage de Quatre Vaux. Note two phases of folding preserved by the quartz veins (1/17).

Pnte de Tiqueras, north from Plage de Quatre Vaux.

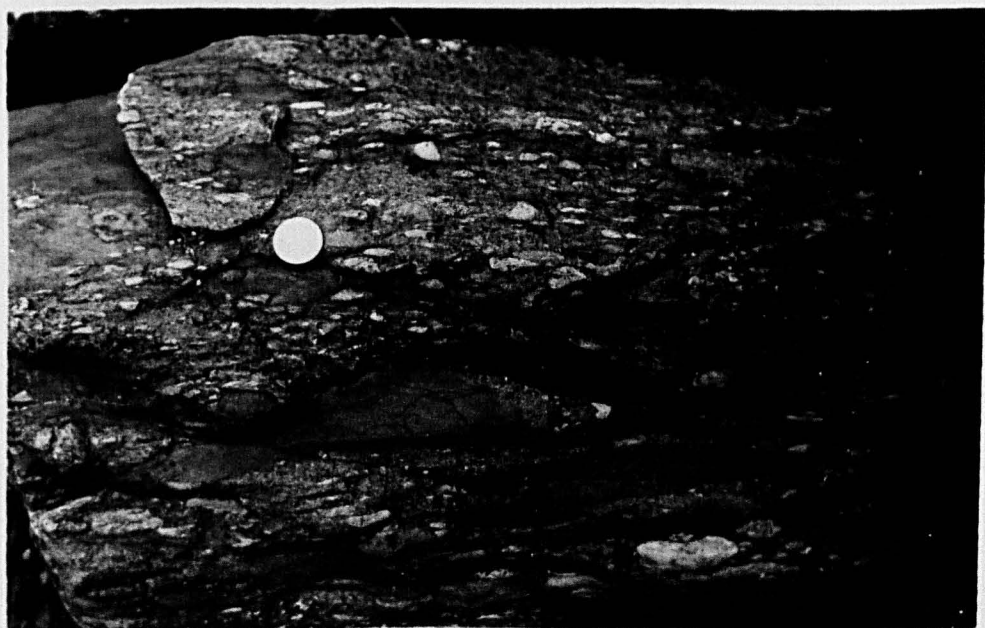
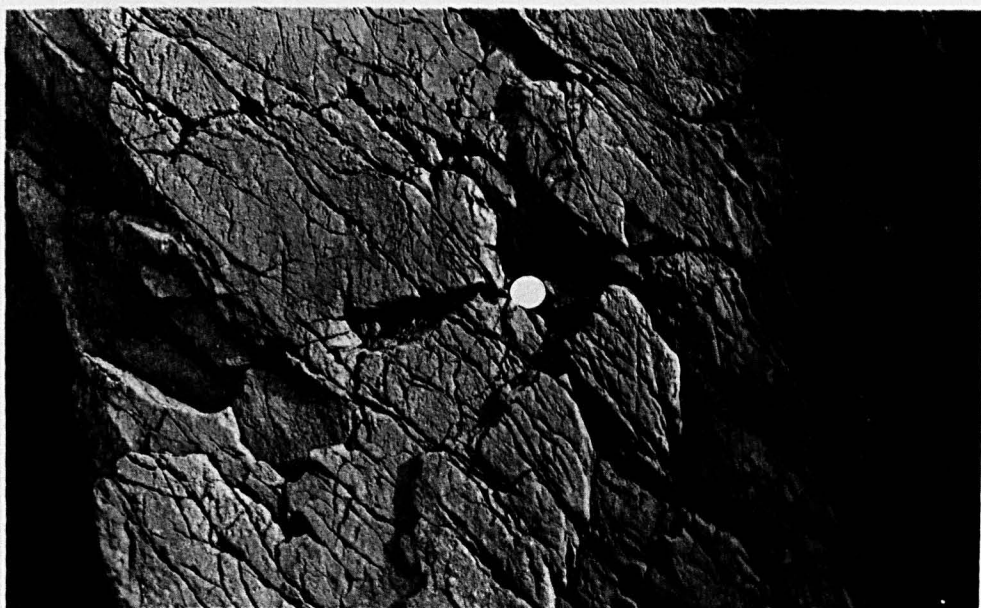
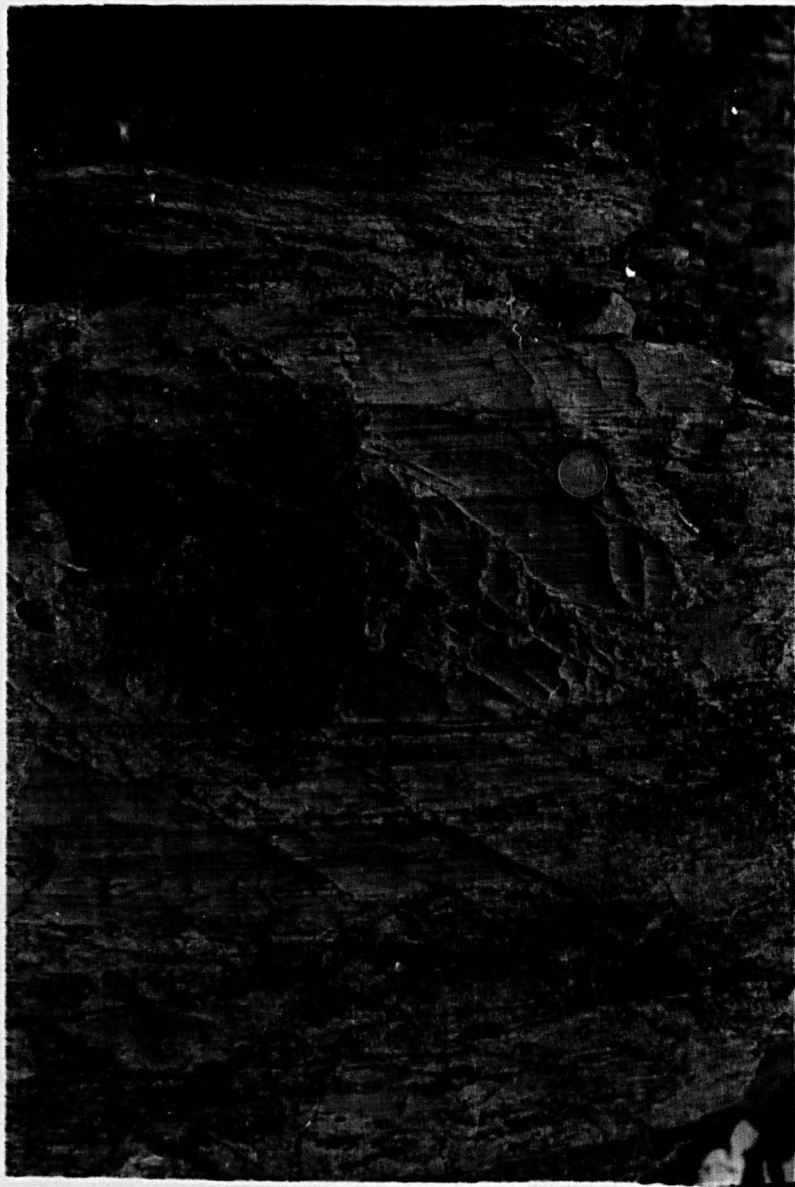


Plate II.46

a: Turbidite units ca 10 cm thick showing graded, parallel laminated and ripple laminated divisions (26/9).

Port a la Duc, Baie de la Fresnaye.

b: Detail from above (26/8).



within the rocks to the south of the pnte du Bay and as far south as the pnte de Tiqueras. At the back of the small bay just north of the pnte de Tiqueras thin conglomerates (Plate II.45b) are found within the succession but recognizable grading in the units is not seen, although there is evidence for contemporaneous slumping. The succession from the southern part of the pnte de Tiqueras to the Plage de Quatre Vaux is dominated by a thick series of dark grey semi-pelites with occasional thin psammites which preserve the tectonic structure (Plate II.45c), though in which sedimentary structures have generally been obliterated.

Turbidite units are again recognized from within the Brioverian sediments exposed at the back of the Baie de la Fresnaye, especially around Port à la Duc, where the units are considerably thinner than those described above from the pnte du Bay and average only about 10 cm in thickness (Plate II.46). Once again it is the coarse part of the unit - divisions A, B and C - which are dominant (see Plate II.46b) but here each of the three divisions is equally developed. The turbidites comprise a buff coloured medium-grained graded sandy A division, a buff-to-grey coloured silty parallel laminated B division and a similar ripple laminated C division. Occasionally the D and E divisions are developed, but this is rare. These features suggest that the turbidite units at Port à la Duc are more distal than those at the pnte du Bay; they are intermediate between typical proximal and typical distal turbidites (Allen, 1970).

The tectonic structures developed within the Brioverian metasediments will be discussed in detail later (Chapter V) and have been briefly summarized by Brown et al (1971). A phase of tight to isoclinal folds with an axial planar metamorphic foliation is followed by a phase of flattening which has tightened the first structures and

folded syntectonic quartz and pegmatite veins. A later phase of open to close folds with an axial planar crenulation cleavage has folded both the bedding and the early metamorphic foliation (Plate II.45c).

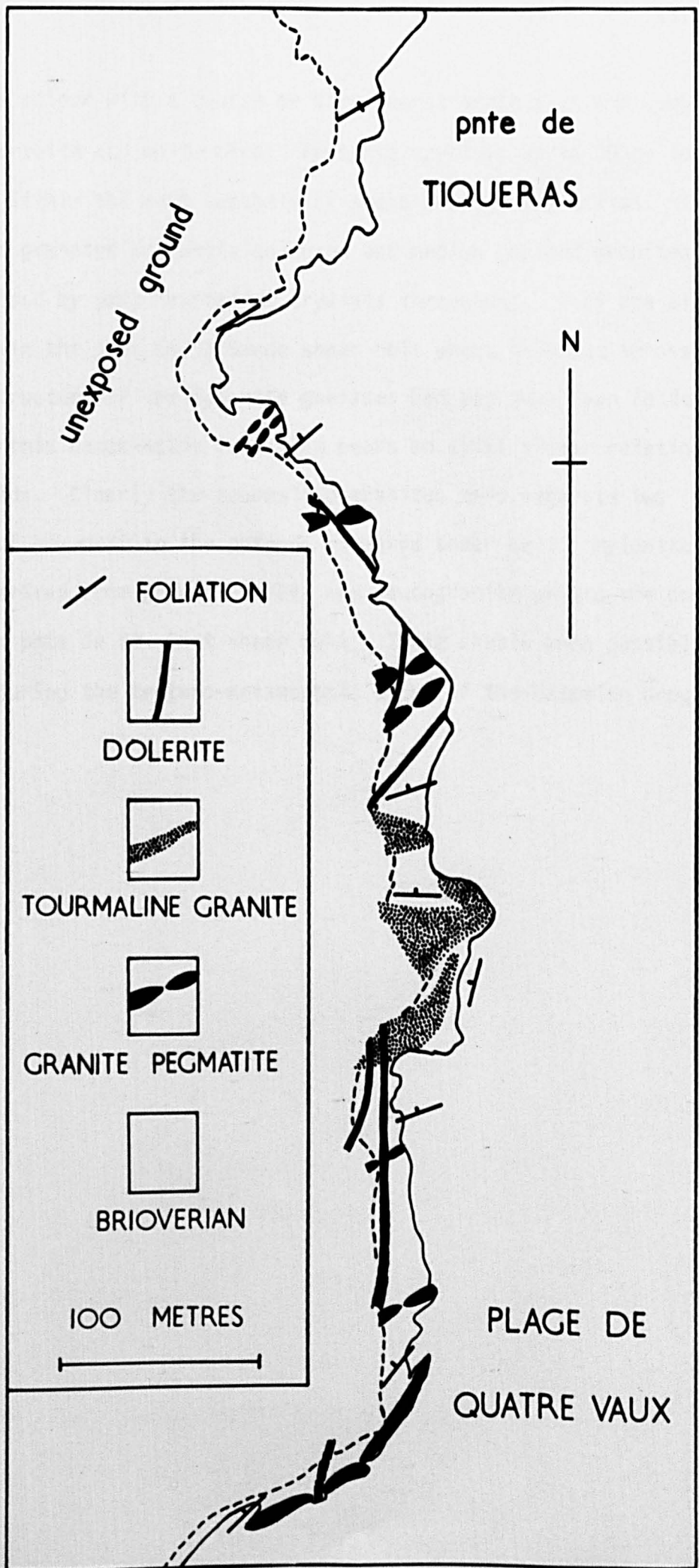
D. The Cadomian Igneous Rocks

Igneous rocks which have been intruded during the tectono-metamorphic phase of the Cadomian orogenic episode are described. It is not the intention of the author to discuss the igneous rocks intruded and extruded during the geosynclinal phase of the Cadomian orogenic episode and the pillow basalts and hyaloclastites which outcrop in the extreme north-west of the area of study (Figure II.2) are not described here. The post-kinematic Bonnemain granite has not been studied in detail by the author and is considered to be outside the scope of this work. Felsic igneous rocks are intruded as sheets into the Brioverian supracrustal rocks between the Plage de Quatre Vaux and the pnte de Tiqueras (Figure II.8) and also into the cataclastic rocks within the pnte de la Garde and pnte de St. Cast shear belts. One concordant mafic sheet, deformed by the late folds, is intruded into the Brioverian metasediments at the pnte de Tiqueras and is exposed on the wave cut platform.

The felsic sheets in the Brioverian metasediments are generally concordant with the lithological lamination and early metamorphic foliation. They are of two types: granite pegmatites and tourmaline granites (see Figure II.8). The thinner granite pegmatites are now preserved as large boudins within this earlier foliation whilst the thicker tourmaline granite sheets have necks separating boudin-like bodies of granite (see Figure II.8). The granite pegmatites are grey

Figure II.8

The Cadomian igneous rocks within the Brioverian supracrustal rocks between the Plage de Quatre Vaux and the pnte de Tiqueras.



or pink in colour with a coarse or very coarse grain size and comprise quartz, perthite and white mica. Perthite crystals up to 30 cm long are found within the most southerly of these granite pegmatites. The tourmaline granites are white coloured and medium grained granites characterised by dark tourmaline crystals throughout. They are also found within the pnte de la Garde shear belt where they cut across the fluxion structure of the mylonite gneisses and yet have been folded such that this cataclastic foliation bears an axial planar relationship to the folds. Clearly the tourmaline granites here separate two episodes of movement in the pnte de la Garde shear belt. Mylonite schists derived from granite sheets and leucogranite sheets are common within the pnte de St. Cast shear belt. These sheets were possibly intruded during the tectono-metamorphic phase of the Cadomian orogenic episode.

Petrography of the Rock Types

A. The Pentevrian Basement

1. The Metasediments

The metasediments which crop out on the south-east side of pnte de la Garde (Figure II.2), along the Rance south of le Minihic (around Langrolay and St. Suliac (Figure II.5), and along the coast around Cancale (Figure II.4) consist of interbedded semi-pelites and psammites with subordinate pelites. They comprise varying amounts of quartz, feldspar and biotite; muscovite may be present and in some bands is in equal proportion to biotite; minor amounts of allanite, zircon, apatite and opaque ore may be present together with occasional tourmaline. The semi-pelites are commonly laminated. This lamination may be due to variation in the amount of biotite or due to quartz-rich layers alternating with biotite + feldspar layers (Plates III.1 and III.2). The grain size varies between 0.02 mm and 0.10 mm but is generally about 0.05 mm. The quartz and feldspar have a granoblastic polygonal texture with curvilinear grain boundaries, which may be diffuse, and a tendency to form triple point junctions. The feldspar is generally turbid in plane light and may be varicized; it is often of indeterminate composition but in some specimens plagioclase, with occasional fine albite twinning, can be identified. Sporadic zoned oligoclase-albite grains and microcline grains occur within the metasediments. The proportion of quartz to feldspar varies from specimen to specimen, sometimes the quartz dominates the felsic component, sometimes the two are present in equal proportion. Biotite (brown or buff to red-brown or dark brown) flakes between 0.05 mm and

Petrography of the Rock Types

A. The Pentevrian Basement

1. The Metasediments

The metasediments which crop out on the south-east side of pnte de la Garde (Figure II.2), along the Rance south of le Minihic (around Langrolay and St. Suliac (Figure II.5), and along the coast around Cancale (Figure II.4) consist of interbanded semi-pelites and psammites with subordinate pelites. They comprise varying amounts of quartz, feldspar and biotite; muscovite may be present and in some bands is in equal proportion to the biotite; minor amounts of allanite, zircon, apatite and opaque ore may be present together with occasional tourmaline. The semi-pelites are commonly laminated. This lamination may be due to variation in the amount of biotite or due to quartz-rich layers alternating with biotite + feldspar layers (Plates III.1 and III.2). The grain size varies between 0.02 mm and 0.10 mm but is generally about 0.05 mm. The quartz and feldspar have a granoblastic polygonal texture with curvilinear grain boundaries, which may be diffuse, and a tendency to form triple point junctions. The feldspar is generally turbid in plane light and may be sericitized; it is often of indeterminate composition but in some specimens plagioclase, with occasional fine albite twinning, can be identified. Sporadic zoned oligoclase-albite grains and microcline grains occur within the metasediments. The proportion of quartz to feldspar varies from specimen to specimen, sometimes the quartz dominates the felsic component, sometimes the two are present in equal proportion. Biotite (straw or buff to red-brown or dark brown) flakes between 0.05 mm and

Plate III.1

- a: Thin psammite layer within semi-pelite representing primary lithological lamination. The metamorphic foliation defined by the orientation of biotite flakes is slightly oblique to the lithological lamination.
Pentevrian metasediments, 1a Rance. (5 cm = 1 mm)
- b: Small-scale kink folding of mica foliation in semi-pelite. The fold limbs are of variable length.
Pentevrian metasediments, 1a Rance. (5 cm = 1 mm)

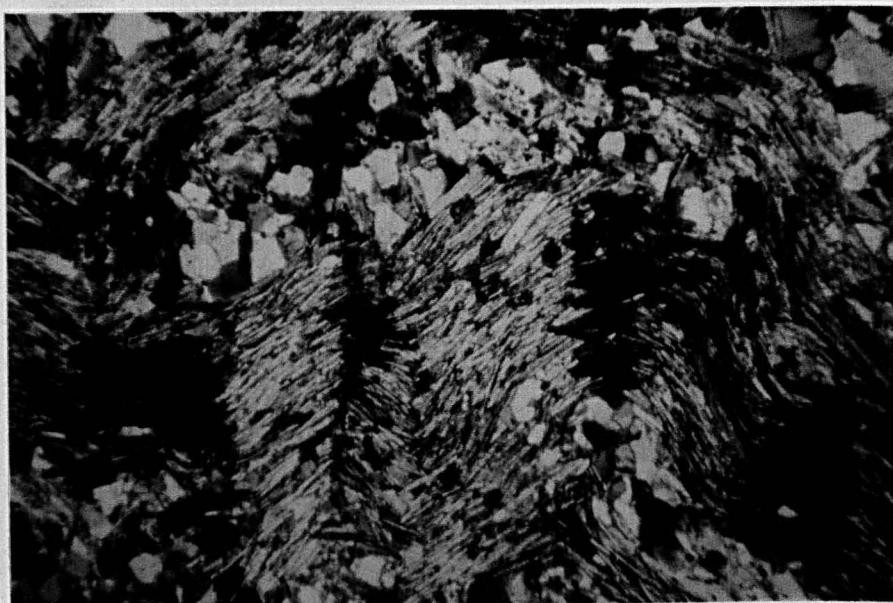
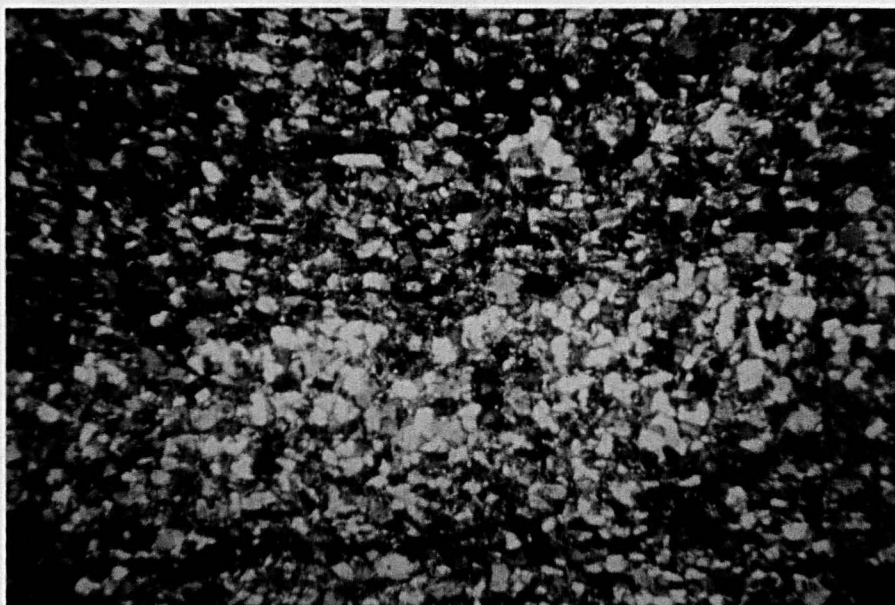
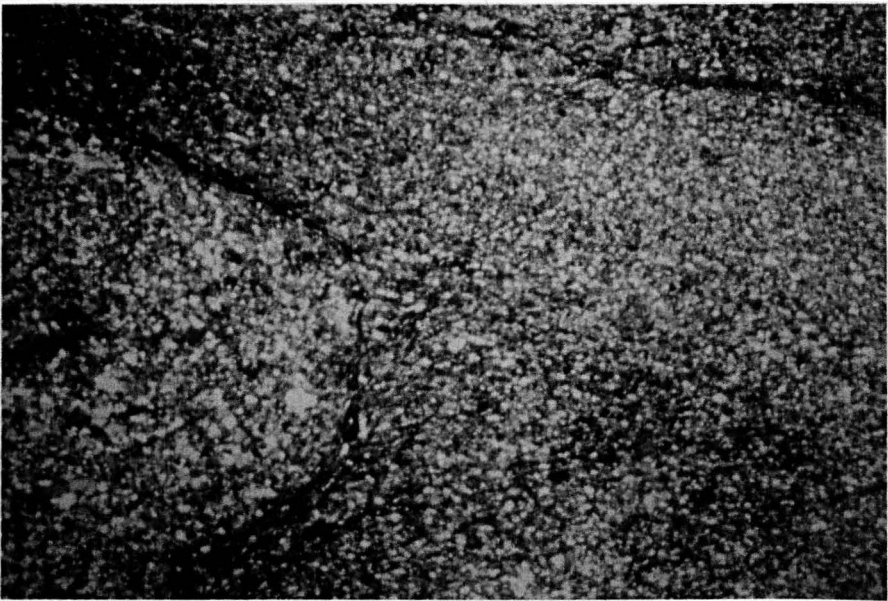


Plate III.2

- a: Folded primary lithological lamination and parallel metamorphic foliation. Reorientation of biotite flakes in the fold hinge has resulted in the local transposition of the metamorphic foliation and the development of an axial plane foliation.
Pentevrian metasediments, south of Cancale. (5 cm = 3.5 mm)

- b: Crenulation and partial transposition of the metamorphic foliation in the closure of a tight fold.
Pentevrian metasediments, south of Cancale. (5 cm = 3.5 mm)

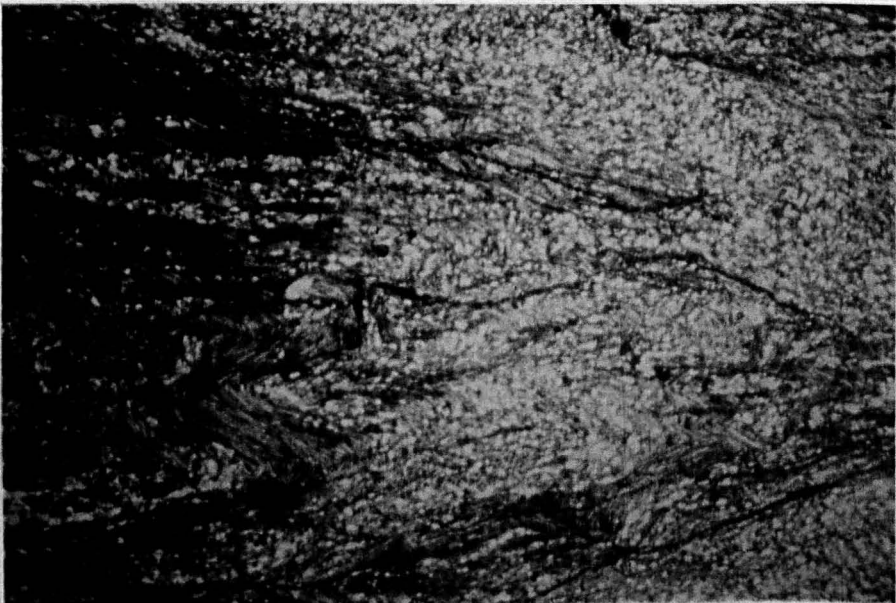
- c: Metamorphic foliation defined by the biotite flakes and at a high angle to poorly defined primary lithological lamination in the hinge zone of tightly folded semi-pelite.
Pentevrian metasediments, south of Cancale. (5 cm = 1 mm)



0.10
orient
is us
lamina
lamina
deform
be pr
musca
with

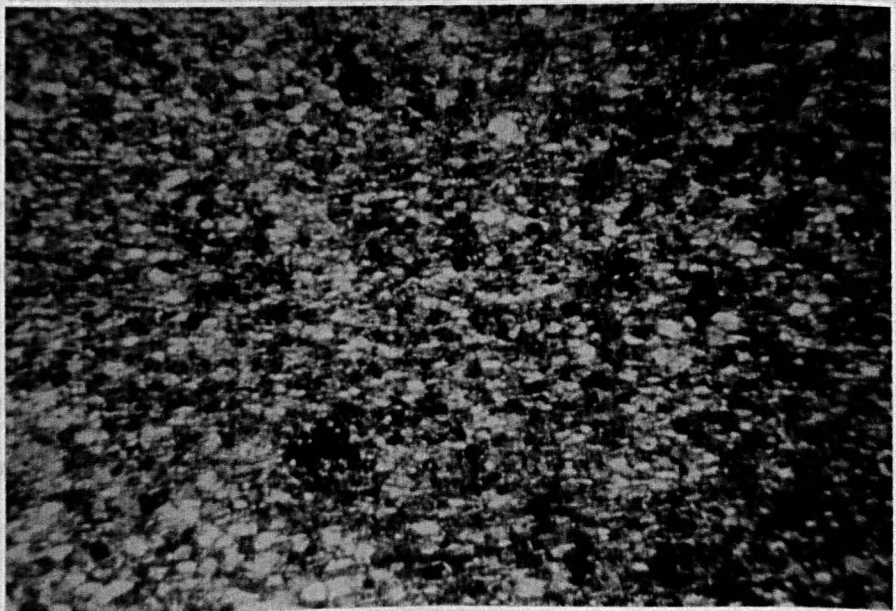
their
ation
cut this
logical
later
akes may
at a
onship
ases of

folding and is commonly crystallized; it may be partly transposed (see
Plates III and IIIA). Minerals present in this is the dominant



access
yellow
aniso
surro
occas
spore
to ye
Cup
2. I

is
it
are is
green



Chapt
betwe
havre
figu
series
of nu
photo
ment

on (see
the coast
of the
Richard's
eriblasts
The
and a

0.10 mm in length are set in the quartz-feldspar matrix and their orientation defines a metamorphic foliation. This biotite foliation is usually parallel to the lithological lamination but it may cut this lamination in some fold hinges. More commonly both the lithological lamination and the biotite foliation have been folded during later deformation; the foliation is often crenulated. Muscovite flakes may be present and in some of the semi-pelites is abundant. Whilst a muscovite foliation has never been seen in axial plane relationship with a set of folds, it has clearly been deformed by later phases of folding and is commonly crenulated; it may be partly transposed (see Plates III.1 and III.2). Partially metamict allanite is the dominant accessory mineral in some of the semi-pelites. It varies from yellow-orange to orange-red in colour and from isotropic to anisotropic; when associated with biotite strong pleochroic haloes surround the allanite. Apatite may or may not be present, it is occasionally pale yellow; zircon is generally present; opaque ore is sporadically present and occasionally tourmaline (pale yellow-green to yellow-green) occurs.

2. The Metatexites

The metatexites are variable in structure and composition (see Chapter II). However, the metatexites which outcrop along the coast between Plage de Quatre Vaux and Dinard (Figure II.3), around the Havre de Rotheneuf (Figure II.4) and by the Rance around la Richardais (Figure II.5) have many features in common. The palaeosome is normally a biotite schist with characteristic large late poikiloblasts of muscovite and intermittent sillimanite (see Plate III.3). The neosome commonly consists of a biotite melanosome or selvedge and a granitic leucosome (see Plate III.4).

The biotite schist palaeosome comprises biotite, plagioclase feldspar within the oligoclase range, quartz and late muscovite with, locally, sillimanite and yellow tourmaline, and minor amounts of opaque ore, zircon and apatite and occasional microcline. The texture is always strongly foliated but within which quartz and plagioclase may exhibit a granoblastic polygonal structure. Small scale folding of the foliation is common. Biotite (pale buff to orange-brown or red-brown) flakes vary between 0.1 mm and 1 mm in length; inclusions of zircon are ubiquitous. The quartz and the plagioclase, which is frequently untwinned, have curvilinear grain boundaries and triple point junctions. Around St. Jacut-de-la-Mer on the western side of the St. Malo migmatite belt anhedral poikiloblasts of oligoclase up to 2 mm across are developed in leucocratic segregations within biotite schists which carry sillimanite (Plate III.3). The sillimanite occurs both as fibrolite sheafs and as prismatic aggregates within quartz or sometimes within the late muscovite (Plate III.3). Large poikiloblasts of muscovite are present within the biotite schist palaeosome of the metatexites. The muscovites vary from 2 mm to 10 mm in length (and rarely up to 20 mm in length) and are frequently elongate in the 'c' crystallographic direction. The muscovites may overgrow fold hinges and are clearly of late origin. They may be intergrown with quartz, especially at the edges of the flakes, in a symplectite although this is by no means common.

The neosome is normally composed of a biotite selvage and a granite leucosome. The biotite (pale buff to orange-brown or red-brown) flakes which make up the selvage are generally coarser than those in the adjacent palaeosome; they generally interlock in a decussate texture (Plate III.4a). As the proportion of palaeosome to

Plate III.3

- a: Plagioclase porphyroblasts in leucocratic segregations within biotite schists which carry sillimanite.

Sillimanite schist, Plage de Quatre Vaux. (5 cm = 1 mm)

- b: Fine prismatic sillimanite within mica and quartz from biotite schists.

Sillimanite schist, Plage de Quatre Vaux. (5 cm = 0.25 mm)

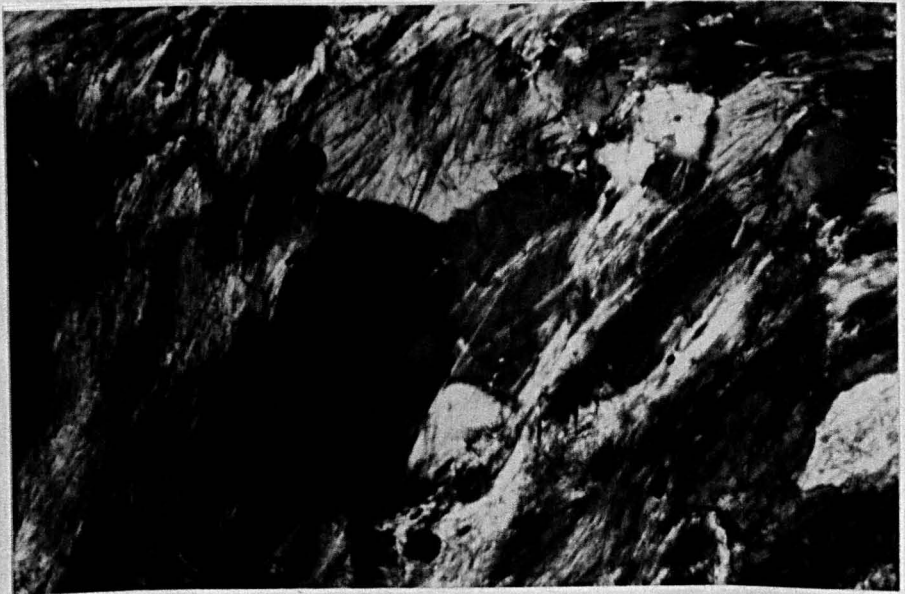
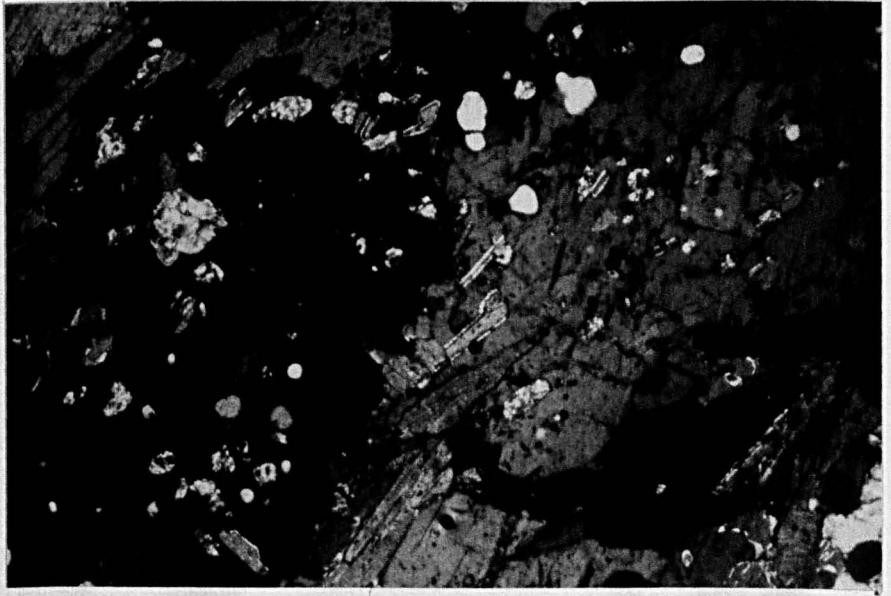


Plate III.4

a: Granitic leucosome and biotite melanosome comprising the neosome of a typical metatexite.

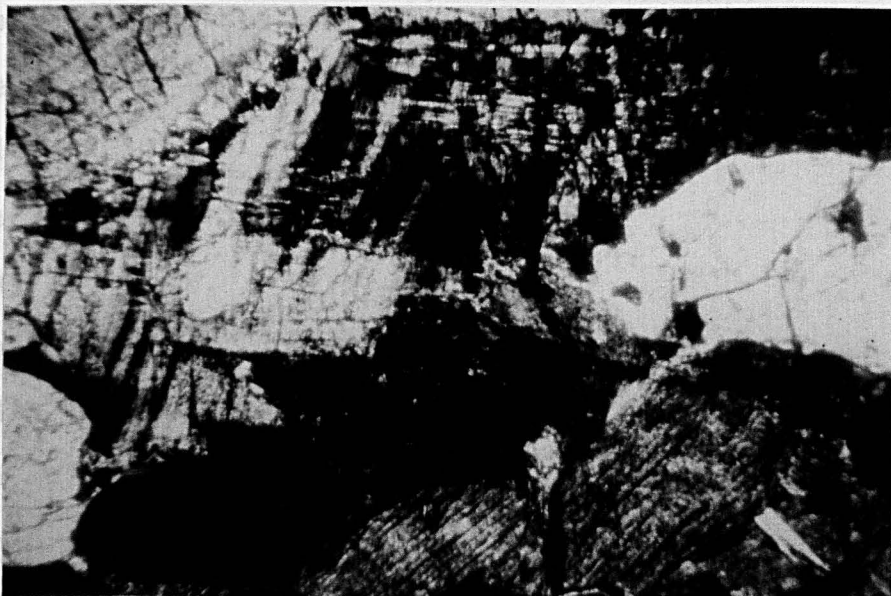
Metatexite, pnte de la Garde Guérin. (5 cm = 1 mm)

b: Typical texture of a granitic leucosome (compare with Plate III.7).

Metatexite, pnte de la Garde Guérin. (5 cm = 1 mm)

neosome decreases with increasing metatexis so the biotite selvage becomes a biotite layer separating two granite layers and finally breaks up to form the skeleton of the inhomogeneous diatexites. The

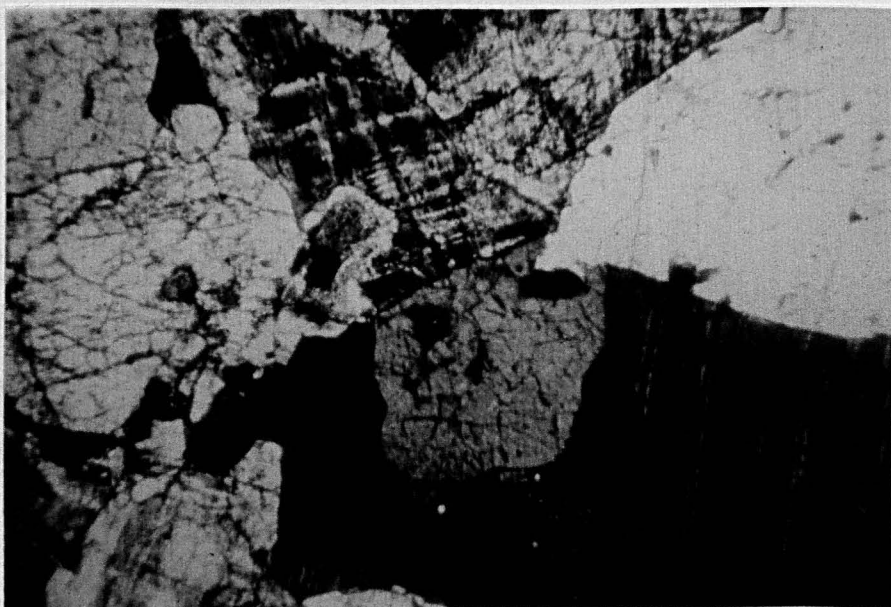
leucocrystalline granite
in which the plagioclase
The albite rims
frequently
common
is associated
oligoclase
twinned



granite
comprise
biotite.
and are
feldspar
the
ly
ms

microperthitization occurring parallel to the foliation. There are numerous inclusions of plagioclase with perthitized cores and clear albite rims (Plate III.4b). Drop-like inclusions of quartz are common in the microcline and may be present in some of the plagioclase. Interstitial quartz aggregates are inclosed into thin feldspars.

2. In
granite
foliation
through
various
From
plagioclase



to
swirling
structure
per
achmen and
net of
which may

be microperthitic, quartz, zircon, and monazite together with minor amounts of allanite, monazite, zircon, apatite, and sporadic titanite. The plagioclase texture is generally

neosome decreases with increasing metatexis so the biotite selvage becomes a biotite layer separating two granite layers and finally breaks up to form the schlieren of the inhomogeneous diatexites. The leucosomes have a variable composition but are most commonly granite in well developed metatexites (eg. Lancieux to Dinard). They comprise plagioclase, microcline and quartz with rare single flakes of biotite. The anhedral plagioclase grains commonly average 1 mm across and are frequently zoned from a sodic oligoclase to albite. They are commonly extensively embayed by replacive quartz. When the K-feldspar is adjacent to the plagioclase lobes of microcline penetrate the oligoclase in a replacive manner. The microcline is frequently twinned in the characteristic gridiron pattern and is sometimes microperthitic (string perthite). There are numerous inclusions of plagioclase with sericitized cores and clear albite rims (Plate III.4b). Drop-like inclusions of quartz are common in the microcline and may be present in some of the plagioclase. Interstitial quartz aggregates are lobate into both feldspars.

3. The Diatexites

The inhomogeneous diatexites are medium grained granitic to granodioritic rocks with schlieren of biotite which define a swirling foliation. They are remarkably uniform in composition and texture throughout the St. Malo migmatite belt, although alkali feldspar varies in amount from section to section of the same hand specimen and from specimen to specimen. The inhomogeneous diatexites consist of plagioclase feldspar within the oligoclase range, microcline which may be microperthitic, quartz, biotite and muscovite together with minor amounts of sillimanite and/or fibrolite, zircon, apatite, opaque ore and sporadic tourmaline. The plagioclase feldspar is generally

oligoclase (between An_{18} and An_{22}) but may be calcic oligoclase or sodic oligoclase (see later section). Its form varies from subhedral to (less commonly) anhedral and may occur as rectangular crystals or (less commonly) equant crystals; albite twinning is normally present. The rectangular plagioclases vary from 1 mm to 3 mm in length whilst the equant grains are between 1 mm and 2 mm across, smaller grains of plagioclase occur as inclusions within the alkali feldspar (see below). The plagioclase is often slightly sericitised and in some specimens of inhomogeneous diatexite may be zoned to clear albite rims, although this is a ubiquitous feature of included plagioclase it is only a rare feature of the plagioclase outside the alkali feldspar. Inclusions of quartz within the plagioclase are common. Quartz-plagioclase grain boundaries are often lobate and suggest some replacement of the plagioclase by the quartz. A myrmekite-like intergrowth between plagioclase and quartz is sometimes present in plagioclase adjacent to grain boundaries with quartz and some plagioclases are riddled with quartz blebs. Post-crystalline deformation is reflected by kink folding or microfaulting of the albite twin lamellae. The alkali feldspar is microcline with coarse to fine wedge-shaped albite and pericline twinning which give the characteristic gridiron pattern; it is occasionally microperthitic. The microcline is present as irregular anhedral areas from 1 mm to 10 mm across which appear to be of relatively late origin and replacive. Inclusions of plagioclase, quartz and biotite are present within the microcline; it is the plagioclase together with some quartz which seems to have suffered replacement. The small plagioclase inclusions consist of slightly sericitized oligoclase cores with clear albite rims which often merge into the surrounding microcline (see Plate III.5a). The grain boundaries between microcline and plagioclase are strongly lobate with the microcline apparently replacing the plagioclase. Sometimes quartz

has been replaced by microcline. In Plate III.5b microcline can be seen to have nucleated along a plagioclase-quartz grain boundary and replaced both. Biotite (straw yellow or buff to orange-brown or red-brown) is present both as discrete flakes and as aggregates (schlieren) up to 10 mm long in thin section (see Plates III.6 and III.7) but considerably larger in hand specimen (see frontispiece 2 and Chapter II). The biotite flakes vary in shape from rectangular to square and in size from 0.5 mm to 2 mm in length. The cleavage ends are frequently ragged and on occasion the biotite has been replaced by chlorite along the cleavage or by muscovite and opaque ore. Sometimes the cleavage ends of the biotite are intergrown with quartz in a symplectite and more rarely the edges of the biotite flakes are embayed by quartz. The biotites have suffered strong kinking in response to post-crystalline deformation. Tourmaline (colourless or pale yellow to yellow or yellow brown - dravite) occurs sporadically in the biotite schlieren from inhomogeneous diatexites around St. Jacut-de-la-Mer. Small randomly orientated flakes of muscovite frequently occur within the biotite schlieren cross cutting the biotites and possibly of later origin. There are abundant zircons with strong pleochroic haloes within the biotites (see Plate III.7a). Muscovite is subordinate to biotite in the inhomogeneous diatexites and appears to be of relatively late origin. It is typically present as ragged flakes up to 3 mm in length and is occasionally elongate parallel to the 'c' crystallographic direction. The muscovite is frequently riddled with quartz around the edges in symplectitic intergrowth, this is always the case when the muscovite is adjacent to microcline. Prismatic sillimanite is sporadically included within the late muscovite and on occasions the muscovite appears to replace areas of fibrolite. Prismatic sillimanite may also be found enclosed in quartz (see Plate III.7b). Quartz occurs as drop-like inclusions

Plate III.5

- a: Equant grain of oligoclase with albite rim (in extinction) included within poorly twinned microcline. Note the slightly ragged and embayed biotite flake. Inhomogeneous diatexite, St. Jacut. (5 cm = 1 mm)
- b: Typical inhomogeneous diatexite texture. Notice the nucleation of microcline along the quartz-oligoclase boundary and the subsequent replacement of both minerals; there is a thin reaction rim between the microcline and the oligoclase. Inhomogeneous diatexite, St. Jacut. (5 cm = 1 mm)

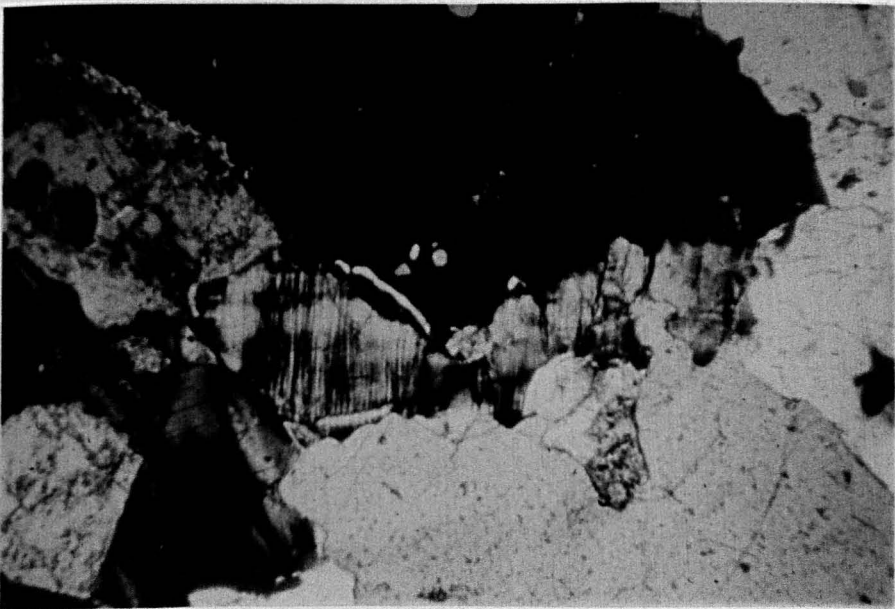


Plate III.6

a: Typical inhomogeneous diatexite texture with small
biotite schlieren.

Inhomogeneous diatexite, St. Jacut. (5 cm = 2.5 mm)

b: Large biotite schlieren. Note the presence of both
tourmaline and muscovite.

Inhomogeneous diatexite, St. Jacut. (5 cm = 2.5 mm)



Plate III.7

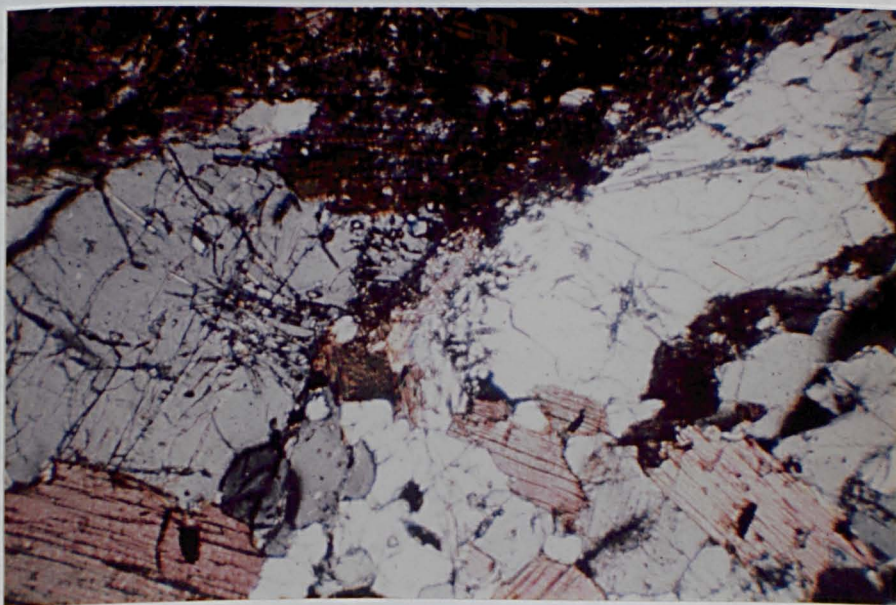
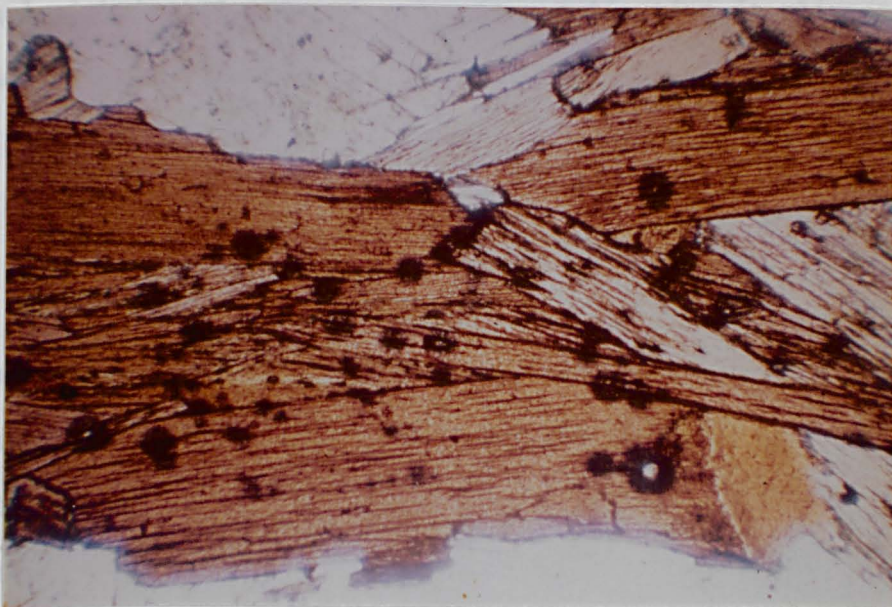
- a: Small biotite schlieren with decussate texture typical of the inhomogeneous diatexites. Note the numerous pleochroic haloes surrounding small zircons.

Inhomogeneous diatexite, St. Jacut. (5 cm = 1 mm)

- b: Scattered prismatic sillimanite needles within both the quartz and the muscovite.

Inhomogeneous diatexite, le Guildo. (5 cm = 1 mm)

in both feldspars and as subhedral-grain aggregates. Some quartz aggregates have slightly sutured grain boundaries superimposed on a triple point texture but more commonly show grain boundaries and



in both feldspars and as anhedral grain aggregates. Some quartz aggregates have slightly sutured grain boundaries superimposed on a triple point texture but more commonly the grain boundaries are strongly lobate and sutured. Undulose extinction is ubiquitous. Much of the quartz appears to be replacive, embayments of quartz into plagioclase are common and, although infrequent, embayments of quartz into biotite do occur.

The homogeneous diatexites are medium grained granitic to granodioritic rocks with a poorly defined swirling biotite foliation. The homogeneous diatexite which crops out on the Presqu'île de St. Jacut-de-la-Mer (Figure II.6) comprises plagioclase feldspar within the oligoclase range, microcline which may be microperthitic, quartz, biotite and muscovite with minor amounts of opaque ore, apatite and zircon and rare rutile and topaz. Plagioclase is subordinate in quantity to the microcline in the central parts of the outcrop but this relationship is reversed in the marginal parts of the body of homogeneous diatexite. The plagioclase feldspar is commonly of middle oligoclase composition but may be zoned to sodic oligoclase and occasionally to albite at the rim. The plagioclases vary from slightly sericitized to completely sericitized but when zoned to albite the rims are clear. The form of the plagioclase is generally subhedral and from 1 mm to 2 mm long in the central part of the body but up to 4 mm in length in specimens from the margins of the body. The edges of the crystals are frequently embayed by both microcline and quartz, especially in specimens from the central part of the body, suggesting that the microcline and some of the quartz are of relatively late origin and replacive. The alkali feldspar is microcline generally with the characteristic cross hatched twinning and often microperthitic (mainly string or rod perthite but less commonly film perthite) (see

Plate III.8a). It occurs as large anhedral areas up to 7 mm across (although more commonly between 3 mm and 5 mm across) and may replace both plagioclase and quartz (see Plates III.8 and III.9) giving textures similar to those figured by Marmo (1971), Pitcher and Berger (1972) and Augustithis (1973). Inclusions of plagioclase are ubiquitous within the microcline and the largest areas of microcline may contain all the other constituent minerals of the rock as inclusions. The plagioclase inclusions have a subhedral to anhedral rectangular to equant form with a sericitized oligoclase core zoned to a clear albite rim which often merges into the enclosing microcline (see Plates III.8 and III.9). Biotite (neutral or straw yellow to red-brown or brown) is present as discrete ragged flakes and small aggregates of flakes. They rarely exceed 2 mm in length. Slight chloritization or muscovitization of the biotite along the cleavages is common. Zircon, with its characteristic pleochroic haloes, and fine rutile needles are included within the biotite. Muscovite is present as small flakes cutting through the biotites and as much larger ragged flakes intergrown with quartz in a symplectite. The micas are cut by kink folds due to post-crystalline deformation. Quartz is found as inclusions in both feldspars, intergrown with muscovite and as anhedral grain aggregates up to 5 mm across. Quartz-quartz grain boundaries are always sutured and undulose extinction is ubiquitous. Quartz-plagioclase grain boundaries, however, may be straight or lobate, when lobate it is the plagioclase which is embayed by and replaced by the quartz. In places the texture is equigranular and hypidiomorphic (see Plate III.8).

The homogeneous diatexite which crops out on the north side of Port Briac and along the coast northwards (Figure II.4) consists of large crystals of microcline which is commonly microperthitic in a

Plate III.8

a: Cross hatched twinning in microcline which is seen to enclose and replace plagioclase. The included plagioclase grains have slightly sericitized oligoclase cores and clear albite rims.

Homogeneous diatexite, St. Jacut. (5 cm = 1 mm)

b: Typical equigranular hypidiomorphic homogeneous diatexite texture.

Homogeneous diatexite, St. Jacut. (5 cm = 1 mm)

c: Typical microcline-plagioclase-quartz relationships. Notice the clear albite rim to the included plagioclase grain.

Homogeneous diatexite, St. Jacut. (5 cm = 1 mm)

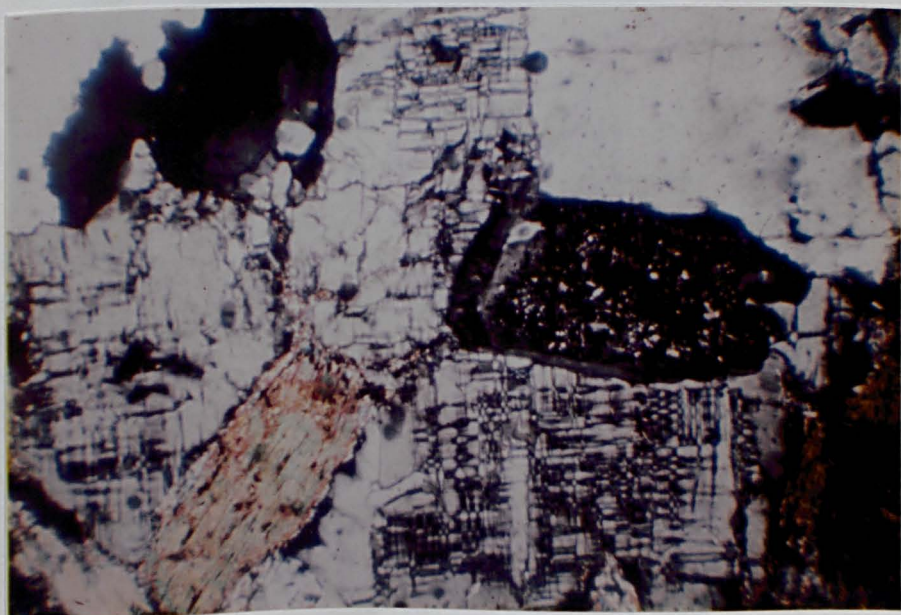
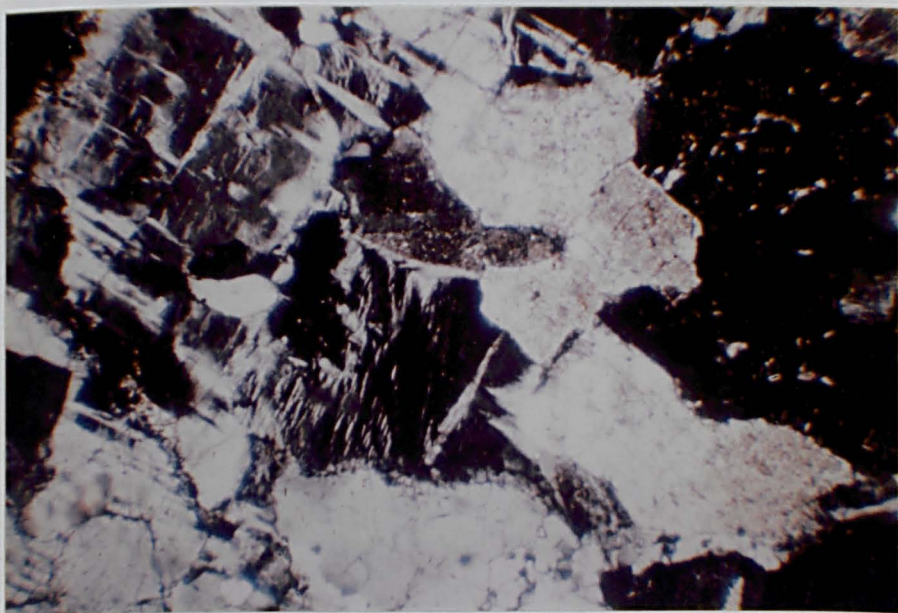
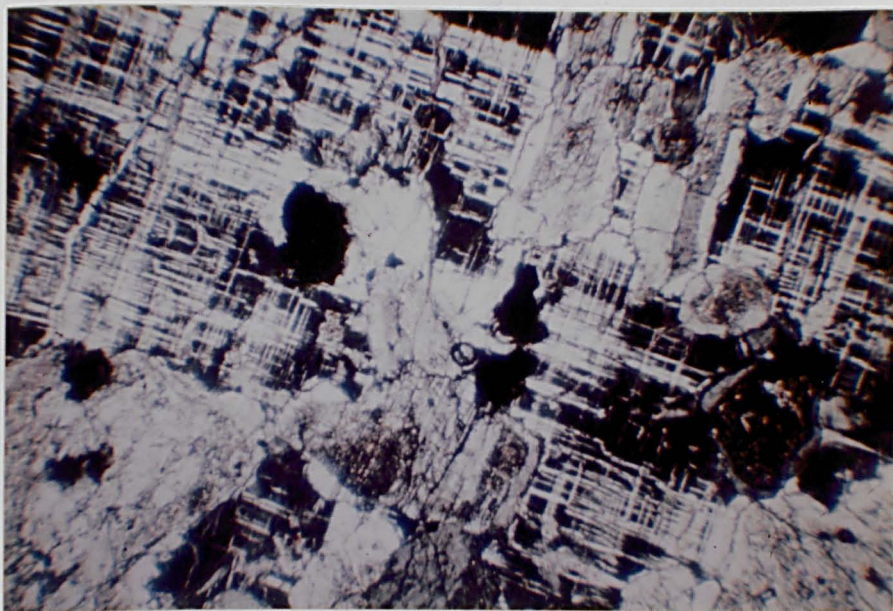
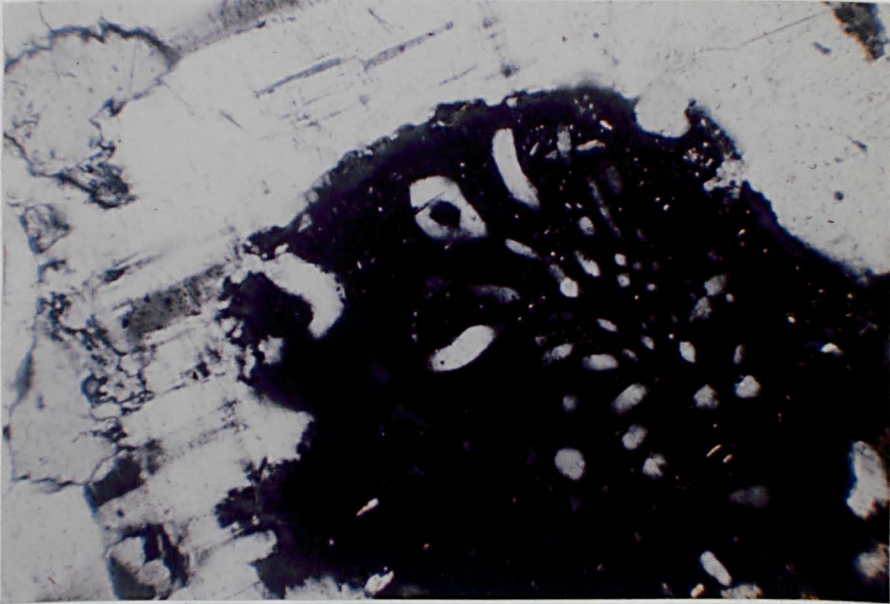


Plate III.9

- a: Oligoclase grain (dark) embayed by microcline (light) and containing rhabditiform microcline. There is a reaction zone 0.025 mm wide on the oligoclase side of the microcline-oligoclase grain boundary and a diffuse edge to the microcline adjacent to the grain boundary. Homogeneous diatexite, St. Jacut. (5 cm = 0.35 mm)
- b: Oligoclase grain (mid grey) embayed by microcline (twinned) and containing rhabditiform microcline. Notice the diffuse nature of the microcline-oligoclase grain boundary and the optical continuity of the microcline. Homogeneous diatexite, St. Jacut. (5 cm = 0.35 mm)

medium grained groundmass of plagioclase feldspar within the
of eclogite range, quartz, biotite and muscovite with minor amounts of
pyroxene ore, zircon, apatite, garnet and in some cases epidote and sphene. The
rock is strongly foliated due to a concentration of the alignment of



aligned by the surrounding matrix. The inclusion appears to have partially
replaced the plagioclase (see Plate III, fig. 1). Kynmekite is
occasionally developed in the outer part of the plagioclase inclusions.
The plagioclases in the groundmass of the rock are medium sized (from
1 to 2 mm long) and often slightly rounded by the wide cataclasts.



... contains a variable foliation or is small aggregates of
... with a mosaic texture. The flakes, which vary from 0.1 mm to

medium grained groundmass of plagioclase feldspar within the oligoclase range, quartz, biotite and muscovite with minor amounts of opaque ore, apatite, zircon and on occasion epidote and sphene. The rock is strongly foliated due to a combination of the alignment of biotites and a poorly developed cataclastic fluxion structure. In some zones the rock could be called a protomylonite. The large microcline crystals vary from 3 mm to 10 mm in length with a mean dimension of 5 mm. The characteristic cross hatched twinning is ubiquitous and carlsbad twinning is commonly present (see Plate III.10a). Small drop-like inclusions of quartz up to 0.3 mm across and subhedral to rounded inclusions of plagioclase up to 1 mm in length are frequent within the microcline. The plagioclase inclusions are zoned from middle or sodic oligoclase to albite and are often embayed by the surrounding microcline which appears to have partially replaced the plagioclase (see Plate III.10a). Myrmekite is occasionally developed in the outer part of the plagioclase inclusions. The plagioclases in the groundmass of the rock are medium sized (from 1 mm to 2 mm long) and often slightly rounded by the mild cataclasis. They have sericitized cores of middle to sodic oligoclase and often clear albite rims, some appear to have patchy zoning. A few of the plagioclases contain rhabdites of quartz in a myrmekite-like intergrowth which appears unrelated to the proximity of the alkali feldspar. Quartz in the groundmass may be present as grain aggregates up to 5 mm across commonly with triple point junctions between grains but with sutured grain boundaries but can also be present in elongate zones of ribbon quartz where the rock has suffered cataclasis (see Plate III.10b). Undulose extinction is ubiquitous. The biotite flakes (straw yellow to deep red-brown) may be present as individual flakes, in layers defining a variable foliation or in small aggregates of flakes with a decussate texture. The flakes, which vary from 0.1 mm to

1 mm in length, are generally ragged and may be partially chloritized. Flakes of muscovite, subordinate to the biotite, are commonly associated with the biotite layers and aggregates. The micas are always kinked in response to post-crystalline deformation.

To the west of pnte de Grouin the diatexites have suffered cataclasis and contain augen-like pods of foliated garnet granite. In thin section these garnet granites are seen to have been sheared as well and in places are seen to carry a cataclastic fluxion structure. They comprise plagioclase, microcline, quartz, garnet, biotite and muscovite. The plagioclase is very strongly sericitized and only rarely are albite twin lamellae visible; it appears to be sodic oligoclase in composition. Undulose extinction is ubiquitous. The microcline occurs as equant anhedral areas approximately 1 mm across which occasionally appear to be of relatively late origin and replacive but most of the original textural relationships have been destroyed by the cataclasis. The garnet may be present as large crystals up to 20 mm across intergrown with quartz in a symplectite (Plate III.10c). More commonly the garnet crystals have been broken into numerous fragments by the cataclasis. Biotite (pale brown to very dark brown) flakes define a poor foliation. Garnet may be partially replaced by biotite. Small random muscovite flakes are scattered through the rock. Quartz areas have often been polygonized into fine grained unstrained aggregates. Those areas which have not been recrystallized have strongly sutured grain boundaries and show undulose extinction.

Plate III.10

a: Perthitic microcline exhibiting both the characteristic albite-pericline twinning and carlsbad twinning. There are numerous inclusions of albite rimmed oligoclase feldspar.

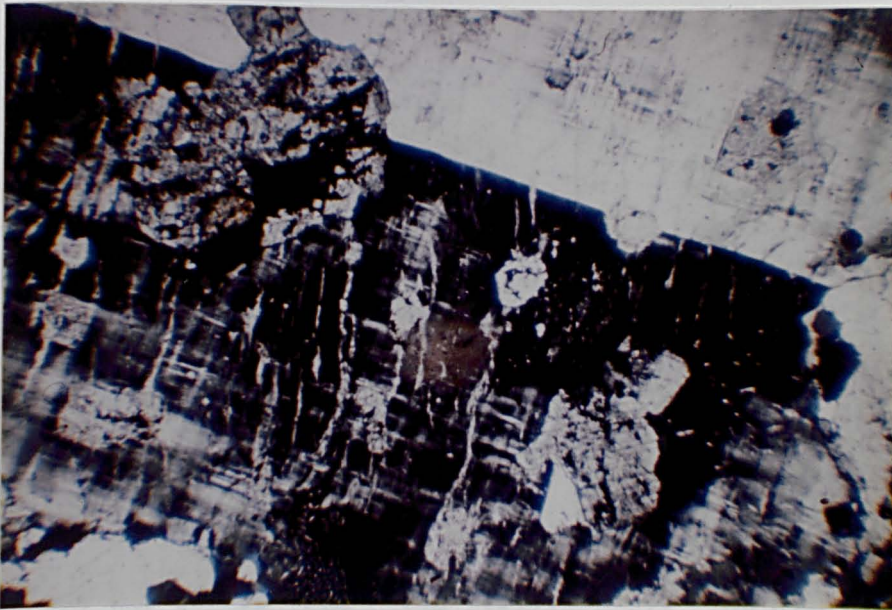
Homogeneous diatexite, Port Briac. (5 cm = 1 mm)

b: Mild cataclasis of the diatexite has resulted in the local development of a cataclastic fluxion structure and a protomylonite.

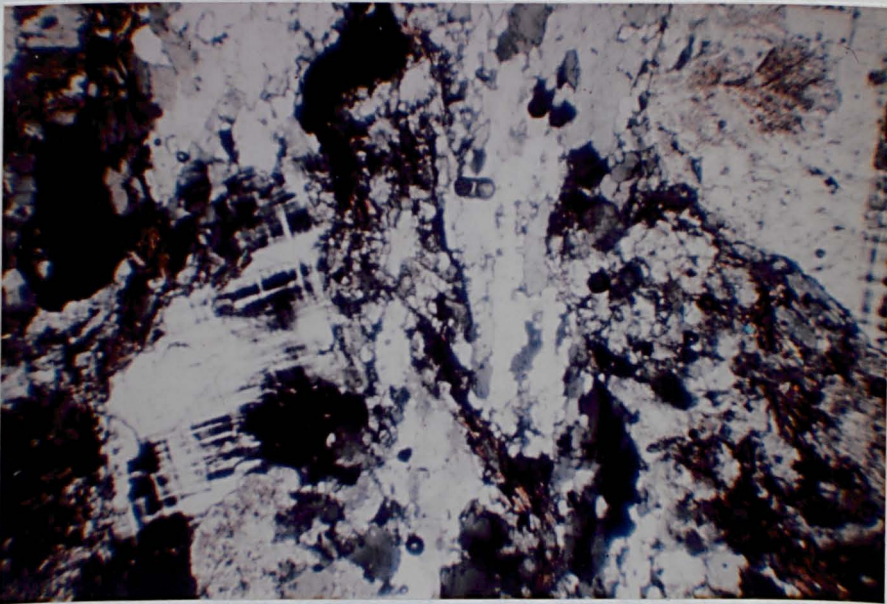
Homogeneous diatexite, Port Briac. (5 cm = 1 mm)

c: Garnet-quartz symplectite within poorly foliated granitic pod.

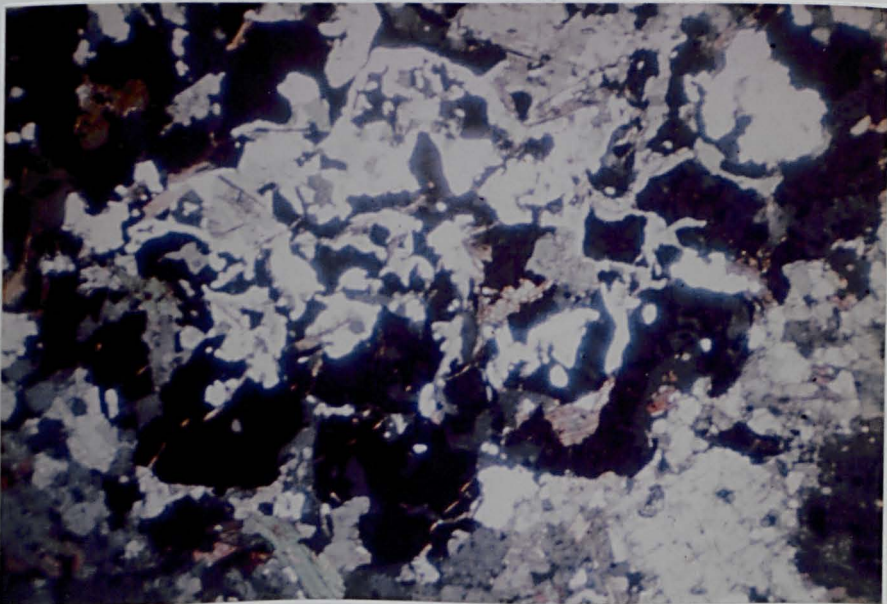
Foliated granite, west of pnte de Grouin. (5 cm = 3.5 mm)



Slightly serrated, ...



... ..



4. The Colombière Granite

The Colombière Granite (Figure II.7) is a medium grained cream to buff rock comprising plagioclase, microperthitic microcline, quartz, biotite and muscovite with minor amounts of zircon. The plagioclase is a sodic oligoclase (between An_{10} and An_{14}) which is sometimes zoned to albite, and rare albite. The grains are anhedral and equant in shape and from 1 mm to 3 mm across; they are extensively embayed by both microcline and quartz (see Plate III.11a & b). The plagioclase is often slightly sericitized; sometimes the central part of the plagioclase is partly replaced by flakes of muscovite (see Plate III.11c). On rare occasions myrmekite is developed in plagioclase at junctions with microcline. The microcline occurs as anhedral areas from 2 mm to 6 mm across and appears to be relatively late and replacive. It embays and replaces the plagioclase and contains inclusions of embayed plagioclase with albite rims which grade into the microcline. Both the characteristic cross hatched twinning and carlsbad twinning are present in the microcline; microperthite (string perthite and patch perthite) is common. Biotite (buff to red-brown) is present as individual flakes which are occasionally included in the microcline. Zircons with strong pleochroic haloes are contained within the biotites. There are rare flakes of muscovite within the rock; more commonly this mineral is located as a replacement feature in plagioclase cores (see Plate III.11c). Quartz occurs as anhedral grain aggregates up to 5 mm across, the grains have ubiquitous undulose extinction and strongly sutured grain boundaries. Quartz is lobate against plagioclase and frequently embays the plagioclase suggesting some replacement. There are drop-like inclusions of quartz within the plagioclase feldspar.

Plate III.11

a: Typical texture in the Colombière granite. Note the replacement of the plagioclase by both microcline and quartz.

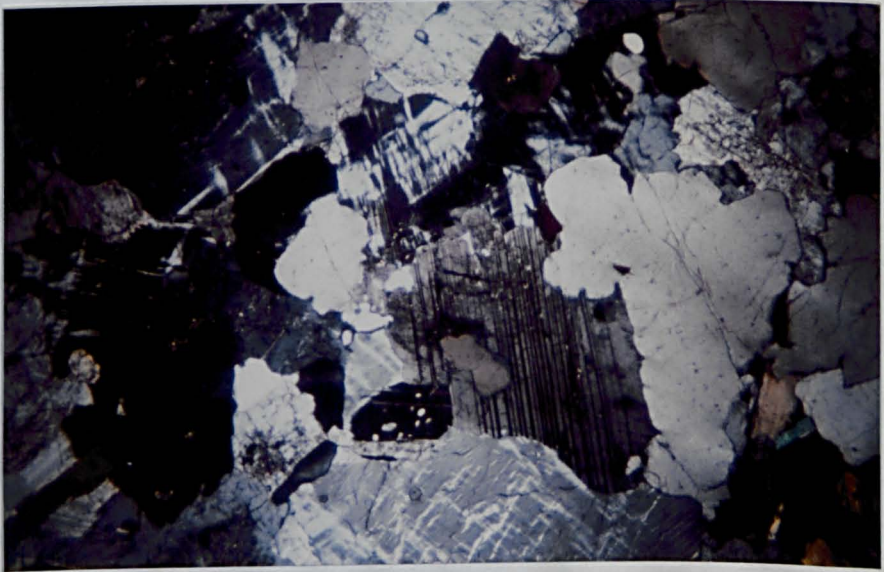
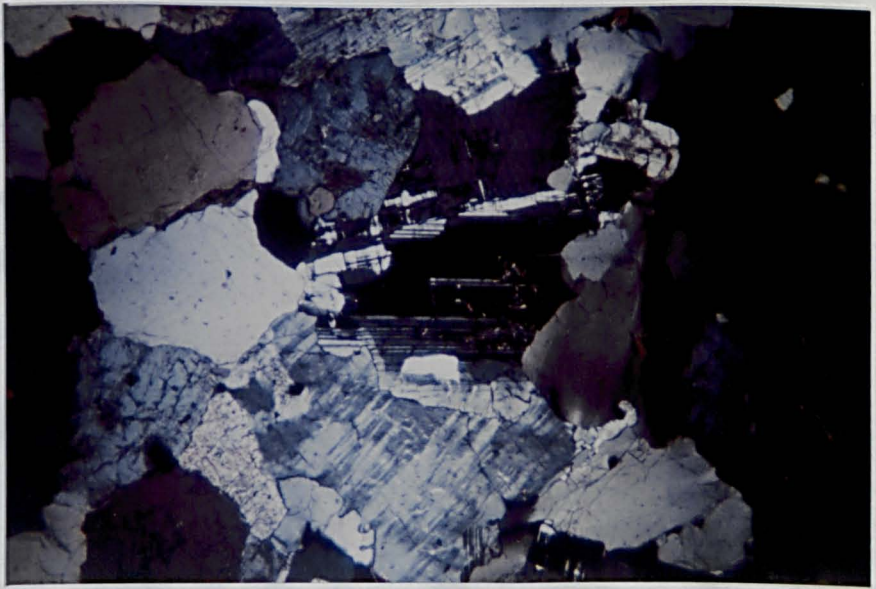
Colombière granite, Ile de la Colombière. (5 cm = 2.5 mm)

b: Typical texture in the Colombière granite. Note the replacement of the plagioclase by both microcline and quartz.

Colombière granite, Ile de la Colombière. (5 cm = 2.5 mm)

c: Muscovite flakes replacing the core of a plagioclase grain.

Colombière granite, Ile de la Colombière. (5 cm = 2.5 mm)



5. The Granitoid Sheets

Concordant and slightly discordant sheets of medium grained buff granite and (less commonly) coarse grained white granite pegmatite occur within the metatexites on the north-western side of the St. Malo migmatite belt.

The buff granites comprise plagioclase within the oligoclase range, microcline, quartz, biotite, muscovite and tourmaline with minor amounts of zircon and rutile (Plate III.12a). The plagioclase is present either as ragged laths up to 3 mm long or as equant grains between 1 mm and 2 mm across, albite twinning is commonly present. Its composition is sodic oligoclase (An_{10} to An_{18}); moderate sericitization is common. Some of the plagioclases are normally zoned to an albite rim. Both microcline and quartz have embayed the plagioclase and partially replaced it. Anhedral irregular areas of microcline, which is often microperthitic, enclose both plagioclase and quartz as inclusions. The microcline commonly has diffuse grain boundaries with both the plagioclase and the quartz and the overall texture, although partly obscured by mild cataclasis, suggests a relatively late and replacive origin. The biotite (straw yellow to deep red-brown) occurs as individual somewhat ragged flakes. Zircon, with strong pleochroic haloes, and rutile needles are included within the biotite. Muscovite is scattered through the rock as ragged flakes which sometimes penetrate the biotite. Fragmented tourmaline occurs in some of the granites, it is slightly zoned dravite (pale yellow to orange-yellow but with a green tint in the core). Irregular areas of quartz have strongly sutured grain boundaries and ubiquitous undulose extinction, occasionally large quartz crystals are partly polygonized into unstrained aggregates. Some of the quartz embays the plagioclase and is clearly relatively late and replacive.

The white granite pegmatites comprise plagioclase within the oligoclase range, microcline, quartz, muscovite and minor amounts of chlorite, zircon and rutile (Plate III.12b). The plagioclase, sodic oligoclase (An_{10} to An_{18}), may occur as laths up to 5 mm long but more commonly is present as equant grains about 2 mm across. It is moderately sericitized. The plagioclase has lobate embayments of both microcline and quartz; there is often a narrow albite rim separating the sodic oligoclase from the replacing microcline. Many of the plagioclases have blebs of quartz as inclusions. The microcline forms irregular anhedral areas which appear to be relatively late and replacive. Strong tartan twinning is ubiquitous but microperthite (string perthite and patch perthite) is only sporadically developed. Ragged muscovite flakes, often associated with the microcline and occasionally intergrown with the microcline, are scattered throughout the rock. There are rare flakes of chlorite (brownish-green) with inclusions of rutile and zircon. The quartz is interstitial forming anhedral grain aggregates with sutured grain boundaries and ubiquitous undulose extinction. Shallow lobes of quartz penetrate and replace the plagioclase.

Concordant to strongly discordant sheets of medium grained cream to buff trondhjemite occur within the metatexites and metasediments on the southern side of the St. Malo migmatite belt (exposed along the Rance south of Ia Richardais). They comprise plagioclase within the oligoclase range, quartz, biotite and muscovite with minor amounts of zircon (Plate III.12c). The equant plagioclase grains are from 0.5 mm to 2 mm across. They are calcic oligoclase in composition (from An_{22} to An_{30}) but variably developed twinning, slight zoning and undulose extinction (see Plate III.12c) often combine to render exact determination difficult. Combined carlsbad-albite twinning is common

Plate III.12

a: Typical texture of a granite sheet.

Granite, St. Jacut.

(5 cm = 2.5 mm)

b: Typical texture of a granite pegmatite sheet.

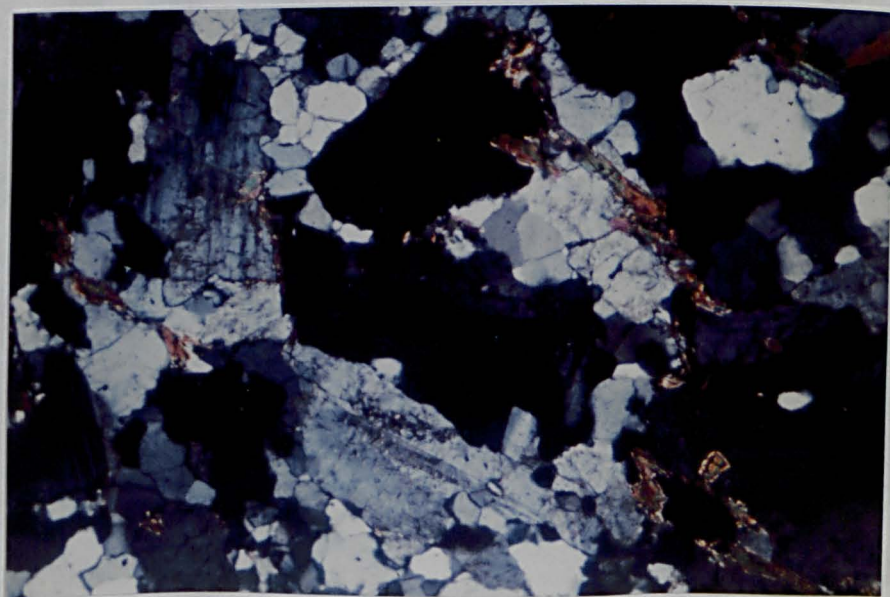
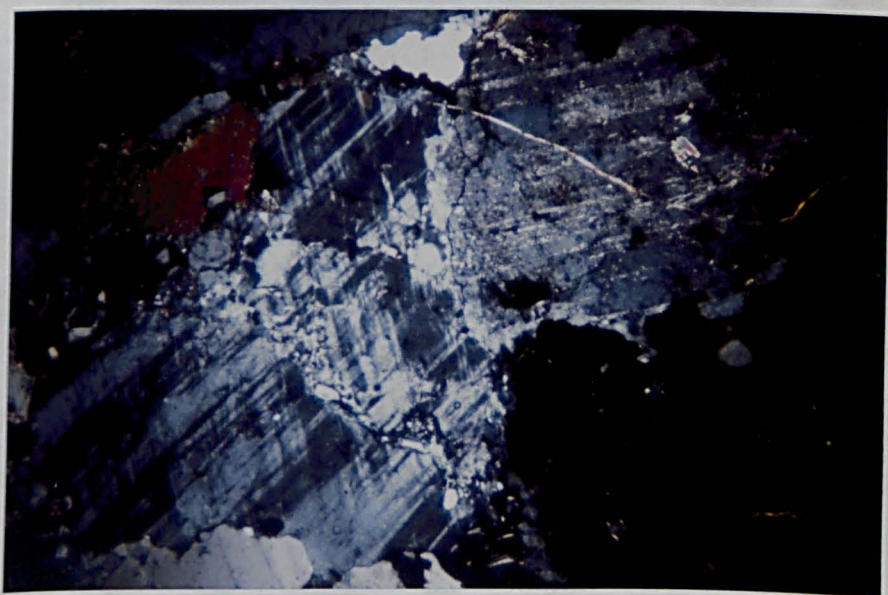
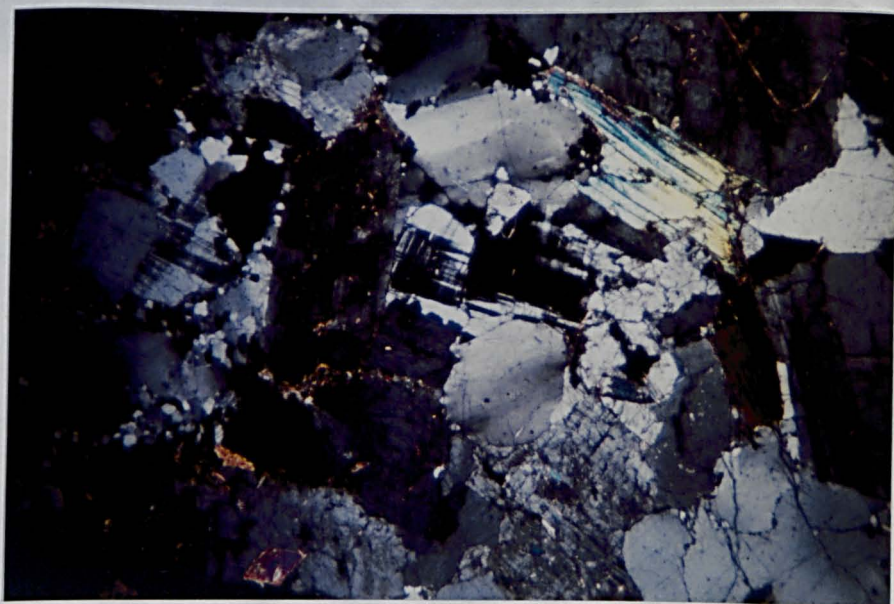
Granite pegmatite, Lancieux.

(5 cm = 2.5 mm)

c: Typical texture of a trondhjemite sheet.

Trondhjemite, le Minihic.

(5 cm = 1 mm)



whilst pericline twinning may also be present and completely untwinned grains do occur. Slight normal zoning is ubiquitous (from calcic oligoclase to middle oligoclase) whilst zoning to sodic oligoclase (An_{15} to An_{18}) may occur and on rare occasions slight oscillatory zoning (only 1 or 2% An) has been detected. There are numerous drop-like inclusions of quartz in the plagioclase. Ragged laths of biotite (buff or golden brown to brown or dark brown) between 0.05 mm and 0.5 mm in length are dispersed throughout the rock. They contain numerous inclusions of zircon in strong pleochroic haloes. There are a few small ragged muscovite flakes. Quartz is present in small (under 1 mm) polygonal aggregates with triple point junctions and slightly sutured grain boundaries in response to cataclastic deformation.

B. The Cataclastic Rocks

1. Plage de Quatre Vaux

It was evidence from this bay on the north-west side of the St. Malo migmatite belt (Figure II.3) that enabled Brown, Barber and Roach (1971) to demonstrate the Pentevrian age of the migmatites. The structural relationships between the rocks exposed at the two ends of the bay will be discussed in detail in Chapter V. Cataclasis has affected the diatexites which crop out on the south side of the Plage de Quatre Vaux and to the south. The diatexites are variably inhomogeneous with small to large biotite schlieren and sporadic mesoscopic patches of homogeneous diatexite or zones of metatexite. Even the apparently unshered medium grained buff granodioritic diatexites are seen to have suffered mild cataclasis when examined in thin section. This cataclasis is not sufficient to warrant the rocks

being termed protomylonites and the original textural relationships between the minerals are still apparent (see Plate III.13a). The rocks comprise plagioclase of variable composition within the oligoclase range, occasional microcline, quartz, biotite and muscovite with minor amounts of zircon, apatite and opaque ore and rare sillimanite and tourmaline. The plagioclase is generally middle oligoclase (from An_{18} to An_{22}) which may be slightly normally zoned to sodic oligoclase (from An_{15} to An_{18}); albite twinning is frequent. The shape of the plagioclase varies from rectangular to equant and the size from 1 mm to 5 mm in length. Drop-like inclusions of quartz are common within the plagioclase and there are infrequent biotite flakes included. Embayments of quartz invade and replace the plagioclase. Small grains of microcline microperthite (string perthite) with inclusions of plagioclase, biotite and quartz are occasionally present, often nucleated at quartz junctions, and become ubiquitous in the diatexites to the south of the bay. Biotite (straw yellow to orange brown) occurs as small flakes from 1 mm to 3 mm long with grains of ore in the cleavages and rare chlorite. Small schlieren comprising about a dozen flakes of biotite are frequent. Muscovite appears to replace the biotite and often grows through the biotite flakes at a low angle to the cleavage. It also occurs as ragged flakes intergrown with quartz in a symplectite. Anhedral quartz aggregates have strongly sutured grain boundaries and ubiquitous undulose extinction. They may be partly polygonised to relatively strain free aggregates. There are narrow irregular zones of movement within the rocks filled by fine quartz and sericite.

With increased cataclasis the rocks become protomylonites (Higgins, 1971) (see Plates III.13 and III.14). Porphyroclasts of plagioclase, rectangular to oblong in shape and from 1 mm to 4 mm in

length, lie within a thoroughly cataclastic fluxion structure (Plate III.13b & c). They are generally slightly sericitized, often have fine albite twin lamellae and invariably have undulose extinction. The twin lamellae may be kinked or cut by micro-faults (see Plate III.14a). The fluxion structure represents the movement zones within the rock and comprises a mixture of fine grained quartz, sericite and opaque ore. Some recrystallized biotite (straw yellow to dark brown) occurs within the foliation and random flakes of new muscovite cut across the fluxion structure. Frequent small subhedral grains of tourmaline (colourless to deep golden yellow-brown - dravite) are present in the foliation. The anhedral quartz aggregates of the diatexites are now represented by streaked out lenticular areas of fine grained polygonal quartz aggregates.

Further cataclasis resulting in more than 50% of the rock being broken down produces the mylonites (see Plate III.15). The large plagioclase porphyroclasts of the protomylonites become broken into smaller fragments which have often been rounded to oval shapes averaging 1 mm across. The matrix is similar to the protomylonites and comprises fine grained quartz, pale brown sericite and opaque ore. Compositional layering 0.2 mm thick may develop with quartz layers alternating with more micaceous layers to emphasise the cataclastic fluxion structure. Ultramylonite is occasionally produced. The ultramylonites have a few oval plagioclase porphyroclasts up to 1 mm across preserved within a finely laminated fluxion structure. Compositional layering from 0.1 mm to 0.4 mm thick defines the foliation.

Plate III.13

- a: Mild cataclastic texture superimposed upon a typical inhomogeneous diatexite texture.

Inhomogeneous diatexite, Plage de Quatre Vaux. (5 cm = 3.5 mm)

- b: Protomylonite with well developed cataclastic fluxion structure and rounded porphyroclasts of oligoclase feldspar.

Protomylonite, Plage de Quatre Vaux. (5 cm = 3.5 mm)

- c: Protomylonite with well developed cataclastic fluxion structure and large porphyroclasts of oligoclase.

Protomylonite, Plage de Quatre Vaux. (5 cm = 3.5 mm)

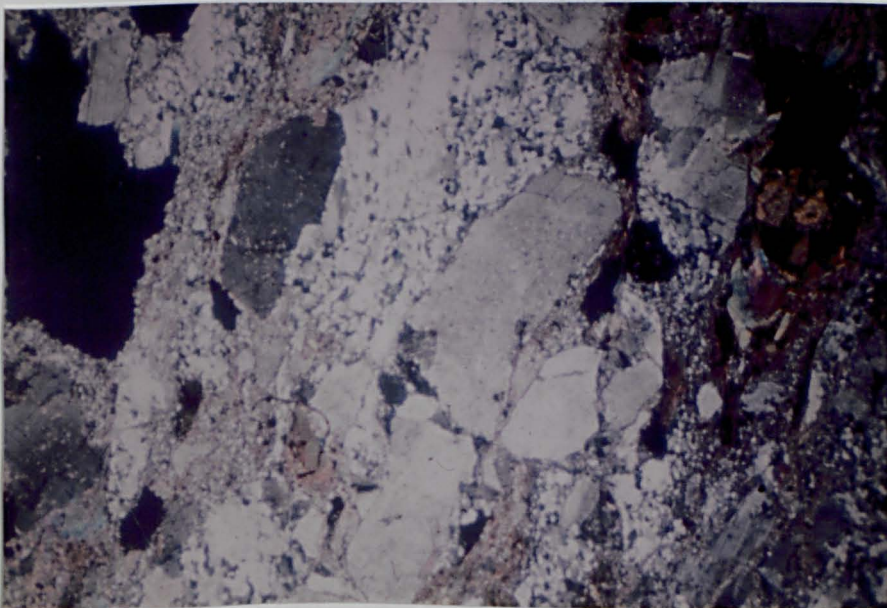
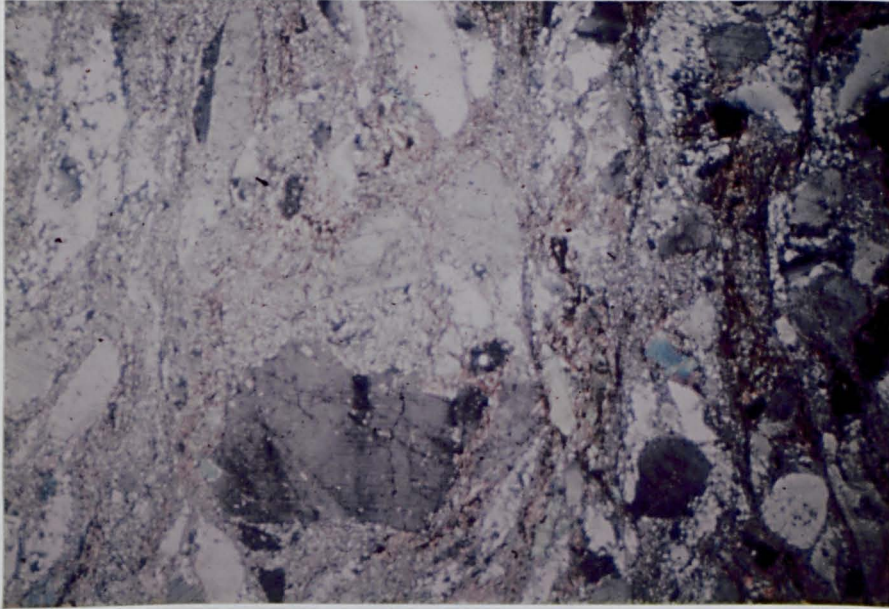
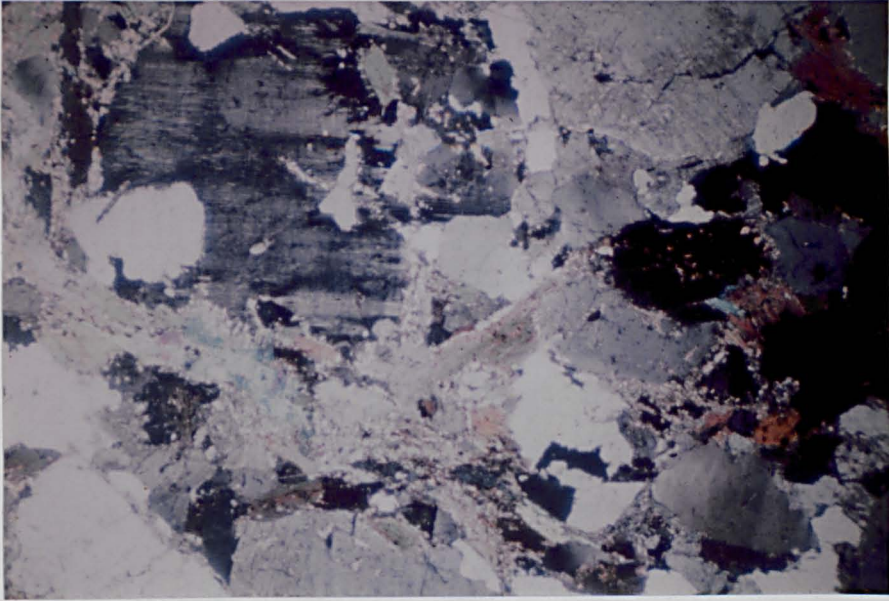


Plate III.14

- a: Plagioclase porphyroclast with fine deformation twin lamellae which have been kinked and cut by microfaults.
Protomylonite, Plage de Quatre Vaux. (5 cm = 1 mm)
- b: Porphyroclasts and grain aggregates within a cataclastic fluxion structure.
Protomylonite, Plage de Quatre Vaux. (5 cm = 1 mm)

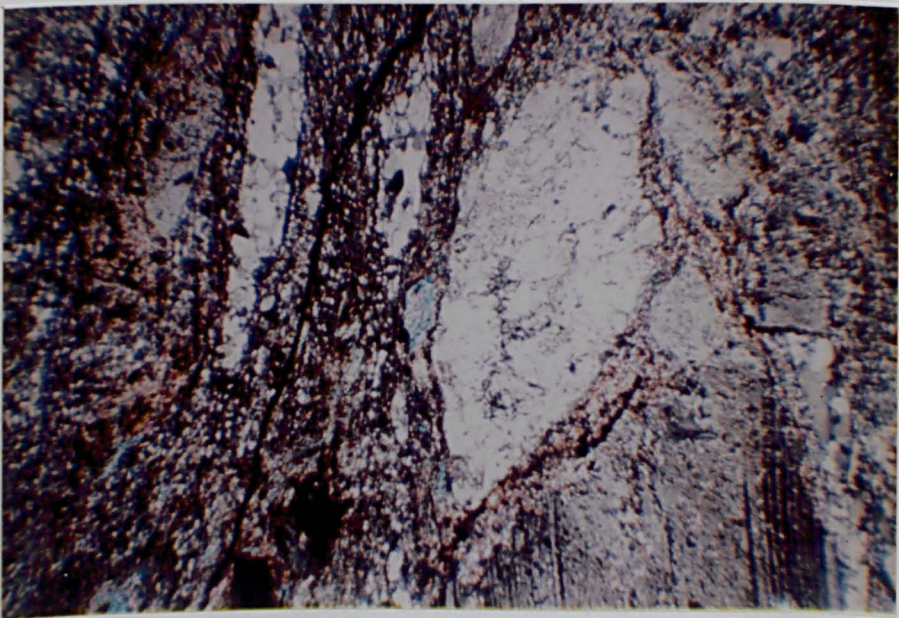
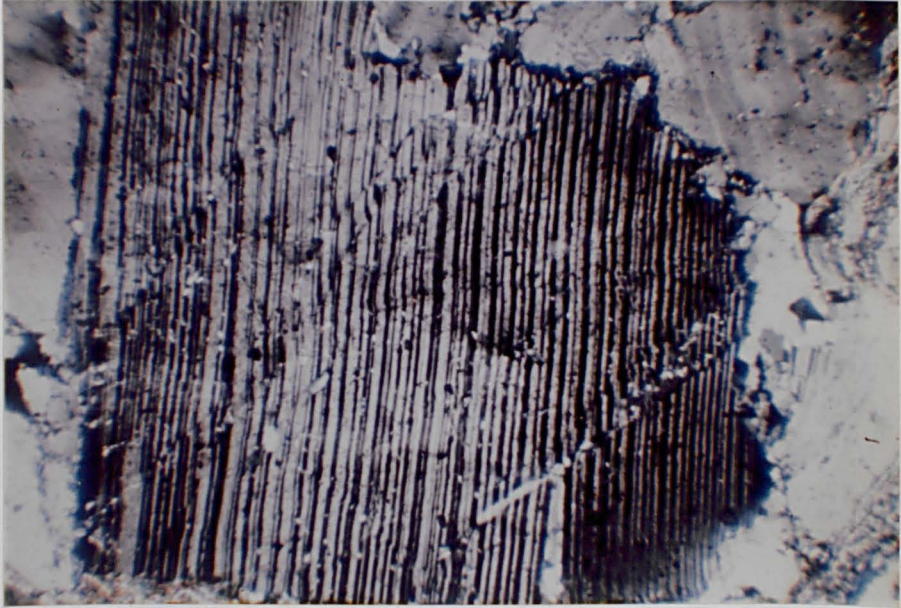


Plate III.15

- a: Cataclastic fluxion structure in mylonite. Large porphyroclasts are rare but when present are often highly strained.

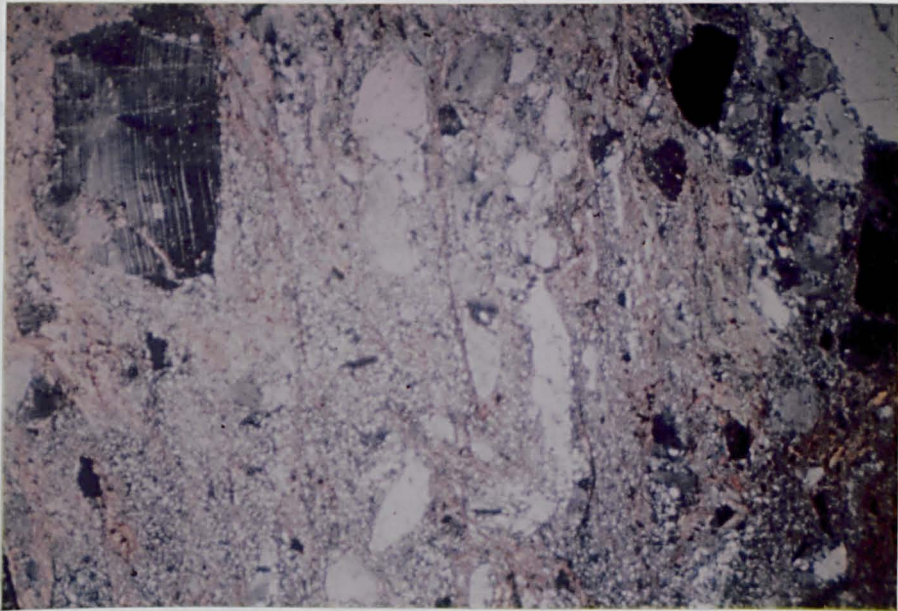
Mylonite, Plage de Quatre Vaux. (5 cm = 3.5 mm)

- b: Detail of the mylonite fluxion structure.

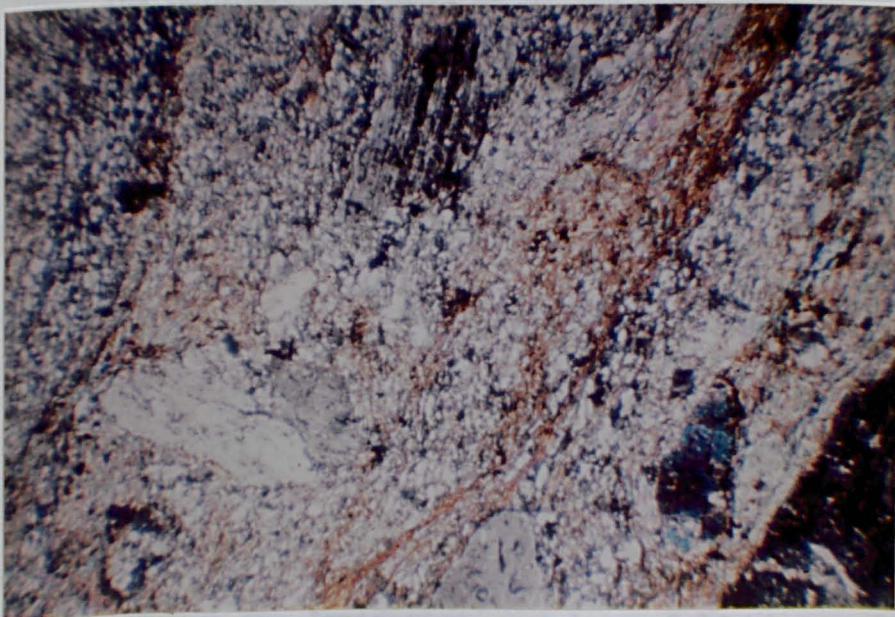
Mylonite, Plage de Quatre Vaux. (5 cm = 1 mm)

2. Pate de la Serpe

The general appearance of the rocks exposed around the pate de la Serpe is shown in figure 11 (see page 9).



The feldspar and quartz are the main constituents. The matrix is a fine-grained, crystalline rock with a granitic appearance. A folded face of a rock is visible. The flysch is situated above the cataclastic rocks in a zone close to the fold. The spatial relationships between these various units are complex - a summary has been presented above.



The texture is similar to that of the flysch, but the feldspar is more abundant. It has been transformed or where a crystalline cleavage is seen.

2. Pnte de la Garde

The general field relationships of the rocks exposed around the pnte de la Garde have been described in Chapter II (Section B). Multiply folded Pentevrian metasediments cut by narrow shear zones outcrop on the south-east side of the headland. A variety of cataclastic rocks outcrop in the central part and on the north-west side of the headland. These cataclastic rocks within the pnte de la Garde shear belt may be grouped into four varieties: mylonite gneisses with preserved augen of metatexite and diatexite; dark grey-green mylonite schists with red garnet and cream feldspar porphyroclasts; grey mylonite schists some of which contain large retrogressed porphyroclasts after garnet(?); and buff to grey mylonite schists with cream feldspar and sometimes red garnet porphyroclasts. The cataclastic rocks are cut by white tourmaline granite sheets which have a folded form and a cataclastic fabric. The fluxion structure within the cataclastic rocks is axial plane to the folded granite sheets. The spatial relationships between these various mylonite schists are complex - a summary has been presented above (Chapter II, p.26). The deformational history of the shear zone will be considered later (Chapter V).

The Pentevrian metasediments comprise semi-pelitic schists with thin psammite ribs. They generally show mild effects of cataclastic deformation but in shear zones may be transposed to mylonite schists. The least cataclased metasediments (Plates III.16 and III.17) have a grain size of between 0.05 mm and 0.1 mm although muscovite flakes may exceed this limit by a factor of 10. A metamorphic foliation generally parallels the lithological lamination except in early fold hinges, where it may cut the lamination, and later fold hinges where the foliation has been transposed or where a crenulation cleavage has been

developed. The metamorphic foliation is defined by small flakes of biotite (colourless or pale straw yellow to golden brown or brown) and muscovite, which may be considerably larger than the biotite. Quartz often exhibits a slight dimensional preferred orientation in the foliation plane and frequently tends towards a granoblastic polygonal texture; undulose extinction is frequent. Small untwinned feldspar grains are scattered throughout the rocks. Opaque ore, the apatite and zircon are present in small amounts.

The augen of metatexite and diatexite within the mylonite gneisses clearly demonstrate the parent lithology of some of the cataclastic rocks within the shear belt. The mylonite gneiss has a strong fluxion structure defined by recrystallized biotite and muscovite (Plate III.18b). These micaceous layers 'flow' around porphyroclasts of plagioclase feldspar and quartz aggregates (Plate III.18b). The biotite (colourless or pale straw yellow to orange-brown or brown) occurs as small flakes up to 0.25 mm long which are often in layers two or three biotites thick. Small muscovite flakes up to 0.15 mm long are associated with the biotite layers. The micaceous layers and schlieren of the migmatites have been completely transposed by the new foliation of the mylonite gneiss. Porphyroclasts of plagioclase feldspar within the oligoclase range frequently have narrow multiple twin lamellae and slight undulose extinction in response to the deformation; a few appear to have oscillatory zoning. The original rectangular to equant shape of the feldspar has generally been preserved. The porphyroclasts are commonly between 0.5 mm and 1 mm across but clasts up to 3 mm long have been observed. Recrystallized quartz with straight to slightly curved grain boundaries meeting in triple point junctions infills pressure shadow areas associated with the plagioclase porphyroclasts. The quartz in augen-like aggregates

also has straight to slightly curved grain boundaries which meet in triple point junctions although a fine suturing has often been superimposed on the grain boundaries. Folded quartz veins some 5 mm thick comprise dimensionally orientated grains parallel to the cataclastic fluxion structure and axial planar to the folds. Subhedral equidimensional crystals of tourmaline (pale yellow to dark yellow or yellow-brown - dravite) up to 1 mm across are ubiquitous within the mylonite gneisses. There are rare perthite porphyroclasts and some neomineralization of microcline which may replace quartz. Fine prismatic sillimanite enclosed within muscovite (Plate III.18a) may occur in the less deformed augen of metatexite. There are minor quantities of zircon, opaque ore and apatite.

The dark grey-green mylonite schists which carry red garnet and cream feldspar porphyroclasts are of uncertain parentage. The distinctive features of this lithology are the frequent red garnets or garnet aggregates in hand specimen and the blue-green amphibole lying within the foliation in thin section (Plate III.19). These grey-green mylonite schists exhibit a well developed fluxion structure defined by green chlorite and brown biotite which has been overgrown by blue-green amphibole. The chlorite (colourless or pale green to green) exhibits anomalous interference tints and is length slow. It is probably pennine. Biotite (colourless or straw yellow to brown or dark brown) occurs as discrete flakes some of which have been partly replaced by the chlorite. The amphibole (α = very pale green, β = green and γ = blue-green - hornblende) occurs as subhedral to euhedral stumpy crystals about 0.5 mm across which have neomineralised after the chlorite and biotite. The cream feldspar porphyroclasts are plagioclase of oligoclase-andesine composition with narrow multiple twin lamellae and undulose extinction (Plate III.19c). They vary in

shape from rectangular to oval according to the degree of cataclasts and are up to 2.5 mm in length. The red garnet porphyroclasts are seen to be either cracked and slightly broken or aggregates of broken garnet fragments (see Plate III.19a). The porphyroclasts are generally up to 2 mm across but the aggregates of garnet fragments may be up to 6 mm across. The aggregates of garnet fragments are associated with replacive chlorite and occasionally quartz, biotite and opaque ore. There are rare small equidimensional grains of tourmaline (yellow to yellow-brown - dravite), stumpy apatite grains, large zircons and grains of opaque ore within these mylonite schists. Quartz is present throughout the rock as small polygonally recrystallized aggregates with straight grain boundaries and triple point junctions.

The grey mylonite schists, some of which carry large retrogressed porphyroclasts, were probably derived from a metasedimentary or metatextitic parent sequence. Medium sized porphyroclasts of plagioclase feldspar are set in a finer biotite + quartz + chlorite matrix with fluxion structure. The plagioclase porphyroclasts of oligoclase composition show combined carlsbad-albite twinning and vary in shape from rectangular, up to 4 mm in length, to round (averaging 1 mm across). The cataclastic fluxion structure is defined by the orientation of pennine (yellow-green to green) and biotite (pale buff to orange-brown or red-brown) flakes. Quartz grains of irregular shape and averaging 0.1 mm across have sutured grain boundaries and undulose extinction. Some of the grey mylonite schists carry dark grey ovoid retrogressed porphyroclasts up to 10 mm in length. They comprise a mat of pale coloured brown-green chlorite with minor amounts of biotite, opaque ore, muscovite and occasional clinozoisite (Plate III.19b). Small broken fragments of garnet are present in some of the chlorite mats suggesting that they represent pseudomorphs after garnet.

Buff to grey mylonite schists outcrop on the north-west side of pnte de la Garde. They carry prominent cream feldspar porphyroclasts and, in places, prominent red garnet porphyroclasts. The feldspar porphyroclasts and slightly sericitized oligoclase with both albite and albite-pericline twinning and undulose extinction. They vary in shape from rectangular (up to 5 mm in length) with quartz aggregates in pressure shadows at the ends through oval shaped clasts (average 3 mm in length) to rounded clasts (from 1 mm to 2 mm across) depending upon the degree of cataclasis. The plagioclase porphyroclasts lie in a fluxion structure comprising small flakes (average 0.2 mm long) of biotite (pale straw yellow to red-brown) and oblong grains of quartz (between 0.1 mm and 0.5 mm in length) which have sutured grain boundaries. Chlorite occasionally replaces some of the biotite but is more commonly present as small knots of pale green pennine which displays anomalous interference tints. Garnet occurs as porphyroclasts (average 1.25 mm diameter) in some specimens but in others it is associated with the chlorite knots together with some biotite and opaque ore suggesting some replacement. There are minor amounts of late muscovite, apatite and zircon.

The white tourmaline granite sheets separate two episodes of deformation within the pnte de la Garde shear belt since they cross cut the fluxion structure but are themselves mylonite schists (see the more detailed discussion in Chapter V). Large porphyroclasts of subhedral tourmaline (pale yellow-green to pale green cores with pale green-yellow to yellow-brown rims) up to 6 mm in length have been fractured and sometimes fragmented by the cataclasis. They are set in a finer matrix of ribbon-like quartz with sutured grain boundaries and undulose extinction and minor irregular feldspar grains of indeterminate composition (see Plate III.20).

Plate III.16

a: Some disruption of layering and transposition of foliation in semi-pelite by mild cataclasis.

Pentevrian metasediments, pnte de la Garde. (5 cm = 1 mm)

b: Conjugate kink folds affecting the micaceous foliation in semi-pelite.

Pentevrian metasediments, pnte de la Garde. (5 cm = 1 mm)

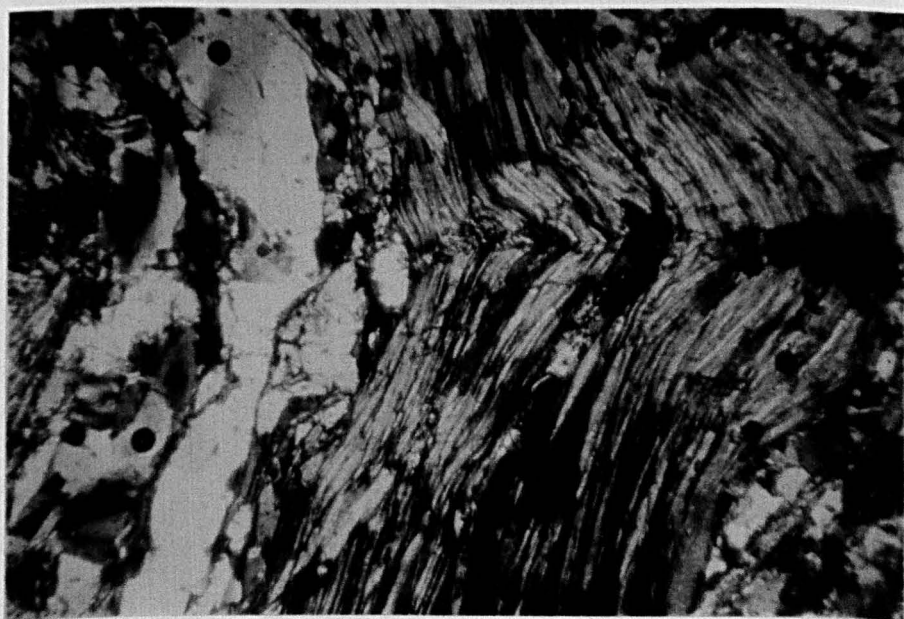
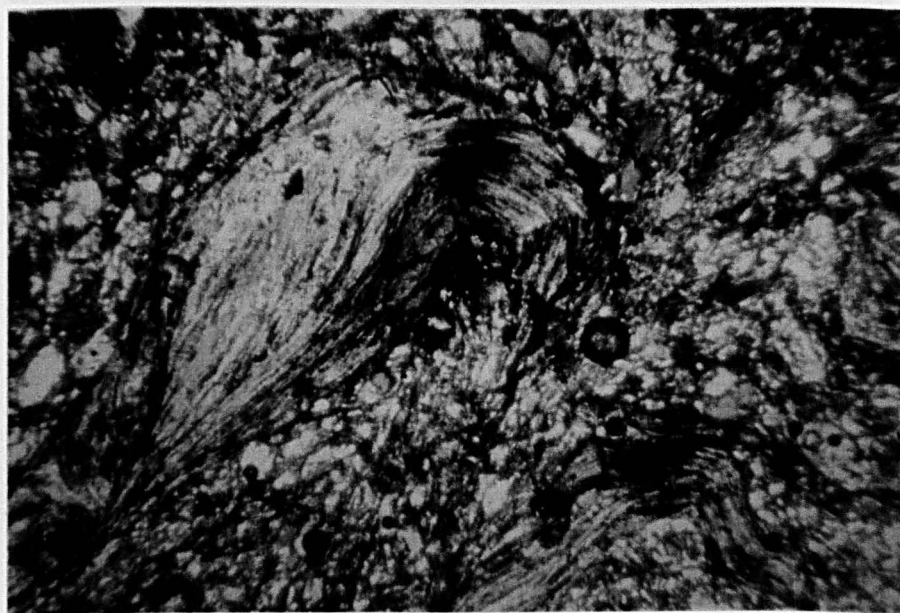


Plate III.17

a: Mildly cataclased semi-pelite.

Pentevrian metasediments, pnte de la Garde. (5 cm = 1 mm)

b: Mildly cataclased semi-pelite.

Pentevrian metasediments, pnte de la Garde. (5 cm = 1 mm)

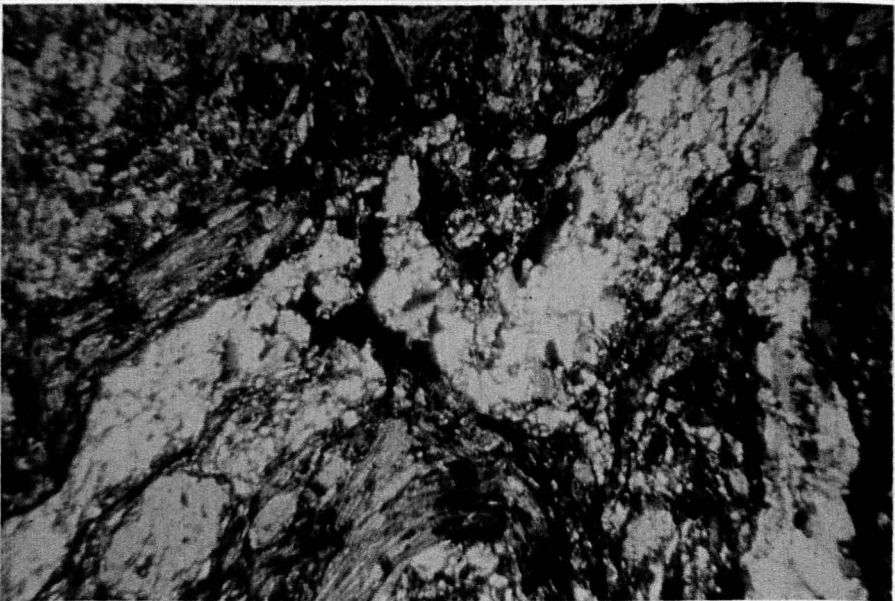


Plate III.18

a: Needles of prismatic sillimanite within large muscovite flake from preserved augen of inhomogeneous diatexite within mylonite gneisses.

Mylonite gneiss, pnte de la Garde. (5 cm = 1 mm)

b: Typical mylonite gneiss texture.

Mylonite gneiss, pnte de la Garde. (5 cm = 1 mm)

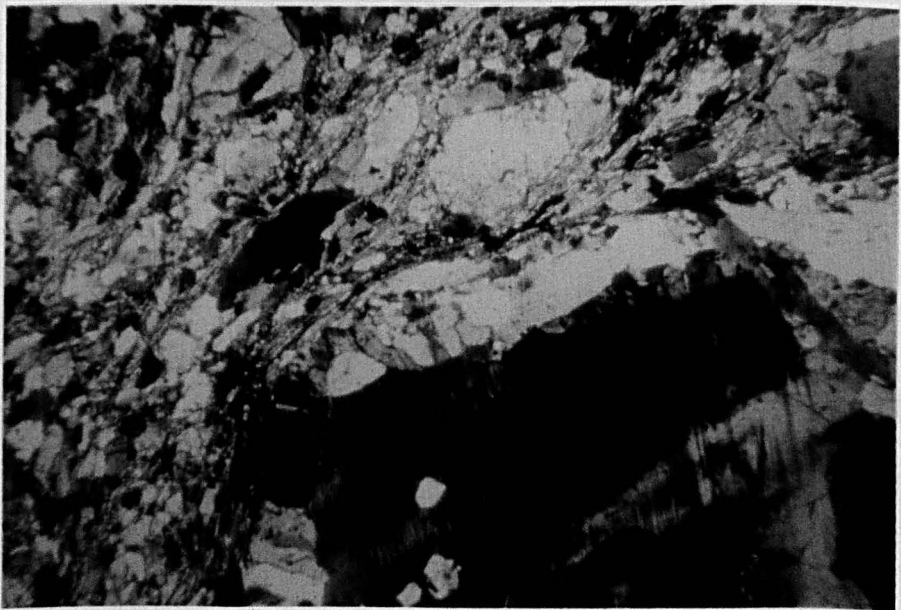
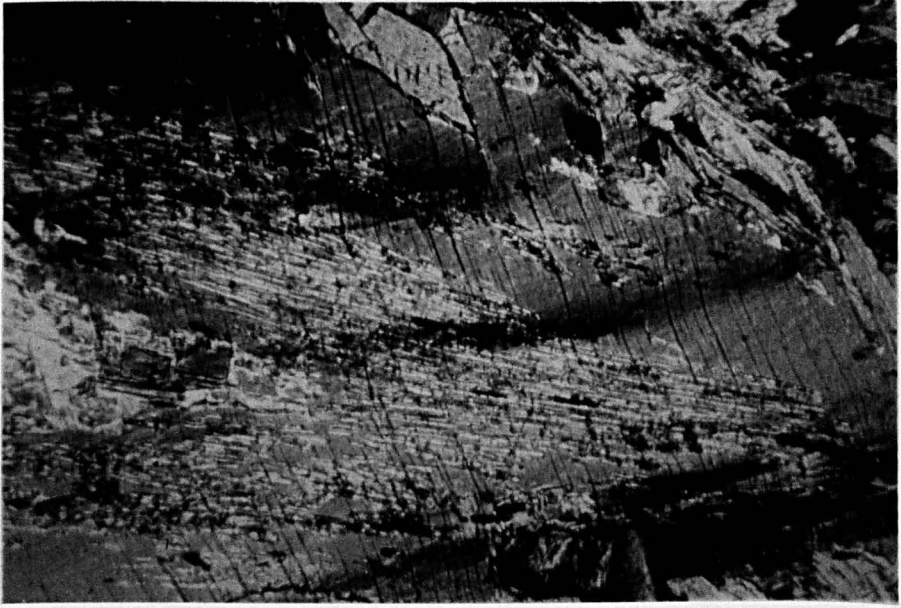


Plate III.19

- a: Mylonite schist with porphyroclasts of garnet and plagioclase within a mica + amphibole cataclastic fluxion structure.

Mylonite schist, pnte de la Garde. (5 cm = 3.5 mm)

- b: Mylonite schist with numerous plagioclase porphyroclasts and large mica + chlorite aggregates possibly as pseudomorphs after garnet.

Mylonite schist, pnte de la Garde. (5 cm = 3.5 mm)

- c: Detail of mylonite schist to illustrate the neomineralisation of amphibole.

Mylonite schist, pnte de la Garde. (5 cm = 1 mm)

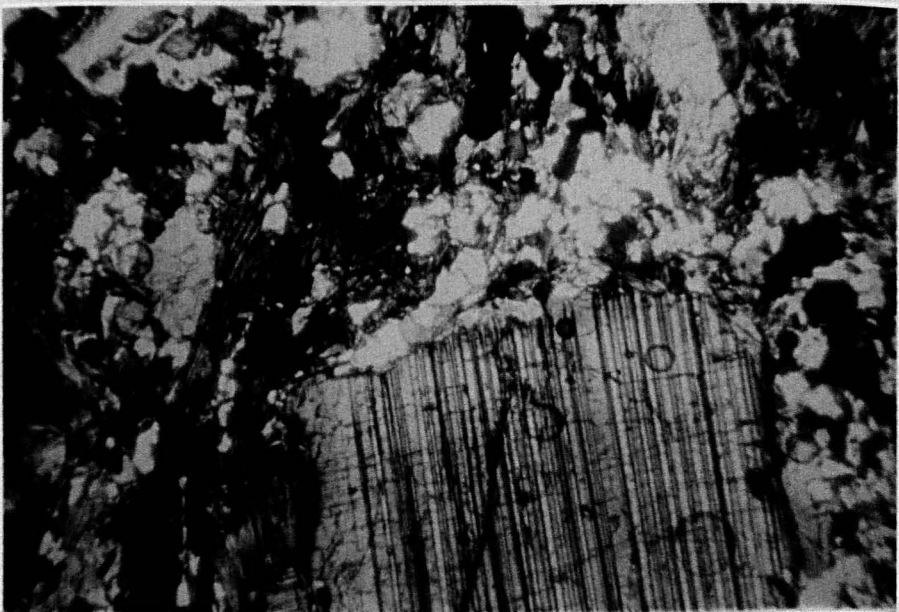
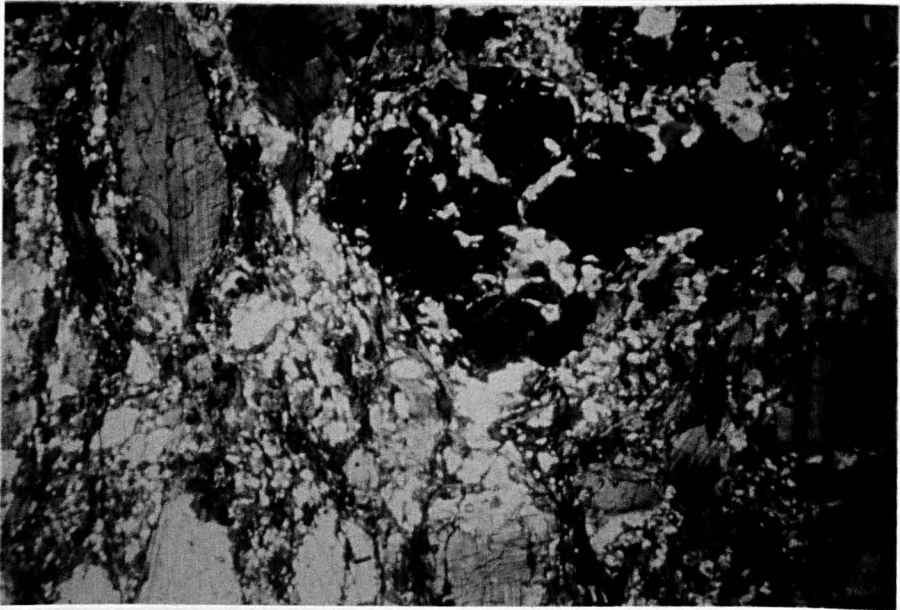


Plate III.20

a: Typical texture of the sheared tourmaline granites -
now mylonite schists.

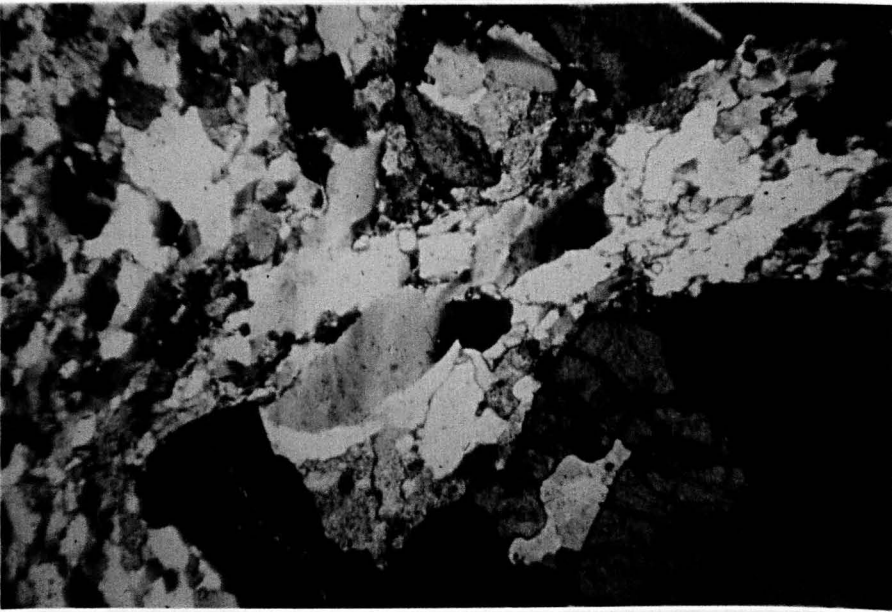
Mylonite schist, pnte de la Garde. (5 cm = 1 mm)

b: Cataclastic fluxion structure and tourmaline
porphyroclasts in sheared tourmaline granite - now
mylonite schist.

Mylonite schist, pnte de la Garde. (5 cm = 3.5 mm)

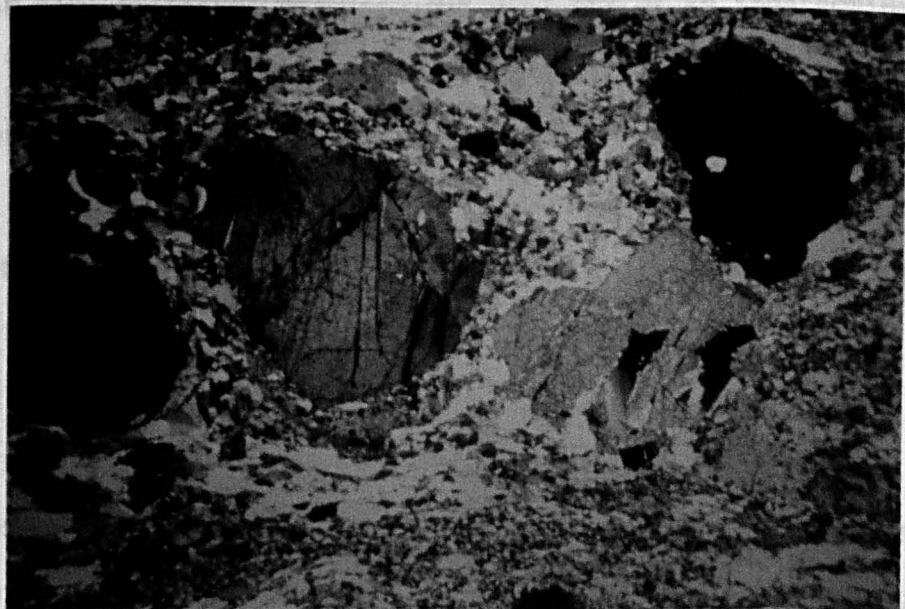
C. The Brioverian Supracrustal Rocks

The B
Quatre Yau
of proxima
with occas
northern s
In thin se
quartz cla
to a lesse
angular to



aggregates and fine grained poly-crystalline aggregates. The clasts
have an approximate length to breadth ratio of 2:1 and range in size
from 1 um to 4 um long. The (red-brown) quartz grains in the quartz
aggregates have ubiquitous undulatory extinction, strongly sutured grain
boundaries and are sometimes partly polygonal and unstrained
aggregates. The fine grained poly-crystalline aggregates may be graphic
granite of

nature.
amounts of
twinning
from 0.4
crystalline
of crystal
although
(colourless
zircons w



the biotite flakes were... accordingly the finer grained quartz... better schistosity... Anhydral quartz

C. The Brioverian Supracrustal Rocks

The Brioverian metasediments which outcrop between Plage de Quatre Vaux and Plage de Pen Guen (Figure II.3) comprise a sequence of proximal turbidites in the north and a sequence of semi-pelites with occasional psammite layers in the south. The turbidites of the northern part of the outcrop are dominated by the graded division. In thin section the turbidites consist of rock fragments, feldspar and quartz clasts, and a fine grained matrix in which biotite, quartz and, to a lesser extent, feldspar are prominent (see Plate III.21). The angular to poorly rounded rock fragments are of two main kinds: quartz aggregates and fine grained polycrystalline aggregates. The clasts have an approximate length to breadth ratio of 2:1 and range in size from 1 mm to 4 mm long. The individual quartz grains in the quartz aggregates have ubiquitous undulose extinction, strongly sutured grain boundaries and are sometimes partly polygonized into unstrained aggregates. The fine grained polycrystalline aggregates may be graphic granite or fine schistose material but most are of an indeterminate nature. The feldspar clasts are mainly oligoclase but there are small amounts of alkali feldspar often with the cross hatched microcline twinning. The feldspar clasts vary from angular to oval in shape and from 0.4 mm to 2 mm in long dimension. The fine grained matrix has crystallized to a metamorphic mineralogy and texture with a high degree of crystallinity and a grain size of between 0.02 mm and 0.1 mm, although some biotite laths may reach 0.2 mm in length. Biotite (colourless or straw yellow to dark tan or brown) contains abundant zircons with surrounding pleochroic haloes. It is the orientation of the biotite flakes which defines the schistosity seen in the field, accordingly the finer grained parts of the graded units carry the better schistosity (see Plate III.21 and Chapter II). Anhedral quartz

Plate III.21

a: The coarse grained base of a graded division from the thick turbidite units within the Brioverian supracrustal sequence.

Brioverian, pnte du Bay. (5 cm = 1 mm)

b: The fine grained top of a graded division from the thick turbidite units within the Brioverian supracrustal sequence. Notice that there is a well developed biotite schistosity.

Brioverian, pnte du Bay. (5 cm = 1 mm)

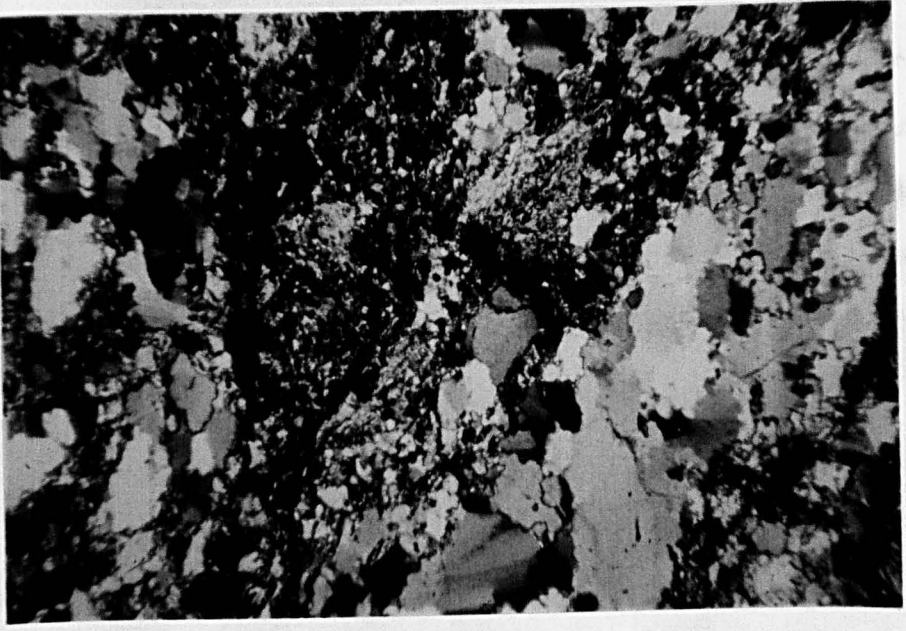
c: The middle part of a graded division from the thick turbidite units within the Brioverian supracrustal sequence.

Brioverian, pnte du Bay. (5 cm = 1 mm)

and with
other
epidote
metamorphic
metasand
greenish

the
bits of
igneous
granite

D. The



pegmatite

Plage

The

tourmaline

4 mm to

occasional

zircon

lobate

(An₇)

which are strongly

pressure

have

quarters

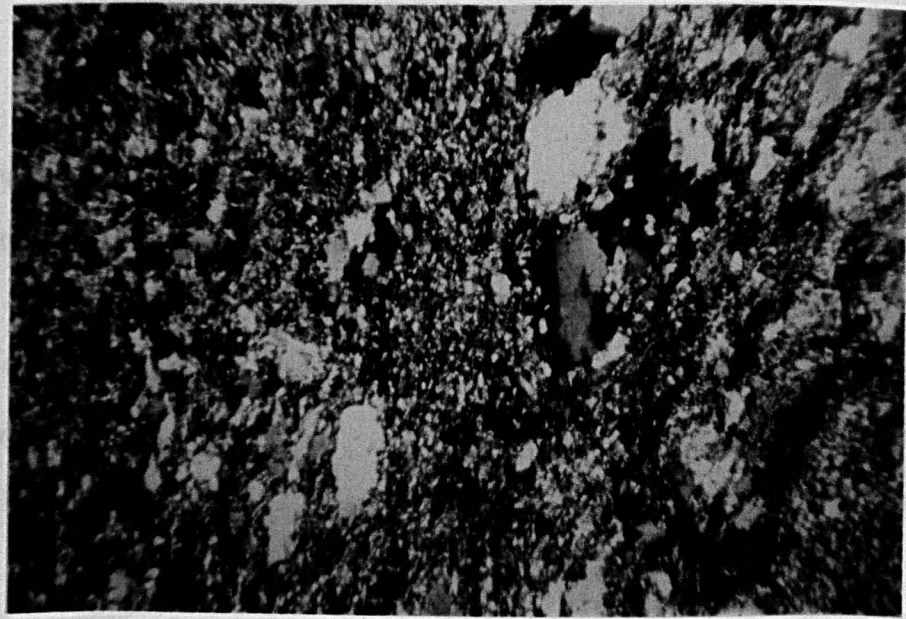
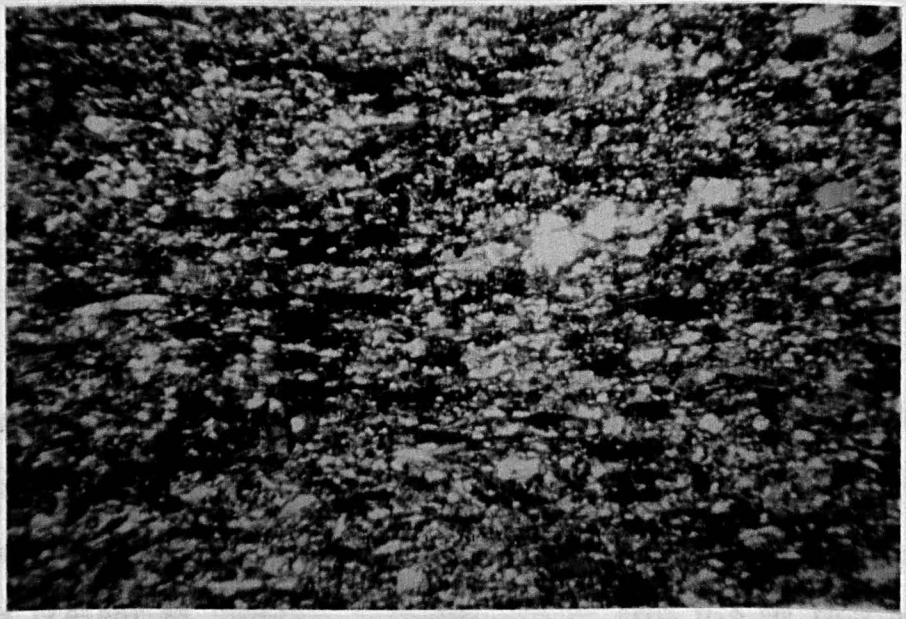
uniquely

character

boundaries

the

show



and anhedral untwinned feldspar of indeterminate composition are the other prominent minerals in the matrix together with minor amounts of epidote (epidote sensu stricto with infrequent clinozoisite and rare metamict allanite), opaque ore and infrequent topaz. The Brioverian metasediments in this area were subjected to metamorphism under greenschist facies conditions.

D. The Cadomian Igneous Rocks

Boudinaged white tourmaline granite sheets and grey granite pegmatite sheets occur within the Brioverian metasediments north of Plage de Quatre Vaux (Figure II.8).

The tourmaline granites comprise microcline, albite, quartz, tourmaline and muscovite. The microcline occurs as anhedral areas from 4 mm to 8 mm across with variably developed tartan twinning and occasional microperthite (string perthite). There are inclusions of albite and drop-like quartz; occasionally the microcline is strongly lobate against the albite which it appears to replace. The albite (An_7) is present as sporadic anhedral grains from 0.5 mm to 1 mm across which are strongly embayed by quartz; fine albite twinning is generally present (see Plate III.22a). Quartz grains average 1 mm across and have an irregular anhedral form. Quartz clearly replaces albite. Quartz-quartz grain boundaries are lobate; undulose extinction is ubiquitous and deformation bands are often developed in the strained quartz. Fine granular quartz is commonly present along grain boundaries reflecting mild cataclastic deformation which accompanied the extension and boudinage. Subhedral to anhedral grains of tourmaline (colourless or very pale grey-green to pale grey-green, a yellow-green

Plate III.22

a: Typical tourmaline granite texture.

Tourmaline granite, Plage de Quatre Vaux. (5 cm = 2.5 mm)

b: Microcline with veins of albite.

Granite pegmatite, Plage de Quatre Vaux. (5 cm = 2.5 mm)

or yellow-brown, but may be present in 0.1 mm to 0.5 mm across
scattered throughout the matrix. They are commonly broken with quartz
filling the cracks.

present
response

The
perthite
microclines
several
forming
Plate 1



included. In some specimens, however, a regular array of parallel
slits may be seen in the matrix. They are usually
perpendicular to lines of reflective quartz. In some cases, the
various elements occur within the same field of view as
interstitial aggregate. Quartz grains are commonly
the commonest extraction is always present. The quartz is
found along grain boundaries and is often well developed. Quartz
ragged



of
from a variety

or yellow-brown core may be present) from 0.5 mm to 2.5 mm across are scattered throughout the granite. They are commonly broken with quartz filling tension cracks. Ragged flakes of muscovite are occasionally present. Sericite occurs along many of the grain boundaries in response to the mild cataclasis.

The granite pegmatites comprise large crystals of microcline perthite, quartz, sporadic albite, muscovite and rare tourmaline. The microcline perthite may occur up to 30 cm in length and is commonly several centimetres in length. It has the characteristic tartan twinning and contains exsolved veins of twinned albite as perthite (Plate III.22b) together with albite, quartz and muscovite as inclusions. In less pegmatitic examples irregular anhedral grains of albite with fine twin lamellae are present. They are commonly penetrated by lobes of replacive quartz. Anhedral grains of quartz of variable dimension occur within the microcline perthite and as interstitial aggregates. Quartz-quartz grain boundaries are lobate and undulose extinction is always present. Fine granular quartz is common along grain boundaries reflecting mild cataclasis. Sporadic ragged flakes of muscovite may be present.

The Feldspars

Alkali feldspar

The alkali feldspars from the various rock types comprising the St. Malo migmatite belt exhibit variable development of microcline 'cross-hatched' twinning and the occasional development of micro-perthite. 14 alkali concentrates were separated from a variety of rock

types from the St. Malo belt and analysed by X-ray diffraction to determine their structural state. The techniques employed have been summarised briefly in Chapter I and are similar to those recommended by Wright and Stewart (1968). The diffraction data discussed below are given in Table III.1.

In Figure III.1 the St. Malo alkali feldspars (14 K-feldspar phases and 5 perthitic Na-feldspar phases) are shown plotted on the 2θ (060) - 2θ ($\bar{2}04$) diagram of Wright (1968). The majority of the K-feldspar phases plot around the low structural state position of pure KAlSi_3O_8 (maximum microcline) and have a structural state similar to the Spencer U feldspar (Wright, op.cit.). Three of the K-feldspar phases plot between the maximum microcline - low albite and the orthoclase series and have a structural state similar to the Spencer B feldspar (Wright, op.cit.). The Na-feldspar of the perthitic intergrowths have a structural state intermediate between low albite and albite III (Wright, op.cit.). The co-existing K-feldspar phases and Na-feldspar phases have similar structural states with the sole exception of specimen 701 where slight disequilibrium between the structural states of the two phases might reflect included remnants of replaced plagioclase.

Two measures of structural state of the potassic phase in these microcline perthites are used to supplement the initial comparison with standard feldspars given in the previous paragraph. The first measure of structural state is the degree of triclinicity or obliquity which is defined by Goldsmith and Laves (1954) as:

$$\Delta = 12.5 \{d(131) - d(\bar{1}\bar{3}1)\}$$

The maximum separation between the (131) and ($\bar{1}\bar{3}1$) peaks is about 0.08 Å yielding an obliquity of 1.00 which corresponds to triclinic

Table III.1

Summary of the X-ray diffraction data for 14 alkali feldspars from the St. Malo belt (comprising 14 K-feldspar of which 5 show albite on the diffractograms (perthitic intergrowths)).

Specimen 309: inhomogeneous diatexite, le Guildo.

Specimen 761: metatexite, pnte de la Garde Guérin.

Specimen 207: inhomogeneous diatexite, road cutting, la barrage.

Specimen 210: inhomogeneous diatexite, quarry, Montagne St. Joseph.

Specimen 701: homogeneous diatexite, St. Jacut.

Specimen 704: inhomogeneous diatexite, St. Jacut.

Specimen 708: granite sheet, St. Jacut.

Specimen 745: granite pegmatite sheet, Lancieux.

Specimen 746: granite sheet, Lancieux.

Specimen 757: inhomogeneous diatexite, Ile des Hébihens.

Specimen 346: Colombière granite, la Nellière.

Specimen 360: Colombière granite, Ile de la Colombière.

Specimen 758: homogeneous diatexite, St. Briac.

Specimen 759: inhomogeneous diatexite, pnte de la Garde Guérin.

K - FELDSPAR

	$2\theta(\bar{2}01)$	$2\theta(060)$	$2\theta(\bar{2}04)$	Δ	δ	TYPE
309	20.87	41.76	50.69		0.391	I
761	20.90	41.78	50.585	0.74	0.759	I
207	20.885	41.74	50.62		0.529	I
210	20.95	41.75	50.675		0.406	I
701	20.84	41.775	50.505	0.91	0.979	II
704	20.92	41.77	50.545	0.83	0.847	II
708	20.95	41.77	50.50	0.93	0.979	II
745	21.01	41.81	50.565	0.84	0.906	II
746	20.90	41.765	50.50	0.89	0.965	II
757	21.02	41.795	50.56	0.91	0.876	II
346	20.93	41.79	50.555	0.95	0.876	II
360	20.94	41.79	50.55	0.84	0.891	II
758	20.87	41.795	50.495	1.00	1.068	II
759	20.88	41.755	50.525	0.81	0.862	II

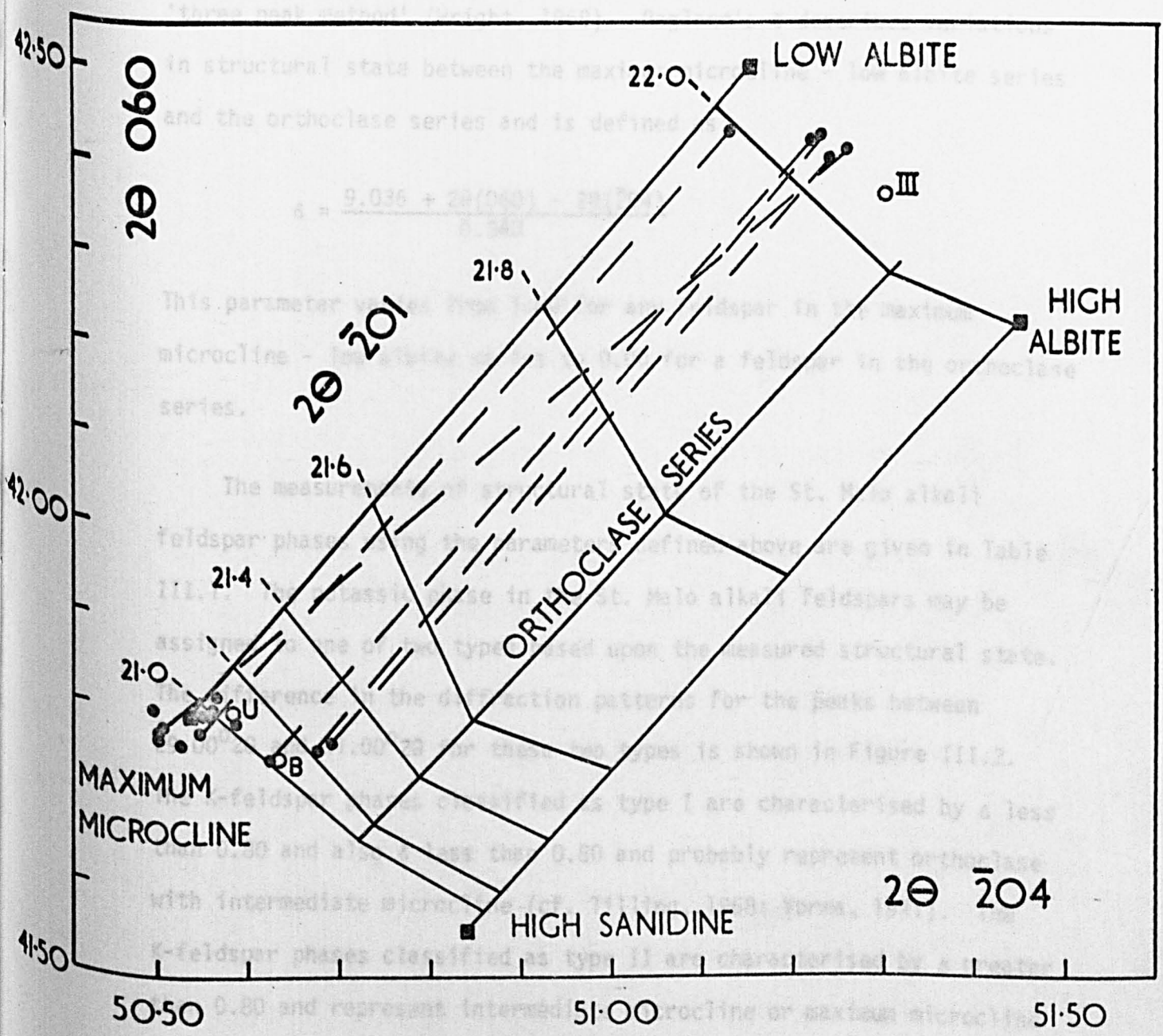
Na - FELDSPAR

	$2\theta(\bar{2}01)$	$2\theta(060)$	$2\theta(\bar{2}04)$	δ
309	21.97	42.40	51.24	0.656
207	22.00	42.42	51.22	0.774
210	22.075	42.425	51.23	0.759
701	22.02	42.41	51.26	0.626
704	22.05	42.43	51.13	1.068

Figure III.1

Plot of 2θ (060) against 2θ ($\bar{2}04$) for alkali feldspars simplified slightly after Wright (1968, figure 3).

U = Spencer U feldspar; B = Spencer B feldspar; and III = Albite III feldspar (all from Wright). Small solid circles represent the St. Malo K-feldspars and the Na-feldspar component where present on the diffractogram.



During measurement of the (201) peaks it was noticed that several of the K-feldspar phases showed a broad or double peak in this position (see figure III.3). This phenomenon has been examined by Vogel (1970) in his study of the alkali feldspars from the Saenereville amphibole

maximum microcline. With increasing disorder of Si-Al the obliquity decreases to 0.00 which corresponds to monoclinic orthoclase. The second measure of structural state of alkali feldspars is Ragland's δ (Ragland, 1970) which is based upon the quantification of Wright's 'three peak method' (Wright, 1968). Ragland's δ describes variations in structural state between the maximum microcline - low albite series and the orthoclase series and is defined as:

$$\delta = \frac{9.036 + 2\theta(060) - 2\theta(\bar{2}04)}{0.340}$$

This parameter varies from 1.00 for any feldspar in the maximum microcline - low albite series to 0.00 for a feldspar in the orthoclase series.

The measurements of structural state of the St. Malo alkali feldspar phases using the parameters defined above are given in Table III.1. The potassic phase in the St. Malo alkali feldspars may be assigned to one of two types based upon the measured structural state. The difference in the diffraction patterns for the peaks between $29.00^{\circ}2\theta$ and $31.00^{\circ}2\theta$ for these two types is shown in Figure III.2. The K-feldspar phases classified as type I are characterised by Δ less than 0.80 and also δ less than 0.80 and probably represent orthoclase with intermediate microcline (cf. Tilling, 1968; Vorma, 1971). The K-feldspar phases classified as type II are characterised by Δ greater than 0.80 and represent intermediate microcline or maximum microcline only (cf. Vorma, op.cit.; Gorbatshev, 1972).

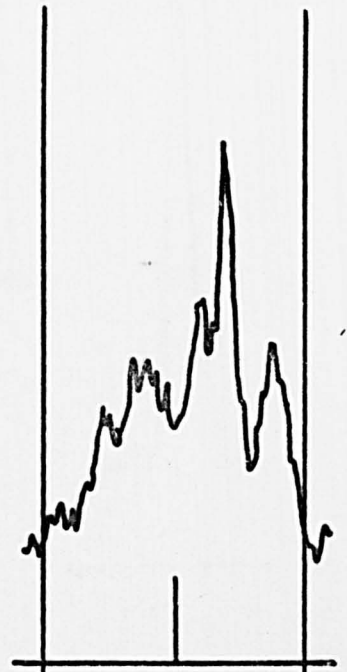
During measurement of the ($\bar{2}01$) peaks it was noticed that several of the K-feldspar phases showed a broad or double peak in this position (see Figure III.3). This phenomenon has been examined by Vogel (1970) in his study of the alkali feldspars from the Beemerville nepheline

Figure III.2

Typical X-ray diffractogram for the two types of
K-feldspar:

Type I = orthoclase with intermediate microcline.

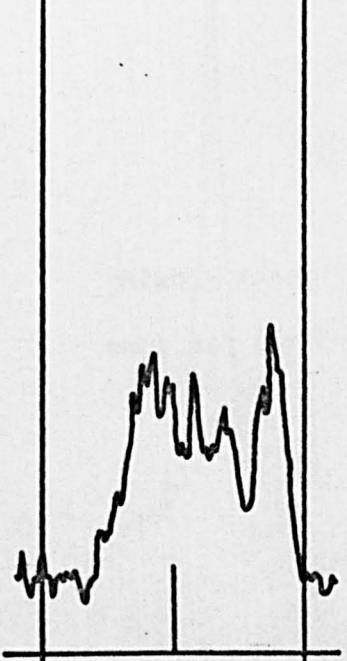
Type II = intermediate microcline or maximum microcline.



309



701



207



360



761



746

29° 30° 31°

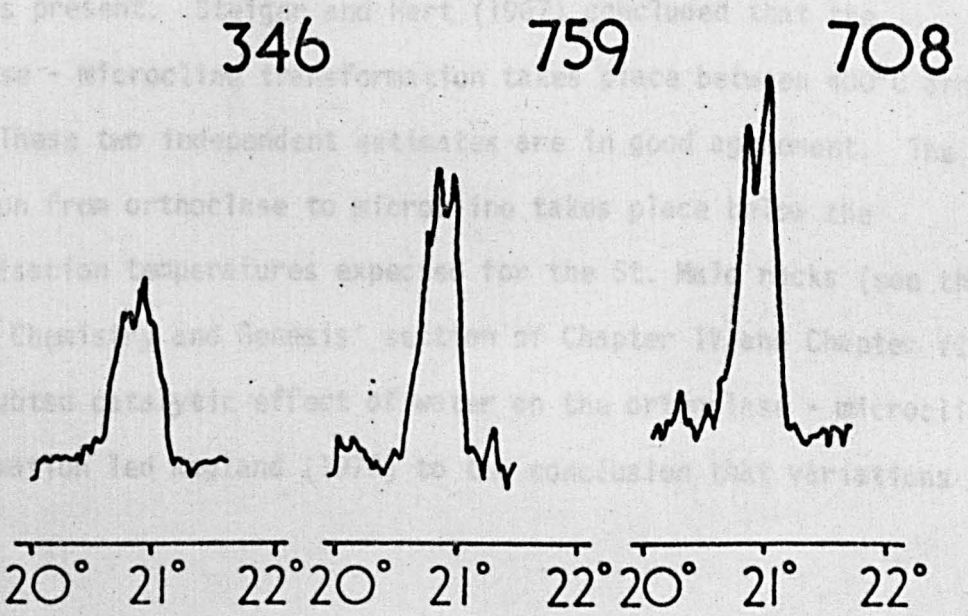
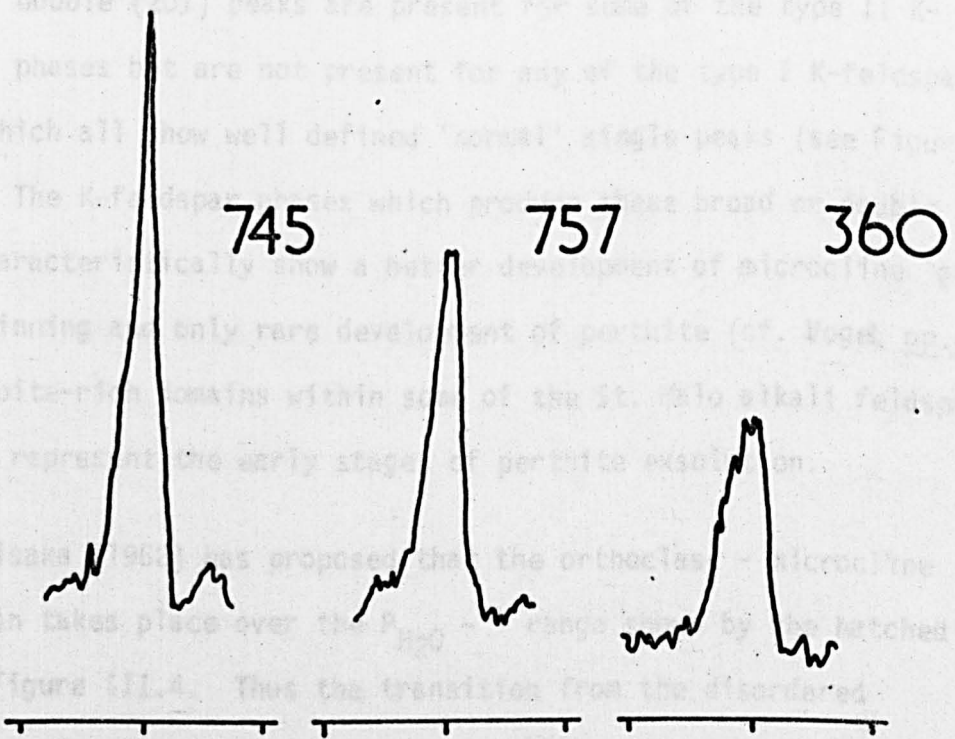
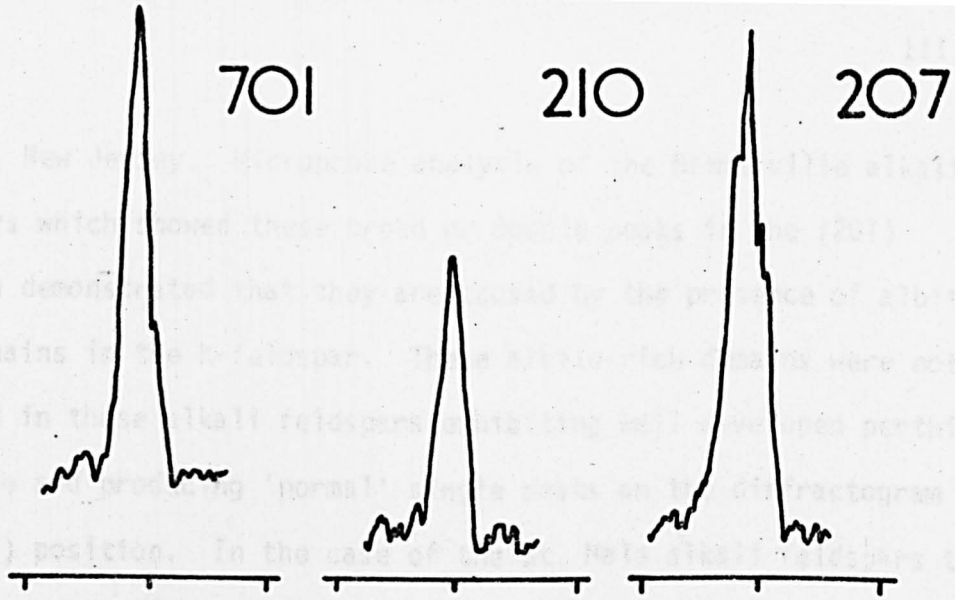
I

29° 30° 31°

II

Figure III.3

Typical X-ray diffractograms for the (201) peaks showing the development of broad peaks in this position for some of the type II K-feldspars.

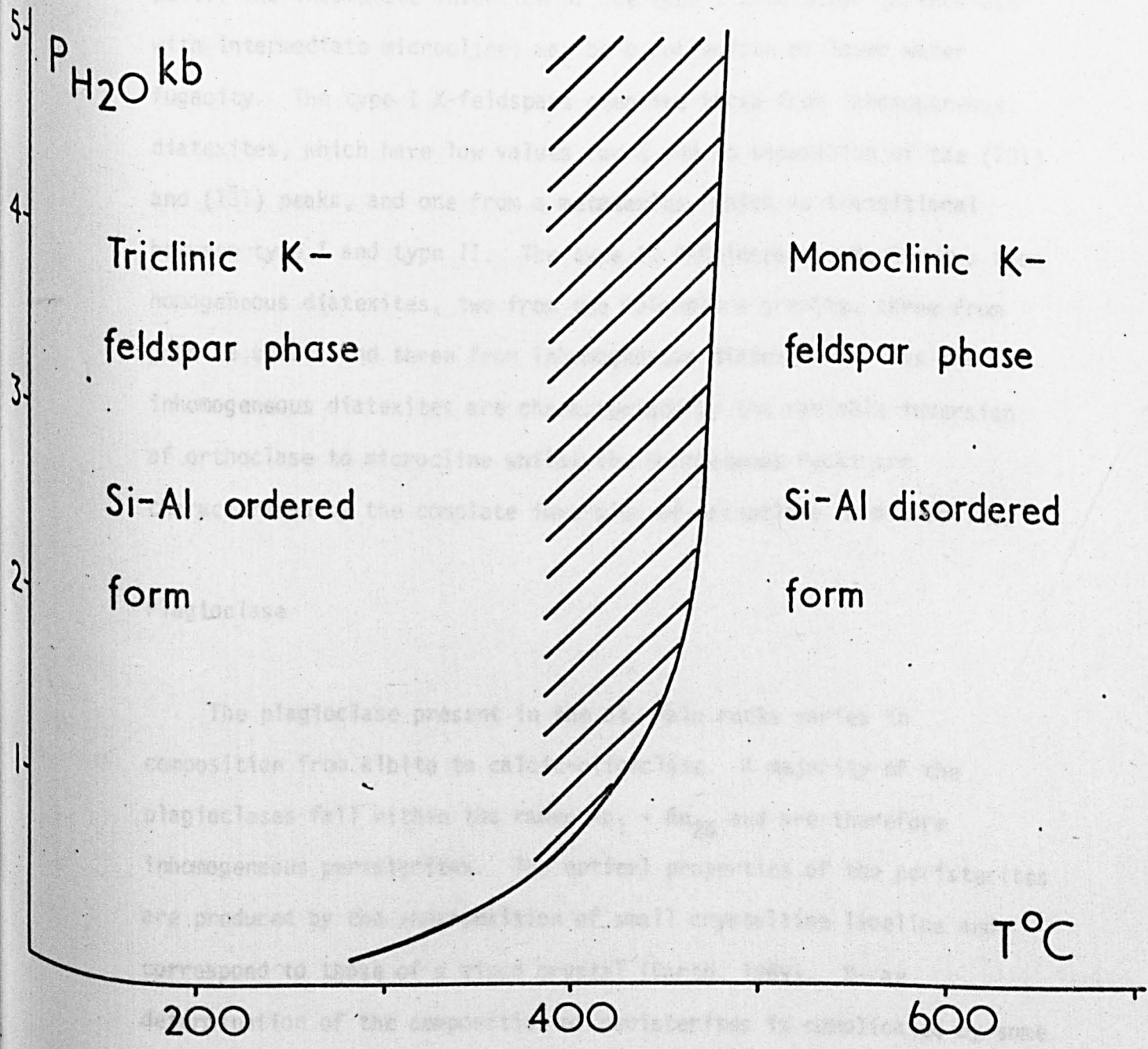


syenite, New Jersey. Microprobe analysis of the Beemerville alkali feldspars which showed these broad or double peaks in the ($\bar{2}01$) position demonstrated that they are caused by the presence of albite-rich domains in the K-feldspar. These albite-rich domains were not detected in those alkali feldspars exhibiting well developed perthitic structure and producing 'normal' single peaks on the diffractogram in the ($\bar{2}01$) position. In the case of the St. Malo alkali feldspars the broad or double ($\bar{2}01$) peaks are present for some of the type II K-feldspar phases but are not present for any of the type I K-feldspar phases which all show well defined 'normal' single peaks (see Figure III.3). The K-feldspar phases which produce these broad or double peaks characteristically show a better development of microcline 'grid-iron' twinning and only rare development of perthite (cf. Vogel, op.cit.). These albite-rich domains within some of the St. Malo alkali feldspars probably represent the early stages of perthite exsolution.

Tomisaka (1962) has proposed that the orthoclase - microcline transition takes place over the P_{H_2O} - T range shown by the hatched area in Figure III.4. Thus the transition from the disordered orthoclase structure to the ordered microcline structure at P_{H_2O} of 2 to 5 kilobars would take place over the temperature interval between 460-480°C and 380°C. No appreciable transition occurs unless water vapour is present. Steiger and Hart (1967) concluded that the orthoclase - microcline transformation takes place between 400°C and 350°C. These two independent estimates are in good agreement. The transition from orthoclase to microcline takes place below the crystallisation temperatures expected for the St. Malo rocks (see the 'Biotite Chemistry and Genesis' section of Chapter IV and Chapter VI). The undoubted catalytic effect of water on the orthoclase - microcline transformation led Ragland (1970) to the conclusion that variations in

Figure III.4

P-T diagram showing the stability relations of monoclinic - triclinic potassium feldspars according to Tomisaka (1962). The hatched area represents the P-T range where the transition from the triclinic to the monoclinic phase is possible.



the structural state of alkali feldspars might be related to variations in water fugacity.

Biotite data, to be presented in Chapter IV, suggest variations in the fugacity of water throughout the rocks comprising the St. Malo belt. The incomplete inversion of the type I K-feldspar (orthoclase with intermediate microcline) may be a reflection of lower water fugacity. The type I K-feldspars comprise three from inhomogeneous diatexites, which have low values for δ and no separation of the (131) and ($\bar{1}\bar{3}1$) peaks, and one from a metatexite, which is transitional between type I and type II. The type II K-feldspars comprise two from homogeneous diatexites, two from the Colombière granite, three from granite sheets and three from inhomogeneous diatexites. Thus the inhomogeneous diatexites are characterised by the variable inversion of orthoclase to microcline whilst the homogeneous rocks are characterised by the complete inversion of orthoclase to microcline.

Plagioclase

The plagioclase present in the St. Malo rocks varies in composition from albite to calcic-oligoclase. A majority of the plagioclases fall within the range $An_1 - An_{24}$ and are therefore inhomogeneous peristerites. The optical properties of the peristerites are produced by the superposition of small crystalline lamellae and correspond to those of a mixed crystal (Barth, 1969). X-ray determination of the composition of peristerites is complicated by some lattice distortion and the presence of two components within the structure - albite and calcic-oligoclase. Bambauer, Corlett, Eberhard and Viswanathan (1967) state "It is usually difficult or indeed impossible to examine both the components of peristerites sufficiently

by means of powder methods". This will result in broader peaks on X-ray diffractograms.

The composition of the plagioclases separated from some of the St. Malo rocks was determined from the following two pairs of reflections: (111) and ($1\bar{1}1$), and (131) and ($1\bar{3}1$), using the curves of Smith (1956) and Bambauer et al (op.cit.) which relate the difference in 2θ between the reflections in each pair to composition. Although the peaks were generally broad, due to the peristerite structure, the An contents determined from the two different pairs of reflections are often in reasonable agreement (see Table III.2). It is thought that the composition obtained from the average of these two determinations represents a good estimate of the An content of the plagioclase. The complete data and plagioclase compositions together with the normative Ab/An ratios where they are available are given in Table III.2).

Table III.2

Summary of the composition of 24 plagioclase feldspars determined by X-ray diffraction from the St. Malo belt.

- Specimen 701: homogeneous diatexite, St. Jacut.
- Specimen 758: homogeneous diatexite, St. Briac.
- Specimen 710: homogeneous diatexite, pnte de Grouin.
- Specimen 309: inhomogeneous diatexite, le Guildo.
- Specimen 757: inhomogeneous diatexite, Ile des Hébihens.
- Specimen 704: inhomogeneous diatexite, St. Jacut.
- Specimen 759: inhomogeneous diatexite, pnte de la Garde Guérin.
- Specimen 760: inhomogeneous diatexite, pnte de la Garde Guérin.
- Specimen 207: inhomogeneous diatexite, road cutting, la barrage.
- Specimen 210: inhomogeneous diatexite, quarry, Montagne St. Joseph.
- Specimen 320: sheared diatexite, west of pnte de Grouin.
- Specimen 324: sheared diatexite, west of pnte de Grouin.
- Specimen 761: metatexite, pnte de la Garde Guérin.
- Specimen 346: Colombière granite, la Nellière.
- Specimen 360: Colombière granite, Ile de la Colombière.
- Specimen 708: granite sheet, St. Jacut.
- Specimen 745: granite pegmatite, Lancieux.
- Specimen 746: granite sheet, Lancieux.
- Specimen 740: trondhjemite sheet, pnte du Crapaud.
- Specimen 742: trondhjemite sheet, pnte du Crapaud.
- Specimen 706: metasediment, St. Jacut.
- Specimen 766: metasediment, la Richardais.
- Specimen 733: metasediment, north of St. Suliac.
- Specimen 224: metasediment, from raft at Port Briac.

PLAGIOCLASE

	2 θ (111)- 2 θ (1 $\bar{1}\bar{1}$)	%An	2 θ (131)- 2 θ (1 $\bar{3}\bar{1}$)	%An	Av. %An	NORMATIVE Ab/An RATIO*
701	0.66	24.0	1.45	16.5	20.25	4.8
758	0.65	23.0	1.55	21.5	22.25	5.7
710	0.54	9.0	1.30	9.0	9.00	

309	0.68	26.5	1.60	23.5	25.00	
757	0.62	19.0	1.50	18.5	18.75	9.6
704	0.60	16.5	1.38	13.0	14.75	159.4
759	0.63	20.0	1.45	16.5	18.25	10.7
760	0.65	22.5	1.45	16.5	19.50	12.4
207	0.63	20.0	1.45	16.5	18.25	10.9
210	0.65	22.5	1.46	17.0	19.75	10.1
320	0.62	19.0	1.51	19.0	19.00	
324	0.55	10.0	1.32	10.0	10.00	
761	0.60	16.5	1.48	17.5	17.00	

346	0.53	8.0	1.27	8.0	8.00	
360	0.55	10.0	1.23	7.0	8.50	24.0
708	0.57	13.0	1.40	14.0	13.50	10.2
745	0.59	15.0	1.40	14.0	14.50	11.6
746	0.55	10.0	1.30	9.0	9.50	
740	0.70	29.0	1.60	23.5	26.25	4.1
742	0.71	30.0	1.68	28.0	29.00	2.8

706			1.67	27.5	27.50	3.2
766	0.68	26.5	1.60	23.5	25.00	5.7
733			1.65	26.0	26.00	4.2
224	0.57	13.0	1.34	11.0	12.00	

* Barth mesonorm.

Whole-rock Major and Trace Element Chemistry

Thirty two rocks have been selected from the area studied and analysed for twenty three major and trace elements. The rocks chosen were: 5 homogeneous diatexites from the St. Malo belt; 3 inhomogeneous diatexites from the St. Malo belt; 2 inhomogeneous diatexites and 1 sheared biastic schist from the northern part of the St. Malo belt; 1 metatexite from the St. Malo belt; 3 metasediments from the St. Malo belt; 2 homogeneous granites from the St. Malo belt; 2 gabbro dykes and 2 trondhjemite sheets from the St. Malo belt; and 10 horned felsic sheets from within the Brittishia Supracrustal Suite in the north-west of the St. Malo belt. These **CHAPTER IV** rocks were selected to try and give a representative sample of the major rock types occurring in the St. Malo igneous belt and adjacent areas. However, it was not possible to collect more than one specimen of fresh material which was large enough to overcome sample inhomogeneity. In addition, the sample is not truly representative of the rock types in the area, due to a bias towards the diatexites which were the most abundant and reduced to manageable proportions. The selection of samples suitable for chemical analysis is further hampered by the fact that the rocks to which was sampling by marine agencies was very limited. The greatest care was given to collecting the freshest possible material which was likely to be used for chemical analysis. The preparation of samples for analysis and the techniques employed in analysis have been described in Chapter 1.

The analyses are presented in the form of tables arranged according to rock type and also containing the data necessary for the calculation of cation percentages for the major elements in small rocks.

Whole-rock Major and Trace Element Chemistry

Thirty two rocks have been selected from the area studied and analysed for twenty three major and trace elements. The rocks chosen were: 6 homogeneous diatexites from the St. Malo belt; 9 inhomogeneous diatexites from the St. Malo belt; 2 inhomogeneous diatexites and 1 sheared blastic schist from the northern part of the Dinan belt; 1 metatexite from the St. Malo belt; 5 metasediments from the St. Malo belt; 2 homogeneous granites from the St. Malo belt; 2 granite sheets and 2 trondhjemite sheets from the St. Malo belt; and 2 Cadomian felsic sheets from within the Brioverian supracrustal rocks to the north-west of the St. Malo belt. These thirty two rocks were selected to try and give a representative sample of the major rock types comprising the St. Malo migmatite belt and adjacent areas. However, it proved impossible to collect more than one specimen of fresh metatexite which was large enough to overcome sample inhomogeneity. Accordingly, the sample is not truly representative of the rock types within the area but has a bias towards the diatexites where problems of sample inhomogeneity are reduced to manageable proportions. Collection of specimens suitable for chemical analysis is further hampered by the extent and depth to which weathering by marine agencies has penetrated. Much attention was given to collecting the freshest possible material when it was likely to be used for chemical analysis. The preparation of specimens for analysis and the techniques employed in analysis have been summarised in Chapter I.

The analyses are presented in the form of tables grouped according to rock type and also containing the Barth mesonorm and the C.I.P.W. norm, cation percentages for the major elements and Niggli numbers

calculated from the analyses. Graphical methods have been employed to supplement much of the tabled data. The analyses are arranged into the following groups: homogeneous diatexites - Table IV.1; inhomogeneous diatexites and related rocks - Table IV.2; the metasediments - Table IV.3; the granitic rocks - Table IV.4. Some analyses from the literature of greywacke-type and arkose-type sediments and of typical plutonic rocks are given in Tables IV.5 and IV.6 for comparison with the analyses from north-eastern Brittany. The arithmetic mean of the 6 homogeneous diatexites is compared with the arithmetic mean of the 9 inhomogeneous diatexites from the St. Malo belt in Table IV.7 and the St. Malo inhomogeneous diatexites are compared with the Dinan rocks in Table IV.8. The analyses of the two Cadomian felsic sheets are presented in Table IV.9.

The homogeneous diatexites, the inhomogeneous diatexites from the St. Malo belt, the rocks from the Dinan belt, the metatexite, the metasediments and the two homogeneous granites have a broadly similar chemistry. Upon closer examination, however, there are certain differences in detail between the mean analyses of the St. Malo homogeneous and inhomogeneous diatexites and also between the mean analyses of the St. Malo inhomogeneous diatexites and the Dinan rocks. Differences have accordingly been tested for significance using the Student's t-test and in the discussion which follows are quoted at the 2.5% level. The homogeneous diatexites from the St. Malo belt are significantly richer in SiO_2 and Al_2O_3 and significantly poorer in TiO_2 , Fe_2O_3 , FeO , MnO , MgO , Cu , Y , Zn and Zr than the inhomogeneous diatexites from the St. Malo belt. However, the homogeneous diatexites and the inhomogeneous diatexites are not significantly different in terms of the remaining elements and notably for CaO , Na_2O , K_2O , La , Rb , Sr , Th and U all of which might be expected to be highly

	1	2	3	4	5	6	7	8
	765	701	703	358	758	720		
SiO ₂	68.65	69.85	68.50	69.25	71.20	70.35	69.63	69.20
TiO ₂	0.64	0.46	0.55	0.50	0.32	0.43	0.48	0.50
Al ₂ O ₃	15.10	15.80	15.90	13.65	18.72	15.25	15.64	15.92
Fe ₂ O ₃	1.94	1.47	1.42	1.37	0.54	0.54	1.25	1.41
FeO	2.53	1.94	1.70	1.66	1.16	1.71	1.72	1.63
MnO	0.04	0.04	0.04	0.03	0.09	0.03	0.04	0.04
MgO	1.14	1.35	1.31	0.93	0.63	0.50	0.98	1.20
CaO	1.02	2.00	1.70	1.50	1.50	1.07	1.55	1.92
Na ₂ O	3.19	3.79	3.83	4.29	3.31	3.27	3.61	3.97
K ₂ O	3.52	3.62	3.66	2.85	3.88	4.77	3.65	3.78
H ₂ O	1.27	1.08	1.00	0.52	0.96	1.04	0.99	0.99

Table IV.1

Summary of the geochemical data for the homogeneous diatexites.

Major element composition (oxide %), trace element content (ppm), selected element ratios, the Barth (1960 & 1962) mesonorm, the Kelsey-C.I.P.W. (1965) norm, the major elements as cation percentages and the Niggli numbers are listed in order on the following three pages.

Analysis 1: specimen 765, Plage de Quatre Vaux.

Analysis 2: specimen 701, St. Jacut.

Analysis 3: specimen 703, St. Jacut.

Analysis 4: specimen 358, St. Jacut.

Analysis 5: specimen 758, St. Briac.

Analysis 6: specimen 720, pnte de Grouin.

Analysis 7: arithmetic mean of analyses 1-6.

Analysis 8: arithmetic mean of analyses 2-4.

La	17	20	18	23	14	87	30	20
Pb	57	34	32	69	39	110	57	46
Th	178	154	153	146	111	423	200	163
Th/U	2.71	2.97	2.74	2.88	2.11	2.91	2.30	1.92
Ba/Rb	6.34	3.97	3.23	3.20	5.59	8.23	5.16	3.63
Rb/Sr	0.60	0.85	0.95	0.60	0.65	0.55	0.76	0.82
Ca	0.73	1.43	1.28	1.35	1.07	0.77	1.12	1.37
Ca/Sr	40	96	81	86	72	30	63	87
Ca/Zr	41	93	80	81	97	18	65	85
Ca/Y	429	2050	1792	3370	2144	105	1768	2076
Hf	0.38	0.28	0.33	0.30	0.19	0.26	0.29	0.30
Ti/Zr	22	18	26	18	17	6	13	16
Th/U	5.12	5.24	6.47	7.19	7.14	5.42	6.09	6.30

	1	2	3	4	5	6	7	8
	<u>765</u>	<u>701</u>	<u>703</u>	<u>358</u>	<u>758</u>	<u>720</u>		
SiO ₂	68.65	69.85	68.50	69.25	71.20	70.35	69.63	69.20
TiO ₂	0.64	0.46	0.55	0.50	0.32	0.43	0.48	0.50
Al ₂ O ₃	15.10	15.80	15.90	16.05	15.72	15.25	15.64	15.92
Fe ₂ O ₃	1.94	1.47	1.42	1.33	0.54	0.84	1.26	1.41
FeO	2.53	1.54	1.70	1.66	1.16	1.71	1.72	1.63
MnO	0.04	0.04	0.04	0.03	0.03	0.03	0.04	0.04
MgO	1.14	1.35	1.31	0.93	0.63	0.50	0.98	1.20
CaO	1.02	2.00	1.88	1.89	1.50	1.07	1.56	1.92
Na ₂ O	3.19	3.79	3.83	4.29	3.31	3.27	3.61	3.97
K ₂ O	3.52	3.62	3.66	2.25	4.08	4.77	3.65	3.18
H ₂ O +	1.27	1.08	1.00	0.88	1.04	0.96	1.04	0.99
P ₂ O ₅	0.23	0.18	0.18	0.18	0.17	0.11	0.18	0.18
Total	<u>99.27</u>	<u>101.18</u>	<u>99.97</u>	<u>99.24</u>	<u>99.70</u>	<u>99.29</u>	<u>99.79</u>	<u>100.14</u>
T. Fe	4.75	3.18	3.31	3.18	1.83	2.74	3.17	3.22
Ba	792	580	590	352	715	1152	697	507
Cu	28	10	11	25	7	12	16	15
La	17	20	18	23	14	87	30	20
Pb	57	34	32	69	39	110	57	45
Rb	125	146	158	110	128	140	135	138
Sr	181	149	166	161	150	257	177	159
Th	21	22	22	25	20	45	26	23
U	4.1	4.2	3.4	3.5	2.8	8.3	4.4	3.7
Y	17	5	7.5	4	5	73	19	5.5
Zn	63	62	76	59	47	46	59	66
Zr	178	154	168	166	111	423	200	163
K	2.92	3.00	3.04	1.87	3.39	3.96	3.03	2.62
K/Rb	238	206	183	170	265	283	224	186
Ba/K × 10 ²	2.71	1.93	1.94	1.88	2.11	2.91	2.30	1.92
Ba/Rb	6.34	3.97	3.73	3.20	5.59	8.23	5.16	3.63
Rb/Sr	0.69	0.98	0.95	0.68	0.85	0.55	0.76	0.87
Ca	0.73	1.43	1.34	1.35	1.07	0.77	1.12	1.37
Ca/Sr	40	96	81	84	72	30	63	87
Ca/Zr	41	93	80	81	97	18	65	85
Ca/Y	429	2858	1792	3378	2144	105	1768	2676
Ti	0.38	0.28	0.33	0.30	0.19	0.26	0.29	0.30
Ti/Zr	22	18	20	18	17	6	15	18
Th/U	5.12	5.24	6.47	7.14	7.14	5.42	6.09	6.28

	1	2	3	4	5	6	7
Ap	0.50	0.38	0.38	0.38	0.36	0.24	0.38
Sph	1.39	0.96	1.17	1.07	0.68	0.92	1.02
Mag	2.10	1.54	1.51	1.42	0.58	0.90	1.34
Cor	6.29	3.32	3.72	4.68	4.40	4.01	4.41
Qu	34.15	28.41	27.38	30.79	32.04	29.90	30.45
Alb	29.66	34.16	34.88	39.32	30.35	30.14	33.07
Or	16.56	17.16	17.44	9.95	21.89	25.94	18.13
An	1.38	7.17	6.33	6.60	5.33	3.17	4.99
Bi	7.98	6.89	7.20	5.80	4.37	4.78	6.20
K	4.31	4.30	4.39	2.72	4.93	5.70	4.40
Qtz	42.49	35.63	34.35	38.45	38.02	34.77	37.29
Or	20.60	21.53	21.88	12.43	25.97	30.18	22.21
Ab	36.91	42.84	43.77	49.12	36.01	35.05	40.50
Na	52.56	52.08	52.65	62.95	48.31	46.72	52.52
Or	34.78	29.34	29.73	17.81	38.03	43.78	32.27
Ab	62.32	58.40	59.48	70.39	52.72	50.86	58.85
An	2.89	12.26	10.79	11.81	9.26	5.36	8.88
Fe	22.74	14.50	14.86	15.09	9.27	12.93	14.97
(Na+K)	70.09	72.52	72.99	71.90	79.71	79.72	74.36
Qu	32.45	27.74	26.24	30.22	32.11	29.53	29.73
Cor	4.74	2.44	2.65	3.55	3.54	3.03	3.35
Or	20.80	21.39	21.63	13.30	24.11	28.19	21.57
Alb	26.99	32.07	32.41	36.30	28.01	27.67	30.55
An	3.56	8.75	8.15	8.20	6.33	4.59	6.56
En	2.84	3.36	3.26	2.32	1.57	1.25	2.44
Fs	2.06	0.93	1.11	1.18	1.21	1.80	1.40
Mag	2.81	2.13	2.06	1.93	0.78	1.22	1.83
Il	1.22	0.87	1.04	0.95	0.61	0.82	0.91
Ap	0.54	0.43	0.43	0.43	0.40	0.26	0.43
P	0.47	0.35	0.35	0.35	0.38	0.24	0.37
Qtz	40.44	34.16	32.69	37.86	38.12	34.58	36.32
Or	25.92	26.34	26.94	16.66	28.62	33.01	26.35
Ab	33.64	39.50	40.37	45.48	33.25	32.40	37.33

	1	2	3	4	5	6	7
Si ⁺⁴	65.88	64.97	64.39	65.51	67.37	66.91	65.82
Ti ⁺⁴	0.46	0.32	0.39	0.36	0.23	0.31	0.34
Al ⁺³	17.08	17.32	17.61	17.90	17.53	17.09	17.43
Fe ⁺³	1.40	1.03	1.00	0.95	0.39	0.60	0.90
Fe ⁺²	2.03	1.20	1.34	1.31	0.92	1.36	1.36
Mn ⁺²	0.03	0.03	0.03	0.02	0.02	0.02	0.03
Mg ⁺²	1.63	1.87	1.84	1.31	0.89	0.71	1.38
Ca ⁺²	1.05	1.99	1.89	1.92	1.52	1.09	1.58
Na ⁺	5.94	6.83	6.98	7.87	6.07	6.03	6.62
K ⁺	4.31	4.30	4.39	2.72	4.93	5.79	4.40
P ⁺⁵	0.19	0.14	0.14	0.14	0.14	0.09	0.14

Ca	9.29	15.19	14.28	15.33	12.15	8.45	12.54
Na	52.56	52.08	52.63	62.95	48.51	46.72	52.52
K	38.16	32.73	33.09	21.72	39.34	44.84	34.94

Ca	7.18	12.99	12.16	13.01	11.02	7.36	10.66
Fe	22.74	14.50	14.86	15.09	9.27	12.93	14.97
(Na+K)	70.09	72.52	72.99	71.90	79.71	79.72	74.36

si	338.6	319.3	312.7	331.7	374.3	366.8	338.1
al	43.12	42.56	42.77	45.30	48.70	46.86	44.75
fm	25.72	20.30	20.43	18.20	12.31	14.77	18.84
c	5.30	9.80	9.19	9.70	8.45	5.98	8.11
alk	25.86	27.35	27.60	26.79	30.55	32.39	28.29
k	0.42	0.39	0.39	0.26	0.45	0.49	0.40
mg	0.32	0.45	0.44	0.36	0.40	0.26	0.38
ti	2.33	1.58	1.89	1.80	1.27	1.69	1.75
p	0.47	0.35	0.35	0.36	0.38	0.24	0.37
Qtz I.	129.2	109.9	102.3	124.5	152.1	137.2	124.9

Analysis 20: arithmetic mean of analyses 9-19.

Analysis 21: specimen 906, Port St. Hubert, la Rance.

Analysis 22: specimen 761, pnte de la Garde Guérin.

9
757

SiO₂ 67.00
TiO₂ 0.30
Al₂O₃ 14.50
FeO 8.07
CaO 3.34
MgO 3.74
K₂O 3.37
Total 99.98
Ba 346
Cu 16
Rb 151
Ba/Rb 3.62
Nb/Sr 1.17
Ca/Zr 32
Ca/Ti 307
Ti 0.40
Ti/Zr 10
Th/U 7.61

Table IV.2

Summary of the geochemical data for the 11 inhomogeneous diatexites (analyses 9-19), 1 sheared blastic schist (analysis 21), and 1 metatexite (analysis 22). Major element composition (oxide %), trace element content (ppm), selected element ratios, the Barth (1960 & 1962) mesonorm, the Kelsey-C.I.P.W. (1965) norm, the major elements as cation percentages and the Niggli numbers are listed in order on the following three pages.

Note: * signifies that the trace element concerned is present in an amount below the calculated lower limit of detection.

- Analysis 9: specimen 757, Ile des Hébihens.
- Analysis 10: specimen 704, St. Jacut.
- Analysis 11: specimen 759, pnte de la Garde Guérin.
- Analysis 12: specimen 760, pnte de la Garde Guérin.
- Analysis 13: specimen 205, road cutting, la Barrage.
- Analysis 14: specimen 207, road cutting, la Barrage.
- Analysis 15: specimen 208, quarry, Montagne St. Joseph.
- Analysis 16: specimen 210, quarry, Montagne St. Joseph.
- Analysis 17: specimen 721, pnte de Grouin.
- Analysis 18: specimen 902, Port St. Jean, la Rance.
- Analysis 19: specimen 915, road cutting, Taden, la Rance.
- Analysis 20: arithmetic mean of analyses 9-19.
- Analysis 21: specimen 905, Port St. Hubert, la Rance.
- Analysis 22: specimen 761, pnte de la Garde Guérin.

	9	10	11	12	13	14	15	16	17	18	19	20	21	22
	<u>757</u>	<u>704</u>	<u>759</u>	<u>760</u>	<u>205</u>	<u>207</u>	<u>208</u>	<u>210</u>	<u>721</u>	<u>902</u>	<u>915</u>		<u>905</u>	<u>761</u>
SiO ₂	67.00	67.20	68.65	67.00	69.25	67.30	69.95	66.90	67.30	66.25	66.30	67.46	66.62	69.45
TiO ₂	0.86	0.81	0.68	0.78	0.74	0.84	0.64	0.77	0.67	0.87	0.86	0.77	0.96	0.76
Al ₂ O ₃	14.50	15.55	14.80	15.35	14.35	14.80	14.65	15.10	16.40	15.10	15.20	15.07	15.15	13.80
Fe ₂ O ₃	2.07	2.78	1.82	1.84	1.25	1.45	1.79	1.53	2.33	2.28	1.87	1.91	3.31	1.66
FeO	3.53	2.78	3.13	3.30	3.62	3.82	2.93	4.08	2.92	2.88	3.57	3.32	2.03	2.97
MnO	0.06	0.04	0.04	0.05	0.05	0.04	0.04	0.05	0.05	0.04	0.04	0.05	0.04	0.04
MgO	1.05	1.44	1.16	1.34	1.52	1.93	1.03	1.88	1.47	1.15	1.40	1.40	1.14	1.10
CaO	1.81	0.92	1.17	1.29	1.18	1.25	1.25	1.43	1.97	1.12	0.82	1.29	1.28	1.10
Na ₂ O	3.74	3.09	3.24	3.55	3.14	2.95	3.25	3.12	3.16	2.87	2.83	3.18	2.41	3.41
K ₂ O	4.14	3.50	3.54	3.62	3.79	3.79	3.79	3.74	3.15	4.44	4.30	3.80	4.19	3.67
H ₂ O +	1.02	1.53	1.05	1.23	1.43	1.60	1.47	1.45	1.44	1.28	1.45	1.36	1.85	0.95
P ₂ O ₅	0.38	0.24	0.11	0.17	0.13	0.13	0.27	0.25	0.36	0.20	0.19	0.22	0.19	0.12
Total	<u>99.98</u>	<u>99.88</u>	<u>99.39</u>	<u>99.52</u>	<u>100.45</u>	<u>99.90</u>	<u>100.06</u>	<u>100.30</u>	<u>101.22</u>	<u>98.48</u>	<u>98.83</u>	<u>99.83</u>	<u>99.17</u>	<u>99.03</u>
T. Fe	5.99	5.87	5.30	5.50	5.27	5.70	5.05	6.06	5.58	5.48	5.84	5.60	5.56	4.96
Ba	846	574	800	674	1065	890	740	700	630	930	858	792	822	888
Cu	16	30	32	24	39	41	20	52	31	26	38	32	6	11
La	28	19	22	16	22	15	18	22	20	27	21	21	19	26
Pb	38	86	27	26	35	27	30	29	43	36	56	39	97	31
Rb	151	143	138	139	134	129	147	152	131	153	156	143	170	133
Sr	129	123	180	181	191	178	166	174	229	180	150	171	143	183
Th	26	24	24	23	22	22	22	22	23	28	24	24	23	22
U	3.5	5.8	3.0	2.8	3.8	2.8	4.9	4.4	4.0	4.9	3.5	3.9	3.8	*
Y	34	16	19	15	15	20	18	18	20	16	15	19	20	15
Zn	103	90	75	73	84	93	68	99	68	82	145	89	132	75
Zr	410	218	218	208	252	228	194	189	178	220	215	230	230	247
K	3.44	2.91	2.94	3.00	3.15	3.15	3.15	3.10	2.61	3.69	3.57		3.48	3.05
K/Rb	228	203	213	216	235	244	214	204	200	241	229		205	229
Ba/Kx10 ²	2.46	1.98	2.72	2.24	3.39	2.83	2.35	2.26	2.41	2.52	2.40		2.36	2.91
Ba/Rb	5.60	4.01	5.80	4.85	7.95	6.90	5.03	4.61	4.81	6.08	5.50		4.84	6.68
Rb/Sr	1.17	1.16	0.77	0.77	0.70	0.73	0.89	0.87	0.57	0.85	1.04		1.19	0.73
Ca	1.29	0.66	0.84	0.92	0.84	0.89	0.89	1.02	1.41	0.80	0.59		0.92	0.72
Ca/Sr	100	54	47	51	44	50	54	59	62	45	39		64	43
Ca/Zr	32	30	38	44	34	39	46	54	79	36	27		40	29
Ca/Y	381	411	440	615	562	447	496	568	704	500	391		458	477
Ti	0.40	0.49	0.41	0.47	0.44	0.50	0.38	0.46	0.40	0.52	0.52		0.58	0.46
Ti/Zr	10	22	19	23	18	22	20	24	23	24	24		25	19
Th/U	7.43	4.14	8.00	8.21	5.79	7.85	4.49	5.00	5.75	5.71	6.86		6.05	

	9	10	11	12	13	14	15	16	17	18	19	20	21	22
Ap	0.81	0.52	0.24	0.37	0.28	0.28	0.58	0.54	0.77	0.44	0.48	0.47	0.42	0.26
Sph	1.84	1.75	1.47	1.68	1.59	1.81	1.38	1.65	1.42	1.90	1.89	1.66	2.11	1.64
Mag	2.21	3.01	1.97	1.98	1.34	1.56	1.93	1.64	2.48	2.49	2.04	2.06	3.64	1.80
Cor	2.88	7.47	5.24	5.23	4.70	5.59	4.94	5.49	6.59	5.86	6.73	5.51	6.89	3.93
Qu	25.81	33.69	33.10	29.38	33.14	32.49	32.57	31.05	32.21	30.44	31.71	31.39	34.19	32.75
Alb	34.30	28.69	30.04	32.80	28.90	27.33	30.06	28.72	28.85	26.95	26.50	29.42	22.75	31.69
Or	19.01	15.86	15.71	15.49	15.26	14.25	17.75	13.67	12.97	22.11	19.40	16.48	22.48	16.80
An	3.58	0.18	2.81	2.65	2.49	2.51	2.28	2.85	5.18	1.28	0.00	2.35	1.86	2.10
Bi	9.56	8.83	9.43	10.44	12.32	14.17	8.51	14.39	9.54	8.52	11.36	10.66	5.67	9.03
K ⁺	5.00													
Qtz	32.62	43.06	41.98	37.83	42.88	43.86	40.52	42.28	43.51	38.28	40.85	40.61	43.05	40.31
Or	24.03	20.27	19.92	19.94	19.74	19.24	22.08	18.61	17.51	27.82	24.99	21.32	28.31	20.68
Ab	43.35	36.66	38.10	42.23	37.38	36.90	37.40	39.11	38.98	33.90	34.14	38.07	28.64	39.01
Na	30.11													
Or	33.42	35.46	32.35	30.41	32.71	32.33	35.44	30.21	27.59	43.93	42.27	34.15	47.75	33.21
Ab	60.29	64.13	61.87	64.39	61.95	61.99	60.02	63.49	61.40	53.54	57.73	60.98	48.31	62.64
An	6.29	0.41	5.78	5.20	5.34	5.68	4.54	6.30	11.01	2.54	0.00	4.87	3.94	4.15
Fe	23.43													
(Na+K)	66.31													
Qu	23.45	31.69	30.88	26.69	30.01	28.40	30.76	26.98	30.37	28.09	28.41	28.67	32.66	30.59
Cor	1.49	5.58	3.77	3.65	3.25	3.88	3.58	3.92	5.07	4.02	4.85	3.91	4.78	2.51
Or	24.47	20.68	20.92	21.39	22.40	22.40	22.40	22.10	18.61	26.24	25.41	22.46	24.76	21.69
Alb	31.65	26.15	27.42	30.04	26.57	24.96	27.50	26.40	26.74	24.29	23.95	26.91	20.39	28.86
An	6.50	3.00	5.09	5.29	5.00	5.35	4.44	5.46	7.42	4.25	2.83	4.96	5.11	4.67
En	2.62	3.59	2.89	3.34	3.79	4.81	2.57	4.68	3.66	2.86	3.49	3.49	2.84	2.74
Fs	3.46	1.54	3.20	3.34	4.49	4.50	2.92	5.05	2.42	2.04	3.67	3.34	0.00	2.90
Mag	3.00	4.03	2.64	2.67	1.81	2.10	2.60	2.22	3.38	3.31	2.71	2.77	3.89	2.41
Il	1.63	1.54	1.29	1.48	1.41	1.60	1.22	1.46	1.27	1.65	1.63	1.46	2.45**	1.44
Ap	0.90	0.57	0.26	0.40	0.31	0.31	0.64	0.59	0.85	0.47	0.45	0.52	0.45	0.28
Ca	0.70													
Qtz	29.47	40.35	38.98	34.16	38.00	37.49	38.13	35.75	40.11	35.73	36.53	36.73	41.98	37.70
Or	30.75	26.36	26.40	27.38	28.36	29.56	27.77	29.27	24.58	33.38	32.67	28.78	31.82	26.73
Ab	39.77	33.29	34.62	38.45	33.64	32.95	34.10	34.98	35.31	30.89	30.79	34.48	26.20	35.57

** includes 0.63% haematite.

	9	10	11	12	13	14	15	16	17	18	19	20	21	22
Si ⁺⁴	63.41	64.38	65.69	63.88	65.77	64.36	65.81	63.56	63.42	64.21	64.13	64.42	64.89	66.61
Ti ⁺⁴	0.61	0.58	0.49	0.56	0.53	0.60	0.46	0.55	0.48	0.63	0.63	0.55	0.70	0.55
Al ⁺³	16.18	17.56	16.69	17.25	16.06	16.68	16.48	16.91	18.21	17.25	17.33	16.96	17.39	15.60
Fe ⁺³	1.47	2.00	1.31	1.32	0.89	1.04	1.29	1.09	1.65	1.66	1.36	1.37	2.43	1.20
Fe ⁺²	2.79	2.23	2.51	2.63	2.88	3.06	2.34	3.24	2.30	2.34	2.89	2.65	1.65	2.38
Mn ⁺²	0.05	0.03	0.03	0.04	0.04	0.03	0.03	0.04	0.04	0.03	0.03	0.04	0.03	0.03
Mg ⁺²	1.48	2.06	1.66	1.90	2.15	2.75	1.47	2.66	2.07	1.66	2.02	1.99	1.66	1.57
Ca ⁺²	1.84	0.94	1.20	1.32	1.20	1.28	1.28	1.46	1.99	1.16	0.85	1.32	1.34	1.13
Na ⁺	6.86	5.74	6.01	6.56	5.78	5.47	6.02	5.75	5.77	5.39	5.31	5.89	4.55	6.34
K ⁺	5.00	4.28	4.32	4.40	4.59	4.62	4.62	4.53	3.79	5.49	5.31	4.63	5.21	4.49
P ⁺⁵	0.30	0.20	0.09	0.14	0.11	0.11	0.22	0.20	0.29	0.16	0.16	0.18	0.16	0.10

Ca	13.40	8.62	10.40	10.73	10.37	11.26	10.74	12.40	17.22	9.66	7.41	11.15	12.04	9.45
Na	50.11	52.36	52.13	53.43	49.96	48.09	50.51	48.97	49.09	44.77	46.30	49.74	41.03	53.01
K	36.49	39.02	37.47	35.85	39.67	40.65	38.75	38.62	32.79	45.57	46.29	39.11	46.93	37.54

Ca	10.26	6.27	7.87	8.17	7.87	8.34	8.28	9.11	12.88	7.33	5.47	8.38	8.91	7.33
Fe	23.43	27.25	24.32	23.87	24.16	25.94	22.86	26.55	25.24	24.14	26.26	24.86	25.98	22.49
(Na+K)	66.31	66.49	67.81	67.96	67.97	65.72	68.86	64.34	61.88	68.54	68.27	66.76	65.11	70.19

Note: * signifies that the trace element is present

si	292.9	305.8	325.0	299.6	322.7	298.7	329.7	287.8	289.1	306.9	303.6	305.1	313.8	341.0
al	37.35	41.70	41.29	40.45	39.41	38.70	41.29	38.27	41.52	41.23	41.02	40.16	42.05	39.93
fm	26.78	30.02	27.22	27.65	29.25	31.94	25.67	31.86	27.62	27.31	29.83	28.68	27.89	26.55
c	8.48	4.49	5.93	6.18	5.89	5.94	6.41	6.59	9.07	5.56	4.02	6.25	6.46	5.79
alk	27.39	23.79	25.56	25.71	25.45	23.42	26.63	23.27	21.79	26.01	25.13	24.90	23.59	27.73
k	0.42	0.43	0.42	0.40	0.44	0.46	0.43	0.44	0.40	0.50	0.50	0.44	0.53	0.41
mg	0.26	0.33	0.30	0.32	0.36	0.40	0.29	0.38	0.34	0.29	0.32	0.33	0.29	0.30
ti	2.83	2.77	2.42	2.62	2.59	2.80	2.30	2.49	2.16	3.03	2.96	2.62	3.40	2.81
p	0.70	0.46	0.22	0.32	0.26	0.24	0.55	0.46	0.65	0.39	0.37	0.42	0.38	0.25
Qtz I.	83.3	110.7	122.8	96.8	120.9	105.0	123.3	94.7	102.0	102.9	103.1	105.5	119.4	130.1

Table IV.3

Summary of the geochemical data for the 2 metasediment enclaves (analyses 23 & 24), the 2 metasediments from within the zone of metatexis (analyses 25 & 26), and the unaltered metasediment (analysis 27). Major element composition (oxide %), trace element content (ppm), selected element ratios, the Barth (1960 & 1962) mesonorm, the Kelsey-C.I.P.W. (1965) norm, the major elements as cation percentages and the Niggli numbers are listed in order on the following three pages.

Note: * signifies that the trace element concerned is present in an amount below the calculated lower limit of detection.

Analysis 23: specimen 706, St. Jacut.

Analysis 24: specimen 718, Havre de Rotheneuf.

Analysis 25: specimen 766, la Richardais.

Analysis 26: specimen 204, quarry, le Minihic.

Analysis 27: specimen 733, north of St. Suliac.

	23	24	25	26	27
	<u>706</u>	<u>718</u>	<u>766</u>	<u>204</u>	<u>733</u>
SiO ₂	71.40	67.25	69.15	67.25	69.95
TiO ₂	0.78	0.77	0.74	0.96	0.69
Al ₂ O ₃	12.50	15.65	13.75	15.60	13.50
Fe ₂ O ₃	2.10	3.00	1.62	1.60	1.83
FeO	2.39	2.70	2.98	3.96	2.57
MnO	0.06	0.04	0.04	0.03	0.05
MgO	1.00	1.77	1.23	2.00	1.16
CaO	2.38	0.32	1.51	1.12	2.25
Na ₂ O	2.92	0.40	2.54	1.50	3.66
K ₂ O	1.83	5.51	4.45	4.69	2.80
H ₂ O +	2.41	2.57	1.66	1.63	0.98
P ₂ O ₅	0.13	0.23	0.14	0.16	0.14
Total	<u>99.90</u>	<u>100.21</u>	<u>99.81</u>	<u>100.50</u>	<u>99.58</u>
T. Fe	4.75	6.00	4.93	6.00	4.69
Ba	822	805	1602	1115	712
Cu	20	56	21	40	*
La	28	22	27	27	33
Pb	34	42	39	42	32
Rb	92	181	136	167	122
Sr	398	52	275	175	343
Th	23	22	29	25	27
U	4.3	2.7	3.3	3.7	4.6
Y	17	25	15	20	18
Zn	72	78	82	129	81
Zr	307	274	277	242	237
K	1.52	4.57	3.69	3.89	2.32
K/Rb	165	253	272	233	190
Ba/K ^{x102}	5.41	1.76	4.34	2.87	3.07
Ba/Rb	8.94	4.45	11.78	6.68	5.84
Rb/Sr	0.23	3.48	0.50	0.95	0.36
Ca	1.70	0.23	1.08	0.80	1.61
Ca/Sr	43	44	39	46	47
Ca/Zr	55	8	39	33	68
Ca/Y	1001	92	719	400	893
Ti	0.47	0.46	0.44	0.58	0.42
Ti/Zr	15	17	16	24	18
Th/U	5.35	8.15	8.79	6.76	5.87

	23	24	25	26	27
Ap	0.29	0.30	0.30	0.35	0.30
Sph	1.72	1.61	1.61	2.08	1.48
Mag	2.31	1.76	1.76	1.73	1.97
Cor	3.10	3.74	3.74	8.64	1.77
Qu	42.23	33.79	33.79	37.81	32.48
Alb	27.60	23.70	23.70	13.96	33.82
Or	6.92	21.31	21.31	19.58	11.89
An	8.68	4.16	4.16	1.21	8.07
Bi	7.15	9.63	9.63	14.64	8.22
K ⁺	2.29	6.90	5.47	5.28	3.43
Qtz	55.02	42.87	42.87	52.99	41.54
Or	9.01	27.05	27.05	27.44	15.21
Ab	35.97	30.08	30.08	19.57	43.25
Na	53.68	40.30	40.30	28.87	34.25
Or	16.01	43.34	43.34	56.34	22.11
Ab	63.90	48.20	48.20	40.17	62.88
An	20.09	8.46	8.46	3.48	15.01
Fe	24.43	34.40	27.67	30.22	20.81
(Na+K)	57.30	62.84	67.09	61.49	64.59
Qu	40.52	40.58	31.31	33.64	30.81
Cor	1.70	9.00	2.34	6.40	0.69
Or	10.81	32.56	26.30	27.72	16.55
Alb	24.71	3.38	21.49	12.69	30.97
An	10.96	0.08	6.58	4.51	10.25
En	2.49	4.41	3.06	4.98	2.89
Fs	1.48	1.28	2.99	4.42	2.16
Mag	3.04	4.35	2.35	2.32	2.65
Il	1.48	1.46	1.41	1.82	1.31
Ap	0.31	0.54	0.33	0.38	0.33
P	0.29	0.47	0.29	0.30	0.20
Qtz I.	191.1	150.0	132.8	121.2	131.5

- Analysis 24 is deficient in CaO

	23	24	25	26	27
Si ⁺⁴	69.66	66.06	66.60	64.60	66.70
Ti ⁺⁴	0.57	0.57	0.54	0.69	0.50
Al ⁺³	14.37	18.12	15.61	17.66	15.17
Fe ⁺³	1.54	2.22	1.17	1.16	1.31
Fe ⁺²	1.95	2.22	2.40	3.18	2.05
Mn ⁺²	0.05	0.03	0.03	0.02	0.04
Mg ⁺²	1.45	2.59	1.77	2.86	1.65
Ca ⁺²	2.49	0.34	1.56	1.15	2.30
Na ⁺	5.52	0.76	4.74	2.79	6.77
K ⁺	2.29	6.90	5.47	5.75	3.41
P ⁺⁵	0.11	0.19	0.11	0.13	0.11
Ca	24.18	4.21	13.24	11.89	18.43
Na	53.68	9.52	40.30	28.82	54.25
K	22.14	86.27	46.46	59.29	27.31
Ca	18.27	2.76	10.24	8.30	14.60
Fe	24.43	34.40	22.67	30.22	20.81
(Na+K)	57.30	62.84	67.09	61.49	64.59
si	375.1	325.6	335.7	300.8	333.1
al	38.70	44.65	39.33	41.11	37.89
fm	26.90	34.80	27.08	33.64	25.23
c	13.40	1.66	7.85	5.37	11.48
alk	21.00	18.89	25.73	19.88	25.40
k	0.29	0.90	0.54	0.67	0.33
mg	0.29	0.37	0.33	0.40	0.33
ti	3.08	2.80	2.70	3.23	2.47
p	0.29	0.47	0.29	0.30	0.28
Qtz I.	191.1	150.0	132.8	121.2	131.5

	28	29	30	31	32	33
	345	360	708	745	740	742
SiO ₂	72.15	72.40	72.20	74.00	71.30	71.30
TiO ₂	0.25	0.17	0.22	0.16	0.28	0.27
Al ₂ O ₃	14.35	14.30	15.50	15.40	15.30	16.20
Fe ₂ O ₃	0.90	0.24	0.78	0.21	0.40	0.75
FeO	1.58	1.69	0.54	0.31	1.30	1.03
MnO	0.04	0.05	0.05	0.03	0.02	0.03
PbO	0.15	0.09	0.33	1.07	0.44	0.32
CaO	0.68	0.57	1.14	0.54	0.31	0.41

Table IV.4

Summary of the geochemical data for the 2 homogeneous granites (Colombière Granite) (analyses 28 & 29), 2 granite sheets (analyses 30 & 31), and 2 trondhjemite sheets (analyses 32 & 33). Major element composition (oxide %), trace element content (ppm), selected element ratios, the Barth (1960 & 1962) mesonorm, the Kelsey-C.I.P.W. (1965) norm, the major elements as cation percentages and the Niggli numbers are listed in order on the following three pages.

Note: * signifies that the trace element concerned is present in an amount below the calculated lower limit of detection.

Analysis 28: specimen 345, la Nellière.

Analysis 29: specimen 360, Ile de la Colombière.

Analysis 30: specimen 708, St. Jacut.

Analysis 31: specimen 745, Lancieux.

Analysis 32: specimen 740, pnte du Crapaud.

Analysis 33: specimen 742, pnte du Crapaud.

Th/Sr	3.04	5.57	0.63	0.43	0.30	0.16
Ce	0.49	0.41	0.82	0.48	1.02	2.44
Ca/Sr	90	116	43	80	31	21
Ca/Zr	19	25	97	133	130	254
Ca/Y	63	56	1630	329	2240	4074
Th	0.15	0.10	0.73	0.08	0.37	0.17
Th/Zr	6	6	16	15	37	17
Th/U	5.63	4.58	4.35	—	10.73	—

	28	29	30	31	32	33
	<u>345</u>	<u>360</u>	<u>708</u>	<u>745</u>	<u>740</u>	<u>742</u>
SiO ₂	72.15	72.60	72.20	74.00	71.30	70.70
TiO ₂	0.25	0.17	0.22	0.10	0.28	0.29
Al ₂ O ₃	14.35	14.30	15.50	15.40	15.30	16.20
Fe ₂ O ₃	0.90	0.24	0.76	0.21	0.98	0.75
FeO	1.69	1.69	0.54	0.31	1.03	1.03
MnO	0.04	0.05	0.03	0.01	0.03	0.03
MgO	0.15	0.09	0.33	0.07	0.44	0.53
CaO	0.68	0.57	1.14	0.69	2.36	3.41
Na ₂ O	3.70	4.76	4.02	2.62	4.67	4.83
K ₂ O	5.06	4.64	4.02	5.26	1.47	1.26
H ₂ O +	0.46	0.57	1.25	0.34	0.62	0.57
P ₂ O ₅	0.10	0.07	0.21	0.16	0.08	0.10
Total	<u>99.53</u>	<u>99.75</u>	<u>100.22</u>	<u>99.17</u>	<u>98.56</u>	<u>99.70</u>
T. Fe	2.78	2.12	1.36	0.55	2.12	1.89
Ba	755	434	865	1600	320	172
Cu	3	2	*	2	6	*
La	56	35	9	*	20	14
Pb	42	47	116	54	38	17
Rb	164	195	118	105	65	57
Sr	54	35	188	246	330	356
Th	27	22	17	13	15	13
U	4.8	4.8	3.9	*	1.4	*
Y	77	73	5	15	7.5	5
Zn	62	71	30	4	36	30
Zr	263	160	84	37	130	114
K	4.20	3.85	3.34	4.37	1.22	1.05
K/Rb	256	198	283	416	188	184
Ba/Kx10 ²	1.80	1.13	2.59	3.66	2.62	1.64
Ba/Rb	4.60	2.23	7.33	15.24	4.93	3.02
Rb/Sr	3.04	5.57	0.63	0.43	0.20	0.16
Ca	0.49	0.41	0.82	0.49	1.69	2.44
Ca/Sr	90	116	43	20	51	69
Ca/Zr	19	25	97	133	130	214
Ca/Y	63	56	1630	329	2249	4874
Ti	0.15	0.10	0.13	0.06	0.17	0.17
Ti/Zr	6	6	16	16	13	15
Th/U	5.63	4.58	4.36	--	10.71	--

	28	29	30	31	32	33
Ap	0.21	0.15	0.45	0.34	0.17	0.21
Sph	0.53	0.36	0.47	0.21	0.60	0.61
Mag	0.96	0.25	0.81	0.22	1.05	0.79
Cor	2.35	0.88	3.60	5.20	2.56	1.44
Qu	28.57	24.53	29.83	35.76	32.19	28.98
Alb	33.81	43.04	36.58	24.08	42.95	43.76
Or	28.34	25.28	23.00	31.36	7.04	5.34
An	1.88	1.79	3.57	2.08	10.46	15.39
Bi	3.35	3.73	1.71	0.74	2.97	3.48
Qtz	31.50	26.42	33.36	39.21	39.17	37.12
Or	31.24	27.23	25.73	34.38	8.57	6.84
Ab	37.27	46.36	40.91	26.41	52.26	56.04
Or	44.26	36.06	36.43	54.52	11.65	8.28
Ab	52.80	61.39	57.92	41.87	71.05	67.85
An	2.94	2.56	5.65	3.61	17.31	23.87
Qu	28.95	24.76	31.07	37.39	32.72	29.58
Cor	1.79	0.59	2.97	4.53	1.93	0.93
Or	29.90	27.42	23.76	31.08	8.69	7.45
Alb	31.31	40.28	34.02	22.17	39.52	40.87
An	2.72	2.37	4.28	2.38	11.19	16.26
En	0.37	0.22	0.82	0.17	1.10	1.32
Fs	2.02	2.72	0.06	0.25	0.68	0.85
Mag	1.30	0.35	1.10	0.30	1.42	1.09
Il	0.47	0.32	0.42	0.19	0.53	0.55
Ap	0.24	0.17	0.50	0.38	0.19	0.24

	28	29	30	31	32	33
Si ⁺⁴	68.04	67.74	67.80	70.20	67.68	66.10
Ti ⁺⁴	0.18	0.12	0.16	0.07	0.20	0.20
Al ⁺³	15.95	15.73	17.15	17.22	17.12	17.85
Fe ⁺³	0.64	0.17	0.54	0.15	0.70	0.53
Fe ⁺²	1.33	1.32	0.42	0.25	0.82	0.81
Mn ⁺²	0.03	0.04	0.02	0.01	0.02	0.02
Mg ⁺²	0.21	0.13	0.46	0.10	0.62	0.74
Ca ⁺²	0.69	0.57	1.15	0.70	2.40	3.42
Na ⁺	6.77	8.61	7.32	4.82	8.60	8.76
K ⁺	6.09	5.52	4.82	6.37	1.78	1.50
P ⁺⁵	0.08	0.06	0.17	0.13	0.06	0.08
Listed in order on the following three pages						
Ca	5.08	3.88	8.64	5.90	18.79	24.98
Na	49.97	58.56	55.11	40.44	67.29	64.03
K	44.96	37.56	36.26	53.55	13.93	10.99
Analysis 35: average of 30 gneisses						
Ca	4.44	3.52	8.06	5.71	16.83	22.77
Fe	12.55	9.15	6.68	3.16	10.42	8.84
(Na+K)	83.01	87.33	85.26	91.13	72.75	83.25
Analysis 37: average of 61 gneisses						
si	393.2	395.0	393.3	455.7	369.6	337.8
al	46.09	45.83	49.76	55.88	46.74	45.62
fm	12.80	9.63	8.39	3.26	11.82	10.71
c	3.97	3.32	6.65	4.55	13.11	17.46
alk	37.14	41.20	35.20	36.30	28.33	26.21
k	0.47	0.39	0.40	0.57	0.17	0.15
mg	0.10	0.08	0.32	0.20	0.29	0.35
ti	1.02	0.70	0.90	0.46	1.09	1.04
p	0.23	0.16	0.48	0.42	0.18	0.20
Qtz I.	144.7	130.1	152.5	210.5	156.3	133.0

34 35 36 37 38 39 40 41 42

SiO ₂	64.70	68.10	64.20	66.75	71.72	68.15	75.57	73.32	76.33
TiO ₂	0.50	0.70	0.60	0.63	0.35	0.92	0.42	0.00	0.41
Al ₂ O ₃	14.80	15.40	13.30	13.54	13.23	15.05	11.38	11.31	10.63
Fe ₂ O ₃	1.50	1.40	3.40	3.30	3.30	1.61	0.82	3.54	2.12
FeO	3.90	3.40	2.00	3.54	2.58	4.14	1.62	0.72	1.22
MnO	0.10	0.20	0.00	0.12	0.00	0.08	0.05	0.00	0.25

Table IV.5

Summary of the geochemical data for various greywacke and arkose analyses from the literature. Major element composition (oxide %), the Barth (1960 & 1962) mesonorm, the Kelsey-C.I.P.W. (1965) norm, major elements as cation percentages and the Niggli numbers are listed in order on the following three pages.

- Analysis 34: average of 23 greywackes, Pettijohn (1957).
- Analysis 35: average of 30 greywackes, Tyrrell (1933).
- Analysis 36: combination of 2 parts average shale and 1 part average arkose, Pettijohn (1957).
- Analysis 37: average of 61 greywackes, Tobschall (1971).
- Analysis 38: fresh Franciscan greywacke, Taliaferro (1943).
- Analysis 39: average of 9 non-garnetiferous pelitic and semi-pelitic schists, Brown (1967).
- Analysis 40: average of 3 Torridonian arkoses, Kennedy (1951).
- Analysis 41: Lower Old Red Sandstone, Mackie (1905).
- Analysis 42: average arkose, Pettijohn (1957).

	34	35	36	37	38	39	40	41	42
SiO ₂	64.70	68.10	64.20	66.75	71.72	66.15	75.57	73.32	76.37
TiO ₂	0.50	0.70	0.60	0.63	0.35	0.92	0.42	0.00	0.41
Al ₂ O ₃	14.80	15.40	13.80	13.54	13.23	15.05	11.38	11.31	10.63
Fe ₂ O ₃	1.50	1.40	3.40	1.60	0.30	1.61	0.82	3.54	2.12
FeO	3.90	3.40	2.00	3.54	3.58	4.14	1.63	0.72	1.22
MnO	0.10	0.20	0.00	0.12	0.00	0.09	0.05	0.00	0.25
MgO	2.20	1.80	1.70	2.15	1.81	2.35	0.72	0.24	0.23
CaO	3.10	2.30	2.50	2.54	1.80	1.61	1.69	1.53	1.30
Na ₂ O	3.10	2.60	1.50	2.93	2.72	2.43	2.45	2.34	1.84
K ₂ O	1.90	2.20	3.80	1.99	1.29	4.60	3.35	6.16	4.99
H ₂ O	2.40	2.10	3.60	2.42	2.53	0.74	1.06		
P ₂ O ₅	0.20	0.20	0.20	0.16	0.09	0.16	0.30	0.00	0.21
HF	45.57	35.31	29.52	31.24	32.87	32.87	25.25	31.15	32.15
Br	4.45	13.93	43.38	7.79	5.41	41.29	1.11	1.11	35.37
As	66.21	64.79	33.30	48.09	27.49	37.31	3.32	2.32	43.19
Ag	29.34	27.28	22.29	24.25	22.29	2.29	2.29	2.29	2.29
Ge	27.54	35.55	33.61	31.91	42.72	40.87	42.93	40.87	40.87
Co	2.49	5.04	3.15	2.33	4.33	2.72	2.72	2.72	2.72
Cr	11.23	13.00	22.46	11.76	2.82	2.82	2.82	2.82	2.82
Alb	26.23	22.00	12.65	24.79	21.22	27.25	25.25	25.25	25.25
Ru	14.07	10.10	11.10	13.10	12.10	12.10	12.10	12.10	12.10
Er	5.48	4.48	4.28	5.28	4.28	4.28	4.28	4.28	4.28
Fe	5.28	4.30	5.28	4.28	4.28	4.28	4.28	4.28	4.28
Mg	2.17	2.03	2.17	2.17	2.17	2.17	2.17	2.17	2.17
Li	0.95	1.33	1.33	1.33	1.33	1.33	1.33	1.33	1.33
Mo	0.47	0.47	0.47	0.47	0.47	0.47	0.47	0.47	0.47

** Includes ...

*** Includes ...

+ Analytical ...

Of 1.000 ...

	34	35	36	37	38	39	40	41	42
Ap	0.44	0.43	0.46	0.36	0.20	0.34	0.65	+	0.46
Sph	1.10	1.52	1.38	1.40	0.77	1.97	0.92	+	0.89
Mag	1.66	1.52	3.90	1.77	0.33	1.73	0.89	+	2.30
Cor	3.61	6.72	4.70	3.64	5.47	5.27	2.17	+	0.98
Qu	32.99	39.17	37.25	36.95	45.89	30.51	44.51	+	43.03
Alb	29.39	24.22	14.79	27.91	25.73	22.37	22.94	+	17.16
Or	1.98	5.21	19.69	3.20	0.00	17.68	17.15	+	29.39
An	13.03	7.96	9.89	9.93	7.51	3.83	5.18	+	3.79
Bi	15.81	13.25	7.94	14.84	12.85	16.30	5.59	+	1.99
K ⁺	2.37	2.70	4.93	2.50	1.61	5.57	4.13	7.53	6.73
Qtz	51.26	57.10	51.93	54.30	64.07	43.24	52.61	+	48.04
Or	3.07	7.59	27.46	4.70	0.00	25.06	20.27	+	32.80
Ab	45.67	35.31	20.62	41.01	35.93	31.70	27.12	+	19.16
Na	51.13	48.89	27.87	51.92	59.60	38.29	43.84	32.23	31.50
Or	4.45	13.93	43.38	7.79	0.00	40.29	37.89	+	58.37
Ab	66.21	64.79	33.33	68.00	77.41	50.97	50.68	+	34.09
An	29.34	21.28	22.29	24.21	22.59	8.74	11.43	+	7.53
Fe	26.19	26.76	27.03	26.47	25.73	27.10	14.95	18.47	18.23
(Na+K)	52.96	55.74	54.24	55.24	58.08	62.58	70.04	72.06	71.73
Qu	27.64	35.55	33.61	31.91	42.05	25.67	43.87	33.67	43.91
Cor	2.49	5.04	3.15	2.33	4.30	3.53	1.37	0.00 ⁺	0.34
Or	11.23	13.00	22.46	11.76	7.62	27.18	19.80	36.40	29.49
Alb	26.23	22.00	12.69	24.79	23.02	20.56	20.73	19.80	15.57
An	14.07	10.10	11.10	11.56	8.34	6.94	6.42	2.16	5.08
En	5.48	4.48	4.23	5.36	4.51	5.85	1.79	0.00	0.57
Fs	5.28	4.30	0.00	4.36	5.75	4.92	1.72	0.00	0.28
Mag	2.17	2.03	4.71	2.32	0.43	2.33	1.19	2.32	3.07
Il	0.95	1.33	1.29**	1.20	0.66	1.75	0.80	1.94 ^{'''}	0.78
Ap	0.47	0.47	0.47	0.38	0.21	0.38	0.71	0.00	0.50

** includes 0.15% haematite

''' includes 1.94% haematite

+ Analysis 41 is Al₂O₃ deficient and also contains
Di 1.29% and Wo1 1.57%

	34	35	36	37	38	39	40	41	42
Si ⁴⁺	63.31	65.48	65.32	65.62	70.03	62.84	73.03	70.29	73.52
Ti ⁴⁺	0.37	0.51	0.46	0.47	0.26	0.66	0.31	0.00	0.30
Al ³⁺	17.07	17.45	16.55	15.69	15.23	16.85	12.96	12.78	12.06
Fe ³⁺	1.10	1.01	2.60	1.18	0.22	1.15	0.60	2.55	1.54
Fe ²⁺	3.19	2.73	1.70	2.91	2.92	3.29	1.32	0.58	0.98
Mn ²⁺	0.08	0.16	0.00	0.10	0.00	0.07	0.04	0.00	0.20
Mg ²⁺	3.21	2.58	2.58	3.15	2.63	3.33	1.04	0.34	0.33
Ca ²⁺	3.25	2.37	2.73	2.68	1.88	1.64	1.75	1.57	1.34
Na ⁺	5.88	4.85	2.96	5.58	5.15	4.48	4.59	4.35	3.43
K ⁺	2.37	2.70	4.93	2.50	1.61	5.57	4.13	7.53	6.13
P ⁵⁺	0.16	0.16	0.17	0.13	0.07	0.13	0.25	0.00	0.17
Ca	28.25	23.90	25.67	24.87	21.80	14.02	16.71	11.68	12.30
Na	51.13	48.89	27.87	51.92	59.60	38.29	43.84	32.33	31.50
K	20.62	27.22	46.46	23.20	18.60	47.69	39.44	55.99	56.20
Ca	20.86	17.50	18.73	18.29	16.19	10.22	14.21	9.53	10.06
Fe	26.19	26.76	27.03	26.47	25.73	27.10	14.95	18.41	18.23
(Na+K)	52.96	55.74	54.24	55.24	58.08	62.68	70.84	72.06	71.71
si	269.4	306.6	299.3	299.6	375.5	274.1	468.7	404.5	483.5
al	36.32	40.86	37.91	35.81	40.81	36.74	41.59	36.77	39.66
fm	32.29	30.39	31.53	33.53	30.98	34.19	19.20	19.99	20.07
c	13.83	11.09	12.49	12.21	10.10	7.15	11.23	9.04	8.82
alk	17.56	17.66	18.08	18.44	18.11	21.92	27.98	34.19	31.45
k	0.29	0.36	0.63	0.31	0.24	0.55	0.47	0.63	0.64
mg	0.42	0.40	0.37	0.43	0.46	0.42	0.35	0.10	0.11
ti	1.57	2.37	2.10	2.13	1.38	2.87	1.96	0.00	1.95
p	0.35	0.38	0.39	0.30	0.20	0.28	0.79	0.00	0.56
Qtz I.	99.2	135.9	126.9	125.8	203.0	86.4	256.7	167.7	257.8

	43	44	45	46	47
SiO ₂	69.96	65.90	65.47	73.40	76.54
TiO ₂	0.70	0.62	0.88	0.20	0.19
Al ₂ O ₃	16.66	16.75	14.26	14.10	11.85
Fe ₂ O ₃	2.67	1.07	2.61	0.70	0.59
FeO	2.90	3.00	3.00	1.70	1.22
MnO	0.00	0.00	0.11	0.02	0.03
MgO	2.42	1.76	0.90	0.40	0.30

Table IV.6

Summary of the geochemical data for various plutonic rocks from the literature. Major element composition (oxide %), the Barth (1960 & 1962) mesonorm and the Kelsey-C.I.P.W. (1965) norm are listed in order on the following two pages.

Total	100.00	100.00	99.35	99.82	99.42
-------	--------	--------	-------	-------	-------

Analysis 43: biotite-plagioclase paragneiss, Mehnert (1968).

Analysis 44: biotite-plagioclase-quartz diatexite,
Mehnert (1968).

Analysis 45: synkinematic granodiorite, Marmo (1962).

Analysis 46: average Woodson Mountain granodiorite,
Larsen (1948).

Analysis 47: Roblar leucogranite, Larsen (1948).

	43	44	45	46	47
SiO ₂	69.96	65.90	65.47	73.40	76.54
TiO ₂	0.70	0.62	0.88	0.20	0.19
Al ₂ O ₃	16.66	16.75	14.26	14.10	11.86
Fe ₂ O ₃	2.07	1.07	2.61	0.70	0.59
FeO	2.98	3.72	3.89	1.70	1.22
MnO	0.00	0.00	0.11	0.02	0.03
MgO	2.42	1.76	0.96	0.40	0.30
CaO	2.73	2.83	2.78	2.10	1.10
Na ₂ O	3.48	4.30	3.05	3.40	3.06
K ₂ O	2.03	2.25	4.85	3.50	4.29
H ₂ O +	0.82	0.68	0.43	0.30	0.22
P ₂ O ₅	0.15	0.12	0.10	0.00	0.02
Total	<u>100.00</u>	<u>100.00</u>	<u>99.39</u>	<u>99.82</u>	<u>99.42</u>

Or	8.38	9.25	27.58	20.00	20.00
Ab	69.19	70.40	58.44	50.00	50.00
An	22.43	20.37	14.00	15.00	15.00
Qu	27.79	21.89	20.00	16.00	15.00
Cor	4.13	2.38	0.00	0.00	0.00
Or	12.00	13.30	28.00	0.00	0.00
Alh	29.45	36.39	25.81	0.00	0.00
An	12.56	13.26	10.00	0.00	0.00
En	6.03	4.38	2.02**	0.00	0.00
Fs	2.61	4.92	3.16**	0.00	0.00
Mag	3.00	1.55	3.78	0.00	0.00
Il	1.23	1.18	1.67	0.00	0.00
Ap	0.36	0.28	0.24	0.00	0.00

** Anal. 44, 45, 46, 47

	43	44	45	46	47
Ap	0.32	0.25	0.22	0.00	0.04
Sph	1.49	1.31	1.89	0.43	0.41
Mag	2.20	1.13	2.81	0.74	0.63
Cor	5.58	3.50	0.34	1.29	0.53
Qu	30.52	24.65	22.70	33.23	37.84
Alb	31.76	38.95	28.19	31.07	28.18
Or	3.85	5.11	23.47	18.27	23.99
An	10.30	11.20	10.37	9.90	4.79
Bi	13.36	13.28	9.65	4.45	3.22
Qtz	46.16	35.88	30.52	40.25	42.03
Or	5.81	7.44	31.56	22.12	26.65
Ab	48.03	56.69	37.91	37.63	31.31
Or	8.38	9.25	37.84	30.84	42.12
Ab	69.19	70.49	45.44	52.45	49.48
An	22.43	20.27	16.72	16.71	8.40
Qu	27.73	21.69	20.85	34.11	38.90
Cor	4.13	2.38	0.00**	0.90	0.23
Or	12.00	13.30	28.86	20.68	25.35
Alb	29.45	36.39	25.81	28.77	25.89
An	12.56	13.26	10.90	10.42	5.33
En	6.03	4.38	2.02**	1.00	0.75
Fs	2.61	4.92	3.16**	2.25	1.49
Mag	3.00	1.55	3.78	1.01	0.86
Il	1.33	1.18	1.67	0.30	0.36
Ap	0.36	0.28	0.24	0.00	0.05

** Analysis 45 also contains Di 1.88%

Table IV.7

The comparison between the arithmetic mean of the 6 homogeneous diatexites and the arithmetic mean of the 9 inhomogeneous diatexites from the St. Malo belt.

S.D. = standard deviation.

MAX. = maximum value, MIN. = minimum value.

RANGE = the difference between the maximum and minimum values.

	MEAN	S.D.	MAX.	MIN.	RANGE
SiO ₂	69.63	1.04	71.20	68.30	2.90
TiO ₂	0.48	0.11	0.64	0.30	0.34
Al ₂ O ₃	15.64	0.38	16.05	15.20	0.85
Fe ₂ O ₃	1.26	0.50	1.94	0.50	1.44
FeO	1.72	0.45	2.53	1.19	1.34
Ca	697	269	1152	362	790
Co	16	9	29	7	22
La	18*	3	23	14	9
Pb	46*	16	69	30	39
Sm	135	17	158	110	48
Y	177	41	257	135	122
Zn	22	2	25	20	5
Zr	3.6*	0.5	4.2	2.8	1.4
Y ₂ O ₃	8*	5	17	4	13
ZnO	99	11	76	46	30
ZrO ₂	155*	26	178	111	67

* Analysis 6 (specimen 72) omitted from mean calculations
 La 97, Pb 110, Y 71 & Zr 423.

THE ST. MALO DIATEXITES

HOMOGENEOUS DIATEXITE

INHOMOGENEOUS DIATEXITE

	MEAN	S.D.	MAX.	MIN.	RANGE	MEAN	S.D.	MAX.	MIN.	RANGE
SiO ₂	69.63	1.04	71.20	68.50	2.70	67.73	0.94	69.25	66.90	2.35
TiO ₂	0.48	0.11	0.64	0.32	0.32	0.75	0.08	0.86	0.64	0.22
Al ₂ O ₃	15.64	0.38	16.05	15.10	0.95	15.06	0.64	16.40	14.35	2.05
Fe ₂ O ₃	1.26	0.50	1.94	0.54	1.40	1.87	0.47	2.78	1.25	1.53
FeO	1.72	0.45	2.53	1.16	1.37	3.35	0.45	4.08	2.78	1.30
MnO	0.04	0.01	0.04	0.03	0.01	0.05	0.01	0.06	0.04	0.02
MgO	0.98	0.35	1.35	0.50	0.85	1.42	0.33	1.93	1.03	0.90
CaO	1.56	0.43	2.00	1.02	0.98	1.36	0.33	1.97	0.92	1.05
Na ₂ O	3.61	0.43	4.39	3.19	1.10	3.25	0.25	3.74	2.95	0.79
K ₂ O	3.65	0.83	4.77	2.25	2.52	3.67	0.27	4.14	3.15	0.99
P ₂ O ₅	0.18	0.04	0.23	0.11	0.12	0.23	0.10	0.38	0.11	0.27
T. Fe	3.17	0.95	4.75	1.83	2.92	5.59	0.35	6.06	5.05	1.01
Ba	697	269	1152	352	800	769	150	1065	574	491
Cu	16	9	28	7	21	32	11	52	16	36
La	18*	3	23	14	9	20	4	28	15	13
Pb	46*	16	69	32	37	38	19	86	26	60
Rb	135	17	158	110	48	140	8	152	129	23
Sr	177	41	257	149	108	172	32	229	123	106
Th	22	2	25	20	5	23	1	26	22	4
U	3.6*	0.6	4.2	2.8	1.4	3.9	1.0	5.8	2.8	3.0
Y	8*	5	17	4	13	19	6	34	15	19
Zn	59	11	76	46	30	84	13	103	68	35
Zr	155*	26	178	111	67	233	70	410	178	232

* Analysis 6 (specimen 720) omitted from mean calculation:
La 87, Pb 110, U 8.3, Y 73 & Zr 423.

ST. MALO AND DINAN

9 ST. MALO INHOMOGENEOUS DIATEXITES

3 DINAN ROCKS

Table IV.8

	MEAN	S.D.	MAX.	MIN.	RANGE	MEAN	S.D.	MAX.	MIN.	RANGE
S ₁₀	67.73	0.94	69.25	66.90	2.35	66.39	0.20	66.62	66.25	0.37
T ₁₀	0.75	0.08	0.86	0.64	0.22	0.90	0.06	0.96	0.86	0.10
Al ₂ O ₃	15.06	0.64	16.40	14.35	2.05	15.75	0.05	15.20	15.10	0.10
Fe ₂ O ₃	1.87	0.47	2.79	1.25	1.54	2.49	0.74	3.91	1.87	1.44
FeO	3.35	0.45	4.08	2.78	1.30	2.83	0.77	3.57	2.03	1.54
MgO	1.42	0.33	1.93	1.03	0.90	1.23	0.75	1.40	1.14	0.26
CaO	1.35	0.33	1.97	0.92	1.05	1.07	0.23	1.28	0.82	0.46
Na ₂ O	3.25	0.25	3.74	2.95	0.79	2.70	0.25	2.87	2.41	0.46
K ₂ O	4.31	0.13	4.44	4.19	0.25	4.31	0.13	4.44	4.19	0.25
P ₂ O ₅	0.19	0.01	0.20	0.18	0.02	0.19	0.01	0.20	0.18	0.02
T. Fe	5.59	0.35	6.06	5.05	1.01	5.63	0.19	5.84	5.48	0.36
Ba	769	150	1069	574	491	870	55	930	822	108
Cu	32	11	52	16	36	23	16	38	6	32
La	20	4	28	15	13	22	4	27	19	8
Pb	38	19	86	25	60	63	31	97	36	61
Rb	140	8	152	129	23	160	9	170	153	17
Sr	172	32	220	123	106	158	19	180	140	37
Th	23	1	26	22	4	25	3	28	23	5
U	3.9	1.0	5.8	2.8	3.0	4.1	0.7	4.9	3.5	1.4
Y	19	6	34	15	19	17	3	20	15	5
Zn	84	13	103	68	35	120	33	145	82	63
Zr	233	70	410	178	232	222	5	230	215	15

The comparison between the arithmetic mean of the 9 St. Malo inhomogeneous diatexites and the arithmetic mean of the 3 Dinan rocks.

S.D. = standard deviation.

MAX. = maximum value, MIN. = minimum value.

RANGE = the difference between the maximum and minimum values.

ST. MALO AND DINAN

9 ST. MALO INHOMOGENEOUS DIATEXITES

3 DINAN ROCKS

	MEAN	S.D.	MAX.	MIN.	RANGE	MEAN	S.D.	MAX.	MIN.	RANGE
SiO ₂	67.73	0.94	69.25	66.90	2.35	66.39	0.20	66.62	66.25	0.37
TiO ₂	0.75	0.08	0.86	0.64	0.24	0.90	0.06	0.96	0.86	0.10
Al ₂ O ₃	15.06	0.64	16.40	14.35	2.05	15.15	0.05	15.20	15.10	0.10
Fe ₂ O ₃	1.87	0.47	2.78	1.25	1.53	2.49	0.74	3.31	1.87	1.44
FeO	3.35	0.45	4.08	2.78	1.30	2.83	0.77	3.57	2.03	1.54
MnO	0.05	0.01	0.06	0.04	0.02	0.04	0.00	0.04	0.04	0.00
MgO	1.42	0.33	1.93	1.03	0.90	1.23	0.15	1.40	1.14	0.26
CaO	1.36	0.33	1.97	0.92	1.05	1.07	0.23	1.28	0.82	0.46
Na ₂ O	3.25	0.25	3.74	2.95	0.79	2.70	0.25	2.87	2.41	0.46
K ₂ O	3.67	0.27	4.14	3.15	0.99	4.31	0.13	4.44	4.19	0.25
P ₂ O ₅	0.23	0.10	0.38	0.11	0.27	0.19	0.01	0.20	0.19	0.01
T. Fe	5.59	0.35	6.06	5.05	1.01	5.63	0.19	5.84	5.48	0.36
Ba	769	150	1065	574	491	870	55	930	822	108
Cu	32	11	52	16	36	23	16	38	6	32
La	20	4	28	15	13	22	4	27	19	8
Pb	38	19	86	26	60	63	31	97	36	61
Rb	140	8	152	129	23	160	9	170	153	17
Sr	172	32	229	123	106	158	19	180	143	37
Th	23	1	26	22	4	25	3	28	23	5
U	3.9	1.0	5.8	2.8	3.0	4.1	0.7	4.9	3.5	1.4
Y	19	6	34	15	19	17	3	20	15	5
Zn	84	13	103	68	35	120	33	145	82	63
Zr	233	70	410	178	232	222	8	230	215	15

	48	49
	<u>211</u>	<u>212</u>
SiO ₂	72.25	73.00
TiO ₂	0.01	0.01
Al ₂ O ₃	16.25	16.00
Fe ₂ O ₃	0.30	0.32
FeO	0.18	0.38
MnO	0.05	0.08
MgO	0.55	0.59
CaO	0.36	0.30
Na ₂ O	5.10	4.33
K ₂ O	3.45	3.73
H ₂ O +	1.02	0.62
P ₂ O ₅	0.27	0.22
Total	<u>100.29</u>	<u>99.95</u>

Table IV.9

The chemical composition of the 2 Cadomian felsic sheets.

The major element composition (oxide %), trace element content (ppm) and selected element ratios are listed in order.

Note: * signifies that the trace element concerned is present in an amount below the calculated lower limit of detection.

Sr	82	80
Th	12	12
Zn	4	51
Zr	20	29
K	2.85	3.10
K/Rb	123	101
Ba/Kx10 ²	0.26	0.13
Ba/Rb	0.35	0.15
Rb/Sr	2.83	3.84
Ca	0.26	0.21
Ca/Sr	31	27
Ca/Zr	129	76
Ca/Y	536	435
Ti	0.008	0.006
Ti/Zr	3	2
Th/U	0.00	4.14

Analysis 48: specimen 211, granite pegmatite, Plage de Quatre Vaux.

Analysis 49: specimen 212, tourmaline granite, Plage de Quatre Vaux.

	48	49
	<u>211</u>	<u>212</u>
SiO ₂	72.25	73.00
TiO ₂	0.01	0.01
Al ₂ O ₃	16.25	16.00
Fe ₂ O ₃	0.30	0.32
FeO	0.18	0.38
MnO	0.05	0.08
MgO	0.55	0.59
CaO	0.36	0.30
Na ₂ O	5.10	4.33
K ₂ O	3.45	3.73
H ₂ O +	1.02	0.62
P ₂ O ₅	0.77	0.62
Total	<u>100.29</u>	<u>99.95</u>
T. Fe	0.50	0.74
Ba	80	45
Cu	*	5
La	*	*
Pb	25	41
Rb	232	307
Sr	82	80
Th	12	12
U	1.5	2.9
Y	3	4
Zn	4	51
Zr	20	29
K	2.86	3.10
K/Rb	123	101
Ba/Kx10 ²	0.28	0.15
Ba/Rb	0.35	0.15
Rb/Sr	2.83	3.84
Ca	0.26	0.21
Ca/Sr	31	27
Ca/Zr	129	74
Ca/Y	856	535
Ti	0.006	0.006
Ti/Zr	3	2
Th/U	8.00	4.14

mobile during ultrametamorphism. The oxides and trace elements which are significantly lower for the homogeneous diatexites (ie. the inhomogeneous diatexites are relatively enriched in these oxides and trace elements) are those that might be expected to behave in a refractory manner during anatexis and thus this difference between the rock types might be expected. The St. Malo inhomogeneous diatexites are significantly richer in SiO_2 , MnO and Na_2O and significantly poorer in TiO_2 , K_2O and Rb than the rocks from the Dinan belt. These differences are the type that might be expected from minor variation in the source material for anatexis (eg. the SiO_2 and Na_2O) and minor variation in the degree of late muscovitisation (ie. K metasomatism causing significant variation in K_2O and Rb). The differences between these two rock groups, especially for the alkali elements, are reflected in normative plots on the Q-Ab-Or face of the Q-Ab-Or-An tetrahedron and will be discussed further in Chapter VI.

In a consideration of the whole spectrum of St. Malo rocks¹ there is a general increase of CaO content with increasing Na_2O whilst Na_2O generally decreases with increasing K_2O content (Figure IV.1). Moreover, the bulk of the St. Malo rocks plot in the region of quartz dioritic to granodioritic rocks (2.5-3.5% Na_2O and 3.0-5.0% K_2O) but between the fields of greywackes (2.5-4.0% Na_2O and 1.7-2.5% K_2O) and arkoses (1.5-2.5% Na_2O and 3.0-6.0% K_2O) in terms of alkali contents. The higher alkali content of the homogeneous granites and the high CaO - low K_2O content of the two trondhjemite sheets are apparent.

1. The phrase 'St. Malo rocks' is taken to include the three analyses of specimens from the Dinan belt for the remainder of this section.

Figure IV.1

Plots of CaO against Na_2O and Na_2O against K_2O for the diatexites, metatexite and metasediments (solid circles), the unaltered metasediment (open circle), the homogeneous granites (diagonal crosses) and the granitoid sheets (upright crosses).

Figure IV.2 shows the St. Malo rocks plotted on K-Na-Ca and Fe-Na+K-Ca diagrams together with some averages from the literature. Again the St. Malo rocks are seen to plot between the greywackes and the arkoses. However, it is more useful to examine similarities and differences between the St. Malo rocks and the averages from the literature by looking at their Niggli numbers which, in a general way, characterise a rock (see Tables IV.1-IV.5 and Figures IV.3 & IV.4). It is apparent that the arkoses given for comparison with the St. Malo rocks are far too rich in silica and that there is a closer affinity, in terms of silica content, with the greywackes. But, whilst the arkoses are also too alkali-rich the greywackes are alkali-poor and have higher fm and c than the St. Malo rocks. Thus the St. Malo rocks generally plot between the arkoses and the greywackes on all the diagrams comprising Figures IV.3 & IV.4 except that of Niggli alk against Niggli c, where the depleted nature of the St. Malo rocks in CaO compared with the greywackes is emphasised. It is interesting that the mean of the 11 inhomogeneous diatexites (large solid circle - K) plots close to the centroid of the St. Malo analyses in Figures IV.3 & IV.4. This raises the possibility that this mean value approximates to the average composition of the early Pentevrian crust in this part of the Armorican Massif. This is discussed more fully later in this section (page IV.6). There are four possible interpretations of the above data:

1. The St. Malo rocks might have been produced by extensive segregation and anatexis (=metatexis and diatexis) of a sequence of feldspathic greywackes (which were accordingly alkali-rich) during an episode of high-grade metamorphism and without extensive metasomatism. The common development of large unorientated (late ?) muscovites suggests some addition of K^+ (probably in a hydrous solution) and argues against true isochemical metamorphism.

Figure IV.2

K-Na-Ca and Fe-Na+K-Ca plots for the diatexites, metatexite and metasediments (small solid circles), the unaltered metasediment (open circle), the homogeneous granites (diagonal crosses) and the granitoid sheets (upright crosses). The following are also plotted for comparison:

- A. Average of 23 greywackes, Pettijohn (1957).
- B. Average of 30 greywackes, Tyrrell (1933).
- C. The combination of 2 parts average shale and 2 parts average arkose, Pettijohn (1957).
- D. Average of 61 greywackes, Tobschall (1971).
- E. Fresh Franciscan greywacke, Taliaferro (1943).
- F. Average of 9 non-garnetiferous schists, Brown (1967).
- G. Average of 3 Torridonian arkoses, Kennedy (1951).
- H. Lower Old Red Sandstone, Mackie (1905).
- I. Average arkose, Pettijohn (1957).
- J. Average of 6 homogeneous diatexites, this work.
- K. Average of 11 inhomogeneous diatexites, this work.

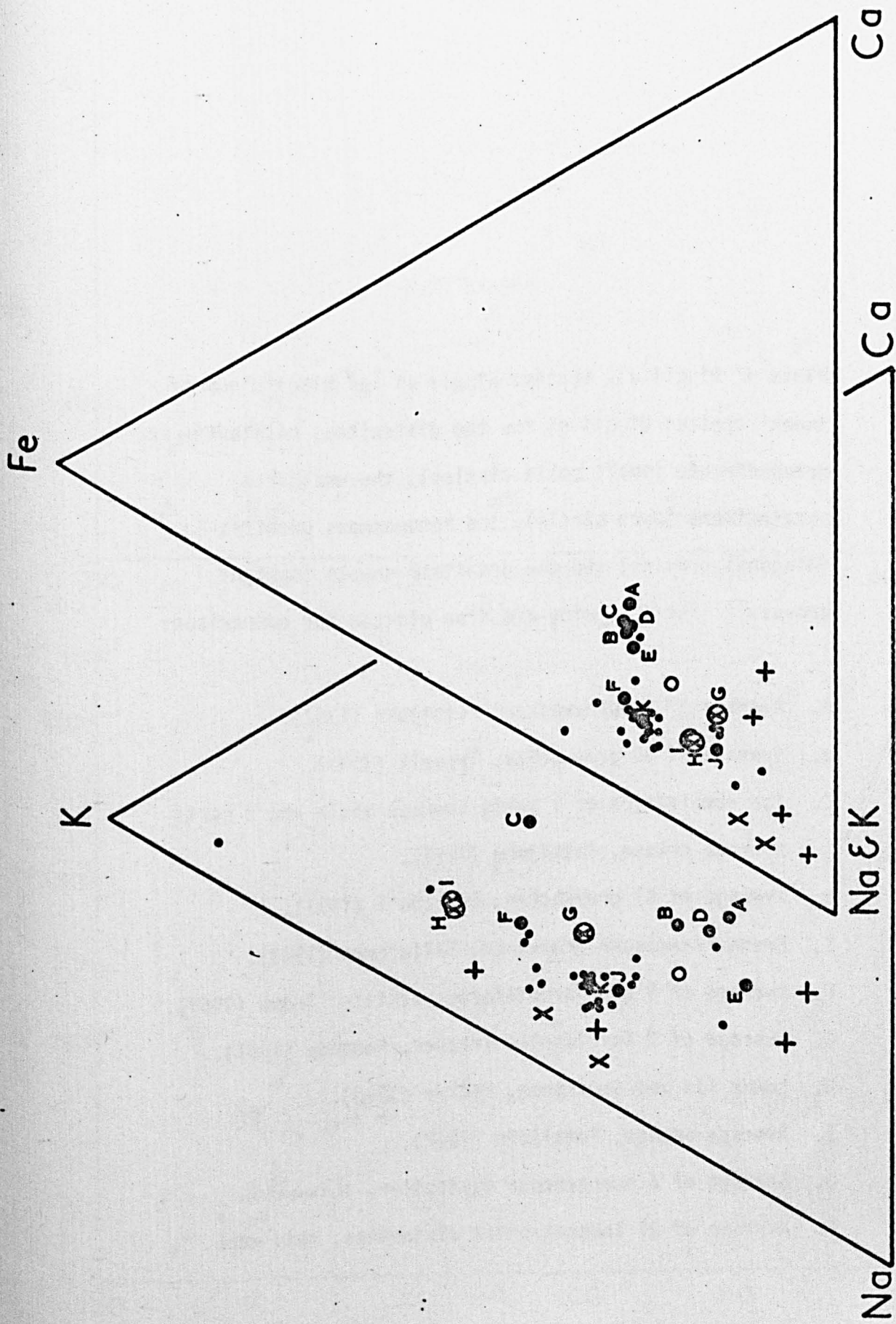


Figure IV.3

Plots of Niggli alk against Niggli si and Niggli 'quartz index' against Niggli si for the diatexites, metatexite and metasediments (small solid circles), the unaltered metasediment (open circle), the homogeneous granites (diagonal crosses) and the granitoid sheets (upright crosses). The following are also plotted for comparison:

- A. Average of 23 greywackes, Pettijohn (1957).
- B. Average of 30 greywackes, Tyrrell (1933).
- C. The combination of 2 parts average shale and 2 parts average arkose, Pettijohn (1957).
- D. Average of 61 greywackes, Tobschall (1971).
- E. Fresh Franciscan greywacke, Taliaferro (1943).
- F. Average of 9 non-garnetiferous schists, Brown (1967).
- G. Average of 3 Torridonian arkoses, Kennedy (1951).
- H. Lower Old Red Sandstone, Mackie (1905).
- I. Average arkose, Pettijohn (1957).
- J. Average of 6 homogeneous diatexites, this work.
- K. Average of 11 inhomogeneous diatexites, this work.

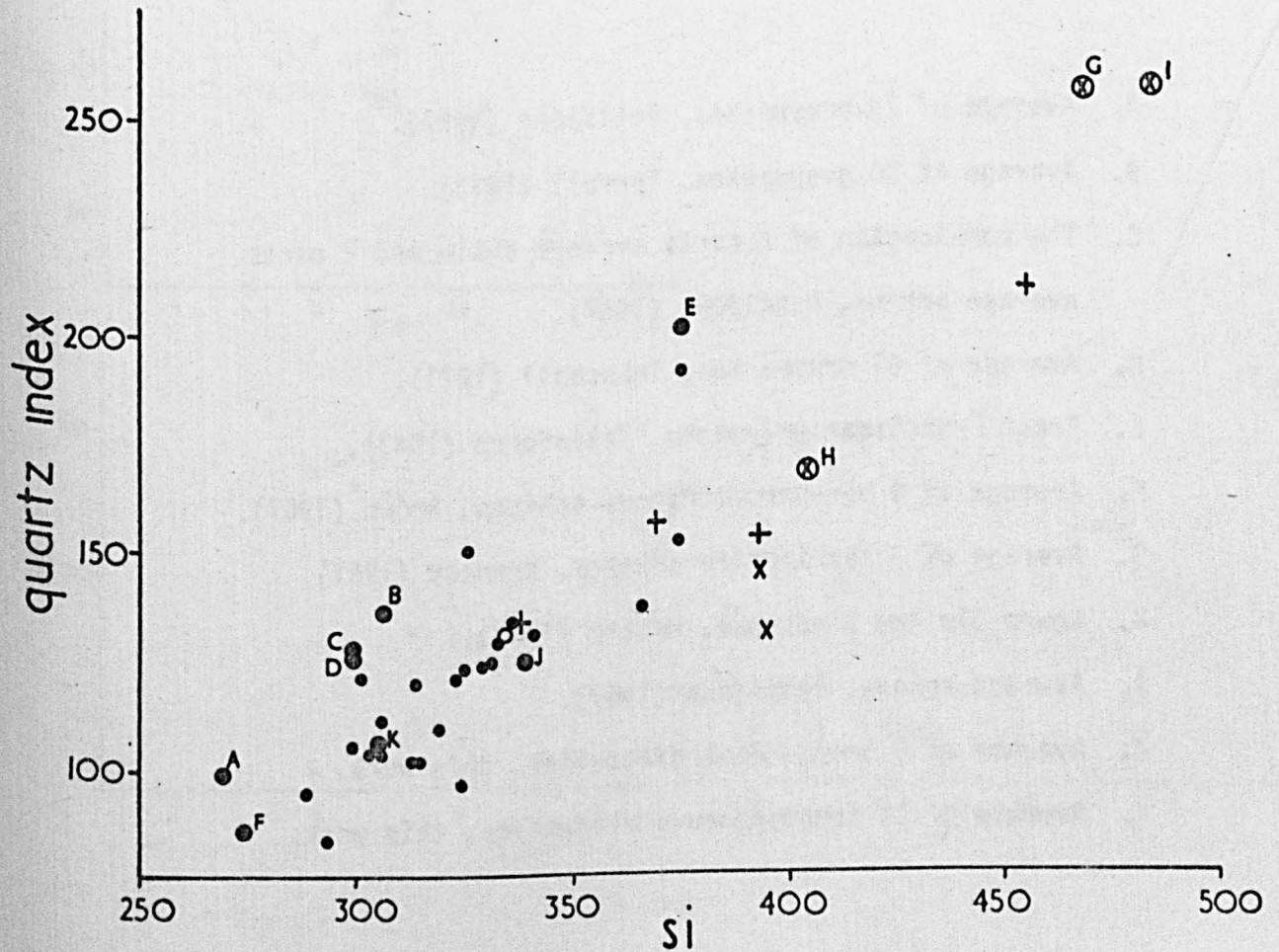
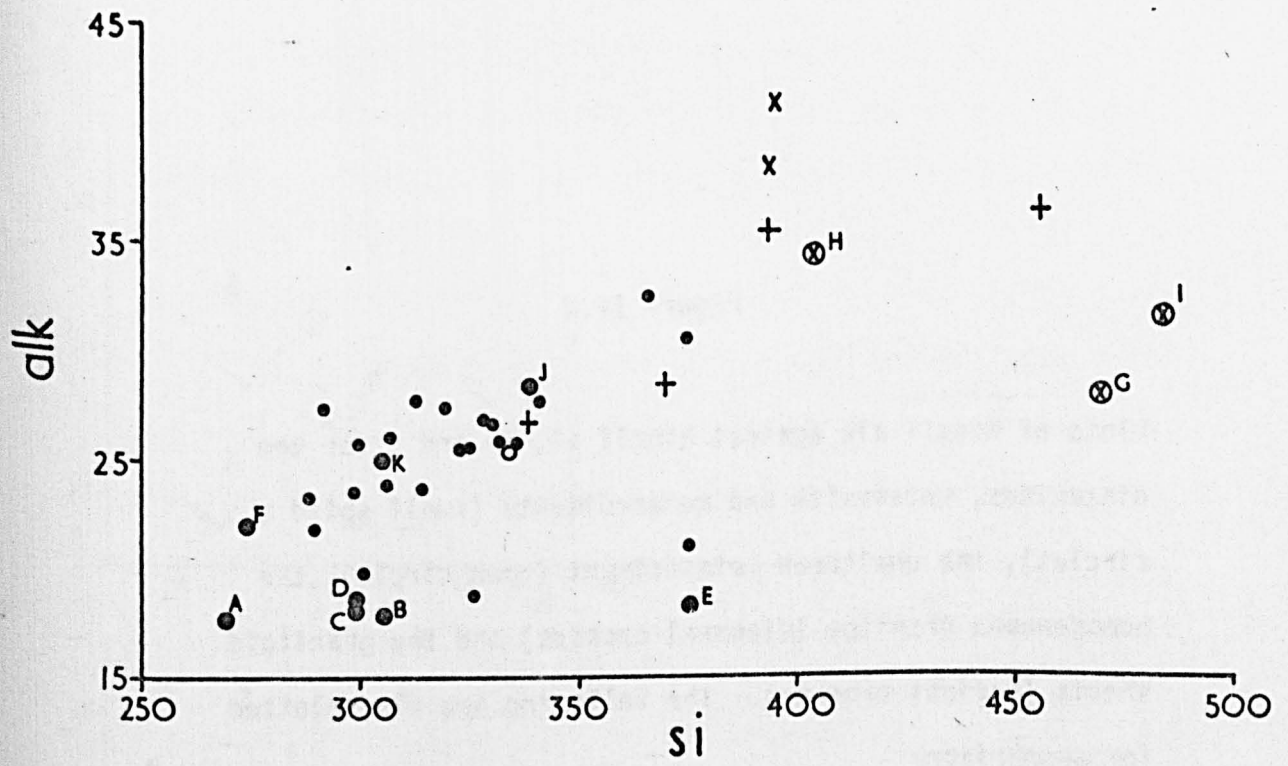
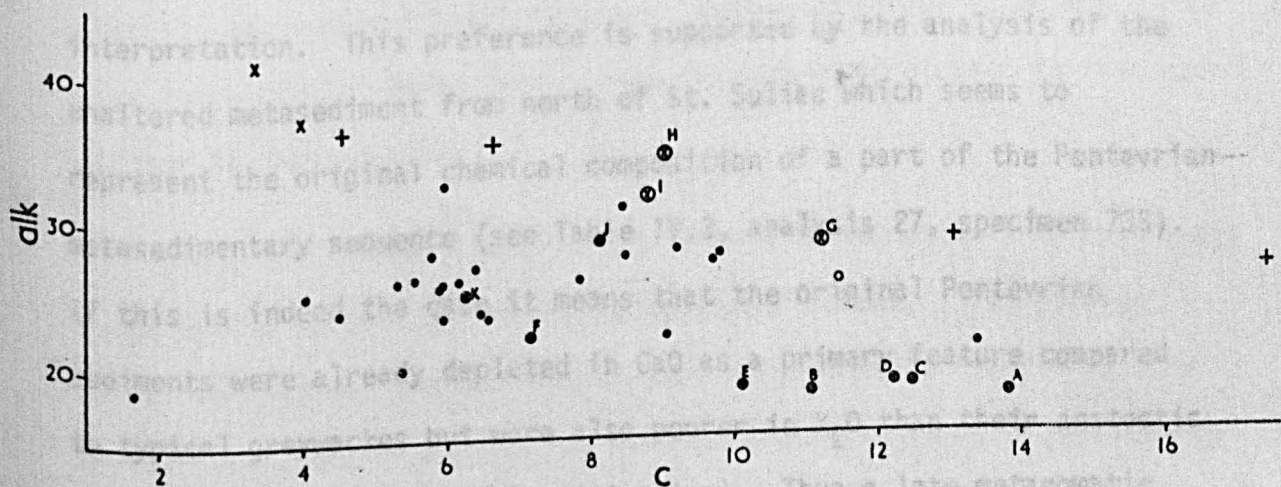
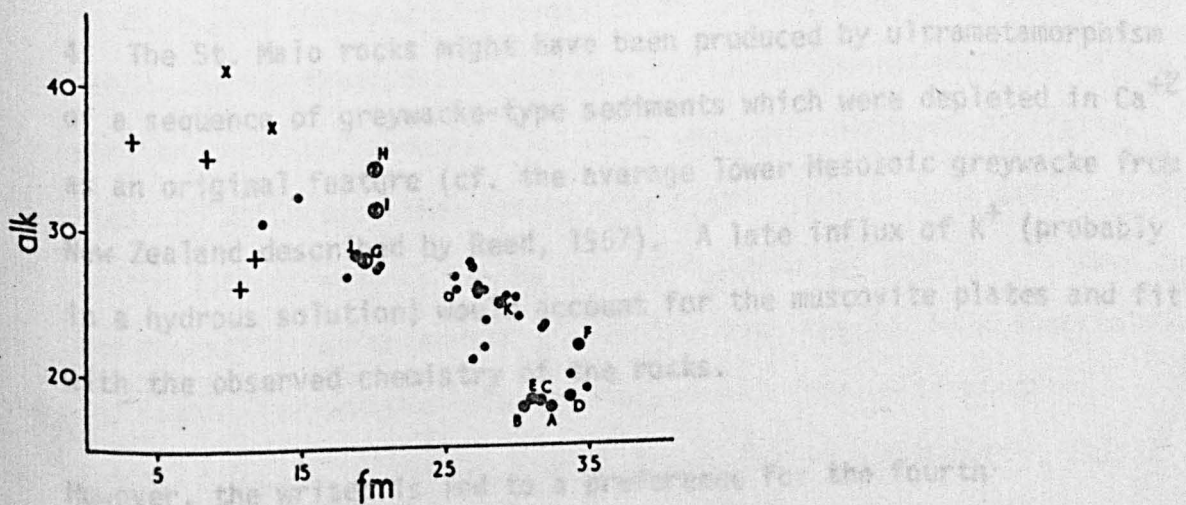
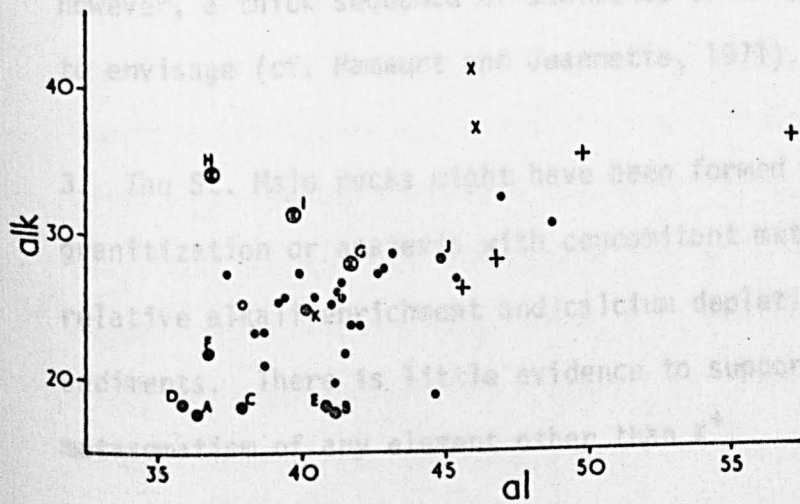


Figure IV.4

Plots of Niggli alk against Niggli al, fm and c for the diatexites, metatexite and metasediments (small solid circles), the unaltered metasediment (open circle), the homogeneous granites (diagonal crosses) and the granitoid sheets (upright crosses). The following are also plotted for comparison:

- A. Average of 23 greywackes, Pettijohn (1957).
- B. Average of 30 greywackes, Tyrrell (1933).
- C. The combination of 2 parts average shale and 2 parts average arkose, Pettijohn (1957).
- D. Average of 61 greywackes, Tobschall (1971).
- E. Fresh Franciscan greywacke, Taliaferro (1943).
- F. Average of 9 non-garnetiferous schists, Brown (1967).
- G. Average of 3 Torridonian arkoses, Kennedy (1951).
- H. Lower Old Red Sandstone, Mackie (1905).
- I. Average arkose, Pettijohn (1957).
- J. Average of 6 homogeneous diatexites, this work.
- K. Average of 11 inhomogeneous diatexites, this work.

2. The St. Maie rocks could represent the results of differential anatexis and concomitant homogenization (especially of the alkali elements) of a sequence of greywacke-type and arkose-type sediments. However, a thick sequence of sediments of this type is difficult to envisage (cf. Massart and Veinotte, 1971).



However, the widespread preference for the fourth interpretation. This preference is supported by the analysis of the altered metasediment from north of St. Sulpice which seems to represent the original chemical composition of a part of the Pontevrian-sedimentary sequence (see Table 1, analysis 27, specimen 735). This is indeed the case, it means that the original Pontevrian elements were already depleted in CaO as a primary feature compared to the bulk of the St. Maie rocks. Thus a late metamorphic addition of H_2O (or K^+ probably in a hydrous phase), as required by interpretation 4, seems likely to account for the higher H_2O contents of the bulk of the St. Maie rocks.

2. The St. Malo rocks could represent the results of differential anatexis and concomitant homogenization (especially of the alkali elements) of a sequence of greywacke-type and arkose-type sediments. However, a thick sequence of sediments of this type is difficult to envisage (cf. Hameurt and Jeannette, 1971).
3. The St. Malo rocks might have been formed by metasomatic granitization or anatexis with concomitant metasomatism resulting in relative alkali enrichment and calcium depletion of greywacke-type sediments. There is little evidence to support large scale (regional) metasomatism of any element other than K^+ .
4. The St. Malo rocks might have been produced by ultrametamorphism of a sequence of greywacke-type sediments which were depleted in Ca^{+2} as an original feature (cf. the average lower Mesozoic greywacke from New Zealand described by Reed, 1957). A late influx of K^+ (probably in a hydrous solution) would account for the muscovite plates and fit with the observed chemistry of the rocks.

However, the writer is led to a preference for the fourth interpretation. This preference is supported by the analysis of the unaltered metasediment from north of St. Suliac which seems to represent the original chemical composition of a part of the Pentevrian metasedimentary sequence (see Table IV.3, analysis 27, specimen 733). If this is indeed the case it means that the original Pentevrian sediments were already depleted in CaO as a primary feature compared to typical greywackes but were also poorer in K_2O than their anatectic equivalents (eg. the St. Malo diatexites). Thus a late metasomatic addition of K_2O (or K^+ probably in a hydrous phase), as required by interpretation 4, seems likely to account for the higher K_2O contents of the bulk of the St. Malo rocks.

It has been suggested (Condie, 1967) that the composition of Precambrian greywackes reflects the composition of the ancient crust that was being eroded. Table IV.10 compares the St. Malo diatexites and the Dinan diatexites with Poldervaart's (1955) average composition for the surface rocks of continental shield areas and with Eade and Fahrig's (1971) average composition of the Proterozoic. The overall similarity between these average values is quite remarkable and only SiO_2 , CaO and MgO show any marked dissimilarity. This supports the suggestion made above (page IV.4) that the average inhomogeneous diatexite might reflect the composition of the early Pentevrian crust in this part of the Armorican Massif. The diatexites were produced by extensive anatexis of a sequence of Ca-poor greywacke-type sediments (above) which themselves would have reflected the composition of the earlier gneissic basement from which they were derived by erosion. Chemical differentiation during this cycle seems to have been restricted to the loss of some Ca and Mg and the addition of some K. Metasediments and migmatites which possibly correlate with the St. Malo metasediments and migmatites occur within the metamorphic complex of southern Guernsey (eg. at Vason Bay and at Castle Cornet - see Roach, 1966). The Guernsey metasediments must have been deposited before 2,700 m.y. ago (see Roach et al., 1972, 248). This tentative correlation is discussed further in Chapter VII.

Since "diatexites lie within the field of magmatism and accordingly ought to lie outside the migmatite spectrum" (Brown, 1973) it might be useful to consider the St. Malo diatexites, the Dinan diatexites, the homogeneous granites and the two granite sheets in terms of the chemical classification of igneous rocks into 'magma types' proposed by Burri and Niggli (1945; in Burri, 1964). This classification is based on the Niggli numbers, especially 'fm', 'al', 'alk' and 'c'. The average

	1	2	3	4	5	6
SiO_2	69.6	67.7	66.4	67.5	68.4	65.0
TiO_2	0.5	0.8	0.9	0.8	0.6	0.6
Al_2O_3	15.6	15.7	15.2	15.1	15.5	18.0
Fe_2O_3	1.3	1.9	2.5	1.9	1.8	4.9*
MnO	0.1	0.1	0.1	0.1	0.1	0.1

Table IV.10

Mean composition of the diatexites and crustal rocks.

- 1 = Average of 6 homogeneous diatexites, this work.
- 2 = Average of 9 inhomogeneous diatexites (St. Malo), this work.
- 3 = Average of 2 inhomogeneous diatexites (Dinan), this work.
- 4 = Average of 11 inhomogeneous diatexites, this work.
- 5 = Average surface rock of continental shield areas, Poldervaart (1955).
- 6 = Average chemical composition of the Proterozoic, Eade and Fahrig (1971).

composition of crustal igneous rocks is taken as the common reference point and other magma types are defined according to their departure from this reference composition. The St. Malo diatexites and associated rocks may be considered, in terms of their chemical classification, as semisialic (fm=30; al = 37-45), intermediate to alkali-rich (ak = 2/2), c 3 poor (4/5) and 5 similar 6 to the granitic

SiO ₂	69.6	67.7	66.4	67.5	66.4	65.0
TiO ₂	0.5	0.8	0.9	0.8	0.6	0.6
Al ₂ O ₃	15.6	15.1	15.2	15.1	15.5	16.0
Fe ₂ O ₃	1.3	1.9	2.5	1.9	1.8	4.9*
FeO	1.7	3.4	2.8	3.3	2.8	
MnO	0.1	0.1	0.1	0.1	0.1	0.1
MgO	1.0	1.4	1.2	1.4	2.0	2.1
CaO	1.6	1.4	1.1	1.3	3.8	3.3
Na ₂ O	3.6	3.3	2.7	3.2	3.5	3.5
K ₂ O	3.7	3.7	4.3	3.8	3.3	3.5
P ₂ O ₅	0.2	0.2	0.2	0.2	0.2	0.2

* total iron as Fe₂O₃

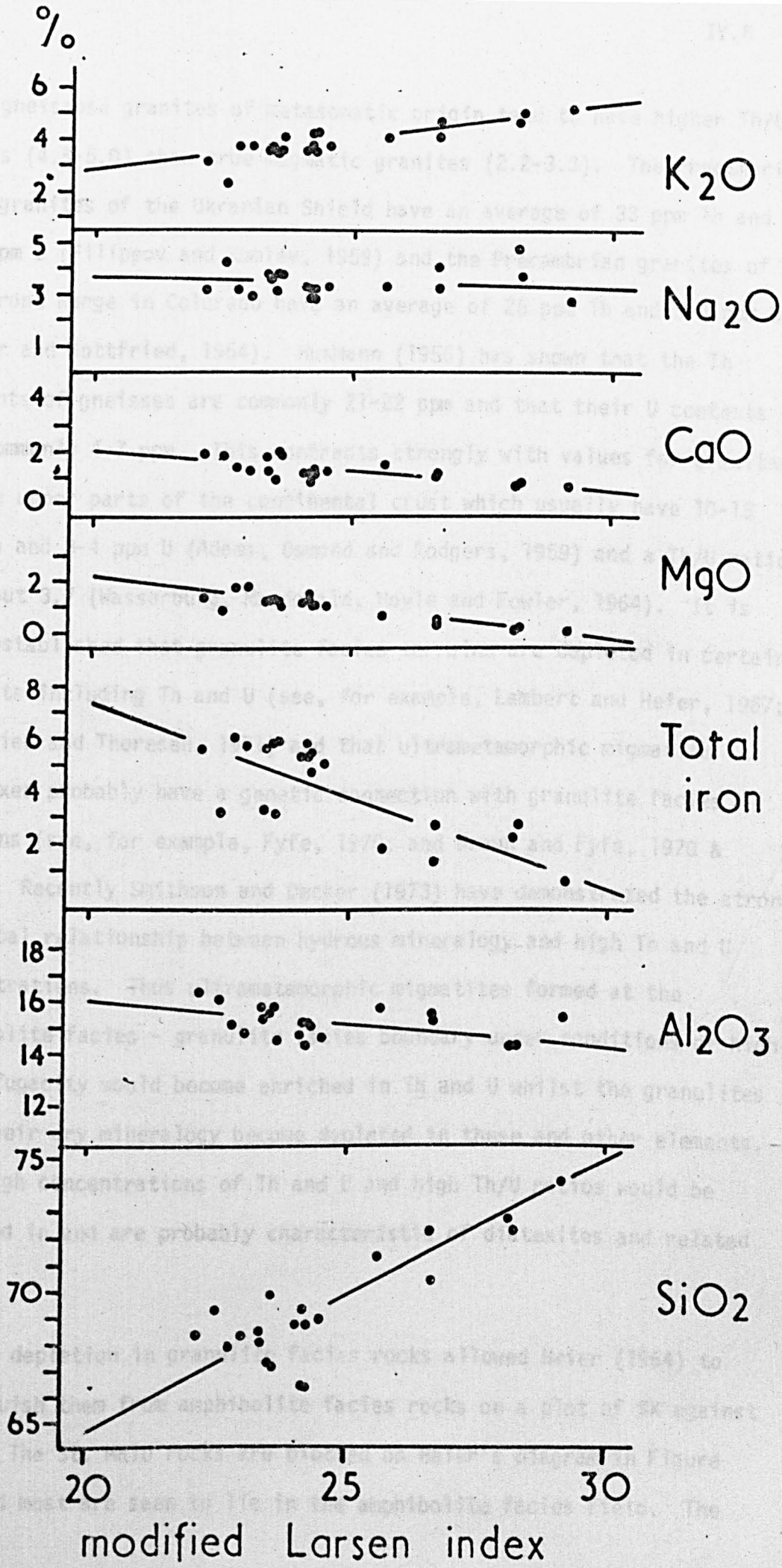
The U contents of the St. Malo rocks is generally 3-5 ppm (average of 6 homogeneous diatexites - 4.4 ppm; average of 3 homogeneous diatexites from St. Jacut - 3.7 ppm; and the average of 11 inhomogeneous diatexites - 3.3 ppm) and the Th contents 20-23 ppm (average of 6 homogeneous diatexites - 26 ppm; average of 3 homogeneous diatexites from St. Jacut - 23 ppm; and the average of 11 inhomogeneous diatexites - 24 ppm). The homogeneous granites have similar values but the granitoid sheets generally have both lower U and lower Th contents (see Tables IV.1 - IV.4). The Th/U ratios for the St. Malo rocks may be regarded as high and lie between 4 and 8 (average of 6 homogeneous diatexites - 5.9; average of 3 homogeneous diatexites from St. Jacut - 6.2; and the average of 11 inhomogeneous diatexites - 6.2). Precambrian granites are often characterised by high Th/U ratios (see Whitfield, Rogers and Adams, 1959) and Kolbe and Taylor (1966) have suggested

composition of crustal igneous rocks is taken as the common reference point and other magma types are defined according to their departure from this reference composition. The St. Malo diatexites and associated rocks may be considered, in terms of their chemical classification, as semisialic (f_{m^30} ; $a_1 = 37-45$), intermediate to alkali-rich ($alk = 2/3a_1$), 'c' poor ($c < 15$) and similar to the granitic and leucogranitic magma types of the calc-alkali series (in Burri, 1964). In Figure IV.5 the 'modified Larsen Index' ($(1/3Si + K) - (Ca + Mg)$) has been plotted against the main oxide percentages. Approximately linear variation trends are considered to be typical of a single suite of co-magmatic rocks. The St. Malo diatexites, the Dinan diatexites, the homogeneous granites and the two granite sheets all plot close to a linear trend in Figure IV.5 which suggests that they have a similar and related mode of origin. This is discussed more fully in Chapter VI.

The U contents of the St. Malo rocks is generally 3-5 ppm (average of 6 homogeneous diatexites - 4.4 ppm; average of 3 homogeneous diatexites from St. Jacut - 3.7 ppm; and the average of 11 inhomogeneous diatexites - 3.9 ppm) and the Th contents 20-29 ppm (average of 6 homogeneous diatexites - 26 ppm; average of 3 homogeneous diatexites from St. Jacut - 23 ppm; and the average of 11 inhomogeneous diatexites - 24 ppm). The homogeneous granites have similar values but the granitoid sheets generally have both lower U and lower Th contents (see Tables IV.1 - IV.4). The Th/U ratios for the St. Malo rocks may be regarded as high and lie between 4 and 8 (average of 6 homogeneous diatexites - 5.9; average of 3 homogeneous diatexites from St. Jacut - 6.2; and the average of 11 inhomogeneous diatexites - 6.2). Precambrian granites are often characterised by high Th/U ratios (see Whitfield, Rodgers and Adams, 1959) and Kolbe and Taylor (1966) have suggested

Figure IV.5

Plot of the 'modified Larsen Index' ($(\frac{1}{3}\text{Si} + \text{K}) - (\text{Ca} + \text{Mg})$) against the main oxide percentages (total iron as Fe_2O_3) for the St. Malo diatexites, the homogeneous granites and the two granite sheets together with the two Dinan diatexites.



that gneissose granites of metasomatic origin tend to have higher Th/U ratios (4.5-5.0) than true magmatic granites (2.2-3.3). The Precambrian mica granites of the Ukrainian Shield have an average of 33 ppm Th and 5.7 ppm U (Filippov and Komlev, 1959) and the Precambrian granites of the Front Range in Colorado have an average of 25 ppm Th and 5.0 ppm U (Phair and Gottfried, 1964). Husmann (1956) has shown that the Th contents of gneisses are commonly 21-22 ppm and that their U contents are commonly 4-7 ppm. This contrasts strongly with values for granites in the upper parts of the continental crust which usually have 10-15 ppm Th and 3-4 ppm U (Adams, Osmond and Rodgers, 1959) and a Th/U ratio of about 3.7 (Wasserburg, Macdonald, Hoyle and Fowler, 1964). It is well established that granulite facies terrains are depleted in certain elements including Th and U (see, for example, Lambert and Heier, 1967; and Heier and Thoresen, 1971) and that ultrametamorphic migmatite complexes probably have a genetic connection with granulite facies terrains (see, for example, Fyfe, 1970; and Brown and Fyfe, 1970 & 1972). Recently Smithson and Decker (1973) have demonstrated the strong empirical relationship between hydrous mineralogy and high Th and U concentrations. Thus ultrametamorphic migmatites formed at the amphibolite facies - granulite facies boundary under conditions of high water fugacity would become enriched in Th and U whilst the granulites with their dry mineralogy become depleted in these and other elements. Thus high concentrations of Th and U and high Th/U ratios would be expected in and are probably characteristic of diatexites and related rocks.

Rb depletion in granulite facies rocks allowed Heier (1964) to distinguish them from amphibolite facies rocks on a plot of %K against Rb/Sr. The St. Malo rocks are plotted on Heier's diagram in Figure IV.6 and most are seen to lie in the amphibolite facies field. The

Figure IV.6

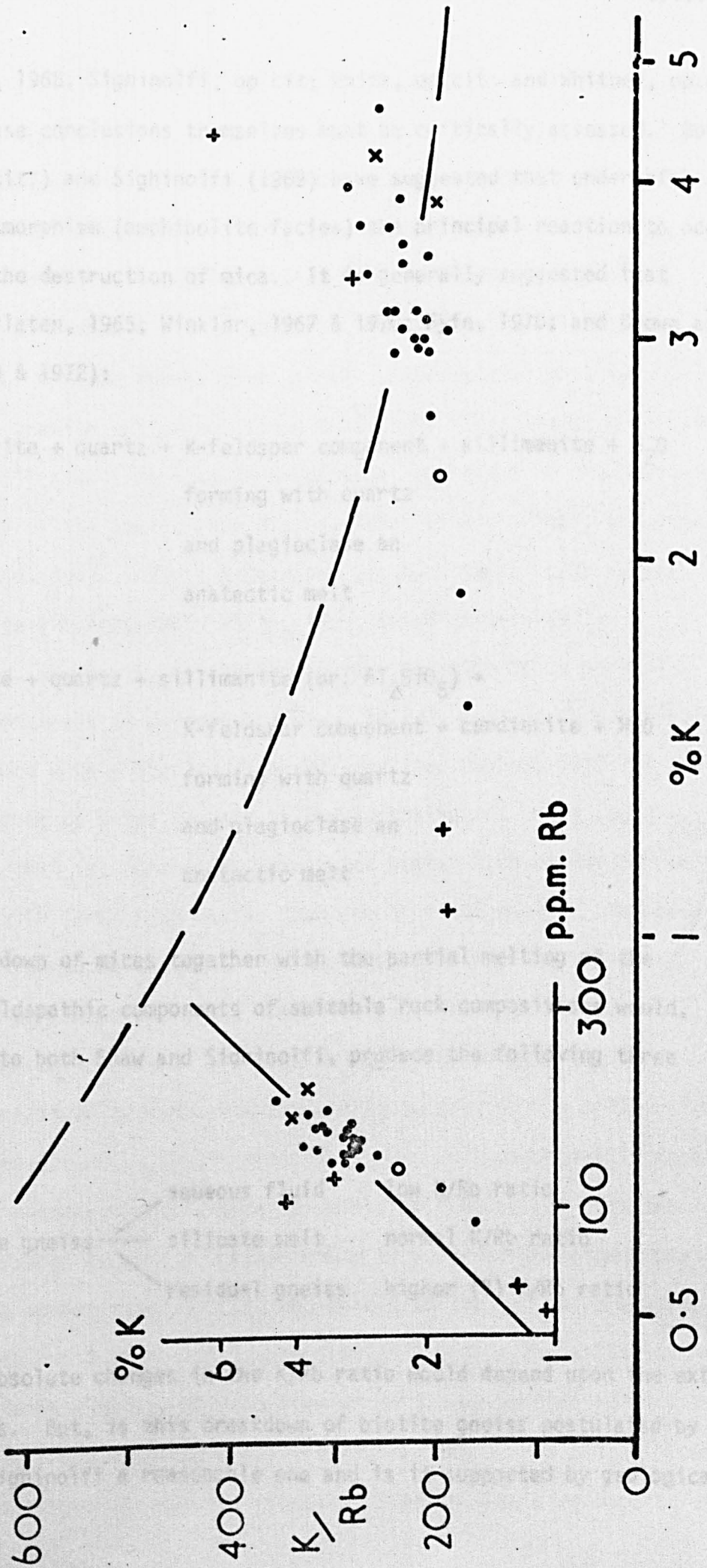
Plot of $\log. K$ against $\log. Rb/Sr$ for the diatexites, metatexite and metasediments (solid circles), the unaltered metasediment (open circle), the homogeneous granites (diagonal crosses) and the granitoid sheets (upright crosses). The dashed line dividing the field of granulite facies rocks from the field of amphibolite facies rocks is taken from Heier (1964).

relationship between K and Rb for the St. Malo rocks is shown in Figure IV.7. The positive correlation between K and Rb is demonstrated by the inset diagram of log. K against log. Rb and emphasises the grouping of K/Rb ratios around the M Trend of Shaw (1968) of 230. The K/Rb ratios of the St. Malo rocks (eg. average of 6 homogeneous diatexites - 224 and average of 11 inhomogeneous diatexites - 221) are also close to the crustal average of 229 (Heier and Adams, 1964), the average for the Canadian Shield of 219 (Shaw, Reilly, Muysson, Pettenden and Campbell, 1967) and the value of 231 found to characterise amphibolite facies rocks (from the West Alps, Sighinolfi, 1969 and from the Northwest Adirondacks, Whitney, 1969). This contrasts with the PH Trend of Shaw (1968) with K/Rb ratios from 150 down to as little as 20 and which exhibits great enrichment of Rb relative to K and it is ratios within this Trend that would be expected from granitoid rocks which had been produced by some process of metasomatic granitization, eg. by some hydrous vapour phase such as that investigated by Luth and Tuttle (1969). The St. Malo rocks have K/Rb ratios that are consistent with an origin by anatexis during amphibolite facies metamorphism but which are inconsistent with regional granitization. The plot of K/Rb ratio against log. %K for the St. Malo rocks which forms the larger diagram in Figure IV.7 demonstrates that the K/Rb ratio remains essentially constant with increasing K content. This is in contrast to the relationship suggested by Sighinolfi that the K/Rb ratio decreases with increasing K content which is represented by the dashed line (see Sighinolfi, 1969).

K-Rb data have often been used in the past to support or deny various petrogenetic processes for the formation of migmatitic rocks (see White, 1966 and Whitney, 1969). Thus the K-Rb data for the St. Malo rocks must be examined in the light of recent work and conclusions

Figure IV.7

Plot (inset) of $\log. K$ against $\log. Rb$ (solid line for $K/Rb = 230$) and plot of K/Rb against $\log. K$ (dashed line represents the relationship between K/Rb and K content suggested by Sighinolfi, 1969) for the diatexites, the metatexite and metasediments (solid circles), the unaltered metasediment (open circle), the homogeneous granites (diagonal crosses) and the granitoid sheets (upright crosses).



(see Shaw, 1968; Sighinolfi, op.cit; White, op.cit; and Whitney, op.cit.), though these conclusions themselves must be critically assessed. Both Shaw (op.cit:) and Sighinolfi (1969) have suggested that under high-grade metamorphism (amphibolite facies) the principal reaction to occur would be the destruction of mica. It is generally suggested that (eg. Von Platen, 1965; Winkler, 1967 & 1970; Fyfe, 1970; and Brown and Fyfe, 1970 & 1972):

muscovite + quartz \rightarrow K-feldspar component + sillimanite + H₂O

forming with quartz

and plagioclase an

anatectic melt

biotite + quartz + sillimanite (or: Al₂SiO₅) \rightarrow

K-feldspar component + cordierite + H₂O

forming with quartz

and plagioclase an

anatectic melt

This breakdown of micas together with the partial melting of the quartzo-feldspathic components of suitable rock compositions would, according to both Shaw and Sighinolfi, produce the following three phases:

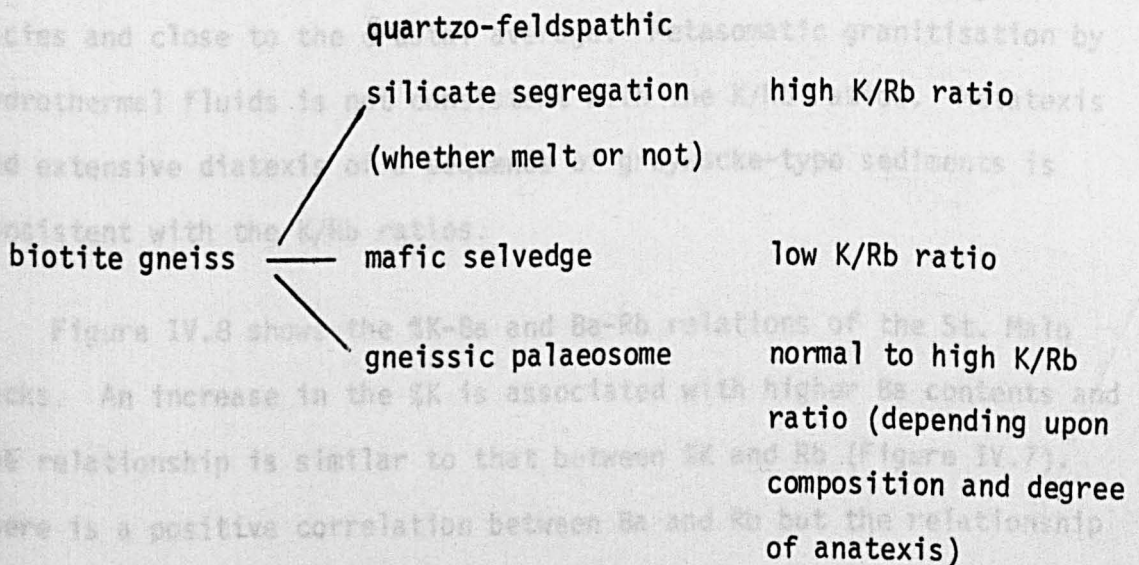
biotite gneiss		aqueous fluid	low K/Rb ratio
		silicate melt	normal K/Rb ratio
		residual gneiss	higher (?) K/Rb ratio

although absolute changes in the K/Rb ratio would depend upon the extent of anatexis. But, is this breakdown of biotite gneiss postulated by Shaw and Sighinolfi a reasonable one and is it supported by geological evidence?

White (1966) has argued against an origin by partial melting for the Palmer migmatites in Australia. One of White's arguments for an origin by metamorphic differentiation was the high K/Rb ratios of the granitic veins. It is argued that Rb would be expected to concentrate in early formed granitic melts giving rise to low K/Rb ratios compatible with Shaw's (1968) PH Trend, ie. consistent with the breakdown of biotite gneiss given above. Experimental work in the quaternary granite system has shown that early formed melts produced by anatexis will always be rich in K-feldspar regardless of the initial Ab/An ratio of the gneiss (Von Platen, 1965; Winkler, 1967; and James and Hamilton, 1969). Since K-feldspar has much higher K/Rb ratios than biotite (Taylor, 1965; White, 1966; and Blattner, 1971) segregation, whether by metamorphic differentiation or by partial melting (metatexis as defined by Brown, 1973), must produce a K-feldspar-rich metatect with a biotite-rich selvage (see Hughes, 1970) of the type described by White (op.cit.) from Australia and Brown (op.cit.) from Brittany - that is, 'granitic' veins with higher K/Rb ratios and mafic selvages with lower K/Rb ratios than the original gneiss. The same result is also to be expected from the destruction of muscovite to give the K-feldspar component since muscovite also has high K/Rb ratios. White states that textural evidence in the Palmer migmatites is in accord with the breakdown of muscovite and quartz to provide the sillimanite according to the reaction given earlier. The only petrogenetic process which will produce banded migmatites with low K/Rb ratios for the 'granitic' veins is that of metasomatism by some hydrous vapour phase of the type investigated by Luth and Tuttle in the synthetic granite system (Luth and Tuttle, 1969). Thus White's high K/Rb ratios in the veins are to be expected as much from an origin by partial melting as from an origin by metamorphic differentiation especially if, as Brown (1973) has suggested, the two processes overlap (see also Hughes, op.

cit.). Whitney (1969) arrived at a similar conclusion and wrote of the migmatitic paragneisses of the Northwest Adirondacks "the K/Rb data do not permit an unequivocal choice between anatexis and metamorphic differentiation as a mechanism of origin for the migmatites".

From the above discussion it is apparent that the breakdown of biotite gneiss suggested by Shaw (1968) and adhered to by Sighinolfi (1969) is untenable since it is not supported by theoretical considerations or by geological evidence. During metatexis the following situation will exist:



During diatexis most of the original constituents of the gneiss have melted and the melt will have K/Rb ratios similar to the original gneiss (if melting is complete) or lower than the original gneiss (if some restite with high K/Rb ratios remains). Upon crystallization this diatexite melt will give rise to a diatexite with K/Rb ratios around the M Trend of Shaw (1968) and probably some hydrous vapour phase with low K/Rb ratios within the PH Trend of Shaw (op.cit.). Granulite facies terrains are generally depleted in Rb relative to K (Heier, 1964; Whitney, 1969; and Sighinolfi, 1969). Fyfe (1970) and Brown and Fyfe (1972) have suggested that granulite facies rocks represent the

residues of melting to produce various members of the granite family. As such, high K/Rb ratios are to be expected. High K/Rb ratios will be further emphasised by the mineralogical control over the chemistry suggested by Leake (1972) since characteristic minerals of granulite facies rocks do not easily accommodate K or Rb (eg. Whitney suggested that the appearance and growth of almanditic garnet was responsible for the high K/Rb ratios of the granulite facies paragneisses in the Northwest Adirondacks; Whitney, 1969).

The following conclusions may be drawn from the St. Malo rocks K-Rb data. The rocks have K/Rb ratios characteristic of the amphibolite facies and close to the crustal average. Metasomatic granitisation by hydrothermal fluids is not consistent with the K/Rb ratios. Metatexis and extensive diatexis of a sequence of greywacke-type sediments is consistent with the K/Rb ratios.

Figure IV.8 shows the %K-Ba and Ba-Rb relations of the St. Malo rocks. An increase in the %K is associated with higher Ba contents and the relationship is similar to that between %K and Rb (Figure IV.7). There is a positive correlation between Ba and Rb but the relationship is considerably blurred by the scatter of points. There are also positive correlations between %TiO₂ and both Y and Zr for the St. Malo rocks (Figure IV.9). The Y values are slightly lower than values quoted by Taylor (1965) for granodiorite (30 ppm), granite (40 ppm) and greywacke (30 ppm). The good correlation between %TiO₂ and Zr signifies that the Ti/Zr ratio remains fairly constant throughout the St. Malo rocks (Figure IV.9; Tables IV.1, IV.2, IV.3 and IV.4). The Zr values for the homogeneous diatexite (average 200 ppm), the inhomogeneous diatexite (average 230 ppm) and for the metasediments (237-307 ppm) are higher than the values given by Taylor (op.cit.) for igneous rocks (granodiorite - 140 ppm; granite - 180 ppm) and also

Figure IV.8

Plots of K against Ba and Ba against Rb for the diatexites, the metatexite and metasediments (solid circles), the unaltered metasediment (open circle), the homogeneous granites (diagonal crosses) and the granitoid sheets (upright crosses).

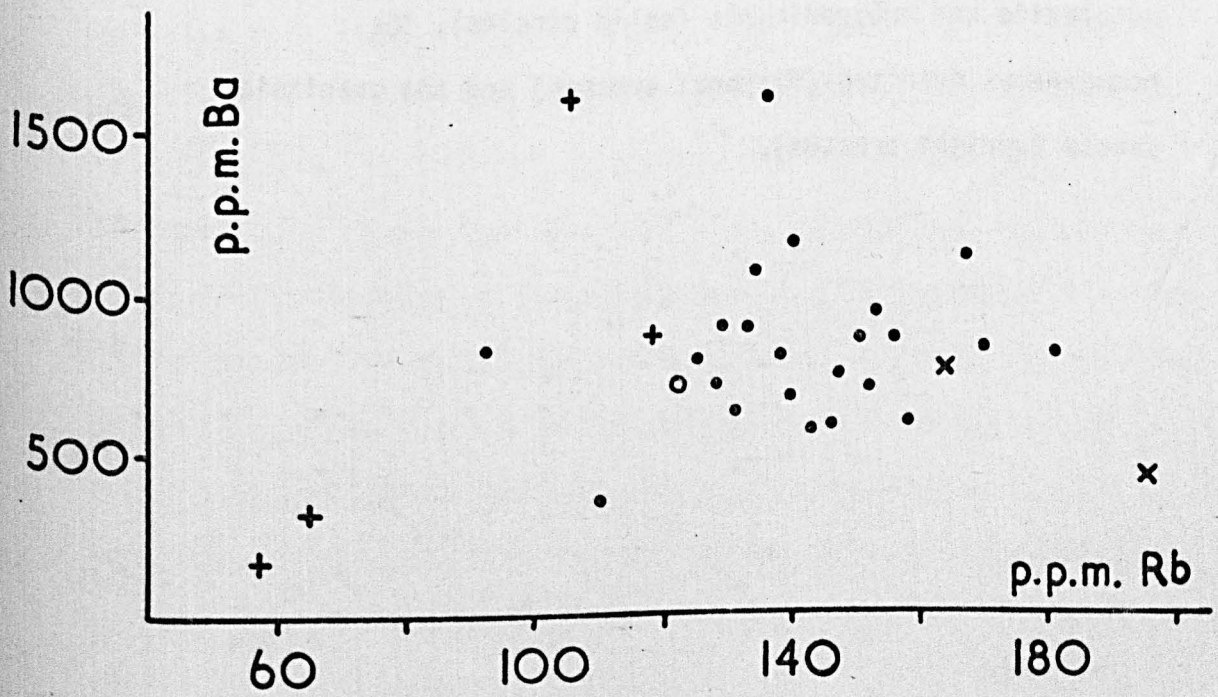
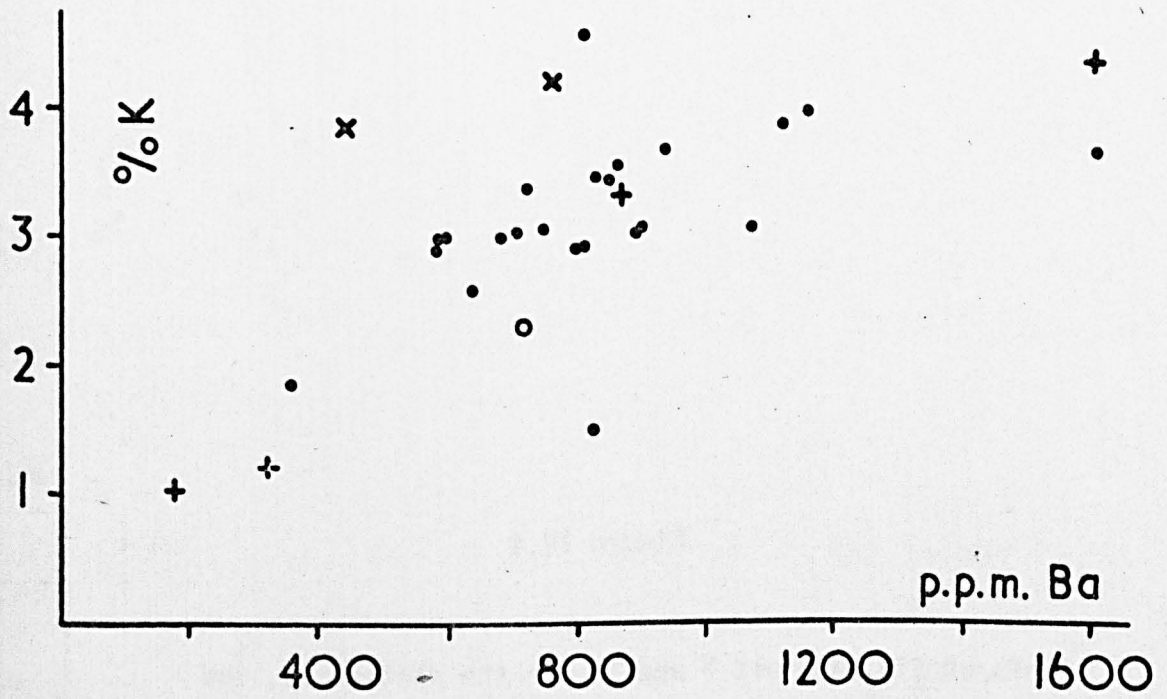
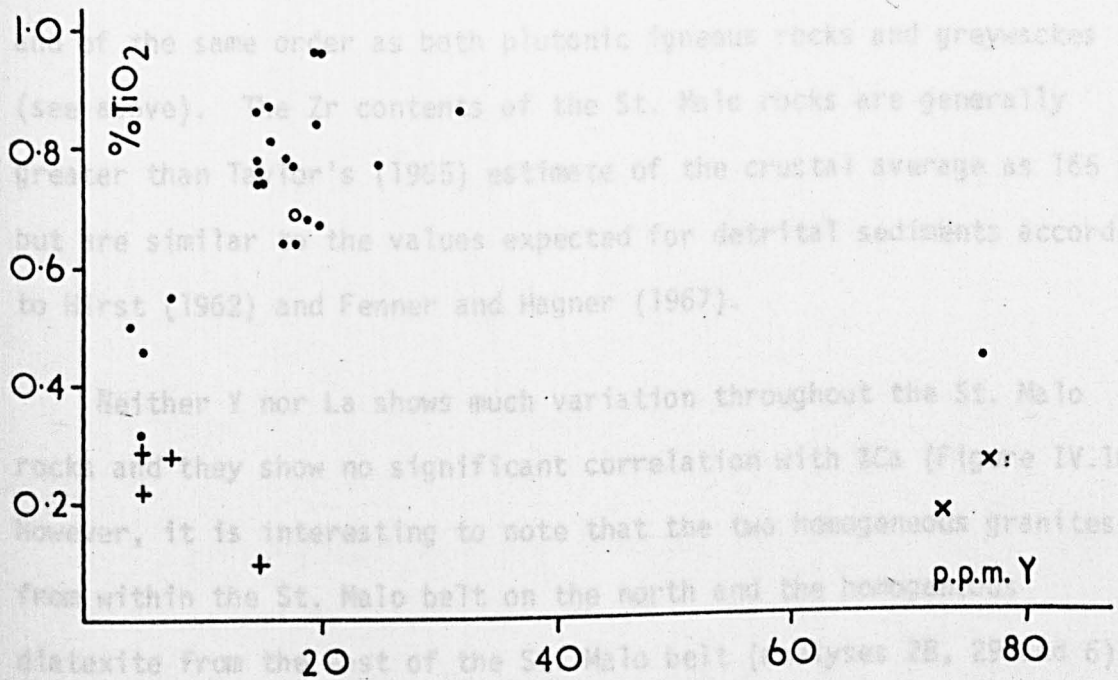


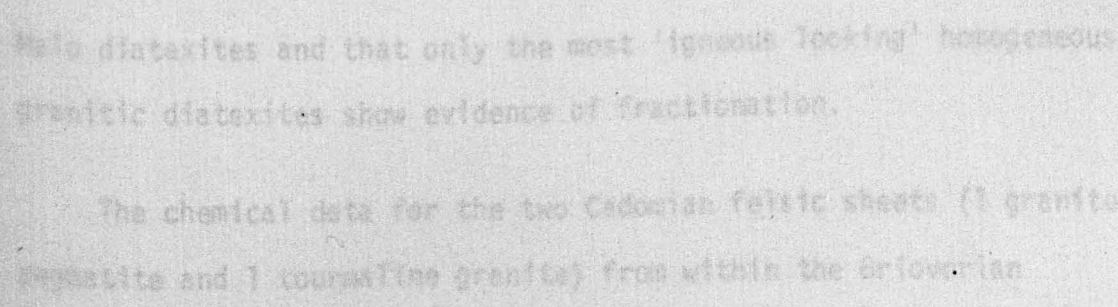
Figure IV.9

Plots of TiO_2 against Y and Zr for the diatexites, the metatexite and metasediments (solid circles), the homogeneous granites (diagonal crosses) and the granitoid sheets (upright crosses).

higher than the value he gives for greywackes (140 ppm), but they are of the same order as the Zr contents of quartzites (250 ppm). However, the average Zr content for the homogeneous diatexites without analysis 6 (which is considerably higher than the other 5 analyses) is 155 ppm



Neither Y nor La shows much variation throughout the St. Malo rocks and they show no significant correlation with ΣCa (Figure IV.10). However, it is interesting to note that the two homogeneous granites from within the St. Malo belt on the north and the homogeneous diatexite from the east of the St. Malo belt (analyses 2B, 2C, 6) have higher Y and La values than the bulk of the St. Malo rocks (analyses 6 also has high Zr) (see Figure IV.10; Tables IV.1, IV.2, IV.4). These high values of Y and La probably represent some degree of fractionation of the homogeneous granites compared with the diatexites and other rocks. There is a moderate positive correlation between ΣCa and Sr for the St. Malo rocks (Figure IV.10) which is to be expected from their chemical properties. As with the Ti/Zr ratio, the Ca/Sr ratio remains fairly constant throughout the St. Malo rocks. Since decrease of these two ratios (Ti/Zr and Ca/Sr) with a related sequence of rocks is indicative of fractionation it is concluded that extensive fractionation has been observed in the St. Malo diatexites and that only the most 'igneous looking' homogeneous granitic diatexites show evidence of fractionation.



The chemical data for the two Cadomian felsic sheets (1 granite gneiss and 1 coarse-grained granite) from within the orogenic belt are shown in Figure IV.11. The granite gneiss has a Ti/Zr ratio of 1.2 and a Ca/Sr ratio of 1.2, which are similar to the values for the St. Malo rocks.

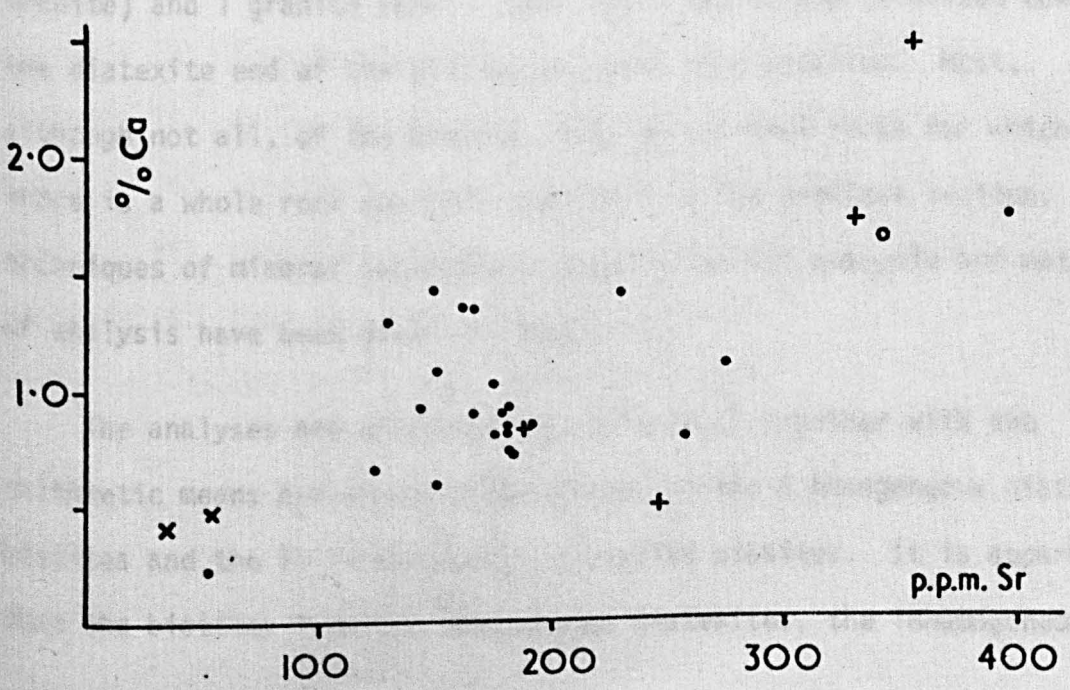
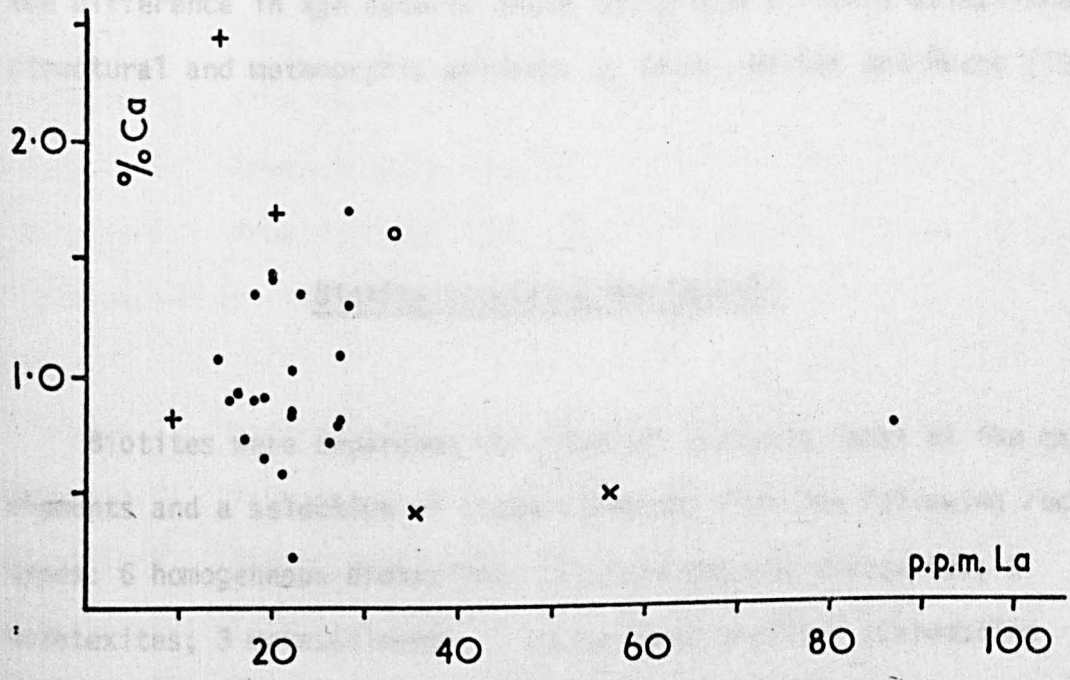
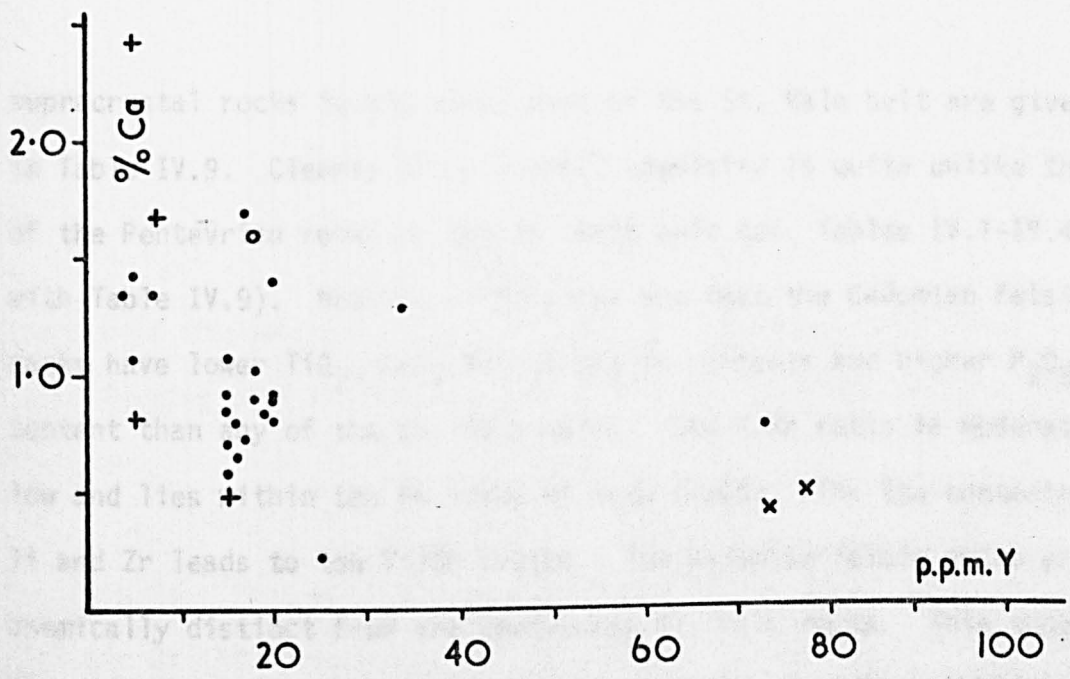
higher than the value he gives for greywackes (140 ppm), but they are of the same order as the Zr contents of quartzites (250 ppm). However, the average Zr content for the homogeneous diatexites without analysis 6 (which is considerably higher than the other 5 analyses) is 155 ppm and of the same order as both plutonic igneous rocks and greywackes (see above). The Zr contents of the St. Malo rocks are generally greater than Taylor's (1965) estimate of the crustal average as 165 ppm but are similar to the values expected for detrital sediments according to Hirst (1962) and Fenner and Hagner (1967).

Neither Y nor La shows much variation throughout the St. Malo rocks and they show no significant correlation with %Ca (Figure IV.10). However, it is interesting to note that the two homogeneous granites from within the St. Malo belt on the north and the homogeneous diatexite from the east of the St. Malo belt (analyses 28, 29 and 6) have higher Y and La values than the bulk of the St. Malo rocks (analysis 6 also has high Zr) (see Figure IV.10; Tables IV.1, IV.2, IV.3 and IV.4). These high values of Y and La probably represent some degree of fractionation of the homogeneous granites compared with the bulk of the diatexites and other rocks. There is a moderate positive correlation between %Ca and Sr for the St. Malo rocks (Figure IV.10) which is to be expected from their chemical properties. As with the Ti/Zr ratio, the Ca/Sr ratio remains fairly constant throughout the St. Malo rocks. Since decrease of these two ratios (Ti/Zr and Ca/Sr) within a related sequence of rocks is indicative of fractionation it is concluded that there has been no extensive fractionation of the St. Malo diatexites and that only the most 'igneous looking' homogeneous granitic diatexites show evidence of fractionation.

The chemical data for the two Cadomian felsic sheets (1 granite pegmatite and 1 tourmaline granite) from within the Brioverian

Figure IV.10

Plots of Ca against Y, La and Sr for the diatexites, the metatexite and metasediments (solid circles), the unaltered metasediment (open circle), the homogeneous granites (diagonal crosses) and the granitoid sheets (upright crosses).



supracrustal rocks to the north-west of the St. Malo belt are given in Table IV.9. Clearly their overall chemistry is quite unlike that of the Pentevrian rocks of the St. Malo belt (cf. Tables IV.1-IV.4 with Table IV.9). Notable differences are that the Cadomian felsic rocks have lower TiO_2 , CaO, Ba, La and Zr contents and higher P_2O_5 content than any of the St. Malo rocks. The K/Rb ratio is moderately low and lies within the PH Trend of Shaw (1968). The low contents of Ti and Zr leads to low Ti/Zr ratios. The Cadomian felsic rocks are chemically distinct from the Pentevrian St. Malo rocks. This supports the difference in age between these two groups of rocks established on structural and metamorphic evidence by Brown, Barber and Roach (1971).

Analysis 1: from specimen 705, Prie de Brucin.
 Analysis 2: from specimen 706, St. Brieuc.
 Analysis 3: from specimen 707, St. Brieuc.
 Analysis 4: from specimen 708, St. Brieuc.
 Analysis 5: from specimen 758, St. Brieuc.
 Analysis 6: from specimen 720, prie de Brucin.
 Analyses 1-6 are from Biotite Chemistry and Genesis

Biotites were separated for chemical analysis (most of the major elements and a selection of trace elements) from the following rock types: 6 homogeneous diatexites; 10 inhomogeneous diatexites; 2 metatexites; 3 metasediments; 2 homogeneous granites (Colombière Granite) and 1 granite sheet. Once again the sample is biased towards the diatexite end of the ultrametamorphic rock spectrum. Most, although not all, of the biotite analysed are from rocks for which there is a whole rock analysis available in the previous section. The techniques of mineral separation, preparation for analysis and methods of analysis have been given in Chapter I.

The analyses are presented in Table IV.11 together with the arithmetic means and standard deviations of the 6 homogeneous diatexite biotites and the 10 inhomogeneous diatexite biotites. It is apparent that the biotites from the homogeneous diatexites, the inhomogeneous

Table IV.11

Summary of the geochemical data for the biotites separated from rocks forming part of the Pentevrian basement in north-eastern Brittany.

Analysis 1: from specimen 765, Plage de Quatre Vaux.

Analysis 2: from specimen 701, St. Jacut.

Analysis 3: from specimen 703, St. Jacut.

Analysis 4: from specimen 358, St. Jacut.

Analysis 5: from specimen 758, St. Briac.

Analysis 6: from specimen 720, pnte de Grouin.

Analyses 1-6 are from homogeneous diatexites.

Analysis 7: from specimen 309, le Guildo.

Analysis 8: from specimen 757, Ile des Hebihens.

Analysis 9: from specimen 704, St. Jacut.

Analysis 10: from specimen 759, pnte de la Garde Guérin.

Analysis 11: from specimen 760, pnte de la Garde Guérin.

Analysis 12: from specimen 205, road cutting, la Barrage.

Analysis 13: from specimen 207, road cutting, la Barrage.

Analysis 14: from specimen 208, quarry, Montagne St. Joseph.

Analysis 15: from specimen 210, quarry, Montagne St. Joseph.

Analysis 16: from specimen 721, pnte de Grouin.

Analyses 7-16 are from inhomogeneous diatexites.

Analysis 17: from specimen 761, pnte de la Garde Guérin.

Analysis 18: from specimen 731, pnte du Nid.

Analyses 17 and 18 are from metatexites.

Analysis 19: from specimen 706, St. Jacut.

Analysis 20: from specimen 766, la Richardais.

Analysis 21: from specimen 204, quarry, le Minihic.

Analyses 19-21 are from metasediments.

Analysis 22: from specimen 708, St. Jacut.

Analysis 22 is from a granite sheet.

Analysis 23: from specimen 345, la Nellière.

Analysis 24: from specimen 360, Ile de la Colombière.

Analyses 23 and 24 are from the Colombière Granite.

Analysis 25: mean and standard deviation of the 6
homogeneous diatexite biotites.

Analysis 26: mean and standard deviation of the 10
inhomogeneous diatexite biotites.

	1	2	3	4	5	6	7	8	9	10	11	12	13	14	15	16	17	18	19	20	21	22	23	24	25	26		
	765	701	703	358	758	720	309	757	704	759	760	205	207	208	210	721	761	731	706	766	204	708	345	360	MEAN	S.D.	MEAN	S.D.
SiO ₂	36.22	35.78	34.58	35.10	37.04	35.35	35.76	35.76	34.97	36.02	35.90	32.35	34.51	35.17	37.12	35.89	35.50	36.43	34.93	36.85	35.74	36.88	32.91	34.56	35.68	0.87	35.35	1.26
TiO ₂	2.30	1.84	2.07	2.39	2.08	2.61	2.60	2.76	2.45	2.35	2.81	2.54	2.47	2.54	2.36	2.45	2.89	2.93	2.89	2.63	2.49	1.81	1.99	1.95	2.22	0.27	2.53	0.15
Al ₂ O ₃	18.03	18.30	19.40	18.35	18.90	19.00	19.22	18.05	20.45	18.95	18.71	19.64	19.73	19.97	19.12	18.55	18.75	19.00	18.27	18.85	18.75	18.00	18.71	18.03	18.66	0.52	19.24	0.76
Fe ₂ O ₃	4.91	4.65	4.28	4.35	3.30	3.88	3.36	5.41	4.97	3.09	3.43	2.25	1.98	2.10	2.32	3.48	2.87	2.65	6.54	5.02	2.33	12.84	5.57	3.55	4.23	0.57	3.24	1.18
FeO	17.89	15.78	16.05	15.56	19.95	21.38	17.92	20.72	18.56	19.95	19.56	20.47	20.45	20.81	21.16	19.47	19.45	19.47	17.47	17.63	20.96	8.71	26.94	27.30	17.77	2.43	19.91	1.00
MnO	0.24	0.24	0.23	0.23	0.25	0.23	0.26	0.28	0.23	0.19	0.19	0.20	0.18	0.27	0.25	0.28	0.18	0.27	0.37	0.25	0.25	0.42	0.48	0.67	0.24	0.01	0.23	0.04
MgO	8.78	11.50	11.50	10.80	9.25	8.00	9.00	5.75	8.75	9.00	9.45	9.75	9.75	9.25	9.35	9.25	9.00	9.25	8.25	9.26	9.50	8.50	2.93	2.93	9.97	1.50	8.93	1.16
Na ₂ O	0.15	0.12	0.18	0.23	0.15	0.21	0.23	0.20	0.23	0.15	0.14	0.16	0.16	0.18	0.16	0.16	0.14	0.16	0.16	0.23	0.15	0.22	0.18	0.13	0.17	0.04	0.18	0.03
K ₂ O	9.50	9.00	9.06	9.10	8.90	7.80	9.50	8.90	7.40	9.40	10.50	9.20	8.94	9.10	9.10	9.24	9.60	9.54	8.74	8.90	9.56	7.60	7.40	8.90	8.89	0.57	9.13	0.76
Ba	538	388	330	402	272	380	550	590	382	633	582	1130	1030	590	905	785	730	1290	3600	660	1175	272	260	255	385	89	718	237
Cr	260	320	270	277	235	176	290	274	290	300	395	462	345	309	362	335	300	382	390	392	290	161	40	70	256	48	326	76
Cs	34	50	37	37	40	45	45	35	48	34	38	23	19	42	35	35	22	28	30	28	36	58	50	79	41	6	35	9
Cu	57	48	40	31	9	38	24	60	62	44	48	27	21	14	18	43	16	11	65	41	8	20	25	9	37	16	36	18
Li	168	215	280	250	199	163	182	200	235	158	180	139	153	259	222	149	163	135	244	176	181	282	577	1228	213	46	188	40
Ni	64	120	128	80	108	52	71	51	117	64	57	124	95	97	112	56	85	94	164	81	95	68	29	40	92	31	84	28
Rb	724	940	900	696	912	854	865	801	648	822	869	702	657	787	735	774	725	699	717	685	765	824	929	1090	838	103	766	79
Sc	27	22	26	33	27	48	49	51	38	38	32	51	48	43	50	39	43	44	56	28	24	14	79	74	31	9	44	7
Sr	16	13	9	8	8	19	10	12	13	11	11	11	13	9	12	14	7	11	20	23	11	29	10	7	12	5	12	2
V	380	262	287	287	227	285	550	345	402	420	410	540	620	505	502	440	430	410	532	310	310	155	168	170	288	51	473	84
Zr	170	162	162	136	190	595	152	371	316	145	110	242	245	216	203	273	151	187	183	176	179	323	502	315	164*	19	227	80

* analysis 6 (specimen 720) omitted

diatexites and the metatexites are broadly similar in chemical composition and are Fe^{+2} biotites as defined by Foster (1960). The homogeneous granite biotites are actually lepidomelanes as defined by Foster. The homogeneous diatexite biotites and the inhomogeneous diatexite biotites were tested for significant differences using the Student's t test. Taking differences as significant at the 2.5% level the homogeneous diatexite biotites have significantly lower TiO_2 , Al_2O_3 , Ba, Sc and V than the inhomogeneous diatexite biotites and significantly higher Fe_2O_3 . The difference in FeO may also be significant. The differences in Fe_2O_3 and FeO are discussed later in this section.

The St. Malo biotites are plotted in terms of $\text{FeO} + \text{MnO} - \text{Fe}_2\text{O}_3 + \text{TiO}_2 - \text{MgO}$ in Figure IV.11 after Heinrich (1946). Most of the biotites (the exceptions are the biotite from the granite sheet and the two lepidomelanes from the homogeneous granites) plot within the field of biotites from granites (after Heinrich) and a large number of these also fall within the overlapping field of biotites from schists and gneisses (after Heinrich). The two lepidomelanes from the two homogeneous granites fall just outside the field of biotites from granites but within the field of biotites from granitic pegmatites (after Heinrich). The biotite from the granite sheet from St. Jacut has a very high ferric iron content and plots in the field of biotites from extrusive rocks (after Heinrich).

The structural formulae of the biotites from the St. Malo rocks were calculated using the method recommended by Foster (1960). Foster states that "the negative inherent charge on the unit layers and the positive charge on the interlayer cations should be close to 2.00 for trioctahedral micas like the phlogopites and the biotites. In ... this study a variation of plus or minus 0.20 was permitted in these values".

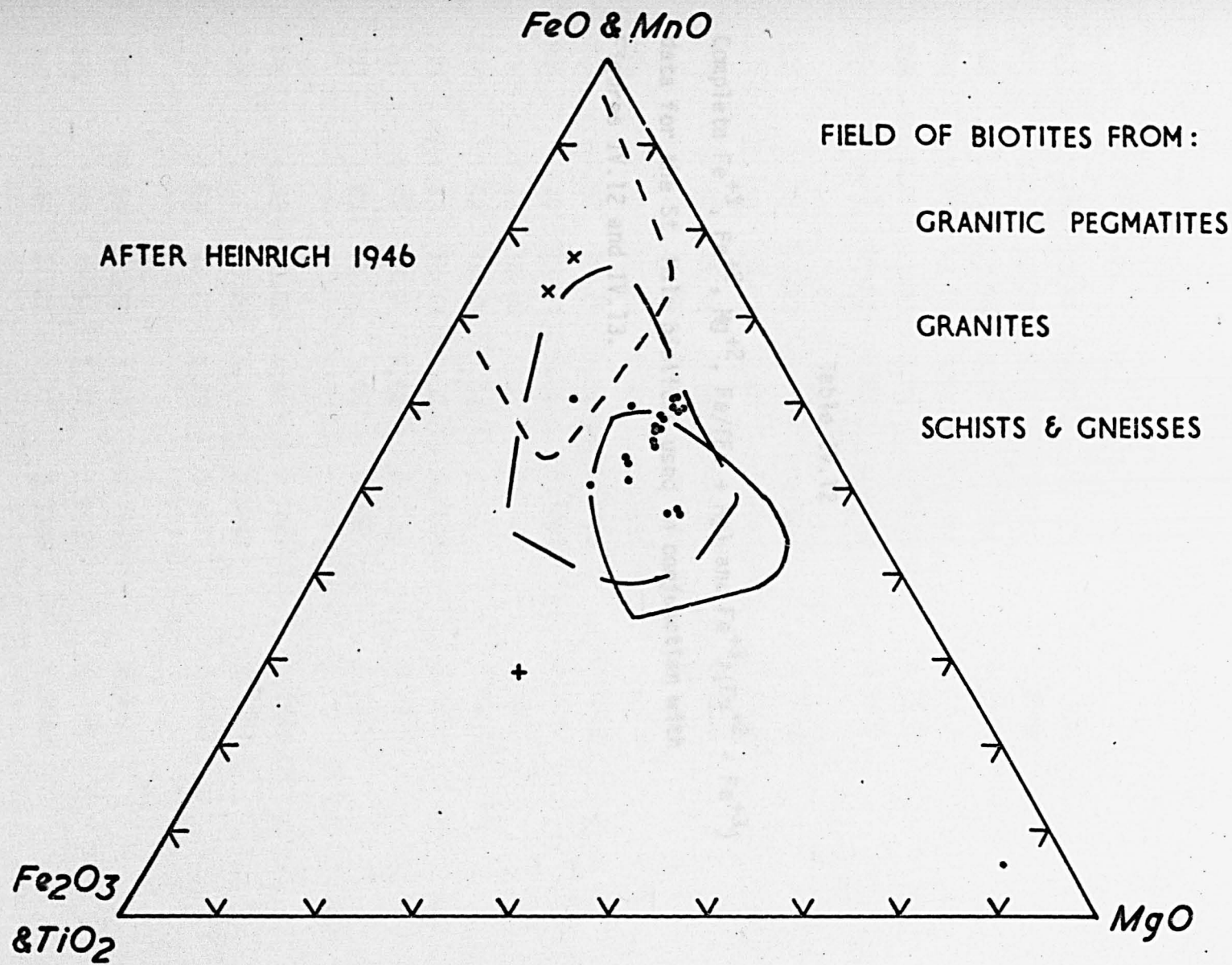
The charge values for the St. Malo biotites were not within this permitted variation and accordingly have not been presented. It is felt that the reasons for this excess variation in charge are twofold. Firstly, the SiO_2 and Al_2O_3 contents are critical in calculating the composite layer charge and the interlayer cationic charge and any inaccuracy in the determination of these oxides is reflected in the charge balance. Secondly, the analyses are not complete and minor amounts of oxides such as CaO would also alter the charge balance.

The experimental work of Eugster and Wones (1962), Wones (1963) and Wones and Eugster (1965) demonstrates the effect of the three independent intensive variables temperature, fugacity of water ($f_{\text{H}_2\text{O}}$) and fugacity of oxygen (f_{O_2}) on the formation and resultant composition of biotites within the ternary system $\text{KFe}^{+2}_3\text{AlSi}_3\text{O}_{10}(\text{OH})_2$ (annite) - $\text{KMg}^{+2}_3\text{AlSi}_3\text{O}_{10}(\text{OH})_2$ (phlogopite) - $\text{KFe}^{+3}_3\text{AlSi}_3\text{O}_{12}(\text{H}_{-1})$ ("oxybiotite"). If it is assumed that substitutions other than Fe-Mg will not materially influence biotite stability (see Wones and Eugster, 1965, pp.1257-1258) then the St. Malo biotites can be interpreted in the light of, and using conclusions based on the results of, this experimental work. Estimates can be made concerning the fugacity of oxygen or the fugacity of water at the time of crystallisation of the biotites. The Fe^{+3} , Fe^{+2} and Mg^{+2} values, the $\text{Fe}/(\text{Fe} + \text{Mg})$ and the $\text{Fe}^{+3}/(\text{Fe}^{+2} + \text{Fe}^{+3})$ ratios for the biotites from the St. Malo rocks are given in Table IV.12.

If the equilibrium assemblage sanidine-magnetite-biotite is present a determination can be made of the divariant $f_{\text{O}_2} - f_{\text{H}_2\text{O}} - T$ conditions at the time of crystallisation of the mineral assemblage which contains biotite of a given composition (Wones and Eugster, op.cit.). The majority of the St. Malo rocks contain the mineral assemblage K-feldspar-ore-biotite and only the biotites from the

Figure IV.11

FeO + MnO - Fe₂O₃ + TiO₂ - MgO plot of the St. Malo biotites. The fields of biotites from granitic pegmatites, granites and schists and gneisses are taken from Heinrich (1946). Biotites from the diatexites, metatexites and metasediments - solid circles, biotite from the granite sheet - upright cross and the two biotites from the homogeneous granites - diagonal crosses.



	Fe ⁺³	Fe ⁺²	Mg ⁺²	Fe/(Fe+Mg)	Fe ⁺³ /(Fe ⁺² +Fe ⁺³)
765	3.43	13.91	5.30	0.7659	0.1976
701	3.25	12.27	6.94	0.6910	0.2094
703	2.99	12.48	6.94	0.6904	0.1932
358	3.04	12.10	6.51	0.6992	0.2008
758	2.31	15.51	3.58	0.7615	0.1296
720	2.71	16.52	4.83	0.6000	0.1400

Table IV.12

309	2.35	13.93	5.43	0.7500	0.1444
757	3.75	16.12	3.45	0.8520	0.1901

Complete Fe⁺³, Fe⁺², Mg⁺², Fe/(Fe + Mg) and Fe⁺³/(Fe⁺² + Fe⁺³)

data for the St. Malo biotites used in conjunction with Figures IV.12 and IV.13.

360	2.30	15.20	5.70	0.7554	0.1304
205	1.57	16.91	5.98	0.7493	0.0898
207	1.38	15.90	5.88	0.7461	0.0799
208	1.47	16.18	5.58	0.7598	0.0823
210	1.62	16.45	5.64	0.7621	0.0696
721	2.43	15.13	5.58	0.7589	0.1384
761	2.01	15.12	5.43	0.7593	0.1173
731	1.85	15.13	5.58	0.7527	0.1089
706	4.57	13.58	4.98	0.7847	0.2518
766	3.51	13.70	5.59	0.7548	0.2039
204	1.63	16.29	5.73	0.7577	0.0909
708	8.98	6.77	5.13	0.7543	0.5702
345	3.90	20.94	1.77	0.9335	0.1570
360	2.48	21.22	1.77	0.9305	0.1047

metasediments (which do not contain K-feldspar), the biotite from homogeneous diatexite specimen 765 (which does not contain K-feldspar) and the biotite from the granite sheet from St. Jacut (which have high Fe₂O₃) are excluded from the discussions comprising the remainder of this section.

	Fe ⁺³	Fe ⁺²	Mg ⁺²	Fe/(Fe+Mg)	Fe ⁺³ /(Fe ⁺² +Fe ⁺³)
765	3.43	13.91	5.30	0.7659	0.1978
701	3.25	12.27	6.94	0.6910	0.2094
703	2.99	12.48	6.94	0.6904	0.1932
358	3.04	12.10	6.51	0.6992	0.2008
758	2.31	15.51	5.58	0.7615	0.1296
720	2.71	16.62	4.83	0.8000	0.1400
309	2.35	13.93	5.43	0.7500	0.1444
757	3.78	16.12	3.45	0.8520	0.1901
704	3.48	14.43	5.28	0.7723	0.1942
759	2.16	15.51	5.43	0.7650	0.1222
760	2.40	15.20	5.70	0.7554	0.1364
205	1.57	15.91	5.88	0.7493	0.0898
207	1.38	15.90	5.88	0.7461	0.0799
208	1.47	16.18	5.58	0.7598	0.0833
210	1.62	16.45	5.64	0.7621	0.0896
721	2.43	15.13	5.58	0.7589	0.1384
761	2.01	15.12	5.43	0.7593	0.1173
731	1.85	15.13	5.58	0.7527	0.1089
706	4.57	13.58	4.98	0.7847	0.2518
766	3.51	13.70	5.59	0.7548	0.2039
204	1.63	16.29	5.73	0.7577	0.0909
708	8.98	6.77	5.13	0.7543	0.5702
345	3.90	20.94	1.77	0.9335	0.1570
360	2.48	21.22	1.77	0.9305	0.1047

biotites from the St. Jacut homogeneous diatexite can be made. Their Fe/(Fe + Mg) ratios are 0.68, 0.69 and 0.70 (from Table IV.12) which yield temperature estimates of 640°C from Figure IV.12, lower. The

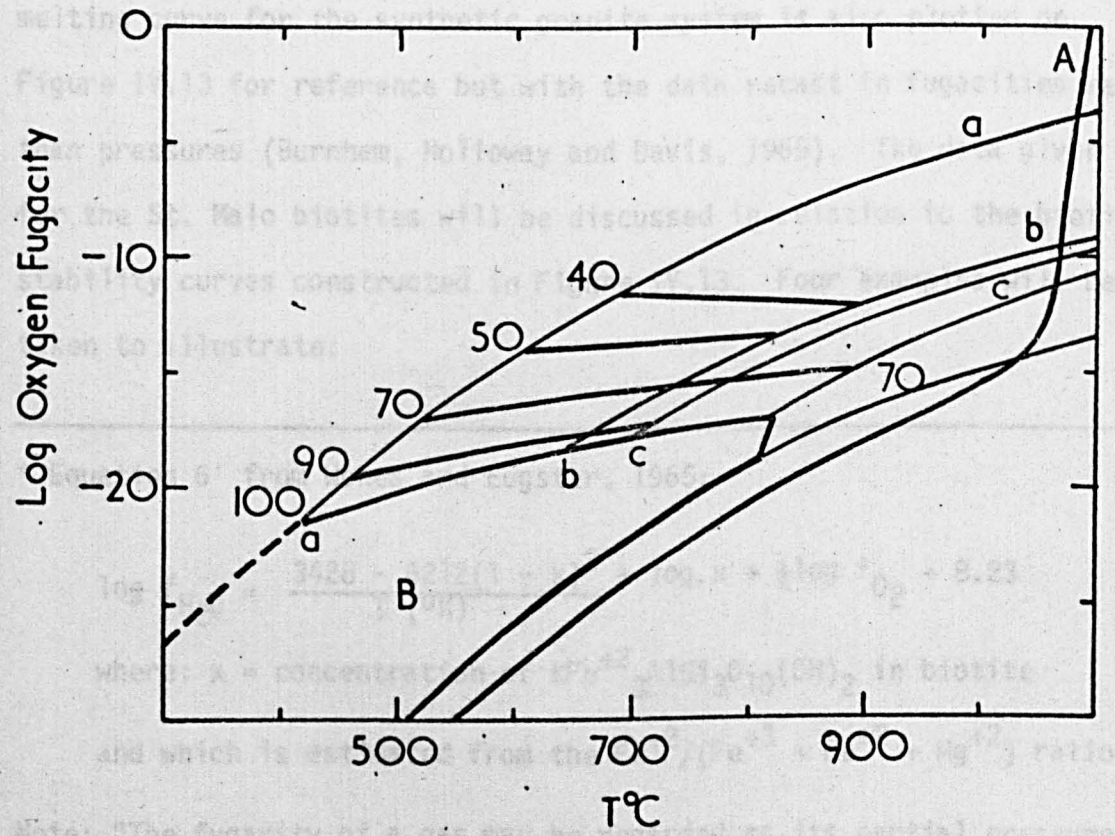
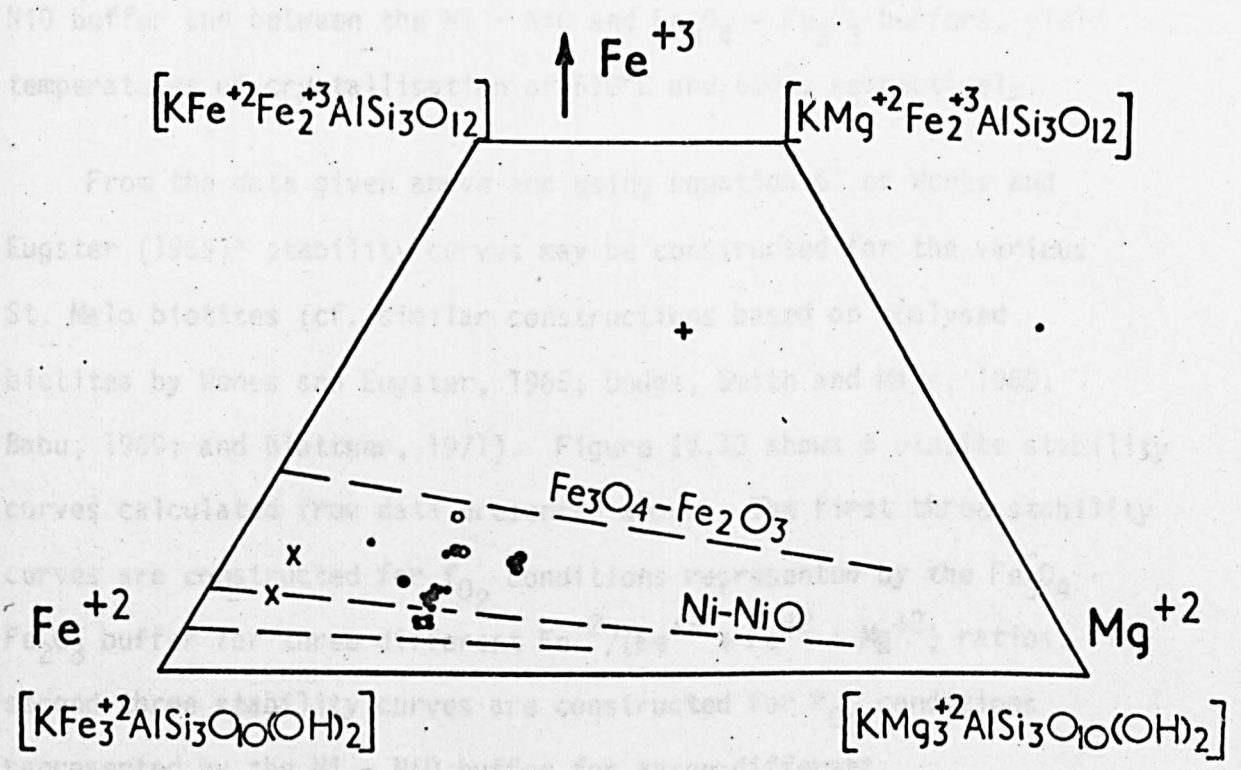
metasediments (which do not contain K-feldspar), the biotite from homogeneous diatexite specimen 765 (which does not contain K-feldspar) and the biotite from the granite sheet from St. Jacut (which have high Fe_2O_3) are excluded from the discussions comprising the remainder of this section.

According to Wones (1963) the $\text{Fe}^{+3}/(\text{Fe}^{+2} + \text{Fe}^{+3})$ ratio of suitable biotites may serve as an indicator of variations in the oxygen fugacity of the environment in which a biotite crystallises or recrystallises in the case of medium-to-high-grade metamorphic rocks. The plot of the suitable St. Malo analyses within the compositional triangle $\text{Fe}^{+3} - \text{Fe}^{+2} - \text{Mg}^{+2}$ (Figure IV.12, upper) demonstrates the close relationship between these biotites and Wones and Eugster's (1965) estimated compositions of biotite solid solution in the ternary system $\text{KFe}^{+3}_3\text{AlSi}_3\text{O}_{12}(\text{H}_{-1}) - \text{KFe}^{+2}_3\text{AlSi}_3\text{O}_{10}(\text{OH})_2 - \text{KMg}^{+2}_3\text{AlSi}_3\text{O}_{10}(\text{OH})_2$ which are stable at oxygen fugacities controlled by individual buffer equilibria (Figure IV.12, upper). Expressed in terms of the $\text{Fe}^{+3}/(\text{Fe}^{+2} + \text{Mg}^{+2})$ ratio (from Table IV.12), many of the biotites (especially those from the inhomogeneous diatexites and the two metatexites) have a ratio close to that for the Ni - NiO buffer of 0.10 whilst the remainder of the biotites have ratios intermediate between the Ni - NiO buffer and the $\text{Fe}_3\text{O}_4 - \text{Fe}_2\text{O}_3$ buffer ie. between 0.10 and 0.25 (Wones and Eugster, 1965). From Figure IV.12, lower, it can be estimated that the biotites which cluster across the Ni - NiO buffer (Figure IV.12, upper), and which have $\text{Fe}/(\text{Fe} + \text{Mg})$ ratios in the region of 0.75 (see Table IV.12), would have crystallised at temperatures of about 720°C . In the same way an estimate of the temperature of crystallisation for the three biotites from the St. Jacut homogeneous diatexite can be made. Their $\text{Fe}/(\text{Fe} + \text{Mg})$ ratios are 0.69, 0.69 and 0.70 (from Table IV.12) which yield temperature estimates of 640°C from Figure IV.12, lower. The

Figure IV.12

Upper: The St. Malo biotites plotted in terms of Fe^{+3} - Fe^{+2} - Mg^{+2} contents. The dashed lines represent compositions of buffered biotites determined experimentally by Wones and Eugster (1965) in the ternary system $\text{KFe}^{+3}_3\text{AlSi}_3\text{O}_{12}(\text{H}_{-1})$ - $\text{KFe}^{+2}_3\text{AlSi}_3\text{O}_{10}(\text{OH})_2$ - $\text{KMg}^{+2}_3\text{AlSi}_3\text{O}_{10}(\text{OH})_2$ (after Wones and Eugster, figure 1). Compositions on the unlabelled dashed line are buffered by Fe_2SiO_4 - Fe_3O_4 - SiO_2 .

Lower: The stability of biotites with specific $\text{Fe}/(\text{Fe} + \text{Mg})$ values as a function of oxygen fugacity and temperature at 2070 bars total pressure. Heavy lines represent contours of constant 100 $\text{Fe}/(\text{Fe} + \text{Mg})$ values. Light lines depict buffer curves: a = Fe_3O_4 - Fe_2O_3 ; b = Ni - NiO; c = Fe_2SiO_4 - Fe_3O_4 - SiO_2 . The heavy curve A represents maximum stability of phlogopite and the field B is the annite stability field. This diagram is after Wones and Eugster (1965, figure 4) but has been simplified for clarity.



Note: "The fugacity of a gas may be regarded as its partial pressure corrected for deviation from perfect gas behavior" (Krusup, 1959).

two lepidomelanes from the homogeneous granites, which have Fe/(Fe + Mg) ratios of 0.93 and oxygen fugacities similar to the Ni - NiO buffer and between the Ni - NiO and Fe₃O₄ - Fe₂O₃ buffers, yield temperatures of crystallisation of 670°C and 620°C respectively.

From the data given above and using equation 6' of Wones and Eugster (1965)* stability curves may be constructed for the various St. Malo biotites (cf. similar constructions based on analysed biotites by Wones and Eugster, 1965; Dodge, Smith and Mays, 1969; Babu, 1969; and Blattner, 1971). Figure IV.13 shows 6 biotite stability curves calculated from data presented above. The first three stability curves are constructed for f_{O_2} conditions represented by the Fe₃O₄ - Fe₂O₃ buffer for three different $Fe^{+2}/(Fe^{+3} + Fe^{+2} + Mg^{+2})$ ratios. The second three stability curves are constructed for f_{O_2} conditions represented by the Ni - NiO buffer for three different $Fe^{+2}/(Fe^{+3} + Fe^{+2} + Mg^{+2})$ ratios. Tuttle and Bowen's (1958) minimum melting curve for the synthetic granite system is also plotted on Figure IV.13 for reference but with the data recast in fugacities rather than pressures (Burnham, Holloway and Davis, 1969). The data given above for the St. Malo biotites will be discussed in relation to the biotite stability curves constructed in Figure IV.13. Four examples will be taken to illustrate:

* Equation 6' from Wones and Eugster, 1965:

$$\log f_{H_2O} = \frac{3428 - 4212(1 - x)^2}{T (^{\circ}K)} + \log x + \frac{1}{2} \log f_{O_2} + 8.23$$

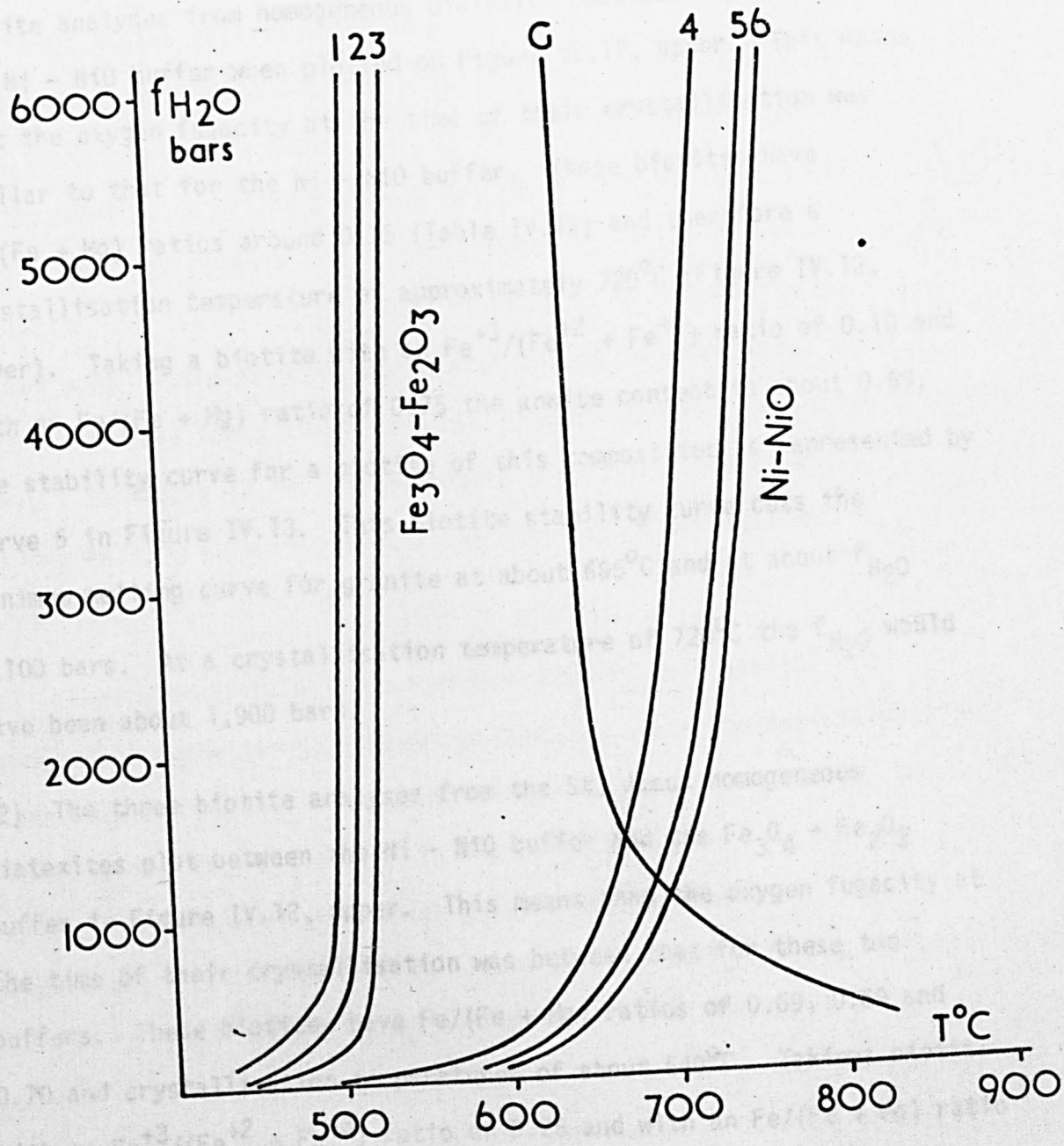
where: x = concentration of $KFe^{+2}_3AlSi_3O_{10}(OH)_2$ in biotite

and which is estimated from the $Fe^{+2}/(Fe^{+3} + Fe^{+2} + Mg^{+2})$ ratio.

Note: "The fugacity of a gas may be regarded as its partial pressure corrected for deviation from perfect gas behaviour" (Krauskopf, 1969).

Figure IV.13

Plot of $f_{\text{H}_2\text{O}}$ against T. Curve G represents the 'granite minimum' melting curve as determined by Tuttle and Bowen (1958) but with their data recast in fugacities rather than in pressures, using the fugacity values of Burnham, Holloway and Davis (1969). Curves 1, 2 and 3 represent biotite stability curves for f_{O_2} conditions represented by the $\text{Fe}_3\text{O}_4 - \text{Fe}_2\text{O}_3$ buffer and with annite contents (using the $\text{Fe}^{+2}/(\text{Fe}^{+3} + \text{Fe}^{+2} + \text{Mg}^{+2})$ ratio) of: 0.70 (curve 1); 0.60 (curve 2); and 0.52 (curve 3). Curves 4, 5 and 6 represent biotite stability curves for f_{O_2} conditions represented by the Ni - NiO buffer and with annite contents (using the $\text{Fe}^{+2}/(\text{Fe}^{+3} + \text{Fe}^{+2} + \text{Mg}^{+2})$ ratio) of: 0.84 (curve 4); 0.72 (curve 5); and 0.69 (curve 6). Stability curves constructed from equation 6' of Wones and Eugster (1965), $\log f_{\text{O}_2}$ was calculated for 5 kilobars total pressure.



1) A large number of the biotite analyses from the inhomogeneous diatexites, the two biotite analyses from the metatexites and the biotite analyses from homogeneous diatexite specimen 758 cluster across the Ni - NiO buffer when plotted on Figure IV.12, upper. This means that the oxygen fugacity at the time of their crystallisation was similar to that for the Ni - NiO buffer. These biotites have Fe/(Fe + Mg) ratios around 0.75 (Table IV.12) and therefore a crystallisation temperature of approximately 720°C (Figure IV.12, lower). Taking a biotite with an $\text{Fe}^{+3}/(\text{Fe}^{+2} + \text{Fe}^{+3})$ ratio of 0.10 and with an Fe/(Fe + Mg) ratio of 0.75 the annite content is about 0.69. The stability curve for a biotite of this composition is represented by curve 6 in Figure IV.13. This biotite stability curve cuts the minimum melting curve for granite at about 695°C and at about $f_{\text{H}_2\text{O}}$ 1,100 bars. At a crystallisation temperature of 720°C the $f_{\text{H}_2\text{O}}$ would have been about 1,900 bars.

2) The three biotite analyses from the St. Jacut homogeneous diatexites plot between the Ni - NiO buffer and the $\text{Fe}_3\text{O}_4 - \text{Fe}_2\text{O}_3$ buffer in Figure IV.12, upper. This means that the oxygen fugacity at the time of their crystallisation was between that for these two buffers. These biotites have Fe/(Fe + Mg) ratios of 0.69, 0.69 and 0.70 and crystallisation temperatures of about 640°C. Taking a biotite with an $\text{Fe}^{+3}/(\text{Fe}^{+2} + \text{Fe}^{+3})$ ratio of 0.25 and with an Fe/(Fe + Mg) ratio of 0.69 the annite content is about 0.52. The stability curve for a biotite of this composition is represented by curve 3 in Figure IV.13. Also, taking a biotite with an $\text{Fe}^{+3}/(\text{Fe}^{+2} + \text{Fe}^{+3})$ ratio of 0.10 and with an Fe/(Fe + Mg) ratio of 0.69 the annite content is about 0.69. The stability curve for a biotite of this composition is represented by curve 6 in Figure IV.13. The stability curve for the St. Jacut homogeneous diatexite biotites will lie between these two calculated

stability curves and will cut the minimum melting curve for granite at about 640°C and at about $f_{\text{H}_2\text{O}}$ 3,000 - 5,000 bars.

3) Biotite analysis 24 (from specimen 360) is of a biotite from the homogeneous granite to the north of St. Jacut (Colombière Granite). This biotite analysis plots close to the Ni - NiO buffer in Figure IV.12, upper. It has an Fe/(Fe + Mg) ratio of 0.93 which gives a crystallisation temperature of 670°C from Figure IV.12, lower. Taking a biotite with an $\text{Fe}^{+3}/(\text{Fe}^{+2} + \text{Fe}^{+3})$ ratio of 0.10 and with an Fe/(Fe + Mg) ratio of 0.93 the annite content is about 0.84. The stability curve for a biotite of this composition is represented by curve 4 in Figure IV.13. This biotite stability curve cuts the minimum melting curve for granite at about 670°C and at about $f_{\text{H}_2\text{O}}$ 1,500 bars.

4) Biotite analysis 6 (from specimen 720) is of a biotite from homogeneous diatexite just north of Cancale. This biotite analysis plots between the Ni - NiO buffer and the Fe_3O_4 - Fe_2O_3 buffer, but closer to the Ni - NiO buffer in Figure IV.12, upper. It has an Fe/(Fe + Mg) ratio of 0.80 which gives a crystallisation temperature of about 655°C from Figure IV.12, lower. Taking a biotite with an $\text{Fe}^{+3}/(\text{Fe}^{+2} + \text{Fe}^{+3})$ ratio of 0.10 and with an Fe/(Fe + Mg) ratio of 0.80 the annite content is about 0.72. The stability curve for a biotite of this composition is represented by curve 5 in Figure IV.13. The stability curve for biotite analysis 6 will lie to the left of this since it plots slightly away from the Ni - NiO buffer in Figure IV.12, upper. A stability curve in this position would cut the minimum melting curve of granite at about 655°C and at about $f_{\text{H}_2\text{O}}$ 2,000 bars.

Three assumptions have been made in the above analysis. Firstly, that the $\text{Fe}^{+2}/(\text{Fe}^{+3} + \text{Fe}^{+2} + \text{Mg}^{+2})$ ratio is equivalent to the mole fraction annite in the biotite (see Wones and Eugster, 1965). Secondly, that the activities of KAlSi_3O_8 and Fe_3O_4 are equal to unity for the St. Malo rocks. Thirdly, that the melting curve for the metasediments from which the St. Malo metatexites, diatexites and granites were produced is comparable to the 'granite minimum' melting curve of Tuttle and Bowen (1958). Changes in these assumptions do not give rise to significant changes in either the results presented above or the conclusions drawn from those results.

CHAPTER V

Structural Geology

Preliminary Statement

The methods employed in the elucidation of the tectonic histories within the rocks comprising and associated with the ... belt are those in common use (see Turner ... 1967). Descriptive terminology of folds ... (Pansay *op. cit.*). The problems of correlation ... in metamorphic belts have been critically examined ... to the conclusion that "there are thus ... methods of correlating deformation phases ... country ... All that can be **CHAPTER V**

events in small areas". The approach ... establish structural sequences in ... relative ages upon the major rock units ... these structural sequences have ... although the validity of such correlations ... rock units within the research area have ... Fundamental tectonic units within the ... Massif (Cogné, 1959 & 1962; Roach, Adams, ... 1972; and Bishop, Roach and Adams, in press). ... concerning the relative ages of the ... and adjacent metasediments from one critical area (Place ... and the regional implications of these age relationships ... by Brown, Barber and Roach (1971).

The principal technique used to establish a structural sequence within an area is that of superposition of structures - structure C

Structural Relationships

Preliminary Statement

The methods employed in the elucidation of the structural histories within the rocks comprising and associated with the St. Malo migmatite belt are those in common use (see Turner and Weiss, 1963 and Ramsay, 1967). Descriptive terminology of folds follows Fleuty (1964) and Ramsay (op.cit.). The problems of correlation of structural sequences in metamorphic belts have been critically examined by Park (1969) who came to the conclusion that "there are thus no reliable structural methods of correlating deformation phases across large tracts of country All that can be achieved with confidence is the ordering of events in small areas". The approach adopted in this study has been to establish structural sequences in critical areas in order to place relative ages upon the major rock units. Similarities between some of these structural sequences have enabled correlation between them, although the validity of such correlation may be questioned. The major rock units within the research area have been correlated with the fundamental tectonic units within the Precambrian of the Armorican Massif (Cogné, 1959 & 1962; Roach, Adams, Brown, Power and Ryan, 1972; and Bishop, Roach and Adams, in press). A preliminary statement concerning the relative ages of the St. Malo migmatite belt and adjacent metasediments from one critical area (Plage de Quatre Vaux) and the regional implications of these age relationships has been presented by Brown, Barber and Roach (1971).

The principal technique used to establish a structural sequence within an area is that of superposition of structures - structure C

affects and therefore post-dates structure B and structure B affects and therefore post-dates structure A. It should be remembered that superimposition of folds is only possible when the direction of compression of the second fold phase is at a high angle to that of the first fold phase, otherwise the first folds rotate and tighten (Ghosh and Ramberg, 1968). The difficulties of labelling successive foliations and lineations have been commented upon by Park (op.cit.) especially when successive foliations are co-planar and successive lineations are co-linear (Coward, 1973). Approximately co-axial folding is encountered within the Pentevrian rocks of the St. Malo region (see below) and has been reported from other areas of Pentevrian basement (Ryan, 1973 and Ryan and Roach, in press). It is thus often difficult to assign fold closures to a particular fold phase unless fold closures of more than one generation are present and interfere such that a structural sequence may be established. It was the failure to recognise the complexities introduced by approximately co-axial folding that led Jeannette (1971) to correlate structures within the St. Malo migmatite belt with those produced by the Cadomian orogenic episode. The problem of identification of fold closures of a particular phase is increased by the poor and sporadic development of axial plane foliations with each fold phase and the general absence of any distinctive fabric or mineral parageneses.

The St. Malo migmatite belt and associated metasediments have been assigned to the Pentevrian basement (Brown et al, op.cit.) and the structures within these rocks are termed pre-Cadomian. Structures produced during the Cadomian orogenic episode are found within Brioverian supracrustal rocks which lie on the north-western side of the St. Malo migmatite belt. Shear belts within the Pentevrian basement are probably of Cadomian age. The structural analysis presented herein is not complete, much work still remains to be done.

A. The Pre-Cadomian Structures

1. The Metasediments

Pentevrian metasediments outcrop on the south-eastern side of pnte de la Garde, near St. Cast (Figure II.2), along the Rance around Langrolay - St. Suliac and downstream within the metatexites as far as la Richardais (Figure II.5) and to the north and south of Cancale (Figure II.4).

The key to the apparently complex structural pattern within the metasediments is found at pnte de la Garde. Here four phases of folding can be established within the metasediments prior to the cataclastic deformation within the pnte de la Garde shear belt (Table V.1). The first deformation episode produced tight to isoclinal folds with a penetrative metamorphic foliation parallel to the lithological lamination ($S_0=S_1$). Fold closures are extremely rare. The closed structure shown in Plate V.1b is interpreted as a section through an F_1 fold closure which has a curvilinear hingeline; the metamorphic foliation is parallel to the long dimension of the structure. The alternative explanation for such a closed structure is the superposition of two phases of folding (Ramsay, 1962 & 1967, Figure 10-5) but folds with a suitable geometrical relationship to each other are not found within the metasediments. Accordingly the simpler explanation for this closed structure has been preferred in this account. Shallow interference structures of Ramsay's (op.cit.) type 2 are shown in Plate V.1c and have been produced by the superposition of the folds developed during the fourth deformation episode upon the postulated first phase folds. These interference structures support the interpretation of the closed structure in Plate V.1b as an F_1 fold closure.

Table V.1: The Pre-Cadomian structural history of the Pentevrian metasediments on the south-eastern side of pnte de la Garde, near St. Cast.

Deform ⁿ episode	Fold phase	Fold type and orientation	Foliation	Lineation
D ₁	F ₁	Tight to isoclinal folds. Closures are only rarely seen. Orientation of fold axes approximately NW-SE.	S ₁	
D ₂	F ₂	Tight, variably inclined sub-horizontal to gently plunging folds. Closures are common. Orientation of fold axes approximately SW.	Locally S ₂	L ₂
D ₃	F ₃	Tight, recumbent to gently inclined sub-horizontal to gently plunging folds. Closures are common. Orientation of fold axes approximately SW.	Locally S ₃	L ₃
D ₄	F ₄	Gentle to open, upright to steeply inclined sub-horizontal to gently plunging folds. Closures are common. Orientation of fold axes approximately SW.		L ₄

Plate V.1

a: The sub-vertical section facing the ruck-sac cuts through an F_1 fold (see b). The gently undulating surface underneath the ruck-sac demonstrates the superimposition of F_4 folds on the F_1 folds (see c). This sub-horizontal surface represents the upper limb of an F_3 fold and the lower limb of an F_2 fold (23/23).

Pnte de la Garde, near St. Cast.

b: Closed structure interpreted as a section through an F_1 fold closure which has a curvilinear hinge line (23/11).

Pnte de la Garde, near St. Cast.

c: Ramsay type 2 interference structures produced by the superimposition of F_4 folds on F_1 folds (23/8).

Pnte de la Garde, near St. Cast.

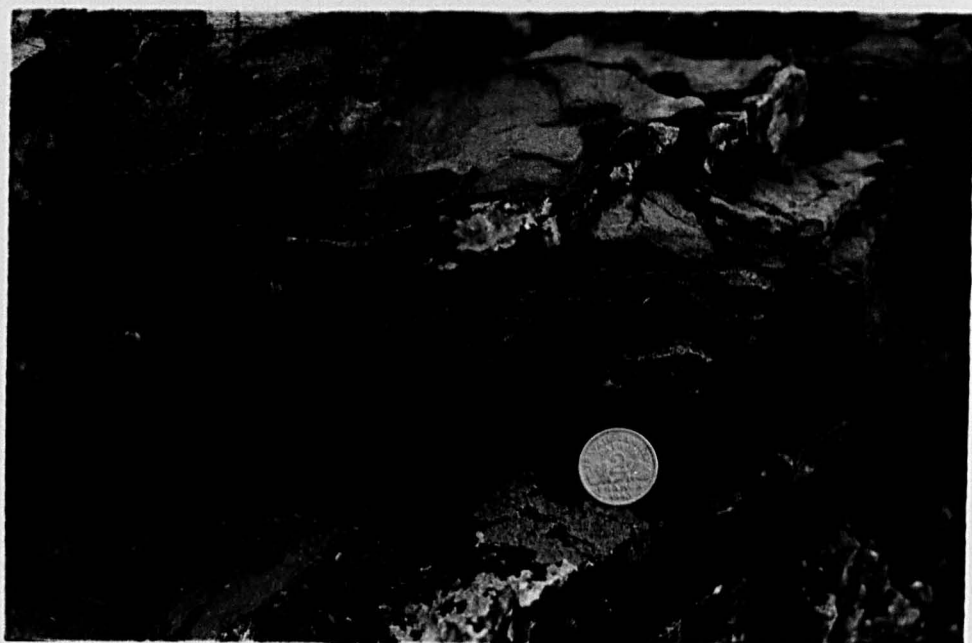
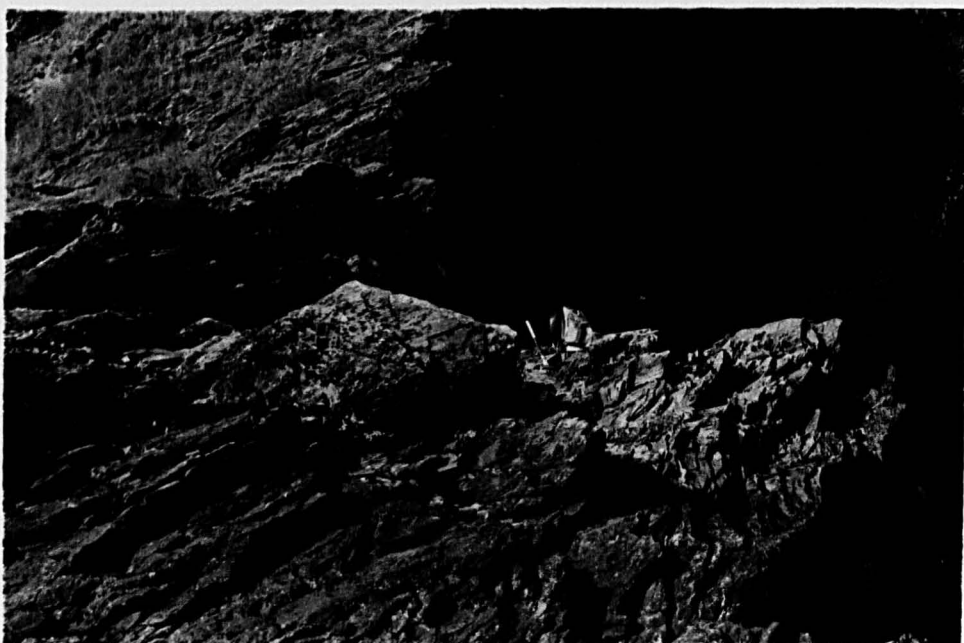


Plate V.2

a: F_2 fold closure. An axial plane foliation, S_2 , is locally developed in the hinge zone (23/29).

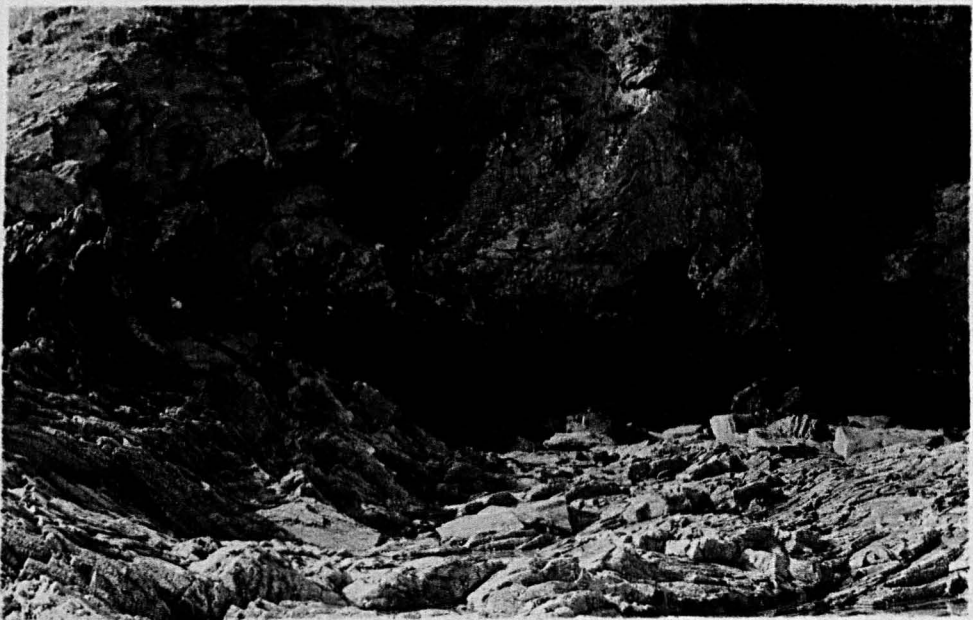
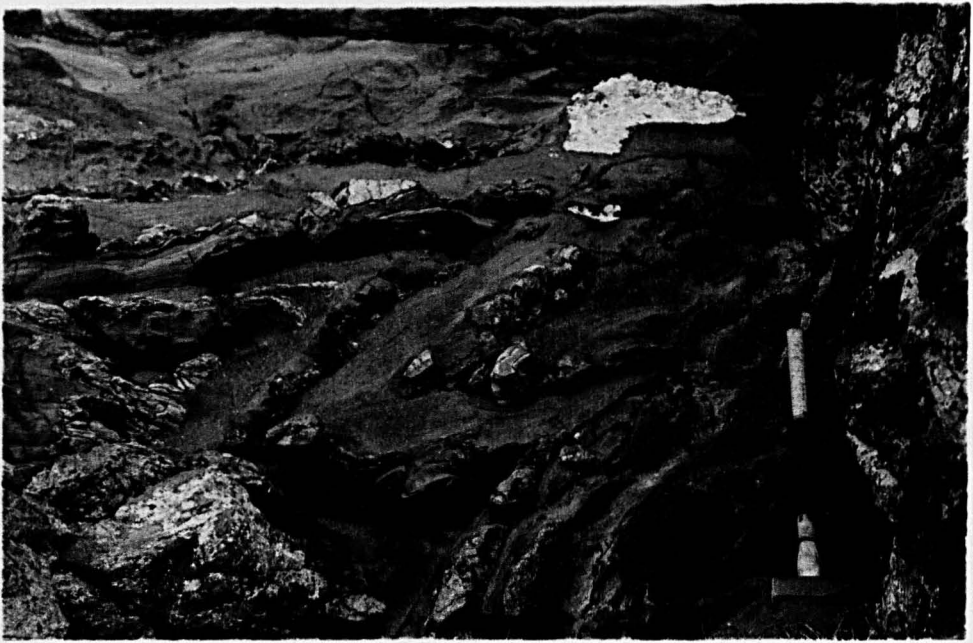
Pnte de la Garde, near St. Cast.

b: Small interference structure produced by the refolding of an F_2 fold by F_3 (23/24).

Pnte de la Garde, near St. Cast.

c: Large F_3 fold closure on the left and gentle F_4 folds in the right foreground (23/22).

Pnte de la Garde, near St. Cast.



The second episode of deformation has produced a phase of tight folds which are locally accompanied by an axial plane foliation in the hinge zones (Plate V.2a). These folds have been refolded during the third episode of deformation to give interference structures of Ramsay's (op.cit.) type 3 (Plate V.2b). The tight folds produced during the third deformation only occasionally have an axial plane foliation developed in the hinge zone. Both the F_2 folds and the F_3 folds may have a crinkle lineation developed parallel to the hinge line of the folds. The F_2 fold axial trend and the F_3 fold axial trend are both gentle and approximately to the south-west. It is a consequence of approximately co-axial folding that the minor structures produced during the successive fold phases are difficult to distinguish with confidence in the absence of a distinctive fabric (a similar problem was encountered by Coward, 1973, in the Laxfordian complex of South Uist).

The fourth deformation episode has produced a phase of open folds (Plate V.2c and the interference structures of Plate V.1c) which also have a gentle plunge approximately to the south-west.

The pre-Cadomian structural history of the metasediments and metasedimentary palaeosome which outcrop along the Rance between la Richardais and St. Suliac is summarized in Table V.2. The sequence of deformation episodes is similar to that established at pnte de la Garde. Within these metasediments it is extremely difficult to differentiate between the minor folds produced during D_2 , D_3 and D_4 . The overall orientation of the lithological lamination, however, has been determined by the large F_4 folds and the local pre- D_4 structural geometry. Typical structures from the Rance section are shown in Plates V.3, V.4 and V.5. No fold closures which could be assigned unequivocally to F_1 have been found from the Rance section. However,

there is the ubiquitous presence of an early metamorphic foliation which is generally parallel to the lithological lamination (S_0-S_1) and which has been folded during the later episodes of deformation. An early lineation (thought to have been produced during D_1 and labelled L_1) is folded by the later deformation episodes (Plate V.3). The F_1 folds must have been large and tight to isoclinal in form. Minor F_2 fold closures may be distinguished with confidence in a few cases (Plate V.3) especially when they have been refolded by folds of the F_3 phase (Plate V.4) although care must be exercised because minor F_4 folds may also refold the earlier fold closures on occasion. Major F_4

Table V.2: The Pre-Cadomian structural history of the Pentevrian metasediments which outcrop along the Rance between Ia Richardais and St. Suliac.

Deform ⁿ episode	Fold phase	Fold type and orientation	Foliation	Lineation
D_1	? F_1	No fold closures which could reliably be ascribed to this episode of deformation have been found. It is inferred that they are tight to isoclinal.	S_1	L_1
D_2	F_2	Tight, variably inclined and variably plunging folds. Orientation of fold axes variable between N and E.	Locally S_2	L_2
D_3	F_3	Close to tight, variably inclined and variably plunging folds which refold F_2 folds. Orientation of fold axes variable between N and E.	Locally S_3	L_3
D_4	F_4	Open to close, upright to steeply inclined gently plunging folds. Orientation of fold axes approximately NE.	Locally S_4	L_4

and orientation of the F_4 folds can be established from area 11 (see Plate 12.2). They are upright folds with a gentle plunge approximately north-east (the x axis for the girdle shown in Figure 2.18 is 15° to $N54^\circ E$). To the north in area 1 the pre- D_4 orientation of S_0-S_1 was more variable but the F_4 folds still dominate the overall orientation of S_0-S_1 (the x axis for the girdle shown in Figure 2.18 is 20° to

there is the ubiquitous presence of an early metamorphic foliation which is generally parallel to the lithological lamination ($S_0=S_1$) and which has been folded during the later episodes of deformation. An early lineation (thought to have been produced during D_1 and labelled L_1) is folded by the later deformation episodes (Plate V.3a). The F_1 folds must have been large and tight to isoclinal in form. Minor F_2 fold closures may be distinguished with confidence in a few cases (Plate V.3) especially when they have been refolded by folds of the F_3 phase (Plate V.4) although care must be exercised because minor F_4 folds may also refold the earlier fold closures on occasion. Major F_4 folds can be identified with relative ease in the metasediments near Langrolay - St. Suliac and sometimes can be identified within the metasediments outcropping within the metatexites to the north (Plate V.4c). Where major F_4 folds cannot be identified with confidence the distinction between minor F_2 , F_3 and F_4 folds is difficult. An intermittent crinkle lineation is associated with the F_2 , F_3 and F_4 folding and a foliation may be developed in F_2 and F_3 fold closures. Late conjugate kink folds are developed sporadically within the Rance metasediments (Plate V.5c).

Figure V.1 shows the orientation of $S_0=S_1$ along the Rance. In area I minor F_2 folds and F_3 folds and both major and minor F_4 folds are all present. In area II both major and minor F_4 folds are present but minor F_2 folds and F_3 folds are generally absent. Thus the style and orientation of the F_4 folds can be established from area II (see Plate II.2). They are upright folds with a gentle plunge approximately north-east (the π axis for the girdle shown in Figure V.1B is 15° to $N54^\circ E$). To the north in area I the pre- D_4 orientation of $S_0=S_1$ was more variable but the F_4 folds still dominate the overall orientation of $S_0=S_1$ (the π axis for the girdle shown in Figure V.1A is 20° to

Plate V.3

a: Strong L_1 lineation refolded by later deformation
(21/32).

Pnte du Crapaud, la Rance.

b: F_2 fold closure. L_1 is at a high angle to the F_2 hinge
line and is folded by F_2 (21/28).

North of pnte du Crapaud, la Rance.

c: F_2 fold closure. An axial plane foliation is developed
in the hinge zone (9/4).

West of le Val es Bouillis, la Rance.



Plate V.4

- a: An F_2 fold which has been refolded by F_3 (24/9).
Les Hures, la Rance.
- b: Small interference structure produced by the refolding
of an F_2 fold by F_3 (12/36).
East of le Val es Bouillis, la Rance.
- c: The overall orientation of $S_0=S_1$ is dominated by F_4
although both F_2 and F_3 folds may be distinguished
(23/34).
East of le Val es Bouillis, la Rance.

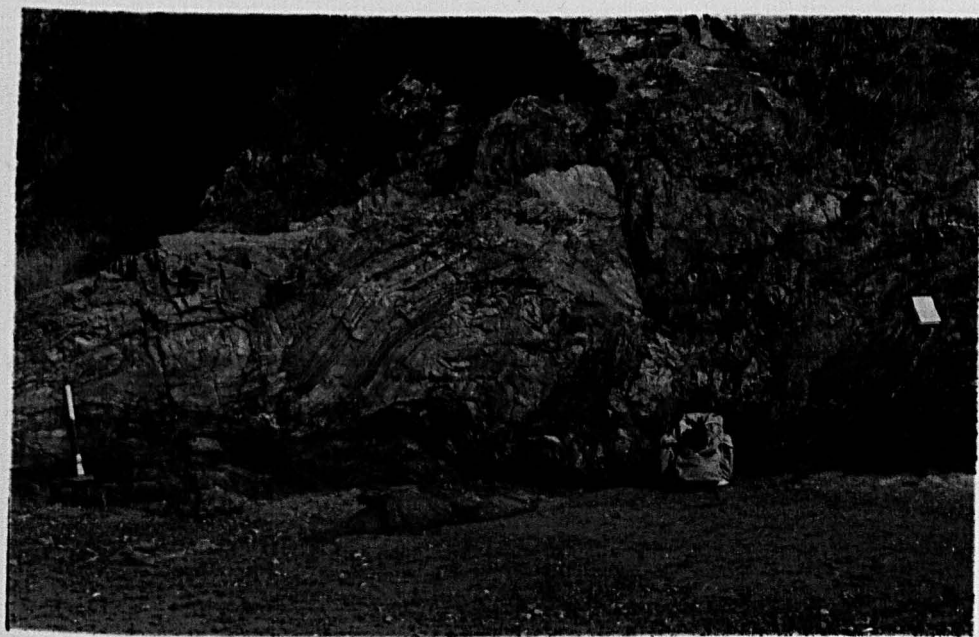
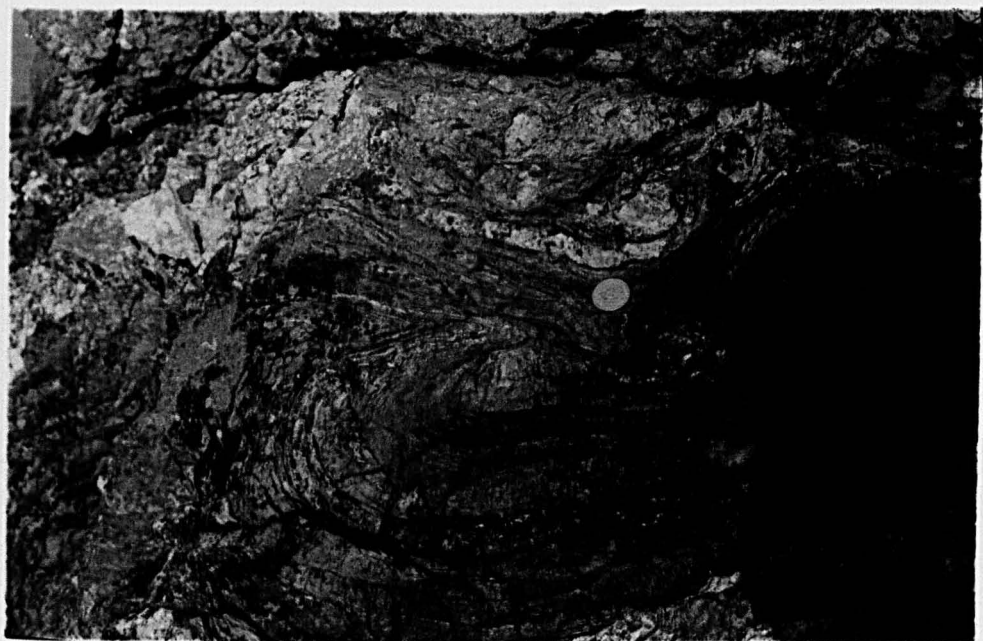


Plate V.5

- a: Gentle F_4 folds. There is a crinkling lineation parallel to the hammer handle (1/20).
South of pnte de Chatelet, la Rance.
- b: Gentle to open F_4 folds (12/28).
Vge de Grainfolet, la Rance.
- c: Late conjugate kink folds (9/17).
Pnte de Gareau, la Rance.

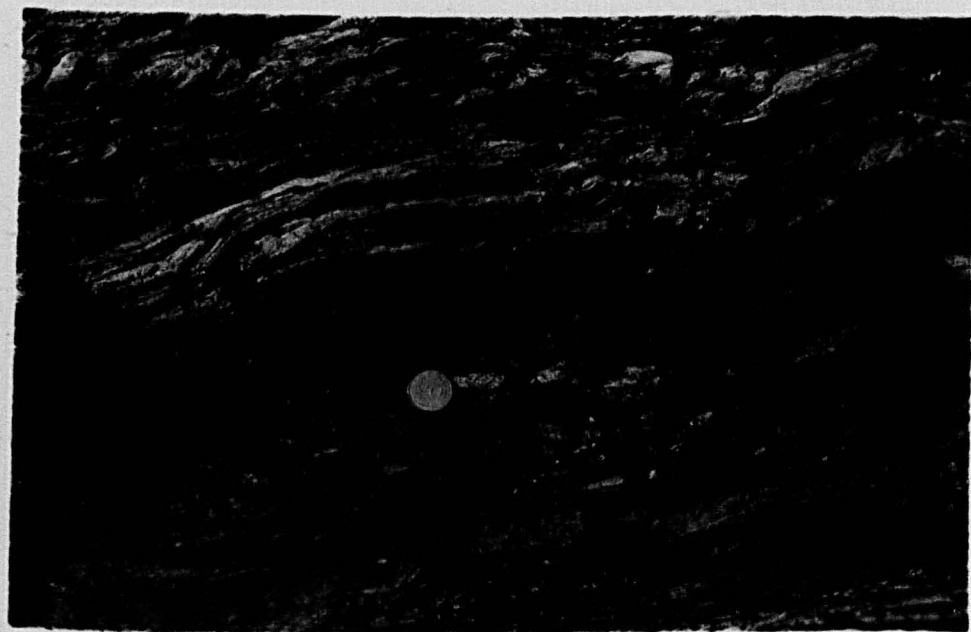
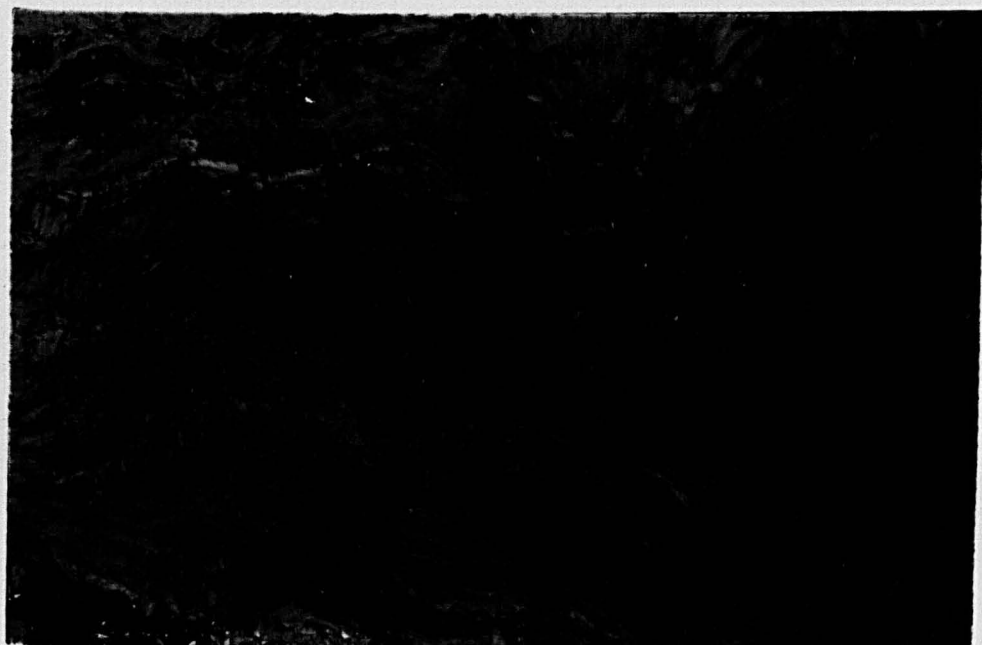
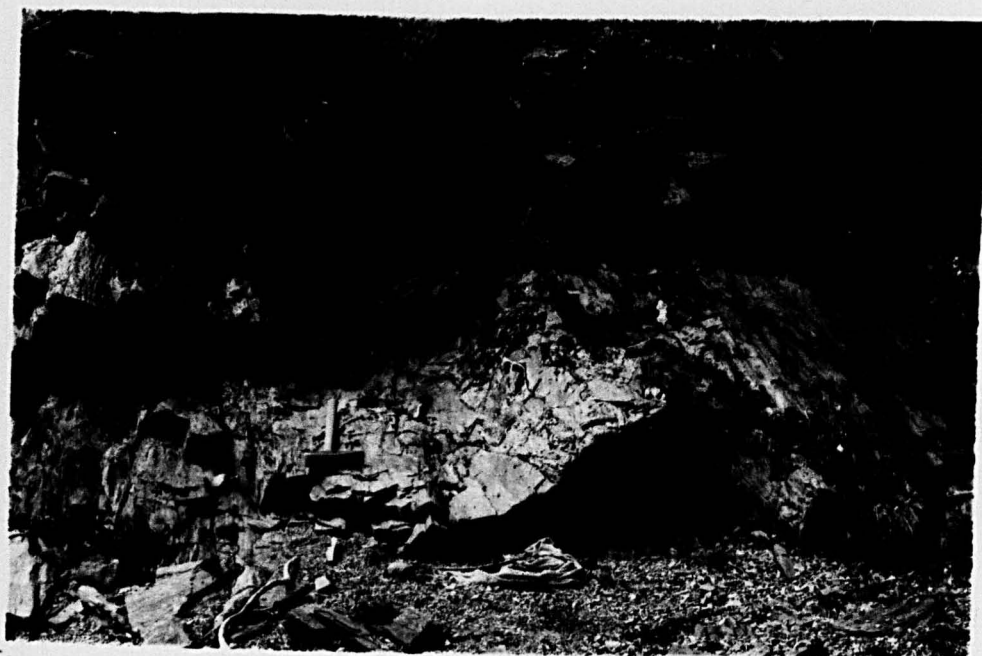


Figure V.1

- A. Orientation diagram for metasediments and metasedimentary palaeosome from area I along the Rance; 410 poles to $S_0=S_1$. Contours 3%, 2%, 1% and 0.25% per 1% area, equal area projection from the lower hemisphere.
- B. Orientation diagram for metasediments from area II along the Rance; 190 poles to $S_0=S_1$. Contours 8%, 4% and 0.5% per 1% area, equal area projection from the lower hemisphere.

la Richardais

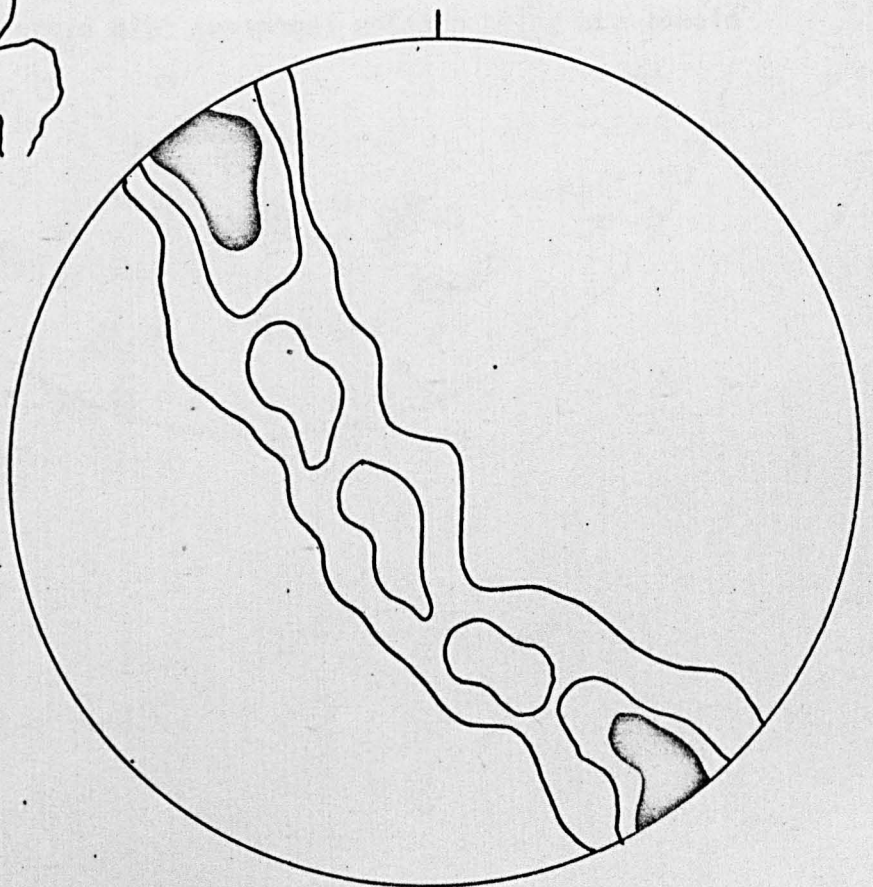
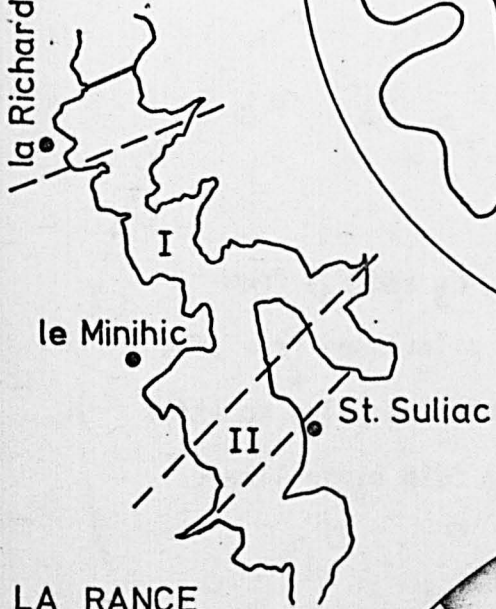


Figure V.2

Orientation diagram for folds (F_2 , F_3 and F_4) from metasediments and metasedimentary palaeosome from area I along the Rance. Open circles represent poles to axial planes and solid circles represent fold hinge lines.

1971). The orientation of microfossils in the ...
supports this contention that the ...
result of the D_2 deformation.

Journé et al. (1971, Part I, Chapter 11, ...
describes the folding of the ...

descriptions it seems that Journé ...
the F_2 folds of this work ...

the F_3 and F_4 folds ...
superimposition ...

The structural history of the ...
with an ...

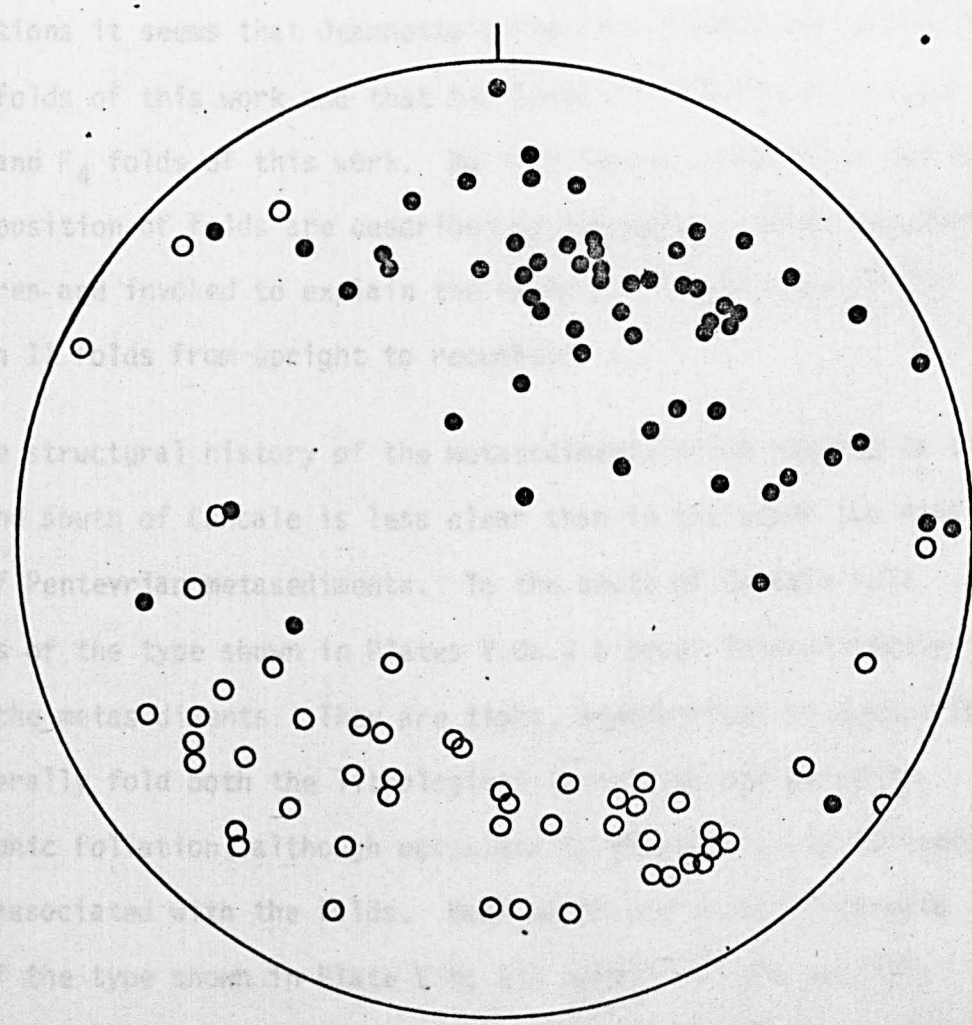
of Penck ...
of the type ...

within the ...
and general ...

of the type ...
equivalent to the F_4 folds ...

showing lineation (Plate V.2) ...
is shown on the south side of ...

of the ...
of the ...



N32°E). The orientation of undifferentiated minor folds (Figure V.2) supports this contention that the overall orientation of $S_0=S_1$ is the result of the D_4 deformation.

Jeannette has examined the Rance metasediments in detail (Jeannette, 1971, Part I, Chapter II, p.21-36) but only recognizes two phases of folding labelled Cadomian I and Cadomian II. From his descriptions it seems that Jeannette's Cadomian I folds correspond to the F_2 folds of this work and that his Cadomian II folds correspond to the F_3 and F_4 folds of this work. No interference structures due to superimposition of folds are described by Jeannette. Large recumbent structures are invoked to explain the variation in attitude of the Cadomian II folds from upright to recumbent.

The structural history of the metasediments which outcrop to the north and south of Cancale is less clear than in the other two main areas of Pentevrian metasediments. To the south of Cancale fold closures of the type shown in Plates V.6a & b occur intermittently within the metasediments. They are tight, asymmetrical or symmetrical and generally fold both the lithological lamination and an early metamorphic foliation, although occasionally an axial plane foliation may be associated with the folds. Both north and south of Cancale folds of the type shown in Plate V.6c are common and are possibly equivalent to the F_4 folds found along the Rance. They fold a steeply plunging lineation (Plate V.7). Their sense of asymmetry changes from 'z' shaped on the south side of Port Briac, north of Cancale, to predominantly 's' shaped south of Cancale and reflects major folding of the metasediments. There is a set of late conjugate folds occasionally associated with a crenulation cleavage (Plates V.7b & c) which is present both north and south of Cancale.

Plate V.6

- a: Pre- D_4 folding of $S_0=S_1$ in the metasediments south of Cancale (19/23).
North of pnte des Roches Noires, south of Cancale.
- b: Disruption of pre- D_4 folding of $S_0=S_1$ in the metasediments south of Cancale (24/22).
South of pnte des Roches Noires, south of Cancale.
- c: D_4 folds within the metasediments south of Cancale (ie. these folds are correlated with F_4 folds developed in the Rance section) (18/20).
North of pnte des Roches Noires, south of Cancale.



Plate V.7

- a: A steep lineation refolded by the folds produced during the Pentevrian D_4 deformation episode (24/19).
Pnte des Roches Noires, south of Cancale.
- b: Late conjugate folds (19/24).
South of pnte des Roches Noires, south of Cancale.
- c: Late conjugate folds (19/10).
South of pnte des Roches Noires, south of Cancale.

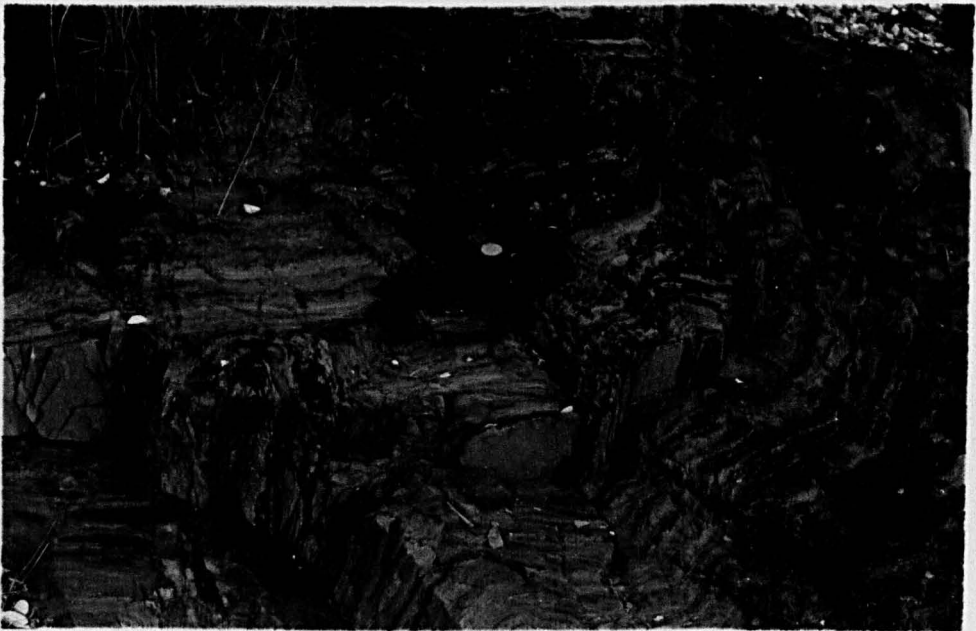
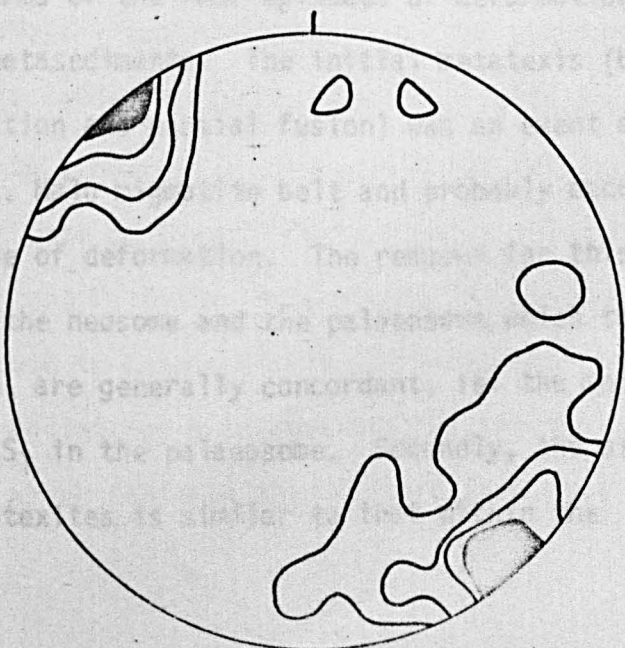
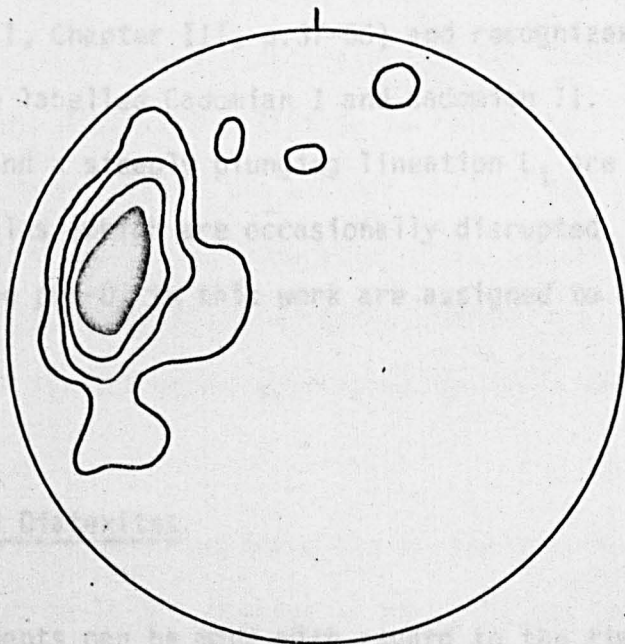
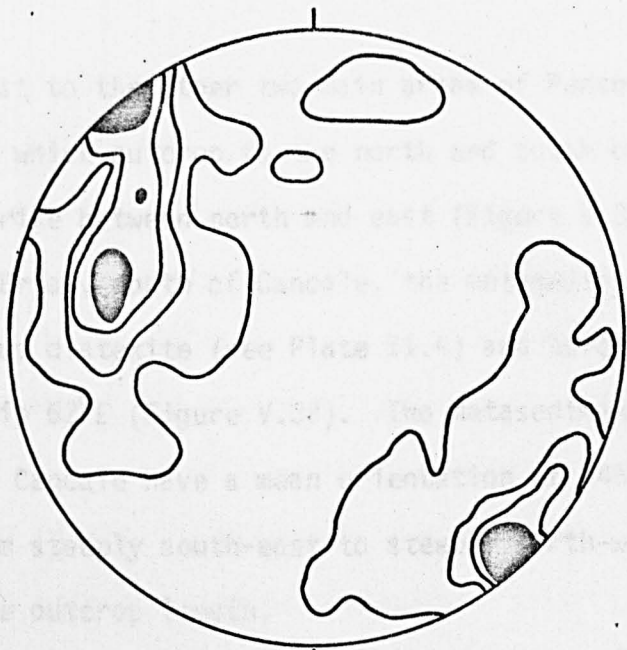


Figure V.3

- A. Orientation diagram for metasediments around Cancale; 200 poles to $S_0=S_1$. Contours 7%, 5%, 3% and 0.25% per 1% area, equal area projection from the lower hemisphere.
- B. Orientation diagram for metasediments on the south side of Port Briac, north of Cancale; 100 poles to $S_0=S_1$. Contours 12%, 8%, 4% and 1% per 1% area, equal area projection from the lower hemisphere.
- C. Orientation diagram for metasediments to the south of Cancale; 100 poles to $S_0=S_1$. Contours 12%, 8%, 4% and 1% per 1% area, equal area projection from the lower hemisphere.



In complete contrast to the other two main areas of Pentevrian metasediments the rocks which outcrop to the north and south of Cancale have a steep dip and strike between north and east (Figure V.3A). On the south side of Port Briac, north of Cancale, the metasediments dip away from the homogeneous diatexite (see Plate II.4) and have a mean orientation of $N15^{\circ}E$, dip $62^{\circ}E$ (Figure V.3B). The metasediments which outcrop to the south of Cancale have a mean orientation of $N45^{\circ}E$ and a dip which changes from steeply south-east to steeply north-west from north to south along the outcrop length.

Jeannette has examined the Cancale metasediments in detail (Jeannette, 1971, Part I, Chapter III, p.37-56) and recognizes two episodes of deformation labelled Cadomian I and Cadomian II. The metamorphic fabric S_1 and a steeply plunging lineation L_1 are assigned to Cadomian I whilst folds (which are occasionally disrupted, cf. Plate V.6b this work) labelled pre- D_4 in this work are assigned to Cadomian II by Jeannette.

2. The Metatexites and Diatexites

Two general statements can be made with regard to the timing of the migmatization in terms of the four episodes of deformation recognized within the metasediments. The initial metatexis (by metamorphic differentiation and partial fusion) was an event early in the evolution of the St. Malo migmatite belt and probably occurred during the first episode of deformation. The reasons for this thinking are twofold. Firstly, the neosome and the palaeosome, which together comprise the metatexite, are generally concordant, i.e. the metatexitic banding is parallel to S_1 in the palaeosome. Secondly, the structural history within the metatexites is similar to that within the

metasediments, a fact which suggests a common development (see Plates II.6 to II.12 inclusive and Plates V.8 & V.9). Diatexis (substantial anatexis) occurred later in the evolution of the St. Malo migmatite belt since the diatexite has clearly disrupted the metatexite in places (eg. Frontispiece 1 and Plates V.9c & V.10a) and was probably post D_2 in the metasediments. The reason for placing the diatexis post D_2 in the sequence of events is the common occurrence of metasedimentary enclaves within the diatexite which preserve F_2 folds (Plate V.10). Moreover, some enclaves have preserved interference structures of Ramsay's (1962 & 1967) type 3 which are generally produced by the superimposition of F_3 folds on F_2 folds in the metasediments. The evidence suggests that diatexis was broadly concomitant with D_3 . The diatexite foliation is folded by the D_4 deformation. The structures within the western part of the St. Malo migmatite belt, that is around the Presqu'Isle de St. Jacut-de-la-Mer and le Guildo (Figures II.3 & II.6), and within the eastern part of the belt, that is north of Port Briac (Figure II.4), will be examined in more detail.

Within the metatexites which dominate the northern part of the Presqu'Isle de St. Jacut-de-la-Mer (Figure II.6) $S_0=S_1$ has been affected by a sequence of deformation episodes similar to that established within the Pentevrian metasediments. The metatextitic banding has been tightly folded during D_2 and these folds have been refolded during D_3 (Plate V.8b). A major F_3 fold has determined the orientation of $S_0=S_1$ at pnte du Chevet (Plate V.8a). The effect of the gentle to open, upright F_4 folds found within the Pentevrian metasediments is difficult to assess within the metatexites of St. Jacut since the metatextitic banding has a predominantly steep dip (Figure V.4A). The diatexites which dominate the southern part of the

Plate V.8

- a: Major F_3 fold in metatexite palaeosome (25/25).
Pnte du Chevet, St. Jacut-de-la-Mer.
- b: Minor F_2 fold on the left and minor F_3 folds on the
right in metatexite palaeosome (4/6).
North of le Chef de l'Isle, St. Jacut-de-la-Mer.
- c: Minor folds ($?F_3$) in metatexite palaeosome (2/16).
Pnte de Lancieux, Lancieux.

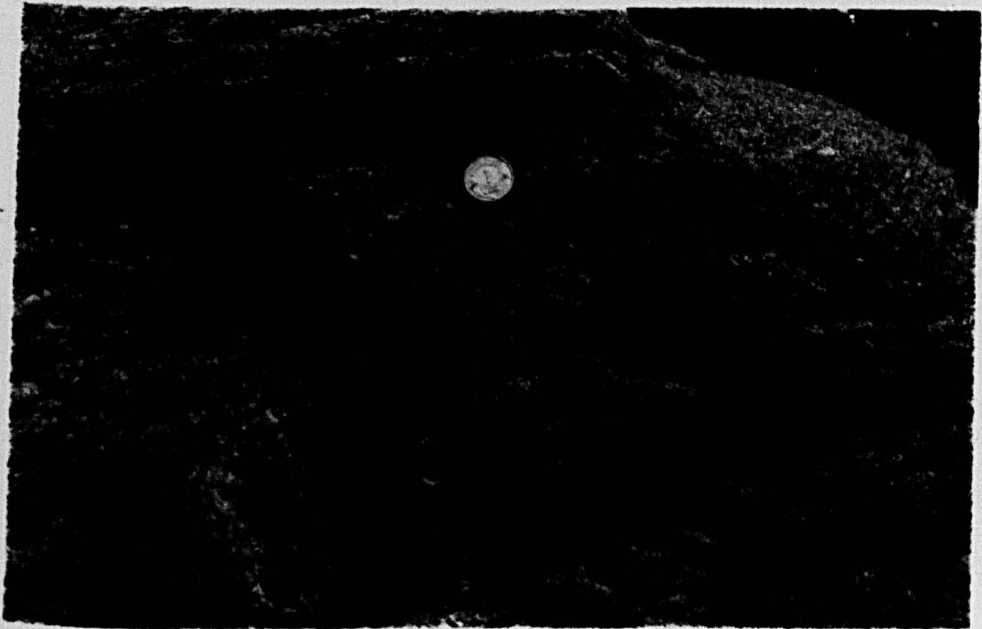
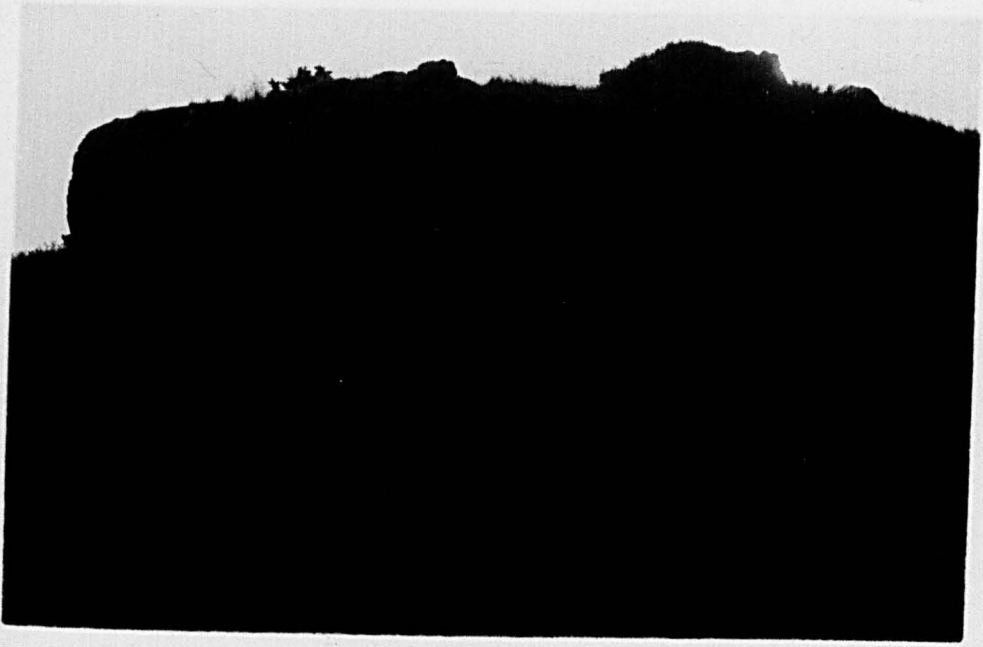


Plate V.9

a: Minor folds (?F₃) in metatexite (5/27).

Ile Besnard, near Rotheneuf.

b: Minor folds (?F₃) in metatexite (5/30).

Ile Besnard, near Rotheneuf.

c: Mobile diatexite cross-cutting earlier metatexite
(11/2).

South of pnte de la Haye, near St. Briac.

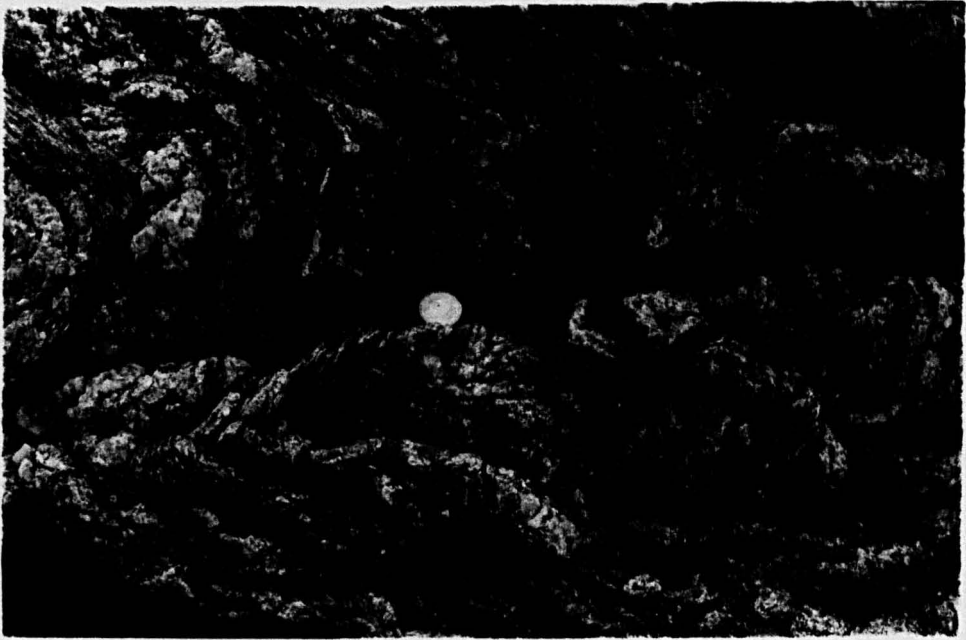


Plate V.10

- a: Diatexite which has disrupted the metatexite (4/21).
Port Blanc, west of Dinard.
- b: Psammite enclave with F_2 folds preserved enclosed
within foliated inhomogeneous diatexite (1/26).
Pnte du Bechet, St. Jacut-de-la-Mer.
- c: Enclave with F_2 folds and local S_2 foliation enclosed
within foliated inhomogeneous diatexite (3/11).
South of pnte du Chateau Parlant, St. Jacut-de-la-Mer.

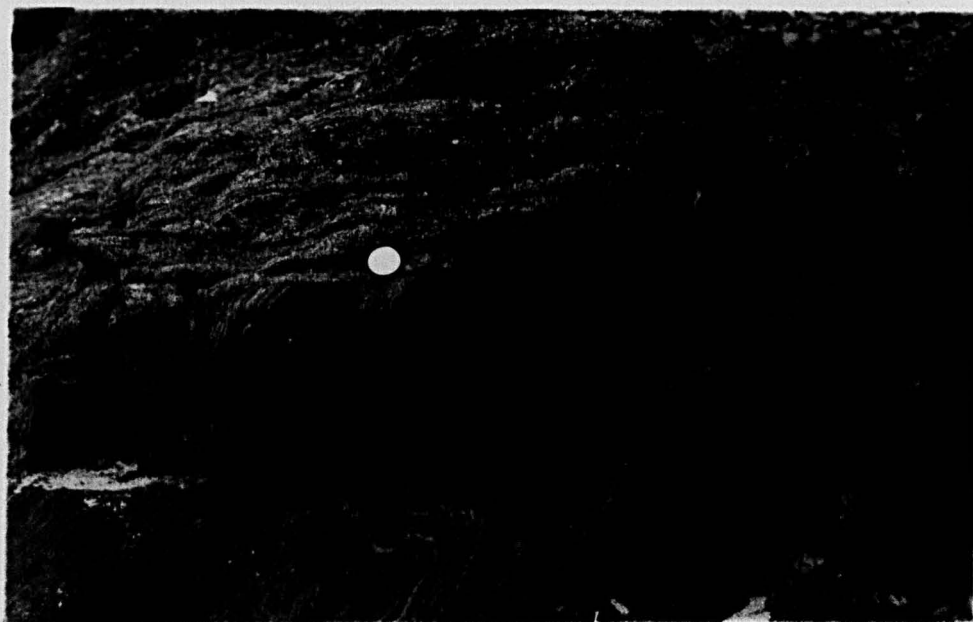
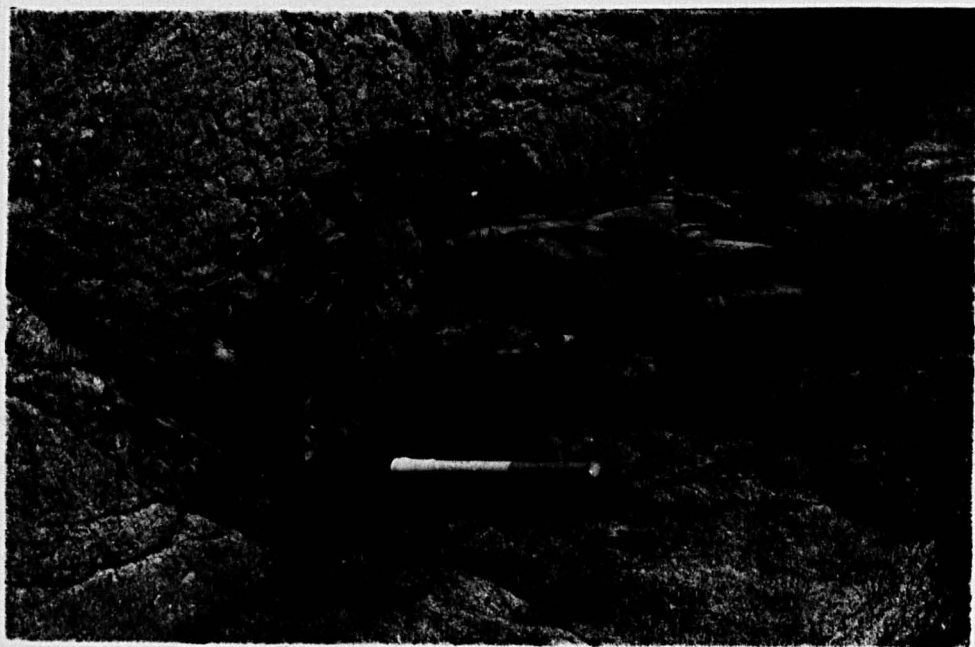


Figure V.4

- A. Orientation diagram for metatexites from St. Jacut-de-la Mer; 198 poles to metatextitic banding. Contours 6%, 4%, 2% and 0.5% per 1% area, equal area projection from the lower hemisphere.

- B. Orientation diagram for inhomogeneous diatexites between le Guildo and Plage de Quatre Vaux and from St. Jacut-de-la-Mer; 167 poles to diatexite foliation. Contours 8%, 6%, 4%, 2% and 0.67% per 1% area, equal area projection from the lower hemisphere.

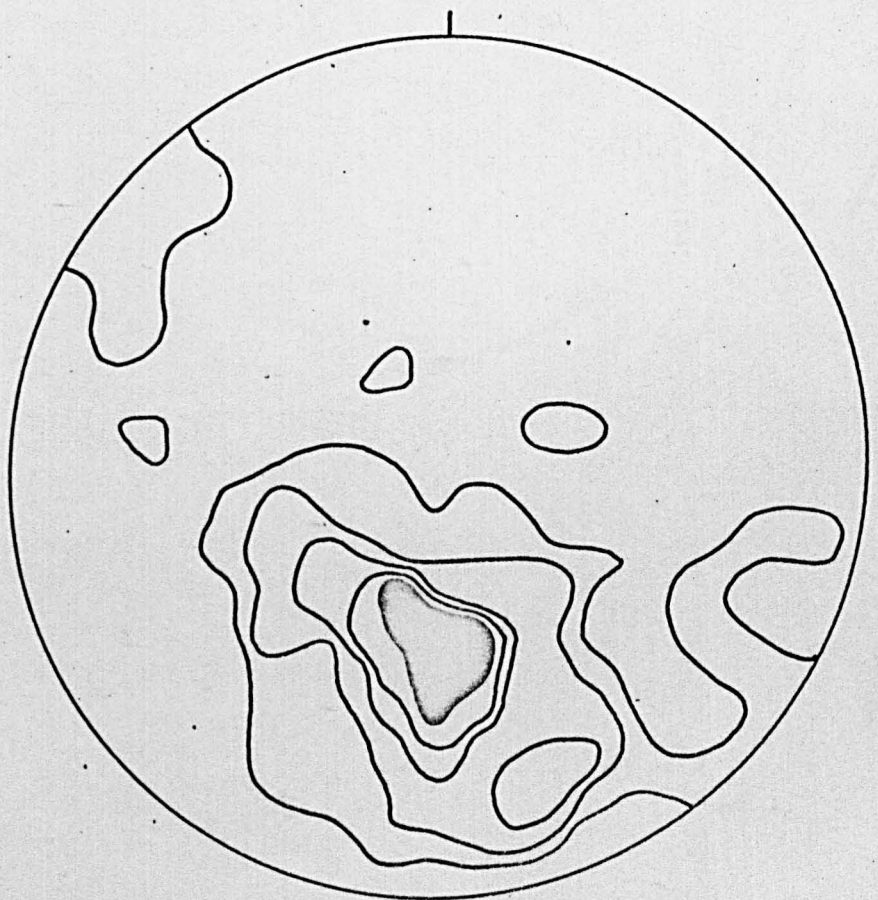
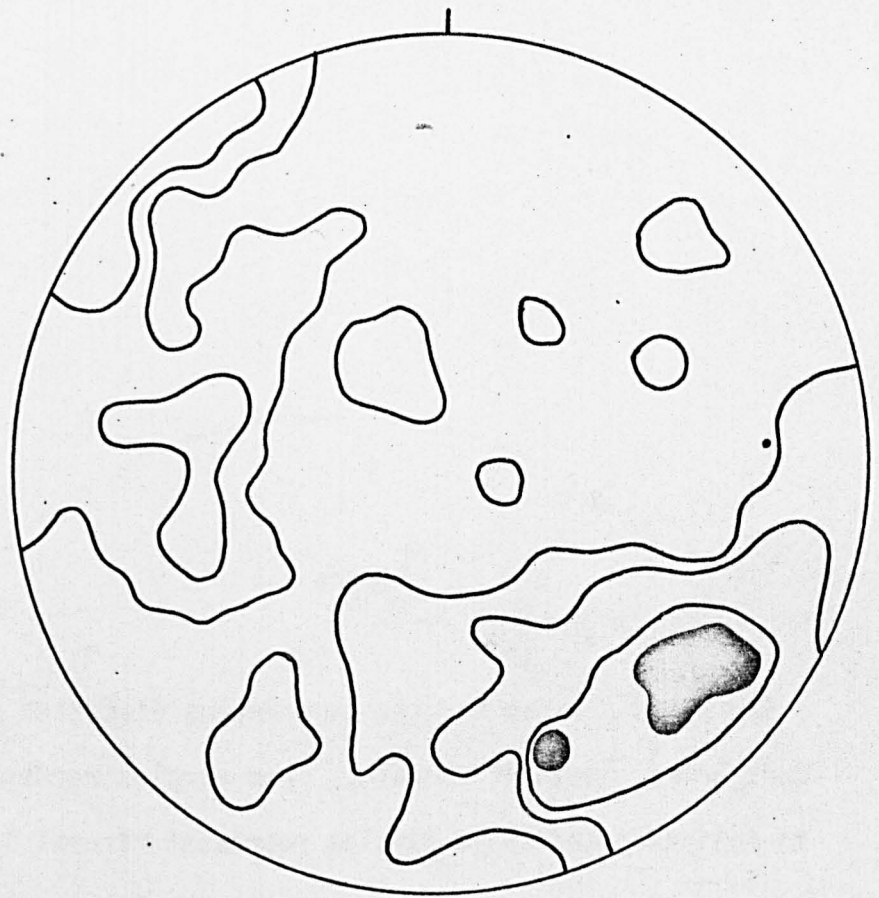
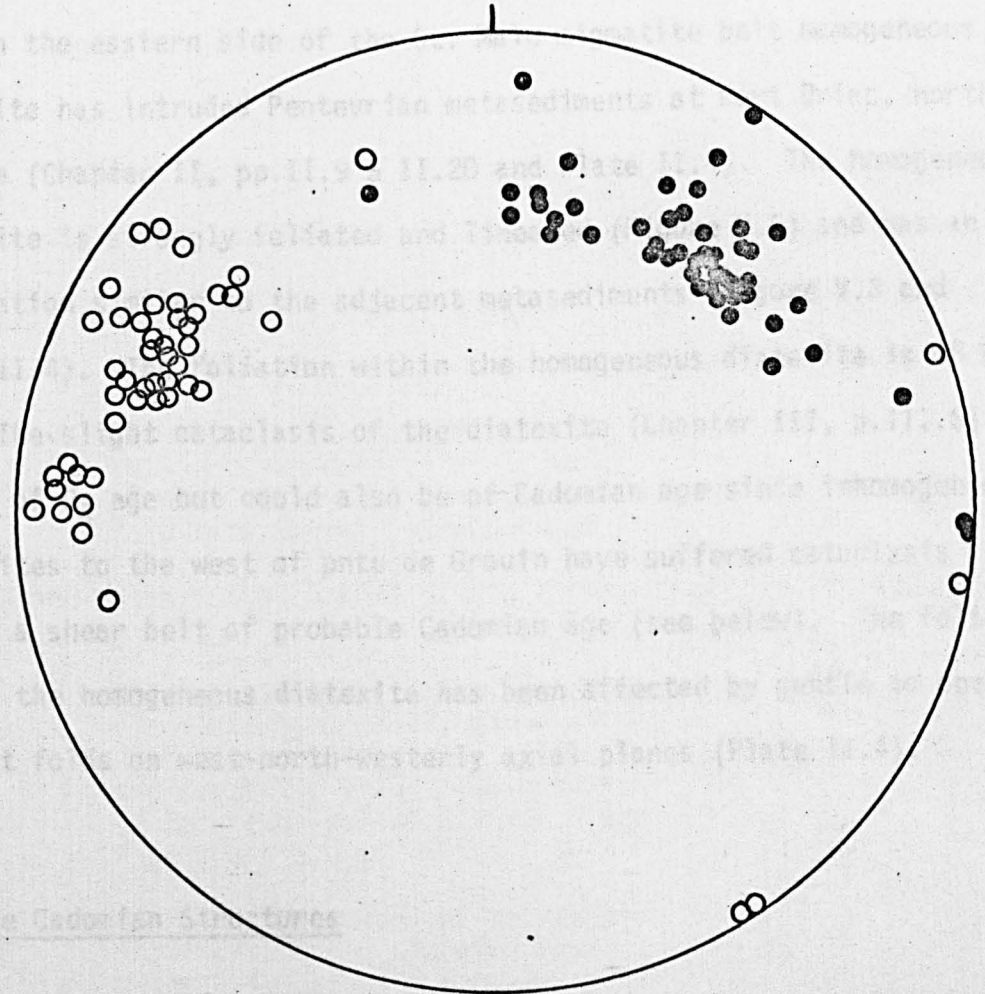


Figure V.5

Orientation diagram for the homogeneous diatexite north of Port Briac, north of Cancale. Open circles represent poles to foliation and solid circles represent mineral lineations.

... preserved (Plate V, figs 2, 3) and rarely with interference structures produced by F_2 folds on F_1 folds... This foliation has a moderate to steep dip and a variable strike (Figure 4, 4B) and was produced during D_2 and folded during D_3 .



6. The Cadomian structures

1. The Brivoerian Supracrustal Rocks

The Cadomian structural history for the Brivoerian supracrustals which outcrop between Plage de Quatre Vaux and Plage de la Pointe (Figure 11.2) is summarized in Table 11.3. Three episodes of deformation are recognized. The first deformation episode, which some have considered responsible for the development of close to right, west to east

Presqu'Isle de St. Jacut-de-la-Mer contain enclaves with F_2 folds preserved (Plates V.10a & b) and rarely with interference structures produced by F_3 folds on F_2 folds preserved. The diatexite foliation diverges around the enclaves to enclose them in large scale augen structures. This foliation has a moderate to steep dip and a variable strike (Figure V.4B) and was produced during D_3 and folded during D_4 .

On the eastern side of the St. Malo migmatite belt homogeneous diatexite has intruded Pentevrian metasediments at Port Briac, north of Cancale (Chapter II, pp.II.9 & II.20 and Plate II.4). The homogeneous diatexite is strongly foliated and lineated (Figure V.5) and has an orientation similar to the adjacent metasediments (Figure V.3 and Plate II.4). The foliation within the homogeneous diatexite is of D_4 age. The slight cataclasis of the diatexite (Chapter III, p.III.8) may be of D_4 age but could also be of Cadomian age since inhomogeneous diatexites to the west of pnte de Grouin have suffered cataclasis within a shear belt of probable Cadomian age (see below). The foliation within the homogeneous diatexite has been affected by gentle to open, upright folds on west-north-westerly axial planes (Plate II.4).

B. The Cadomian Structures

1. The Brioverian Supracrustal Rocks

The Cadomian structural history for the Brioverian metasediments which outcrop between Plage de Quatre Vaux and Plage de Pen Guen (Figure II.3) is summarized in Table V.3. Three episodes of deformation are recognized. The first deformation episode within these rocks was responsible for the development of close to tight, upright to steeply

Table V.3: The Cadomian structural history of the Brioverian supracrustal rocks between Plage de Quatre Vaux and Plage de Pen Guen.

Deform ⁿ episode	Fold phase	Fold type and orientation	Foliation	Lineation
D ₁	F _{1A}	Close to tight, upright to steeply inclined sub-horizontal to gently plunging folds. Orientation of fold axes varies between N and E.	S ₁	L _{1A}
SEGREGATION AND INTRUSION OF QUARTZ VEINS, INTRUSION OF GRANITE PEGMATITE AND GRANITE				
D ₂	F _{1B}	Flattening of F _{1A} folds. Open to close, upright to steeply inclined variably plunging folds in quartz and pegmatite veins. Orientation of fold axes varies between N and E or S and W.	S ₁	L _{1B}
D ₃	F ₂	Open to close, upright to steeply inclined steeply plunging folds. Orientation of fold axes approximately NW or SE.	S ₂	L ₂

inclined folds with a gentle plunge between north and east (Plate V.11). An axial plane metamorphic foliation is associated with these F_{1A} folds (biotite grade, greenschist facies). This foliation is now generally parallel to the bedding within the metasediments except in the F_{1A} hinge zones. The orientation of $S_0=S_1$ is sub-vertical with a variable strike due to the later F_2 folds but a mean strike of north-east (Figure V.6A). The orientation of the F_{1A} folds is shown in Figure V.6B. Segregation and intrusion of numerous quartz veins and the intrusion of several granite pegmatite and tourmaline granite sheets occurred between the first and second deformations. The quartz veins have been folded or boudinaged (depending upon their initial orientation with respect to the D_2 strain ellipsoid) by the second episode of deformation (Plates V.11 & V.12) whilst the granite pegmatite and tourmaline granite sheets have suffered boudinage and mild cataclasis (Figure II.8 and Plate III.22). During D_2 the F_{1A} folds were flattened and tightened to their present form whilst F_{1B} folds were developed in the quartz veins and one thin pegmatite vein (Plate V.12c). The quartz veins and the thin pegmatite vein are oblique to S_1 and yet S_1 has an axial plane relationship with the F_{1B} folds. The plunge of the F_{1B} folds is variable in amount and either north-east or south-west (depending upon their initial orientation with respect to the D_2 strain ellipsoid). The third episode of deformation recognized within the Brioverian metasediments produced a set of open to close, upright folds with an associated axial plane crenulation cleavage (Plate V.13) which is sub-vertical and strikes north-west (Figure V.6C).

Plate V.11

- a: F_{1A} fold in Brioverian supracrustal rocks with axial plane S_1 foliation (1/16).
Pnte de Tiqueras, north of Plage de Quatre Vaux.
- b: F_{1A} fold in Brioverian supracrustal rocks with axial plane S_1 foliation and F_{1B} fold in quartz vein also with axial plane S_1 foliation (17/13).
Between pnte de Tiqueras and Plage de Quatre Vaux.
- c: F_{1A} folds in Brioverian supracrustal rocks with axial plane S_1 foliation and quartz vein boudinaged during F_{1B} flattening deformation (24/28).
Between pnte de Tiqueras and Plage de Quatre Vaux.

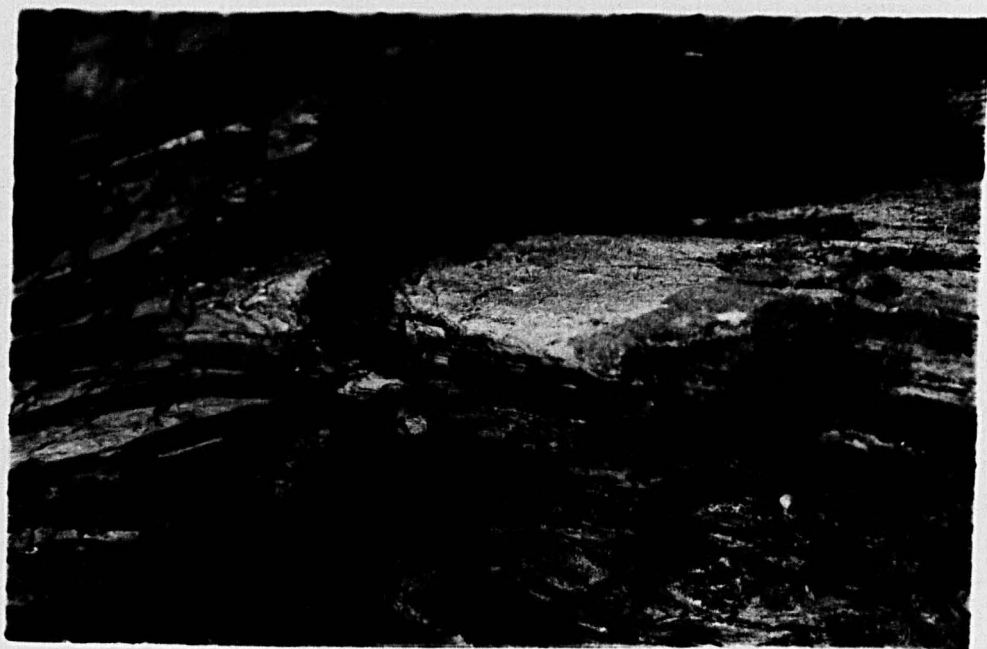


Plate V.12

a: F_{1A} folds in Brioverian supracrustal rocks with axial plane S_1 foliation and quartz vein boudinages during the D_2 flattening event (24/27).

Between pnte de Tiqueras and Plage de Quatre Vaux.

b: F_{1B} folds in quartz veins and D_2 boudinage of quartz veins. Contraction or extension of the quartz veins depends upon their initial orientation with respect to the strain ellipsoid (24/30).

Between pnte de Tiqueras and Plage de Quatre Vaux.

c: F_{1B} folds in pegmatite vein with axial plane fracture cleavage. The pegmatite vein is later than the quartz veins (20/16).

Pnte de Tiqueras, north of Plage de Quatre Vaux.

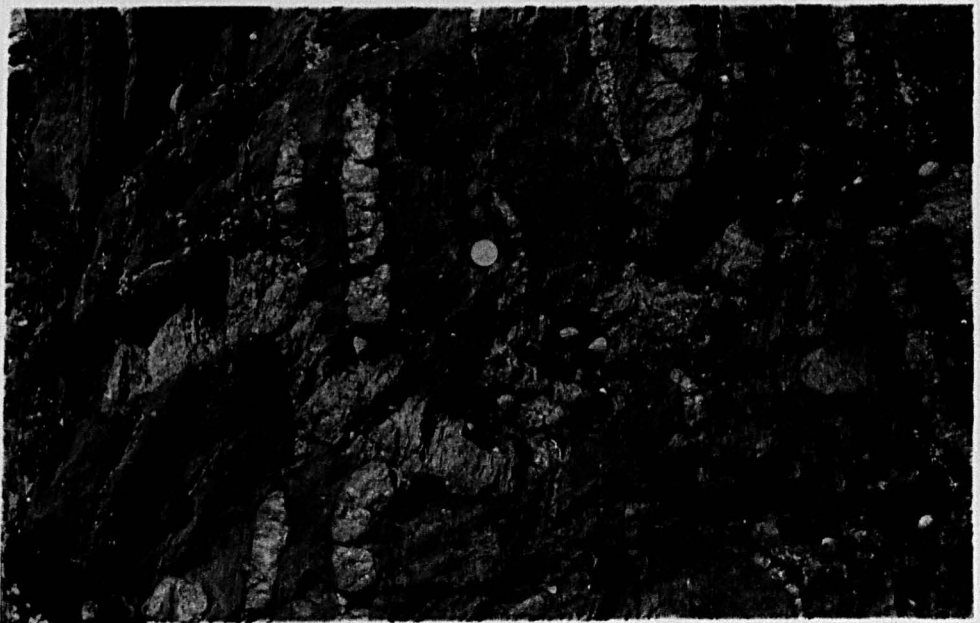


Plate V.13

a: F_{1A} folds in Brioverian supracrustal rocks, F_{1B} folds in quartz veins and F_2 folds in both the Brioverian and the quartz veins (1/17).

Pnte de Tiqueras, north of Plage de Quatre Vaux.

b: F_2 folds in Brioverian supracrustal rocks and quartz veins with axial plane S_2 crenulation foliation (17/36).

Pnte de Tiqueras, north of Plage de Quatre Vaux.

c: Coarse S_2 crenulations in Brioverian supracrustal rocks (7/21).

North-western side of Plage de Quatre Vaux.

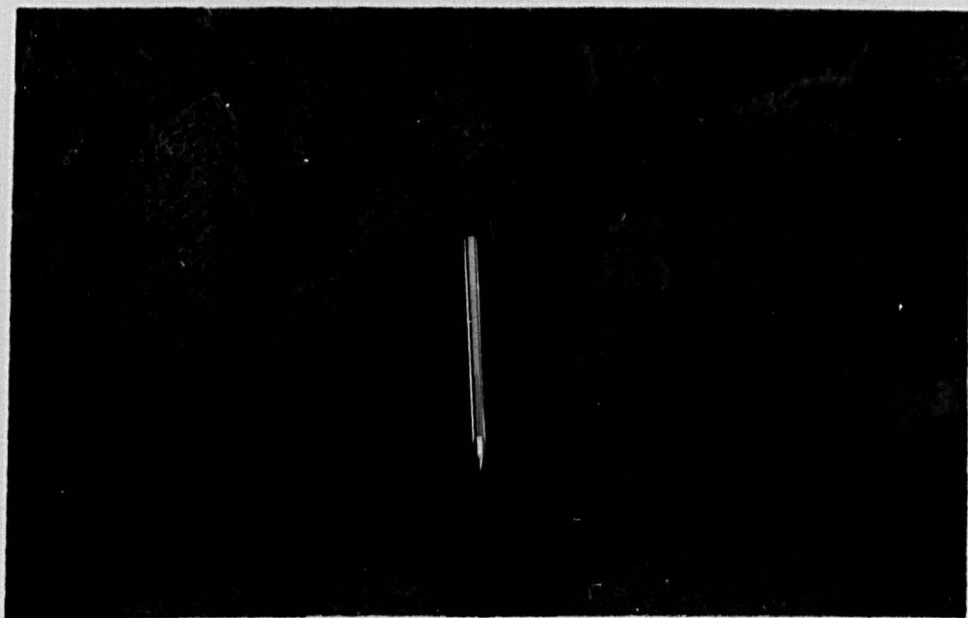
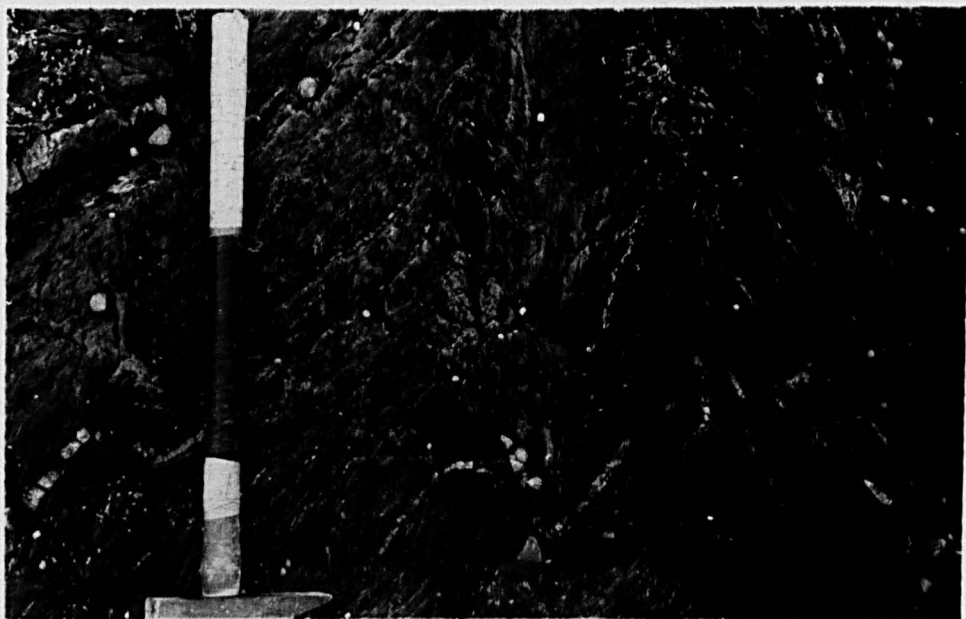
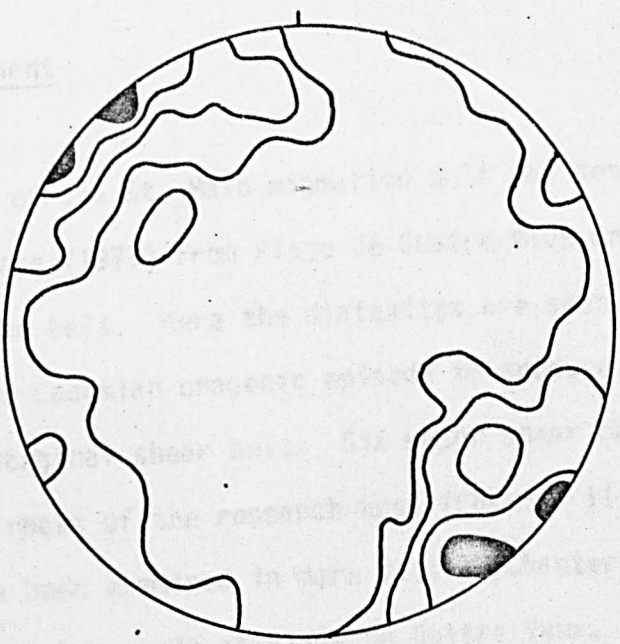


Figure V.6

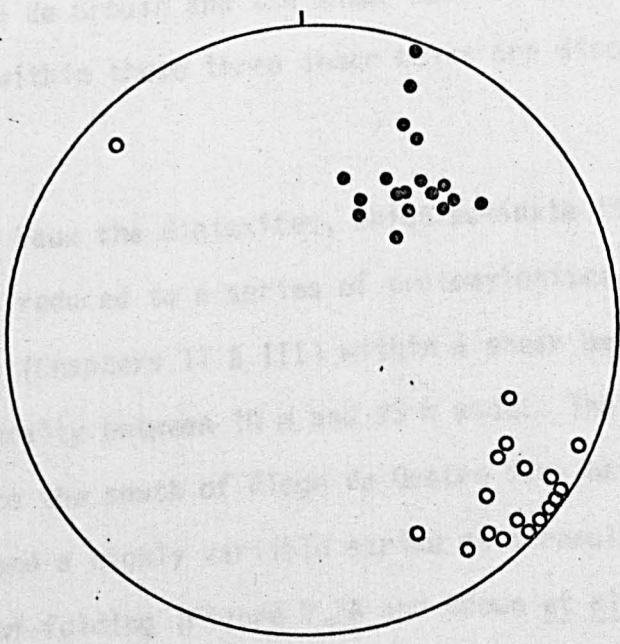
- A. Orientation diagram for the Brioverian supracrustal rocks between Plage de Quatre Vaux and Plage de Pen Guen; 152 poles to $S_0=S_1$. Contours at 8%, 5%, 2% and 0.67% per 1% area, equal area projection from the lower hemisphere.
- B. Orientation diagram for F_{1A} folds from the Brioverian supracrustal rocks between Plage de Quatre Vaux and Plage de Pen Guen. Open circles represent poles to fold axial planes and solid circles represent fold hinge lines.
- C. Orientation diagram for the Brioverian supracrustal rocks between Plage de Quatre Vaux and Plage de Pen Guen; 19 poles to S_2 .

2. The Pentavrian Belt

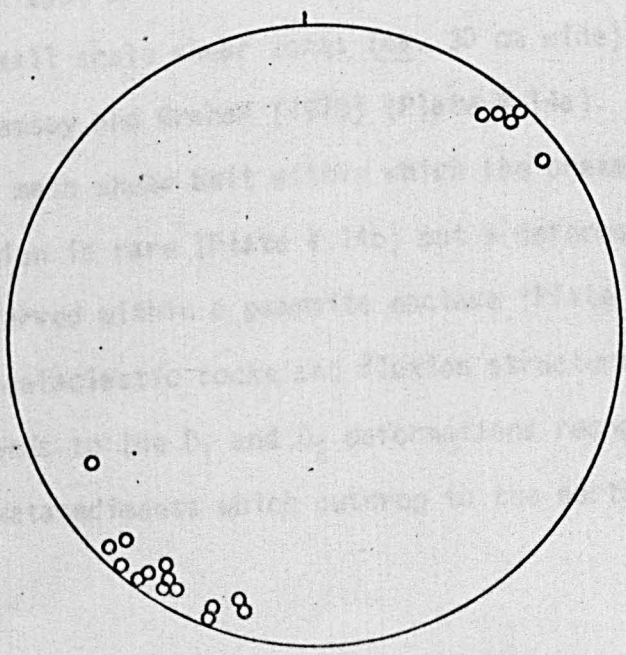
The Pentavrian age is described by Brown, Barber and ... north-western side of ... been deformed during ... of sylvanites with ... through the Pentavrian ... and three of these ... p. 111, 15). They are the ...



belt to the west of ... The structures within ... below.



At Place de ... to the south, have ... and rare ... within the ... moderately ... pre-Columbian ...



At the base of the ... distances are out of ... to those described by ... give way ... of the ... structure ... The development of the ... the ... with the ...

2. The Pentevrian Basement

The Pentevrian age of the St. Malo migmatite belt was demonstrated by Brown, Barber and Roach (1971) from Plage de Quatre Vaux on the north-western side of the belt. Here the diatexites are seen to have been deformed during the Cadomian orogenic episode to produce a series of mylonites within a marginal shear belt. Six major shear belts cut through the Pentevrian rocks of the research area (Chapter II, p.II.24) and three of these have been examined in more detail (Chapter III, p.III.15). They are the shear belt at Plage de Quatre Vaux, the shear belt to the west of pnte de Grouin and the shear belt at pnte de la Garde. The structures within these three shear belts are discussed below.

At Plage de Quatre Vaux the diatexites, which dominate the cliffs to the south, have been reduced to a series of protomylonites, mylonites and rare ultramylonites (Chapters II & III) within a shear belt of variable width but generally between 10 m and 25 m wide. The foliation within the diatexites to the south of Plage de Quatre Vaux has a moderate to steep dip and a highly variable strike as a result of the pre-Cadomian F_4 phase of folding (Figure V.7A and Brown et al, op.cit.). At the back of the south-east end of the Plage de Quatre Vaux the diatexites are cut by small scale shear zones (ca. 30 cm wide) similar to those described by Ramsay and Graham (1970) (Plate V.14a). These give way rapidly to the main shear belt within which the preservation of the diatexite foliation is rare (Plate V.14b) but a deformed linear structure has been preserved within a psammite enclave (Plate V.14c). The development of the cataclastic rocks and fluxion structure within the shear belt corresponds to the D_1 and D_2 deformations recognised within the Brioverian metasediments which outcrop to the north of Plage

Plate V.14

- a: Transposive cataclastic fluxion structure in protomylonite. The migmatitic foliation apparent on the right is destroyed by the cataclasis which has produced the S_1 (Cadomian) foliation on the left (24/36).
South-eastern side of Plage de Quatre Vaux.
- b: The S_1 (Cadomian) cataclastic fluxion structure (24/31).
South-eastern side of Plage de Quatre Vaux.
- c: Deformed linear structure in preserved psammitic enclave within protomylonites (16/22).
South-eastern side of Plage de Quatre Vaux.

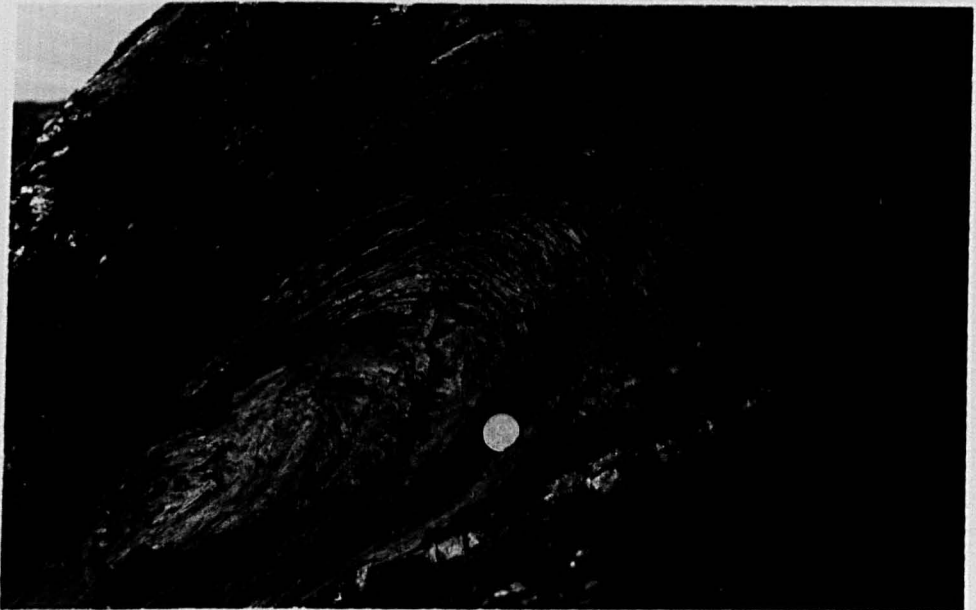
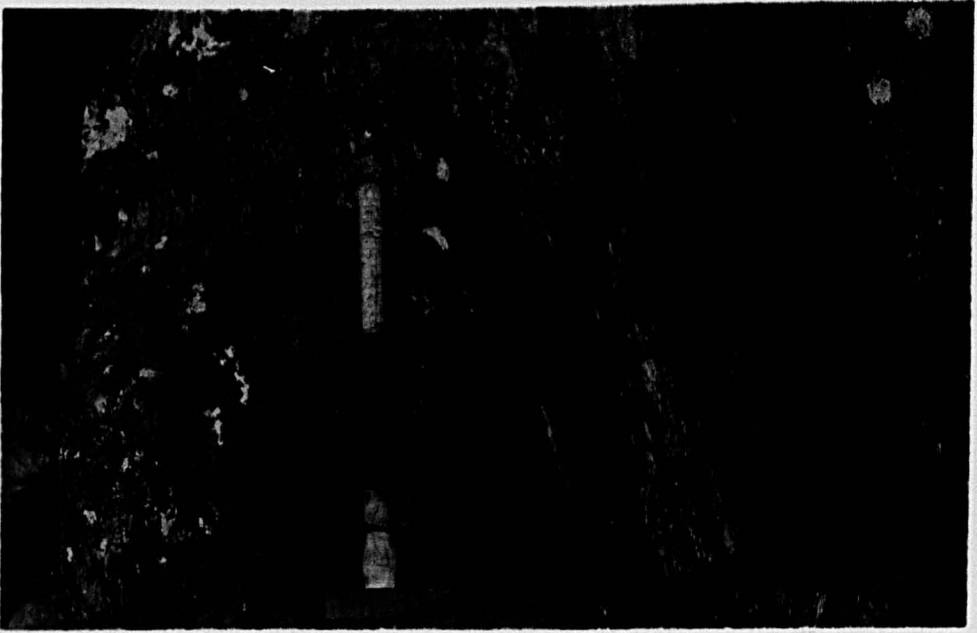
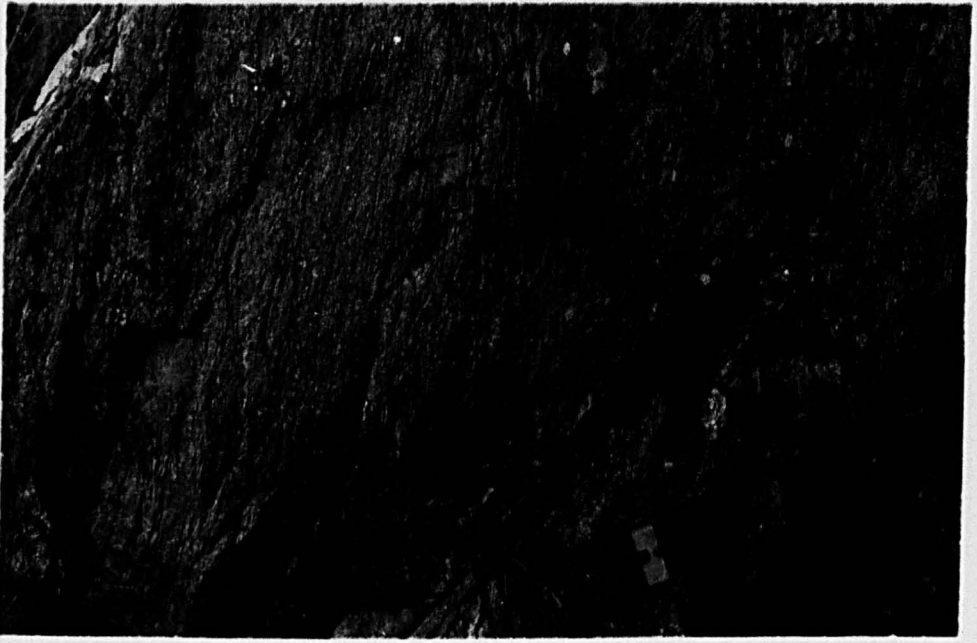
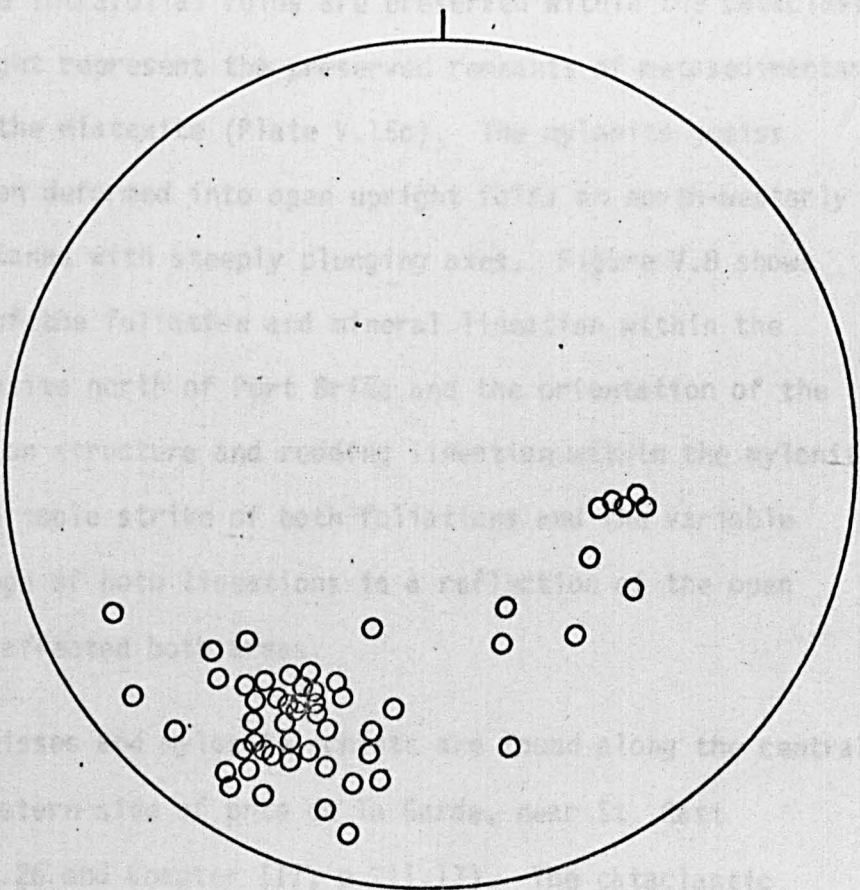
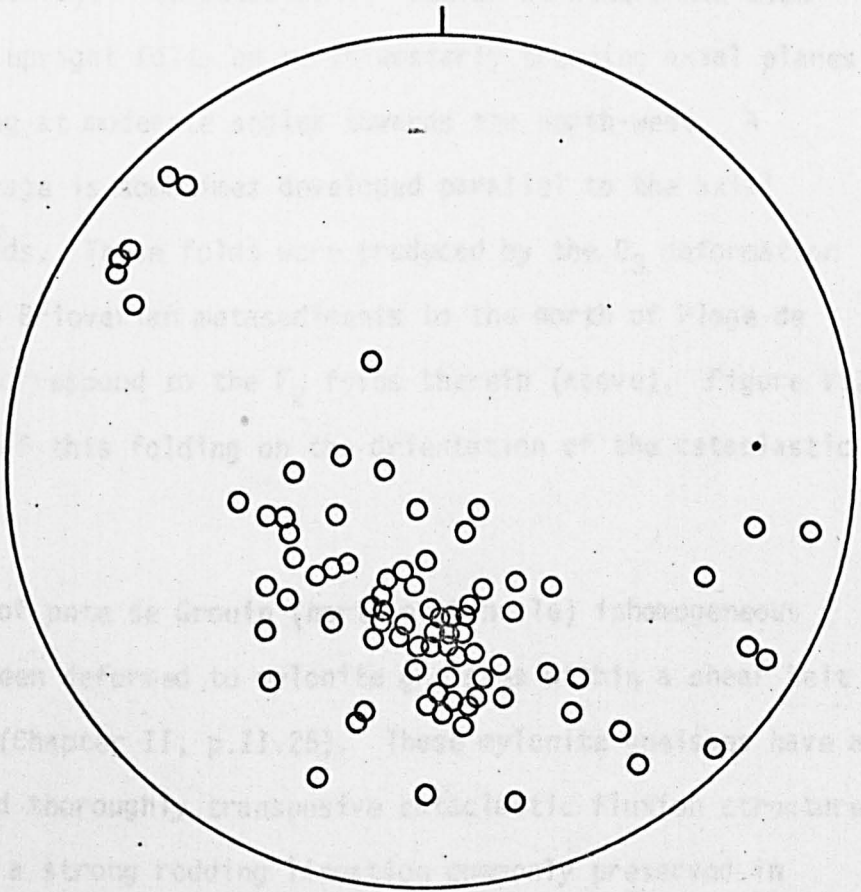


Figure V.7

- A. Orientation diagram for the inhomogeneous diatexites between le Guildo and Plage de Quatre Vaux; 82 poles to diatexite foliation.

- B. Orientation diagram for the protomylonites and mylonites south of Plage de Quatre Vaux; 55 poles to cataclastic fluxion structure.



de Quatre Vaux (above). The cataclastic fluxion structure has been affected by open upright folds on north-westerly trending axial planes with axes plunging at moderate angles towards the north-west. A crenulation cleavage is sometimes developed parallel to the axial planes of the folds. These folds were produced by the D_3 deformation recognized in the Brioverian metasediments to the north of Plage de Quatre Vaux and correspond to the F_2 folds therein (above). Figure V.7B shows the effect of this folding on the orientation of the cataclastic fluxion structure.

To the west of pnte de Grouin (north of Cancale) inhomogeneous diatexites have been deformed to mylonite gneisses within a shear belt about 500 m wide (Chapter II, p.II.25). These mylonite gneisses have a well developed and thoroughly transposive cataclastic fluxion structure (Plate V.15a) and a strong rodding lineation commonly preserved in quartz veins (Plate V.15b) suggesting movement of fluid within the shear belt. Rare intrafolial folds are preserved within the cataclastic foliation and might represent the preserved remnants of metasedimentary enclaves within the diatexite (Plate V.15c). The mylonite gneiss foliation has been deformed into open upright folds on north-westerly trending axial planes with steeply plunging axes. Figure V.8 shows the orientation of the foliation and mineral lineation within the homogeneous diatexite north of Port Briac and the orientation of the cataclastic fluxion structure and rodding lineation within the mylonite gneisses. The variable strike of both foliations and the variable direction of plunge of both lineations is a reflection of the open folding that has affected both areas.

Mylonite gneisses and mylonite schists are found along the central part and north-western side of pnte de la Garde, near St. Cast (Chapter II, p.II.26 and Chapter III, p.III.17). The cataclastic

Plate V.15

a: Cataclastic fluxion structure within mylonite gneisses
(21/35).

West of pnte de Grouin, near Cancale.

b: Strong rodding lineation within mylonite gneisses
(21/36).

West of pnte de Grouin, near Cancale.

c: Intrafolial fold within mylonite gneisses (12/16).

West of pnte de Grouin, near Cancale.

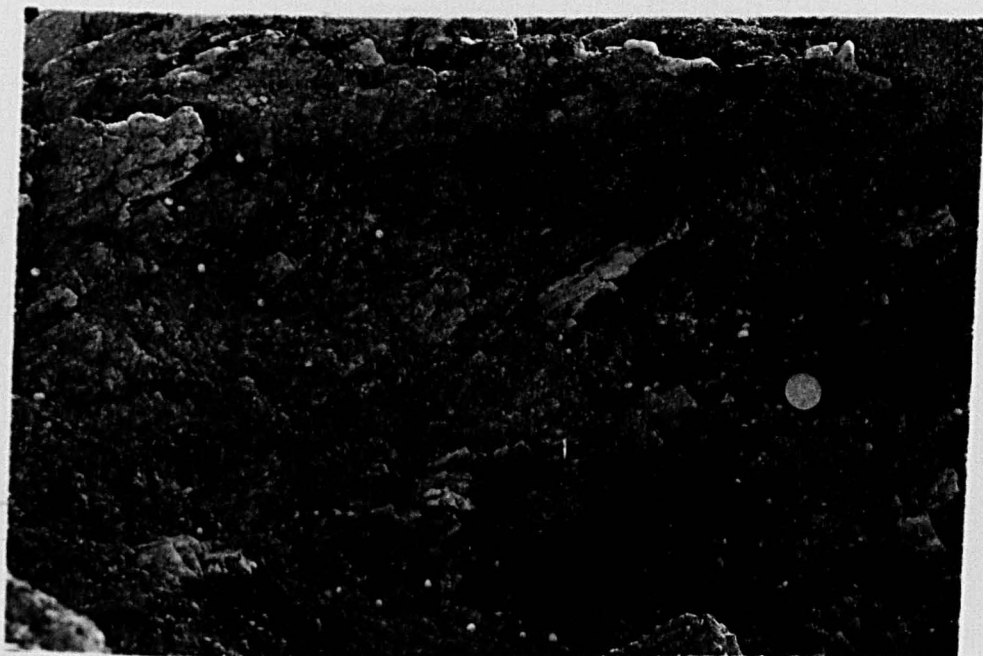
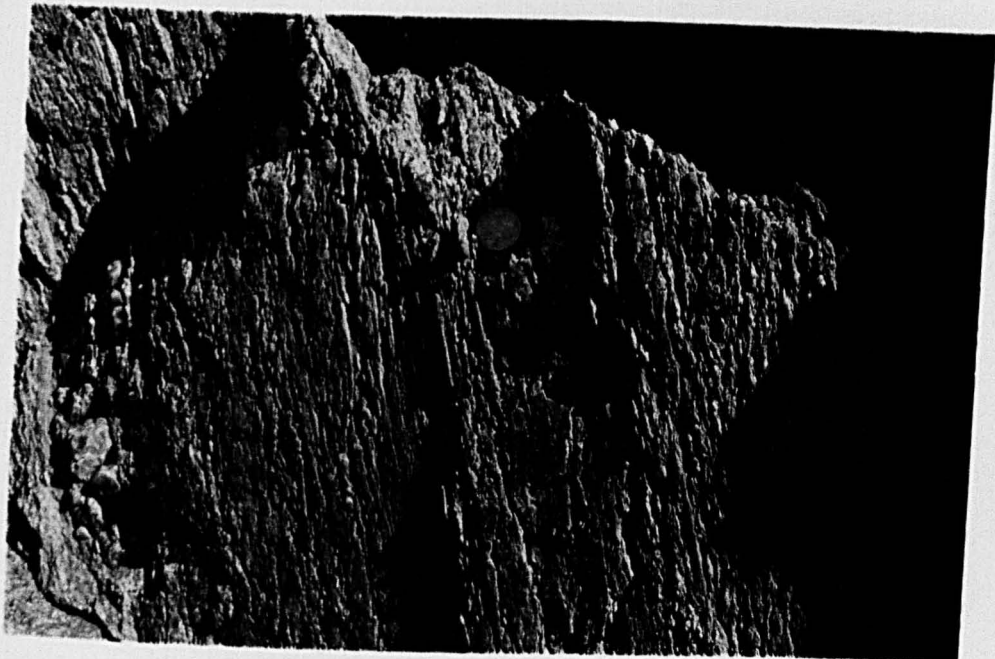
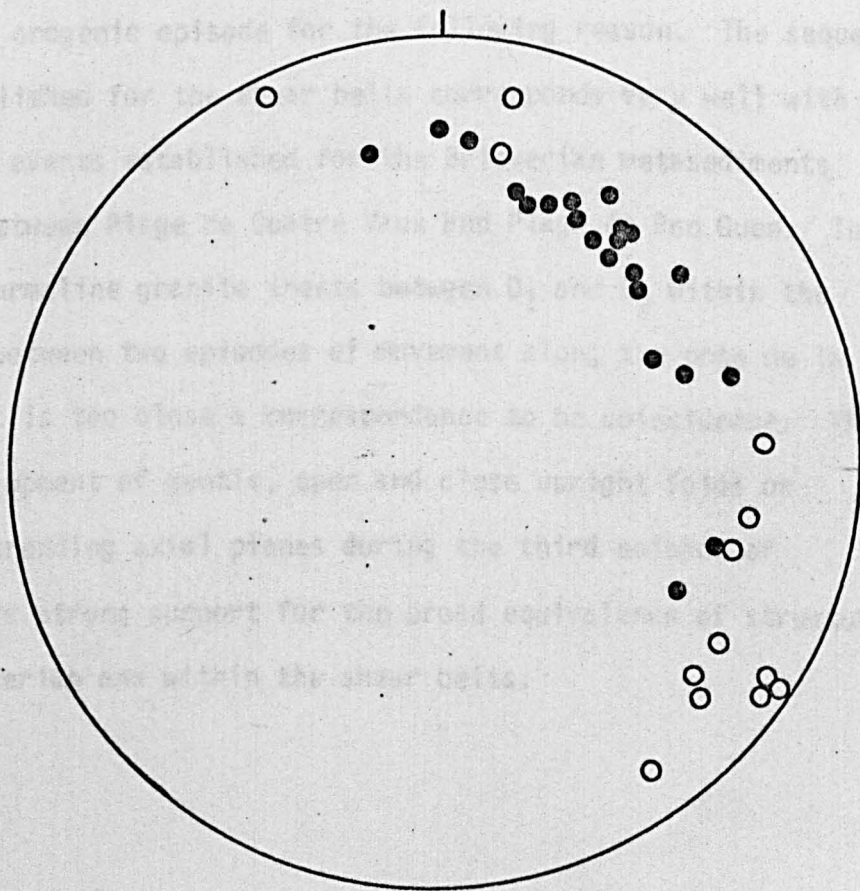
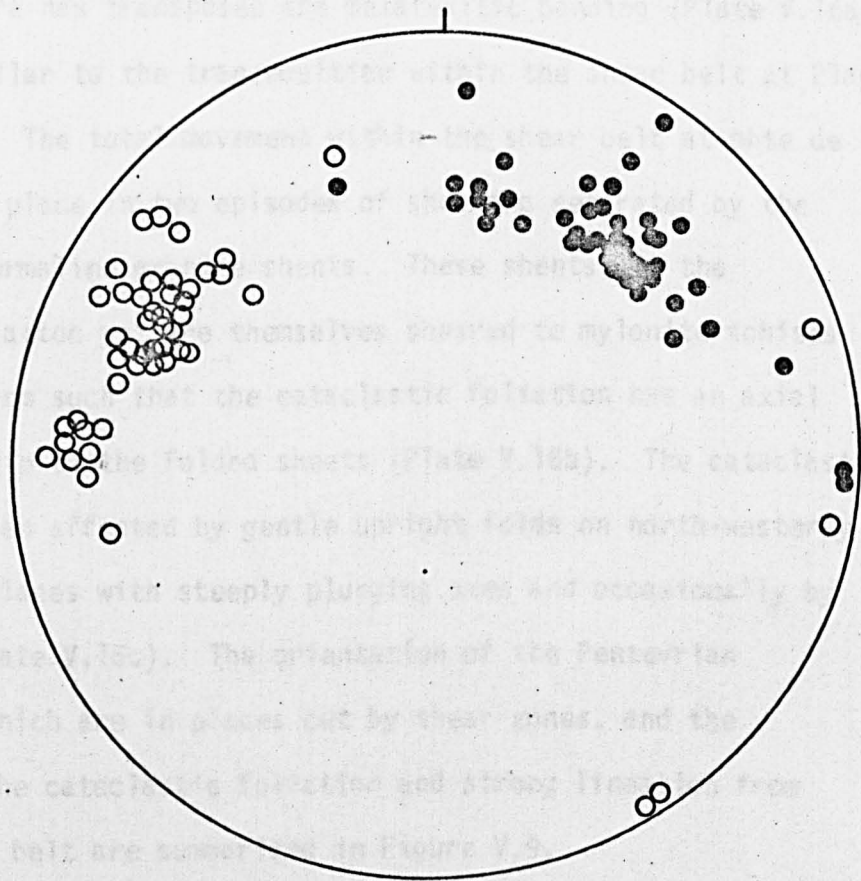


Figure V.8

- A. Orientation diagram for the homogeneous diatexites north of Port Briac, north of Cancale. Open circles represent poles to foliation and solid circles represent mineral lineations.

- B. Orientation diagram for the sheared inhomogeneous diatexite west of pnte de Grouin, north of Cancale. Open circles represent poles to the cataclastic fluxion structure and solid circles represent rodding lineations.



fluxion structure has transposed the metatexitic banding (Plate V.16a) in a manner similar to the transposition within the shear belt at Plage de Quatre Vaux. The total movement within the shear belt at pnte de la Garde has taken place in two episodes of shearing separated by the intrusion of tourmaline granite sheets. These sheets cut the cataclastic foliation yet are themselves sheared to mylonite schists with a folded form such that the cataclastic foliation has an axial plane relationship to the folded sheets (Plate V.16b). The cataclastic foliation has been affected by gentle upright folds on north-westerly trending axial planes with steeply plunging axes and occasionally by kink folding (Plate V.16c). The orientation of the Pentevrian metasediments, which are in places cut by shear zones, and the orientation of the cataclastic foliation and strong lineation from within the shear belt are summarized in Figure V.9.

The shear belts within the Pentevrian basement have been attributed to the Cadomian orogenic episode for the following reason. The sequence of events established for the shear belts corresponds very well with the sequence of events established for the Brioverian metasediments which outcrop between Plage de Quatre Vaux and Plage de Pen Guen. The intrusion of tourmaline granite sheets between D_1 and D_2 within the Brioverian and between two episodes of movement along the pnte de la Garde shear belt is too close a correspondence to be coincidence. The ubiquitous development of gentle, open and close upright folds on north-westerly trending axial planes during the third episode of deformation lends strong support for the broad equivalence of structures within the Brioverian and within the shear belts.

Plate V.16

- a: Folded metatextitic banding transposed by the cataclastic fluxion structure in mylonite gneisses (23/16).
South-eastern side of pnte de la Garde, near St. Cast.
- b: Cataclastic fluxion structure in mylonite schists. Note the deformed tourmaline granite sheet (20/13).
South-eastern side of pnte de la Garde, near St. Cast.
- c: Kink bands deforming the cataclastic fluxion structure (23/32).
South-eastern side of pnte de la Garde, near St. Cast.

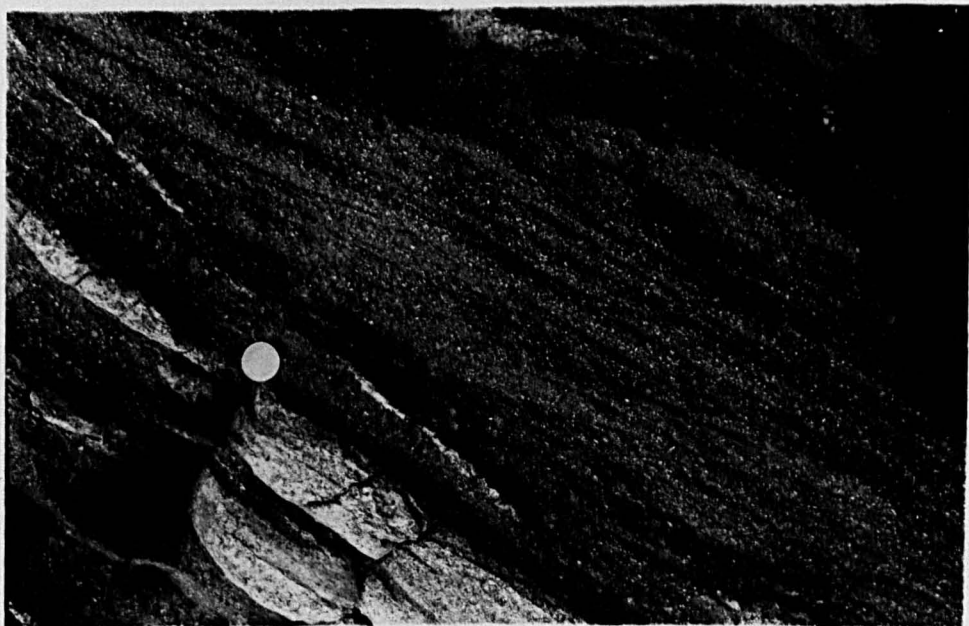
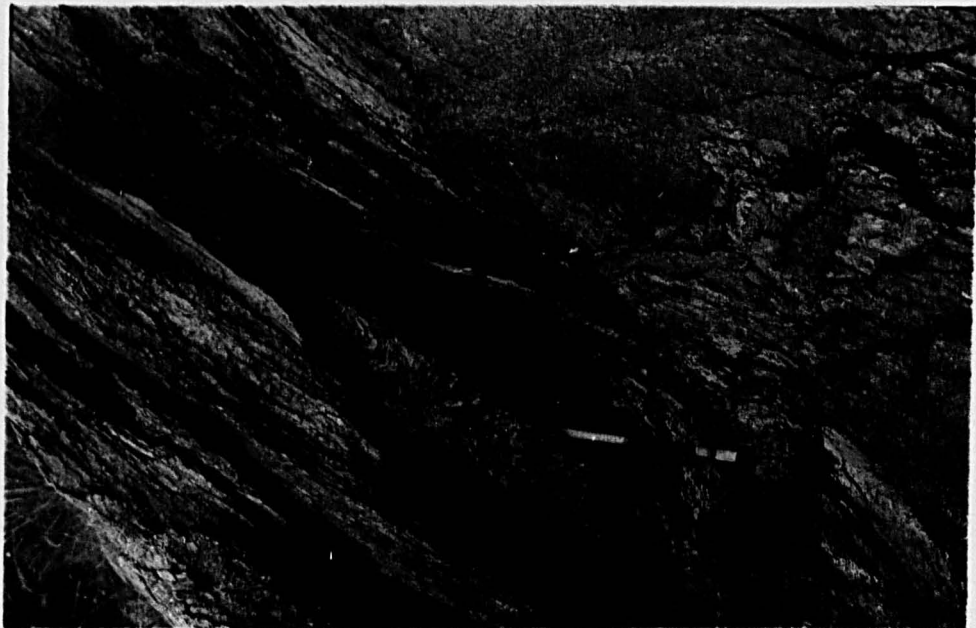
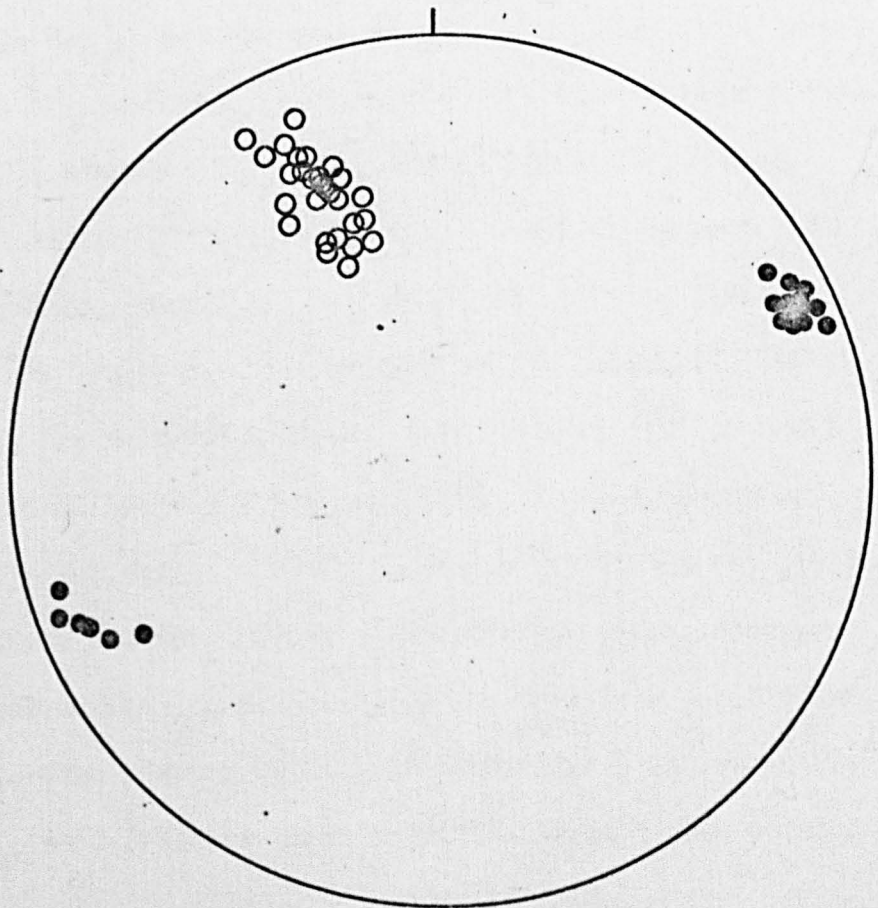
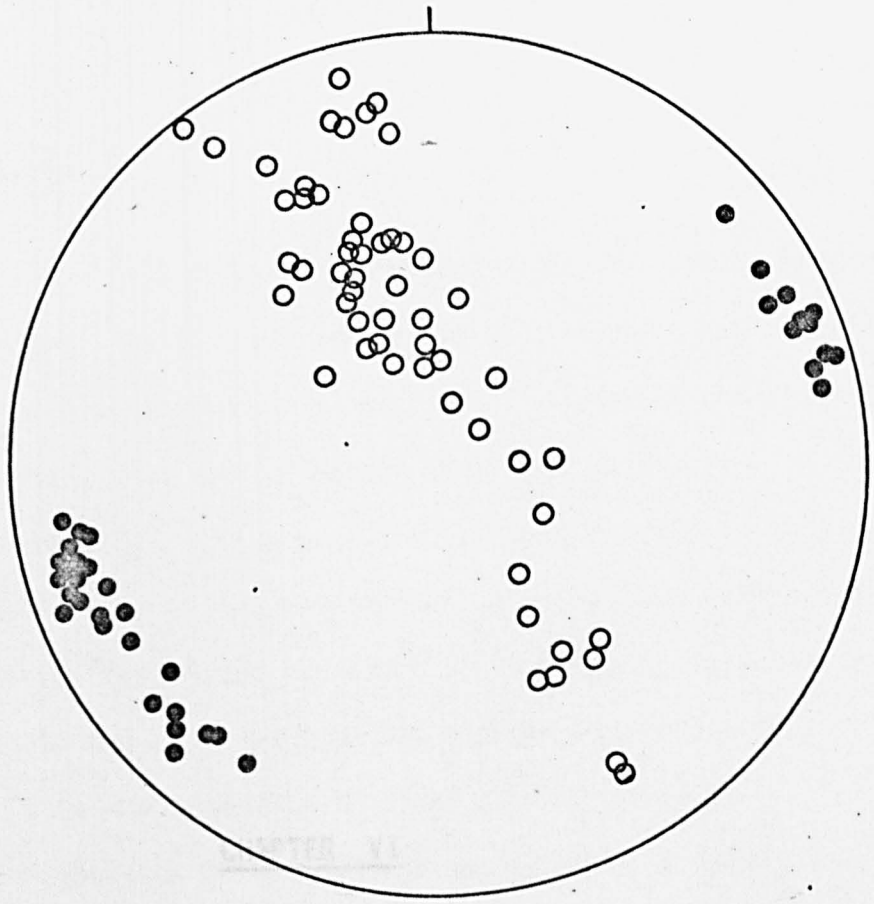


Figure V.9

- A. Orientation diagram for the Pentevrian metasediments which outcrop on the south-eastern side of pnte de la Garde. Open circles represent poles to $S_0=S_1$ and solid circles represent lineations (L_2 , L_3 and L_4).
- B. Orientation diagram for the mylonite gneisses and mylonite schists of the pnte de la Garde shear belt. Open circles represent poles to the cataclastic fluxion structure and solid circles the lineations.



Introductory Statement

Field relationships between the metasediments, the metatexites and the diatexites within the St. Malo migmatite belt suggest mobilization of material, extensive anatexis and intrusion of magma (Chapter II). Textures in the diatexites are in accord with crystal-liquid equilibria (Chapter III). The presence of sillimanite within the schistose palaeosome of the metatexites and muscovites within the inhomogeneous diatexites argues for conditions of temperature and load pressure similar to the upper part of the amphibolite facies of metamorphism. It is now generally accepted that granulites of metasediments and gneisses developed as a consequence of burial under conditions of temperature and load pressure similar to the upper part of the amphibolite facies providing that a fluid phase is present (although P_{fluid} may be less than P_{total} and a solid phase is present (mica or amphibole), for example: Stüwe and Buser (1968); Von Platen (1965); Kleemann (1965); Von Platen and Richter (1966); Lundgren (1966); White (1966); Winkler (1966); Plattner (1966); Weill and Kudo (1968); Sharma (1969); Ghent and Swanson (1969); Fyfe (1970 & 1973); Brown and Fyfe (1971); Fyfe (1971); Tobi (1971); Plattner (1971); Sisson (1972); Mader and Sisson (1972); Drury (1973); Huang and Fyfe (1973); Fyfe and Sisson (1973); Sisson, Busch and Schneider (1973); Fyfe and Sisson (1974); Harris (1974a & b); and Leonardos and Fyfe (1974). Fyfe (1971) considers that "assemblages containing quartz, sillimanite and K-feldspar could undergo initial H_2O saturated melting with the formation of melt at temperatures as low as 650°C at $P_{H_2O} = P_{total}$ of 3.5 kb. or lower pressures at higher pressures".

CHAPTER VI

The St. Malo Rocks and the Petrogenesis

Introductory Statement

Field relationships between the metasediments, the metatexites and the diatexites within the St. Malo migmatite belt suggest mobilization of material, extensive anatexis and intrusion of material (Chapter II). Textures in the diatexites are in accord with crystal-liquid equilibria (Chapter III). The presence of prismatic sillimanite within the schistose palaeosome of the metatexites and sometimes within the inhomogeneous diatexites argues for conditions of temperature and load pressure similar to the upper part of the amphibolite facies of metamorphism. It is now generally accepted that anatexis of metasediments and gneisses of appropriate composition is likely under conditions of temperature and load pressure attributed to the upper part of the amphibolite facies providing that either a fluid phase is present (although P_{fluid} may be less than P_{load}) or a hydrated phase is present (mica or amphibole), for example: Tuttle and Bowen (1958); Von Platen (1965); Kleeman (1965); Von Platen and Holler (1966); Lundgren (1966); White (1966); Winkler (1967 & 1970); Mehnert (1968); Weill and Kudo (1968); Sharma (1969); James and Hamilton (1969); Fyfe (1970 & 1973); Brown and Fyfe (1970 & 1972); Tobschall (1971); Blattner (1971); Sutton (1972); Winkler and Lindeman (1972); Drury (1973); Huang and Wyllie (1973); Joyce (1973); Mehnert, Busch and Schneider (1973); Rutishauser (1973); Thompson (1974); Harris (1974a & b); and Leonardos and Fyfe (1974). Thompson (op.cit.) considers that "assemblages containing $Ms+Ab+Or+Q$ or $Ab+Or+Sill+Q$ could undergo initial H_2O saturated minimum melting at temperatures as low as $650^{\circ}C$ at $P_{H_2O} = P_{\text{total}}$ of 3.5 kb, or lower temperatures at higher pressures".

The St. Malo Rocks and the System Q-Ab-Or-An-H₂O

It is well known that if granitic rocks in which sialic components comprise more than 80% of the norm are plotted on the anhydrous base of the Q-Ab-Or-H₂O tetrahedron then they cluster around the centre of the Q-Ab-Or triangle (Figure VI.1A) and straddle the line joining the experimentally determined quaternary minima (Tuttle and Bowen, 1958) and eutectics (Luth, Jahns and Tuttle, 1964) for various water vapour pressures in the Q-Ab-Or-H₂O system (compare Figure VI.1A with Figure VI.2A). Similarly, if alumina oversaturated (corundum normative) rocks in which the sialic components comprise more than 80% of the norm are plotted on the anhydrous base of the Q-Ab-Or-H₂O tetrahedron then they cluster around the centre of the Q-Ab-Or triangle (Figure VI.1B and Luth et al, op.cit.) and straddle the line joining the experimentally determined quaternary minima and eutectics for various water vapour pressures in the Q-Ab-Or-H₂O system (compare Figure VI.1B with Figure VI.2A). With the logical extension of experimental investigation into the quinary system Q-Ab-Or-An-H₂O (Von Platen, 1965; Von Platen and Holler, 1966; Winkler, 1967; Weill and Kudo, 1968; and James and Hamilton, 1969) it has become apparent that normative Q-Ab-Or ratios of granites and alumina oversaturated rocks overlap with normative Q-Ab-Or ratios of "minimum melt" compositions in the Q-Ab-Or-An-H₂O system and other experimentally produced anatectic melts (compare Figures VI.1A & B with Figure VI.2B; see Brown and Fyfe, 1970). The St. Malo diatexites are granitic to granodioritic in composition and corundum normative - their normative Q-Ab-Or ratios ought to overlap with the normative Q-Ab-Or ratios of granites, alumina oversaturated rocks and experimentally produced anatectic melts.

In order to compare rock compositions with the results of experimental and theoretical work in the Q-Ab-Or-An-H₂O system (and

Figure VI.1

- A. Solid lines represent contours at >5%, >10% and >15% per 1% area of 507 granitic rocks from Washington (1917). Dotted lines represent, from outer to inner, 86% of all granites, 53% of all granites and 14% of all granites (based upon 1190 granite compositions - from Winkler, 1967).
- B. Lines represent contours at >5%, >10% and >15% per 1% area of 281 plutonic rocks with normative corundum from Washington (1917).

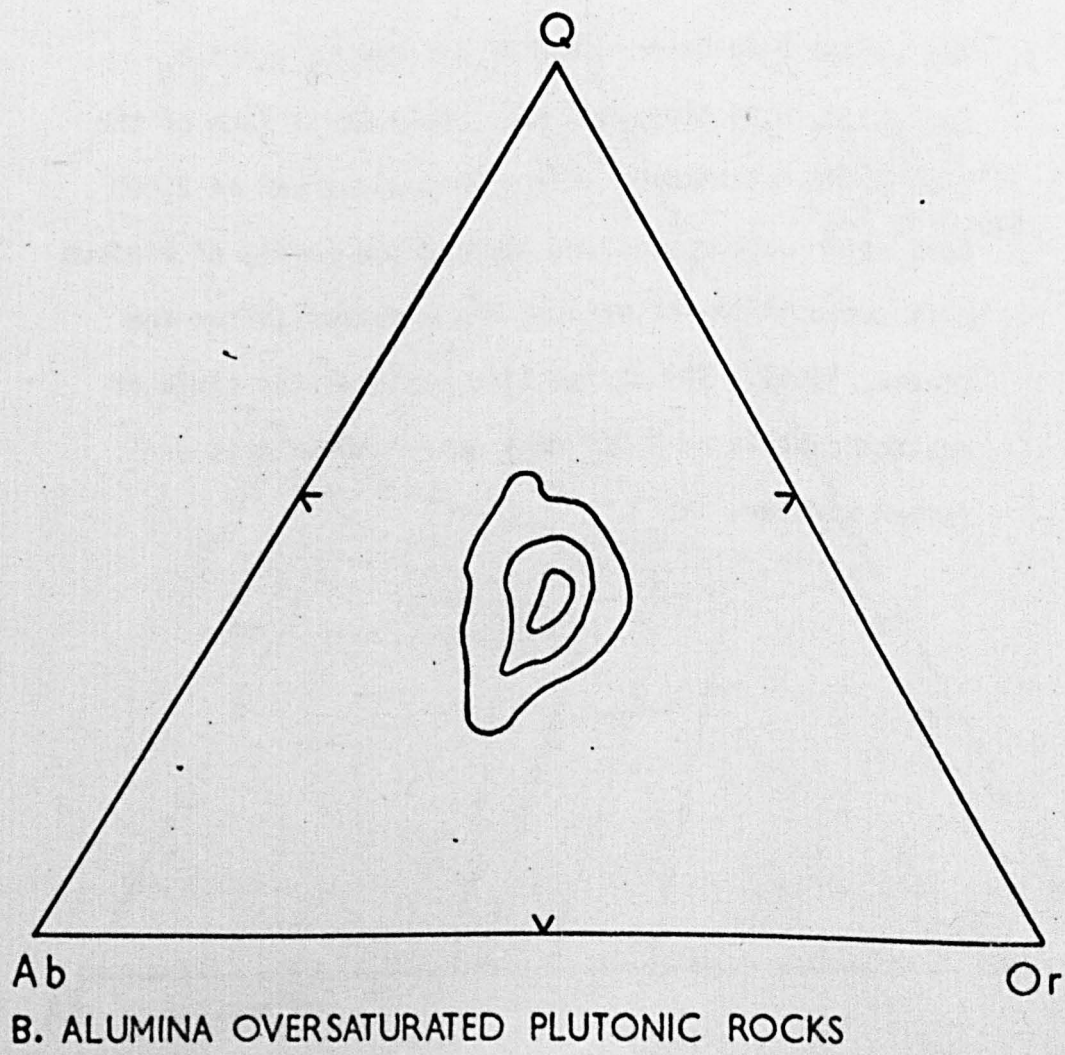
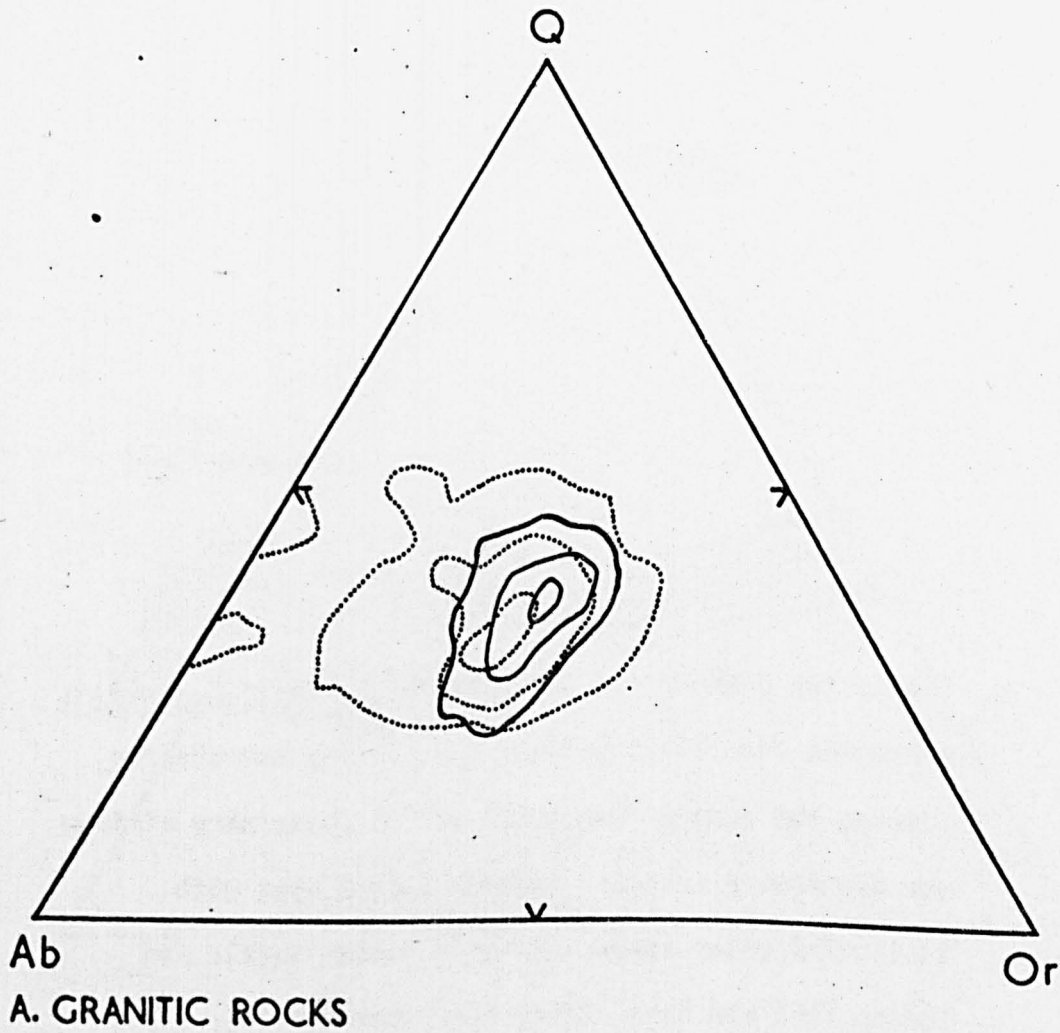
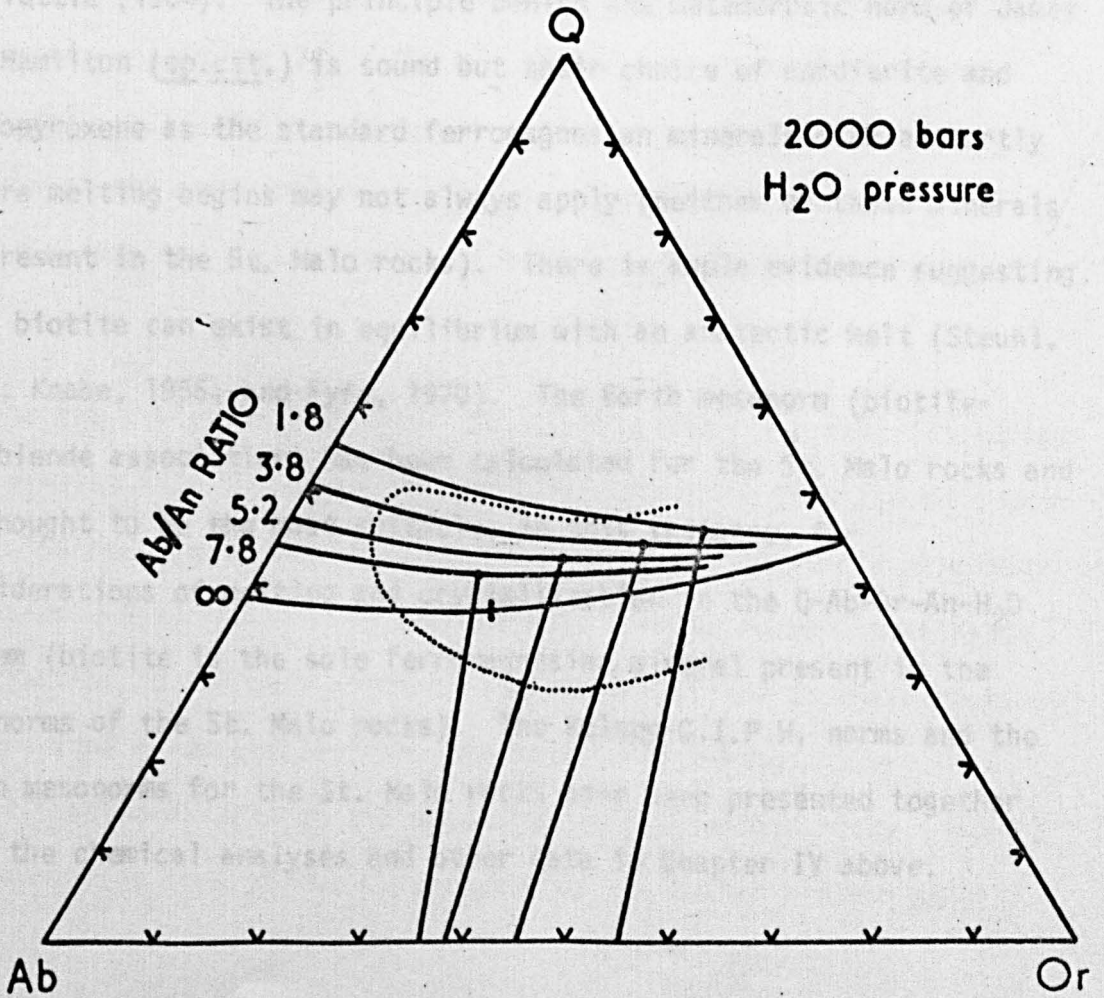
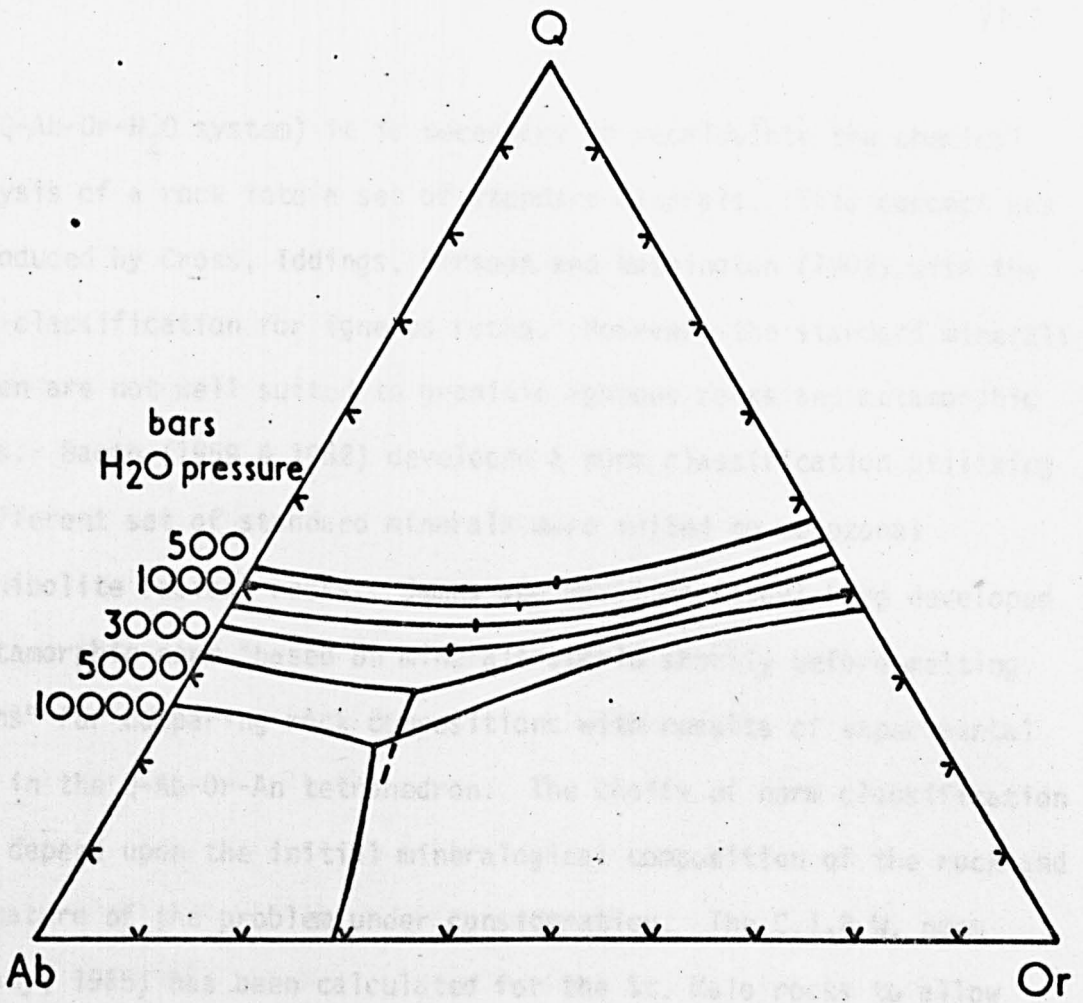


Figure VI.2

- A. The system $Q\text{-Ab-Or-H}_2\text{O}$ ($\text{SiO}_2\text{-NaAlSi}_3\text{O}_8\text{-KAlSi}_3\text{O}_8\text{-H}_2\text{O}$) projected onto the anhydrous base of the tetrahedron showing the progressive shift of the quaternary minimum and quaternary eutectic towards the Ab apex with increasing water vapour pressure (after Tuttle and Bowen, 1958 and Luth, Jahns and Tuttle, 1964).
- B. The system $Q\text{-Ab-Or-An-H}_2\text{O}$ ($\text{SiO}_2\text{-NaAlSi}_3\text{O}_8\text{-KAlSi}_3\text{O}_8\text{-CaAl}_2\text{Si}_2\text{O}_8\text{-H}_2\text{O}$) projected onto the $Q\text{-Ab-Or}$ face of the $Q\text{-Ab-Or-An}$ tetrahedron with excess water and at 2,000 bars water vapour pressure showing the points of minimum melt composition for various Ab/An ratios (after Von Platen, 1965). The dotted line encloses the field of anatectic melts at 2,000 bars water vapour pressure (after Winkler, 1967).



the Q-Ab-Or-H₂O system) it is necessary to recalculate the chemical analysis of a rock into a set of standard minerals. This concept was introduced by Cross, Iddings, Pirsson and Washington (1902) with the norm classification for igneous rocks. However, the standard minerals chosen are not well suited to granitic igneous rocks and metamorphic rocks. Barth (1959 & 1962) developed a norm classification utilizing a different set of standard minerals more suited to mesozonal (amphibolite facies) rocks. James and Hamilton (1969) have developed a metamorphic norm "based on minerals stable shortly before melting begins" for comparing rock compositions with results of experimental work in the Q-Ab-Or-An tetrahedron. The choice of norm classification will depend upon the initial mineralogical composition of the rock and the nature of the problem under consideration. The C.I.P.W. norm (Kelsey, 1965) has been calculated for the St. Malo rocks to allow comparison with the work of Tuttle and Bowen (1958) and Luth, Jahns and Tuttle (1964). The principle behind the metamorphic norm of James and Hamilton (op.cit.) is sound but their choice of cordierite and orthopyroxene as the standard ferromagnesian minerals stable shortly before melting begins may not always apply (neither of these minerals is present in the St. Malo rocks). There is ample evidence suggesting that biotite can exist in equilibrium with an anatectic melt (Steuhl, 1962; Knabe, 1966; and Fyfe, 1970). The Barth mesonorm (biotite-hornblende association) has been calculated for the St. Malo rocks and is thought to be the most suitable, in this instance, for considerations of melting and crystallization in the Q-Ab-Or-An-H₂O system (biotite is the sole ferromagnesian mineral present in the mesonorms of the St. Malo rocks). The Kelsey-C.I.P.W. norms and the Barth mesonorms for the St. Malo rocks have been presented together with the chemical analyses and other data in Chapter IV above.

Experimental and theoretical work in the Q-Ab-Or-An-H₂O system (eg. Von Platen, 1965; Von Platen and Holler, 1966; Kleeman, 1965; Weill and Kudo, 1968; James and Hamilton, 1969; Brown and Fyfe, 1970; Winkler and Lindeman, 1972; and Presnall and Bateman, 1973) has resulted in a better understanding of the origin of migmatites and granites. Most of the authors quoted above are in general agreement about the conclusions which may be drawn from the various studies, although there may be differences in detail. Thus James and Hamilton (op.cit.) compare their results with those obtained by Von Platen (op.cit.) and write "if the differences in working pressure and starting materials are considered, the results of the two studies compare favourably". They suggest that since "at higher water vapour pressures the position of the granite minimum is known to shift towards the Ab apex in the granite system. It is reasonable to expect that the isobaric univariant line in the quaternary system will show a similar trend" (see also Von Platen and Holler, op.cit. who have demonstrated this trend experimentally). The use of the term "eutectic" by Von Platen (op.cit.) and the subsequent criticism by Weill and Kudo (op.cit.) and James and Hamilton (op.cit.) is outside the scope of this discussion and the phrase "point of minimum melt composition" will be used.

For the analysed rocks from the St. Malo migmatite belt (including three samples from the Dinan belt) sialic components comprise more than 80% of the norm (both the Kelsey-C.I.P.W. norm and the Barth mesonorm). The system Q-Ab-Or-An-H₂O may therefore be considered as a reasonable approximation to the bulk chemical composition of the St. Malo rocks and thus provides a reasonable framework to discuss the possible crystallization history of the diatexites and granitoid rocks. Figure VI.3 summarizes some of the experimentally determined minimum melt

compositions in the quinary system and the minima and eutectics in the quaternary system. Figures VI.4 to VI.12 inclusive show the St. Malo rocks plotted in terms of both the C.I.P.W. norm and the mesonorm on the Q-Ab-Or face and the Ab-Or-An face of the vapour saturated Q-Ab-Or-An tetrahedron. Table VI.1 lists the normative Ab/An ratios of the St. Malo rocks. The vapour saturated equilibrium diagram for the system Q-Ab-Or-An-H₂O at 5 kb is given for reference in Figure VI.13.

The normative Q-Ab-Or ratios of the diatexites show a close association with points of minimum melt composition determined experimentally in the Q-Ab-Or-An-H₂O system at 2 kb P_{H₂O} (Von Platen, 1965) and the quaternary minimum in the Q-Ab-Or-H₂O system at 2 kb P_{H₂O} (Tuttle and Bowen, 1958) (Figures VI.4 and VI.5). When the diatexites are projected from Q in the Q-Ab-Or-An tetrahedron onto the Ab-Or-An face together with the isobaric univariant curve at 1 kb P_{H₂O} (ie. the intersection of the two-feldspar surface with the quartz-feldspar surface - James and Hamilton, 1969) they are seen to lie on the plagioclase side of the boundary curve in a zone extending towards the Ab-An side of the ternary feldspar face (Figure VI.6). The water vapour pressure during formation of the diatexites by anatexis is not known. An estimate of the prevailing water vapour pressure, however, may be made from the f_{H₂O} during biotite crystallization or recrystallization (Chapter IV) using the fugacity data of Burnham, Holloway and Davis (1969). The water vapour pressure during crystallization of the diatexites was probably between 2.5 and 5.5 kb. Water vapour pressures in excess of 2 kb would move the points of minimum melt composition determined by Von Platen towards the Ab apex of the Q-Ab-Or face of the Q-Ab-Or-An tetrahedron. Thus the diatexite compositions (mesonorms) lie within the quartz primary phase volume in

Figure VI.3

Summary of some of the results in the Q-Ab-Or-H₂O and Q-Ab-Or-An-H₂O systems. Curves join:

1. The isobaric quaternary minimum at 2 kb P_{H₂O} (Tuttle and Bowen, 1958) and the isobaric quaternary eutectics at 5 kb and 10 kb P_{H₂O} (Luth, Jahns and Tuttle, 1964) for an Ab/An ratio of ∞.
2. The points of minimum melt composition for Ab/An ratios of 7.8, 5.2, 3.8 and 1.8 at 2 kb P_{H₂O} (Von Platen, 1965).
3. The piercing points for Ab/An ratios of 10.4, 4.0 and 1.4 at 1 kb P_{H₂O} (James and Hamilton, 1969).
4. The points of minimum melt composition for a gneiss with an Ab/An ratio of 2.9 at P_{H₂O} of 2, 4, 7 and 10 kb (Von Platen and Holler, 1966).

Q 60%

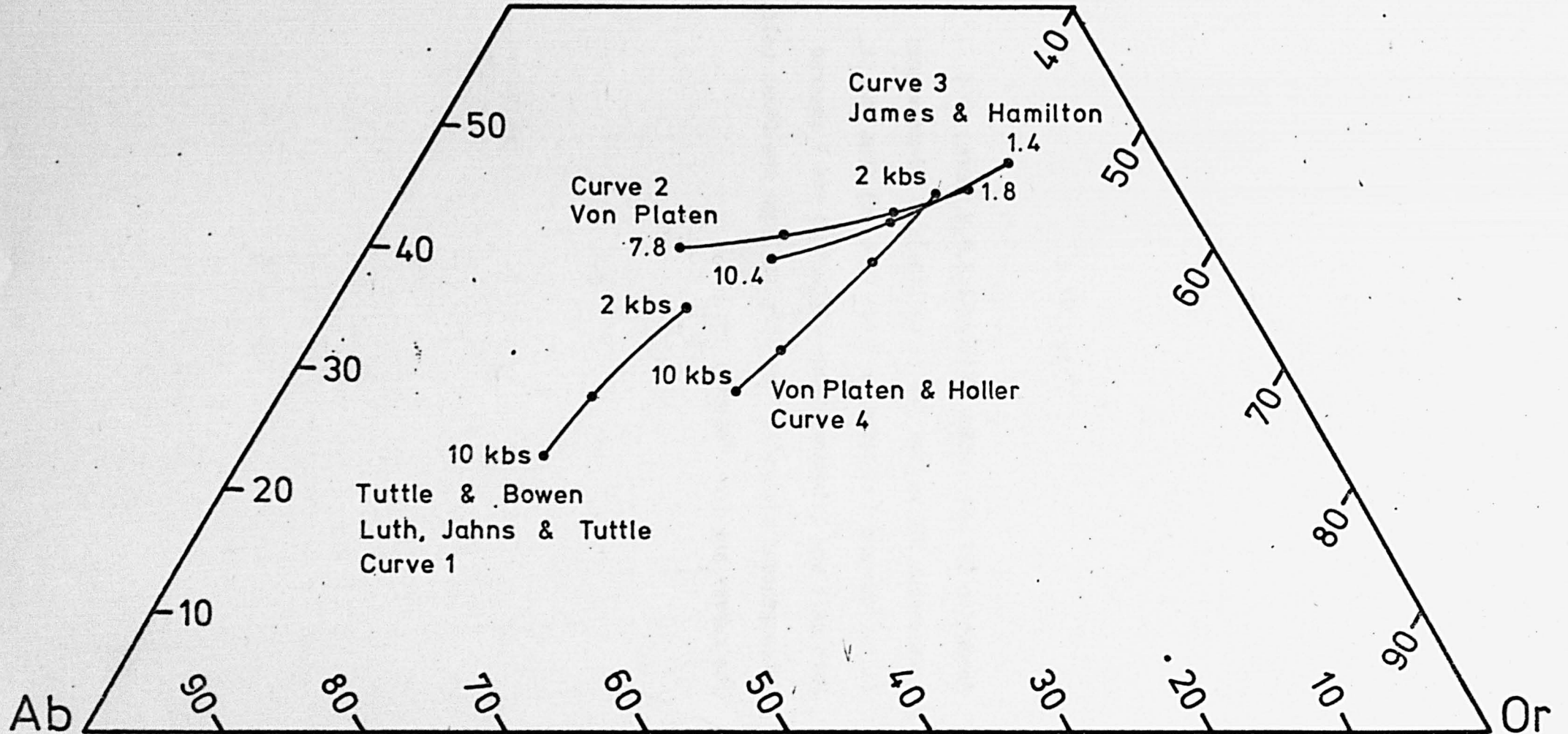
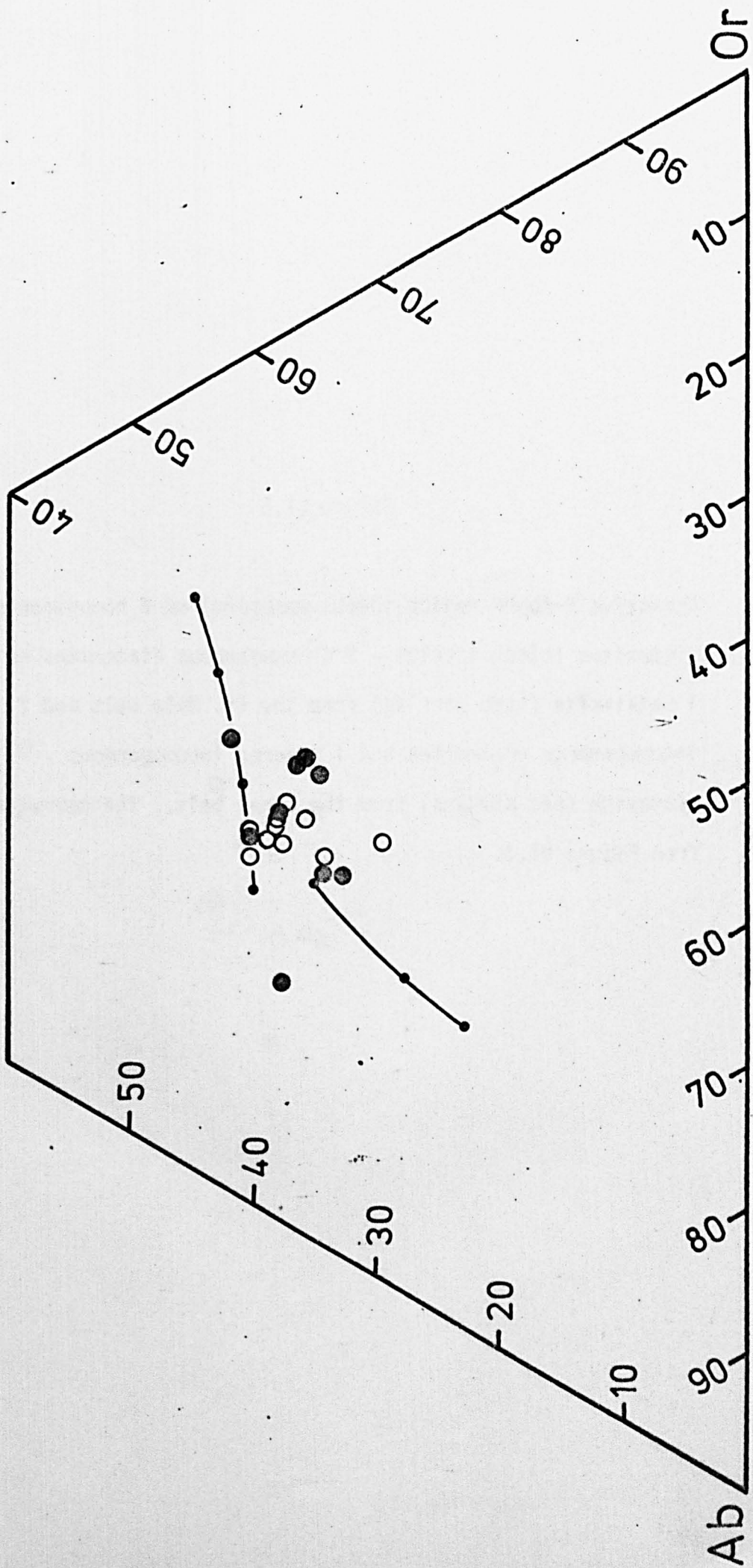


Figure VI.4

Normative Q-Ab-Or ratios (Kelsey-C.I.P.W. norm) of 6 homogeneous diatexites (solid circles), 9 inhomogeneous diatexites and 1 metatexite (open circles) from the St. Malo belt and 2 inhomogeneous diatexites and 1 sheared inhomogeneous diatexite (red circles) from the Dinan belt. The curves are from Figure VI.3.

Q 60%



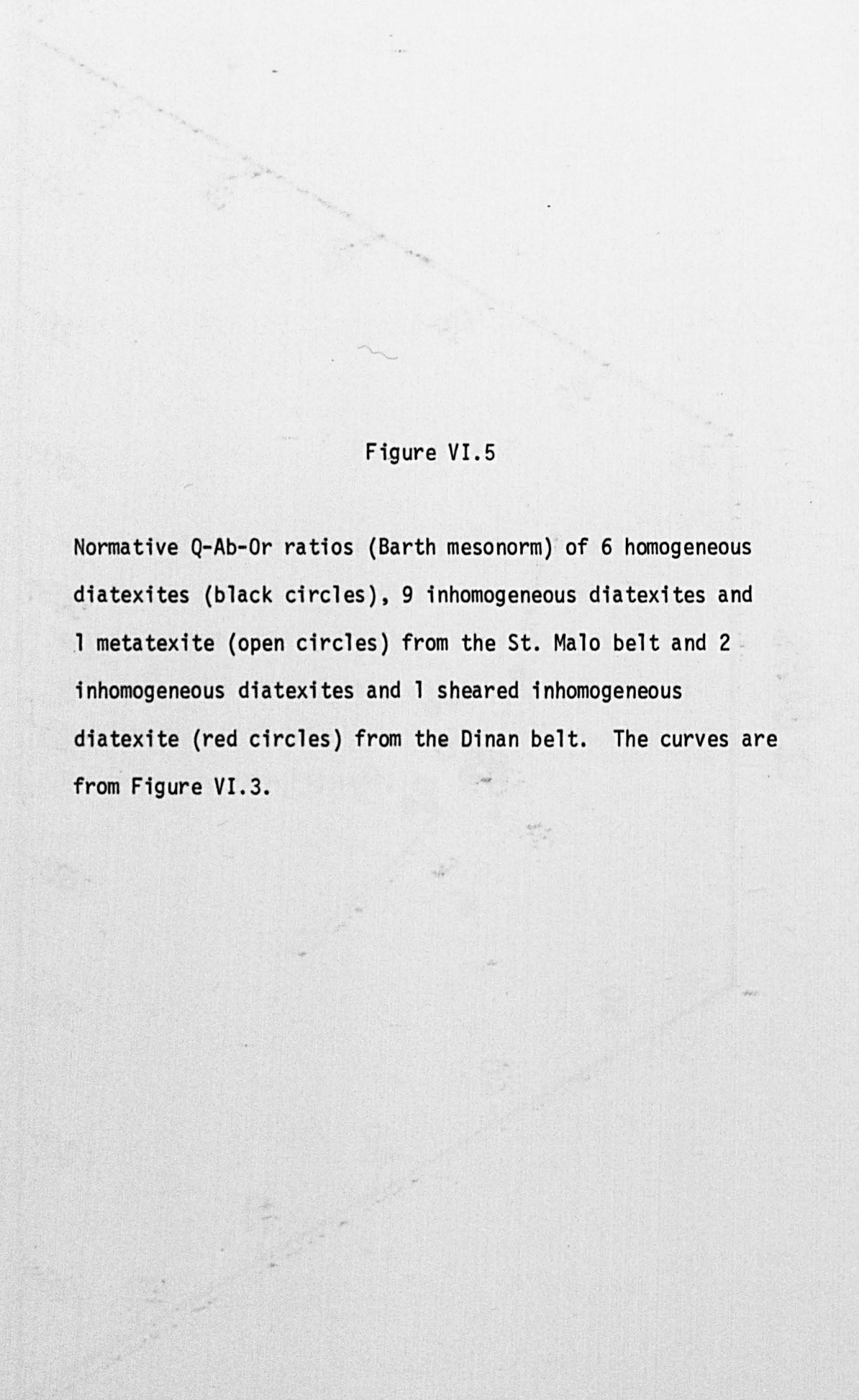


Figure VI.5

Normative Q-Ab-Or ratios (Barth mesonorm) of 6 homogeneous diatexites (black circles), 9 inhomogeneous diatexites and 1 metatexite (open circles) from the St. Malo belt and 2 inhomogeneous diatexites and 1 sheared inhomogeneous diatexite (red circles) from the Dinan belt. The curves are from Figure VI.3.

Q 60%

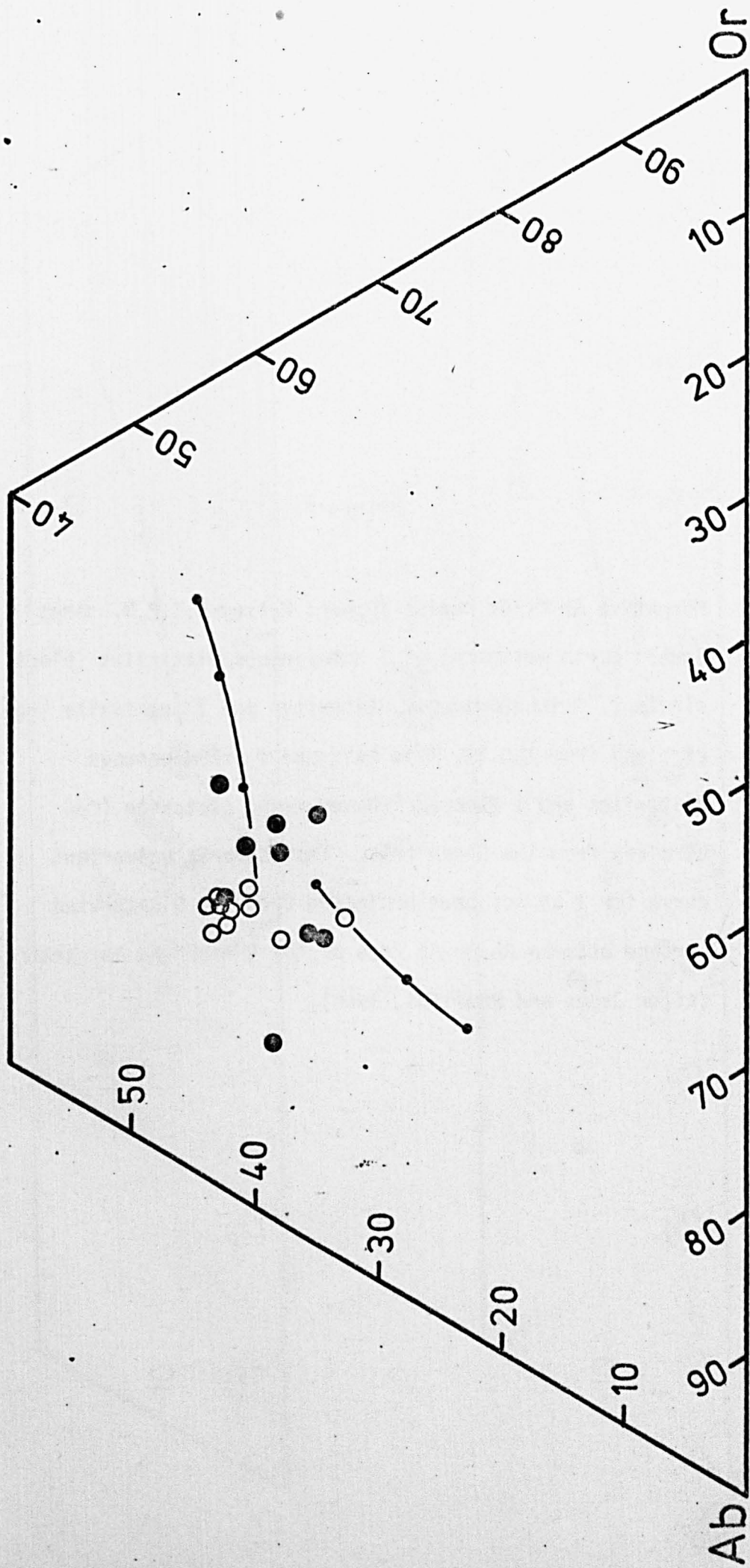
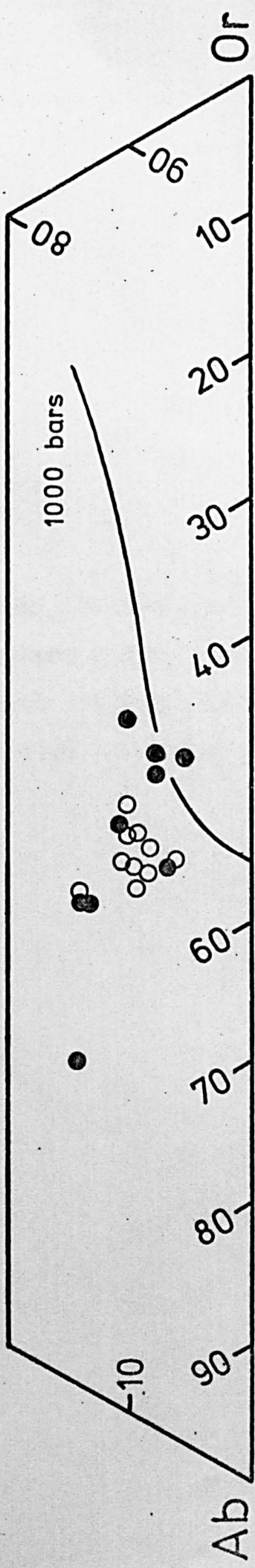


Figure VI.6

Normative Ab-Or-An ratios (upper: Kelsey-C.I.P.W. norm; lower: Barth mesonorm) of 6 homogeneous diatexites (black circles), 9 inhomogeneous diatexites and 1 metatexite (open circles) from the St. Malo belt and 2 inhomogeneous diatexites and 1 sheared inhomogeneous diatexite (red circles) from the Dinan belt. The isobaric univariant curve for 1 kb has been projected from the Q saturated surface onto the Ab-Or-An face of the Q-Ab-Or-An tetrahedron (after James and Hamilton, 1969).

An 20%



An 20%

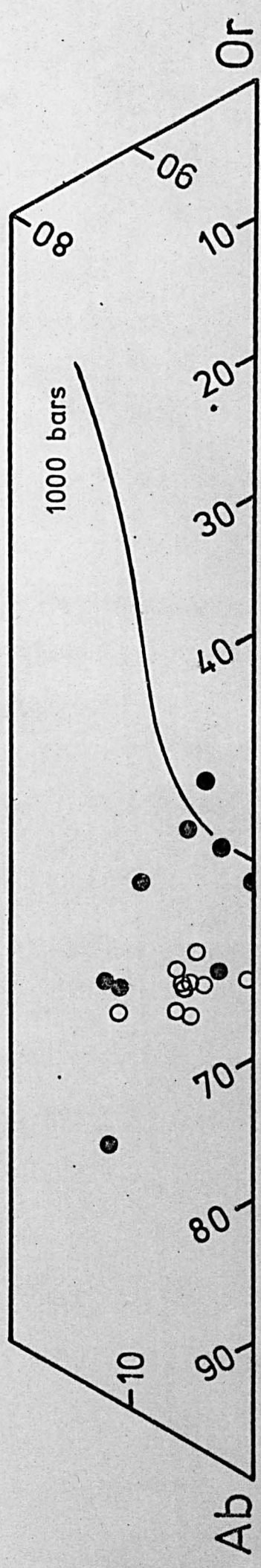
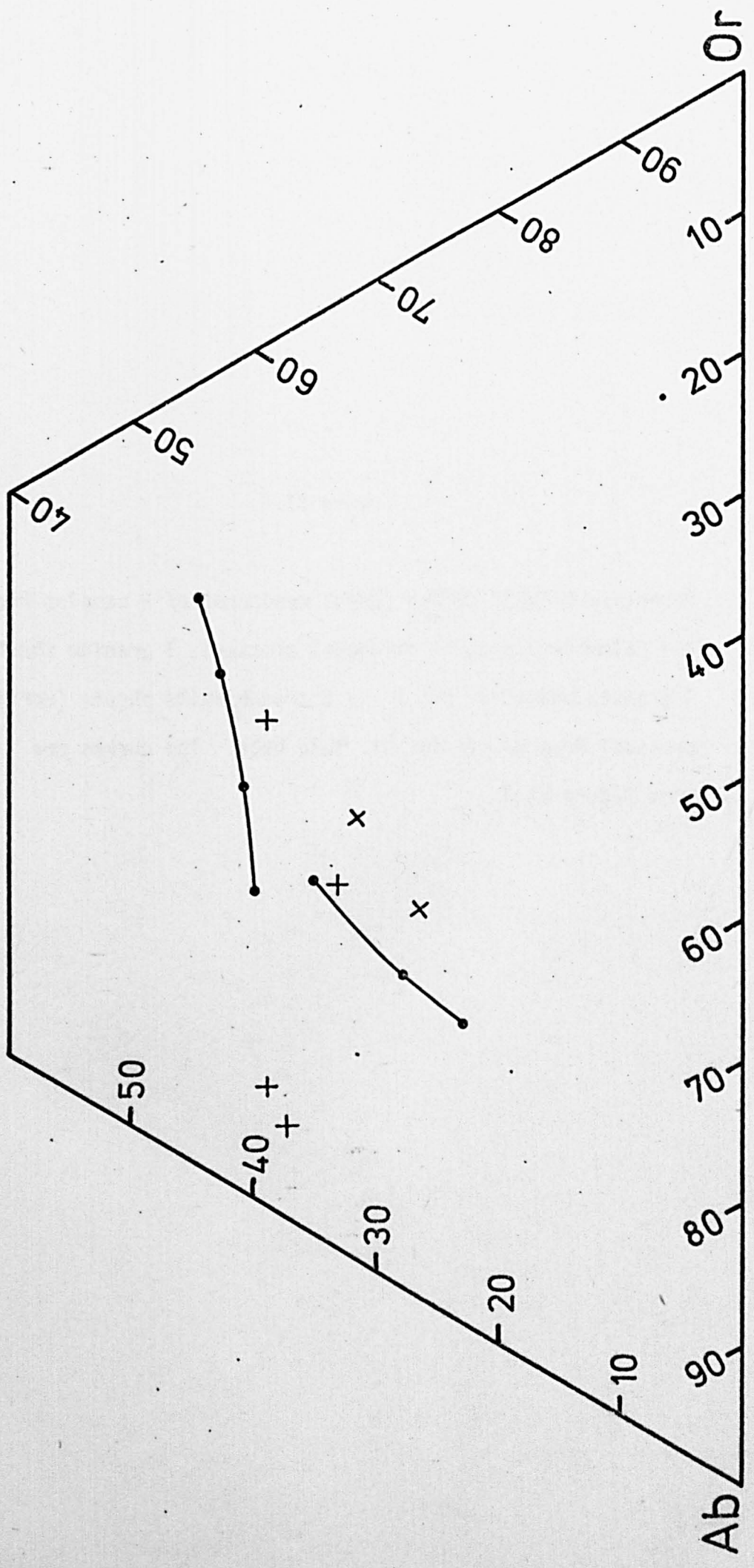


Figure VI.7

Normative Q-Ab-Or ratios (Kelsey-C.I.P.W. norm) of 2 samples from the Colombière granite (diagonal crosses), 1 granite sheet, 1 granite pegmatite sheet and 2 trondhjemite sheets (upright crosses) from within the St. Malo belt. The curves are from Figure VI.3.

Q 60%



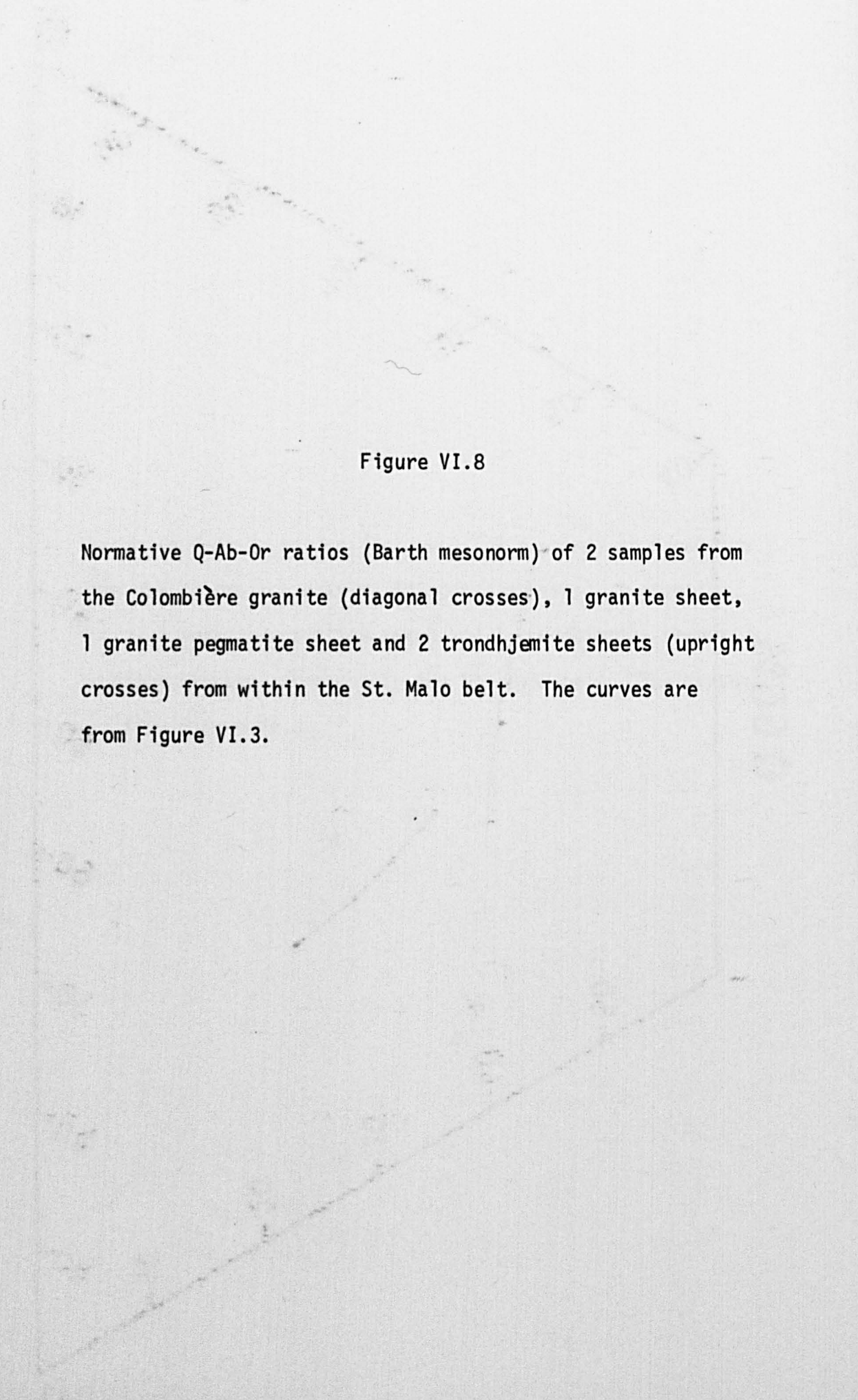


Figure VI.8

Normative Q-Ab-Or ratios (Barth mesonorm) of 2 samples from the Colombière granite (diagonal crosses), 1 granite sheet, 1 granite pegmatite sheet and 2 trondhjemite sheets (upright crosses) from within the St. Malo belt. The curves are from Figure VI.3.

Q 60%

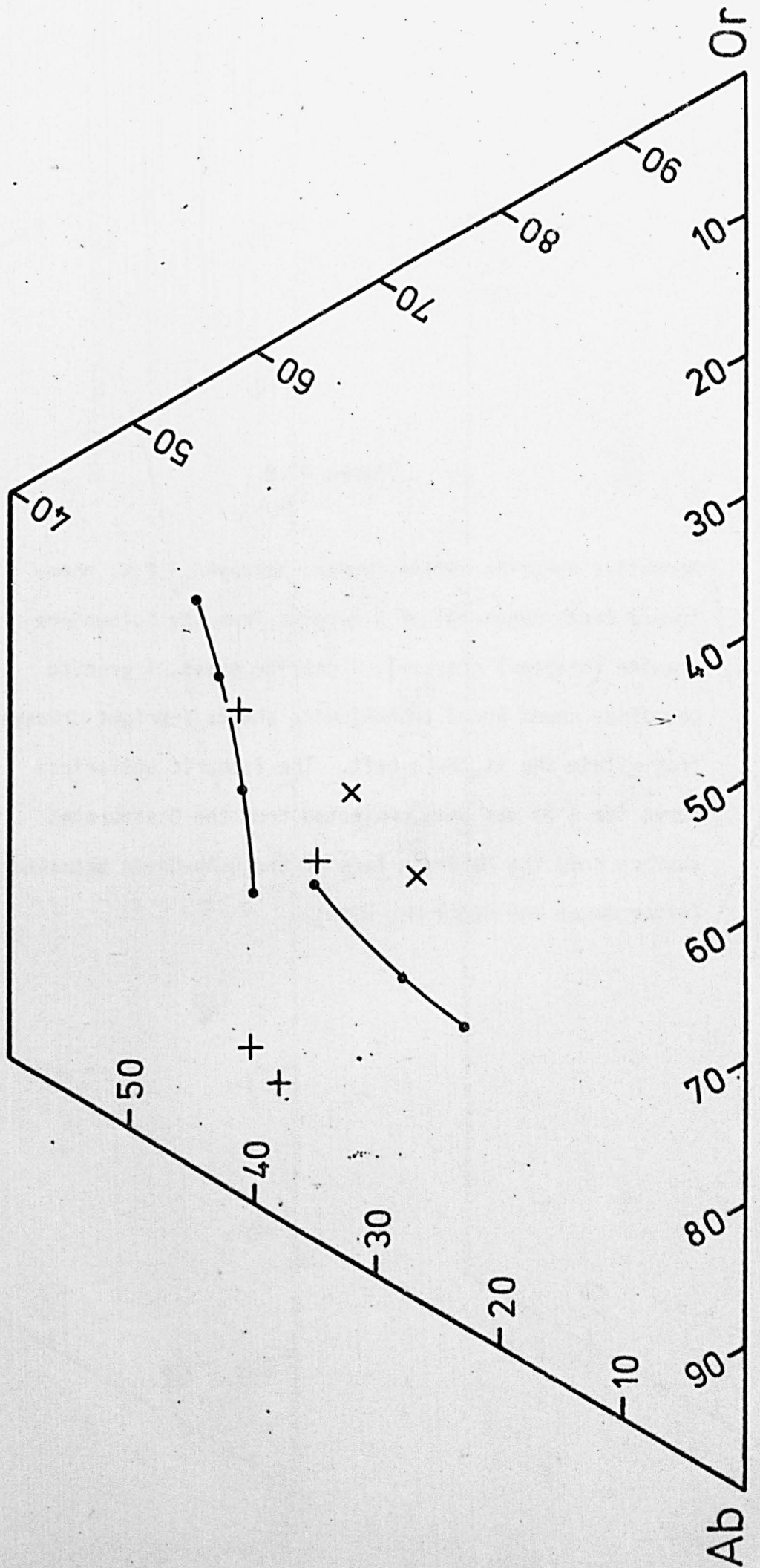
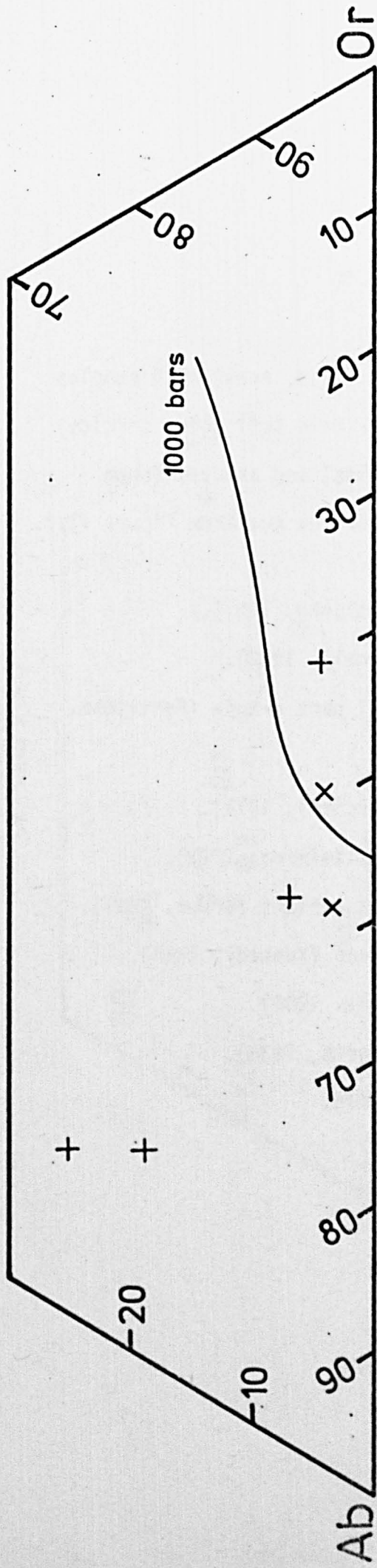


Figure VI.9

Normative Ab-Or-An ratios (upper: Kelsey-C.I.P.W. norm; lower: Barth mesonorm) of 2 samples from the Colombière granite (diagonal crosses), 1 granite sheet, 1 granite pegmatite sheet and 2 trondhjemite sheets (upright crosses) from within the St. Malo belt. The isobaric univariant curve for 1 kb has been projected from the Q saturated surface onto the Ab-Or-An face of the Q-Ab-Or-An tetrahedron (after James and Hamilton, 1969).

An 30%



An 30%

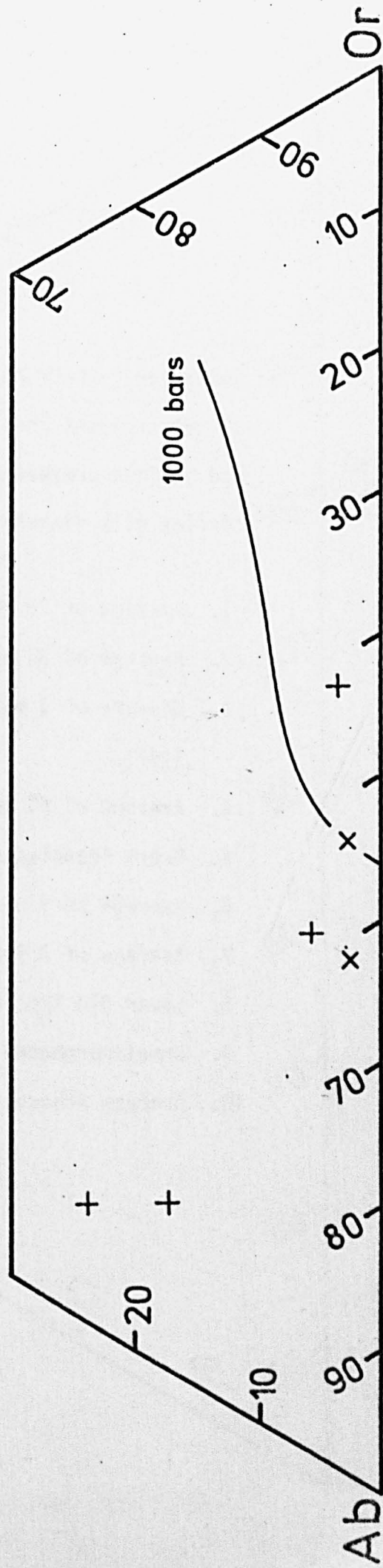


Figure VI.10

Normative Q-Ab-Or ratios (Kelsey-C.I.P.W. norm) of 5 samples of metasediment from within the St. Malo belt (blue circles) and various greywackes (black circles) and arkoses (open circles with diagonal line). The curves are from Figure VI.3.

1. Average of 23 greywackes (Pettijohn, 1957).
2. Average of 30 greywackes (Tyrrell, 1933).
3. Mixture of 2 parts shale and 1 part arkose (Pettijohn, 1957).
4. Average of 61 greywackes (Tobschall, 1971).
5. Fresh Franciscan greywacke (Taliaferro, 1943).
6. Average of 9 non-garnetiferous schists (Brown, 1967).
7. Average of 3 Torridonian arkoses (Kennedy, 1951).
8. Lower Old Red Sandstone (Mackie, 1905).
9. Unmetamorphosed sparagmite (Barth, 1938).
10. Average arkose (Pettijohn, 1957).

Q 65%

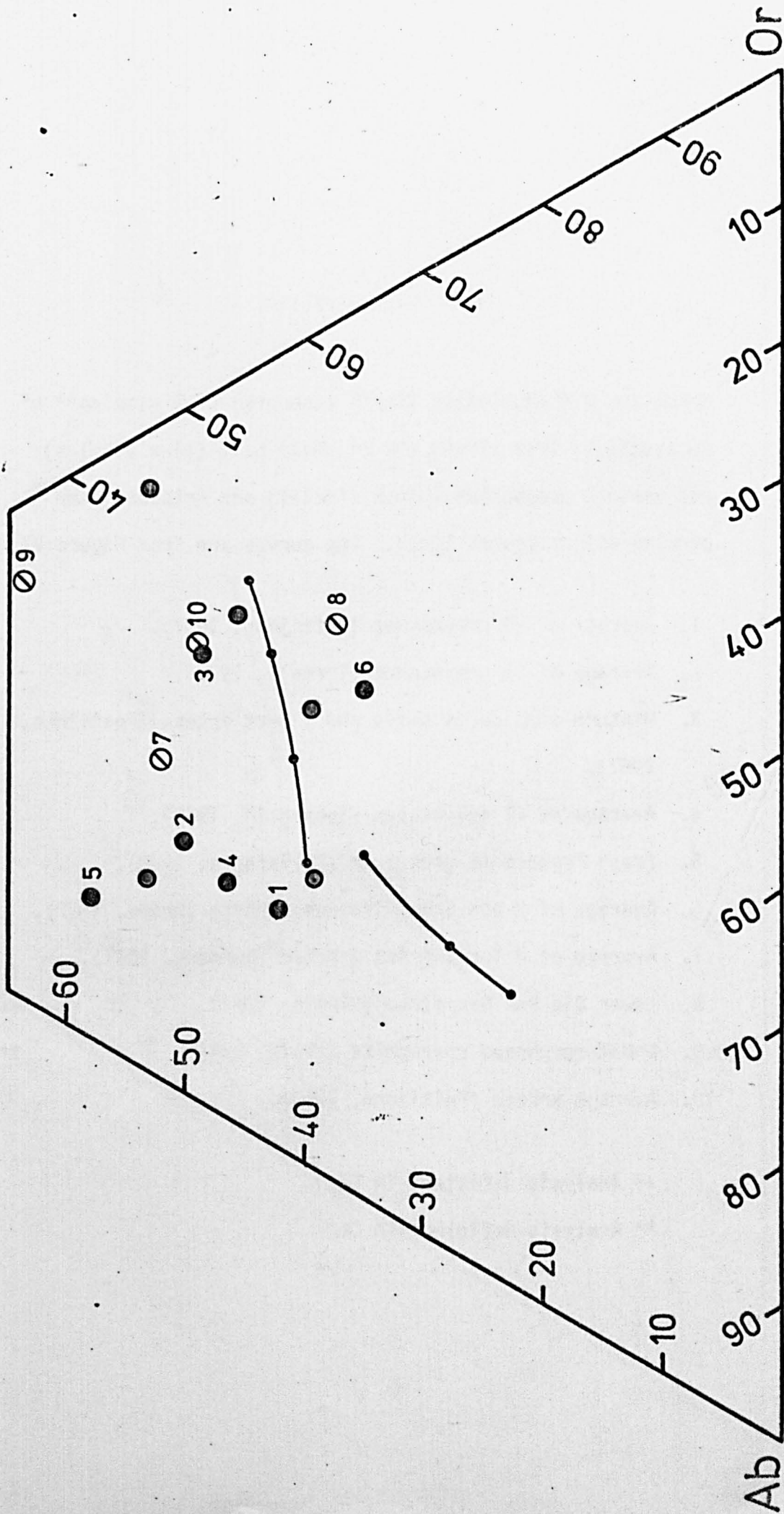


Figure VI.11

Normative Q-Ab-Or ratios (Barth mesonorm) of 5 samples** of metasediment from within the St. Malo belt (blue circles) and various greywackes (black circles) and arkoses (open circles with diagonal line). The curves are from Figure VI.3.

1. Average of 23 greywackes (Pettijohn, 1957).
2. Average of 30 greywackes (Tyrrell, 1933).
3. Mixture of 2 parts shale and 1 part arkose (Pettijohn, 1957).
4. Average of 61 greywackes (Tobschall, 1971).
5. Fresh Franciscan greywacke (Taliaferro, 1943).
6. Average of 9 non-garnetiferous schists (Brown, 1967).
7. Average of 3 Torridonian arkoses (Kennedy, 1951).
8. Lower Old Red Sandstone (Mackie, 1905). ++
9. Unmetamorphosed sparagmite (Barth, 1938). **
10. Average arkose (Pettijohn, 1957).

++ Analysis deficient in Al_2O_3

** Analysis deficient in CaO

Q 65%

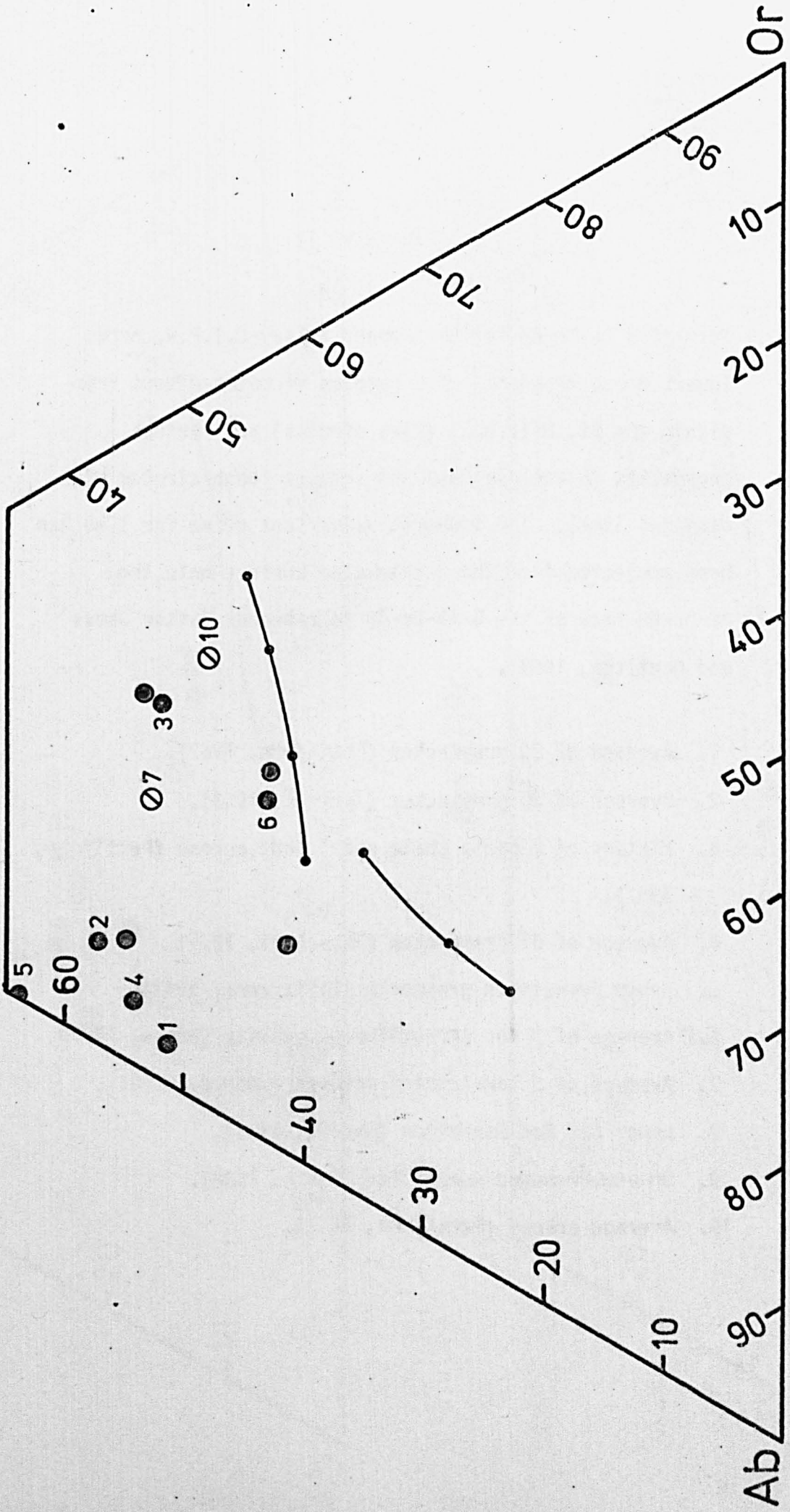
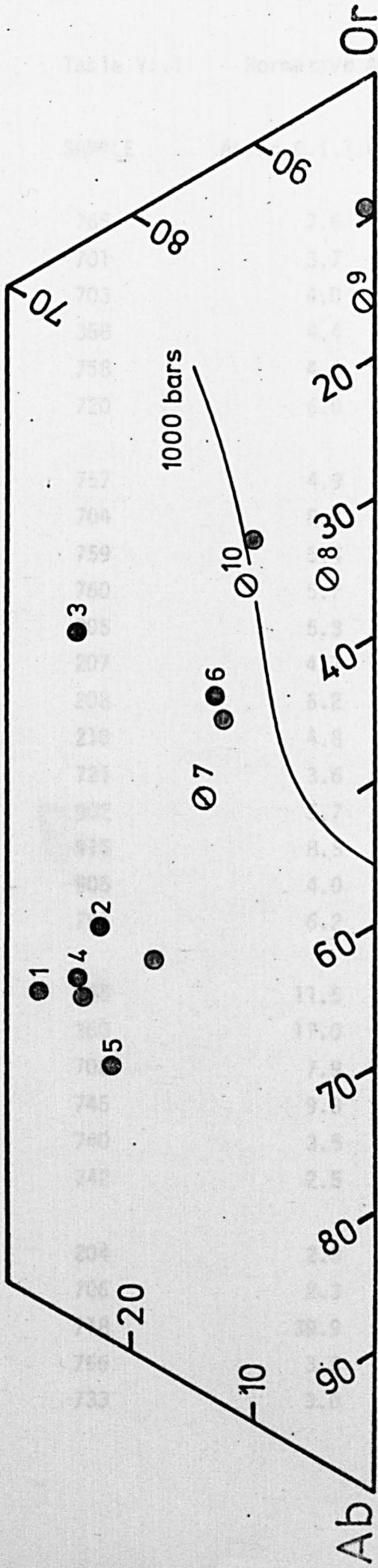


Figure VI.12

Normative Ab-Or-An ratios (upper: Kelsey-C.I.P.W. norm; lower: Barth mesonorm) of 5 samples of metasediment from within the St. Malo belt (blue circles) and various greywackes (black circles) and arkoses (open circles with diagonal line). The isobaric univariant curve for 1 kb has been projected from the Q saturated surface onto the Ab-Or-An face of the Q-Ab-Or-An tetrahedron (after James and Hamilton, 1969).

1. Average of 23 greywackes (Pettijohn, 1957).
2. Average of 30 greywackes (Tyrrell, 1933).
3. Mixture of 2 parts shale and 1 part arkose (Pettijohn, 1957).
4. Average of 61 greywackes (Tobschall, 1971).
5. Fresh Franciscan greywacke (Taliaferro, 1943).
6. Average of 9 non-garnetiferous schists (Brown, 1967).
7. Average of 3 Torridonian arkoses (Kennedy, 1951).
8. Lower Old Red Sandstone (Mackie, 1905).
9. Unmetamorphosed sparagmite (Barth, 1938).
10. Average arkose (Pettijohn, 1957).

An30%



An30%

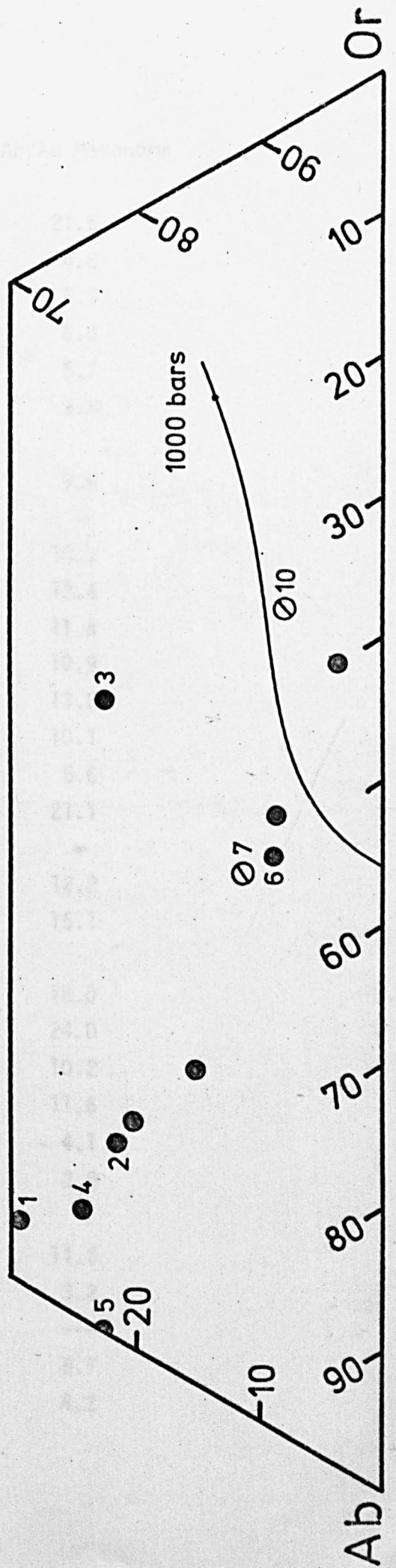


Table VI.1 Normative Ab/An ratios.

SAMPLE	Ab/An C.I.P.W. norm	Ab/An Mesonorm
765	7.6	21.5
701	3.7	4.8
703	4.0	5.5
358	4.4	6.0
758	4.4	5.7
720	6.0	9.5
757	4.9	9.6
704	8.7	∞
759	5.4	10.7
760	5.7	12.4
205	5.3	11.6
207	4.7	10.9
208	6.2	13.2
210	4.8	10.1
721	3.6	5.6
902	5.7	21.1
915	8.5	∞
905	4.0	12.2
761	6.2	15.1
345	11.5	18.0
360	17.0	24.0
708	7.9	10.2
745	9.3	11.6
740	3.5	4.1
742	2.5	2.8
204	2.8	11.5
706	2.3	3.2
718	39.9	---
766	3.3	5.7
733	3.0	4.2

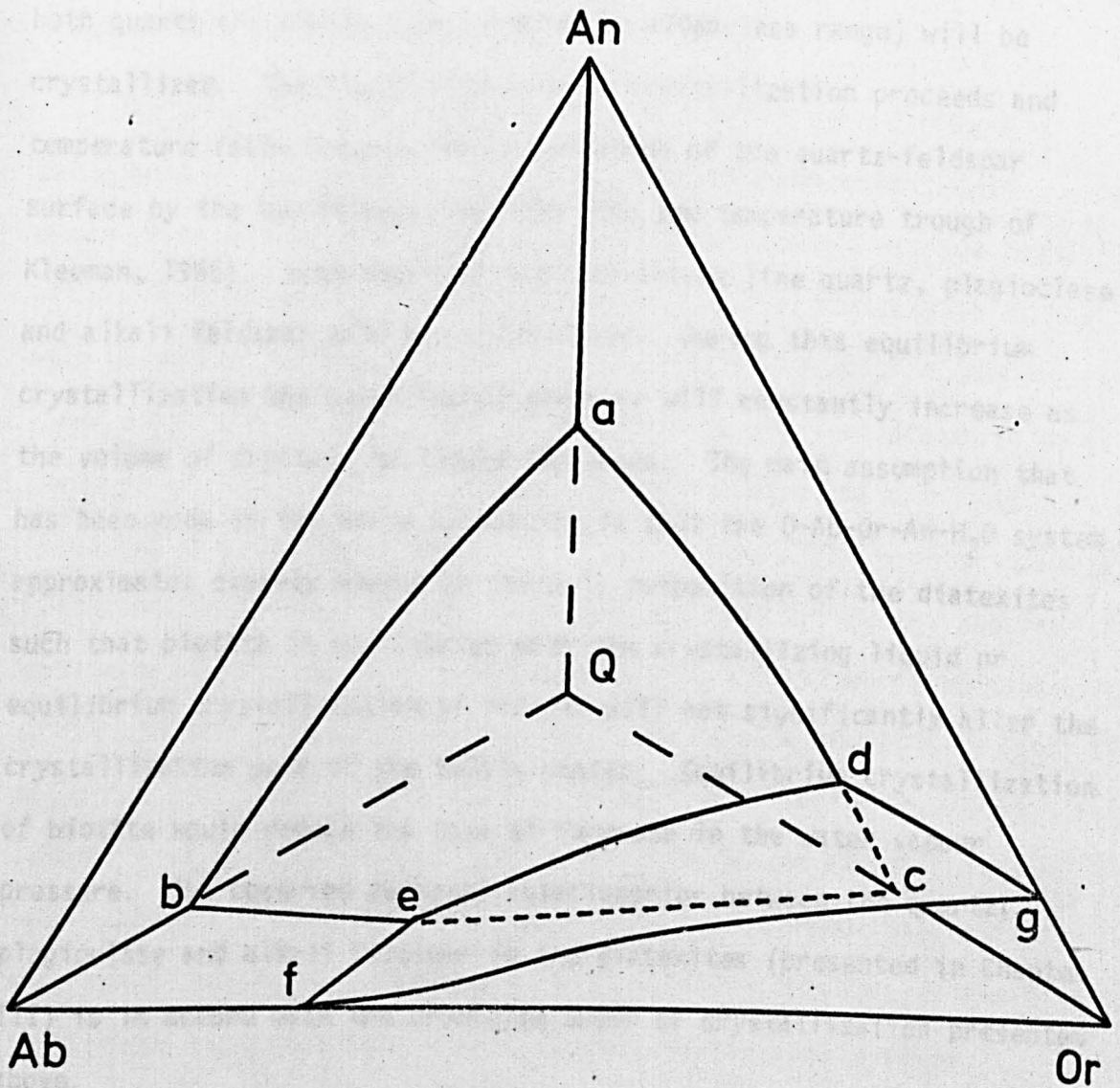
Figure VI.13

Vapour-saturated equilibrium diagram for the system SiO_2 (Q) - $\text{NaAlSi}_3\text{O}_8$ (Ab) - KAlSi_3O_8 (Or) - $\text{CaAl}_2\text{Si}_2\text{O}_8$ (An) - H_2O at 5 kb (based on Carmichael, 1963 and Presnall and Bateman, 1973 after data given by Yoder, Stewart and Smith, 1957; Yoder, 1968; Stewart, 1967; Morse, 1970; and Luth, Jahns and Tuttle, 1964). Within the tetrahedron two curved surfaces are of interest:

1. The surface a-b-c is the boundary separating the primary phase volume of quartz from that of feldspar. This is the quartz-feldspar surface (James and Hamilton, 1969). Liquid compositions on this surface will be in equilibrium with both quartz and feldspar.

2. The surface d-e-f-g is the boundary separating the primary phase volume of plagioclase from that of alkali feldspar. This is the two-feldspar surface (James and Hamilton, op.cit.). Liquids on this surface will be in equilibrium with both plagioclase and alkali feldspar.

The line d-e is the locus of liquids in equilibrium with quartz, plagioclase and alkali feldspar.



the Q-Ab-Or-An tetrahedron and although some of the diatexites lie close to the quartz-feldspar surface most lie well into the quartz volume. It is possible to predict the order of crystallization of the felsic phases during equilibrium crystallization of the diatexite compositions from the phase relations within the vapour saturated Q-Ab-Or-An tetrahedron (Figure VI.13). The diatexites will crystallize quartz until the liquid reaches the quartz-feldspar surface whereupon both quartz and plagioclase (within the oligoclase range) will be crystallized. The liquid will move as crystallization proceeds and temperature falls towards the intersection of the quartz-feldspar surface by the two-feldspar surface (the low temperature trough of Kleeman, 1965). Upon reaching this univariant line quartz, plagioclase and alkali feldspar will be crystallized. During this equilibrium crystallization the water vapour pressure will constantly increase as the volume of crystals to liquid increases. The main assumption that has been made in the above discussion is that the Q-Ab-Or-An-H₂O system approximates closely enough to the bulk composition of the diatexites such that biotite in equilibrium with the crystallizing liquid or equilibrium crystallization of biotite will not significantly alter the crystallization path of the felsic phases. Equilibrium crystallization of biotite would reduce the rate of increase in the water vapour pressure. The observed textural relationships between the quartz, plagioclase and alkali feldspar in the diatexites (presented in Chapter III) is in accord with the predicted order of crystallization presented above.

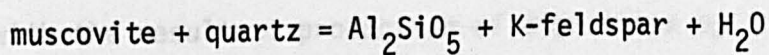
Brown (1970a & b; and in: Brown and Fyfe, 1970) has undertaken an experimental investigation into the production of granites and related rocks during ultrametamorphism. There is considerable similarity between the normative Q-Ab-Or ratios of early liquid compositions resulting from

hydrate induced melting (muscovite and biotite) within granitic and dioritic mineral mixtures at temperatures between 690°C and 760°C and pressures of 2 kb to 4 kb and some of the St. Malo diatexites (compare Tables III.1 & III.2 and Figures VI.4 and VI.5 with Brown and Fyfe, op.cit., Table 2 and Fig. 3).

The Genesis of the St. Malo Rocks

The presence of prismatic sillimanite within the schistose palaeosome of the metatexites suggests metamorphism under upper amphibolite facies conditions. Andalusite and kyanite are not found within rocks of the St. Malo migmatite belt. Thus sillimanite is the only polymorph of Al_2SiO_5 within the St. Malo rocks which allows a lower limit and an upper limit to be placed on the load pressures at the time of the metamorphic climax. Unfortunately, the stability fields of the aluminosilicates are uncertain (Zen, 1969). The stability fields determined by Richardson, Gilbert and Bell (1969) are popular with some authors whilst the stability fields determined by Holdaway (1971) are preferred by other authors. The results of Holdaway (op.cit.) are preferred in this study. At 600°C sillimanite is the stable polymorph of Al_2SiO_5 between 2.25 kb and 5.75 kb and at 700°C it is stable between 0.75 kb and 7.75 kb. The general absence of cordierite and garnet from the St. Malo rocks is unhelpful but Dallmeyer and Dodd (1971) have suggested that $Bi+Sill+Q$ might remain stable above pressures around 3.5 kb until temperatures in excess of 750°C (see also Steuhl, 1962 and Knabe, 1966). The presence of late poikiloblastic muscovite and muscovite-quartz symplectites (Chapter III) demands a water vapour pressure of at least 3.5 kb to 4 kb (Evans, 1965).

The upper part of the amphibolite facies of metamorphism is characterised by the breakdown of micas, especially muscovite (see the experimental work of Segnit and Kennedy, 1961; Evans, 1965; Velde, 1966; Althaus, Karotke, Nitsch and Winkler, 1970; Kerrick, 1972; Storre, 1972; and Day, 1973). One reaction is:



and the stability curve for this reaction is well established. In the more complex systems represented by rocks, however, the reaction for the breakdown of muscovite may well be more complex. Guidotti (1963) has suggested a reaction between muscovite+sodic plagioclase+quartz to produce an aluminosilicate+K-feldspar+ a more calcic plagioclase+water. Winkler (1970) has suggested that water vapour pressure must exceed 3.5 kb to 4 kb with temperatures between 625°C and 675°C for the first entry of the isograd "K-feldspar+Al₂SiO₅ in anatectic (migmatitic) areas". This is in good agreement with Lundgren's (1966) estimate of 650°C for the appearance of the sillimanite-orthoclase isograd in south-eastern Connecticut. It is considered that temperatures in excess of 650°C at load pressures of 4 kb to 6.5 kb represent the conditions prevailing during the metamorphic climax that affected the St. Malo migmatite belt.

Water is critical during ultrametamorphism although agreement on whether a vapour phase is present in amphibolite facies rocks has not been reached. Huang and Wyllie (1973) consider that a pore fluid would be present at the beginning of melting but Fyfe (1970) and Brown and Fyfe (1970) consider that the only water present at the beginning of melting would be that held in hydrated phases such as mica and amphibole. Experimental work has concentrated on the situation for $P_{\text{H}_2\text{O}} = P_{\text{total}}$ (Tuttle and Bowen, 1958; Luth, Jahns and Tuttle, 1964;

Von Platen, 1965; Winkler, 1967; James and Hamilton, 1969; Piwinski, 1968; and Piwinski and Wyllie, 1968) although Brown (1970a & b; Brown and Fyfe, 1970 & 1972) has considered the situation when P_{H_2O} is less than P_{total} .

The elimination of muscovite in an area of high-grade metamorphic rocks with the resultant production of migmatites by anatexis has been discussed by Lundgren (1966). If a vapour phase was present, muscovite breakdown would have started with the liquid absent reaction albite+muscovite+quartz = sillimanite+K-feldspar+vapour (see Evans, 1965). Since the rocks would have contained only a little vapour most of the muscovite breakdown would have occurred through the vapour absent reaction albite+muscovite+quartz = sillimanite+K-feldspar+liquid (see Segnit and Kennedy, 1961) with concomitant migmatization (Kerrick, 1972). Lundgren (op.cit.) considers that in addition to partial melting of rocks in which muscovite was being eliminated there was intrusion of material from deeper zones in which biotite was being eliminated. Both Lundgren and Blattner (1971) have suggested that although P_{H_2O} may initially be less than P_{total} the destruction of micas with the liberation of water should serve to raise the P_{H_2O} to P_{total} . Fyfe (1970) has suggested that the mineralogy of migmatites (eg. the occurrence of garnet) indicates that granitic liquids are not generally water saturated and do not form on minimum melting curves. Garnet is present in the migmatites studied by Lundgren (op.cit.) but not in those studied by Blattner (op.cit.).

At low P_{total} the decomposition of muscovite in the presence of quartz proceeds by one of the liquid absent reactions $Ab+Ms+Q = Sill+K-f+V$ or $Ms+Q = Sill+K-f+V$ which occur before the melting of $Q+Ab+Or+V$ (Figure VI.14). Above 3.5 kb ($P_{total} = P_{H_2O}$) at temperatures of 650°C the assemblage $Ms+Ab+Or+Q+V$ melts (Figure VI.14). Fyfe (1970),

Figure VI.14

P_{H_2O} -T diagram for quartz saturated phase relations.

Based upon data from: Althaus et al, 1970; Day, 1973;

Evans, 1965; Holdaway, 1971; Huang and Wyllie, 1973;

Kerrick, 1972; Lambert, Robertson and Wyllie, 1969;

Merrill, Robertson and Wyllie, 1970; Richardson et al,

1969; Storre, 1972; and Thompson, 1974.

H = Aluminosilicate triple point after Holdaway.

RGB = Aluminosilicate triple point after Richardson et al.

And = andalusite, Sill = sillimanite, Ky = kyanite,

Ms = muscovite, Ab = albite, Or = K-f = K-feldspar,

Q = quartz, V = vapour, and L = liquid.

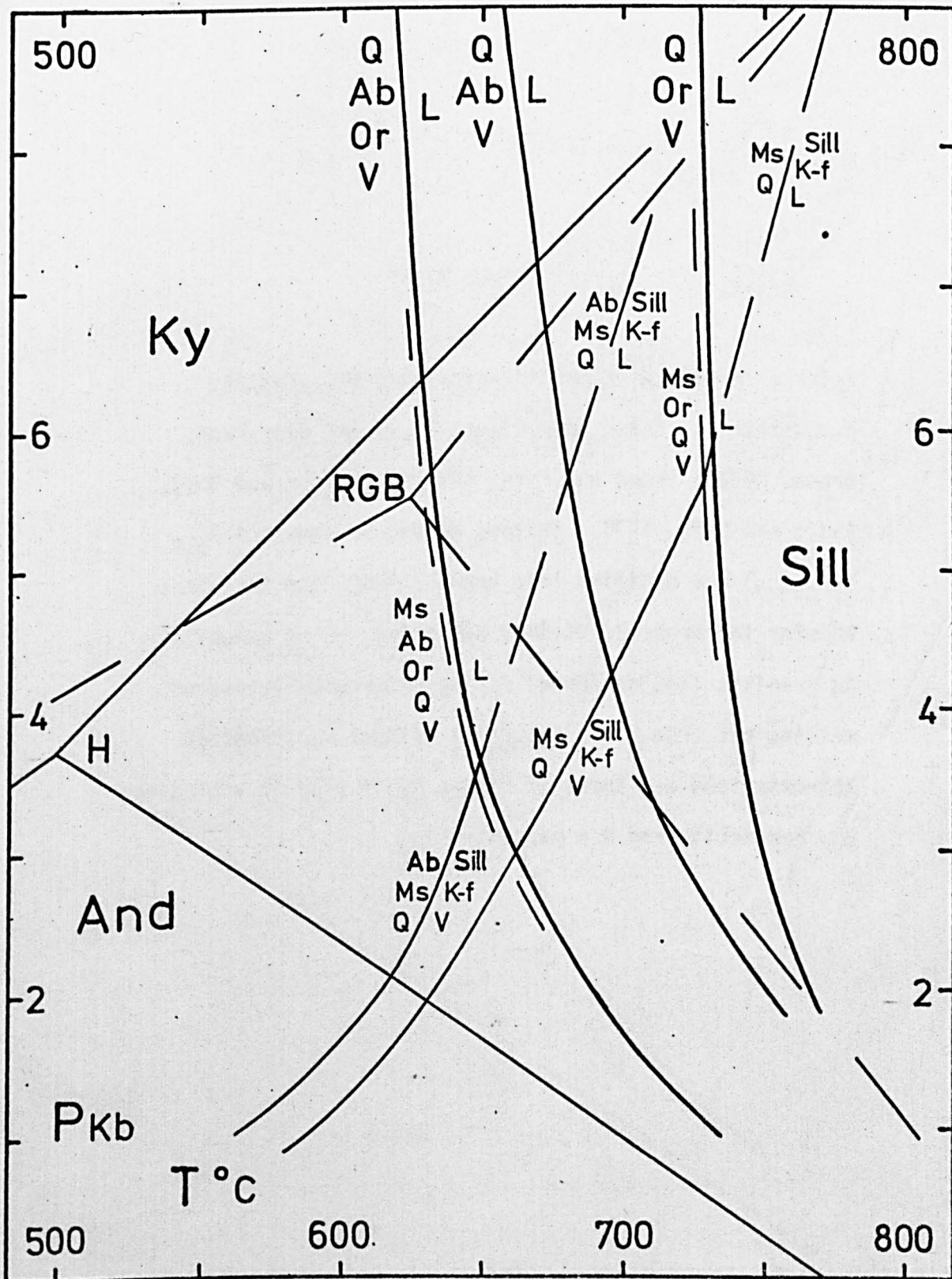
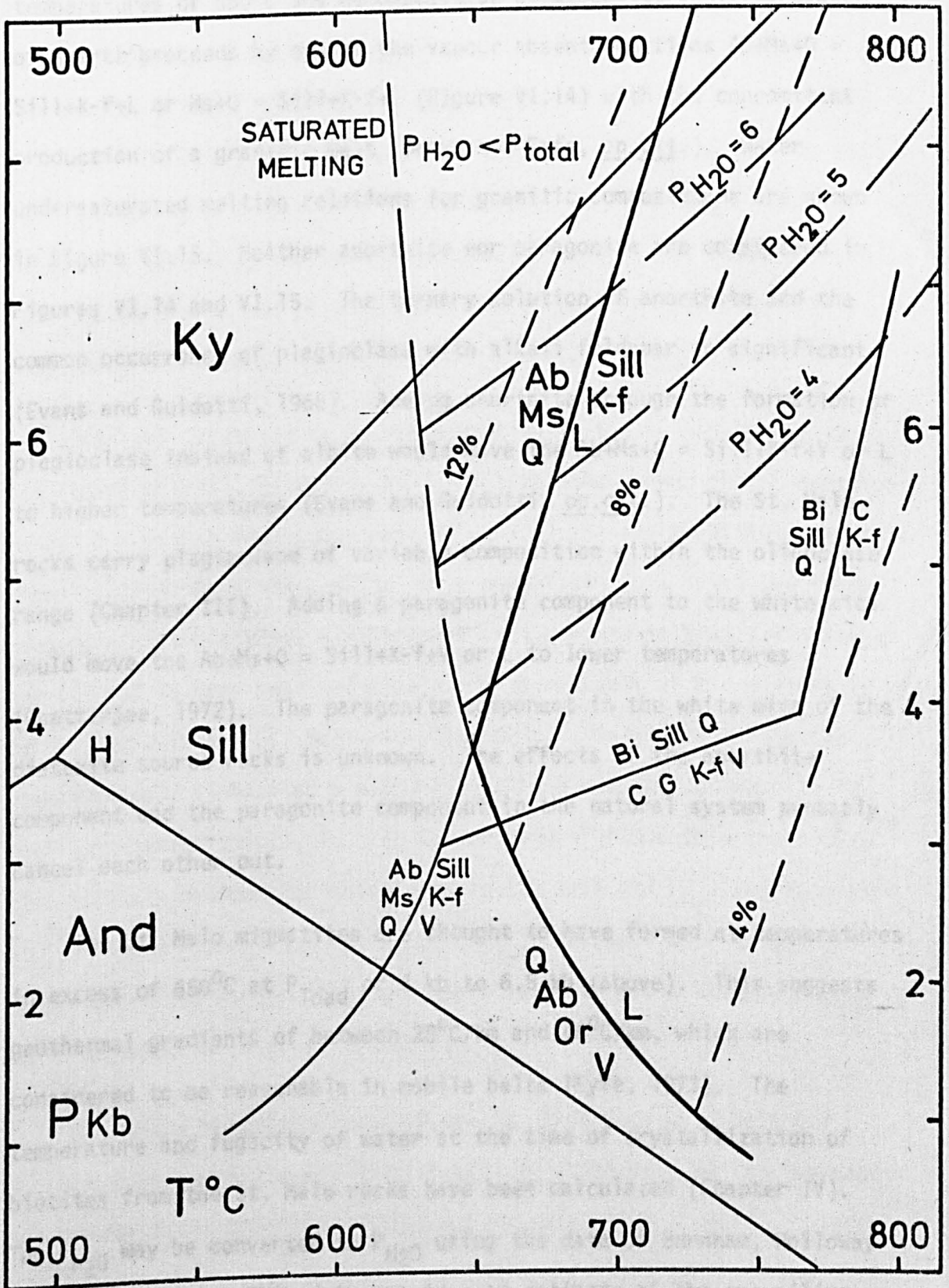


Figure VI.15

Water undersaturated melting relations for granitic compositions. Based upon Figure VI.14 and data from: Brown, 1970b; Brown and Fyfe, 1970; Dallmayer and Dodd, 1971; and Fyfe, 1970. Melting curves of constant P_{H_2O} ($<P_{total}$) are modified from Brown (1970b) and the lines showing the probable minimum percentage water solubility in granitic liquids formed during water undersaturated melting are from Brown (op.cit.) without modification. Abbreviations are those of Figure VI.14 plus Bi = biotite, C = cordierite and G = garnet.



Brown (1970a & b) and Brown and Fyfe (1970) have considered water undersaturated melting in granitic systems. Above 3.5 kb P_{total} at temperatures of 650°C the decomposition of muscovite in the presence of quartz proceeds by one of the vapour absent reactions $\text{Ab} + \text{Ms} + \text{Q} = \text{Sill} + \text{K} + \text{f} + \text{L}$ or $\text{Ms} + \text{Q} = \text{Sill} + \text{K} + \text{f} + \text{L}$ (Figure VI.14) with the concomitant production of a granitic melt (Brown and Fyfe, op.cit.). Water undersaturated melting relations for granitic compositions are shown in Figure VI.15. Neither anorthite nor paragonite are considered in Figures VI.14 and VI.15. The ternary solution of anorthite and the common occurrence of plagioclase with alkali feldspar is significant (Evans and Guidotti, 1966). Adding anorthite through the formation of plagioclase instead of albite would move the $\text{Ab} + \text{Ms} + \text{Q} = \text{Sill} + \text{K} + \text{f} + \text{V}$ or L to higher temperatures (Evans and Guidotti, op.cit.). The St. Malo rocks carry plagioclase of variable composition within the oligoclase range (Chapter III). Adding a paragonite component to the white mica would move the $\text{Ab} + \text{Ms} + \text{Q} = \text{Sill} + \text{K} + \text{f} + \text{V}$ or L to lower temperatures (Chatterjee, 1972). The paragonite component in the white mica of the diatexite source rocks is unknown. The effects of the anorthite component and the paragonite component in the natural system probably cancel each other out.

The St. Malo migmatites are thought to have formed at temperatures in excess of 650°C at P_{load} of 4 kb to 6.5 kb (above). This suggests geothermal gradients of between $28^{\circ}\text{C}/\text{km}$ and $46^{\circ}\text{C}/\text{km}$, which are considered to be reasonable in mobile belts (Fyfe, 1973). The temperature and fugacity of water at the time of crystallization of biotites from the St. Malo rocks have been calculated (Chapter IV). The $f_{\text{H}_2\text{O}}$ may be converted to $P_{\text{H}_2\text{O}}$ using the data of Burnham, Holloway and Davis (1969). This data provides an estimate of the prevailing $P_{\text{H}_2\text{O}}$ during diatexite crystallization. The biotites from typical

inhomogeneous diatexites give a temperature of 720°C and a P_{H_2O} of 2.8 kb. The biotites from the homogeneous diatexite and the Colombiere granite give the following estimates of temperature and water pressure: St. Jacut - 640°C and 4.7 kb to 6.4 kb; north of Port Briac - 665°C and 3.25 kb; and the Colombiere granite - 670°C and 2.45 kb. Fluorine and chlorine have not been determined for the St. Malo rocks, accordingly water is considered to be the main volatile component affecting the temperatures of melting (it is realized that the presence of F and Cl will lower the temperatures for the beginning of melting).

For the estimated P_{load} range of 4 kb to 6.5 kb and temperatures in excess of 650°C (4 kb) to 690°C (6.5 kb) the vapour absent reaction $Ab+Ms+Q = Sill+K-f+L$ is unstable (Figure VI.15) and granitic melts will result (Brown and Fyfe, 1970). If a pore fluid is present the liquid absent reaction $Ab+Ms+Q = Sill+K-f+V$ will precede melting. Biotite is considered to have remained stable during anatexis at the present level of exposure in the St. Malo migmatite belt. The biotites from the inhomogeneous diatexites are thought to have remained in equilibrium with an anatectic melt, i.e. the temperature of 720°C from the biotites represents a maximum for this level in the belt and P_{H_2O} was less than P_{load} . From Figure VI.15 at P_{load} of 5.25 kb (mean of 4 kb and 6.5 kb) water undersaturated melting can begin at about 670°C which allows a 50°C temperature interval to 720°C.

At depths below the level of the St. Malo migmatite belt now exposed both muscovite and biotite will be eliminated by the two vapour absent reactions $Ab+Ms+Q = Sill+K-f+L$ and $Bi+Sill+Q = C+K-f+L$ (Figure VI.15) at temperatures greater than 720°C and P_{load} greater than 5.25 kb. Melts produced at these depths may well be of sufficient quantity to

collect and intrude upward. The high P_{H_2O} suggested by the St. Jacut homogeneous diatexite biotites means that P_{H_2O} must have been close to P_{load} (estimated P_{H_2O} of 4.7 kb to 6.4 kb and estimated P_{load} of 4 kb to 6.5 kb) and accordingly placed severe limitations upon the intrusiveness of the melt (Tuttle and Bowen, 1958). The lower P_{H_2O} and higher temperature suggested for the crystallisation of the biotites from the Colombière granite are in accord with the field evidence suggesting intrusion of material (Chapter II) and imply water undersaturated crystallization. Similarly, the homogeneous diatexite which outcrops to the north of Port Briac, near Cancale, has intruded into Pentevrian metasediments (Chapter II) and again the lower P_{H_2O} and higher temperature suggested for the crystallization of the biotite from these rocks imply water undersaturated crystallization. The St. Jacut homogeneous diatexite has probably not come far. The Colombière granite and the Port Briac homogeneous diatexite, however, are clearly intrusive and were probably derived from depths below the present erosion level.

The temperatures for the onset of melting presented above are in good agreement with experimental work in the Q-Ab-Or-An-H₂O system, experimental melting of mineral mixtures and experimental work on igneous rocks. Von Platen (1965) found that melting was initiated in gneisses with varying Ab/An ratios at temperatures between 690°C and 730°C at 2 kb water pressure, these temperatures would be 40°C lower at 5 kb water pressure. Winkler and Von Platen (quoted, with the revised temperature calibration, by Winkler, 1967) found that melting began in greywackes between 685°C and 715°C at 2 kb water pressure depending upon the Ab/An ratio of the rock, again these temperatures would be 40°C lower at 5 kb water pressure. Between 60% and 80% of the gneiss had melted within 50°C of initial melting (Von Platen, op.cit.). At a

temperature of 770°C the greywackes had produced between 63% and 73% anatectic melt (Winkler, op.cit.). Steuhl (1962) showed that melting commenced between 670°C and 680°C in a biotite paragneiss and that above 690°C plagioclase and, above 700°C, biotite are resolved fractionally by the melt at 2 kb water pressure. Winkler (op.cit.) has summarized the work of Knabe (1966) in the following words "it is certain that, unlike muscovite, not all of the biotite disappears at the beginning of anatexis. Instead, the amount of biotite diminishes as the temperature is increased, and even at temperatures 70-100°C higher than the beginning of anatexis, an appreciable portion of the biotite is still preserved".

Kleeman (1965) has argued that a quartzo-feldspathic rock containing quartz (48%), orthoclase (19%), albite (29%) and anorthite (4%) would begin to melt under a water pressure of 5 kb at 650°C and would continue to melt with increasing temperature until about 61% of the rock had become molten at about 660°C. A 15°C rise in temperature after this would melt a further 12% of the rock but the remainder, all quartz, would require a further rise in temperature of 100°C before it had all melted. Thus, he argues, over 70% of a rock of that composition would melt within a 25°C temperature rise from the beginning of melting.

Experimental work on the beginning of melting in mineral mixtures and igneous rocks is extensive and includes Brown (1970a & b); Brown and Fyfe (1970); Tuttle and Brown (1958); Luth, Jahns and Tuttle (1964); Piwinskii (1968); Piwinskii and Wyllie (1968); and Huang and Wyllie (1973). The beginning of melting in granite at 5 kb water pressure is about 640°C and for granodiorite at 5 kb water pressure is about 665°C. The granite liquidus at 5 kb water pressure is about 670°C, whilst for most granodiorites both K-feldspar and quartz have been eliminated at 700°C under 5 kb water pressure (from Piwinskii, op.cit. and Piwinskii and Wyllie, op.cit.).

The proposed genesis of the St. Malo migmatites is consistent with experimental data. The quantity of melt produced by a rise in temperature depends upon two factors - the magnitude of the rise in temperature and the bulk rock composition, especially the initial Ab/An ratio. Within 50°C of initial melting it is reasonable to expect that between 60% and 80% of the rock will have melted. The initial segregation during D_1 to produce the metatexitic banding (see Chapter V) was probably in response to temperatures only slightly above that required for anatexis to commence. Later diatexis (see Chapter V) accompanied the temperature maximum within the belt. Variation in the amount of melt produced during initial metatexis has resulted in the development of different migmatite structures. Variation in the amount of melt produced during later diatexis has resulted in areas where metatexite and diatexite are frequently intermingled (eg. between St. Briac and Dinard, see Chapter II) and eventually bodies of diatexite with enclaves of metatexite and psammite (eg. St. Jacut-de-la-Mer and St. Briac, see Chapter II). Intrusion of material from lower levels within the metamorphic belt is the logical conclusion of ultrametamorphism (eg. Port Briac, north of Cancale, see Chapter II).

It is thought that the biotite schlieren could represent either broken up melanosome or aggregated biotite flakes. Van Diver (1970) has suggested two possible mechanisms for the origin of biotite-rich orbicles in the "Bullseye Granite" of Craftsbury, Vermont. Either the orbicles formed by the coherence of numerous biotite flakes around biotite nuclei or they formed by the coherence of numerous biotite flakes around gas bubbles migrating up through the magma. Van Diver (op.cit.) preferred the gas bubble hypothesis but in a water undersaturated environment with biotite selvages being destroyed by extensive anatexis the coherence of biotite flakes around biotite aggregates is more likely. The local

presence of tourmaline in the biotite schlieren of the St. Jacut-de-la-Mer inhomogeneous diatexites (Chapter III) suggests that the gas bubble hypothesis may apply when P_{H_2O} approaches P_{load} .

CHAPTER VII

CHAPTER VII

Discussion

The St. Malo migmatite belt is correlated with the Pentevrian basement of the Armorican Massif (see also Brown et al, 1971). The main lithologies within the Pentevrian of the St. Malo area are metasediments, metatexites, diatexites and granitoid sheets. They have been subjected to multiple deformation prior to Brioverian sedimentation. Other areas of Pentevrian basement within the Armorican Massif include the type area along the eastern side of the Baie de St. Briec (Cogné, 1959 & 1964 and Roach et al, 1972); outcrops around la Hague, west of Cherbourg (Graindor, 1960; Roach et al, op.cit.; and Leutwein et al, 1973); parts of Guernsey (Roach, 1966; Roach et al, op.cit.; and Bishop et al, in press), Alderney (Adams, 1967a) and Sark (Power, personal communication) in the Channel Islands; parts of the Trégor (Verdier, 1968 and Auvray, personal communication); and on the western side of the Baie de St. Briec around St. Quay-Portrieux (Ryan, 1973 and Ryan & Roach, in press). These isolated fragments of Pentevrian basement preserve within them a complex history of multiple deformation, metamorphism and magmatism (Roach et al, op.cit.) but to what extent do they have a common orogenic history?

No detailed structural and metamorphic analysis is available for the Pentevrian type area although Roach et al (op.cit. p.248) state "... the Pentevrian orthogneisses and migmatites suffered multiple deformation before intrusion of now poorly foliated granites". It was suggested earlier (Chapter IV, p.IV.6) that the St. Malo Pentevrian metasediments and migmatites might be correlated with similar metasediments and migmatites on Guernsey (Roach, 1966). Migmatized metasediments are also found in the Nez de Jobourg area, la Hague, west of Cherbourg (Power, personal communication).

The work of Adams (1967a) has demonstrated beyond doubt the antiquity of the Guernsey gneisses even though the detailed interpretation of his results is difficult. Roach et al (1972) presented one interpretation based upon a sequence of events for the formation of the metamorphic complex similar to that given by Roach (1966). However, Roach has revised this sequence of events in the light of recent work (personal communication and Roach, Bishop & Adams, in preparation) and the summary presented here is based upon the revised chronology. Roach now regards the older of the two Rb/Sr isochrons for the Icart gneiss (Adams, op.cit. and Roach et al, op.cit.) as the age of its emplacement ($2,620 \pm 50$ m.y. - Icartian event) and the younger Rb/Sr isochron from parts of the Icart gneiss as the age of the production of the main penetrative foliation under amphibolite facies conditions ($1,960 \pm 140$ m.y. - Perellian event). Associated with the emplacement of the Icart gneiss was the development of migmatites within an older supracrustal sequence, both marginal to the Icart gneiss (eg. Vazon Bay) and elsewhere within the metamorphic complex (Pea-Stack and Castle Cornet gneisses). The synkinematic Perelle and Doyle gneisses were emplaced during the tectono-metamorphic event that was responsible for the main penetrative foliation in all the gneisses (Perellian event). This main foliation has been folded under upper greenschist facies conditions (Lihouan event). This sequence differs from that given in Roach et al (1972) mainly in the separation of the Icartian and Perellian events and the correlation of the younger isochron age with the Perellian rather than with the Lihouan event.

On the French mainland at la Hague, west of Cherbourg, the Pentevrian basement comprises similar lithologies to that of the Channel Islands (Graindor, 1960; Roach et al, 1972; and Power, personal

communication). Power has established a sequence of deformational, metamorphic and magmatic events remarkably like that of Guernsey and a common orogenic history for these areas seems likely. In particular, the dominant foliation within the Pentevrian gneisses at Nez de Jobourg, la Hague, is that produced by the second deformation and metamorphism. The correlation with Guernsey is supported by the isotopic work of Leutwein et al (1973) who have obtained an age of $2,500 \pm 100$ m.y. from the gneisses and migmatites.

Ryan's work (1973) on the Precambrian around St. Quay-Portrieux has produced the first detailed description of the Pentevrian basement of northern Brittany. In this area the Pentevrian is represented mainly by complexly deformed and metamorphosed supracrustal rocks. The Port Goret gneisses comprise a sequence of polyphasally folded and migmatitic staurolite-bearing paragneisses and schists. The Plouha Series comprises a supracrustal sequence including volcanics characterised by complex interference structures produced by multiple coaxial folding. Four main episodes of deformation - all of which have produced a set of folds - are recorded by Ryan (op.cit. and Ryan & Roach, in press) from both the Port Goret gneisses and the Plouha Series. Locally, the structural sequence is more complex. The first three sets of folds are tight to isoclinal and approximately coaxial; their interference results in complex outcrop patterns. The main penetrative foliation was developed during D_1 although an axial planar foliation is commonly present in both D_2 and D_3 fold closures. The Port Moguer tonalite was emplaced between the third and fourth deformations. The last major pre-Brioverian deformation has produced large scale folds. The sequence of deformational episodes established by Ryan on the western side of the Baie de St. Briec is similar to that established for the Pentevrian metasediments in the St. Malo area (Chapter V).

This similarity invites correlation and suggests a common orogenic history for these two areas of Pentevrian supracrustal rocks. Such correlation is intuitive and should be treated with due circumspection (see Park, 1969).

The fragments of Pentevrian basement discussed above fall into two groups: the northern group comprising Guernsey, Sark, Alderney and la Hague; and the southern group comprising the St. Quay-Portrieux area, the Pentevrian type area and the St. Malo area. Correlation of these two groups of Pentevrian basement will only be confirmed or denied by future isotopic age determinations. In the absence of strong contradictory evidence the present writer regards these fragments of Pentevrian basement as parts of the same basement complex with a common orogenic history. If valid, such a correlation means that there was an extensive early Pentevrian supracrustal sequence in part derived from and probably in part deposited upon an ancient basement. This supracrustal sequence has suffered multiple deformation and polymetamorphism under low pressure conditions together with concomitant plutonism. It is unfortunate that the Archaean basement to this early Pentevrian supracrustal sequence is nowhere seen.

The Brioverian supracrustal rocks which occur on the north-western side of the St. Malo migmatite belt comprise a sequence of turbidites which have been affected by three episodes of deformation during the Cadomian orogenic episode. The structural sequences within other areas of Brioverian supracrustal rocks are similar although there are sometimes differences in the timing of the main metamorphism (cf. Bradshaw et al, 1967 and Ryan & Roach, in press). A common feature of geographically scattered Brioverian sequences is their general NE-SW to E-W orientation. In the St. Malo area the orientation of Cadomian structures seems to have been determined by the structural

grain of the Pentevrian basement. This basement control over Cadomian structures was first commented upon by Roach (in discussion of Bishop et al, 1969) and may be more significant than Bishop et al were willing to admit in reply. The Pentevrian basement responded heterogeneously to the Cadomian deformations in the St. Malo area - the strain being confined to shear belts up to 500 m in width within which the basement gneisses have been reduced to protomylonites, mylonites and ultramylonites or mylonite schists and mylonite gneisses. The Pentevrian basement/Brioverian cover junction is frequently exposed around the Baie de St. Brieuç and the basement rocks are commonly strongly deformed adjacent to the junction (see, for example, the description by Ryan & Roach, op.cit.). The significance of these Cadomian shear belts has been missed by previous workers who have assigned the deformation to the Hercynian orogenic episode. This has been occasioned in part by the failure of some previous workers to recognize the longer structural history within supracrustal rocks of Pentevrian age than that within supracrustal rocks of Brioverian age.

BRIDGMAN, G. & KEMP, J.W., 1974. *Journal of Metamorphic Geology*, 2, 1-12.

Londres: In *Journal of Metamorphic Geology*, 2, 1-12.

30, 1200-1209.

AUGER, S.S., 1973. *Journal of Metamorphic Geology*, 1, 1-12.

Geology and Petrology, 1973, 1, 1-12.

ADRY, R., 1960. *Le volcanisme de la région de St. Malo*. *Annales de la Société de Géologie de France*, 81, 1-12.

Erzurum (Caucasus), 1960, 81, 1-12.

1960, 81, 1-12.

1960. *Sur la nature des roches métamorphiques de la région de*

Erzurum, 1960, 81, 1-12.

References

- AUVRAY, B., COGNE, J., NAMEURT, J., VIDAL, P. & JEANNETTE, D., 1972. Comments on "P... rocks south of Erquy and around St. Cast, Cotes-du-Nord". *Nature Physical Science*, 239,
- ABRARD, R., 1923. Description Petrographique et Géologique du Massif de St. Malo. *Bull. Soc. géol. Min. de Bretagne*, 4, 54-70.
- ADAMS, C.J.D., 1967a. A geochronological and related isotopic study of rocks from North-Western France and the Channel Islands (United Kingdom). D.Phil. thesis, Univ. of Oxford.
- 1967b. K/Ar ages from the basement complex of the Channel Islands (United Kingdom) and the adjacent French mainland. *Earth and Planet. Sci. Lett.*, 2, 52-56.
- 1969. In discussion of BISHOP et al (see below).
- ADAMS, J.A.S., OSMOND, J.K. & ROGERS, J.J.W., 1959. The geochemistry of thorium and uranium. *Phys. Chem. Earth*, 3, 298-348.
- ALLEN, J.R.L., 1970. *Physical Processes of Sedimentation*. George Allen and Unwin Ltd., London, 188-210.
- ALTHAUS, E., KAROTKE, E., NITSCH, K.H. & WINKLER, H.G.F., 1970. An experimental re-examination of the upper stability limit of muscovite plus quartz. *Neues Jahrb. Mineral.*, 7, 325-336.
- ANDERMAN, G. & KEMP, J.W., 1958. Scattered X-rays as internal standards in X-ray emission spectroscopy. *Analyt. Chem.*, 30, 1306-1309.
- AUGUSTITHIS, S.S., 1973. *Atlas of the Textural Patterns of Granites, Gneisses and Associated Rock Types*. Elsevier, Amsterdam.
- AUVRAY, B., 1968. Le volcanisme spilitique de la Pointe de la Heussaye, Erquy (Cotes-du-Nord). *Bull. Soc. géol. Min. de Bretagne, Nouvelle Série*, 101-118.
- 1969. Sur la nature des roches grenues de la Pointe de Caroual. *Bull. Soc. géol. Min. de Bretagne*, 1, 1-9.

- AUVRAY, B., COGNE, J., HAMEURT, J., VIDAL, P. & JEANNETTE, D., 1972.
Comments on "Precambrian rocks south of Erquy and around
St. Cast, Cotes-du-Nord". *Nature Physical Science*, 239,
73-74.
- BABU, V.R.R.M., 1969. Study of minerals from the pegmatites of the
Nellore mica-belt, Andhra Pradesh, India. Part III -
Biotite. *Mineral. Mag.*, 37, 391-393.
- BACKLUND, H., 1937. Die Umgrenzung der Svekofenniden. *Bull. geol.
Instn. Univ. Upsala*, 27, 219-269.
- BAMBAUER, H.U., CORLETT, M., EBERHARD, E. & VISWANATHAN, K., 1967.
Diagrams for the Determination of Plagioclases using X-ray
Powder Methods. *Schweiz. miner. petrogr. Mitt.*, 7, 333-349.
- BARROIS, C., 1892. Dinan (60) sheet of the "Carte géologique détaillée
de la France au 1.80,000".
----- 1893. Légende de la feuille de Dinan. *Ann. Soc. géol.
Nord.*, 21, 25-40.
----- 1895. Le calcaire de Saint-Thurial. *Ann. Soc. géol. Nord.*,
23, 33-46.
- BARTH, T.F.W., 1938. Progressive metamorphism of sparagmite rocks of
southern Norway. *Norsk. Geol. Tidsskr.*, 18, 54-65.
----- 1959. Principles of classification and norm calculation
of metamorphic rocks. *J. Geol.*, 67, 135-152.
----- 1962. A final proposal for calculating the mesonorm of
metamorphic rocks. *J. Geol.*, 70, 497-498.
----- 1969. Feldspars. Wiley-Interscience, New York.
- BERNAS, B., 1968. A New Method for Decomposition and Comprehensive
Analysis of Silicates by Atomic Absorption Spectroscopy.
Analyt. Chem., 40, 1682-1686.

- BESWICK, A.E., 1973. An experimental study of alkali metal distributions in feldspars and micas. *Geochim. cosmochim. Acta*, 37, 183-208.
- BISHOP, A.C., BRADSHAW, J.D., RENOUF, J.T. & TAYLOR, R.T., 1969. The stratigraphy and structure of part of west Finistère, France. *Quart. J. Geol. Soc. London*, 124, 309-348.
- , ROACH, R.A. & ADAMS, C.J.D., (in press). Precambrian rocks within the variscides. In: *Precambrian of the British Isles*. Geol. Soc. London Special Report.
- BLATTNER, P., 1971. Migmatite by Partial Fusion and Short Range Hydrothermal Transfer, British Columbia. *Schweiz. miner. petrogr. Mitt.*, 51, 155-177.
- BOUMA, A.A., 1962. *Sedimentology of Some Flysch Deposits. A Graphic Approach to Facies Interpretation*. Elsevier, Amsterdam.
- BRADSHAW, J.D., RENOUF, J.T. & TAYLOR, R.T., 1967. The development of Brioverian structures and Brioverian/Palaeozoic relationships in west Finistère (France). *Geol. Rundsch.*, 56, 567-596.
- BROWN, G.C., 1970a. Experimental studies on granites and related rocks. Ph.D. thesis, University of Manchester.
- 1970b. A comment on the role of water in the partial fusion of crustal rocks. *Earth and Planet. Sci. Lett.*, 9, 355-358.
- & FYFE, W.S., 1970. The Production of Granitic Rocks during Ultrametamorphism. *Contr. Mineral. and Petrol.*, 28, 310-318.
- 1972. The Transition from Metamorphism to Melting: Status of the Granulite and Eclogite Facies. 24th I.G.C., Montreal, 2, 27-34.

- BROWN, M., 1973. The Definition of Metatexis, Diatexis and Migmatite. Proc. Geol. Ass., 84, 371-382.
- 1974. Reply by the Author. Proc. Geol. Ass., 85, 114.
- , BARBER, A.J. & ROACH, R.A., 1971. Age of the St. Malo migmatite belt, northern Brittany. Nature Physical Science, 234, 77-79.
- & ROACH, R.A., 1972a. Precambrian rocks south of Erquy and around St. Cast, Cotes-du-Nord. Nature Physical Science, 236, 77-79.
- 1972b. Reply. Nature Physical Science, 239, 74-75.
- BROWN, P.E., 1967. Major Element Composition of the Loch Coire Migmatite Complex, Sutherland, Scotland. Contr. Mineral. and Petrol., 14, 1-26.
- 1971. The origin of the granite sheets and veins in the Loch Coire migmatites, Scotland. Min. Mag., Lond., 38, 446-450.
- BURNHAM, C.W., HOLLOWAY, J.R. & DAVIS, N.F., 1969. Thermodynamic properties of water to 1,000°C and 10,000 bars. Geol. Soc. America Spec. Paper 132, 1-96.
- BURRI, C., 1959. Petrochemische Berechnungsmethoden auf aquivalenter Grundlage. Birkhauser Verlag, Basle. (Petrochemical calculations. 1964 Israel Program for Scientific Translations Ltd.).
- CANN, J.R., 1970. Upward movement of granitic magmas. Geol. Mag., 107, 335-340.
- CHAYES, F., 1952. The staining of potash feldspar. Am. Mineralogist, 37, 357-360.

- CHATTERJEE, N.D., 1972. The upper stability limit of the assemblage paragonite+quartz and its natural occurrence. *Contr. Mineral. and Petrol.*, 34, 288-303.
- CONDIE, K.C., 1967. Geochemistry of early Precambrian greywackes from Wyoming. *Geochim. cosmochim. Acta*, 31, 2135-2149.
- COGNE, J., 1951. Remarques sur les schistes cristallins du cours inférieur de la Rance (Ille-et-Vilaine). *Bull. Soc. géol. Fr.*, 6, 139-145.
- 1959. Données nouvelles sur l'Antécambrien dans l'Ouest de la France: Pentévrien et Briovérien en baie de Saint-Brieuc (Cotes-du-Nord). *Bull. Soc. géol. Fr.*, 7, 112-118.
- 1962. Le Briovérien. Esquisse des caractères stratigraphiques, métamorphiques, structuraux et paléogéographiques de l'Antécambrien récent dans le Massif armoricain. *Bull. Soc. géol. Fr.*, 7, 413-430.
- 1964. In: MICHOT, J. & LAVREAU, J. (see below).
- 1966. Les grands cisaillements Hercyniens dans le Massif armoricain et les phénomènes de granitisation. In: *Etages Tectoniques, à la Baconnière, Neuchatel (Suisse)*, 179-192.
- 1967. Zones stables et zones mobiles au cours de l'orogénèse hercynienne dans le Massif armoricain - relations avec le champ de la pesanteur. In: *Contribution de la carte gravimétrique de la géologie du Massif armoricain. Mém. B.R.G.M.*, 52, 15-23.
- 1970. Le Briovérien et le cycle orogénique cadomien dans le cadre des orogènes fini-précambriens. In: *Colloque international sur les corrélations du Précambrien, Rabat. C.N.R.S., Mém. Serv. géol. Maroc (à l'impression)*.

- 1971. Le Massif armoricain et sa place dans la structure des socles Ouest-Européens: l'Arc hercynien Ibéro-armoricain. In: Histoire structurale du Golfe de Gascogne. Edit. Technip, 1, 1-23.
- COWARD, M.P., 1973. Heterogeneous deformation in the development of the Laxfordian complex of South Uist, Outer Hebrides. *Jl. geol. Soc. Lond.*, 129, 137-160.
- CROSS, W., IDDINGS, J.P., PIRSSON, L.V. & WASHINGTON, H.S., 1902. A quantitative chemico-mineralogical classification and nomenclature of igneous rocks. *J. Geol.*, 10, 555-690.
- DALLMEYER, R.D. & DODD, R.T., 1971. Cordierite in the Hudson Highland gneisses. *Contr. Mineral. and Petrol.*, 33, 289-308.
- DAY, H.W., 1973. The upper stability limit of muscovite plus quartz. *Am. Mineralogist*, 58, 255-262.
- DIETRICH, R.V. & MEHNERT, K.R., 1960. Proposal for the nomenclature of migmatites and associated rocks. 21st I.G.C., Copenhagen, Suppl. Vol. Sect., 1-21, 56-67.
- DODGE, F.C.W., SMITH, V.C. & MAYS, R.E., 1969. Biotites from Granitic Rocks of the Central Sierra Nevada Batholith, California. *J. Petrol.*, 10, 250-271.
- DRURY, S.A., 1972. The Chemistry of Some Granitic Veins from the Lewisian of Coll and Tiree, Argyllshire, Scotland. *Chem. Geol.*, 9, 175-193.
- EADE, K.E. & FAHRIG, W.F., 1971. Geochemical evolutionary trends of continental plates - a preliminary study of the Canadian shield. *Geol. Surv. Canada Bull.*, 179.
- EUGSTER, H.P. & WONES, D.R., 1962. Stability relations of the ferruginous biotite, annite. *J. Petrol.*, 3, 82-125.

- EVANS, B.W., 1965. Application of a reaction-rate method to the breakdown equilibria of muscovite and muscovite plus quartz. *Am. J. Sci.*, 263, 647-667.
- & GUIDOTTI, C.V., 1966. The sillimanite-potash feldspar isograd in western Maine, U.S.A. *Contr. Mineral. and Petrol.*, 12, 25-62.
- FAIRBAIRN, H.W. & HURLEY, P.M., 1971. Evaluation of X-ray fluorescence and mass spectrometric analyses of Rb and Sr in some silicate standards. *Geochim. cosmochim. Acta*, 35, 149-156.
- FENNER, P. & HAGNER, A.F., 1967. Correlation of variation in trace elements and mineralogy of the Esopus Formation, Kingston, New York. *Geochim. cosmochim. Acta*, 31, 237-261.
- FILIPPOV, M.S. & KOMLEV, D.V., 1959. Uranium and Thorium in granitoids of the middle Dnepr region. *Geochemistry (U.S.S.R.)* (English Transl.), 535.
- FLANAGAN, F.J., 1969. U.S.G.S. Standards - II. First compilation of data for the new U.S.G.S. rocks and additional data on rocks G-1 and W-1, 1965-1967. *Geochim. cosmochim. Acta*, 33, 81-120.
- FLEUTY, M.J., 1964. The description of folds. *Proc. Geol. Ass.*, 75, 461-492.
- FOSTER, M.D., 1960. Interpretation of the composition of trioctahedral micas. *U.S. Geol. Surv. Prof. Paper*, 354-B, 1-49.
- FYFE, W.S., 1970. Some thought on granite magmas. In: *Mechanism of Igneous Intrusion*, ed. by G. Newall and N. Rast, *Geol. J. Spec. Issue*, 2, 201-216.
- 1973. The generation of batholiths. In: P.J. Wyllie (Editor), *Experimental Petrology and Global Tectonics*. *Tectonophysics*, 17, 273-283.
- HARKER, A.,

- GHOSH, S.K. & RAMBERG, H., 1968. Buckling experiments on intersecting fold patterns. *Tectonophysics*, 5, 89-105.
- GOLDSMITH, J.R. & LAVES, F., 1954. The microcline-sanidine stability relations. *Geochim. cosmochim. Acta*, 5, 1-19.
- GORBATSHEV, R., 1972. The X-ray obliquity of potassic feldspar in the granites of Jamtland, Northern central Sweden. *Geol. For. Stockh. Forh.*, 94, 213-228.
- GRAINDOR, M.J., 1957. Le Briovérien dans le nord-est du Massif Armoricaïn. *Mém. Serv. Carte géol. Fr.*, 1-211.
- 1960. Existence vraisemblable du Penteévrien dans les Iles Anglo-Normandes et la Hague. *Bull. Soc. linn. Normandie*, 10, 44-47.
- 1962a. Définition du Briovérien sensu stricto. *Bull. Soc. linn. Normandie*, 10, 88-91.
- 1962b. L'age de la migmatite syntectonique de St. Malo. *C.R. Acad. Sci. Fr.*, 254, 3729-2731.
- & WASSERBURG, G.J., 1962. Determinations d'ages absolus dans le Nord du Massif armoricaïn. *C.R. Acad. Sci. Fr.*, 254, 3875-3877.
- GUIDOTTI, C.V., 1963. Metamorphism of pelitic schists in the Bryant Pond quadrangle, Maine. *Am. Mineralogist*, 48, 772-791.
- GURICH, G., 1905. Granit und Gneis. *Himmel Erde*, 17, 241-251.
- HAMEURT, J., 1972. Le Briovérien inférieur et la limite Briovérien-Penteévrien: Problèmes actuels. Unpublished.
- & JEANNETTE, D., 1971. Mise en évidence d'un terme lithostratigraphique nouveau du Briovérien. Le group détritique de St. Cast (Bretagne Septentrionale). *C.R. Acad. Sci. Fr.*, 273, 1767-1770.
- HARKER, A., 1908. The Geology of the Small Isles of Inverness-shire. *Mem. Geol. Surv. U.K.*

- HARRIS, N.B.W., 1974a. The Petrology and Petrogenesis of Some Muscovite Granite Sills from the Barousse Massif, Central Pyrenees. *Contr. Mineral. and Petrol.*, 45, 215-230.
- 1974b. Some migmatite types and their origins, from the Barousse Massif, Central Pyrenees. *Geol. Mag.*, 111, 319-328.
- HARRIS, P.G., KENNEDY, W.Q. & SCARFE, C.M., 1970. Volcanism versus plutonism - the effect of chemical composition. In: *Mechanism of Igneous Intrusion*, ed. by G. Newall and N. Rast, *Geol. J. Spec. Issue*, 2, 187-200.
- HEINRICH, E.Wm., 1946. Studies in the mica group; the biotite-phlogopite series. *Am. J. Sci.*, 244, 836-848.
- HEIER, K.S., 1964. Rubidium/strontium and strontium-87/strontium-86 ratios in deep crustal materials. *Nature*, 202, 477-478.
- & ADAMS, J.A.S., 1964. The geochemistry of the alkali metals. *Phys. & Chem. Earth*, 5, 253-381.
- & THORESEN, K., 1971. Geochemistry of high grade metamorphic rocks, Lofoten-Vesteralen, North Norway. *Geochim. cosmochim. Acta*, 35, 89-99.
- HIGGINS, M.W., 1971. Cataclastic Rocks. U.S. Geol. Surv. Prof. Paper, 687, 1-97.
- HIRST, D.M., 1962. The geochemistry of modern sediments from the Gulf of Paris. *Geochim. cosmochim. Acta*, 26, 1147-1187.
- HOLDAWAY, M.J., 1971. Stability of andalusite and the aluminium silicate phase diagram. *Am. J. Sci.*, 271, 97-131.
- HOLMQUIST, P.J., 1916. Swedish Archaean structures and their meaning. *Bull. geol. Instn. Univ. Upsala*, 15, 125-148.
- 1921. Typen und Nomenklatur der Adergesteine. *Geol. For. Stockh. Forh.*, 43, 612-631.

- HUANG, W.L. & WYLLIE, P.J., 1973a. Muscovite dehydration and melting in deep crust and subducted oceanic sediments. *Earth and Planet. Sci. Lett.*, 18, 133-136.
- 1973b. Melting Relations of Muscovite-Granite to 35 kbar as a Model for Fusion of Metamorphosed Subducted Oceanic Sediments. *Contr. Mineral. and Petrol.*, 42, 1-14.
- HUGHES, C.J., 1970. The significance of biotite selvages in migmatites. *Geol. Mag.*, 107, 21-24.
- HUSMANN, O., 1956. Bestimmungen des Thorium- und Uranium-Gehaltes an Gneisen und magmatischen Gesteinen des mittleren Schwarzwaldes mittels der Koinzidenz-Methode. *Neues Jahrb. Mineral., Monatsh.*, 108-120.
- JAMES, R.S. & HAMILTON, D.L., 1969. Phase Relations in the System $\text{NaAlSi}_3\text{O}_8 - \text{KAlSi}_3\text{O}_8 - \text{CaAl}_2\text{Si}_2\text{O}_8 - \text{SiO}_2$ at 1 kilobar Water Vapour Pressure. *Contr. Mineral. and Petrol.*, 21, 111-141.
- JEANNETTE, D., 1968. Structure du Briovérien à phanites de la baie de la Fresnaye (Cotes-du-Nord, Bretagne). *Bull. Serv. Carte géol. Als. Lorr.*, 21, 163-176.
- 1971. Analyse Tectonique de Formations Antécambriennes. Etude du Nord-est de la Bretagne. Thesis, Univ. of Strasbourg.
- & COGNE, J., 1968. Une discordance majeure au sein du Briovérien au flanc Ouest de la Baie de Saint-Brieuc. *C.R. Acad. Sci. Fr.*, 266, 2211-2214.
- JENKINS, R. & DE VRIES, J.L., 1967/1970. *Practical X-ray Spectrometry*. Macmillan, London.
- JOYCE, A.S., 1973. Petrogenesis of the Murrumbidgee Batholith, A. C. T. *J. geol. Soc. Aust.*, 20, 179-197.

- JUNG, J. & ROQUES, M., 1952. Introduction à l'étude zonéographique des formations crystallophylliennes. Bull. Serv. Carte geol. Fr., 235, 1-62.
- KELSEY, C.H., 1965. Calculation of the C.I.P.W. norm. Min. Mag., 32, 276-282.
- KENNEDY, W.Q., 1951. Sedimentary differentiation as a factor in Moine-Torridonian correlation. Geol. Mag., 88, 257-266.
- KERFORNE, F., 1921. Notice Géologique sur le département d'Ille-et-Vilaine. Bull. Soc. géol. Min. de Bretagne, 3, 49-58.
- KERRICK, D.M., 1972. Experimental determination of muscovite+quartz stability with $P_{H_2O} < P_{total}$. Am. J. Sci., 272, 946-958.
- KLEEMAN, A.W., 1965. The origin of granitic magmas. J. geol. Soc. Aust., 12, 35-52.
- KNABE, W., 1966. Anatektische Schmelzbildung in Quarz-Plagioklas-Biotit Gesteinen. Thesis, Univ. of Gottingen.
- KOLBE, P. & TAYLOR, S.R., 1966. Geochemical investigation of the granitic rocks of the Snowy Mountains area, New South Wales. J. geol. Soc. Aust., 13, 1-25.
- KRAUSKOPF, K.B., 1969. Thermodynamics used in Geochemistry. In: Wedepohl, K.H. (Editor), Handbook of Geochemistry. Springer Verlag, I, 37-77.
- LAETER, J.R. De & ABERCROMBIE, I.D., 1970. Mass spectrometric isotope dilution analyses of rubidium and strontium in standard rocks. Earth and Planet. Sci. Lett., 9, 327-330.
- LAMBERT, I.B. & HEIER, K.S., 1967. The vertical distribution of uranium, thorium and potassium in the Continental Crust. Geochim. cosmochim. Acta, 31, 377-390.
- , ROBERTSON, J.K. & WYLLIE, P.J., 1969. Melting relations in the system $KAlSi_3O_8 - SiO_2 - H_2O$ to 18.5 kilobars. Am. J. Sci., 267, 609-626.

- LARSEN, E.S., 1948. The Batholith and Associated Rocks of Corona, Elsinore and San Luis Rey Quadrangles, Southern California. Geol. Soc. America Mem., 29, 1-182.
- LEAKE, B.E., HENDRY, G.L., KEMP, A., PLANT, A.G., HARVEY, P.K., WILSON, J.R., COATS, J.S., AUCOTT, J.W., LUNEL, T. & HOWARTH, R.J., 1969/1970. The chemical analysis of rock powders by automatic X-ray fluorescence. Chem. Geol., 5, 7-86.
- LEAKE, B.E., 1972. The mineralogical modification of the chemistry of metamorphic rocks. Geol. Mag., 109, 331-337.
- LEONARDOS, O.H., Jr. & FYFE, W.S., 1974. Ultrametamorphism and Melting of a Continental Margin: The Rio de Janeiro Region, Brazil. Contr. Mineral. and Petrol., 46, 201-214.
- LEUTWEIN, F., 1968. Géochronologie et évolution orogénique précambrienne et hercynienne de la partie nord-est du Massif Armoricaïn. Sci. de la Terre, Mém., 11, 1-84.
- & SOMET, J., 1965. Contribution a la Connaissance de l'Evolution Géochronologique de la partie nord-est du Massif Armoricaïn français. Sci. de la Terre, 10, 345-366.
- , POWER, G., ROACH, R. & SOMET, J., 1973. Quelques résultats géochronologique obtenus sur des roches d'age précambrien du Cotentin. C.R. Acad. Sci. Fr., 276, 2121-2124.
- LOEWINSON-LESSING, F., 1899. Studien über die Eruptivgesteine. Zweites Capitel Zur Frage über die Differentiation und Krystallisation der Magmen. C. r. VII I.G.C., St. Petersburg, 308-401.
- LOWMAN, P.D., 1965. Non-anatectic Migmatites in Gilpin County, Colorado. Bull. geol. Soc. Am., 76, 1061-1064.
- LUNDGREN, L.W., 1966. Muscovite Reactions and Partial Melting in South-Eastern Connecticut. J. Petrology, 7, 421-453.

- LUTH, W.C., JAHNS, R.H. & TUTTLE, O.F. 1964. The Granite System at Pressures of 4 to 10 Kilobars. *Journ. Geophys. Res.*, 69, 759-773.
- & TUTTLE, O.F., 1969. The hydrous vapour phase in equilibrium with granite and granite magmas. In: L.H. Larsen (Editor), *Igneous and Metamorphic Geology*. *Geol. Soc. America Mem.*, 115, 513-548.
- MACKIE, W., 1905. Seventy chemical analyses of rocks (chiefly from the Moray area). *Proc. Edinburgh Geol. Soc.*, 8, 58.
- MARMO, V., 1962. On granites. *Bull. Comm. géol. Finlande*, 201, 1-77.
- 1967. On granites; a revised study. *Bull. Comm. géol. Finlande*, 227, 1-83.
- 1971. *Granite Petrology and the Granite Problem*. Elsevier, Amsterdam.
- MATHIEU, G., 1944. *Essai sur les granites du Massif Armoricaïn*. *Revue Sci.*, 3228, 15-24.
- MEHNERT, K.R., 1953-1963. Petrographie und Abfolge der Granitisation im Schwarzwald 1-4. *Neues Jahrb. Mineral.*, 85, 59-140; 90, 39-90; 98, 208-249; and 99, 161-199.
- 1968. *Migmatites and the Origin of Granitic Rocks*. Elsevier, Amsterdam, 1-393.
- , BUSCH, W. & SCHNEIDER, G., 1973. Initial Melting at Grain Boundaries of Quartz and Feldspar in Gneisses and Granulites. *Neues Jb. Miner. Mh.*, 4, 165-183.
- 1974. The Definition of Metatexis, Diatexis and Migmatite. *Written Discussion of a Paper Taken as Read*. *Proc. Geol. Ass.*, 85, 113.

- MERRILL, R.B., ROBERTSON, J.K. & WYLLIE, P.J., 1970. Melting reactions in the system $\text{NaAlSi}_3\text{O}_8 - \text{KAlSi}_3\text{O}_8 - \text{SiO}_2 - \text{H}_2\text{O}$ to 20 kilobars compared with results for other feldspar-quartz- H_2O and rock- H_2O systems. *J. Geol.*, 78, 558-569.
- MICHOT, P. & LAVREAU, J., 1964. Compte Rendu de la session extraordinaire de la Société belge de Géologie, de Paléontologie et d'Hydrologie et de la Société géologique de Belgique. *Bull. Soc. belge de Géol., de Paléontol. et d'Hydrolog.*, 73, 221-254.
- MYERS, J.S., 1971. The Late Laxfordian granite-migmatite complex of Western Harris, Outer Hebrides. *Scott. J. Geol.*, 7, 254-285.
- NOCKOLDS, S.R., 1954. Average chemical compositions of some igneous rocks. *Am. Geol. Soc. Bull.*, 65, 1007-1032.
- PARK, R.G., 1969. Structural correlation in metamorphic belts. *Tectonophysics*, 7, 323-338.
- PETTIJOHN, F.J., 1957. *Sedimentary Rocks*. Harper, New York, 1-718.
- 1963. Data of geochemistry S. Chemical composition of sandstones - excluding carbonate and volcanic sands. *U.S. Geol. Surv. Prof. Paper*, 440-S.
- PHAIR, G. & GOTTFRIED, D., 1964. The Colorado Front Range, Colorado, USA, as a uranium and thorium province. In: Adams, J.A.S. & Lowder, W.M. (Editors), *The natural radiation environment*. Chicago Univ. Press, 7.
- PITCHER, W.S. & BERGER, A.R., 1972. *The Geology of Donegal. A Study of Granite Emplacement and Unroofing*. John Wiley & Sons, New York.
- PIWINSKII, A.J., 1968. Experimental studies of igneous rock series Central Sierra Nevada Batholith, California. *J. Geol.*, 76, 548-570.

- PIWINSKII, A.J. & WYLLIE, P.J., 1968. Experimental studies of igneous rock series: a zoned pluton in the Wallowa Batholith, Oregon. *J. Geol.*, 76, 205-234.
- POLDERVAART, A., 1955. Chemistry of the earth's crust. In: A. RILEY, J.P. Poldervaart (Editor), *Crust of the Earth*. *Geol. Soc. Am. Spec. Paper*, 62, 119-144.
- PRESNALL, D.C. & BATEMAN, P.C., 1973. Fusion Relations in the System $\text{NaAlSi}_3\text{O}_8 - \text{CaAl}_2\text{Si}_2\text{O}_8 - \text{KAlSi}_3\text{O}_8 - \text{SiO}_2 - \text{H}_2\text{O}$ and Generation of Granitic Magmas in the Sierra Nevada Batholith. *Geol. Soc. Am. Bull.*, 84, 3181-3202.
- RAGLAND, P.C., 1970. Composition and structural state of the potassic in perthites as related to petrogenesis of a granite pluton. *Lithos*, 3, 167-189.
- , BILLINGS, G.K. & ADAMS, J.A.S., 1968. Magmatic differentiation and autometasomatism in a zoned granitic batholith from central Texas, USA. In: L.H. Ahrens (Editor), *The Origin and Distribution of the Elements*. Pergamon Press, Oxford, 795-824.
- RAMSAY, J.G., 1962. Interference Patterns Produced by the Superposition of Folds of "Similar" Type. *J. Geol.*, 60, 466-481.
- 1967. *Folding and Fracturing of Rocks*. McGraw-Hill, New York.
- & GRAHAM, R.H., 1970. Strain variation in shear belts. *Can. J. Earth Sci.*, 7, 786-813.
- REED, J.J., 1957. Petrology of the lower Mesozoic rocks of the Wellington District. *N.Z. Geol. Surv. Bull.*, 5, 1-57.
- REED, H.H., 1957. *The Granite Controversy*. Murby, London.
- & WATSON, J., 1968. *Introduction to Geology*, Macmillan, London.

- RICHARDSON, S.W., GILBERT, M.C. & BELL, P.M., 1969. Experimental determination of kyanite-andalusite and andalusite-sillimanite equilibria; the aluminium silicate triple point. *Am. J. Sci.*, 267, 259-272.
- RILEY, J.P., 1958. Rapid analysis of silicate rocks and minerals. *Anal. Chim. Acta*, 19, 413-428.
- ROACH, R.A., 1957. The geology of the Metamorphic Complex of South and Central Guernsey. PhD thesis, University of Nottingham.
- 1966. Outline and guide to the geology of Guernsey. *Rep. Soc. guernés.*, 18, 751-776.
- , ADAMS, C., BROWN, M., POWER, G. & RYAN, P., 1972. The Precambrian Stratigraphy of the Armorican Massif, N.W. France. *Proc. 24th I.G.C. Montreal*, 1, 246-252.
- ROUBAULT, M., LA ROCHE, H. DE & GOVINDARAJU, K., 1968. Report (1966-1968) on geochemical standards: Granites GR, GA, GH; Basalt BR; ferriferous Biotite Mica-Fe; Phlogopite Mica-Mg. *Sci de la Terre*, 13, 379-404.
- RYAN, P.D., 1973. The solid geology of the area between Binic and Bréhec, Cotes-du-Nord, France. PhD thesis, Univ. of Keele.
- & ROACH, R.A., (in press). Pentevrian/Brioverian relationships at Palus Plage, Cotes-du-Nord, N.W. France. *Bull. Soc. géol. Min. de Bretagne*.
- SCHEUMANN, K.H., 1936. Zur Nomenklatur migmatitischer und verwandter Gesteine. *Tschermaks miner. petrogr. Mitt.*, 48, 297-302.
- 1937. Metatexis and Metablastesis. *Tschermaks miner. petrogr. Mitt.*, 48, 402-412.
- SEDERHOLM, J.J., 1907. Om granit och gneis. *Bull. Comm. geol. Finlande*, 23, 1-110.

- SMITH, J.V. 1923. On Migmatites and Associated Pre-Cambrian Rocks of Southwestern Finland. I: The Pellinge Region. Bull. Comm. géol. Finlande, 58, 1-153.
- SMITH, J.V. 1926. On Migmatites and Associated Pre-Cambrian Rocks of Southwestern Finland. II: The Region around Barosundsfjord W. of Helsingfors and Neighbouring Areas. Bull. Comm. géol. Finlande, 77, 1-143.
- STEIGER, R.F. 1967. Selected Works. Oliver and Boyd, Edinburgh and London.
- SEGNET, R.E. & KENNEDY, G.C., 1961. Reactions and melting relations in the system muscovite-quartz at high pressures. Am. J. Sci., 259, 280-287.
- SHAPIRO, L. & BRANNOCK, W.W., 1962. Rapid analysis of silicate, carbonate and phosphate rocks. U.S. Geol. Surv. Bull. 1144A, 1-56.
- SHARMA, R.S., 1969. On Banded Gneisses and Migmatites from Lavertezzo and Roz era (Valle Verzasca, Canton Ticino). Schweiz miner. petrogr. Mitt., 49, 199-276.
- SHAW, D.M. 1968. A review of K-Rb fractionation trends by covariance analysis. Geochim. cosmochim. Acta, 32, 573-601.
- , REILLY, G.A., MUYSSON, J.R., PATTENDEN, G.E. & CAMPBELL, F.E., 1967. The chemical composition of the Canadian Precambrian Shield. Can. J. Earth Sci., 4, 829-853.
- SIGHINOLFI, G.P., 1969. K-Rb Ratio in High Grade Metamorphism: A Confirmation of the Hypothesis of a Continual Crustal Evolution. Contr. Mineral. and Petrol., 21, 346-356.
- SMALES, A.A. & WAGER, L.R., 1960. Methods in Geochemistry. Wiley Interscience, New York.

- SMITH, J.V., 1956. The powder patterns and lattice parameters of plagioclase feldspars: I The soda-rich plagioclases. *Min. Mag.*, 31, 47-68.
- SMITHSON, S.B. & DECKER, E.R., 1973. K, U and Th distribution between dry and wet facies of a syenitic intrusion and the role of fluid content. *Earth and Planet. Sci. Lett.*, 19, 131-134.
- STEIGER, R.H. & HART, S.R., 1967. The microcline - orthoclase transition within a contact aureole. *Am. Mineralogist*, 52, 87-116.
- STEUHL, H.H., 1962. Die experimentelle Metamorphose und Anatexis eines Parabiolithgneises aus dem Schwarzwald. *Chem. Erde*, 21, 413-449.
- STORRE, B., 1972. Dry Melting of muscovite+quartz in the range $P=7$ kb to $P_s=20$ kb. *Contr. Mineral. and Petrol.*, 37, 87-89.
- & KAROTKE, E., 1971. An experimental determination of the upper stability limit of muscovite+quartz in the range 7-20 kb. water pressure. *Neues Jahrb. Mineral.*, 8, 237-240.
- SUTTON, J.S., 1972. The Precambrian Gneisses and Supracrustal Rocks of the Western Shore of Kaipokok Bay, Labrador, Newfoundland. *Can. J. Earth Sci.*, 9, 1677-1692.
- TALIAFERRO, N.L., 1943. Franciscan-Knoxville problem. *Bull. Am. Assoc. Petroleum Geol.*, 27, 109-219.
- TAYLOR, S.R., 1965. The application of trace element data to problems in petrology. *Phys. Chem. Earth*, 6, 133-213.
- THOMPSON, A.B., 1974. Calculation of Muscovite-Paragonite-Alkali Feldspar Phase Relations. *Contr. Mineral. and Petrol.*, 44, 173-194.
- TILLING, R.I., 1968. Zonal Distribution of Variations in Structural State of Alkali Feldspar within the Radar Creek Pluton, Boulder Batholith, Montana. *J. Petrology*, 9, 331-357.

- TOBSCHALL, H.J., 1971. Zur Genese der Migmatite des Baume-Tales (Mittlere Cévennen, Dép. Ardèche). *Contr. Mineral. and Petrol.*, 32, 93-111.
- TOMISKA, T., 1962. On order-disorder transformation and stability range of microcline under high water vapour pressure. *Mineral. J.*, 3, 261-281.
- TURNER, F.J. & WEISS, L.F., 1963. *Structural Analysis of Metamorphic Tectonites*. McGraw-Hill, New York.
- TUTTLE, O.F. & BOWEN, N.L., 1958. Origin of granite in the light of experimental studies in the system $\text{NaAlSi}_3\text{O}_8 - \text{KAlSi}_3\text{O}_8 - \text{SiO}_2 - \text{H}_2\text{O}$. *Geol. Soc. Am. Mem.*, 74, 1-153.
- TYRRELL, G.W., 1933. Greenstones and greywackes. *C.R. réunion intern. pour l'étude du Précambrien*, 24-26.
- VAN DIVER, B.B., 1970. Origin of biotite orbicles in "Bullseye Granite" of Craftsbury, Vermont. *Am. J. Sci.*, 268, 322-340.
- VELDE, B., 1966. Upper stability of muscovite. *Am. Mineralogist*, 51, 924-929.
- VERDIER, P., 1968. *Etude pétrographique et structurale de Trégor occidentale (Baie de Lannion, Cotes-du-Nord-Finistère)*. Thèse de 3^{ème} cycle, Univ. of Strasbourg.
- VIDAL, P., AUVRAY, B., COGNE, J., HAMEURT, J. & JEANNETTE, D., 1971. Données géochronologique sur la série spilitique d'Erquy: problèmes nouveaux à propos du Briovérien de Bretagne Septentrionale. *C.R. Acad. Sci. Fr.*, 273, 132-135.
- VOGEL, T.A., 1969. Albite-rich Domains in Potash Feldspar. *Contr. Mineral. and Petrol.*, 25, 138-143.
- VON PLATEN, H., 1965. Experimental anatexis and genesis of migmatites. In: *Controls of Metamorphism*, ed. by W. Pitcher and G. Flynn, *Geol. J. Spec. Issue*, 1, 203-218.

- & HOLLER, H., 1966. Experimentelle Anatexis des Stainzer Plattengneises von der Koralpe, Steirmark, bei 2, 4, 7 und 10 kb H₂O-Druck. Neues Jahrb. Mineral., 106, 106-130.
- VORMA, A., 1971. Alkali feldspars of the Wiborg rapakivi massif in south-eastern Finland. Bull. Comm. géol. Finlande, 246.
- WASHINGTON, H.S., 1917. Chemical analyses of igneous rocks. U.S. Geol. Surv. Prof. Paper, 99, 1-1201.
- WASSERBURG, G.J., MACDONALD, G.J.F., HOYLE, F. & FOWLER, W.A., 1964. Relative Contributions of Uranium, Thorium and Potassium to Heat Production in the Earth. Science, 143, 465-467.
- WEDEPOHL, K.H., 1969. Handbook of Geochemistry. Springer-Verlag, Berlin-Heidelberg.
- WEILL, D.F. & KUDO, A.H., 1968. Initial melting in alkali feldspat-plagioclase-quartz systems. Geol. Mag., 104, 325-337.
- WHITE, A.J.R., 1966. Genesis of migmatites from the Palmer region of South Australia. Chem. Geol., 1, 165-200.
- WHITFIELD, J.M., RODGERS, J.J.W. & ADAMS, J.A.S., 1959. The relationship between the petrology and the thorium and uranium contents of some granitic rocks. Geochim. cosmochim. Acta, 17, 248-271.
- WHITNEY, P.R., 1969. Variations of the K/Rb ratio in migmatitic paragneisses of the Northwest Adirondacks. Geochim. cosmochim. Acta, 33, 1203-1211.
- WILLIAMS, P.F., 1972. Development of metamorphic layering and cleavage in low-grade metamorphic rocks at Bermagui, Australia. Am. J. Sci., 272, 1-47.
- WINKLER, H.G.F., 1967. Petrogenesis of Metamorphic Rocks. Springer Verlag, New York.

- 1970. Abolition of Metamorphic Facies, Introduction of the Four Divisions of Metamorphic Stage, and a Classification based on Isograds in Common Rocks. Neues Jb. Miner., 5, 189-248.
- & LINDEMANN, W., 1972. The system Qz-Or-An-H₂O within the granitic system Qz-Or-Ab-An-H₂O. Application to granitic magma formation. Neues Jb. Miner., 7, 49-61.
- WRIGHT, T.L., 1968. X-ray and optical study of alkali feldspar: II. An X-ray method for determining the composition and structural state from measurement of 2θ values for three reflections. Am. Mineralogist, 53, 88-104.
- & STEWART, D.B., 1968. X-ray and optical study of alkali feldspar: I. Determination of composition and structural state from refined unit-cell parameters and 2V. Am. Mineralogist, 53, 38-87.
- Zen, E-an., 1969. Stability relations of the polymorphs of aluminium silicates: a survey and some comments. Am. J. Sci., 267, 297-309.